EXPERIMENTAL INVESTIGATION OF INDOOR AIR POLLUTANTS IN THREE RESIDENTIAL BUILDINGS

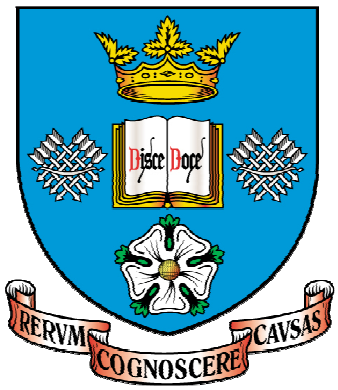

Caren CL Tan, B.Eng., M.Sc
Department of Chemical and Biological Engineering
The University of Sheffield

Supervisors: Prof. V. N. Sharifi & Prof. J. Swithenbank

A thesis submitted to the University of Sheffield for the degree of
Doctor of Philosophy

February 2012

ABSTRACT

We spend about 90% of our time inside buildings, where we control the quality of the environment for health, thermal comfort, security and productivity. The quality of the indoor environment is affected by many factors including the design of the building, ventilation, thermal insulation and energy provision and use. To improve thermal comfort and reduce energy consumption, the inside environment has been almost completely isolated from the outside environment in recent years, through making buildings airtight. However, as dwellings are made more airtight internal pollution sources (such as heating and cooking) can have a greater impact on the indoor air quality and occupants may experience adverse health effects. The main objective of this research was therefore to investigate indoor air pollutant emissions in relation to energy use in residential buildings, with a focus on particulate matter (PM).

Three environments were investigated: (i) a rural house with an electric cooker; (ii) a city-centre flat with a gas cooker; and (iii) an urban flat on a main road, also with gas appliances. Concentrations of PM, carbon monoxide (CO), nitrogen dioxide (NO_2) and volatile organic compounds (VOCs) were measured in the kitchens and enhanced emission rates were calculated for cooking periods. Although there has been a great deal of research examining the effects of gaseous pollutants in the indoor environment, this is the first study to focus on PM.

This study showed that most particulates were small ($\leq$2.5µm) and thus respirable. The elemental analysis of the PM revealed high metal concentrations (Fe/Na/Zn), whilst their morphologies indicated these were present as salt, skin flakes and mineral fibres. Cooking activities were found to directly contribute to $PM_{2.5}$ emissions in the indoor environment. In the kitchen of the rural house with the electrical cooker, $PM_{2.5}$ emission rates ranged from 5 to 22 mg/hr. The city centre flat with a gas cooker had higher $PM_{2.5}$ concentrations and thus also greater emission rates (up to 54 mg/hr). CO concentrations were generally quite low – around 1-2 ppm in all three residential environments. During cooking however, the CO levels became elevated in the kitchens with the gas cookers (Cases 2 and 3), as this was a significant source of this species; levels often peaked at 10-20 ppm during cooking. For Case 1, where an electric cooker was installed, there was no difference in CO levels during cooking and non-cooking periods.

In the rural house (Case 1), since there was no source of NO_2 emissions inside, the indoor and outdoor NO_2 concentrations were the same, around 10-11 $\mu g/m^3$. However in the city-centre flat (Case 2), the gas cooker was found to be a significant source of NO_2 and thus the indoor concentration was much greater than the outdoor levels (47 $\mu g/m^3$ compared to 15 $\mu g/m^3$) and the resultant indoor emission rate was also high – up to 65.5 mg/hr. The VOC concentrations were consistently higher in the indoor environments at all locations compared to outdoor levels. The highest emission rate for VOCs was for the kitchen of Case 2, the city-centre flat (~ 43 mg/hr).

This study has shown that indoor air quality is influenced by fuel, type of cooker, and cooking method. Air quality in residential buildings, especially in the kitchen, was generally poorer when using gas appliances compared to when an electric cooker was used; this was true for both solid and gas-phase pollutants. In addition, indoor air was strongly influenced by outdoor sources of pollution.

ACKNOWLEDGEMENTS

Firstly, I would like to express my grateful appreciation to my supervisors, Professor Jim Swithenbank and Professor Vida Sharifi, for their invaluable guidance, advice, encouragement and inspiration throughout the duration of my work. Without their advice and constructive ideas, this project would not have been successfully accomplished.

My outmost gratitude also goes to Dr Nigel Russel, Dr Karen Finney, Dr Qun Chen, Dr Xiaohui Zhang and Dr Jue Zhou, for their assistance and motivation throughout this learning curve. Without their contributions to the project, this project would not have been possible.

I would like to extend my sincere gratitude to Mr. Alan Cox (Centre for Analytical Sciences) and Dr Cathy Shields (Sorby Centre for Electron Microscopy) for their expertise, support and patience in the usage of analytical equipment. The invaluable advice and suggestions that they gave truly help the progression and smoothness of this project.

Great thanks also go to the UK Engineering and Physical Science Research Council (EPSRC PUrE Intrawise Consortium: Pollutants in the Urban Environment – Integrated Framework for Improving Sustainability of the Indoor Environment) for their financial and technical support for this research study.

Finally, special thanks to my family and friends who have been patient and provided support, understanding, motivation and encouragement. May God bless you abundantly.

Table of Contents

List of Tables

List of Figures

Nomenclature

Symbol	Description
A_p	The projected area of the particle (perpendicular to the flow direction)
a	Air exchange rate (hr^{-1})
a_e	Acceleration of the particle
C_D	Drag coefficient
C_0	The tracer gas concentration at time t=0, $\mu g/m^3$ or ppmv
C_t	The tracer gas concentration at the time t, $\mu g/m^3$ or ppmv
C_{in}	Indoor mass concentration of pollutants ($\mu g/m^3$)
C_{out}	Outdoor mass concentration of pollutants ($\mu g/m^3$)
D_p	Diameter of spherical particle
F_B	The buoyant force
F_D	The drag force
F_e	The external force
k	Pollutant removal rate (hr^{-1})
m	Mass of a particle
n	Air exchange rate, 1/hr or ACH
p	Penetration coefficient across building envelope
Q	Ventilation rate, m^3/hr
S_e	Emission rate ($\mu g/hr$)
t	Sampling time
u	Velocity of the particle relative to the fluid
V	The volume of room space, m^3

Greek Symbols

ρ	Density of the fluid
Δt	Cooking time (corresponding to pollutants emissions)

Abbreviations

ASTM	American Society for Testing and Materials
BSE	Backscattered Electrons
CFD	Computational Fluid Dynamics

CO	Carbon Monoxide
COHb	Carboxyhaemoglobin
COMEAP	Committee on the Medical Effects of Air Pollutants
DEFRA	Department for Environment Food and Rural Affairs
EDS	Energy Dispersion X-ray Spectrometry
HPA	Health Protection Agency
ICP	Inductive Coupled Plasma
I/O	Ratio of Indoor and Outdoor Pollutants Concentrations
ISO	International Organisation for Standardisation
LES	Large Eddy Simulation model
LPG	Liquid Petroleum Gas
NDIR	Nondispersive Infrared Sensor
NIOSH	National Institute of Occupational Safety and Health
NOx	Oxides of Nitrogen
OES	Optical Emission Spectrometry
OSHA	Occupational Safety and Health Administration
PM	Particulate Matter
RNG	Renormalisation Group
RSP	Respirable Suspended Particles
SE	Secondary Electrons
SEM	Scanning Electron Microscopy
TEA	Triethanolamine
USEPA	United State Environmental Protection Agency
VOCs	Volatile Organic Compounds
WHO	World Health Organisation
Σ20 VOCs	The Sum of the Top 20 Volatile Organic Compounds

1

INTRODUCTION

We spend the vast majority of our time indoors – 90% on average – either at home, school or work. We control these indoor environments for health, thermal comfort, productivity and security reasons. However, sustaining the quality of the indoor built environment could impact both human health and the local and global environment. The quality of the indoor environment is affected by many factors, including the design of buildings, ventilation, energy provision or use, thermal insulation and various household activities, such as cleaning.

1.1 BACKGROUND

In recent years, the importance of the indoor air environment has been realised (Zhao *et al*., 2004). Wang *et al* (2007) defined indoor air as the air within non-industrial areas (e.g. dwellings, offices, schools, hospitals etc). Parra *et al* (2008) reported that the concentration of indoor air pollutants is five times higher than outdoor levels. Research has also suggested that indoor air pollution is more serious than outdoor air pollution (USEPA, 2009). In addition, exposure to indoor air pollution was increased as people spend the majority of their time in an indoor environment (Chiang and Lai, 2002; Kumar and Kumar, 2007; Wang *et al*., 2007; USEPA, 2009), including young children (McCormack *et al*., 2008).

One of the methods that people can be easily affected by indoor air pollution is through the inhalation of indoor air. It has been proven that ambient air has a significant impact on the

quality of the indoor environment after several studies were conducted (Parra *et al*., 2008). Approximately 30% of the occupants of new or remodelled buildings may complain about the quality of their indoor environment, according to a 1984 World Health Organization report (USEPA, 2009).

When particles (either in solid or liquid form) and gases contaminate the environment, this phenomenon is known as air pollution. Specifically, indoor air pollution can be defined as the presence of one or more pollutants in the indoor environment, which might affect human health to a certain degree (Kumar and Kumar, 2007). Air pollution has a great impact on human health, either in chronic or acute form. The chronic form arises due to long-term exposure and the acute form tends to occur through accidents (Christoforou, 2007). In the recent past, an abundance of related studies on the indoor environment and its pollutants have been carried out in different situations, such as an office environment (Destaillats *et al*., 2008), care centres for senior citizens (Chiang *et al*., 2001), child care centres (Zuraimi and Tham, 2008) and a primary school (van Dijken *et al*., 2006).

Pollutants which are diffused from natural sources or found in nature are denoted as *natural pollutants*. *Anthropogenic pollutants* are those that are produced by humans or controlled processes (Christoforou, 2007). Air pollutants can be categorized as either primary or secondary pollutants. The pollutants which are released directly from a recognised source to the atmosphere are known as primary pollutants. When these primary pollutants react via chemical or physical processes in the atmosphere, then secondary pollutants will be formed (Christoforou, 2007; HPA, 2012). Several field studies have shown that indoor air can be approximately 20 to 50% (and sometimes exceeding 100%) more polluted than outdoor air (Kumar and Kumar, 2007; Wang *et al*., 2007).

In addition to outdoor sources of pollutants, which ingress to the indoor environment, there are also various indoor sources of air pollution, for example from combustion (from fossil fuels or biomass), building materials (vapours from carpets and pressed wood furniture) and household cleaning products (USEPA, 2009). Parra *et al* (2008) pointed out that indoor air pollution is not only generated by outdoor traffic pollution, but also originates from human activities.

In order to reduce energy consumption while improving the thermal comfort within the buildings, more effort has been put in to increasing the air-tightness of buildings in recent years. The main consequence of making a building more airtight is the aggravation of indoor air pollution issues. Various internal pollution sources (such as heating and cooking systems) can have a greater impact on the indoor air quality and occupants may experience adverse health effects due to the increased exposure. Most indoor air pollution comes from sources inside the building, for instance building materials and various human activities (Agelopoulos *et al*., 2000). These sources generate or release pollutants either continuously or intermittently. Building materials and household fragrance products may release pollutants continuously, whereas smoking or the use of household cleaning solvents would lead to the intermittent release of pollutants. Some of these activities would lead to the pollutants remaining longer in the air (USEPA, 2009).

In addition to the above sources, another major contributor to indoor air pollution is the use of energy, specifically for cooking and heating. When gas cookers are used in kitchens, various pollutants, like carbon monoxide (CO), oxides of nitrogen (NO_x) and particulate matter (PM) can be released. Many different types of appliances are used for heating, cooking and supplying hot water (Godish, 2001). In developed countries, cooking appliances include natural gas or propane-fuelled stoves/ovens, electric stoves/ovens and microwave devices. Gas cooking appliances are not vented to the outdoors and as a result, they are a potentially significant source of indoor air contamination. A numbers of gases (such as volatile organic compounds (VOCs), CO and NO_x) and particles are released during the combustion of various fuels for household heating. The results from studies on indoor air pollution from various heating systems have been published by various authors.

Several studies have been carried out to investigate indoor air pollution from different types of heating system (Yamanaka *et al*., 1979; Traynor *et al*., 1982; Moschandreas *et al*., 1987). Two techniques were developed for emission rate measurements: a direct measurement method and a mass balance method (Moschandreas *et al*., 1987). In the first, pollutant emissions were measured through directing the combustion effluents to an air sampling port. For the second method, indoor air is sampled from selected sampling locations and the pollutant concentrations are measured. Moschandreas *et al*. (1987) compared the emission rates of both NO_x and CO from range-top burners by both methods and concluded that the results were similar under well-defined, controlled conditions.

Indoor air pollutants are the main culprit in threatening human health. $PM_{2.5}$ refers to airborne particles that are less than 2.5 μm in aerodynamic diameter (COMEAP, 2012). It is the pollutant most clearly associated with adverse health outcomes, including death. COMEAP (2008) has reported that about 29,000 deaths could be attributable to exposure to $PM_{2.5}$. Human health may be influenced at the time of exposure or possibly years later (USEPA, 2009). The immediate effects of $PM_{2.5}$ include burning eyes, skin irritation and headaches. Some other possible diseases may include asthma, hypersensitivity pneumonitis and humidifier fever. On the other hand, some of the diseases only affect human health after years of exposure, such as respiratory disease, heart disease and cancer. Therefore, the concentration of pollutants, time of exposure, present health condition and age play a significant role in determining the level of detriment to human health (Kumar and Kumar, 2007; USEPA, 2009).

According to the American Lung Association (2008), various indoor air pollutants (for example combustion byproducts and volatile organic compounds) have been increasingly recognized as respiratory health hazards. Indoor air pollution is the fourth largest threat to the environment in US, according to the United State Environmental Protection Agency. Poor indoor air quality has a significant impact on children, since children are generally more sensitive to environmental pollutants than adults (van Dijken *et al*., 2006; HPA, 2007a). About 6.1 million children below 18 years old suffered with asthma in the US. Children exposed to indoor air pollutants can be easily affected by chronic illness in accordance with American Lung Association (2008). One of the significant causes of hospitalization in children under the age of 15 is asthma (HPA, 2005). Figure 1-1 shows the simulation of the human respiratory system by the Andersen Sampler (Thermo Electron Corp., 2003). The multi-stage and multi-orifice cascade Andersen Sampler will be further discussed in Section 3.3.

In addition, health conditions, such as allergic reactions, including hypersensitivity pneumonitis and allergic rhinitis are all triggered by bioaerosols. Most of the infectious diseases are transmitted through air, such as influenza, measles, chicken pox and others. Hence, it can be concluded that poor indoor air environments have resulted in the deficiency of work performance, poor health and illness (Kumar and Kumar, 2007).

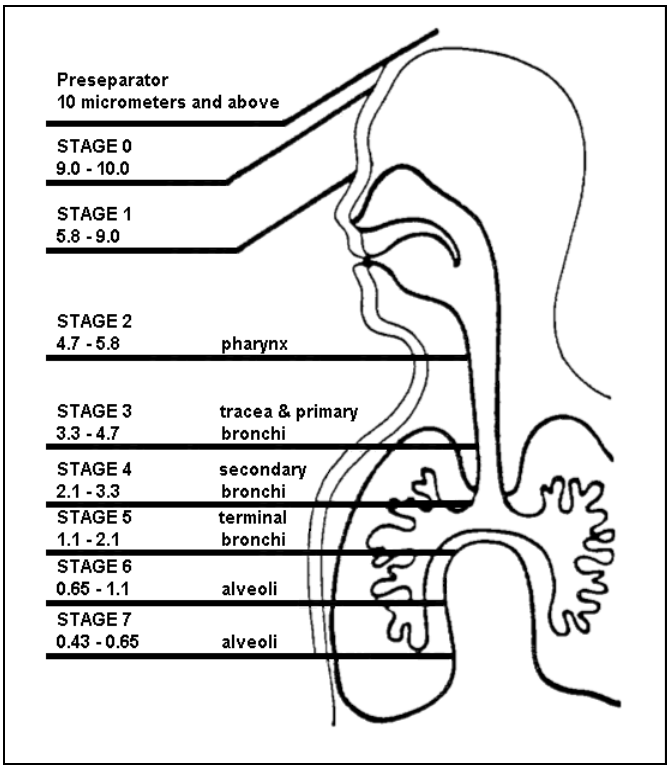

Figure 1-1: Simulation of the Human Respiratory System by the Andersen Sampler (Thermo Electron Corp., 2003)

Not only that, indoor air pollutants from the combustion of various fuels also play an important role in affecting human health in both urban and rural communities, especially in developing countries. Biomass and coal-burning release high concentrations of particles and a large number of people have suffered from these harmful emissions on a daily basis. This has led to detrimental effects on human health, especially those using open fires or low efficiency stoves. Women who are responsible for the cooking activities have become the most affected group by indoor air pollutants after years of exposure. Children who usually accompany their mothers near the cooking area also became part of the affected groups (WHO, 2002).

Indoor air pollution has brought much irritation to people, such as discomfort, ill health and lower productivity. A good indoor environment can minimise the exposure of building occupants to indoor air pollutants and safeguard their comfort and well-being. As explained by Bluyssen and Cox (2002), a healthier indoor environment can be created through reducing the emissions of various pollutants, minimising the exposure to these pollutants and sustaining the comfort of the indoor environment.

1.2 STATEMENT OF PROBLEM

Indoor air pollution has been neglected previously since people are always more concerned about air pollution in the outdoor environment. In the past, people only made use of their resources in order to control outdoor pollution. However, after the emergence of new indoor air pollutants (especially particles emitted from various heating systems), the indoor air pollution issue has now attracted more public concerns. Unfortunately, due to the lack of evidence on the effects of indoor air pollutants on human health, the potential problems that may arise from these new pollutants are becoming more difficult to tackle. Apart from this, the difficulties in measuring air pollutants at low levels have worsened the situation. Under these circumstances, there is an urgent need to study, analyse and investigate the prevailing conditions with a view to identify the problems and formulate solutions, and, if required, to carry out extensive research to upgrade and improve the conditions.

1.3 RESEARCH OBJECTIVE

The main objective of this research was to investigate indoor air pollutants, namely PM, CO, NO_x and VOCs, related to the generation, conservation and use of energy in buildings, focussing especially the particulate matter emitted from various heating and cooking systems.

1.4 RATIONALE FOR THE EXPERIMENTS

Indoor air pollutants, such as those listed above can have significant health implications. CO is highly toxic and even short-term low exposure can negatively impact health. VOCs are also toxic and many are carcinogenic. Acid gas emissions, like NO_x, can dissolve in water to form corrosive acids or can become attached to small particles. It has been suggested that the inhalation of such gases or particles can initiate or exacerbate existing respiratory problems. Particulates, if inhaled, can cause chronic cardiovascular, respiratory and pulmonary illnesses; smaller particles, particularly sub-micron PM, can penetrate deeper into the lungs, having greater health effects. Limited data for indoor air pollutant levels and the associated emission rates from heating or cooking appliances have been reported in the literature. Since we spend most of our time indoors, more detailed information on pollutant levels in homes is vital for understanding how emissions concentrations can be reduced, thus limiting personal exposure and minimising detrimental health impacts.

1.5 LAYOUT OF THESIS

Chapter 1 Introduction describes the background of this study, the statement of the problem, and outlines the research objective and rationale for the experiments.

Chapter 2 Literature Review presents an overview of indoor air pollutants, their effects on human health and the environment, their sources and releases. The chapter also discusses the indoor air pollutants emitted from various heating systems and their emission rates. Pollutant minimization and reduction technologies used in the current market and the indoor air quality guidelines and regulatory limits are introduced. This chapter also investigates the relationship between the indoor and outdoor concentrations. This chapter also outlines relevant computational fluid dynamics procedures and the impact of weather and traffic on indoor air pollution.

Chapter 3 Theoretical Background discusses particle motion theory and the theoretical calculations for this study. This chapter also looks into the principles behind various experimental instruments, e.g. Andersen 8-Stage Ambient Sampler Instrument, Scanning Electron Microscopy with Energy Dispersion X-ray Spectrometry (SEM/EDS), Inductively Coupled Plasma Optical Emission Spectrometry (ICP-OES), DustTrak^{TM} II Aerosol Monitor, IAQ-CALC Indoor Air Quality Meter, Diffusion Tubes and Tenax TA Tubes.

Chapter 4 Experimental Programme discusses the experimental set-up and operating conditions of analytical techniques and equipment for various indoor air pollutants (i.e. $PM_{2.5}$, CO, NO_2 and VOC) for this study. The chapter also describes the sampling locations and measurements.

Chapter 5 Case Study 1: Experiments in a Stone-built Detached House in Hathersage describes the results obtained from the tests carried out in a stone-built detached house in Hathersage. The chapter discusses the particulate measurements, the concentrations of solid-phase particulate matter $\leq$2.5 μm ($PM_{2.5}$) and gaseous pollutants (CO, NO_2 and VOCs). This chapter also discusses the computational fluid dynamic modelling of the particle flowfields inside the kitchen.

Chapter 6 Case Study 2: Experiments in a Residential Flat near Sheffield City Centre shows the results obtained from the tests conducted in a residential flat near Sheffield City Centre. The tests conducted include NO_2, VOCs, CO and $PM_{2.5}$ measurements.

Chapter 7 Case Study 3: Experiments in a Residential Flat on a Main Road in Sheffield shows the results obtained from the tests carried out in a residential flat on a main road in Sheffield. The tests conducted were measurements of $PM_{2.5}$, NO_2, VOCs and CO. This chapter also discusses the additional particulate measurements and analysis.

Chapter 8 Discussion discusses the relationship of indoor and outdoor concentrations of air pollutants, the influence of cooker types and the effect of cooking styles on indoor air quality, the impact of weather on particle size distribution, the elemental composition of PM and the problems and errors encountered in this research study.

Chapter 9 Conclusions and Recommendations for Future Work presents the main conclusions from this study and outlines the recommendations for future work.

2

LITERATURE REVIEW

An extensive literature survey was carried out on the experimental study of indoor air pollutants, particularly in residential buildings. This consisted of a review of various indoor air pollutants, its sources and effects on human health. This literature research also looked into the indoor air pollutants from various heating systems and their emission rates. Pollutant abatement, sampling and analytical technologies, indoor air quality guidelines and regulatory limits of various countries are also presented. The chapter also covered the relationship between the indoor and outdoor concentrations. Computational fluid dynamics used in predicting the particle trajectories is also presented. The chapter concludes with a review of the impacts of traffic and weather on the indoor pollutant concentrations.

2.1 INDOOR AIR POLLUTANTS

While it is recognised that people spend the majority of their time in the indoor environment, much of the attention to date relating to health consequences has been targeted on outdoor airborne pollutants. The following section will discuss the health and environmental effects, sources and releases of various indoor air pollutants, including particulate matter, pesticides, carbon monoxide, dust mites, nitrogen oxides, bacteria, volatile organic compounds, radon, formaldehyde, sulphur dioxide, fungi and ozone. The causes of these indoor air pollutants are summarised by the National Institute of Occupational Safety and Health (NIOSH) in Figure 2-1 and the United States Environmental Protection Agency (USEPA) in Table 2-1.

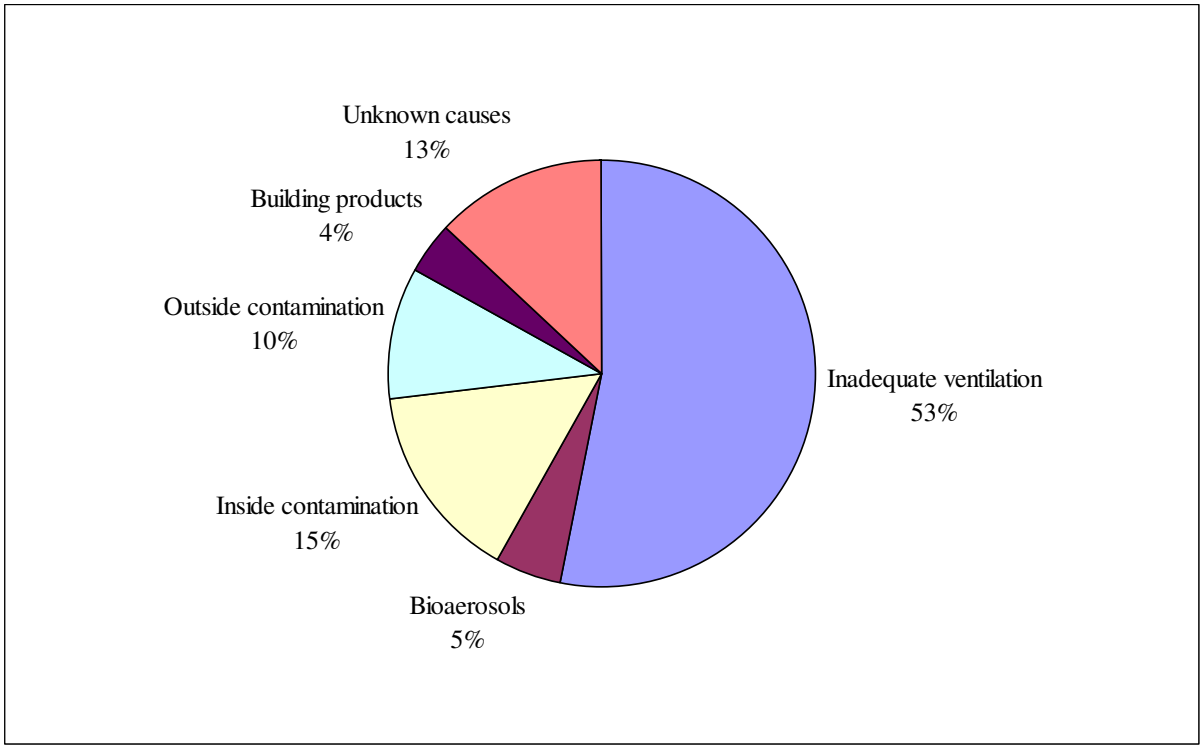

Figure 2-1: Sources of indoor air pollution (after National Institute of Occupational Safety and Health; Kumar and Kumar, 2007)

Table 2-1: Major indoor air pollutants (after Kumar and Kumar, 2007; USEPA, 2009)

Pollutants	Sources
By-products of combustion (e.g. CO, CO_2, NO_x)	Unvented kerosene and gas heaters, gas appliances, wood- and gas-burning fireplaces, leaking chimneys and furnaces, tobacco smoke, automobile exhaust in attached garages
Environmental tobacco smoke	Cigarettes, cigars, pipes
Formaldehyde	Pressed wood products (hardwood, plywood wall panelling, particleboard, fibreboard) used in buildings and furniture, urea-formaldehyde foam insulation, permanent press textiles, glue, environmental tobacco smoke, vehicle exhaust, stoves, fireplaces
Other volatile organic compounds	Paints, solvents, wood preservatives, aerosol sprays, cleaners and disinfectants, moth repellents, air fresheners, hobby supplies, and dry cleaned clothes
Radon	Local geology, soil, water
Pesticides	Garden and lawn chemicals, poisons for pest control
Asbestos	Deteriorating or damaged insulation, fireproofing, or acoustical materials
Heavy metals	Paints, automobiles, tobacco smoke, soil, and dust
Bioaerosols	Humans, pets, moist surfaces, humidifiers, ventilation systems, drip pans, cooling coils in air handling units, plants, outside air

2.1.1 Particulate Matter

Particulate Matter (PM) is referred to as micron-sized solid matter that is suspended in the air (Christoforou, 2007). The particles are varied, from those visible to the naked eye to those only visible under a microscopic. These particles circulate in the air within the indoor environment. The particles can be inhaled and deposited in human respiratory systems (e.g. sinuses, windpipe, etc). The windpipe acts as a filter to ensure the entering of particles into the lungs and damaging its tissues are limited (American Lung Association, 2008).

Particulate matter is often released following the incomplete combustion of fuels (USEPA, 2009). McCormack *et al.* (2008) described a number of studies which have been carried out to look into PM in the home. According to USEPA standard the maximum $PM_{2.5}$ exposure level is 65µg/m^3. However, the WHO guidelines for $PM_{2.5}$ exposure are much lower at 20µg/m^3 but these are for annual mean levels (Jedrychowski *et al*., 2006).

Sources and Mechanism of Formation

PM can originate from various natural or anthropogenic sources, for example cooking stoves, diesel vehicles, industrial processes and coal combustion (Christoforou, 2007). Household activities, such as smoking, sweeping, dusting, vacuuming and cooking can generate significantly higher indoor PM levels (McCormack *et al.*, 2008; American Lung Association, 2008). Van Dijken *et al*. (2006) reported the mass concentration and elemental contents of airborne particles smaller than 10µm in diameter (PM_{10}). With reference to McCormack *et al.* (2008), Figure 2-2 demonstrates the predictors of elevated indoor $PM_{2.5}$ and PM_{10} concentrations over a 3-day period. The indoor PM levels increased with the increase of indoor activities, as presented by the whisker plots. The boxes with the middle 50% of PM values show the median values.

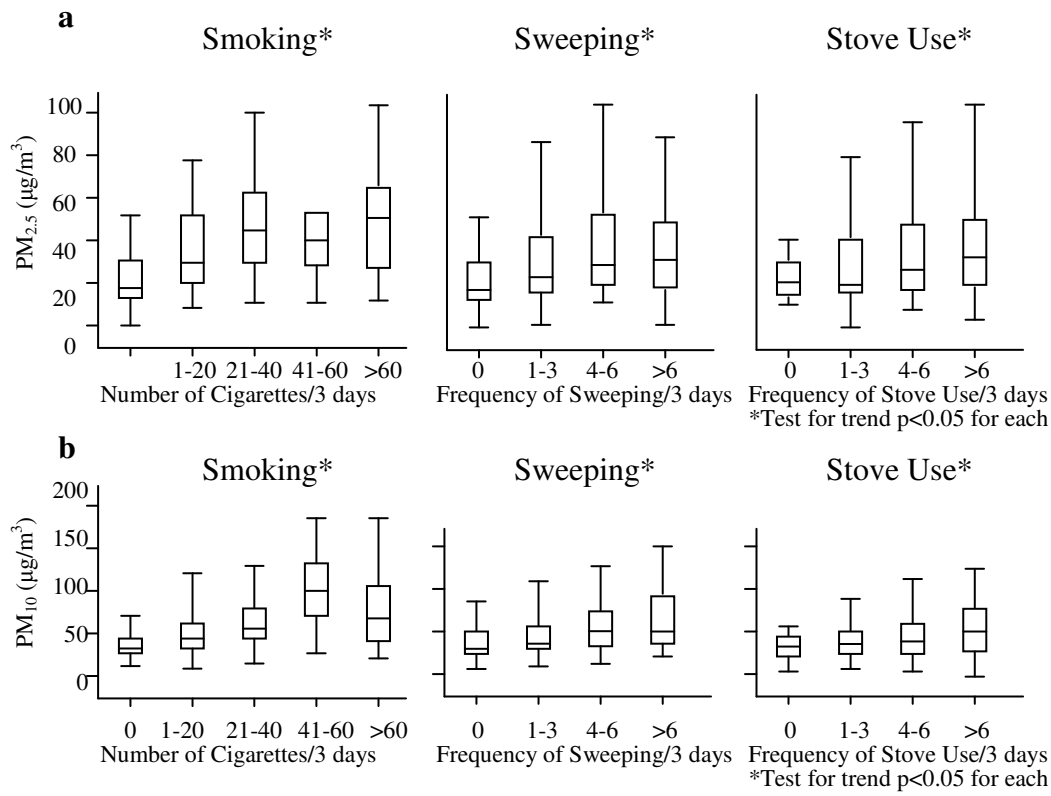

Figure 2-2: Predictors of elevated indoor $PM_{2.5}$ and PM_{10} concentration over a 3-day period (after McCormack *et al*., 2008)

Health Effects / Exposures

Most of the severe respiratory symptoms are linked closely to the airborne PM. These ambient pollutants can decrease lung function among asthmatics and increase mortality in the general population (McCormack *et al.*, 2008). These particles can irritate respiratory tissues and more seriously, decrease lung function and cause cancer. PM can also irritate the human body with allergies or transmittable diseases (American Lung Association, 2008). According to McCormack *et al.* (2008), a study on children revealed that lung fuction decreased with the increase of indoor PM concentrations.

Environmental Effects

PM is the main reason for a reduction in the visibility of the environment. Not only that, it can also affect water, plants and earth. For example, the nutrient balance and acidity level of land or water are affected by acid rain, which is formed from particles with nitrogen and sulphur. This

has caused changes in the composition of the species and buffering capacity. PM also can cause deterioration to materials (Christoforou, 2007).

2.1.2 Carbon Monoxide

Carbon monoxide (CO) is a toxic, yet fairly unreactive gas. It is colourless, odourless and tasteless (HPA, 2007b). It can disrupt the oxygen from being delivered to the human body. It is a by-product of incombustion processes, where it can be produced by any fuel-fired appliance, vehicle, gasoline power tools or other devices (Christoforou, 2007; American Lung Association, 2008; USEPA, 2009).

Sources and Mechanism of Formation

The sources of CO can be various, such as wood and gas stoves, boilers, kerosene heaters, fireplaces, leaking furnaces, vehicle exhaust and environmental tobacco smoke (American Lung Association, 2008). CO is released when the carbon in fuels is not completely burned (Christoforou, 2007).

Health Effects / Exposures

According to USEPA (2009) and Christoforou (2007) CO is an asphyxiant. It has serious health effects on humans. Psychomotor performance will be reduced if humans are exposed to CO (≈50 ppm) for eight hours continuously. CO will cause death if concentrations of 750 ppm are exceeded. Oxygen is transported throughout the body with the help of Haemoglobin. Haemoglobin is part of the blood cell that preferentially binds with CO compared with oxygen (≈240:1). When CO has over accumulated in human bodies, it will combine with haemoglobin, and form carboxyhaemoglobin (COHb). Carboxyhaemoglobin will disrupt the transportation of oxygen in the human body as it limits the haemoglobin to release oxygen. High concentrations of CO can kill in less than five minutes (American Lung Association, 2008).

People with chronic obstructive pulmonary and cardiovascular diseases are easily affected by increased CO levels in the atmosphere. Various household products (i.e. paint strippers etc) can be metabolized to form CO if containing methylene chloride (USEPA, 2009). Figure 2-3 shows the relationship between carbon monoxide concentrations and carboxyhaemoglobin levels

in the blood. The carboxyhaemoglobin levels and its related health effects are tabulated in Table 2-2.

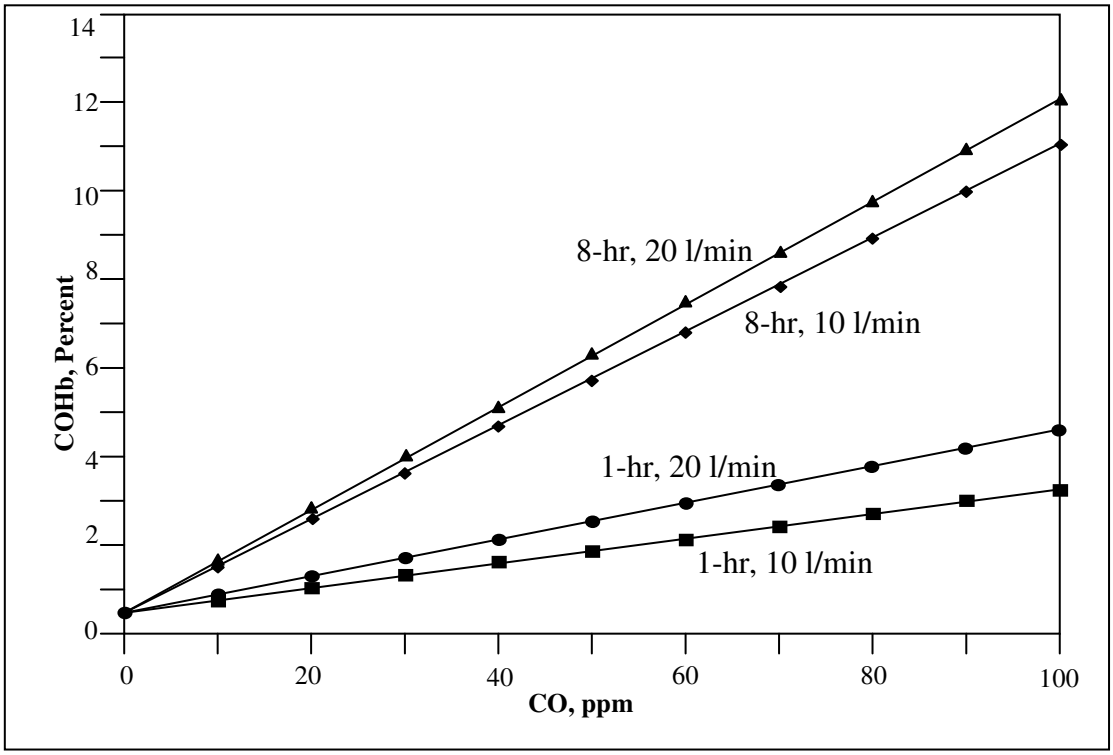

Figure 2-3: Relationship between CO (ppm) and COHb levels in blood (after USEPA, 2009)

Table 2-2: Carboxyhaemoglobin (COHb) levels and related health effects (after USEPA, 2009)

Carboxyhaemoglobin (COHb) levels and related health effects	
% COHb in blood	**Effects Associated with this COHb Level**
80	Death[a]
60	Loss of consciousness; death if exposure continues[a]
40	Confusion; collapse on exercise[a]
30	Headache; fatigue; impaired judgement[a]
7-20	Statistically significant decreased maximal oxygen consumption during strenuous exercise in healthy young men[b]
5-17	Statistically significant diminution of visual perception, manual dexterity, ability to learn, or performance in complex sensorimotor tasks (such as driving)[b]
5-5.5	Statistically significant decreased maximal oxygen consumption and exercise time during strenuous exercise in young healthy men[b]
Below 5	No statistically significant vigilance decrements after exposure to CO[b]
2.9-4.5	Statistically significant decreased exercise capacity (i.e., shortened duration of exercise before onset of pain) in patients with angina pectoris and increased duration of angina attacks[b]
2.3-4.3	Statistically significant decreased (about 3-7%) work time to exhaustion in exercising healthy men[b]
Source: [a] USEPA (1979); [b] USEPA (1985)	

2.1.3 Nitrogen Oxides

Nitrogen dioxide (NO_2) is a reddish-brown gas with an irritating odour. It is the most abundant oxide of nitrogen present in air. It is a lung irritant and not only that, it can cause difficulties in breathing if exposed to high concentrations (Christoforou, 2007). Nitric oxide (NO) and nitrogen dioxide (NO_2) are known as oxides of nitrogen (NO_x).

Sources and Mechanism of Formation

Indoor sources of nitrogen dioxide include gas fireplaces, boilers, hot water heaters, fireplaces and gas ranges (American Lung Association, 2008). Lightning and various biological processes in soils are natural sources of NO_2. Oxides of nitrogen are precursors of acid rain (along with SO_2) and visibility-reducing fine nitrate particles. The main sources of anthropogenic emissions of NO_x are combustion: vehicles and power plants (Christoforou, 2007).

Health Effects / Exposures

Oxides of nitrogen take part in various physiological and pathological mechanisms (e.g. vasodilatation, inflammation and malignant transformation). Several studies have been carried out on the role of oxides of nitrogen in lung carcinogenesis (Chen *et al.*, 2008).

Oxides of nitrogen can damage the lungs and increase susceptibility to colds and respiratory illness (American Lung Association, 2008; HPA, 2011). Evidence shows that continued exposure to low levels of oxides of nitrogen could generate respiratory infection. Various animal studies also proved that continuous exposures to high level of oxides of nitrogen may lead to emphysema. NO_2 is less soluble in water, thus easily irritates the upper airway. Exposure to NO_2 can decrease lung function, increase bronchial reactivity and respiratory infections, even with minimal exposure. This is particularly obvious in young children. Pulmonary oedema and lung injury may occur if exposed to extremely high dose levels of NO_2. Continuous exposure to high level of NO_2 can cause acute or chronic bronchitis (USEPA, 2009).

People with asthma or other respiratory diseases can be easily influenced by the effects of oxides of nitrogen (USEPA, 2009). Studies also showed that the oxidation properties and free radicals of NO_2 can cause lung tissue damage (Chen *et al.*, 2008).

2.1.4 Volatile Organic Compounds

According to the WHO, VOCs are organic chemicals that have varied boiling points, from 50ºC to 200 ºC, except for particles (Wang *et al.*, 2007). VOCs are well-recognized for their malodorousness and toxicity. Some of them are carcinogenic, mutagenic and teratogenic (Vincent *et al.*, 2008). VOCs can not only vaporize easily, but their small organic molecules also easily take part in photochemical reactions in the atmosphere and form smog (Stedman, 2007). The classes of VOCs found in indoor environment are listed in Table 2-3. From the table, it can be noticed that aromatics, aldehydes and halocarbons are most common (Wang *et al.*, 2007).

Table 2-3: The classes of VOCs identified in indoor air (after Wang *et al.*, 2007)

VOC class	Environment and sources
Aliphatic and cyclic hydrocarbons	1, 2, 4, 5, 7, 9-11
Aromatic hydrocarbons	1-7, 9, 11, 12
Aldehydes	1-12
Terpenes	1-4, 7-10
Alcohols	1-9, 11
Esters	1, 2, 4, 7-9
Halocarbons	1, 2, 7, 11
Glycols/glycolethers/glycolesters	1-4, 7, 9
Ketones	1-4, 6-12
Siloxanes	11
Alkene	2, 7
Organic acids	2, 3, 7-9, 11
Ethers	9
Other VOCs	1, 2, 4, 7, 11

1: Established buildings, 2: new and renovated buildings, 3: school, 4: new car interiors, 5: carpets, 6: floor coverings, 7: wood-based panel and furniture, 8: solid woods, 9: paints, 10: cleaning products, 11: unflued gas heaters and electric ovens, 12: office equipment.

Indoor VOC concentrations are often higher than outdoor concentrations (Meininghaus *et al.*, 2000). This was proven by a study carried out by USEPA in six communities in the United States, where the indoor VOC concentration was approximately ten times higher than the outdoor concentration, even at highly polluted outdoor sources, such as petrochemical plants (USEPA, 2009). VOCs are emitted in gas form at room temperature from certain solids or liquids and they include various chemicals (such as formaldehyde, benzene, perchloroethylene), which bring short- and long-term effects (USEPA, 2009). Parra *et al.* (2008) pointed out that the increasing numbers of VOCs and their potential negative consequences on human health have attracted more and more researchers to study them.

Sources and Mechanism of Formation

VOCs are pollutants which can be released from various sources. Tobacco smoke, consumer and cleaning products, combustion by-products, cooking, construction materials and office equipment are some of the sources (Wang *et al.*, 2007; Parra *et al*., 2008). Apart from this, they can be emitted by materials such as carpets, paints, wallpapers or polyvinyl chloride; they may enter a room from outdoors, or they are emitted or generated during human activities (Meininghaus *et al.*, 2000). Geng *et al.* (2008) further indicated that benzene compounds found in ornament painting solvents slowly diffuse into the indoor environment. USEPA (2009) concluded that the main sources of VOCs are dry-cleaning fluids, building materials, personal items, household products, home furnishings, office equipment, graphics and craft materials.

Some specific indoor sources of organic vapours are presented in Table 2-4. VOCs comprise of aromatic compounds, such as benzene, toluene, xylene, dichlorobenzene and others (Sone *et al.*, 2008). The majority of these aromatic compounds are carcinogenetic. They do not have a safety threshold dose for carcinogenic effects. Therefore, exposure to low doses of VOCs could generate significant health impacts.

VOCs exist everywhere in the environment. Therefore, humans can easily come into contact with VOCs. These include breathing, eating and skin contact (Sone *et al.*, 2008). The sources and emission rates are the main factors to determine the exposure level of VOCs indoors. VOCs can be emitted from various sources. However, the most significant source of VOCs is building materials. The total VOCs are much higher in concentration, if compared to individual VOC level ($\leq$ 50$\mu g/m^3$). Therefore, the various emission rates of building materials and coverings make them the main source of indoor VOCs (Wang *et al.*, 2007). The total VOC emission rates from various indoor sources are tabulated in Table 2-5.

From Table 2-5, it can be observed that the most important sources of indoor VOCs are construction coverings and household cleaning products (Wang *et al.*, 2007). The emission rates range from 1.7 x $10^4\mu g/m^2/h$ to 2.6 x $10^8\mu g/m^2/h$ for household cleaning products. The emission rates for construction coverings range from $10\mu g/m^2/h$ to 1.7 x $10^7\mu g/m^2/h$.

Table 2-4: Some specific indoor sources of organic vapours (after Wang *et al.*, 2007)

Compound	Source material (s)
Paradichlorobenzene	Moth crystals, room deodorants
Methylene chloride	Paint removers, solvent usage
Formaldehyde	Pressed wood products, foam
Styrene	Insulation, textiles, disinfectants, plastics, paints
Acetaldehyde	Glues, deodorants, fuels, preventives, mould growth on leathers
Acrolein	Component of oak-wood, by-product of the combustions of wood, kerosene and cotton
Toluene diisocyanate	Polyurethane foam, aerosols
Phthalic acid anhydride **Trimellitic acid** **Triethylene Tetraamine**	Epoxy resins
Benzyl chloride **Benzyl chloride**	Vinyl tiles plasticized with butyl benzyl phthalate
Ethylene Oxide	Sterilizers (hospitals)
Amines (cyclohexyloamine, diethylaminoethanol, morpholine)	Volatilized with the steam boiler systems (corrosion inhibitors of steam pipes and other equipment)
Volatile amines	Putrefactive degradation of casein-containing building materials
Benzene	Smoking
Tetrachloroethylene	Wearing or storing dry-cleaned clothes
Chloroform	Chlorinated water (showering, washing clothes, dishes)
1, 1, 1-trichloroethane	Wearing or storing dry-cleaned clothes, aerosol sprays, fabric protectors
Carbon tetrachloride	Industrial strength cleaners
Aromatic hydrocarbons (toluene, xylene, ethylbenzene, trimethylbenzenes)	Paints, adhesives, gasoline, combustion sources
Aliphatic hydrocarbons (octane, decane, undecane)	Paints, adhesives, gasoline, combustion products
Terpenes (limonene, α-pinene)	Scented deodorizers, polishes, fabrics, fabric softeners, cigarettes, food beverages
Chloropyrifos (Dursban)	Household insecticides
Chlordane, heptachlor	Termicide
Diazinon	Termicide
Polychlorinated Biphenyls	Transformers, PCB-containing fluorescent light ballasts, ceiling tiles
Polycyclic Aromatic Hydrocarbons	Combustion products (smoking, woodburning, kerosene heaters)
Polychlorinated dibenzofurans	Incinerator stack emission
Polychlorinated dibenzo-*p*-dioxins	Contamination of pentachlorophenol used as wood preservative
Acrylic acid esters, epichlorohydin, vinyl chloride	Monomers may escape from polymers
Alcohols	Aerosols, window cleaners, paints, paint thinners, cosmetics and adhesives
Ketones	Lacquers, varnishes, polish removers, adhesives
Ethers	Resins, paints, varnishes, lacquers, dyes, soaps, cosmetics
Esters	Plastics, resins, plasticizers, lacquers solvents, flavours, perfumes
Pentachlorophenol	Wood preservative agent
Lindane	Wood preservative formulations

Table 2-5: Total VOC emission rates for indoor sources (after Wang *et al.*, 2007)

Source description	Emission rate (μg/m^2/h)
Household products ("wet")	
1. Solvent-based waxes/detergents	Up to 2.6 x 10^8
2. Waxes spread on surface	1.0 x 10^6 – 9.4 x 10^7
3. Toilet deodorizers	1.3 x 10^6 – 3.7 x 10^6
4. Room deodorizers	1.6 x 10^5 – 2.0 x 10^6
5. Liquid cleaner/disinfectant	1.1 x 10^6
6. Carpet spray cleaner	1.1 x 10^6
7. Water-based waxes/detergents	1.2 x 10^5 – 1.2 x 10^6
8. Furniture spray polish	3.0 x 10^5
9. Floor cleaners	< 10^4 – 1.5 x 10^5
10.Floor wax paste	6.0 x 10^4
11. Dry-cleaned clothing	2.7 x 10^4
12. Floor wax	2.0 x 10^4
13. Liquid floor detergent	1.7 x 10^4
Construction products ("wet")	
1. Solvent-based adhesives	5.1 x 10^6 – 1.7 x 10^7
2. Water-based adhesives	< 10^4 – 2.1 x 10^6
3. Wall/flooring glue (Ethylene vinyl acetate)	2.7 x 10^5
4. Sealant (including silicones)	300 – 7.2 x 10^4
5. Wood stain	1.7 x 10^4
6. Polyurethane lacquer	6.0 x 10^3
7. Floor varnishes (3 types)	830 – 4.7 x 10^3
8. Polyvinyl acetate glue (water-based)	2.1 x 10^3
Construction products ("dry")	
1. New vinyl flooring	1.9 x 10^4 – 4.3 x 10^4
	120 – 2.3 x 10^3
2. Rubber floor covering	1.4 x 10^3
	410
3. Plywoods	300 – 2.4 x 10^3
4. Polystyrene foam	40
	1.4 x 10^3
	30 - 10^3
5. Textile floor covering	80 – 1.6 x 10^3
6. Plastic floor covering	220 – 590
7. Rubber-backed nylon carpet	300
	50 – 180
8. Felt-carpet	80 – 10
9. paint gypsumboard/particleboard	240 – 260
10. Particleboard	120 – 140
11. Polyurethane foam	120
12. Wallpapers (including vinyl)	30 – 300
13. Gypsumboard	30
14. Glass reinforced plastics sheeting	20
15. Mineral wool	10

Health Effects / Exposures

VOCs can affect human health extensively as they are among the main indoor air pollutants. VOCs can result in sick building syndrome if exposed for a long period of time (Geng *et al.*, 2008). Many VOCs are toxic and they are also carcinogens, mutagens and teratogens.

VOCs are closely related to sick building syndrome (Wang *et al.*, 2007). These compounds can have a negative effect on the occupant's health, since they can act for example as irritants (Meininghaus *et al.*, 2000).

VOCs have primary and secondary negative effects on human health if long-term exposure occurs. The effects may include irritation to the eyes and throat, deterioration of the liver, and in serious circumstances, destruction of the central nervous system (Sone *et al*., 2008). Some other signs and symptoms of VOC exposure are irritation to the airways and respiratory system, rhinitis, dyspnoea and increased allergic sensitisation (USEPA, 2009).

Environmental Effects

VOCs can react with nitrogen oxides and form photochemical smog, to release toxic gases and its byproducts into the atmosphere (Sone *et al.*, 2008). Photochemical smog can cause irritation to eyes, dyspnoea and damage to plants. This has caused a significant reduction in yields due to the damage inflicted on crops (Hastie, 2007). Moreover, many VOCs with low odour thresholds can provoke odour annoyance in the indoor air (Meininghaus *et al.*, 2000).

Trends / Releases

Generally the average VOC concentration in established buildings is below 50µg/m^3. Since the 1970s, various studies have been carried out to determine the indoor VOC concentration. The outcome of these findings are indoor air typically contains higher concentration of VOCs than outdoor air (Wang *et al.*, 2007).

2.1.5 Radon

Radon is an odourless, colourless and tasteless gas (Hamilton, 2007; American Lung Association, 2008; USEPA, 2009). It is radioactive, but chemically unreactive. Radon gas is present everywhere in the natural environment (Hamilton, 2007). The guideline level of radon is four picocuries per litre of air (pCi/L) based on USEPA recommendations (American Lung Association, 2008).

Sources and Mechanism of Formation

There are various sources of radon, such as the earth, uranium and rock beneath homes (American Lung Association, 2008). Radon gas is released when uranium naturally breaks down and it enters through cracks in slabs or walls, unsealed pipes, drains, sumps and crawl spaces (USEPA, 2009; American Lung Association, 2008).

Radon can be found from the anthropogenic environment as well, due to most of the products and food of everyday life originating from the naturally radioactive environment (Hamilton, 2007).

Health Effects / Exposures

Basically, there is no immediate symptom after being exposed to radon. The American Lung Association (2008) estimated that 10% of lung cancer deaths are due to radon. Radon rightfully takes the spotlight as the menacing cause of lung cancer, after smoking. Radon, which breaks down into short-lived radionuclides, can cause damage to lung tissue before removal by clearance mechanisms (USEPA, 2009).

The decay of radon into another element possesses even worse impacts on human health (Hamilton, 2007). The alpha particles emitted by radon decay products can damage lung cells and cause cancer (USEPA, 2009; American Lung Association, 2008). In the United States, it is estimated that about 14,000 lung cancer deaths per year are ascribed to radon—however, this number could vary from 7,000 to 30,000 deaths per year. Smokers have greater risk of suffering from radon-induced lung cancer than non-smokers (USEPA, 2009; American Lung Association, 2008).

2.1.6 Formaldehyde

Formaldehyde originates from either combustion or certain natural processes. It plays an important role in manufacturing various household cleaning products and building materials (USEPA, 2009). However, formaldehyde has been listed as a carcinogen by USEPA (2009).

Sources and Mechanism of Formation

According to Zhao *et al.* (2004), detergents, binders, cosmetics, furniture and environmental tobacco smoke are the main sources of indoor formaldehyde. However, the most important source of formaldehyde is decoration. Based on the research conducted by Zhao *et al.* (2004), indoor formaldehyde concentrations decrease with an increase in the building's age. Nevertheless, elevated indoor air temperatures increase indoor concentrations.

Other sources of formaldehyde include building materials, gas stoves and kerosene space heaters (USEPA, 2009). However, the most important source of indoor formaldehyde is pressed wood products, especially those made using urea-formaldehyde resins contained adhesives. Among those pressed wood products (i.e. particle board, hardwood plywood panelling, fibreboard), medium density fibreboard emits the highest concentration of formaldehyde as it consists of a higher resin-to-wood ratio compared to other pressed wood products (USEPA, 2009; American Lung Association, 2008).

Health Effects / Exposures

Formaldehyde can irritate the eyes and throat, as well as cause nausea and dyspnoea if exposed at above 0.1 parts per million levels. It also possesses harmful effects to asthmatics, and in a more serious way, causes cancer in humans (USEPA, 2009). Some other effects may include airway and respiratory system irritation, rhinitis and increased allergic sensitisation (American Lung Association, 2008).

2.1.7 Sulphur Dioxide

Sulphur dioxide (SO_2) is a colourless, non-flammable, non-explosive gas (Christoforou, 2007).

Sources and Mechanism of Formation

The main anthropogenic sources of SO_2 emissions are coal combustion in power plants and other stationary sources. Volcanic activity is a natural source of SO_2 (Christoforou, 2007).

Health Effects / Exposures

SO_2 can irritate the human respiratory system (Christoforou, 2007). Irritation on mucous membranes easily occurs if exposed to above six parts per million concentrations of SO_2. Epidemiologic studies show that exposure to SO_2 can cause bronchial constriction, particularly for asthmatics even with minimal exposures (≈0.4 parts per million), and chronic obstructive pulmonary disease (USEPA, 2009).

Environmental Effects

The environmental effects caused by SO_2 or sulphate PM are erosion or deterioration of materials (e.g. marble, limestone and mortar). This is due to the fact that water-soluble sulphates (gypsum, $CaSO_4.2H_2O$) have replaced the carbonates (i.e. $CaCO_3$) in these materials (Christoforou, 2007).

2.1.8 Ozone

Ozone (O_3) is formed when molecular oxygen (O_2) reacts with atomic oxygen (O) in the atmosphere. O_3 is also formed naturally in the stratosphere to protect the earth from high ultraviolet rays (Christoforou, 2007).

Sources and Mechanism of Formation

Ozone generators can produce O_3 directly whereas ion generators and electronic air cleaners can produce O_3 indirectly (USEPA, 2009).

Health Effects / Exposures

O_3 can cause irritation to the lungs and eyes. It can also cause asthma attacks in young people (Christoforou, 2007).

Environmental Effects

O_3 is capable of oxidizing materials, decreasing crop yields and stunting the growth of trees (Christoforou, 2007).

2.1.9 Pesticides

Pesticides can be defined as a mixture of chemical and biological substances which were used to repel pests (e.g. bacteria, insects, mites, molluscs etc) that affect human health. Pesticides are useful in disrupting or inactiving the life cycle of pests. Insect attractants, herbicides, plant defoliants, desiccants and plant growth regulators are also considered as pesticides (Edwards, 2007). Some pesticides contain a variety of chemicals thus they are technically categorised as semi-volatile organic compounds (USEPA, 2009).

Sources and Mechanism of Formation

According to American Lung Association (2008), pesticides can be found in insecticides, termiticides and product used on lawning and gardening.

Health Effects / Exposures

Many human illnesses and deaths have occurred over the last fifty years due to exposure to pesticides. Approximately 20,000 deaths were attributed to pesticides each year (Edwards, 2007). Up to 79,000 children were exposed to pesticides in 1990, as reported by the American Association of Poison Control Centres. A survey revealed that 75 percent of the households used at least one pesticide product in the indoor environment. The most common pesticides used are insecticides and disinfectants (USEPA, 2009).

Pesticides possess harmful effects to human health if they are not used properly. Inhalation of spray mists or vapours from pesticides often happen in daily use. Children are suffered from contaminated dusts when in close contact with contaminated surfaces. Exposure to cyclodiene pesticides can cause headaches, dizziness and muscle twitching when misapplication occurs. Long-term exposure to cyclodienes can cause cancer and damage to the liver and the central nervous system (USEPA, 2009).

The small residues of pesticides in both drinking water and food were suspected to disrupt endocrine activities. Numerous cases of pesticide residues in human foods have been reported though stringent regulations were endorsed by various regulatory agencies (Edwards, 2007). Moreover, some of the active components are carcinogenic to human health (USEPA, 2009).

They could cause irritations and damages to kidneys, and moreover cause cancer (American lung Association, 2008).

Environmental Effects

Pesticides are biocides. They are purposely used for killing certain groups of organisms. Therefore, they have diverse negative effects to environment. In spite of these effects are obvious or complex, pesticides are harmful to the flora and fauna, soil and water systems (Edwards, 2007).

2.1.10Dust Mites

Dust mites can be defined as the microscopic animals which can cause irritation to asthmatics and allergic reactions to certain groups of people (American Lung Association, 2008).

Sources

Dust mites always act as a source of house dust allergens. There are various factors that support the growth of biological agents in the air. Normally, house dust mites increase in high relative humidity conditions (USEPA, 2009). The main sources of dust mites include bedding, originated from pets, poorly maintained air conditioners, humidifiers and others (American Lung Association, 2008).

Health Effects / Exposures

Biological agents are the sources of various illnesses and diseases, such as upper respiratory irritations (American Lung Association, 2008). The main health effect caused by biological pollutants is allergic reactions (e.g. rhinitis, nasal congestion, conjunctiva inflammation, urticaria, asthma etc). House dust mites are the notable triggers for these diseases. Several guideline values have been proposed for levels of mite allergens in dust. For chronic exposure, the risk level was set to 2µg Der pI (Dermatophagoides pteronysinus allergen I) per gram of dust (or 100 mites /g or 0.6 mg guanine /g of dust), whereas for acute asthma the risk level is 10µg (Der pI) of the allergen per gram of dust (or 500 mites /g of dust). The mite allergens and Immunoglobulin E (IgE) antibody levels in patients are possible to be measured with the advanced technology available nowadays (USEPA, 2009).

2.1.11 Bacteria

Sources and Mechanism of Formation

The occupant is the main source of airborne bacteria indoors (Pastuszka *et al.*, 2000). Other possible sources include animals, soil and plant debris (USEPA, 2009). Bacteria are released when there is overpopulation of humans or animals. Most of them exist in the outdoor environment. These bacteria are induced indoors through several mechanisms (e.g. natural wind and mechanical ventilation systems). Air conditioning systems, cooling towers, humidifiers and air-distribution ducts become the most suitable breeding places for bacteria. Saliva and dander could be originated from pets (Kumar and Kumar, 2007). Pastuszka *et al.* (2000) proved that the micrococci with Micrococcus and Staphylococcus are the main bacteria dominated in a home.

Health Effects / Exposures

Various infectious diseases (i.e. allergic actions and toxic effects) are caused by airborne bacteria. Sick building syndrome and hypersensitivity diseases (e.g. asthma, humidifier fever etc) are the main health consequences from airborne bacteria (Pastuszka *et al.*, 2000). Besides that, bacteria also can trigger diseases such as hypersensitivity pneumonitis, allergic rhinitis and others. Some of the infectious illnesses caused by the bacteria can be disseminated through air, such as influenza, measles and chicken pox (USEPA, 2009).

The aerodynamic dimensions of the bacteria play an important role in identifying the deposition site of the bacteria and its impacts to the human health. If the aerodynamic dimensions of the bacteria are greater than 10µm, they have a low possibility to deposit in the respiratory naseo-pharyngeal tract. For bacteria sized from 5 to 10µm, they are mostly embedded in the upper respiratory system which can lead to allergic rhinitis. Bacteria which are smaller than 5µm (respirable fraction), can penetrate into the alveoli and cause allergic alveolitis (Pastuszka *et al.*, 2000).

2.1.12 Fungi

Fungi can be defined as a group of parasitic organisms that contain no chlorophyll, such as moulds and mildews (USEPA, 2009).

Sources / Mechanism of Formation

There are several factors affecting the growth of fungi and its release into the air. They can be found especially in high relative humidity places, such as damp surfaces, which allow fungi to grow on it (USEPA, 2009). A moist wall, ceiling, furniture or caspet could be the main source of fungi (American Lung Association, 2008). Fungi can be found in mouldy homes of which the concentration of airborne fungi is elevated to approximately 10^4 CFU m^{-3} (colony-forming units per cubic meter) in some dwellings (Pastuszka *et al*., 2000). It is common that fungi have a higher concentration in indoors compared to outdoors. This has further affirmed that spores play an important part in the indoor microbial pollution (Pastuszka *et al*., 2000).

2.2 INDOOR AIR POLLUTANTS FROM VARIOUS HEATING SYSTEMS AND EMISSION RATES

Prehistoric records showed that people noted down the smoke problems in caves. This proved that indoor air issues have been focused on since the beginning of civilisation. People have become more and more aware of indoor air pollution issues (Kumar and Kumar, 2007). These include the indoor air pollution caused by various heating systems.

Investigations into indoor air pollutants from various heating systems and their emission rates are discussed in this section. The heating systems involved in the discussion include gas-fired heating systems, biomass heating systems, fossil fuel fired heating systems, central heating systems and biofuel heating systems.

2.2.1 Gas Heating Systems

Brown *et al*. (2004) conducted an investigation into the pollutants emitted from unflued gas heaters in Commonwealth Scientific and Industrial Research Organisation's Room Dynamic Environmental Chamber. The temperature, humidity, ventilation and air mixing of the chamber were controlled. The objectives of this research were to measure the concentrations of various pollutants (e.g. respirable suspended particulates, carbon monoxide, nitrogen dioxide, VOCs and formaldehyde). Table 2-6 shows the pollutant emissions from unflued gas heaters and the analytical techniques and instruments used in this study.

Table 2-6: Pollutant emissions from unflued gas heaters and the analytical techniques and instruments (after Brown *et al.*, 2004)

Pollutants	Techniques and Instruments
NO_2	i. ASTM D1607-91 Standard Test Method for Nitrogen Dioxide Content of the Atmosphere (Greiss– Saltzman Reaction). ii. Chemiluminescence NO-NO_2-NO_x analyzer (Thermo Environmental Instruments Inc. Model 42)
Formaldehyde	Australian Standard Method
CO and CO_2	Q-Trak™ Model 8551 IAQ Monitor (TSI Inc., USA)
VOCs	Envirochem multisorbent tubes (containing Tenax TA/Ambersorb/Activated Charcoal)
Respirable suspended particles	Dustrak Model 8520 Aerosol Monitor (TSI Inc., USA)

VOC concentrations ($\mu g/m^3$) in the chamber during the emission tests of Heaters A3, B1 and B2 are presented in Table 2-7. The pollutant emissions from various low-emission unflued gas heaters are presented in Table 2-8.

Table 2-7: VOC concentrations ($\mu g/m^3$) in the chamber during the emission tests (after Brown *et al.*, 2004)

VOC	ID*	Heater A3 after 14.00 h	Heater B1 after 14.00 h	Heater B2 (9-year-old heater)
		Ave±SD	Ave±SD	Ave±SD
Low boiling alkanes	U	27±2	6±1	110±90
Isobutane	U	1±1	3±2	7±5
Butane/methanol	U	11±0	<1	3±3
ΣVVOC (< 5 min)		***38±3***	***10±2***	***110±100***
2-Methylbutane	U	1±0	<1	<1
Acetone/3-methylbutanal	T	12±3	3±2	15±16
2-Chloropentane	U	<1	<1	<1
3-Methylpentane	T	<1	<1	<1
2,4-Dimethylpentane/hexane	T	<1	<1	<1
Methylcyclopentane	T	<1	<1	<1
Acetic acid	C	<2	3±4	10±8
Benzene	C	<1	<1	<2
2-Bromo-2-methylpentane	T	<1	<1	<1
3-Methylhexane	C	<1	<1	<1
Methylcyclohexane	C	<1	<1	<1
Benzaldehyde	C	<1	2±1	3±1
Phenol	T	<1	1±0	3±2
Other VOCs		< 1	< 1	< 1
TVOC (> 5 min)		***11 ± 2***	***33 ± 0***	***25 ± 12***

* Identification of VOCs: C=confirmed, T=tentative, U=unknown

Table 2-8: Emissions from various low-emission unflued gas heaters (after Brown *et al*., 2004)

Pollutant*	Heater	Hours of use	Heating rate	Room conc.	Emission rate
			(MJ/h)	(μg/m^3)	(ng/J)
NO_2	A1	<20	6.8	290	3.0
	A1	1200	6.2	270	3.1
	A2	1400	5.3	190	2.5
	A2(low supply)	<20	5.7	180	2.1
	A3	1400	4.0	230	4.1
	A3(low supply)	<20	5.2	220	3.0
	B1	<20	6.9	520	5.7
	B1	700	6.7	530	5.5
	B1	1400	6.9	530	5.3
	B2(LPG)	9 years	8.7	810	6.6
CO	A1	<20	6.8	4 ppm.	36
	A1	1200	6.2	4 ppm.	40
	A2	1400	5.3	2 ppm.	30
	A2(low supply)	<20	5.7	18 ppm.	260
	A3	1400	4.0	1 ppm.	20
	A3(low supply)	<20	5.2	3 ppm.	36
	B2(LPG)	9 years	8.7	4 ppm.	42
CO/CO_2 ratio	A1	<20	6.8	–	Ratio 0.001
	A1	1200	6.2	–	Ratio 0.001
	A2	1400	5.3	–	Ratio 0.001
	A2(low supply)	<20	5.7	–	Ratio 0.008
	A3	1400	4.0	–	Ratio 0.002
	A3(low supply)	<20	5.2	–	Ratio 0.001
	B2(LPG)	9 years	8.7	–	Ratio 0.001
Formaldehyde	A1	<20	6.8	160	1.6
	A1	1200	6.2	180	1.9
	A2	1400	5.3	97	1.3
	A2(low supply)	<20	5.7	2100	26
	A3	1400	4.0	130	2.5
	A3(low supply)	<20	5.2	370	4.9
	B1	<20	6.9	<10	<0.1
	B1	700	6.7	<10	<0.1
	B1	1400	6.9	<10	<0.1
	B2(LPG)	9 years	8.7	57	0.5

* Indoor respirable particle concentration was 1 μg/m^3 or less for all measurements, except Heater B1 (14 hours of use) which showed a concentration of 4μg/m^3

Gillespie-Bennett *et al.* (2008) conducted a study to look into the effects of heating and household factors on indoor NO_2 in 350 residential houses. They also looked into the reduction of NO_2 emission levels after the heaters were replaced. Passive diffusion tubes were used to

measure the NO_2 concentrations. The average NO_2 levels in living rooms and children's bedrooms are presented in Table 2-9.

From the study, Gillespie-Bennett *et al.* (2008) reported that the level of NO_2 concentrations in homes using unflued gas heaters was three times higher than homes without using unflued gas heaters. They also reported that homes using gas stove-tops have significant increased level of NO_2. However, homes using heat pumps, flued gas heating and enclosed wood burners have lower level of NO_2 concentrations. Another finding from this study is NO_2 levels were reduced by up to 67% in homes using the unflued gas heater intermittenly compared to homes using unflued gas heaters continuously.

Table 2-9: The geometric mean NO_2 levels and geometric mean ratio (95% CIs) of NO_2 levels in living rooms and children's bedrooms by heating type (2006 winter)
(after Gillespie-Bennett *et al.*, 2008)

Type of heating[a]	*N*	µg/m^{3b}	GMR[c]	95% Cl	*P*
Living room					
Enclosed wood burner	45	10.49	0.89	0.67-1.20	0.45
Flued gas	27	18.64	1.68	1.17-2.42	0.006
Heat pump	142	8.47	0.59	0.49-0.72	<0.001
Open fireplace	24	11.12	0.96	0.65-1.42	0.84
Wood pellet burner	29	8.55	0.71	0.50-1.03	0.07
Plug-in electric	286	12.43	1.23	1.00-1.50	0.053
Unflued gas	111	31.79	3.75	3.10-4.52	<0.001
Child's bedroom					
Enclosed wood burner	45	8.10	0.90	0.70-1.16	0.41
Flued gas	27	12.69	1.47	1.07-2.02	0.02
Heat pump	142	7.27	0.71	0.60-0.84	<0.001
Open fireplace	24	7.88	0.88	0.63-1.23	0.45
Wood pellet burner	29	7.25	0.80	0.59-1.09	0.16
Plug-in electric	286	9.14	1.08	0.91-1.29	0.39
Unflued gas	111	18.81	2.67	2.24-3.17	<0.001

GMR, geometric mean ratio.
[a]The reference category for each heating option is all households without that form of heating.
[b]Geometric mean level of those with specified type of heating.
[c]Unadjusted GMR for those homes that had the heating option vs. those homes that did not have the heating option.

2.2.2 Biomass Heating Systems

Mestl *et al.* (2007) conducted a research on the pollutants emitted from domestic biomass and coal burning and their exposures to the urban and rural populations in China. They utilised published indoor air pollution data and time activity patterns for their analysis. Several demographic groups were involved in the exposure assessment. They grouped the indoor air

pollution data according to geographical locations and all demographic groups are subjected to the time activity patterns.

Figures 2-4 and 2-5 show the estimated exposure levels for those living in rural areas of northern and southern China respectively. The estimated exposure levels for those living in urban China are presented in Figure 2-6. The pollutant emission levels, as well as time activity patterns, were used to estimate the exposure levels. Standard deviations were represented by the error bars. From the study, Mestl *et al.* (2007) reported that the average exposure for the rural south is 750 $\mu g/m^3$ and 680 $\mu g/m^3$ in rural north. Their results indicated that the provinces which highly relying on coal turned out to have medium exposure burden only, whilst the largest exposure burden came from those counties which highly dependent on biomass.

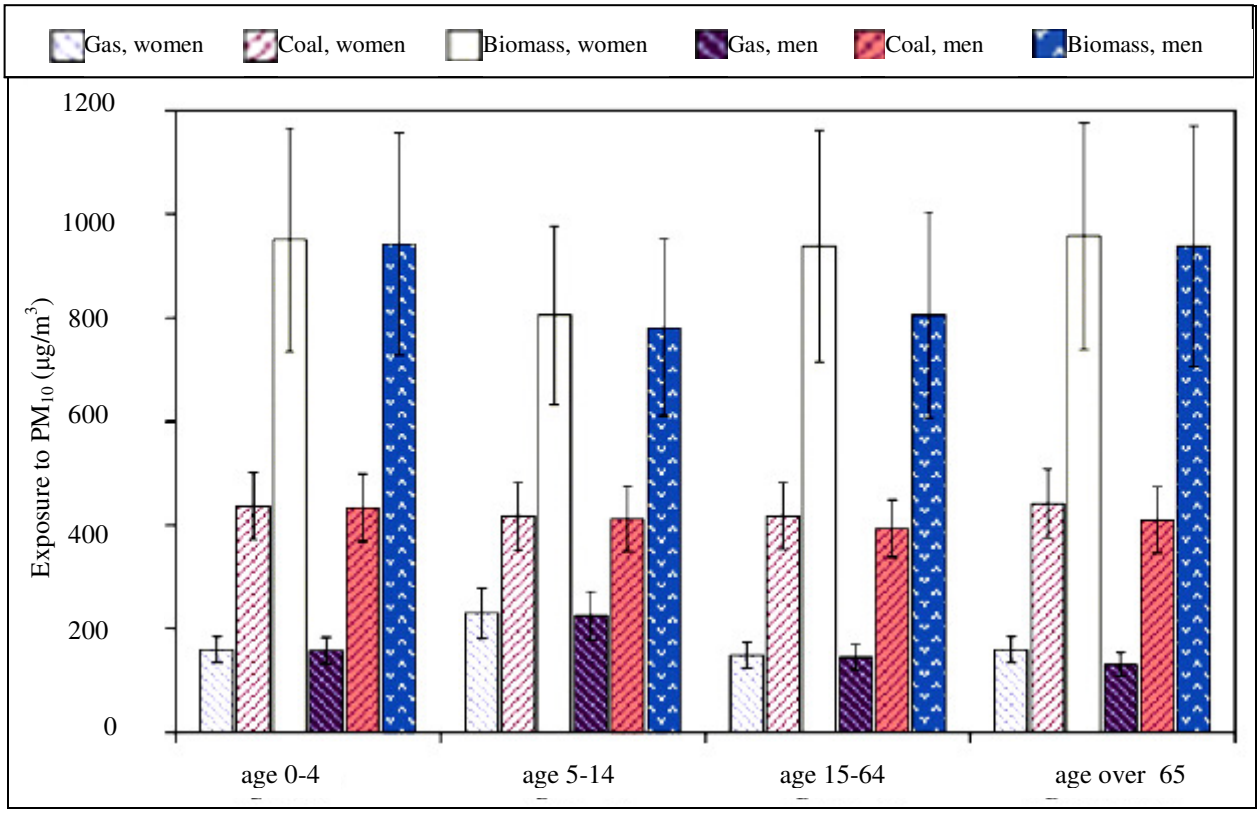

Figure 2-4: Estimated exposure levels ($\mu g/m^3$) for different demographic groups in rural north China (after Mestl *et al.*, 2007)

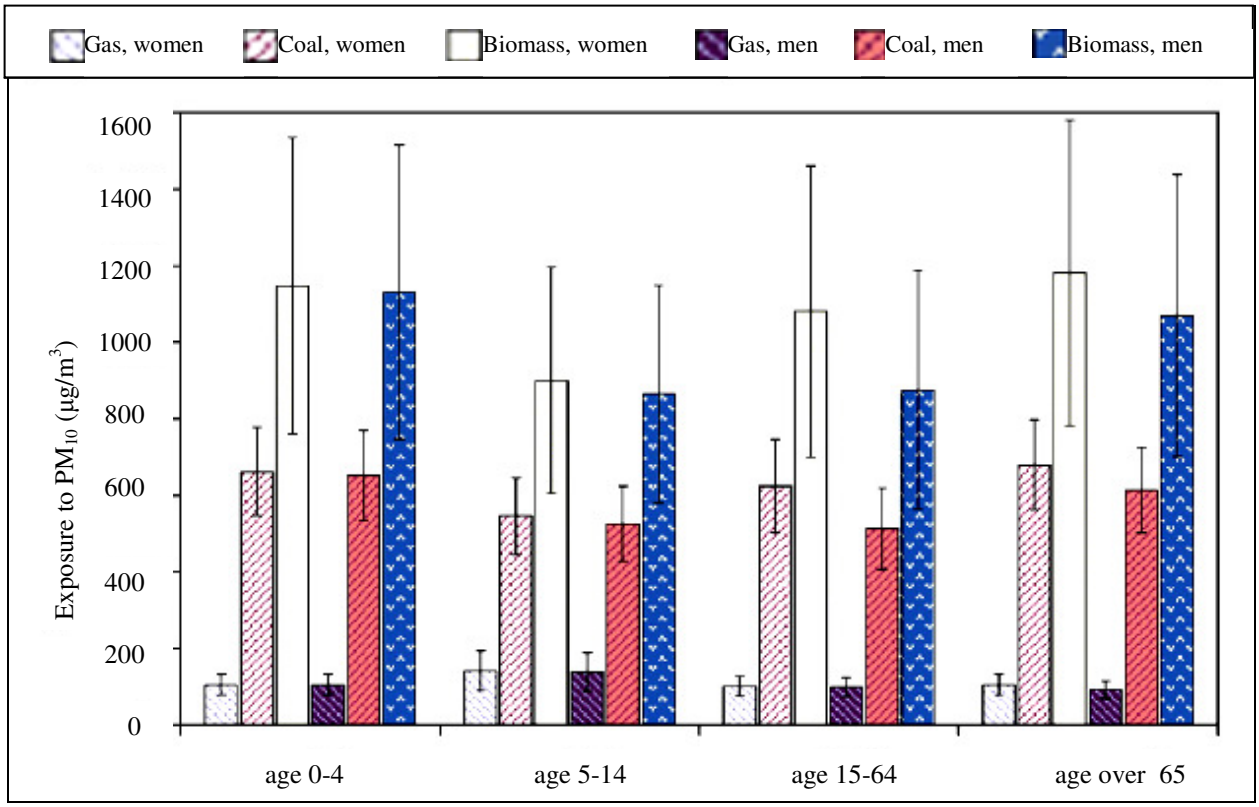

Figure 2-5: Estimated exposure levels (µg/m^3) for different demographic groups in rural south China (after Mestl *et al.*, 2007)

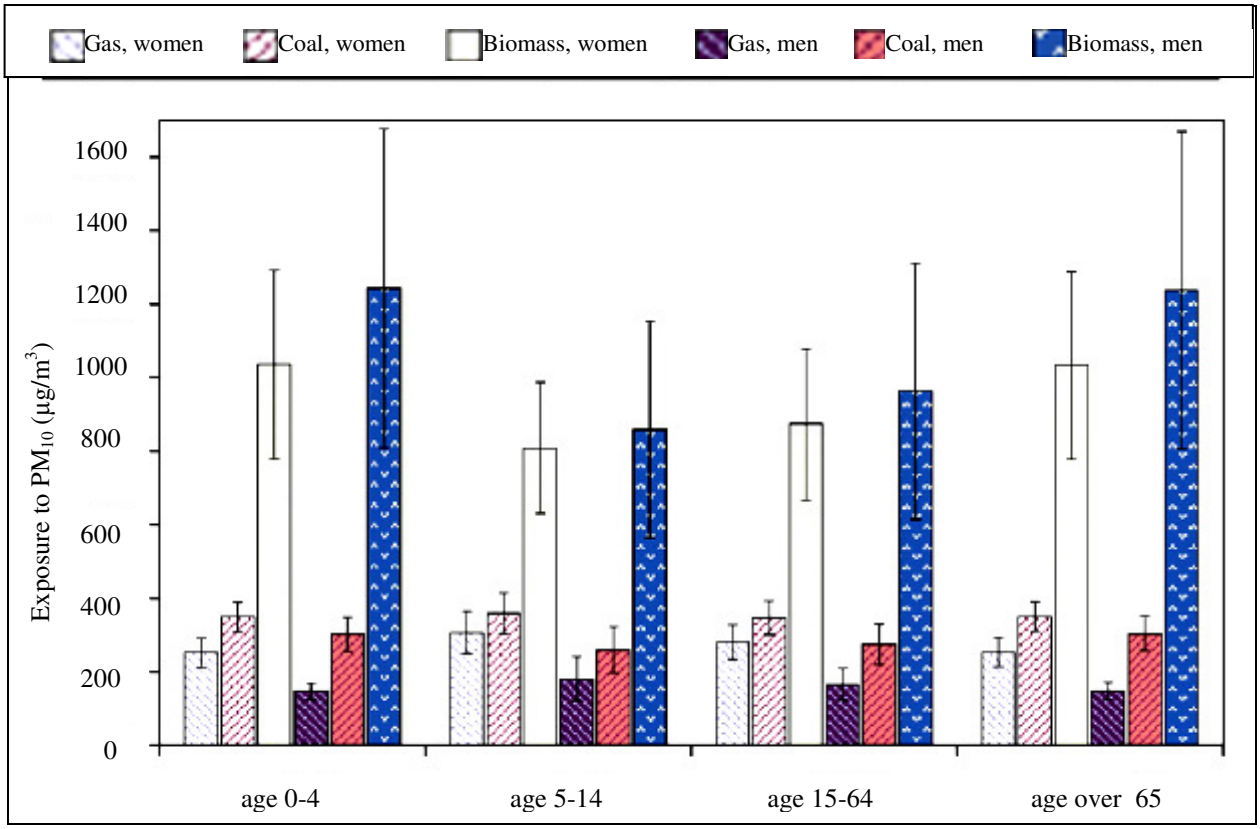

Figure 2-6: Estimated exposure levels (µg/m^3) for different demographic groups in urban China (after Mestl *et al.*, 2007)

To evaluate the effect of the woodstove replacement program for reducing ambient $PM_{2.5}$ levels on indoor air quality, Ward and Noonan (2008) continuously measured $PM_{2.5}$ concentration in 16 homes throughout a 24-h sampling periods in Rocky Mountain valley community during 2005-2007 in the USA. Quartz filters were used to measure the organic carbon, elemental carbon and wood smoke. TSI DustTrak and Leland legacy pump were used to measure the $PM_{2.5}$ concentration.

Figure 2-7 shows the mass results of $PM_{2.5}$ before and after the wood stove replacement. Table 2-10 shows the concentrations of various pollutants before and after the wood stove replacements in 16 homes.

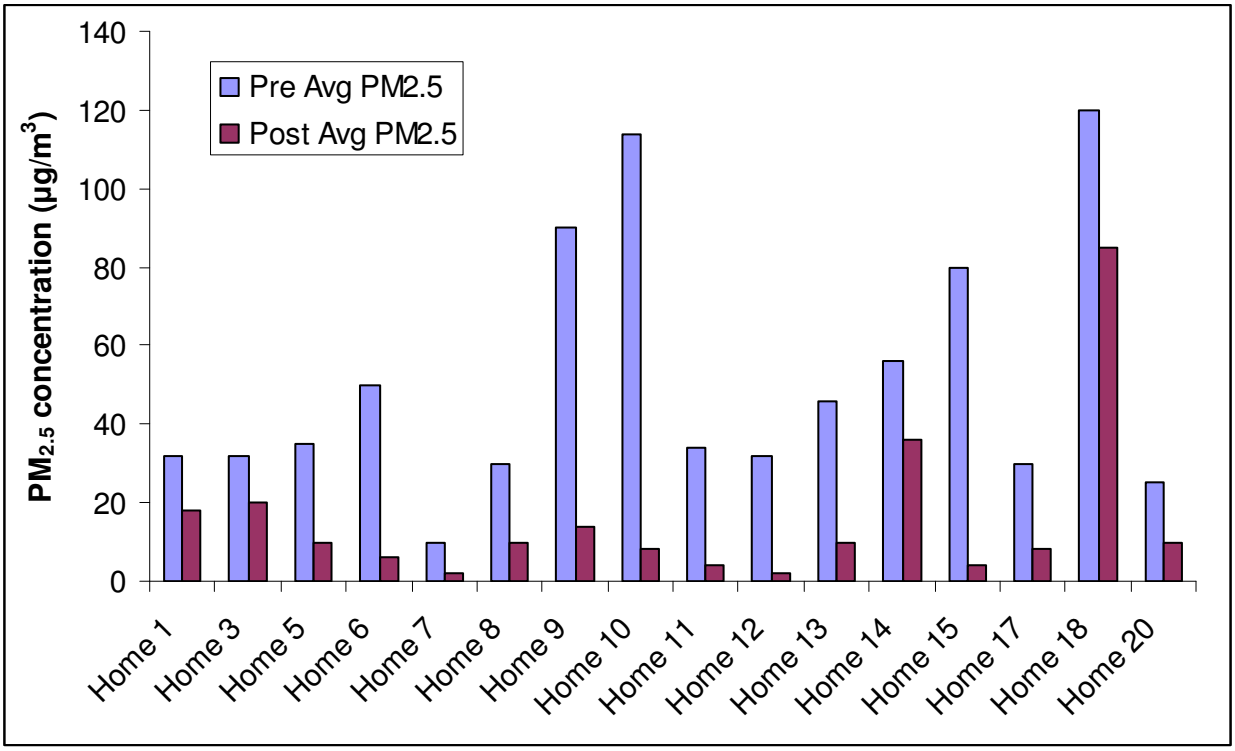

Figure 2-7: $PM_{2.5}$ – mass results, pre- and post-woodstove replacement
(after Ward and Noonan, 2008)

As can be seen from Table 2-10, the average $PM_{2.5}$ concentration was reduced by 71% whereas the maximum $PM_{2.5}$ concentration was reduced by 76%. After the woodstove was replaced, levoglucosan was reduced up to 45%. Another impact from the woodstove replacement program was the increase of resin acids and natural chemicals found in the bark of wood.

Table 2-10: Concentrations and average changes (%) of measured parameters prior to and following woodstove replacements in 16 homes (after Ward and Noonan, 2008)

Parameter	Before Replacement	After Replacement	Percent Change
Average $PM_{2.5}$	34.5	9.5	-71%
Maximum $PM_{2.5}$	266	51.5	-76%
Organic carbon	14.4	9.4	-26%
Elemental carbon	0.68	0.29	-6%
Levoglucosan	652	321	-45%
Dehydroabietic acid	74.1	154	+133%
Abietic acid	2.8	5.2	+292%

Molnar *et al.* (2005) conducted an investigation into personal exposure to $PM_{2.5}$ concentrations from domestic wood burning. They conducted the experiments by using an impactor with cyclones in a residential area which highly relied on wood burning in providing heat. Table 2-11 shows the measurement methodologies and instruments used in the study. Twenty-four-hour samples and a reference group were measured.

Table 2-11: Pollutants emitted from wood-burning households and the measurement methodologies and instruments (after Molnar *et al*., 2005)

Pollutant	Methodologies and Instruments
Mass and elemental concentration	Dispersive X-ray Fluorescence
Black smoke concentration	EEL 43 Reflectometer
$PM_{2.5}$ – PM_{10}	Sierra Andersen series 240, dichotomous virtual impactor
$PM_{2.5}$	EPA-WINS impactor

Both dichotomous virtual impactor (Sierra Andersen, Series 240) and EPA-WINS impactor have a flow rate of 16.7 l/min. A BGI 400S Personal Sampling Pump which connected with a GK2.05 cyclone was used for sampling (Molnar *et al*., 2005). The results from the measurements are presented in Table 2-12.

Table 2-12: Results from measurements of personal exposures and indoor levels (after Molnar *et al.*, 2005)

	Wood burners			Reference group			One-sided p-value[a]
	Median	**Range**	**#>LoD**	**Median**	**Range**	**#>LoD**	
Personal exposure							
$PM_{2.5}$	18	5.3-59	14	12	5.8-46	10	0.115
BS	0.97	0.32-3.0	14	0.74	0.24-0.96	10	0.053
S	880	<210-2000	8	650	<180-2400	6	0.500
Cl	200	140-470	14	160	120-280	9[*c]	0.036
K	240	88-550	14	140	89-360	9[*c]	0.024
Ca	76	36-530	14	43	26-98	10	0.033
Mn	4.8	<1.6-41	9	3.5	<1.6-7.1	6	0.250
Fe	64	22-280	13[*b]	49	14-150	10	0.139
Cu	8.9	<0.83-32	12[*b]	2.4	<0.86-28	6	0.016
Zn	38	18-130	14	22	8.4-67	10	0.033
Br	1.2	0.82-7.1	14	1.2	0.81-2.3	10	0.500
Rb	2.2	1.1-2.5	14	2.3	1.1-2.5	10	0.153
Pb	6.0	3.5-29	14	4.3	<1.7-7.9	9	0.060
Indoor concentration							
$PM_{2.5}$	12	3.9-61	13	9.5	2.9-53	10	0.278
BS	0.64	0.16-2.9	13	0.54	0.12-0.88	10	0.072
S	760	<140-2200	8	590	<160-2600	6	0.488
Cl	190	150-430	13	160	<83-340	8	0.091
K	200	72-600	13	120	70-410	9[*c]	0.026
Ca	44	17-200	13	25	10-49	9[*c]	0.044
Mn	2.6	<1.5-14	8	<1.7	<1.6-7.4	2	0.029
Fe	27	18-120	13	22	3.6-110	10	0.126
Cu	1.7	<0.81-34	7	<0.86	<0.80-7.2	2	0.102
Zn	25	10-100	13	15	7.1-76	10	0.039
Br	1.2	<0.81-9.5	12	1.2	<0.8-2.3	9	0.238
Rb	2.3	2.2-2.4	13	1.2	1.1-2.4	10	0.007
Pb	4.6	<0.84-10	12	3.0	<1.7-11	8	0.258

Median concentration, range, and number of samples above limit of detection (LoD) are presented. Units are $\mu g/m^3$ for PM2.5, ng/m^3 for the elemental concentrations, and $10^{-5}m^{-1}$ for black smoke (BS). An asterisk (*) denotes that one detected value was omitted due to a known major external non-wood-burning source.
[a]Wilcoxom rank-sum test for personal exposure and indoor levels, respectively. Significant P-values are marked in bold. [b]Welding copper pipes, occupational exposure. [c]Use of cleaning detergents at home.

2.2.3 Fossil Fuel Fired Heating Systems

Leaderer *et al*. (1999) conducted a twenty-four-hour investigation to measure PM_{10}, $PM_{2.5}$, particle strong acidity (H^+), sulphate (SO_4^{2-}), nitrate (NO_3^-), ammonia (NH_3), nitrous acid (HONO) and sulfur dioxide in 281 homes during winter and summer periods. Seventy-four of the homes used kerosene heaters. An inertial impactor was used to collect $PM_{2.5}$ and PM_{10} samplings. A Harvard glass honeycomb denuder/filter pack sampler was used to measure the particle sulphate, nitrate, strong acidity and ammonium, as well as gaseous species (nitrous acid, nitric acid, ammonia and sulphur dioxide).

Table 2-13 shows the summary of winter pollutant concentrations. Summary of summer pollutant concentrations is presented in Table 2-14. Figure 2-8 is the comparison of 24-hr indoor and outdoor particle concentrations measured at homes fitted with and without kerosene heaters. Leaderer *et al.* (1999) concluded that indoor concentrations of $PM_{2.5}$, SO_4^{2-} and H^+ were increased in non-smokers homes which installed with a kerosene heater during winter.

Table 2-13: Summary of winter pollutant concentrations (after Leaderer *et al.*, 1999)

Pollutant	Site	n	Mean±SD	Min	Max
PM_{10} (μg/m^3)	Outside all homes	53	23.93±22.21	4.73	112.04
	Inside kerosene-heater homes	42	44.6±30.37	6.45	141.41
	Inside non-kerosene-heater homes	84	25.71±21.12	2.82	181.75
$PM_{2.5}$ (μg/m^3)	Outside all homes	48	12.56±7.27	3.21	43.47
	Inside kerosene-heater homes	71	29.97±23.58	2.13	114.58
	Inside non-kerosene-heater homes	145	17.43±23.63	1.72	207.54
Coarse[a] (μg/m^3)	Outside all homes	46	12.12±22.70	0	105.18
	Inside kerosene-heater homes	41	11.20±8.23	1.86	37.45
	Inside non-kerosene-heater homes	82	12.39±8.85	1.13	48.46
SO_4^{2-}(nmol/m^3)	Outside all homes	52	30.6±14.9	0	66.2
	Inside kerosene-heater homes	74	82.7±76.2	6.1	379.6
	Inside non-kerosene-heater homes	149	21.6±3.37	0	146.5
H^+(nmol/m^3)	Outside all homes	52	6.5±9.8	0	50.3
	Inside kerosene-heater homes	74	5.7±6.9	0	35.8
	Inside non-kerosene-heater homes	149	3.11±5.00	0	21.9
NH_4^+(nmol/m^3)	Outside all homes	52	64.4±38.9	2.2	187.8
	Inside kerosene-heater homes	74	126.1±155.0	0.6	796.7
	Inside non-kerosene-heater homes	147	9.4±21.7	0	125.0
NO_3^-(nmol/m^3)	Outside all homes	52	20.5±22.0	1.8	101.1
	Inside kerosene-heater homes	74	6.5±9.4	0.3	67.2
	Inside non-kerosene-heater homes	149	6.3±9.1	0.3	79.2
NH_3 (ppb)	Outside all homes	52	1.55±4.63	0	33.38
	Inside kerosene-heater homes	74	44.35±45.35	4.06	231.86
	Inside non-kerosene-heater homes	148	37.96±36.02	0.13	234.24
Nitrous acid (ppb)	Outside all homes	53	0.81±1.32	0	9.25
	Inside kerosene-heater homes	74	6.80±6.06	0.15	35.89
	Inside non-kerosene-heater homes	148	3.49±3.61	0.14	20.13
	Inside homes, no kerosene heaters				
	No gas stove	96	2.43±3.05	0.14	20.08
	Gas stove	52	5.45±3.75	0.37	20.14
SO_2 (ppb)	Outside all homes	53	4.00±2.15	0.70	9.59
	Inside kerosene-heater homes	74	16.11±21.34	0.06	107.36
	Inside non-kerosene-heater homes	148	0.83±1.68	0	8.81

Abbreviations: SD, standard deviation; PM_{10}, particle mass ≤10μm in diameter; $PM_{2.5}$, particle mass ≤2.5μm in diameter; coarse, particle mass between 10 and 2.5μm in diameter($PM_{2.5}$- PM_{10}); AC, air conditioned.
[a]This is not a paired comparison, thus there is not always a PM_{10} for every $PM_{2.5}$ and vice versa.

Table 2-14: Summary of summer pollutant concentrations (after Leaderer *et al*., 1999)

Pollutant	Site	n	Mean±SD	Min	Max
PM_{10} (µg/m^3)	Regional site	47	26.0±11.5	10.8	51.9
	Outside all homes	43	28.0±17.7	5.8	112.6
	Inside AC homes	49	28.9±18.7	4.8	97.6
	Inside non-AC homes	8	33.3±14.2	17.7	59.7
$PM_{2.5}$ (µg/m^3)	Regional site	50	20.23±9.9	5.8	42.4
	Outside all homes	43	21.8±14.8	3.8	84.2
	Inside AC homes	49	18.7±13.2	2.5	65.7
	Inside non-AC homes	9	21.1±7.5	9.6	35.3
Coarse[a] (µg/m^3)	Regional site	47	6.3±2.7	1.5	14.3
	Outside all homes	42	7.7±6.2	2.4	34.1
	Inside AC homes	48	10.4±8.5	0	35.1
	Inside non-AC homes	8	11.4±9.7	0.2	32.6
SO_4^{2-}(nmol/ m^3)	Regional site	45	88.4±51.6	14.1	209.0
	Outside all homes	42	83.7±53.7	7.9	230.6
	Inside AC homes	47	47.8±36.3	2.1	137.7
	Inside non-AC homes	9	63.0±37.3	20.9	125.6
H^+(nmol/m^3)	Regional site	47	41.0±28.5	0	136.2
	Outside all homes	45	33.0±36.9	0	208.6
	Inside AC homes	49	12.4±15.3	0	84.5
	Inside non-AC homes	9	16.7±9.4	2.9	34.6
NH_4^+(nmol/m^3)	Regional site	43	124.6±59.0	30.6	293.0
	Outside all homes	45	129.4±87.8	0	338.9
	Inside AC homes	49	78.3±77.2	0	450.6
	Inside non-AC homes	9	96.7±68.9	6.7	214.4
NO_3^-(nmol/m^3)	Regional site	42	10.2±5.0	2.6	20.7
	Outside all homes	42	8.0±5.4	0	22.9
	Inside AC homes	49	5.5±8.9	0	56.1
	Inside non-AC homes	9	6.8±4.6	0.5	12.2
NH_3 (ppb)	Regional site	29	1.7±0.5	0.9	2.7
	Outside all homes	45	2.8±2.5	0	13.2
	Inside AC homes	49	32.1±19.4	1.5	93.0
	Inside non-AC homes	9	27.5±18.4	2.0	49.5
Nitrous acid (ppb)	Regional site	29	0.3±0.4	0	2.1
	Outside all homes	45	0.3±0.4	0	2.1
	Inside AC homes	49	1.6±2.1	0	11.3
	Inside non-AC homes	9	3.5±2.6	0.4	7.5
	Inside homes without gas stoves	39	0.8±0.8	0	2.9
	Inside homes with gas stoves	19	4.0±2.8	0	11.3
SO_2 (ppb)	Regional site	50	1.2±0.6	0.1	2.9
	Outside all homes	45	1.3±1.7	0.02	9.4
	Inside AC homes	49	0.3±0.5	0	3.1
	Inside non-AC homes	7	0.9±1.0	0.1	3.0

Abbreviations: SD, standard deviation; PM_{10}, particle mass ≤10µm in diameter; $PM_{2.5}$, particle mass ≤2.5µm in diameter; coarse, particle mass between 10 and 2.5µm in diameter($PM_{2.5}$- PM_{10}); AC, air conditioned.

[a]This is not a paired comparison, thus there is not always a PM_{10} for every $PM_{2.5}$ and vice versa.

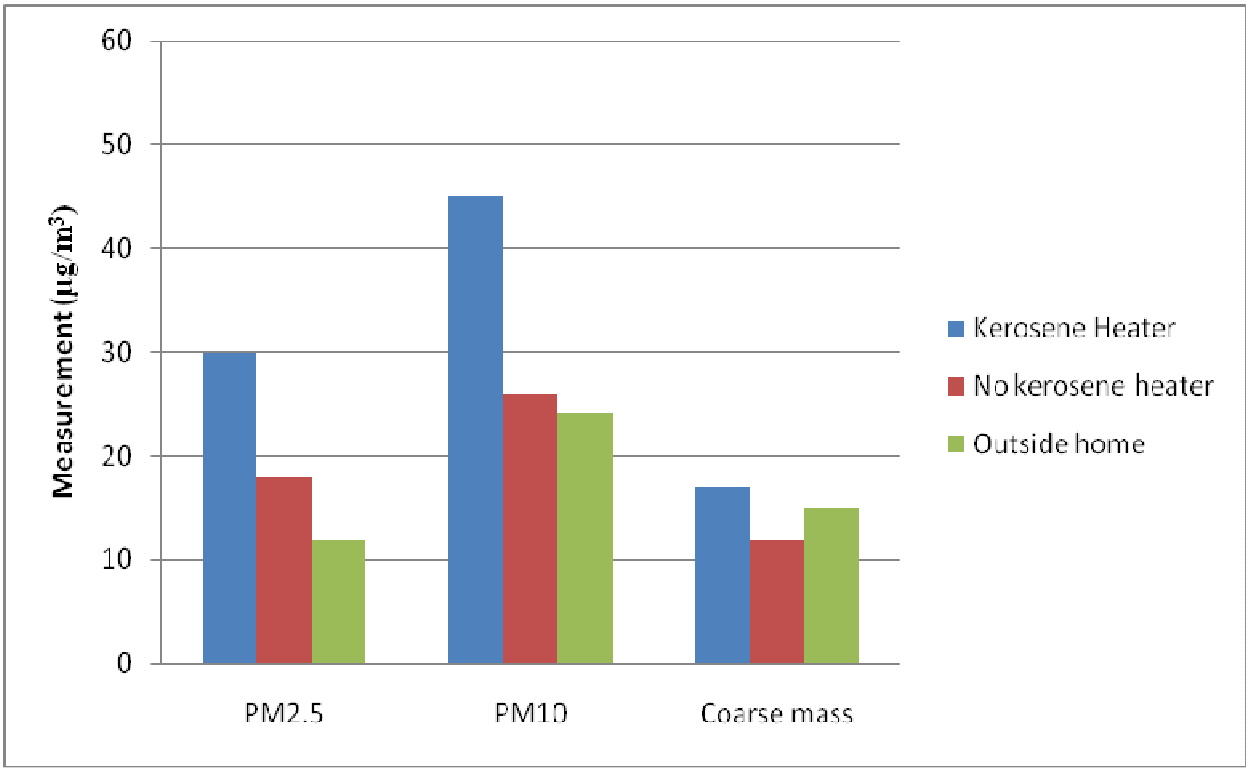

Figure 2-8: Comparison of 24-hr indoor and outdoor PM_{10}, $PM_{2.5}$ and coarse mass measurements made at homes with and without kerosene heaters during winter
(after Leaderer *et al.*, 1999)

Mumford *et al.* (1991) conducted an investigation to assess human exposure to various pollutants emitted from unvented kerosene heaters. PM_{10}, semi-volatile organics and carbon monoxide were monitored in eight electric homes with the kerosene heaters on and off. A particle sampler equipped with a 10-pm inlet separator and a Teflon-coated, glass-fibre filter to collect particles and a stainless steel canister containing XAD-2 resin (65g) were used to collect the PM_{10} and semi-volatile organics at an airflow rate of 12-18 l/min. From the study, it can be noted that the pollutant emissions for four out of eight heaters investigated exceeded the US ambient air standards. Emissions from kerosene heaters can bring significant impacts to the indoor air quality in mobile homes.

Figure 2-9 shows PM_{10} concentrations in eight mobile homes in the kerosene heater emissions study. The results show that there is no significant effect on PM_{10} levels by using kerosene heaters, except in two homes. Figure 2-10 shows the gravimetric organic concentrations and total chromatographable organics concentrations of XAD samples from eight mobile homes in the kerosene heater study. The results show that there is an increase in mutagenicity of particle-phase organics in five homes and little mutagenicity in the semivolatile organics. Figure 2-11 shows average concentrations during sampling (averaging 6.5 h) and 1-h peak CO

concentrations in mobile homes in the kerosene heater study. The results show that there is a significant increase in CO and organic levels.

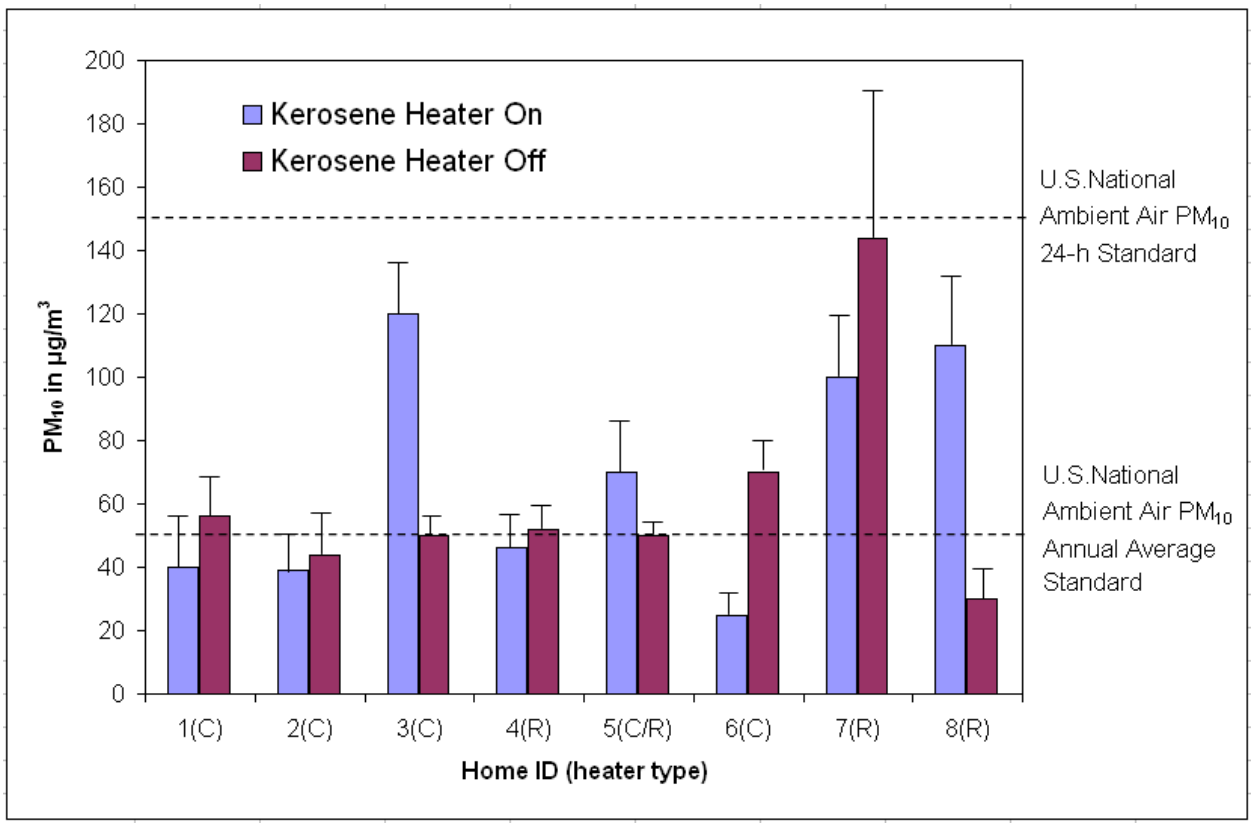

Figure 2-9: PM_{10} concentrations in eight mobile homes in a kerosene heater emission study [C: convective heater; R: radiant heater] (after Mumford *et al.*, 1991)

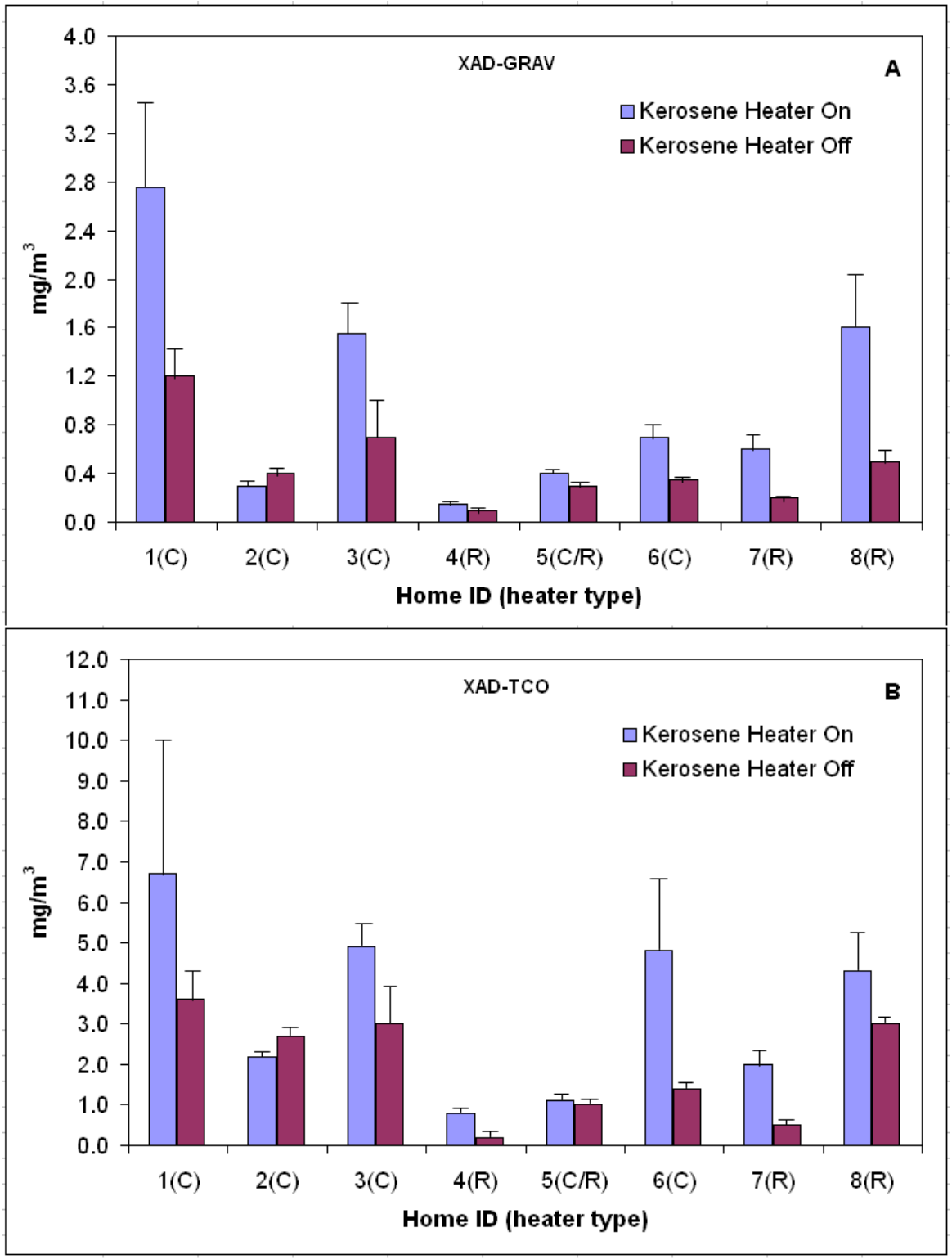

Figure 2-10: Gravimetric organic concentrations (A) and total chromatographable organics concentrations (B) of XAD samples from eight mobile homes in a kerosene heater emission study [C: convective heater; R: radiant heater] (after Mumford *et al.*, 1991)

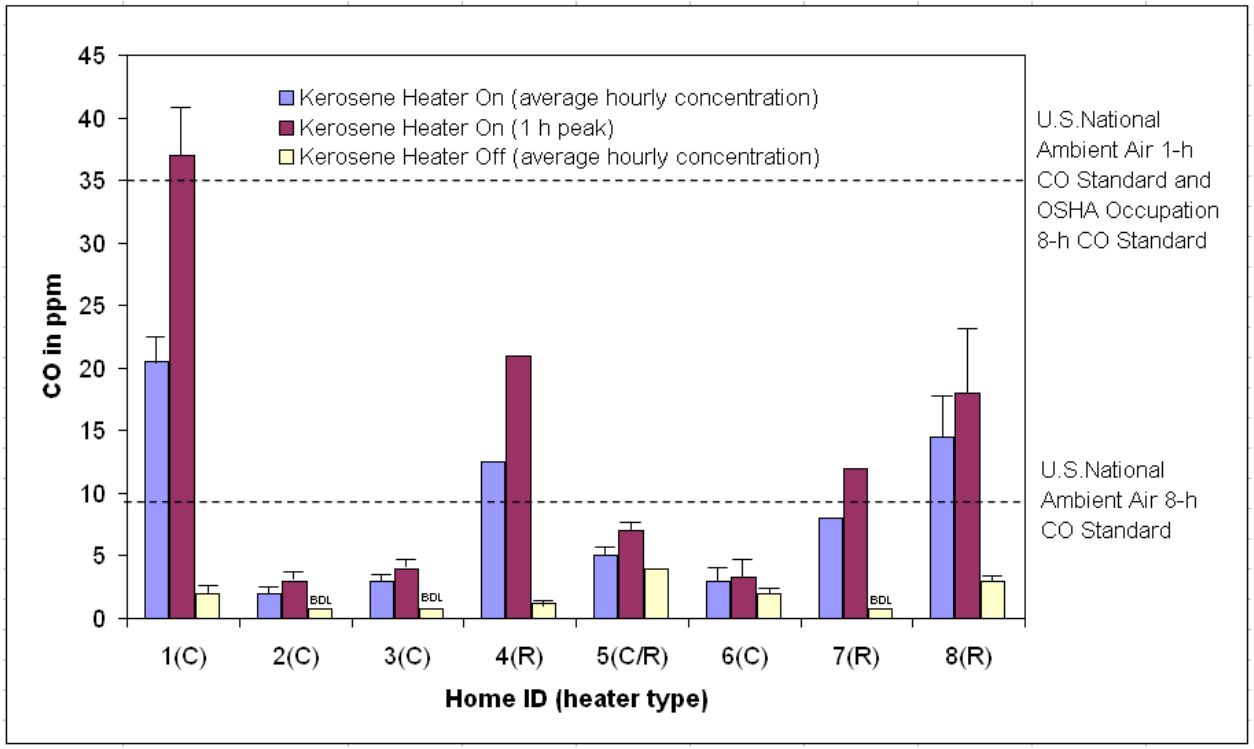

Figure 2-11: Average concentrations during sampling (averaging 6.5 h) and 1-h peak CO concentrations in mobile homes in a kerosene heater emission study
[BDL: below detection limit; C: convective heater; R: radiant heater]
(after Mumford *et al.*, 1991)

2.2.4 Central Heating Systems

Moriske *et al.* (1996) conducted investigations on indoor air quality in sixteen homes with different heating systems (i.e. coal burning fires, open fireplace and central heating). The research objectives were measuring the indoor carbon monoxide, carbon dioxide and sedimented dust concentrations and total suspended particulates, heavy metals and polycyclic aromatic hydrocarbons in both indoor and outdoor air using automatic equipment.

Figure 2-12 shows the indoor CO concentration in different homes. The concentrations of CO_2 in different homes are showed in Figure 2-13. Figure 2-14 shows the concentrations of total suspended particulates in different homes. Figure 2-15 shows the concentrations of sedimented dust material in different homes. Figure 2-16 shows the concentrations of arsenic and heavy metals inside sedimented dust material in different homes. Figure 2-17 shows the concentrations of polycyclic aromatic hydrocarbons in different homes.

As reported by Moriske *et al.* (1996), homes using coal burning and open fireplace generally have more serious indoor air pollution problems when compared to homes with central heating, particularly higher in carbon monoxide, sedimented dust and some of the heavy metals. Home 'S' with central heating system was found most polluted due to the malfunction of its exhaust system.

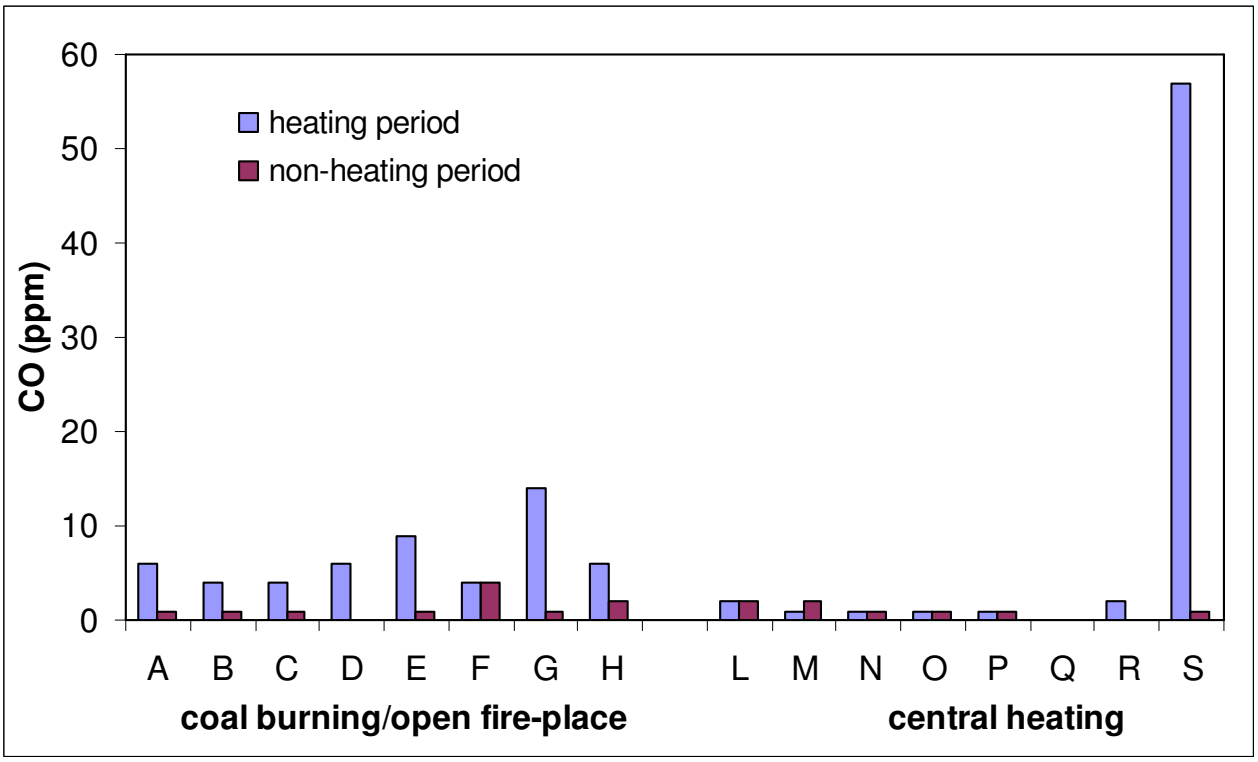

Figure 2-12: Concentrations of carbon monoxide (CO) in different homes (ppm) (after Moriske *et al.*, 1996)

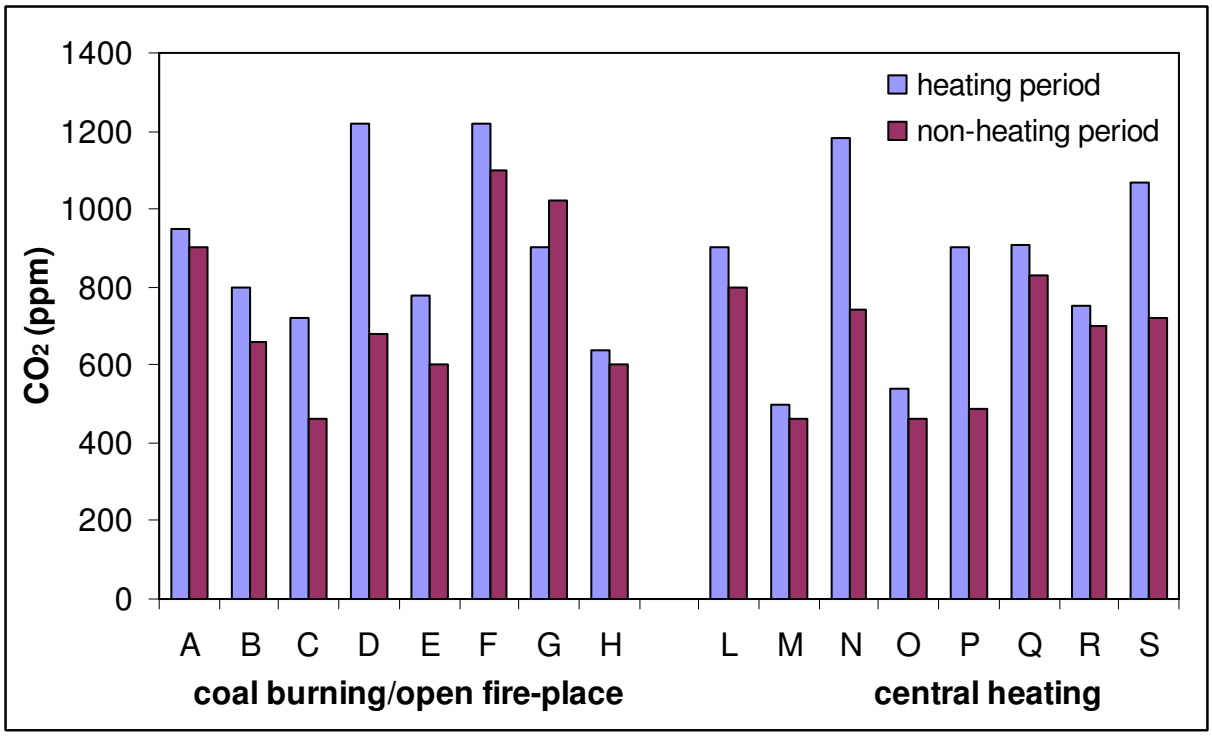

Figure 2-13: Concentrations of carbon dioxide (CO_2) in different homes (ppm)
(after Moriske *et al.*, 1996)

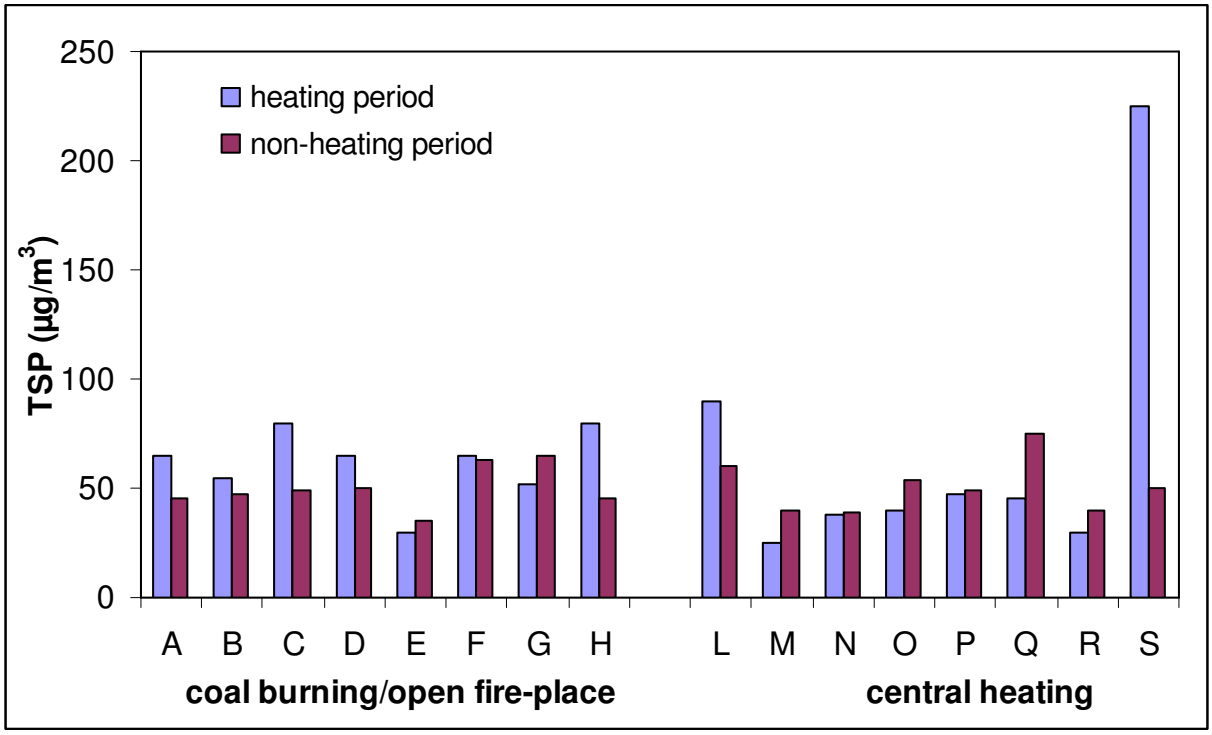

Figure 2-14: Concentrations of total suspended particulates (TSP) in different homes ($\mu g/m^3$)
(after Moriske *et al.*, 1996)

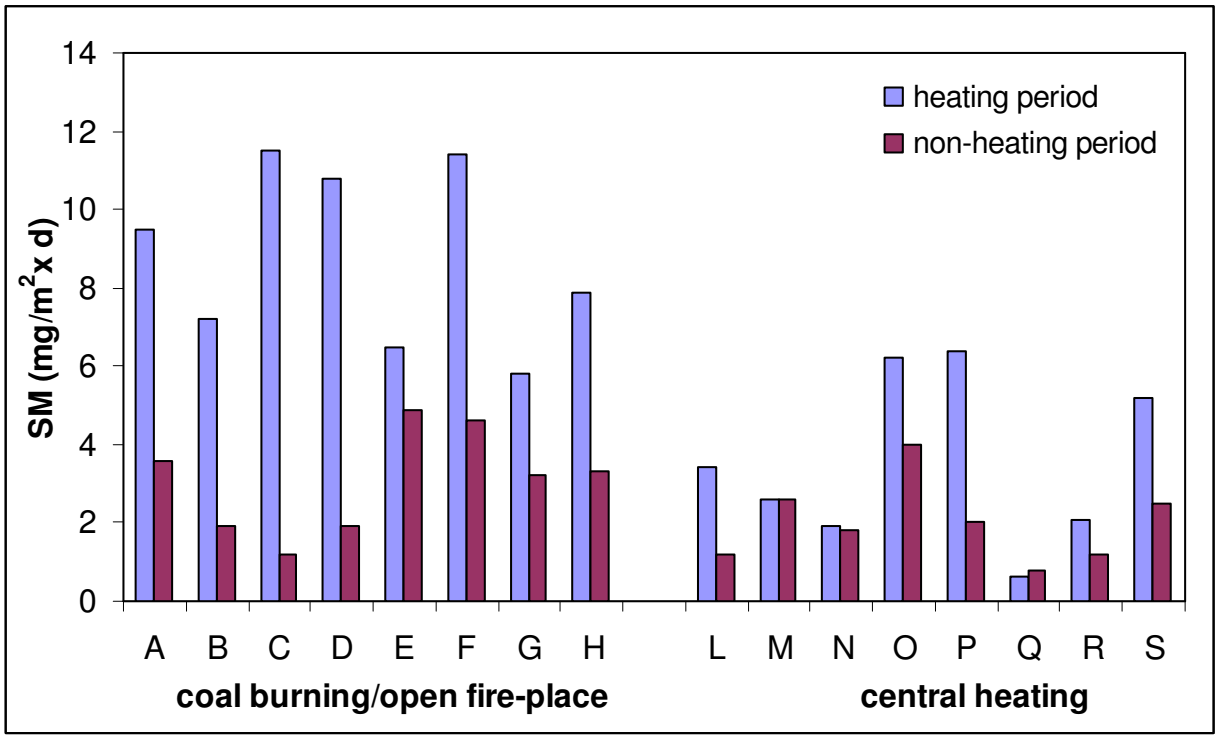

Figure 2-15: Concentrations of sedimented dust material (SM) in different homes (mg/m^2 per day) (after Moriske *et al.*, 1996)

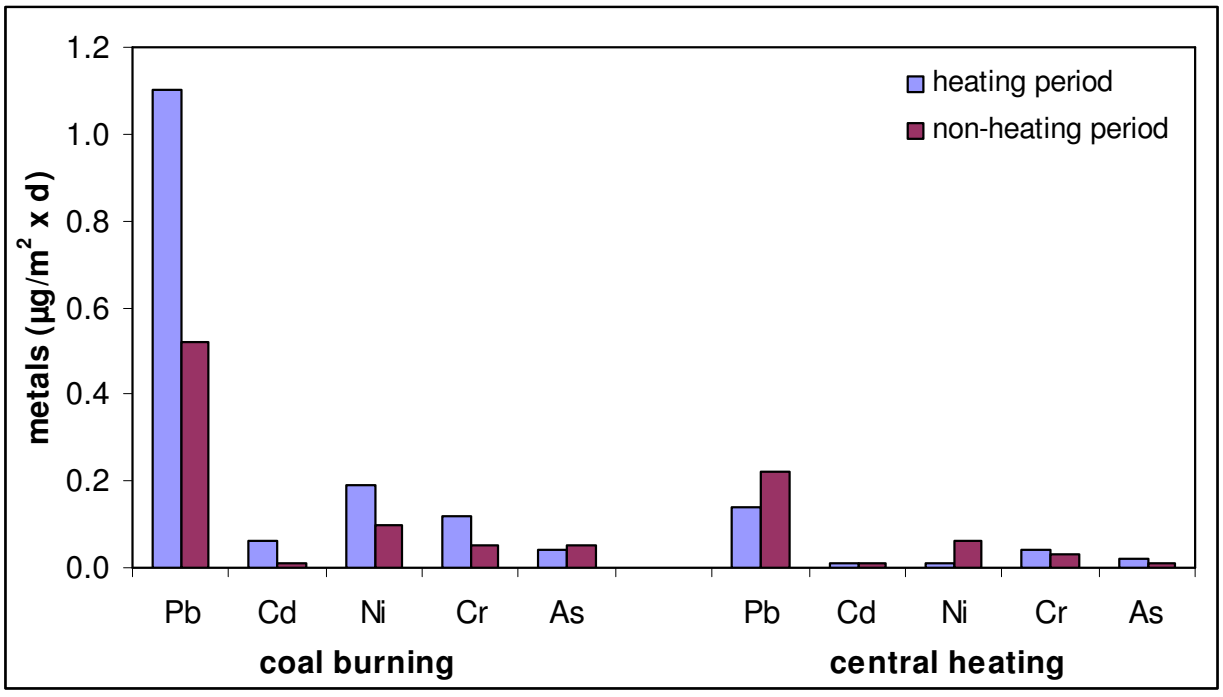

Figure 2-16: Concentrations of arsenic and heavy metals inside sedimented dust material in different homes ($\mu g/m^2$ per day) (after Moriske *et al.*, 1996)

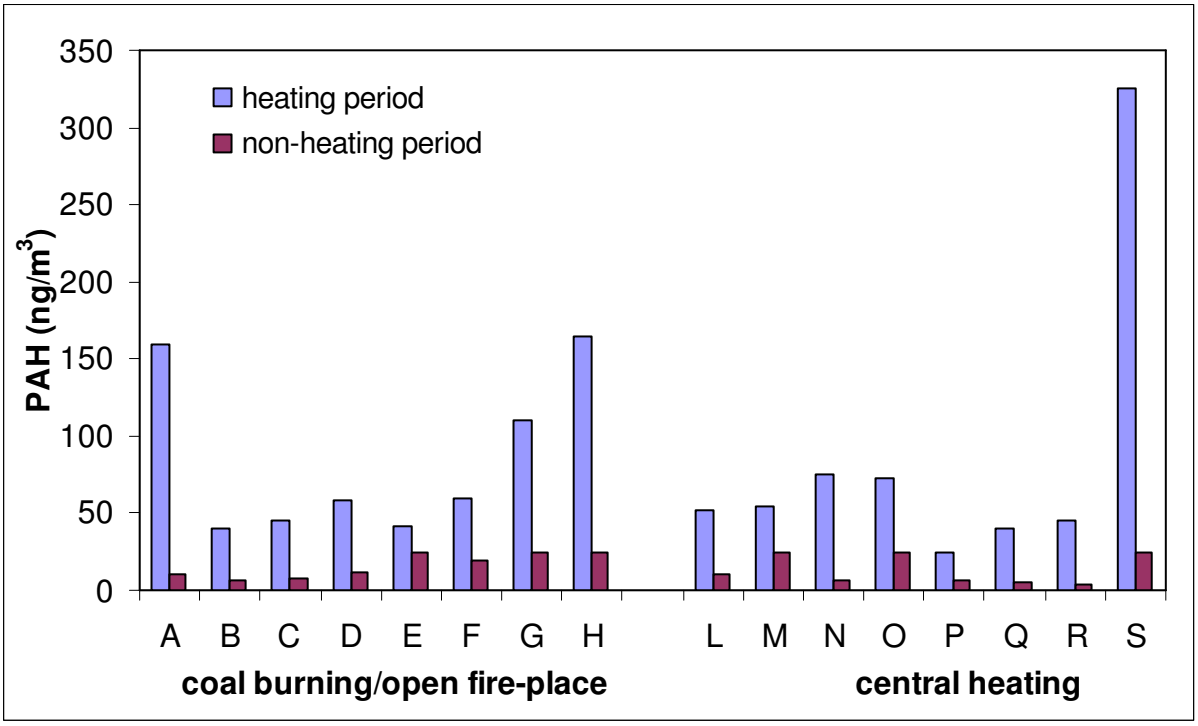

Figure 2-17: Concentrations of polycyclic aromatic hydrocarbons (PAH) in different homes (ng/m^3) (after Moriske *et al.*, 1996)

2.2.5 Biofuel Heating Systems

Parikh *et al.* (2001) carried out a research to study the types of kitchen and fuels used for 418 households in rural Tamil Nadu, India, and their relationships with the pollutant concentration levels in the kitchen by using statistical analysis. 418 households were selected out of 5028 households for the measurement.

As reported by Parikh *et al*. (2001), personal monitors were used to measure the exposures to the female chief cook. The respirable particles (PM_{10}) concentrations from burning biofuels varied from 500-2000$\mu g/m^3$. High concentrations of suspended particles and noxious gases were due to the ineffective ventilation and stoves in the homes. By comparing with modern fuels (e.g. LPG and electricity), unprocessed biomass fuels can produce up to 100 times more particles due to the low efficiencies of the unprocessed biomass fuels.

Cooking with biofuels contributed most respirable particulate matter. Personal exposures ranged from 70$\mu g/m^3$ (with clean fuel) to 2000 $\mu g/m^3$ (with biofuels). The average exposure is 78.16 $\mu g/m^3$. Figure 2-18 shows the mean personal exposures of cooks at different kitchen

locations and fuel types as per sample measurements. Figure 2-19 shows the mean concentration at different kitchen locations and fuel types as per sample measurements.

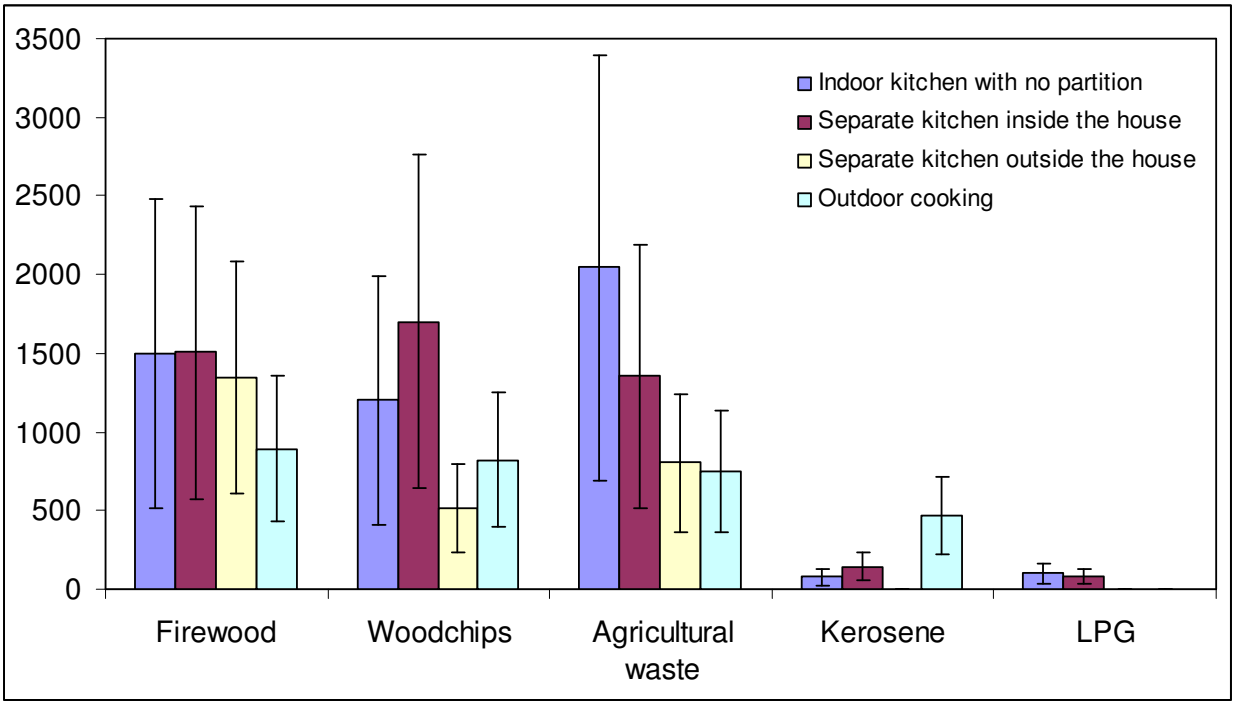

Figure 2-18: Mean personal exposures of cooks at different kitchen locations and fuel types as per sample measurements (after Parikh *et al.*, 2001)

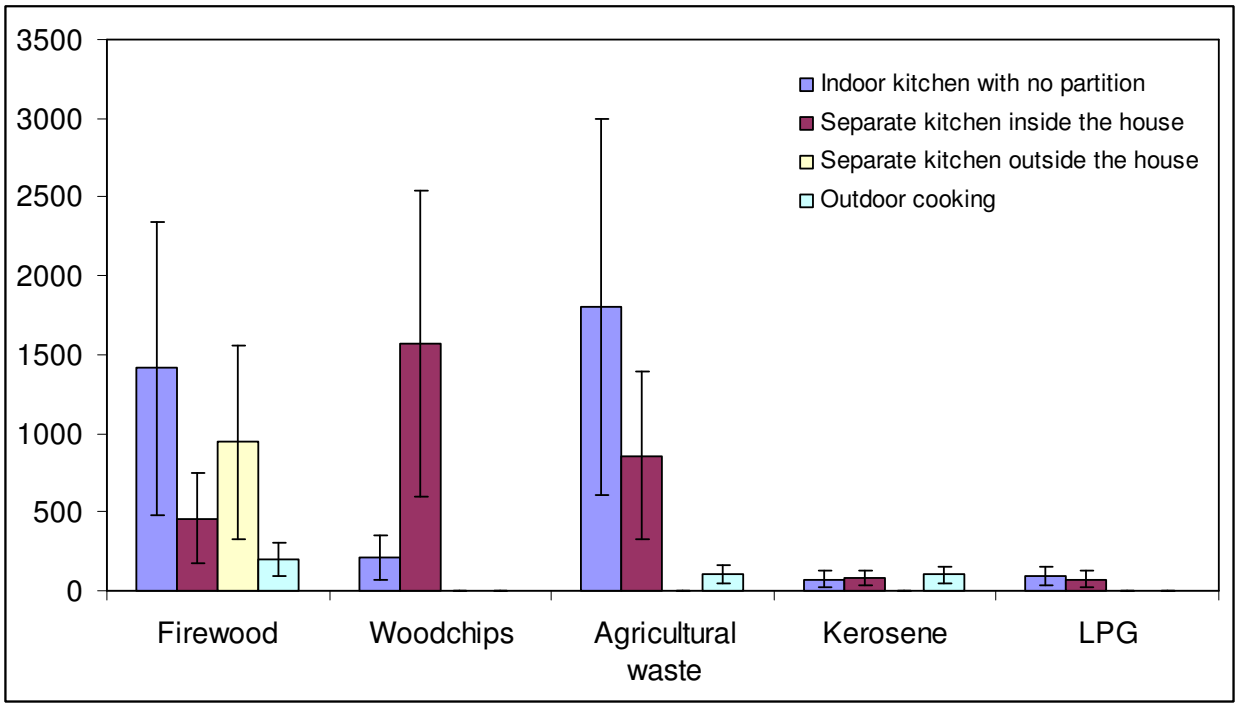

Figure 2-19: Mean concentration at different kitchen locations and fuel types as per sample measurements (after Parikh *et al.*, 2001)

2.3 POLLUTANT MINIMISATION AND REDUCTION TECHNOLOGIES

In order to control indoor air pollution, basic approaches have been suggested, namely source control, increased ventilation and air cleaning. Some other approaches may include source isolation, dehumidification and the use of filters. In this section, several pollutant minimisation and reduction technologies are discussed. Traditionally, it is always difficult to control the sources of various pollution problems in the municipality. More contaminants will be conveyed into the indoor environment if the ventilation indoors was increased. Therefore, air cleaning becomes the most effective solution to minimise the level of pollution in indoor environments (Kumar and Kumar, 2007; Wang *et al.*, 2007).

Adsorption is one of the conventional pollution control methods which can convert gaseous contaminants to solid contaminants. However, Advanced Oxidation has become a promising technology for air purification. Examples of Advanced Oxidation Processes may include Photocatalytic Oxidation and Thermal Oxidation Destruction. Through Advanced Oxidation Process technologies, contaminants can be oxidised to carbon dioxide and water (Wang *et al.*, 2007).

Occasionally, Thermal Oxidation Destruction requires high temperature (200 – 1200 ºC) to operate effectively. This requirement has directly increased the cost of the technology, particularly at low pollutant concentrations. On the contrary, Photocatalytic Oxidation usually happens at room temperature and pressure. Furthermore, the semiconductor catalysts used in this technology are less expensive and they can mineralise organic substances adequately. This technology is definitely more cost-effective when compared to Thermal Oxidation Destruction (Wang *et al.*, 2007).

2.3.1 Photocatalytic Oxidation

Photocatalytic Oxidation is a process to remedy air polluted by VOCs and bacteria (Vincent *et al.*, 2008). This promising process has become a cost-effective technology to remove VOCs in the environment when compared to other technologies, such as thermal catalysis, adsorption and biofiltration (Wang *et al.*, 2007).

A number of research studies on Photocatalytic Oxidation have been carried out in the past few decades. Various types of photocatalyst systems were developed. Most of the investigations are focused on the destruction of VOCs at parts per million (ppm) levels (Wang *et al.*, 2007). An overview of Photocatalytic Oxidation is presented in Figure 2-20.

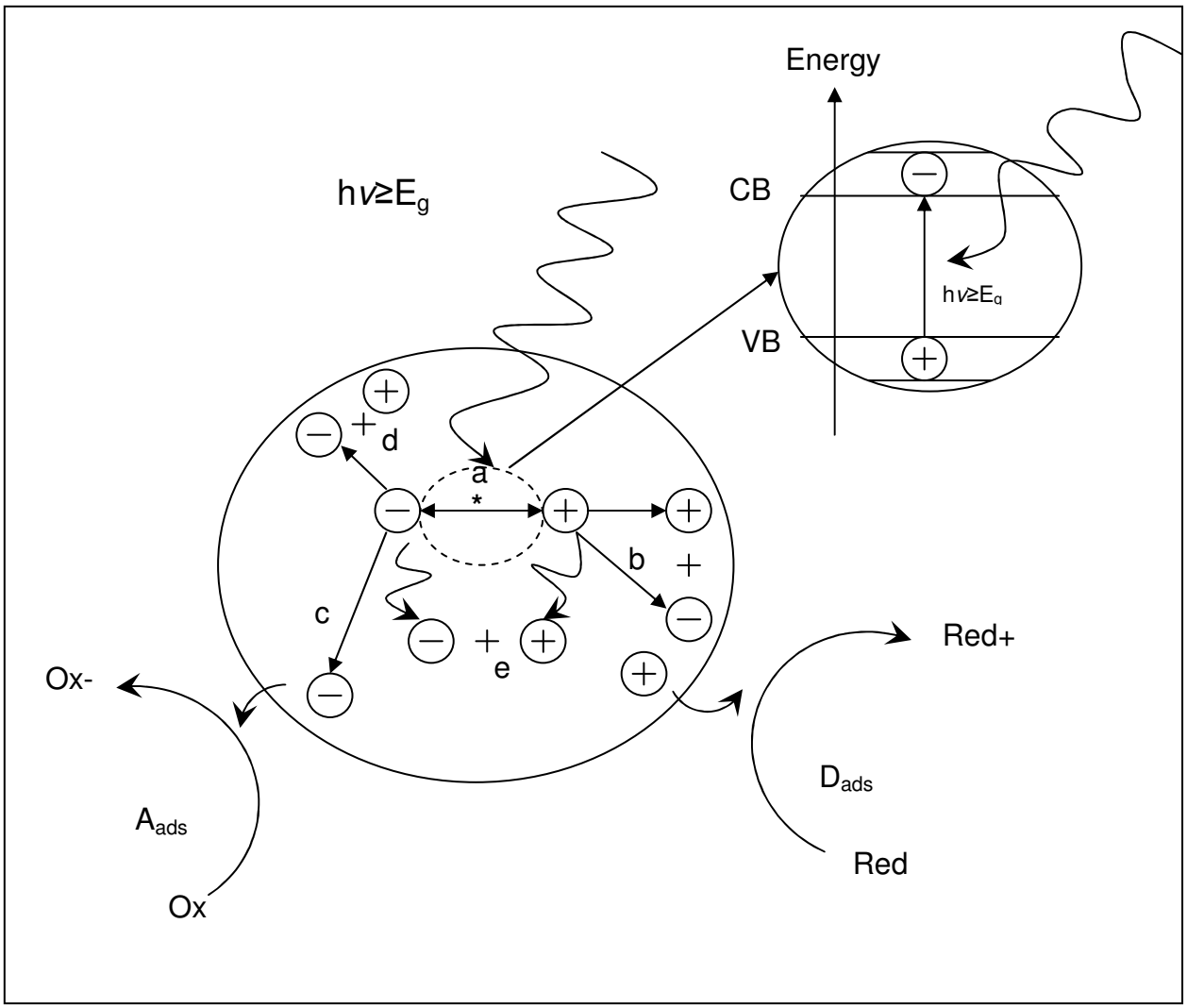

Figure 2-20: A diagram of Photocatalytic Oxidation (after Wang *et al.*, 2007)

In accordance with Geng *et al.* (2008), it is believed that the most effective technology to decompose airborne pollutants nowadays is oxidation. There are various photocatalytic reactors available in the market, such as photocatalytic reactors with fibre optic bundles, flat plate fluidized bed reactors, annular photocatalytic reactors, fixed layer photocatalytic reactors and fluidized bed reactors. The UV source, reactor configuration, catalyst type and interaction behaviors are part of the important reactor parameters for the photocatalytic reactor (Vincent *et al.*, 2008).

Photoreaction occurs when hole-electron pairs are formed in the photocatalytic oxidation process. Energy is provided, so that the band gap between the conduction band and valance band can be overcome in the semiconductor, thus formed pairs of electron-holes. Then the charge will be transferred between the electron-hole pairs and the reactants on the surface of the semiconductor, to enable the photo-oxidation occurs. A good photocatalyst can adsorb two reactants at the same time (Wang *et al.*, 2007).

2.3.2 Ozonation Technology over Different Porous Materials

Ozonation technology is the use of both ozone and porous adsorbents to reduce indoor VOCs. Ozone has a strong oxidizing capability. When the catalytic reaction is taking place in the porous structure, the residual ozone can be minimized as well. Indoor VOCs can be controlled in an effective way with the use of activated carbons or zeolites as they have a larger surface area. This characteristic has enhanced their adsorption capacities (Kwong *et al.*, 2008).

In line with Kwong *et al.* (2008), one of the effective and inexpensive ways to decrease indoor pollutant concentrations is by using the activated carbon. On the other hand, the high selectivity characteristic of a mesoporous molecular sieve can adsorb the VOC effectively, especially under humid condition. With the combination of these two elements, ozone can be degraded and reacted with toluene to form carbon dioxide and water.

2.3.3 Highly Crystalline Multi-Walled Carbon Nanotubes

In the past few decades, various efforts have been made to develop the technology for eliminating VOCs in the indoor environment. One of the developed techniques is by using the carbon nanotubes. According to Sone *et al.* (2008), carbon nanotubes can adsorb the pollutants effectively as they were made of crystalline and amorphous carbon. The proportion of each carbon could determine the adsorption capabilities of the nanotubes.

Carbon nanotubes can be divided into two main types (i.e. multi-walled carbon nanotubes and single-walled carbon nanotubes). Multi-walled carbon nanotubes were introduced to the market earlier than single-walled carbon nanotubes. Typical SEM images of the multi-walled carbon nanotubes at low (upper photo) and high (lower photo) resolutions are shown in Figure 2-21. Based on previous studies, it has been proven that carbon nanotubes can adsorb pollutants

effectively. However, the adsorptive capacities for VOCs will decrease when the temperature increases (Sone *et al.*, 2008).

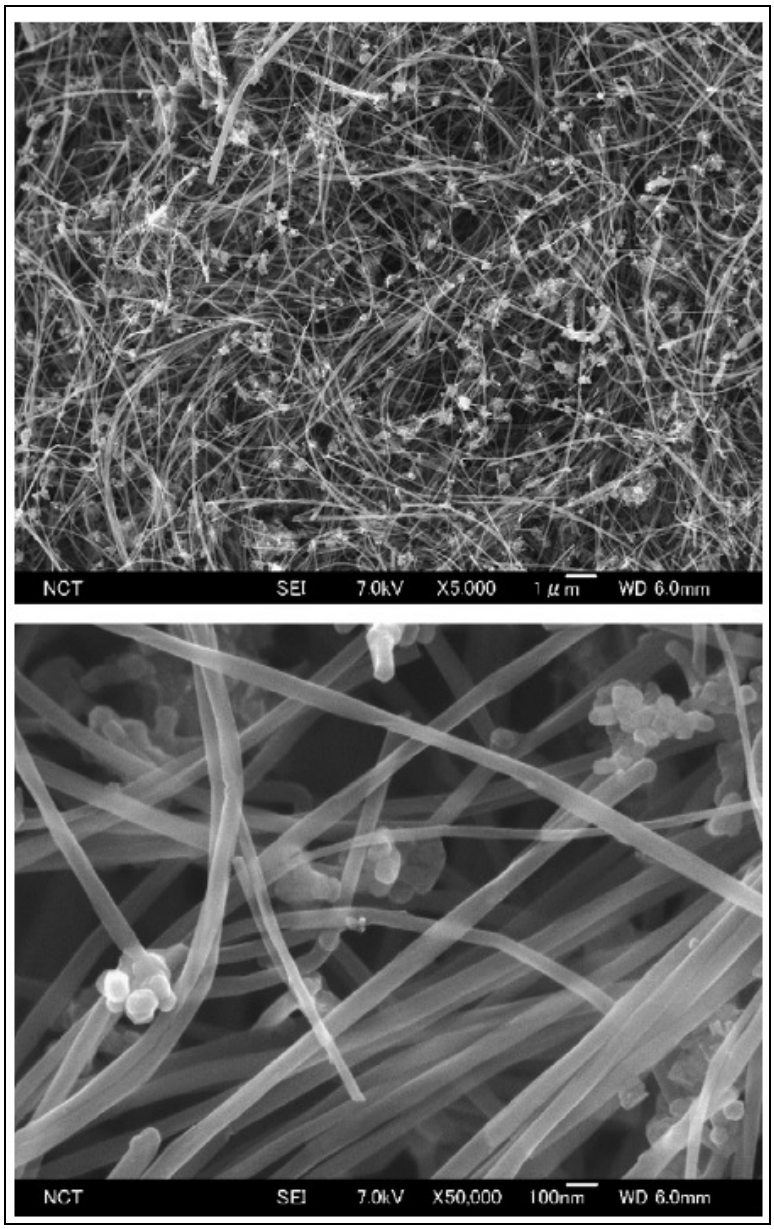

Figure 2-21: Typical SEM images of the highly crystalline multi-walled carbon nanotubes at low (upper photo) and high (lower photo) resolutions (Sone *et al.*, 2008)

2.4 INDOOR AIR QUALITY GUIDELINES AND REGULATORY LIMITS

Nowadays, there are an increasing numbers of people who have become aware of the severity of indoor air pollution. Therefore various indoor air quality guidelines and regulatory limits have been developed to aid current policy development. In 2004, a Committee on the

Medical Effects of Air Pollutants (COMEAP) was formed by the UK government (Department of Health) to develop guidance on the effects of indoor air pollutants on health. Some numerical guidelines are provided and these guidelines only applying to a few air pollutants. These guidelines were targeted to material manufacturers, architects and those who are concerned about indoor air pollution. Pertaining to the COMEAP guidance (2004), several guideline values for indoor air pollutants have been recommended, as tabulated in Table 2-15.

Table 2-15: The guideline values for pollutants found in indoor air (after COMEAP, 2004)

Pollutant	Concentration	Averaging time
Nitrogen dioxide	150 ppb (300 μg/m^3)	1 hour average
	20 ppb (40 μg/m^3)	Annual average*
Carbon monoxide	90 ppm (100 mg/m^3)	15 minutes
	50 ppm (60 mg/m^3)	30 minutes
	25 ppm (30 mg/m^3)	1 hour
	10 ppm (10 mg/m^3)	8 hours
Formaldehyde	0.1 mg/m^3 (0.1 ppm)	30 minutes
Benzene	1.6 ppb (5.0 μg/m^3)	Annual average
Benzo[a]pyrene	0.25 ng/m^3	Annual average*
** Provisional Guidelines*		

Apart from the UK, WHO also developed several guidelines to educate and protect people from the health consequences due to air pollution (WHO, 2000). In 2005, WHO updated the Air Quality Guidelines by including the guideline to PM, O_3, NO_2 and SO_2 (WHO, 2005).

The European Commission Joint Research Centre started the INDEX project (2005) which focused on the indoor exposure limits in the European Union. The project aimed to gather all the indoor air pollution scientists from all over the Europe in order to identify a suitable strategy and action plan to minimize pollution and health impacts. The guidelines covered various compounds such as nitrogen dioxide, toluene, styrene, orthoxylene, naphthalene, meta- and para- xylene, formaldehyde, d-limonene, carbon monoxide, benzene, ammonia, alpha-pinene and acetaldehyde. These compounds are categorised into three groups, which are high priority chemicals (Group 1), second priority chemicals and additional chemicals of interest.

Pertaining to the Indoor Air Hygiene Commission (2009), Guide Value I and Guide Value II have been established by the Federal Environment Agency's Indoor Air Hygiene Commission and the Permanent working Group of the Highest State Health Authorities (Germany) in 1996.

According to the Finnish Society of Indoor Air Quality and Climate (FiSIAQ, 2002), the Classification of Indoor Climate, Construction, and Finishing Materials was published in 1995.

The target values of indoor climate in Finland were established according to the Health Protection Act (1994) and the Land Use and Building Act (1999). The classifications include S1 (Individual Indoor Climate), S2 (Good Indoor Climate) and S3 (Satisfactory Indoor Climate). The Finnish Housing and Building Department also developed the Finnish Building Code (2003) which covered the indoor climate and the ventilation of buildings. These guidelines mainly focus on the indoor climate and ventilation of new buildings. On the other hand, the Swedish R1-guideline for the specification of indoor climate requirements has been revised to adapt the Swedish conditions and regulations (Ekberg, 2007).

The Illinois Department of Public Health (2008) established a guideline to improve the quality of air in indoor environment. The Illinois Department of Public Health has also included some occupational standards for working adults.

The Hong Kong Special Administrative Region Government launched the Indoor Air Quality Certification Scheme for Offices and Public Places in September 2003. It features a set of twelve 2-level parameter indoor air quality objectives as a benchmark to assess the quality of indoor air within premises/buildings (Indoor Air Quality Management Group, 2003). These parameters are Excellent Class and Good Class. The objectives of the scheme mainly focus on the air quality standards indoors. The guidelines are designated to maintain good air quality inside the building, hence reducing the health effects on occupants.

The Singapore Ministry of Environment appointed a Technical Advisory Committee to provide advice on the guidelines for good air quality. The objective is to improve the indoor air quality within air-conditioned premises (Institute of Environmental Epidemiology, 1996). It also provides information on the potential health consequences from indoor air pollution.

A Federal-Provincial Working Group on Indoor Air Quality from Canada has investigated the potential health effects caused by 17 chemical substances and one radioactive substance in the indoor environment (Health Canada, 1987). The working group looked into the potential health effects from both long-term (Acceptable Long-Term Exposure Range) and short-term (Acceptable Short-Term Exposure Range) perspectives.

The Institute for Research in Construction, National Research Council Canada launched the second phase of the Material Emissions and Indoor Air Quality Modelling project in 2000. The objectives are to develop the knowledge and tools needed to estimate concentrations of

VOCs and to provide the scientific bases needed to enhance indoor air quality guidelines for offices and residential buildings. This report is simply a summary of the available standards. The organizations cited in this document are shown in Table 2-16.

Table 2-16: Standards and Guidelines Organizations (after Charles *et al.*, 2005)

Acronym	Organization
ACGIH	American Conference of Governmental Industrial Hygienists
ASHRAE	American Society of Heating, Refrigerating, and Air-Conditioning Engineers
	Association of Environmentally Friendly Carpets (Germany)
	Building Information Foundation (Finland)
CRI	Carpet and Rug Institute
CSA	Canadian Standard Association
DFG	Deutsche Forschungs Gemeinschaft (Germany)
DSIC	Danish Society of Indoor Climate (Denmark)
EPA	U.S. Environmental Protection Agency
GEI	GreenGuard Environmental Institute
	Green Seal
GEV	Gemeinschaft Emissionskontrollierter Verlegewerkstoffe (Germany)
	Federal Environmental Agency (Germany), Indoor Air Hygiene Commission (IRK)
HRSDC	Human Resources and Skill Development Canada
MHLW	Ministry of Health, Labour and Welfare (Japan)
	Nordic Council of Ministries
NFICL	Norwegian Forum of Indoor Climate Labeling (Norway)
NIOSH	National Institute for Occupational Safety and Health
OEHHA	Office of Environmental Health Hazard Assessment (California EPAA)
OSHA	Occupational Health and Safety Administration
SCS	Scientific Certification Systems
	TerraChoice Environmental Services
	The Government of the Hong Kong Special Administrative Region (Hong Kong)
WHO	World Health Organization

According to Charles *et al.* (2005), the report has shown a variety of IAQ standards and guidelines for industrial settings (OSHA, MAK, NIOSH, and ACGIH in Table 2-17). The difference becomes greater when values for non-industrial settings are considered. A similar observation can be made for organic compounds, as shown in Appendix II. A wide variety of substances and guide values exist for guidelines intended for non-occupational exposures (OEHHA, WHO, Japan, Hong Kong, and Germany) compared to those for occupational exposures (OSHA and ACGIH).

Table 2-17: Standards and Guidelines for Common Indoor Contaminants (after Charles *et al.*, 2005)

Unless otherwise specified, values are given in parts per million (ppm). Number in brackets [ ] refers to either a ceiling or to averaging times of less than or greater than eight hours (min=minutes; hr=hours; yr=year; C=ceiling; L=long term. Where no time is specified, the averaging time is eight hours.

	NAAQS/EPA (2000)[a]	**OSHA[a]**	**MAK (2000)[a]**	**Canadian (1995)[a]**	**WHO/Europe (2000)[a]**	**NIOSH (1992)[a]**	**ACGIH (2001)[a]**	**COSHR**	**HongKong (2003)[i]**	**German[j]**
Carbon dioxide		5,000	5,000 10,000 [1 hr]	3,500 [L]		5,000 30,000 [15 min]	5,000 30,000 [15 min]	refer readers to ACGIH recommendations	800 / 1,000 [8 hr]	
Carbon monoxide	9[d] 35 [1hr][d]	50	30 60 [30 min]	11 [8 hr] 25 [1 hr]	90 [15 min] 50 [30 min] 25 [1 hr] 10 [8 hr]	35 200 [C]	25		1.7 / 8.7 [8 hr]	52 / 5.2 [0.5 h] 13 / 1.3 [8 h]
Formaldehyde	(see note e)	0.75 2[15 min]	0.3 1.0[g]	0.1 [L] 0.05 [L][h]	0.081 (0.1 mg/m^3) [30 min]	0.016 0.1 [15 min]	0.3 [C]		0.024 / 0.081 [8 hr]	
Lead	1.5 µg/m^3 [3 months]	0.05 mg/m^3	0.1 mg/m^3 1 mg/m^3 [30 min]	minimize exposure	0.5 µg/m^3 [1 yr]	0.1 mg/m^3 [10 hr]	0.05 mg/m^3			
Nitrogen dioxide	0.05 [1 yr]	5 [c]	5 10 [5 min]	0.05 0.25 [1 hr]	0.1 [1 hr] 0.004 [1 yr]	1.0 [15 min]	3 5 [15 min]		0.021 / 0.08 [8hr]	0.19 [0.5 h] 0.03 [1 wk]
Ozone	0.12 [1 hr][d] 0.08	0.1	carcinogen – no maximum value established	0.12 [1 hr]	0.064 (120 µg/m^3) [8 hr]	0.1 [C]	0.05 – heavy work 0.08 – moderate work 0.1 – light work 0.2 – any work (2hr)		0.025 / 0.061 [8hr]	
Particles[b] <2.5 µm MMAD[c]	15 µg/m^3 [1 yr][f] 65 µg/m^3 [24 hr][f]	5 mg/m^3	1.5 mg/m^3 for <4 µm	0.1 mg/m^3 [1 hr] 0.04 mg/m^3 [L]			3 mg/m^3			
Particles[b] <10 µm MMAD[c]	50 µg/m^3 [1 yr][f] 150 µg/m^3 [24 hr][f]		4 mg/m^3				10 mg/m^3		0.02 / 0.18 mg/m^3	
Radon	4 pCi/L [1 yr]				2.7 pCi/L [1 yr]				4.1 / 5.4 pCi/L [8 hr]	
Sulfur dioxide	0.03 [1 yr] 0.14 [24 hr][d]	5	0.5 1.0[g]	0.38 [5 min] 0.019	0.048 [24 hr] 0.012 [1 yr]	2 5 [15 min]	2 5 [15 min]			
Total particles[b]		15 µg/m^3								

Table 2-17 (Continued)

Notes:
a: *As reported in: American Society of Heating, Refrigerating and Air-Conditioning Engineers (ASHRAE). (2004). ANSI/ASHRAE Standard-62.1-2004: Ventilation for Acceptable Indoor Air Quality. Atlanta, GA: ASHRAE.*
b: *Nuisance particles not otherwise classified (PNOC), not known to contain significant amounts of asbestos, lead, crystalline silica, known carcinogens, or other particles known to cause significant adverse health effects.*
c: *MMAD = mass median aerodynamic diameter in microns (micrometers). Less that 3.0 um is considered respirable; less than 10 um is considered inhalable.*
d: *Not to be exceeded more than once per year*
e: *The U.S. Department of Housing and Urban Development adopted regulations concerning formaldehyde emissions from plywood and particleboard intended to limit the airborne concentration of formaldehyde in manufactured homes to 0.4 ppm (24 CFR Part 3280, HUD Manufactured Home Construction and Safety Standards).*
f: *62 FR38652 – 38760, July 16, 1997.*
g: *Never to be exceeded.*
h: *Target level is 0.05 ppm because of its potential carcinogenic effects. Total aldehydes limited to 1 ppm.*
i: *Guideline value for Excellent Class / Guideline value for Good Class of IAQ (Hong Kong, 2003)*
j: *Guide Value II / Guide Value I; Values are converted from mg/m3 to ppm at 25ºC and 1 atm.*

2.5 RELATIONSHIP BETWEEN THE INDOOR AND OUTDOOR CONCENTRATIONS

Over the past few decades, people tended to believe that indoors are cleaner than outdoors. People will find it more comfortable in an indoor environment as the building can provide protection to them (Lawrence *et al.*, 2004). In fact, a number of investigations have been conducted to look into the relationship between indoor and outdoor pollution (Leaderer *et al.*, 1999; Roulet, 2001; Jedrychowski *et al.*, 2006; Hoek *et al.*, 2008). People can estimate and improve the exposure levels of pollution concentrations under different environmental conditions through understanding the relationship between the indoor and outdoor environment. Hence, human exposure rates to the pollutants and health risks can be reduced effectively (Lawrence *et al.*, 2004).

Since the 1950s, various studies have been conducted to study the relationship between indoor and outdoor pollutants. The relationship between the indoors and outdoors was defined and represented with the ratios of indoor and outdoor pollutant concentrations (I/Os). Anderson (1972) concluded that there were great variations in I/Os in early studies (Lawrence *et al.*, 2004).

Baek *et al.* (1996) conducted an investigation into the effect of ambient air on indoor air quality. Baek *et al.* (1996) investigated the I/Os for several indoor air pollutants, such as respirable suspended particles, CO, NO_2 and VOCs. This study was conducted not only in homes, but also offices and restaurants in Korea. From this study, Baek *et al.* (1996) concluded that indoor air was more polluted than outdoor air and outdoor sources of pollution have a strong influence on indoor air. Table 2-18 shows the correlations between indoor and outdoor air quality in Korea. The table shows that the data obtained in summer presented a consistent correlation between indoor and outdoor VOC concentrations. Apart from this, the data also demonstrated that the relationships of CO, NO_2 and respirable suspended particles (RSP) are poor between the indoor and outdoor environment. This indicated the important contribution of other sources indoors.

Table 2-18: Correlations between indoor and outdoor air quality in Korean urban area (after Baek *et al.*, 1996)

Air quality parameter	Summer			Winter		
	Home	Office	Restaurant	Home	Office	Restaurant
RSP	0.63	0.17	-0.01	0.76	0.25	0.02
CO	0.37	0.48	-0.04	0.72	0.34	0.32
CO_2	0.96	0.71	0.77	0.18	-0.12	0.41
NO_2	0.79	0.79	0.52	0.42	0.23	0.53
Benzene	0.91	0.56	0.14	0.72	0.70	0.27
Toluene	0.88	0.55	0.75	0.85	0.30	0.85
Ethylbenzene	0.93	0.82	0.33	0.72	0.33	0.84
m + p-Xylene	0.94	0.85	0.89	0.73	0.52	0.67
Styrene	0.78	0.60	0.72	0.51	-0.04	0.37
o-Xylene	0.83	0.92	0.88	0.72	0.34	0.70
1,3,5-Trimethylbenzene	0.99	0.70	0.75	0.47	0.06	0.40
1,2,4-Trimethylbenzene	0.99	0.65	0.70	0.46	0. 11	0.36
Sample size	24	24	24	24	24	24

Wallace (1996) reviewed several studies on indoor particle pollution. It was concluded that indoor fine particle concentrations were 0.65 times that of the outdoor concentration. Indoor coarse particle concentrations were 0.43 times that of the outdoor concentration. This value was estimated under the circumstance that there were no specific sources of indoor particles. As most of the studies had higher ratios than these estimations, it can be inferred that most of the homes were contaminated with significant indoor sources of particles (Kingham *et al.*, 2000).

Kingham *et al.* (2000) investigated the spatial concentration variation of pollutants emitted from traffic in Huddersfield. Pollutants, such as $PM_{2.5}$, PM_{10}, benzene, benzo[a]pyrene and polycyclic aromatic hydrocarbons, were the focus of the study. The location of the sampling sites are shown in Figure 2-22. Table 2-19 represents the I/O ratios and tests for differences between indoor and outdoor concentrations. The results showed that indoor and outdoor air pollutant levels were strongly correlated.

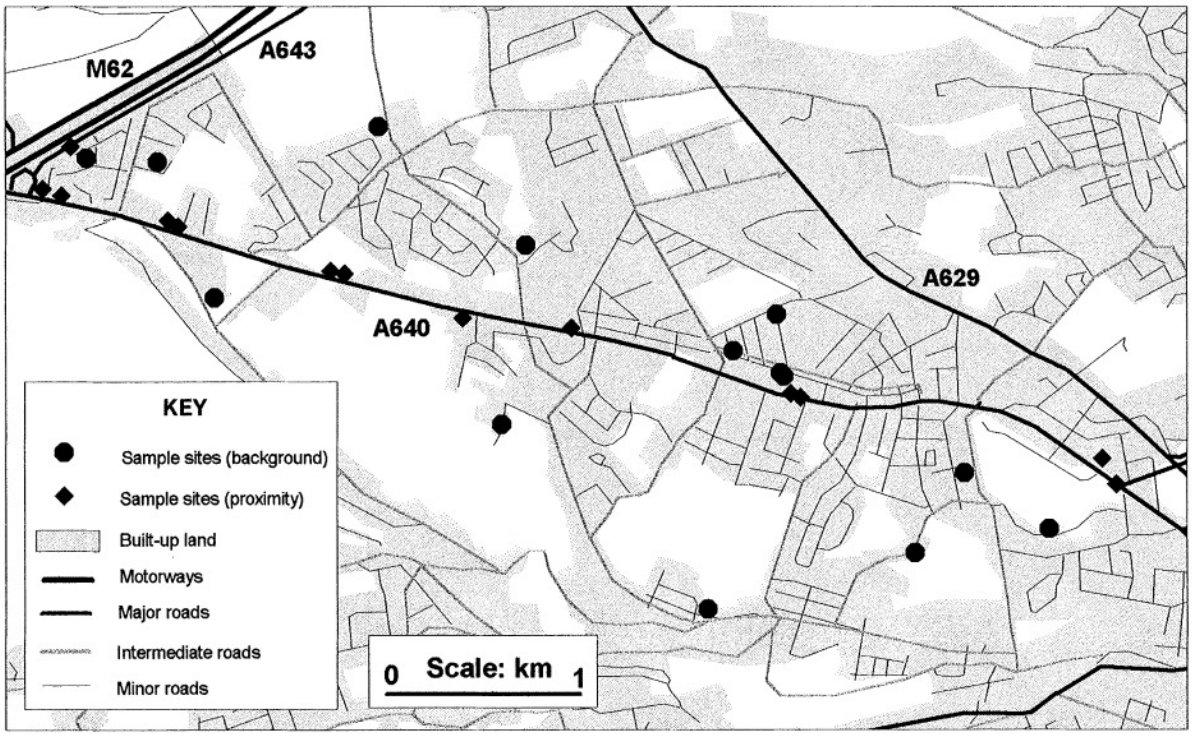

Figure 2-22: Location of sampling sites (Kingham *et al.*, 2000)

Table 2-19: I/O ratios and tests for differences between indoor and outdoor concentrations (after Kingham *et al.*, 2000)

Variable	Ratio						Wilcoxon	
	Mean	Median	SD	Min	Max	M	*p*	N
Mass PM_{10}	1.04	0.81	0.81	0.12	3.28	30	0.023	30
Mass $PM_{2.5}$	0.91	0.73	1.01	0.15	5.22	29	0.002	29
Abs PM_{10}	0.82	0.78	0.27	0.25	1.49	39	0	39
Abs $PM_{2.5}$	0.85	0.79	0.24	0.42	1.71	38	0	38
Benzene	2.73	1.17	5.72	0.12	31	39	0.077	42
B(a)P	22.05	1.00	75.24	0.00	361.00	48	0.100	48
PAH	22.93	0.79	82.13	0.00	390.80	30	0.077	48
B(a)P[a]	0.60	0.27	0.85	0.00	2.67	29	0.003	29
PAH[a]	1.76	0.11	3.49	0.00	17.14	37	0.021	37

a: Excluding ratios for sites below detection limit

2.6 COMPUTATIONAL FLUID DYNAMICS

Computational Fluid Dynamics (CFD) has been expansively adopted in indoor air quality simulations (Chiang *et al.*, 2000; Zhao *et al.*, 2003; Steeman *et al.*, 2009). Various experiments have been modelled using CFD techniques, such as transport mechanisms of airborne particulate matter (Baker *et al.*, 1994a; Zhang and Chen, 2006; Chang and Hu, 2008), particulate concentration simulations (Tian *et al.*, 2006; Nerisson *et al.*, 2011), modelling of gas-phased

reactions in indoor environments (Sorensen and Weschler, 2002), air and contaminant distribution (Fan, 1995; Srebric *et al.*, 2008), indoor air motion (Baker *et al.*, 1994b), indoor ventilation efficiency (Bady *et al.*, 2008), indoor pollutant mixing time (Gadgil *et al.*, 2003), indoor airflow and heat transfer (Stamou and Katsiris, 2006), particle deposition onto indoor surfaces (Zhang and Chen, 2009) and modelling of ultrafine particle dispersion (Zhao *et al.*, 2009).

Apart from this, CFD is also frequently used in prediction models, e.g. prediction of indoor air humidity (Teodosiu *et al.*, 2003) and indoor climate (Rohdin and Moshfegh, 2007). Researchers also use CFD to control and optimise the air quality of the indoor environment (Sun and Wang, 2010). Some of these were conducted in livestock and agricultural buildings (Norton *et al.*, 2010a&b) and offices (Russo and Khalifa, 2010). Several researchers have used CFD to improve the indoor thermal environment (Wang and Wong, 2009) and study the impact of airflow profiles (Sekhar and Willem, 2004). In short, CFD is capable of providing detailed fluid flow information and fluid property distribution (Susin *et al.*, 2009).

As the comparison between the simulation results from the standard k-ε model and the experimental data is always feasible, the standard k-ε model is extensively adopted for indoor air quality simulations (Yan *et al.*, 2009). In this research, the standard k-ε model was selected. Gambit was used to generate the mesh and Fluent was applied to perform calculations in order to evaluate the velocity magnitude, flowfield and particle trajectories within the kitchen.

Zhang and Chen (2006) used the Lagrangian particle tracking method to determine the particle concentration distribution and its flowfield in several ventilated rooms. The particle deposition rate in the rooms was ignored. This research covered three ventilation systems. Underfloor air distribution systems were found to have the best particle removal performance.

Standard k-ε, Renormalisation Group (RNG) k-ε and RNG-based Large Eddy Simulation (LES) models were applied to evaluate the indoor airflow environment. In their study, the researchers validated the CFD model by using data conducted under isothermal ventilated condition which obtained by other researchers. In order to compliment the non-isothermal condition, an additional experiment was carried out. Both monodisperse aerosol generator (TSI 3475, TSI Inc.) and particle counter (PC-2H QCM impactor, California Measurements Inc.) were used to generate 0.7μm Di-Ethyl-Hexyl-Sebacat particles and determine the particles concentration at the outlet respectively.

Figure 2-23 shows experimental arrangements and the environmental chamber configuration and in a ventilated room. Table 2-20 shows the boundary conditions in the room with the underfloor air distribution system. The CFD model consisted of 389, 338 volumes. The researchers assumed the supply air was uniformly distributed in the room.

Table 2-20: Measured boundary conditions in the room with underfloor air distribution system (after Zhang and Chen, 2006)

Surface	Surface temperature (ºC)	Boundary	Surface temperature (ºC)	Heat power (W)
North wall (+ *X*)	24.9	Floor (-Y)	24	-
South wall (- *X*)	25.0	lamps (each)	-	64
East wall (+ *Z*)	25.5	Persons (each)	31.6	100
West wall (- *Z*)	25.3	Supply (north)	20.4	-
Ceiling (+ *Y*)	25.7	Supply (south)	19.9	-

Figure 2-24 shows the measured and predicted particle concentration distribution in the modelled room. Figure 2-24(a) presents the source near the floor centre and Figure 2-24(b) presents the source under one air supply. The particle size was 0.31 μm. Figure 2-25 presents the particle concentration distribution in the scaled model room with side wall air supply. The size of the particle was 4.5 μm. Only drag force and gravity were taken into considerations in this case.

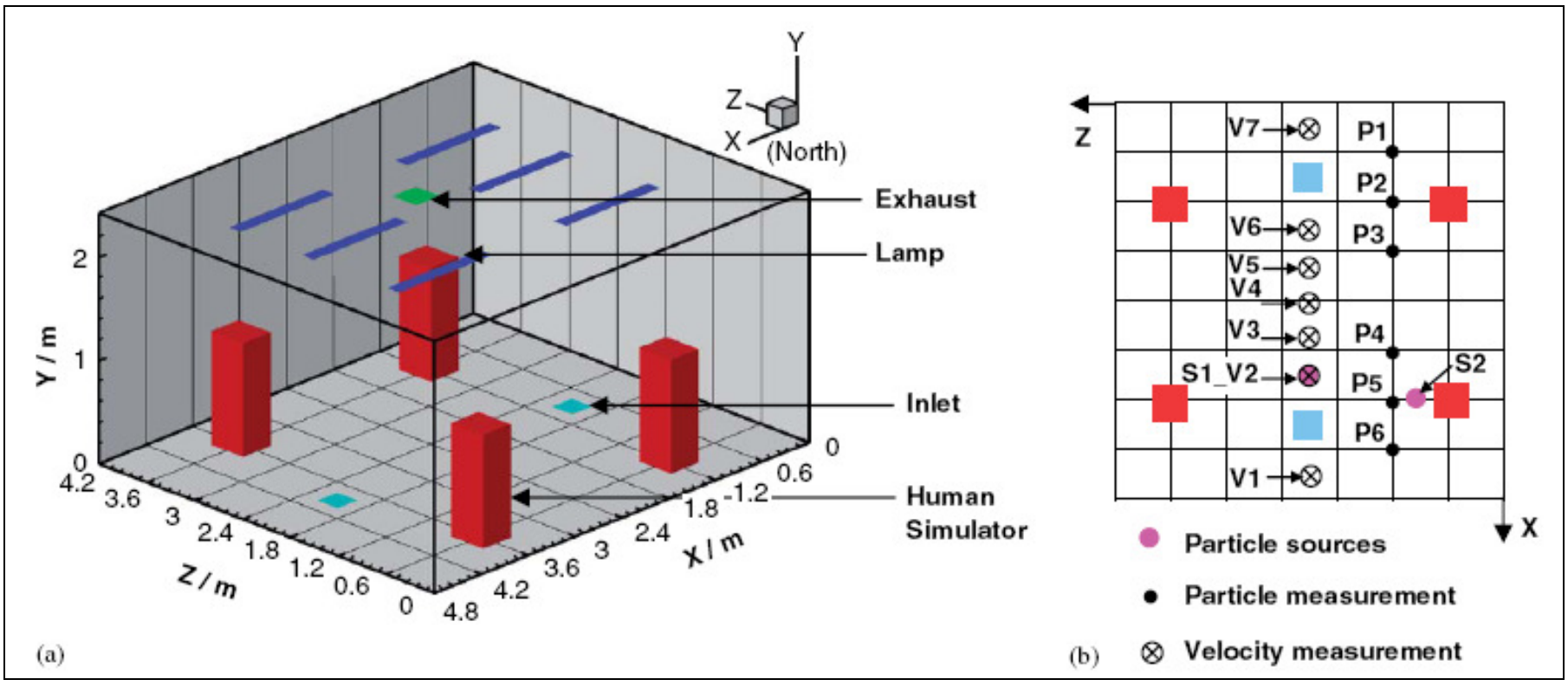

Figure 2-23: A sketch of the environmental chamber configuration and experimental arrangements (Zhang and Chen, 2006)

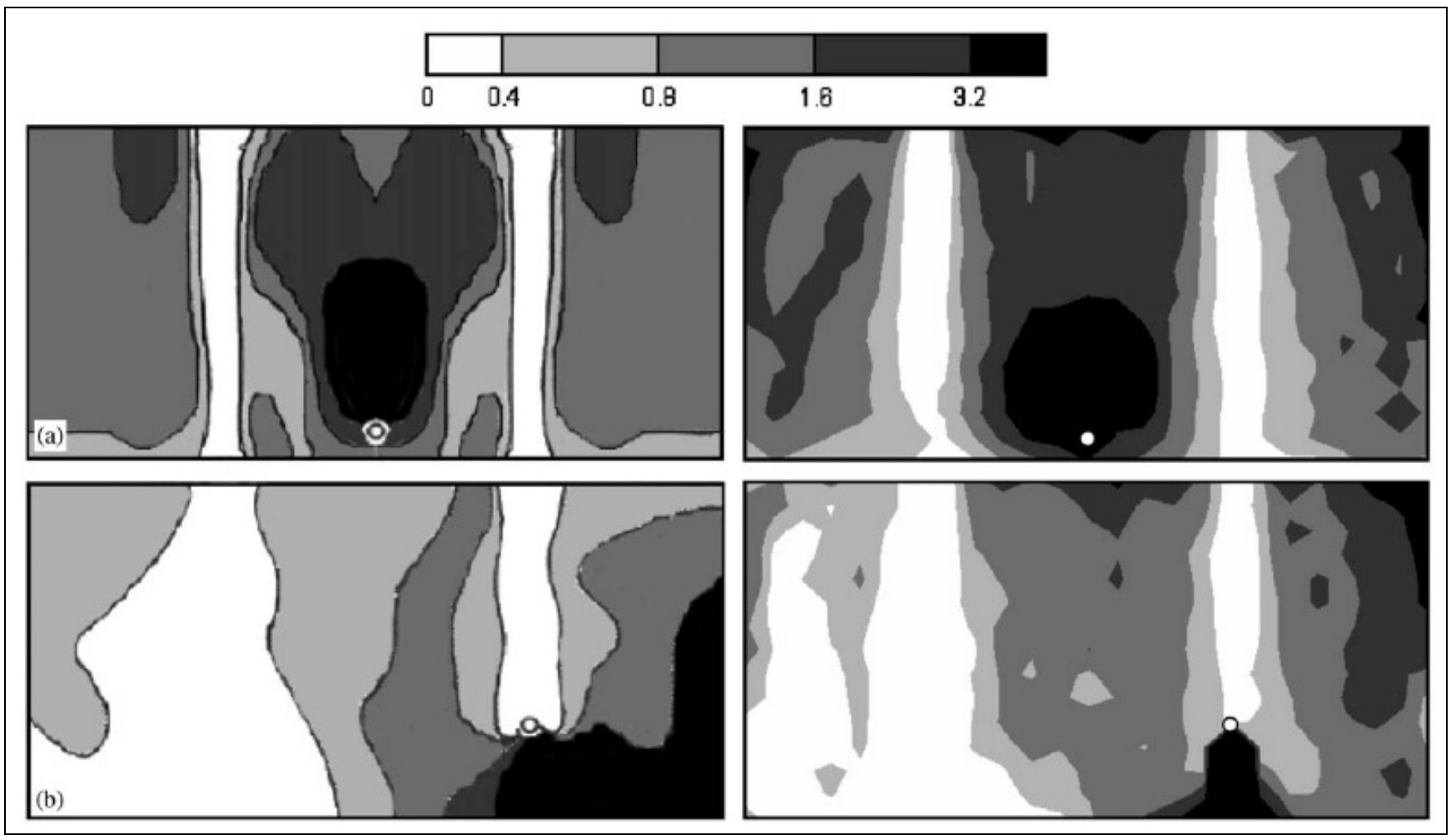

Figure 2-24: Measured and predicted particle concentration distribution in the centre plane of the model room with ceiling air supply: (a) source near the floor centre, and (b) source under one air supply (Zhang and Chen, 2006)

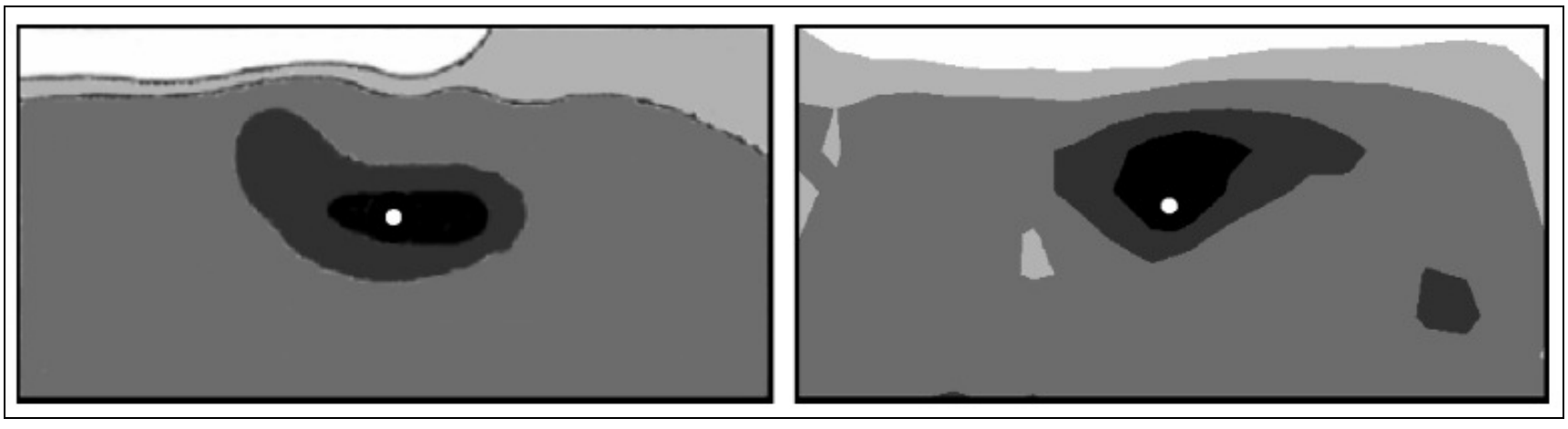

Figure 2-25: Measured and predicted particle concentration distribution in the centre plane of the scaled model room with side wall air supply (left: experimental measurements; right: simulation) (Zhang and Chen, 2006)

The results in both Figures 2-24 & 2-25 showed the feasibility of the model for particle flowfields modelling within an indoor environment since the results from the modelling simulations agree well with the experimental data.

Figure 2-26 shows the airflow pattern in the chamber with an underfloor air distribution system using the validated particle model. The air was well-mixed in the lower part of the chamber, and moved to the upper part through human-generated heat plumes and supply air.

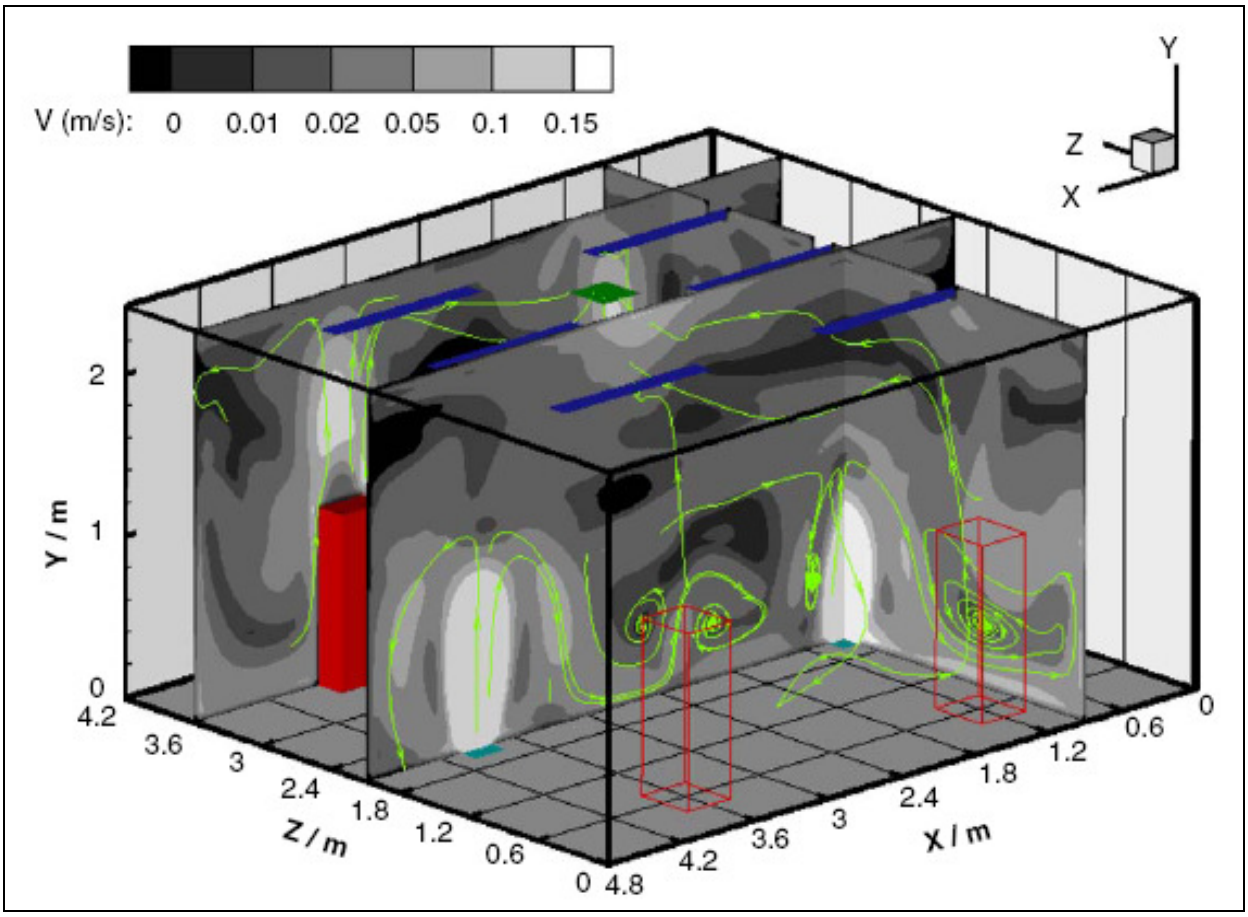

Figure 2-26: Simulated airflow fields in the chamber with the underfloor air distribution system (Zhang and Chen, 2006)

Figure 2-27 shows the particle flowfields in the room with underfloor air distribution. Underfloor air distribution has the lowest normalised average concentration, which means that it is most efficient in removing particles for a ventilation system.

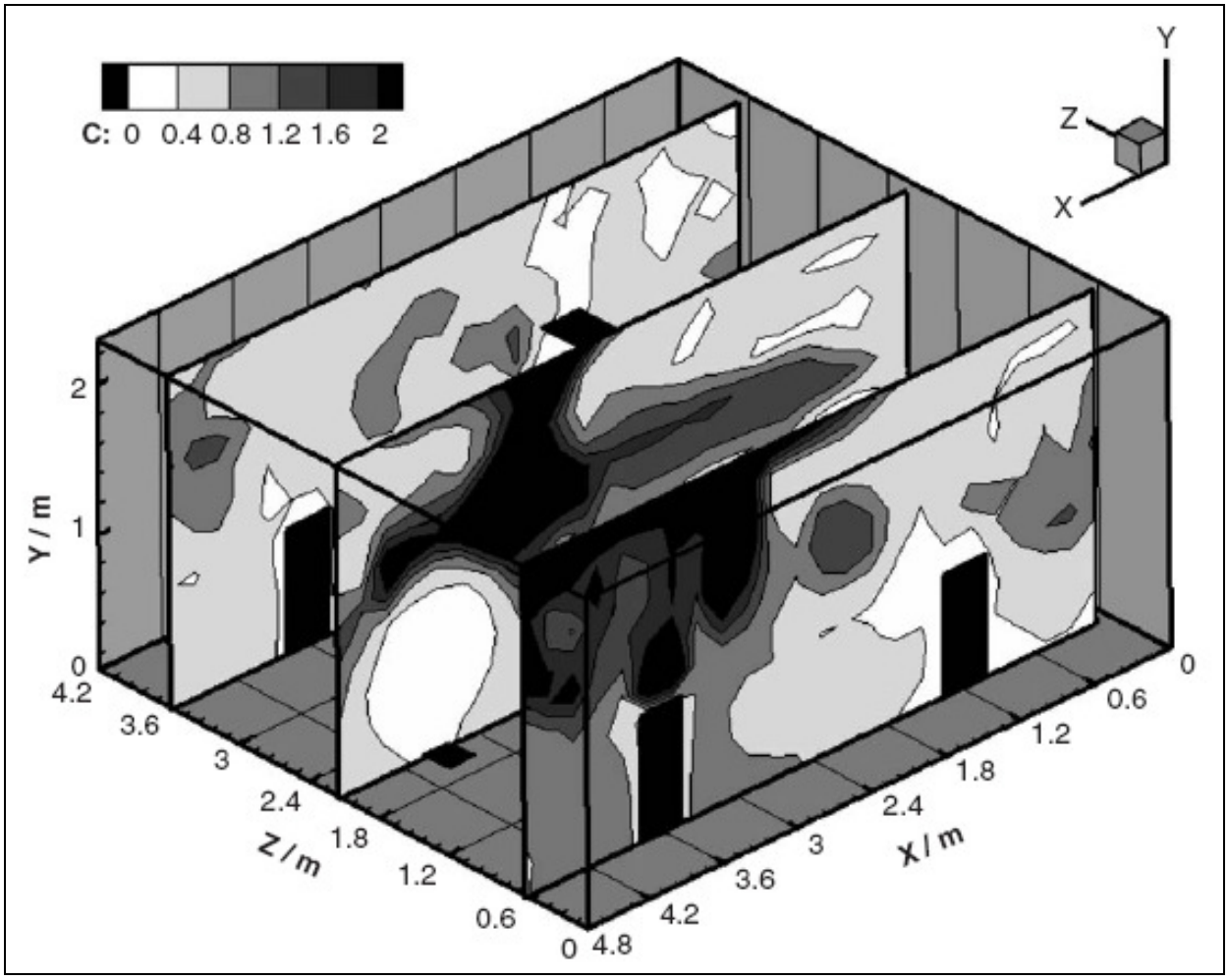

Figure 2-27: Particle concentration distribution with the source near an occupant in the room with the underfloor air distribution system (Zhang and Chen, 2006)

In conclusion, the underfloor air distribution system is efficient in removing occupant-generated particles, but not effective in removing particles which are re-suspended or generated at floor level.

Tian *et al.* (2006) conducted a numerical study on contaminant particle concentrations in indoor airflow. They used three turbulence models to model the particle flowfields (i.e. standard k-ε model, RNG k-ε model and RNG-based LES model). The Lagrangian particle-tracking method was applied. All these models were validated by using the measured air velocity data achieved by other researchers. Among these three models, the RNG-based LES model was proved to be the most effective particle flowfield and concentration distribution model.

Figure 2-28 shows the ventilated room model investigated in this study. The vertical inlet velocity was 0.235m/s. The characteristic length is 0.1m and the Reynolds number at the inlet is 1500. A mesh volume (0.8cm x 0.8cm x 0.8cm) was generated. The mesh was then refined with a

size of 0.5cm x 0.5cm x 0.5cm to achieve grid-independency. When five orders of magnitude were reduced for the iteration residuals, then the model was assumed to be converged. All models were run in unsteady-state conditions.

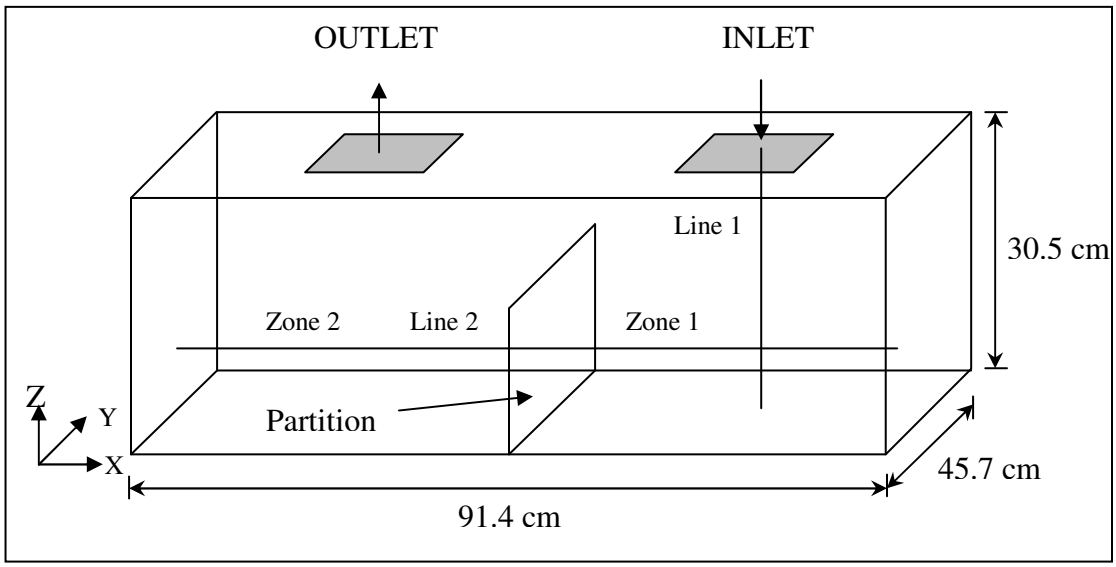

Figure 2-28: Ventilated room model (after Tian *et al.*, 2006)

Figure 2-29 shows the comparison between simulation and measured results for the vertical velocity component. It can be clearly seen that the modelling results agree well with the experimental results from other researchers. These models were validated through these encouraging results. The results from the RNG-based LES model were most similar to the experimental data.

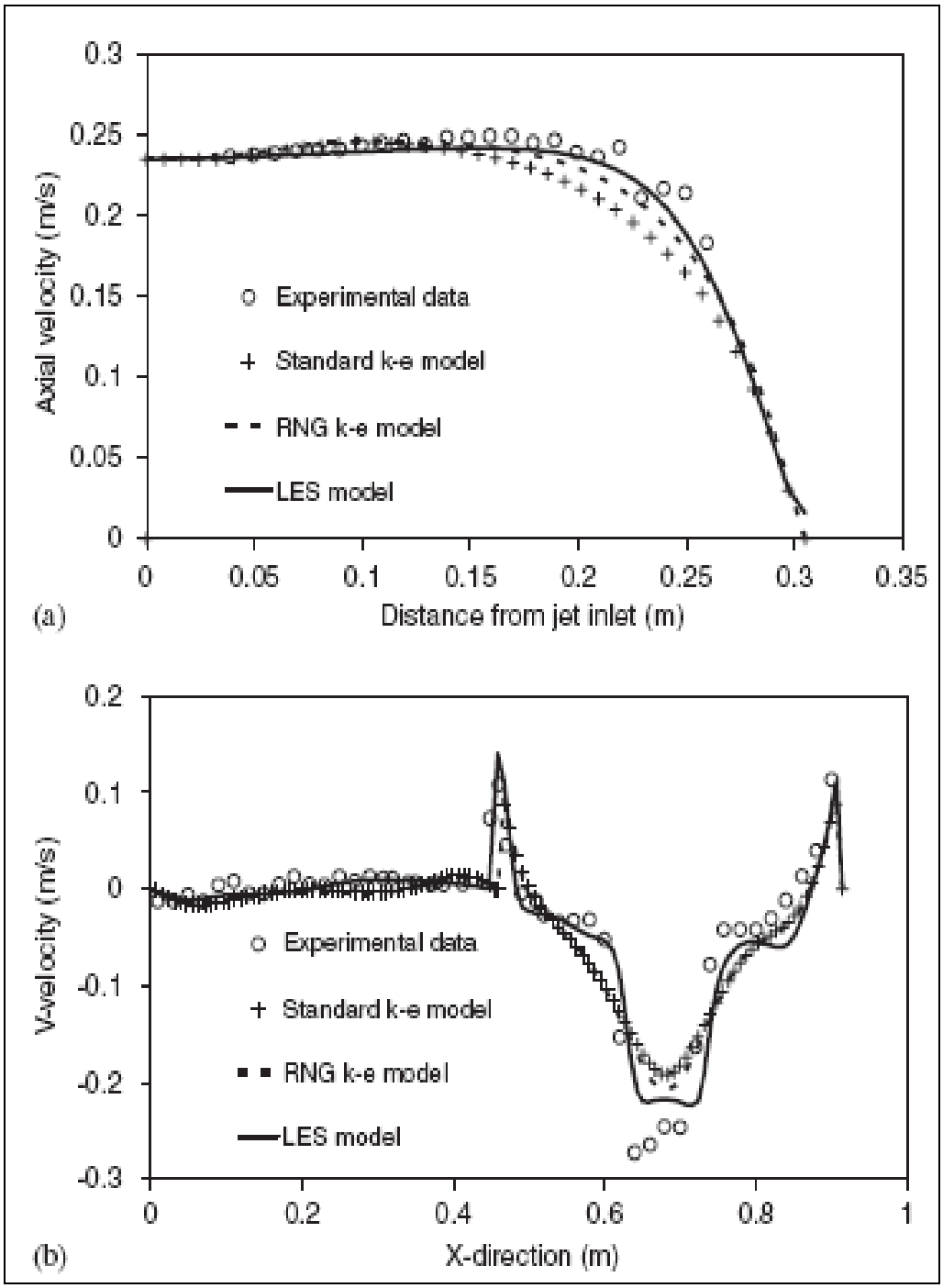

Figure 2-29: Comparison between simulation and measured results for the vertical velocity component: (a) along the vertical inlet jet axis, and (b) along the horizontal line at mid-partition height (Tian *et al.*, 2006)

In order to determine the concentration distribution of particles in the model room, 86,400 particles with 1 μm diameter (of 800 kg/m^3 density) were injected into the room and stopped at elapsed time, 100s. The sample particles were tracked. The comparison of the contaminant particle concentration (d_p = 1μm) simulated by three turbulence models after an elapsed time of 100, 130 and 160s are shown in Figures 2-30, 2-31 and 2-32 respectively.

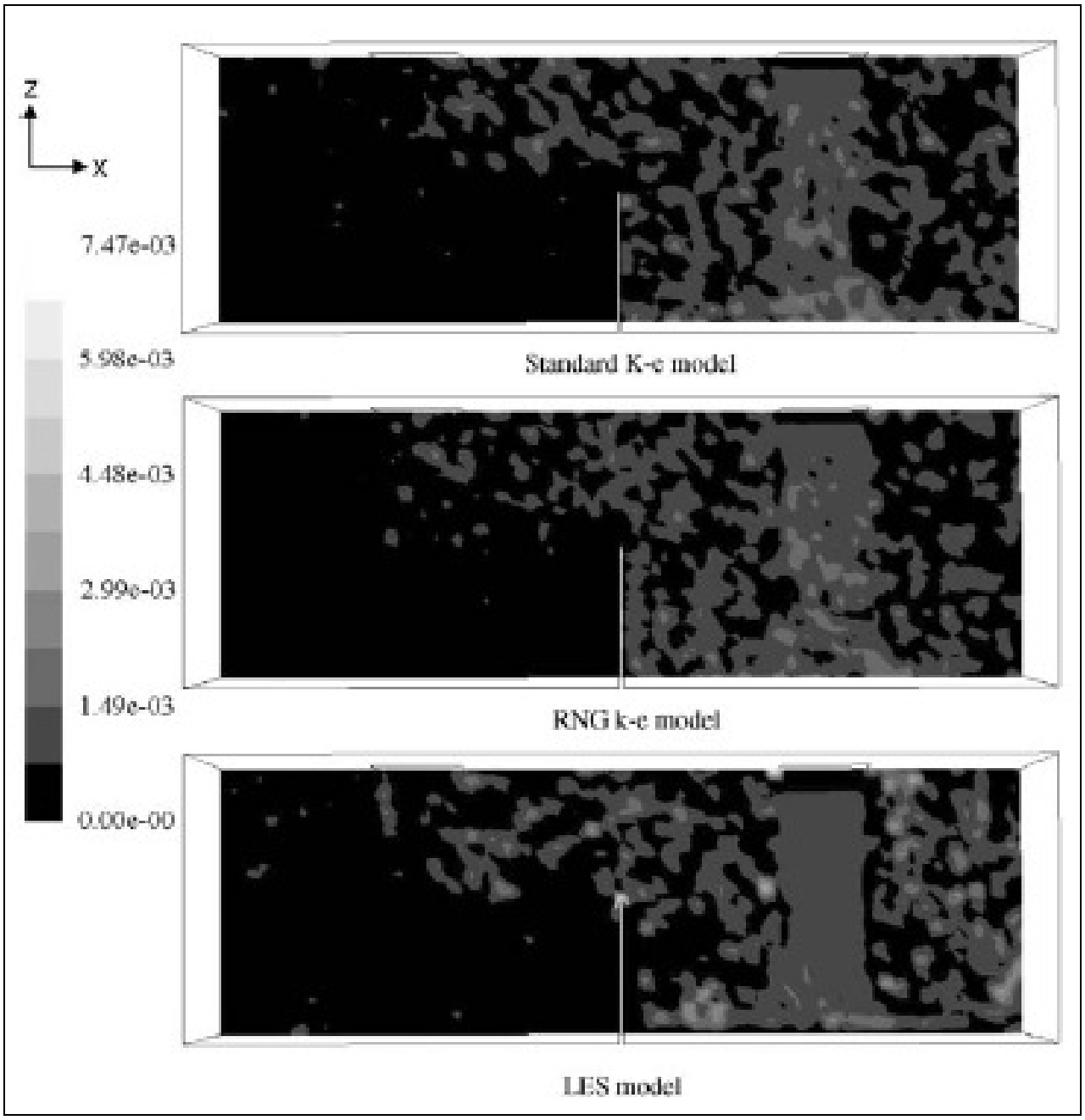

Figure 2-30: The comparison of the contaminant particle concentration (d_p = 1μm) simulated by three turbulence models at the mid-plane of the model room after an elapsed time of 100s (Tian *et al.*, 2006)

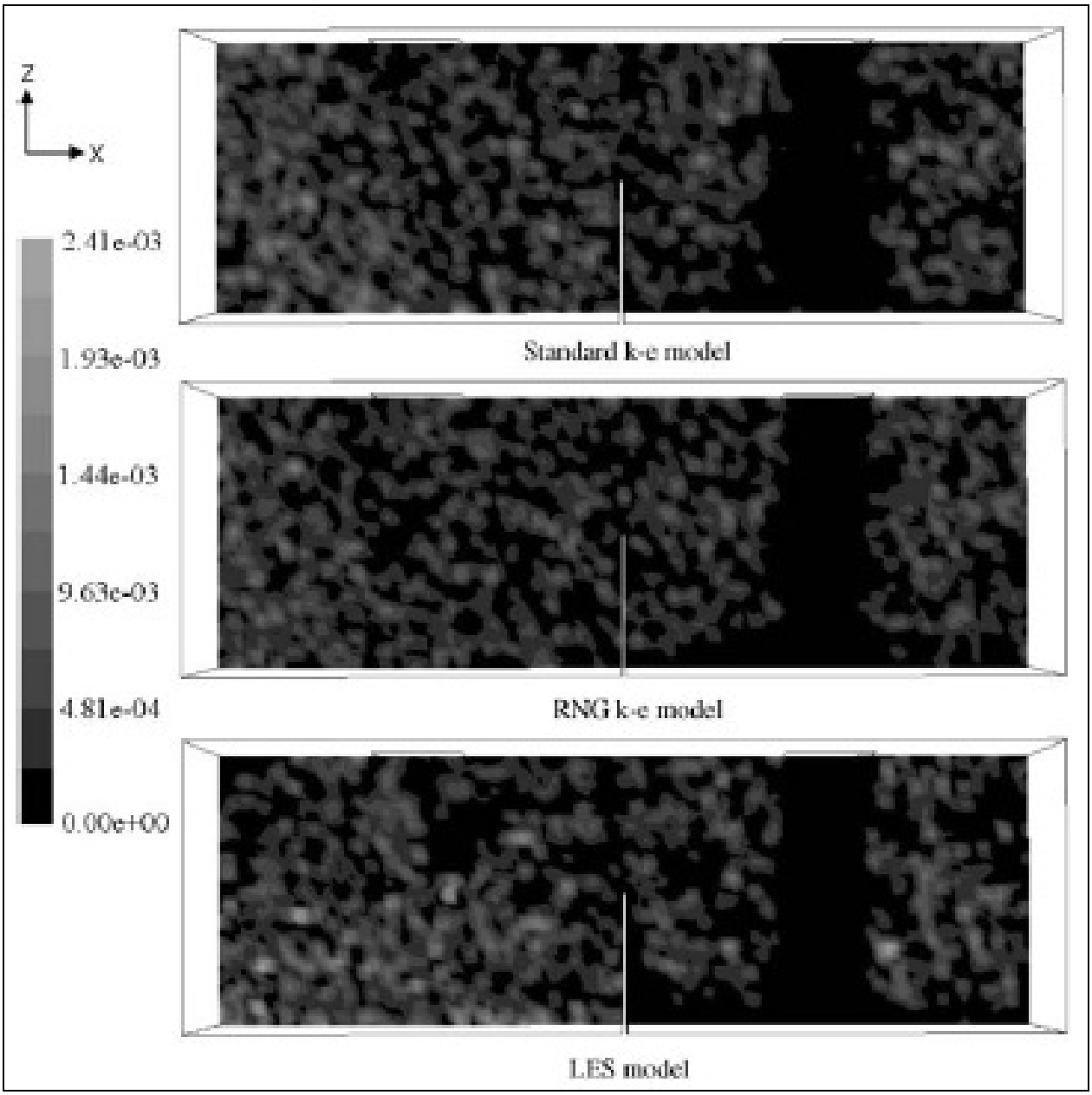

Figure 2-31: The comparison of the contaminant particle concentration (d_p = 1μm) simulated by three turbulence models at the mid-plane of the model room after an elapsed time of 130s (Tian *et al.*, 2006)

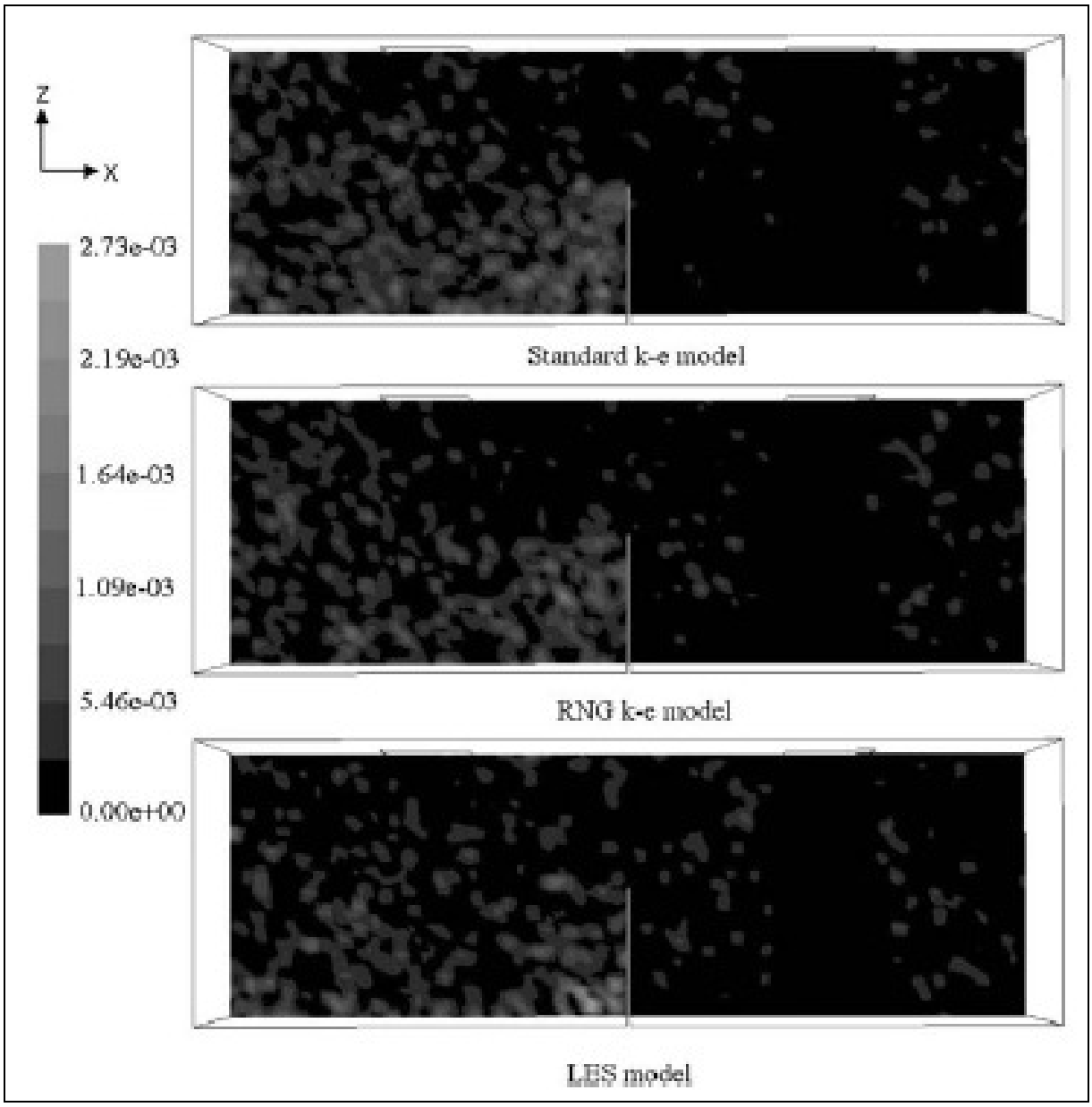

Figure 2-32: The comparison of the contaminant particle concentration (d_p = 1μm) simulated by three turbulence models at the mid-plane of the model room after an elapsed time of 160s (Tian *et al.*, 2006)

In conclusion, the standard and RNG k-ε models and RNG-based LES model were validated by using the air data provided by other researchers. The RNG-based LES model has proved to be the most effective particle flowfield and concentration distribution model among the three.

Chang and Hu (2008) conducted a research to study on the particle transport mechanisms in an indoor environment with partition. The researchers developed a three-dimensional model for their study. The Lagrangian particle tracking method was used. Chang and Hu (2008) have taken the effects of gravitational force, the drag force, the Brownian motion force and the

Saffman lift force into considerations. They looked into particulate matter sizes, ranging from 0.05 to 10μm in diameter.

In this case, two numerical models (i.e. Eulerian indoor airflow model and the Lagrangian particle trajectory-tracking model) were used to determine the particle transport mechanisms indoors. The models were validated by experimental results from other researchers. Figure 2-33 shows the geometry of the building experiment used for this study. The building was divided into two zones. There is a partition and an opening in between the zones.

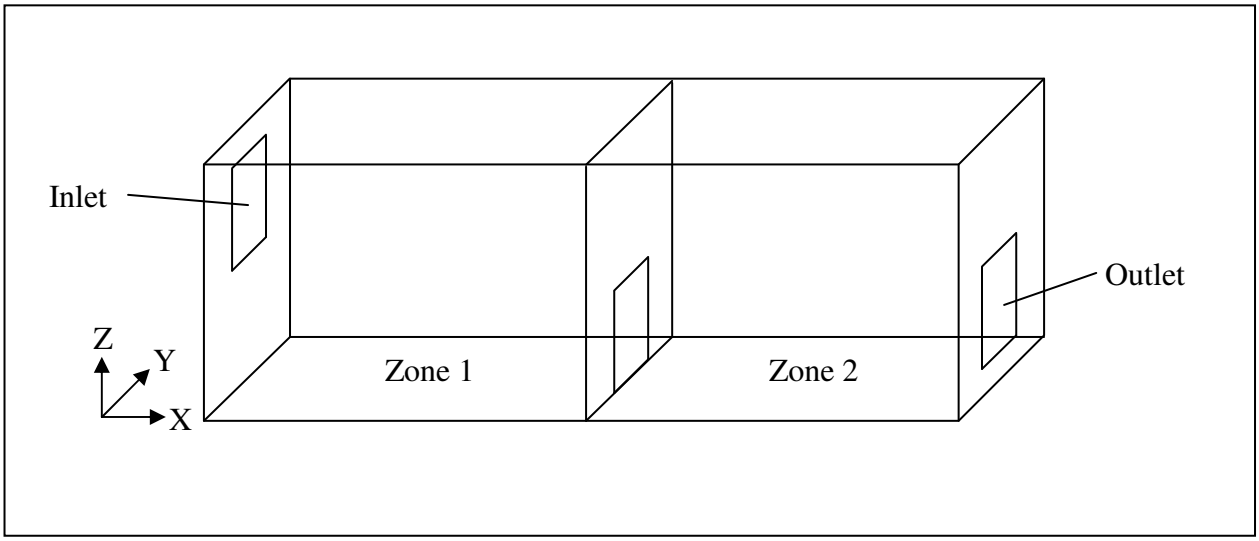

Figure 2-33: Geometry of the two-zone building experiment (after Chang and Hu, 2008)

Six cases with different air exchange rates were conducted. The particle parameters used in the model verification are presented in Table 2-21. The particles, ranging from 1 to 5μm, were injected into Zone 1.

Table 2-21: Particle parameters used in the model verification (after Chang and Hu, 2008)

Case no.	Internal opening size (m x m)	Air change rate (h^{-1})	Reynold number	No. of sample particles	Total initial particle mass (μg)	Particle mass carried by each sample particle (μg)
Case 1	0.70 x 0.20	11.48	1300	2400	152,857	63.69
Case 2	0.70 x 0.20	14.00	1600	2400	104,695	43.62
Case 3	0.70 x 0.30	11.57	1300	2400	119,520	49.80
Case 4	0.70 x 0.30	12.71	1400	2400	94,536	39.39
Case 5	0.70 x 0.95	9.22	1000	2400	117,880	49.12
Case 6	0.70 x 0.95	10.26	1100	2400	147,664	61.53

Figure 2-34 shows the comparison of both simulation results and measured data obtained by other researchers. The particles are dispersed uniformly in Zone 1. Then the particles moved

from Zone 1 to Zone 2. The particle concentration in Zone 2 increased spontaneously at first and then decreased slowly. This scenario occurred in all six case studies. The model has been validated since the simulated results agreed well with the experimental results.

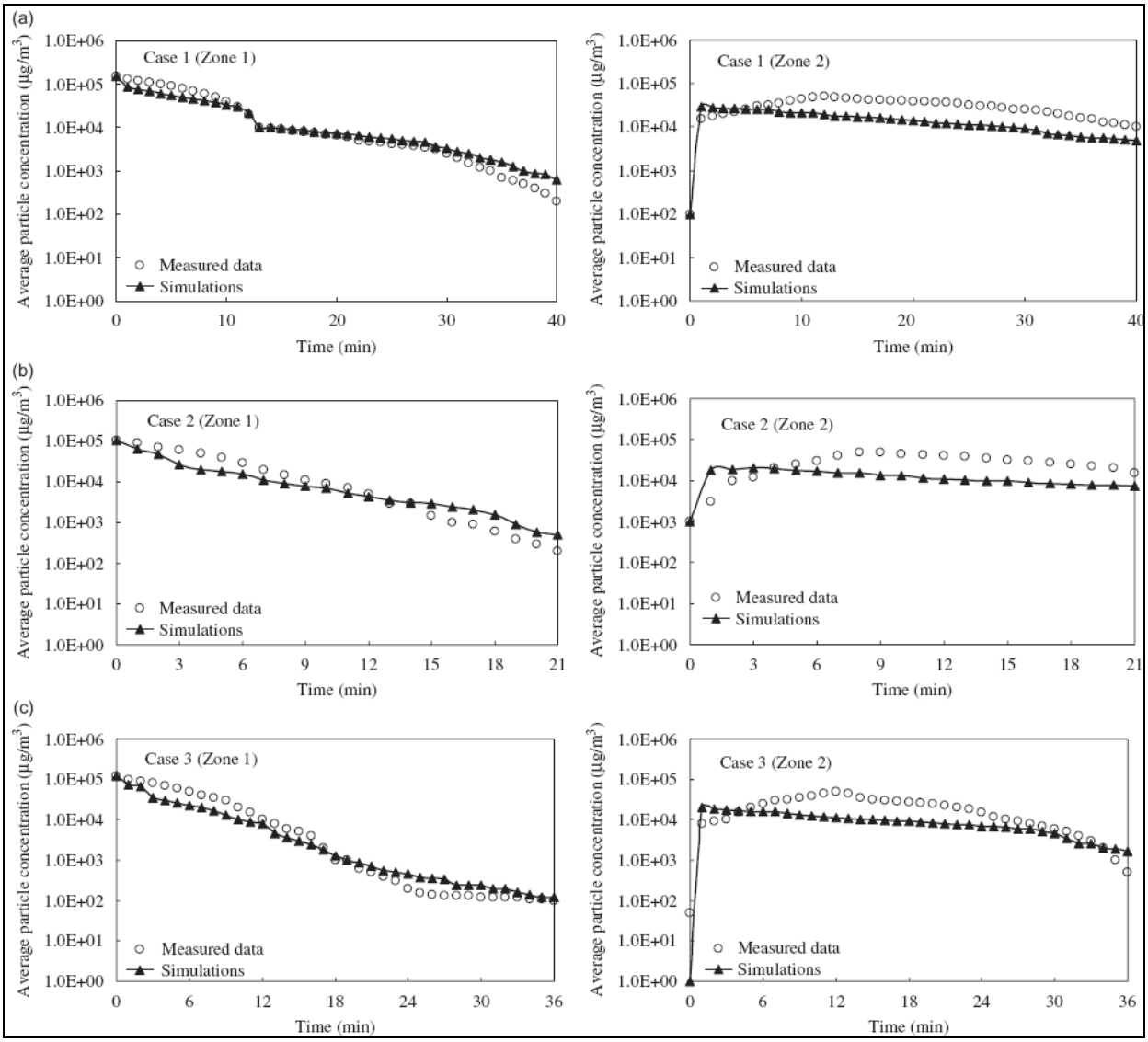

Figure 2-34: Comparison of the simulated particle mass concentrations with the measured data conducted by other researchers (a) ACH = 11.48h^{-1}, (b) ACH = 14.00h^{-1}, and (c) ACH = 11.57h^{-1} [ACH: Air exchange rates] (Chang and Hu, 2008)

Figure 2-34 (continued)

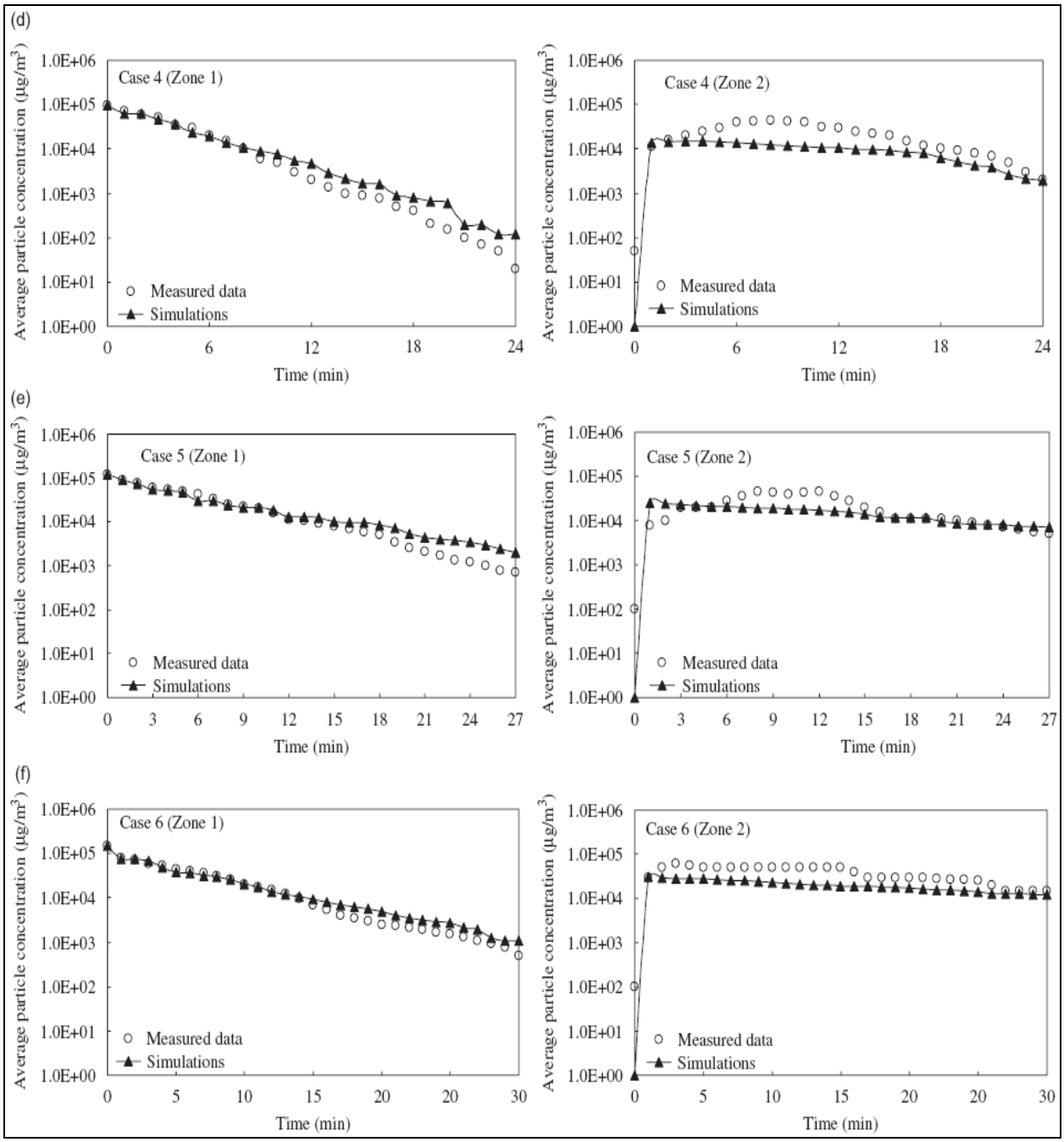

Figure 2-34: Comparison of the simulated particle mass concentrations with the measured data conducted by other researchers (d) ACH = 12.71h^{-1}, (e) ACH = 9.22h^{-1}, and (f) ACH = 10.26h^{-1} [ACH: Air exchange rates] (Chang and Hu, 2008)

The air flowfield within the partitioned environment is depicted in Figure 2-35. Figure 2-35 displays the calculated time-averaged velocity distributions on the X-Z plane at Y = 1.5m and the X-Y plane at Z=0.5m. It can be noted that the air entered Zone 1 through the inlet vent and passed through the opening at the partition to enter Zone 2. From there, the air moved out from Zone 2 through the outlet vent.

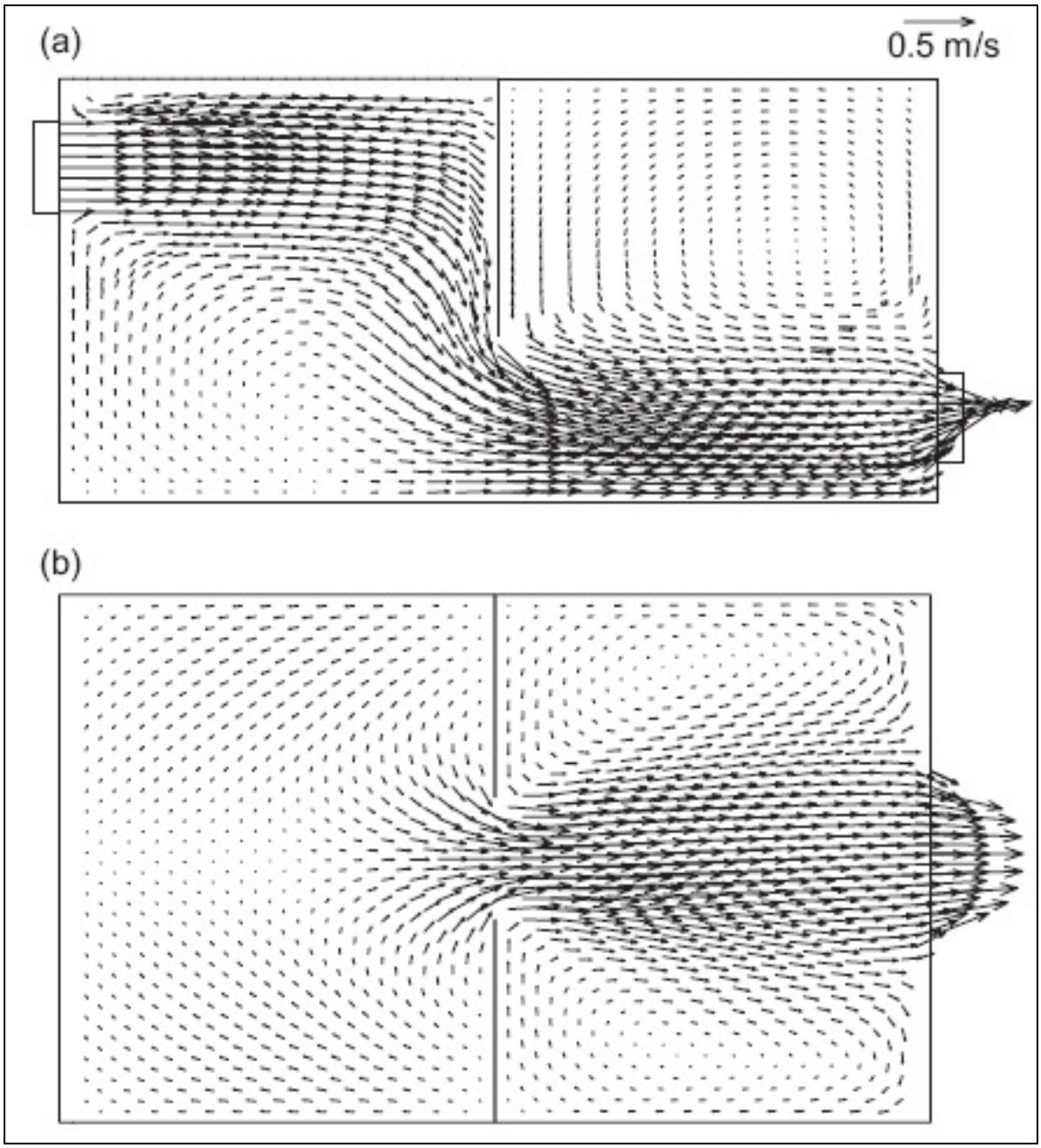

Figure 2-35: The calculated time-averaged velocity distributions on (a) the X-Z plane at Y = 1.5m, and (b) the X-Y plane at Z=0.5m (Chang and Hu, 2008)

Figure 2-36 shows the particle trajectories for various aerodynamic diameters, ranging from 0.05 to 10 μm. 27 particles for each size were injected into the partitioned environment through the inlet vent at Zone 1. From the results, it can be concluded that the airflow patterns within the partitioned environment have a significant impact on the particle transport mechanism, especially for fine particles.

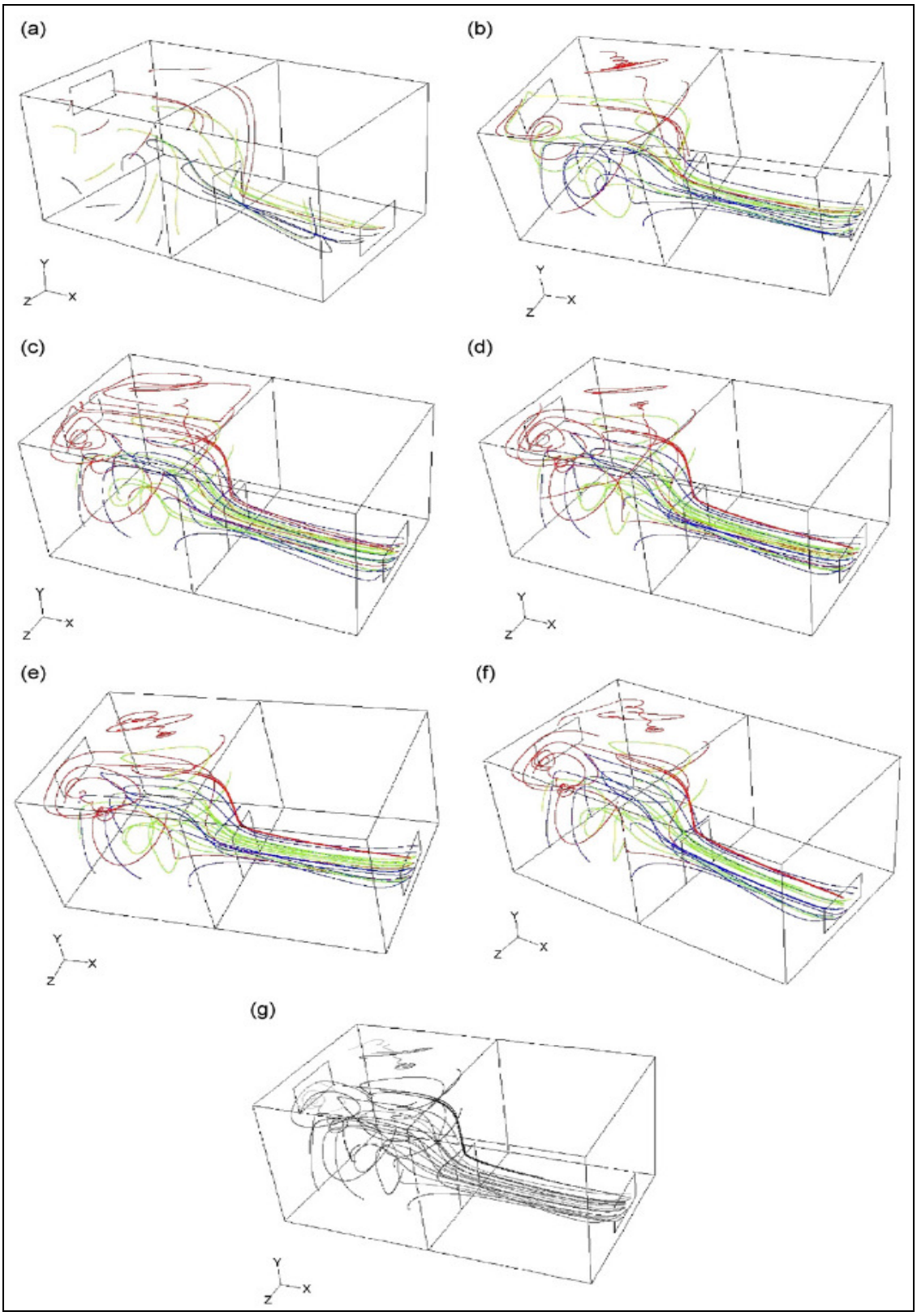

Figure 2-36: Particle trajectories for various aerodynamic diameters, (a) 10, (b) 5, (c) 2.5, (d) 1, (e) 0.5, (f) 0.1, and (g) 0.05μm (Chang and Hu, 2008)

Table 2-22 shows the relative difference of the PM mass concentrations in Zone 1 and Zone 2 between the four scenarios and the dynamic equation scenario aerodynamic diameter at

the 15th minute of the tracking time. It can be seen that the Brownian motion force increases when the particle size become smaller.

Table 2-22: Relative difference of the PM mass concentrations in Zone 1 and Zone 2 between the four scenarios and the dynamic equation scenario aerodynamic diameter at the 15th minute of the tracking time (after Chang and Hu, 2008)

Relative difference (%)	Particle aerodynamic diameter													
	10μm		5 μm		2.5 μm		1 μm		0.5 μm		0.1 μm		0.05 μm	
	Zone 1	Zone 2	Zone 1	Zone 2	Zone 1	Zone 2	Zone 1	Zone 2	Zone 1	Zone 2	Zone 1	Zone 2	Zone 1	Zone 2
Brownian motion force neglected	0.14	0.74	1.31	2.67	1.08	3.14	3.41	4.56	3.91	5.96	4.48	8.20	8.53	15.31
Saffman lift force neglected	2.13	0.14	6.62	17.32	3.82	6.50	3.40	5.02	1.22	4.17	0.70	1.06	0.19	0.24
Drag force neglected	86.36	82.69	34.68	57.42	11.16	22.82	1.65	5.32	2.8	4.91	1.06	1.60	0.14	0.24
Initial force neglected	87.95	84.5	34.14	62.46	62.46	27.29	3.61	8.43	2.84	6.01	0.96	2.03	0.27	0.34

Figure 2-37 presents the average deviations of particle displacement during the tracking period for various aerodynamic diameters, ranging from 0.05 to 10μm. From the figure, it can be concluded that drag force and inertial force have the most substantial impact on particles with a diameter larger than 1 μm. The Brownian motion force has the most influence on particles with a diameter smaller than 0.5 μm and the Sallman lift force is most influential on the particle sizes between 2.5 and 5 μm.

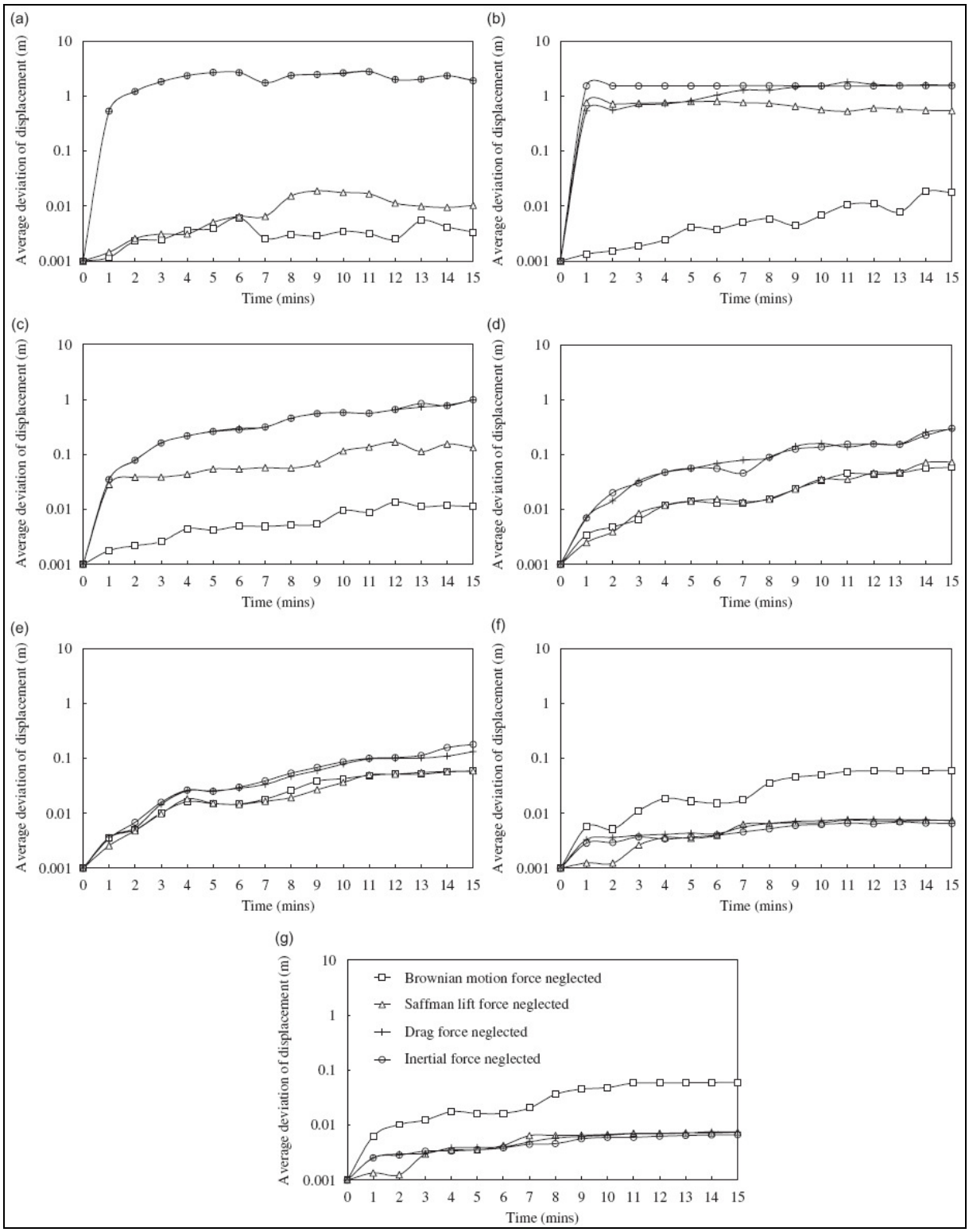

Figure 2-37: The average deviations of particle displacement during the tracking period for various aerodynamic diameters, (a) 10, (b) 5, (c) 2.5, (d) 1, (e) 0.5, (f) 0.1, and (g) 0.05μm (Chang and Hu, 2008)

2.7 IMPACT OF WEATHER ON INDOOR AIR POLLUTION

A large number of investigations have been conducted in the past to look into the effect of weather on air pollution (Lebowitz *et al.*, 1973; Daisey *et al.*, 1982; Hoek *et al.*, 1997; Keatinge and Donaldson, 2001; Noullet *et al.*, 2006; Yi *et al.*, 2010). Park *et al.* (2008) have conducted research on the variation of ultrafine particle concentrations due to seasonal and diurnal variations in Gwangju, Korea. In this study, they measured the particle number concentrations (3–600nm), PM_{10}, NO_x, CO, SO_2, O_3, and meteorological data in all four seasons.

Figure 2-38 shows the diurnal variation of ultrafine particle number concentrations in different seasons. The results indicated that the concentration of ultrafine particle changed with time and seasons due to different sources. The increased ultrafine particle concentration in winter was due to traffic and heating systems, whereas in summer, it was due to photochemical activity.

The correlations between ultrafine particle concentrations and other pollutants were shown in Figure 2-39. The ultrafine particle concentration was consistent with other pollutant concentrations (SO_2 and NO_x). It can be concluded that the three types of ultrafine particles are due to different events, which were traffic event (10-100 nm), residential heating event (50-100 nm) and photochemical event (10-30 nm). The concentration of pollutants was effected by seasonal and diurnal variations.

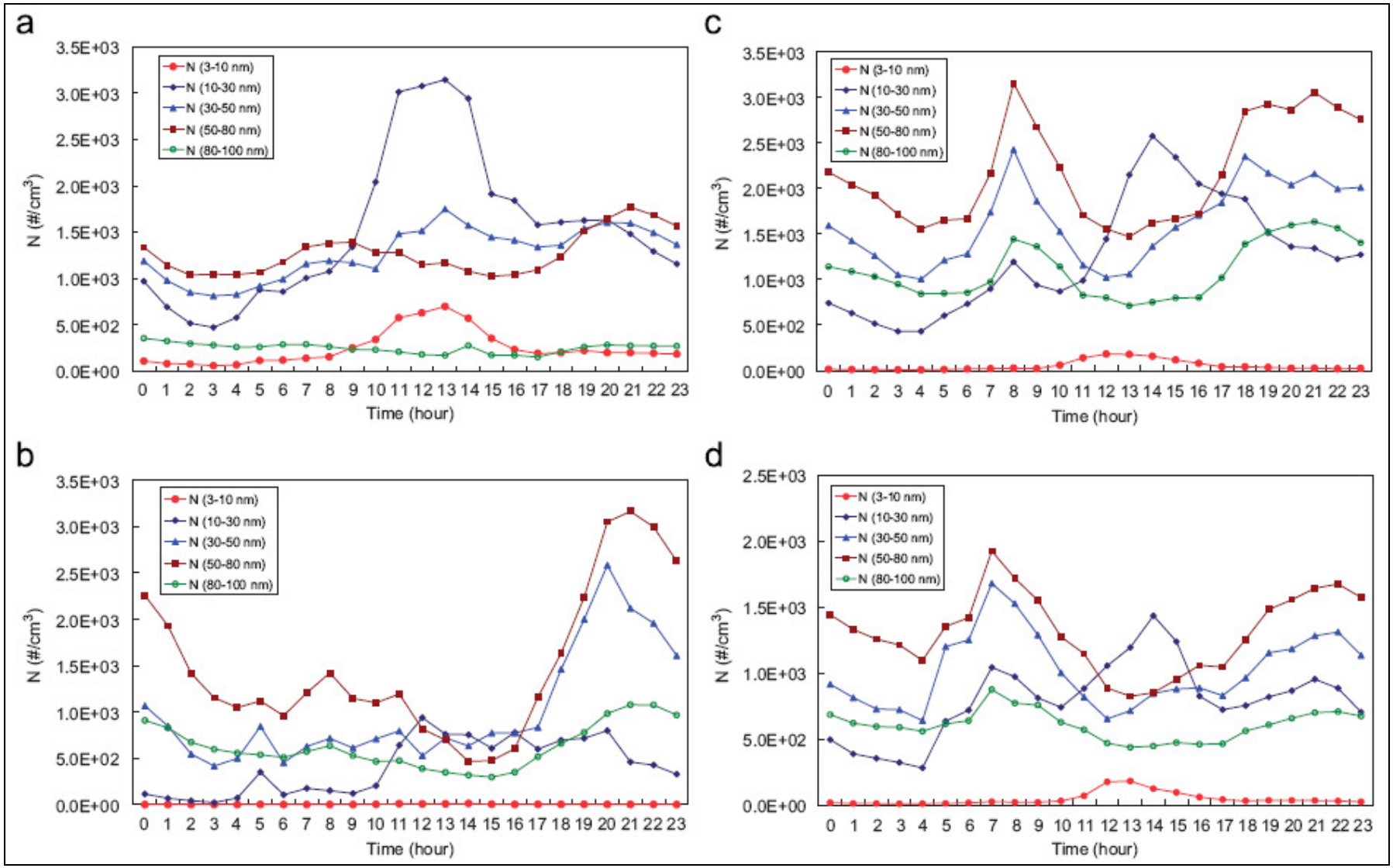

Figure 2-38: Diurnal variation of ultrafine particle number concentrations in different size intervals in different seasons (a) summer, (b) fall, (c) winter, and (d) spring (Park *et al.*, 2008)

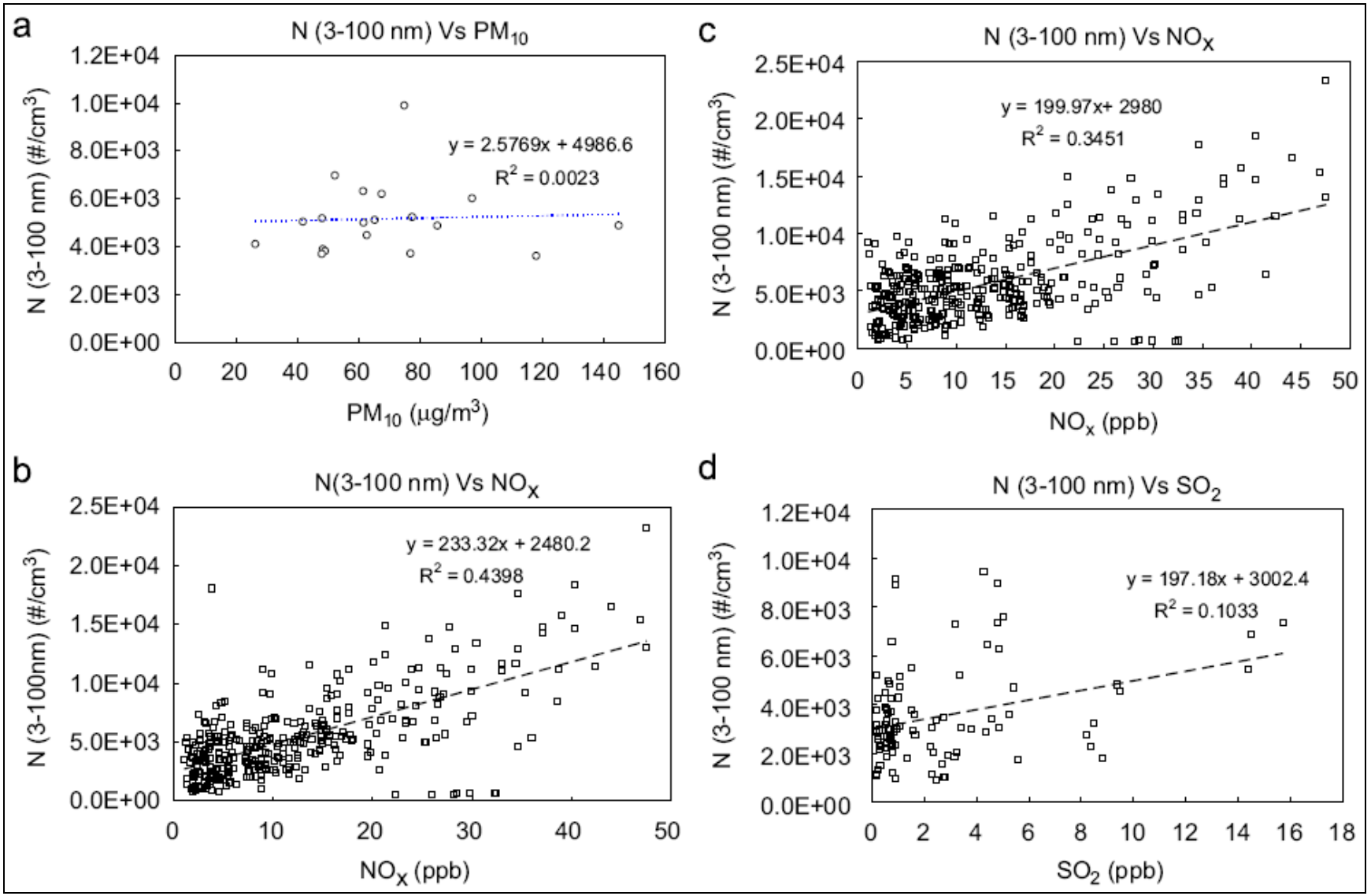

Figure 2-39: Correlations between ultrafine particle concentration and (a) PM_{10}, (b) NO_x (6:00–11:00), (c) NO_x (17:00–23:00), and (d) SO_2 (12:00–17:00) (Park *et al.*, 2008)

Gao *et al.* (2007) also conducted research to measure the aerosol number concentration and size distribution in summer and winter at the urban site of Jinan City, China. Figure 2-40 shows the number size distribution of submicron particles in winter and summer. The results showed that more finer particles were produced in summer. This is due to the strong solar radiation intensity, as well as the high temperatures during summer months. However, there were fewer particles in winter due to the lack of photochemical promotion.

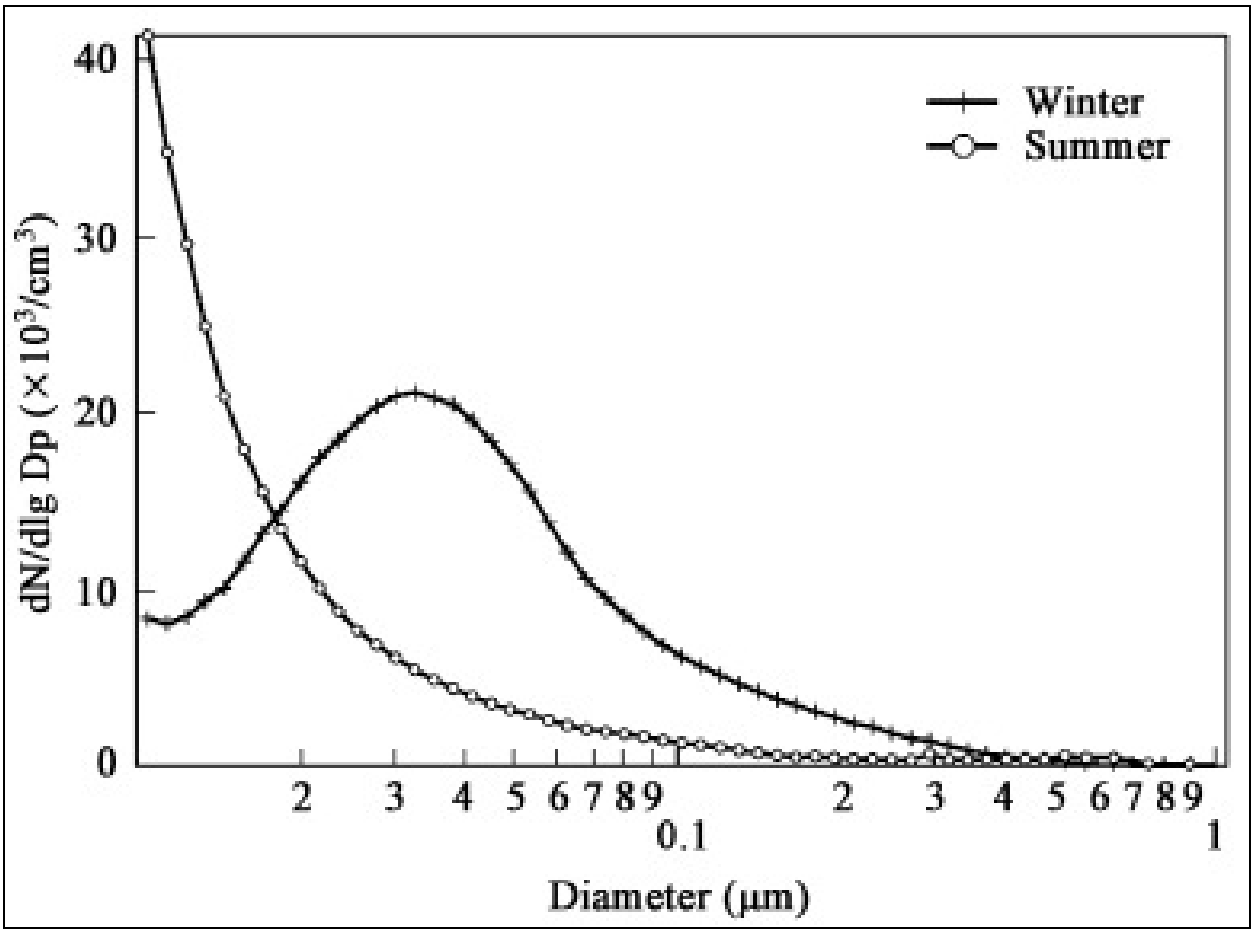

Figure 2-40: Number size distribution of submicron particles in winter and summer (Gao *et al.*, 2007)

Figure 2-41 shows the relationship between the number concentration, the meteorological factors, the trace gases concentration (SO_2, NO_x, CO) and PM_{10} mass concentration due to diurnal variation in summer. The particle concentration peaked at noon due to photochemical events. Figure 2-42 shows the relationship between the number concentration, the meteorological factors, the trace gases concentration (SO_2, NO_x, CO) and PM_{10} mass concentration due to diurnal variation in winter. The cooler weather restricted the formation of new particles due to the lower intensity of solar radiation. A possible source could be diesel engines. This study concluded that the particle number concentration and particle size distribution were strongly correlated with seasonal variation.

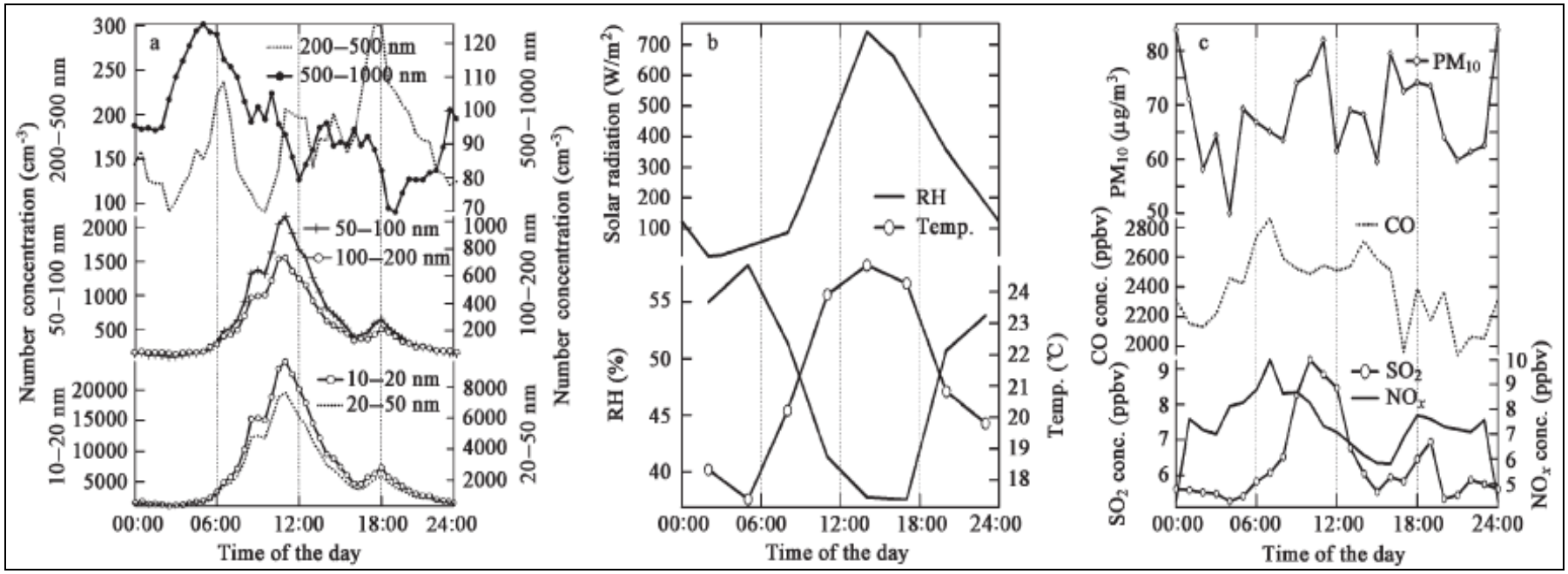

Figure 2-41: Diurnal variation in summer (a) the number concentration, (b) the meteorological factors, and (c) the trace gases concentration (SO_2, NO_x, CO) and PM_{10} mass concentration (Gao *et al.*, 2007)

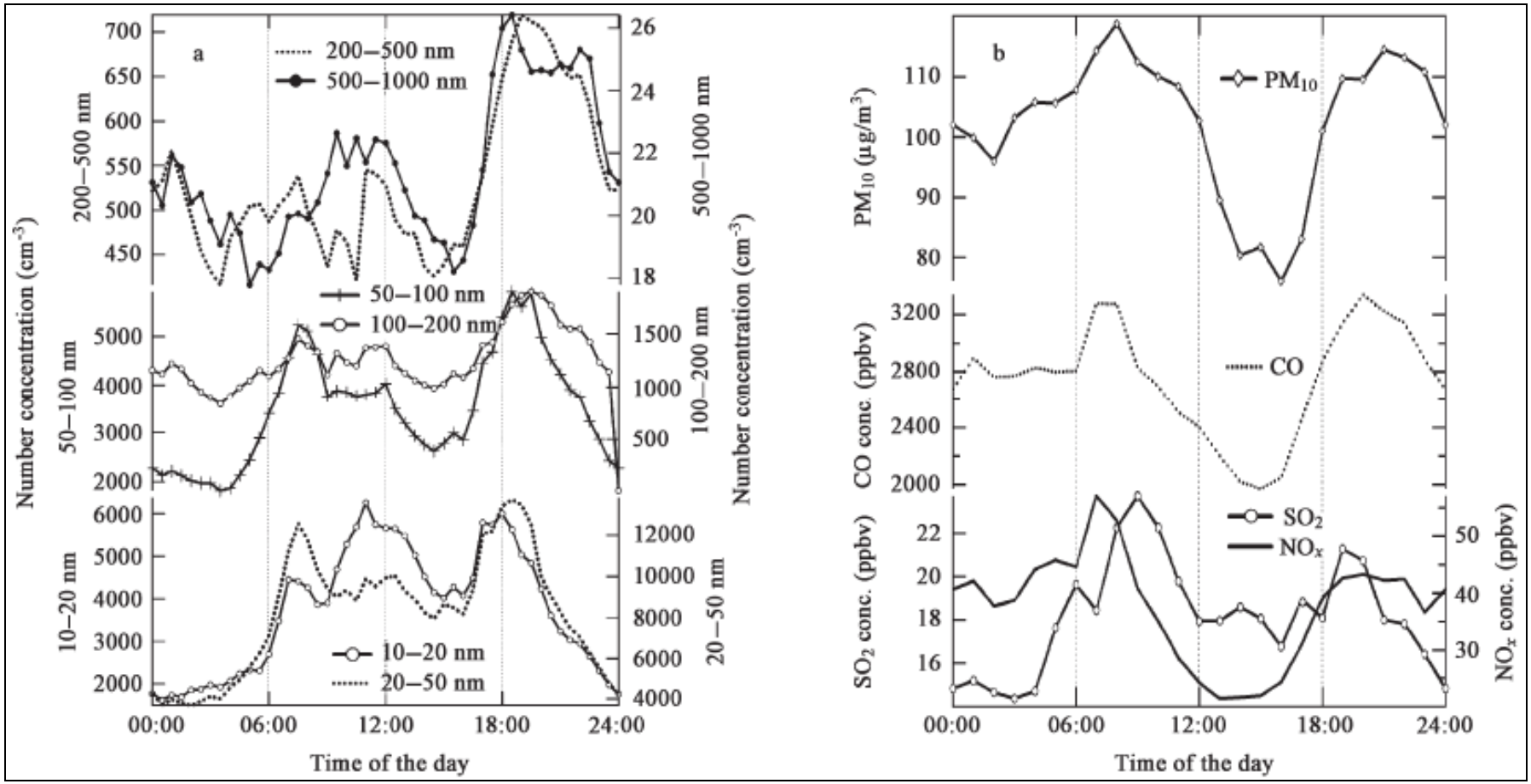

Figure 2-42: Diurnal variation in winter (a) the number concentration, (b) the trace gases concentration (SO_2, NO_x, CO) and PM_{10} mass concentration (Gao *et al.*, 2007)

Shi *et al.* (2007) carried out a research to investigate the particle number concentration and particle size distribution (≈ 5.6–560 nm diameter) in Beijing. Figure 2-43 shows the diurnal variation in number concentration of total particles averaged over the workdays, the non-workdays, and the observation period.

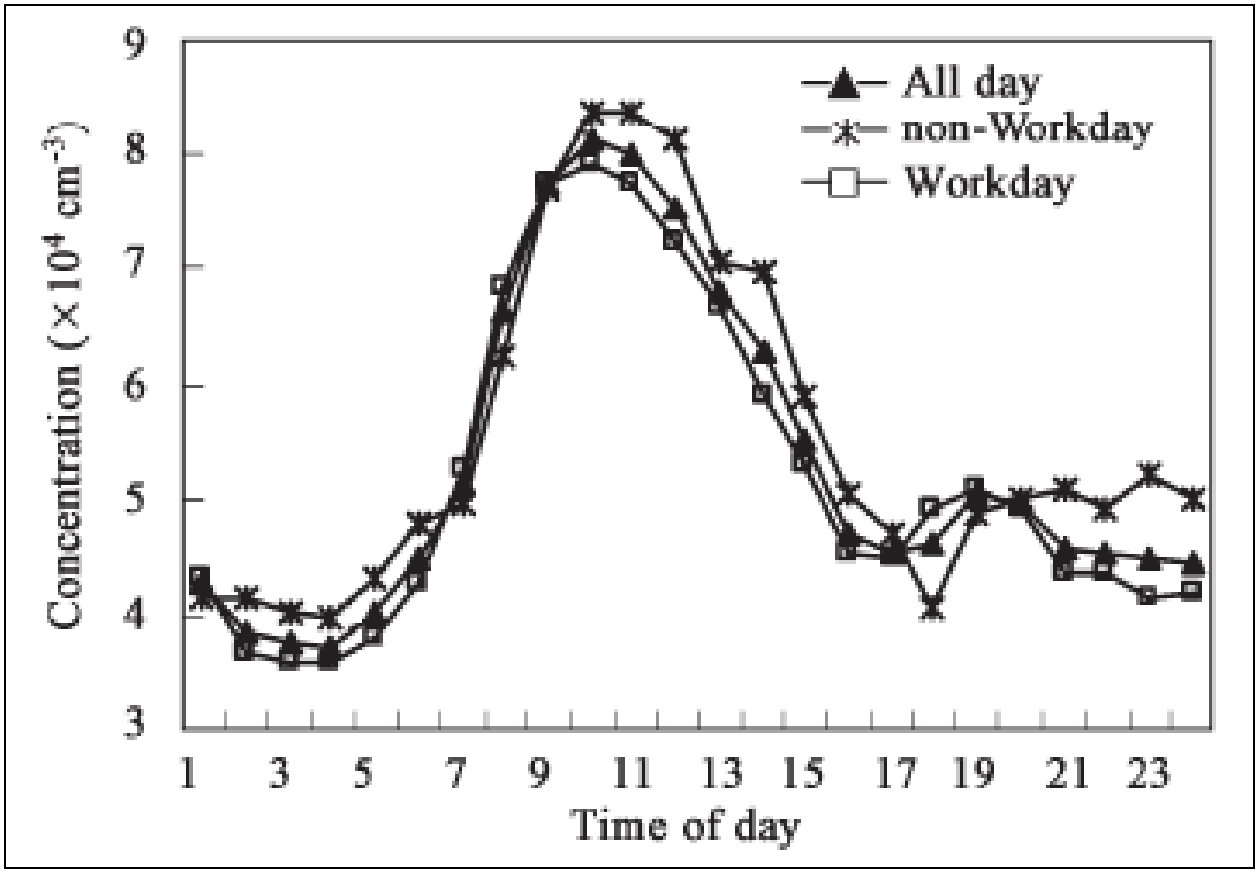

Figure 2-43: Diurnal variation of number concentration of total particles averaged over the workdays, the non-workdays, and the observation period (Shi *et al.*, 2007)

Figure 2-44 presents the diurnal variations of mixing ratios of CO, NO, NO_x, SO_2, and O_3, and the mass level of PM_{10} averaged over the observation period. The elevated NO_x concentration was mainly caused by vehicle emissions. The meteorological conditions were closely related to the emissions of various vehicles. Not only that, the results also showed an inversion can effect the dispersion of air pollutants in the atmosphere.

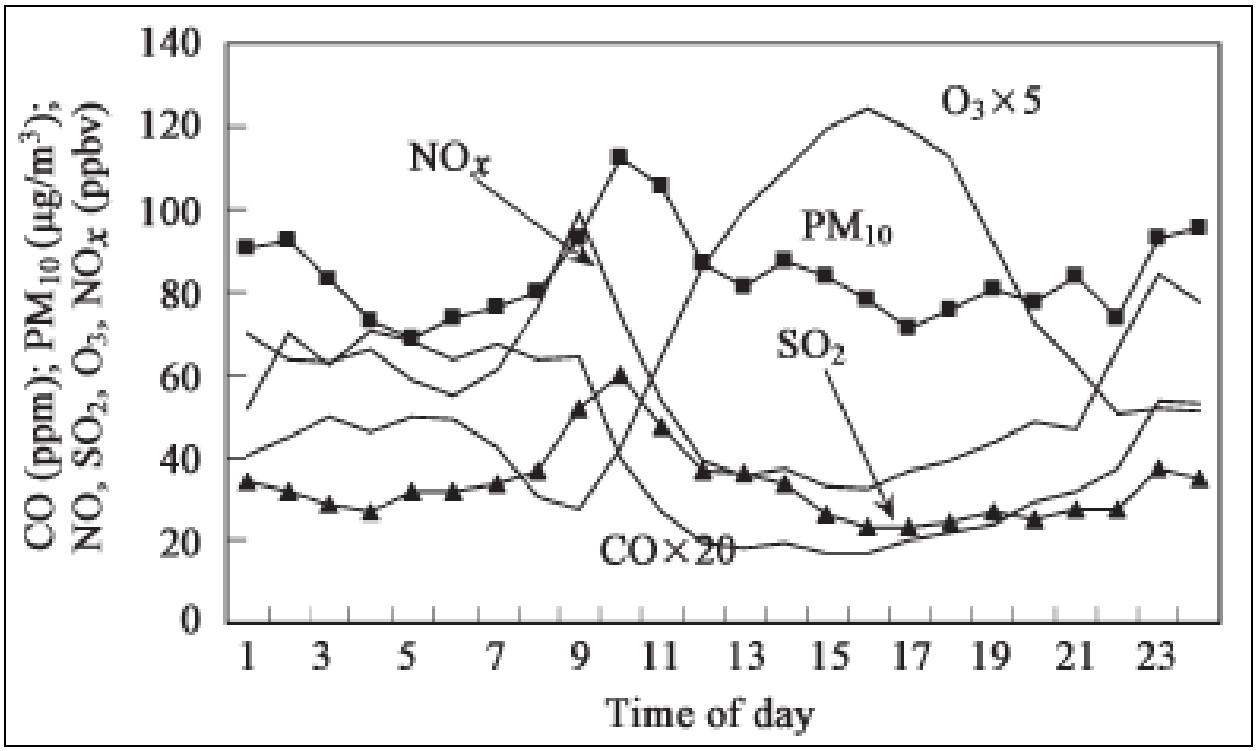

Figure 2-44: Diurnal variations of mixing ratios of CO, NO, NO_x, SO_2, and O_3, and mass level of PM_{10} averaged over the observation period (Shi *et al.*, 2007)

Table 2-23 shows the influence of wind speed and wind direction on the hourly average concentrations of particles in different modes. Wind speed has an impact on the particle concentrations. The results from this study concluded that the particle concentration is strongly affected by the diurnal variation.

Table 2-23: Influence of wind speed and wind direction on hourly average concentrations of particles in different modes (Unit: 10^4 cm^{-3}) (after Shi *et al.*, 2007)

Mode	**Wind speed (m/s)**				**Wind direction* (º)**			
Range	**0–1.0**	**1.0-2.0**	**2.0-3.0**	**>3.0**	**0-90**	**90-180**	**180-270**	**270-360**
Frequency (%)	**38**	**31**	**15**	**16**	**16**	**8**	**15**	**62**
Nucleation (5.6 – 20 nm)	0.97	1.77	2.67	2.24	1.48	0.84	0.76	2.08
Aitken (20 -100 nm)	5.19	3.21	2.66	1.60	3.37	3.88	3.94	2.91
Accumulation (100-560nm)	0.67	0.39	0.24	0.09	0.48	0.74	0.55	0.33
Total particle (5.6 – 560nm)	5.86	5.37	5.57	3.92	5.33	5.46	5.27	5.32

*North is 0º; south is 180º.

2.8 IMPACT OF TRAFFIC ON INDOOR AIR POLLUTION

Some researchers have conducted studies to look into the impact of traffic on air pollution (Giess, 1998; Palmgreen *et al.*, 2003; Milner *et al.*, 2004; O'Connell *et al.*, 2008; Hun *et al.*, 2011; Lawson *et al.*, 2011). Roorda-Knape *et al.* (1998) have investigated the air pollution near major motorways in city districts. This study was conducted in 12 schools, which were located in the west of The Netherlands. They looked into pollutants such as $PM_{2.5}$, PM_{10}, black smoke, benzene and nitrogen dioxide. Figure 2-45(a) showed that the black smoke and NO levels were not affected by the increasing distance from the motorway. The gradient found for these two pollutants was curvilinear, but no gradient was found for particulate matter or benzene (Figure 2-45(b)). These were due to the children's movements in the school.

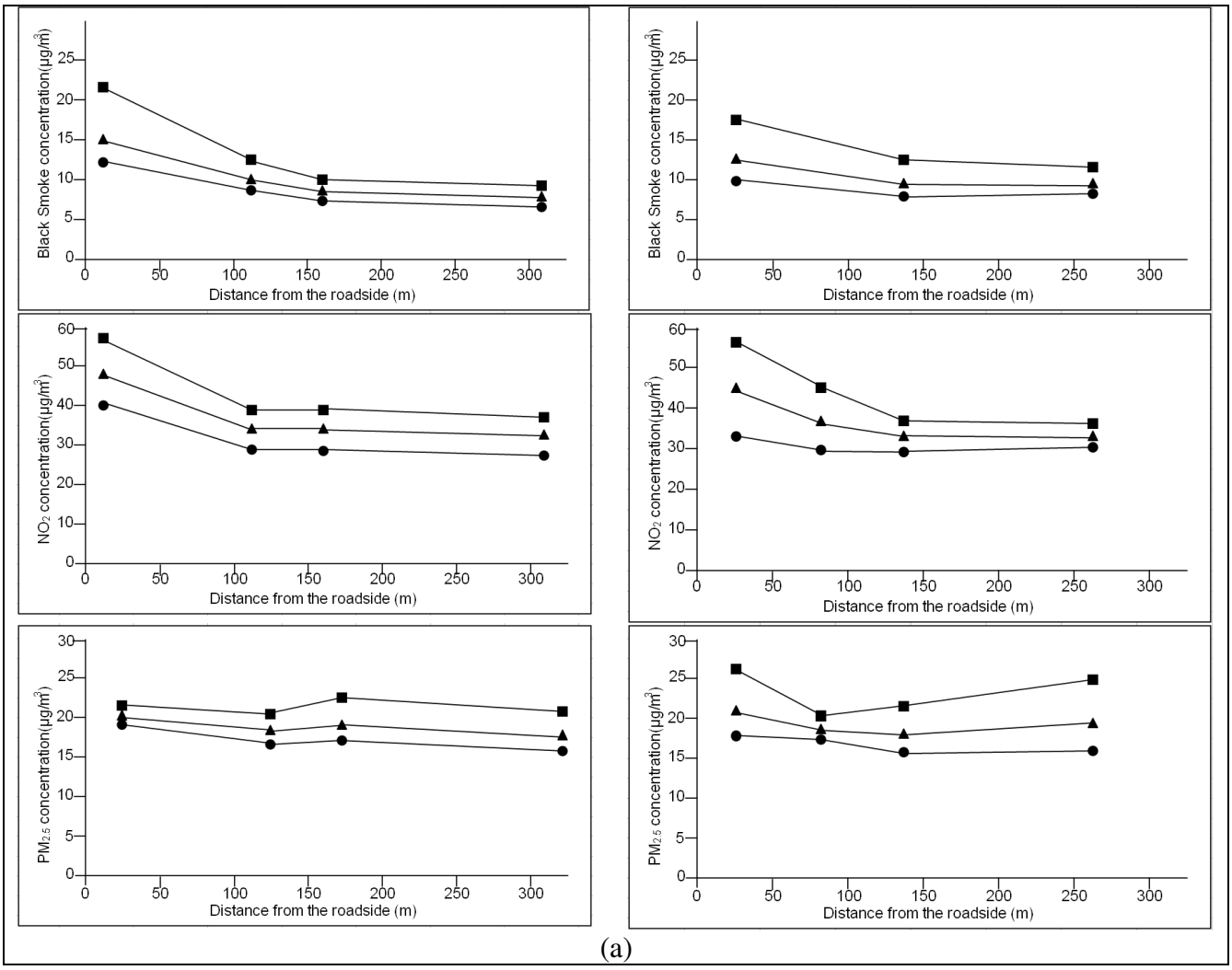

(a)

Figure 2-45(a): Concentrations measured at different distances from the roadside in Delft (left) and Overschie (right) (■ = high exposed periods; ● = low exposed periods; ▲ = all periods) (after Roorda-Knape *et al.*, 1998)

This can be proved by the fact that distance, time downwind and traffic intensity were not correlated with the motorway and indoor levels in buildings. The truck traffic and time period downwind have a significant impact on the black smoke concentrations, as shown in Table 2-24. When the monitored property was downwind of the motorway, the NO_2 concentrations was affected up to 33%. The correlation matrix between air pollution concentrations in schools, traffic intensity, distance from the road side and time downwind of motorway are shown in Table 2-24.

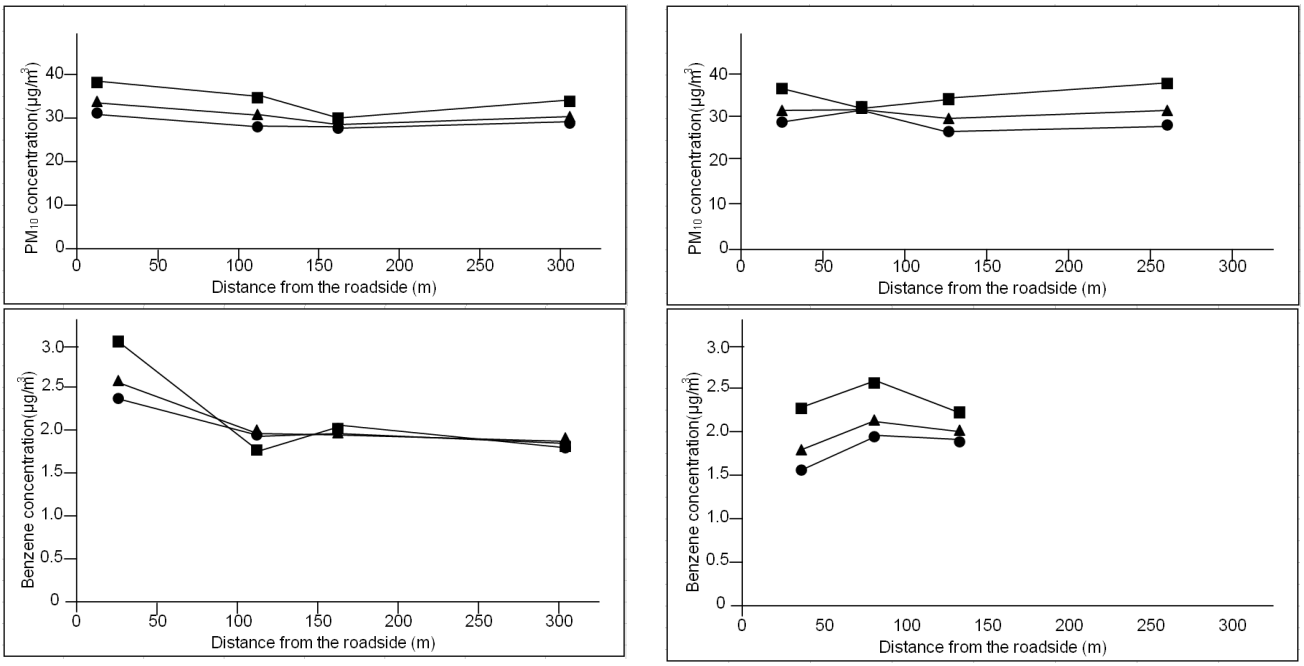

(b)

Figure 2-45(b): Concentrations measured at different distances from the roadside in Delft (left) and Overschie (right) (■ = high exposed periods; ● = low exposed periods; ▲ = all periods) (after Roorda-Knape *et al.*, 1998)

Table 2-24: Correlation matrix between air pollution concentrations in schools, traffic intensity, distance from the road side and % time downwind of motorway (after Roorda-Knape *et al.*, 1998)

Relationships	**Black Smoke**	**NO_2**	**Trucks*** **	**Cars*** **	**Total Traffic**	**ln (distance)**	**% downwind**	
							PM_{10}/BS	**NO_2**
PM_{10}	0.29	0.25	-0.17	-0.04	-0.07	-0.39	-0.05	-
Black Smoke	-	0.74	0.67**	0.15	0.28	-0.46	0.79	-
NO_2	-	-	0.47	0.61**	0.68**	-0.83	-	0.88*
#Trucks* **	-	-	-	-0.00	0.17	-.16	0.77*	0.71*
#Cars* **	-	-	-	-	0.17	-0.59	0.37	0.40
Total Traffic	-	-	-	-	-	-0.61	0.50***	0.52***
ln (distance)	-	-	-	-	-	-	-0.67**	-0.71

Where * = p<0.01, ** = p<0.05, *** = p<0.10, the number of samples taken for PM_{10} and black smoke was 11, while the number of samples for NO_2 was 12.

Kingham *et al.* (2000) conducted an investigation into the spatial variations of traffic-related pollutants concentrations in Huddersfield, England. The objective of the study was to monitor the traffic-related pollutants concentrations in both indoor and outdoor environments and to analyse the relationships between these pollutants. The experiments took place in 27 homes. The first experimental period was conducted in 13 'proximity' homes which were less than 50m from the road and the remaining 14 'background' homes were greater than 50m. The second test period took place in 22 homes, of which 10 'proximity' homes and 12 'background' homes were used.

Table 2-25 shows the measured concentrations in homes in the Huddersfield study. It can be noted that the mean indoor concentrations in the 'proximity' homes are greater than the 'background' homes. The median ratios for the outside measurements exceed one only for the absorbance measures of particles ($PM_{2.5}$ and PM_{10}). The important finding from Table 2-25 was that spatial variations of the traffic-related pollutants occurred at further distances from the road.

Table 2-25: Measured concentrations of pollutants in homes in the Huddersfield study (after Kingham *et al.*, 2000)

Pollutant	No. of Pairs	Proximity Homes		Background homes		Median Ratio
		Mean	StDev	Mean	StDev	
Indoors						
Mass PM_{10} ($\mu g\ m^{-3}$)	13	35.36	27.63	34.91	21.03	0.99
Mass $PM_{2.5}$ ($\mu g\ m^{-3}$)	12	17.81	12.21	19.52	13.58	1.08
Abs PM_{10} ($m^{-1}\ 10^5$)	13	1.25	0.47	1.06	0.44	1.18
Abs $PM_{2.5}$ ($m^{-1}\ 10^5$)	12	1.33	0.69	1.05	0.43	1.1
Benzene ($\mu g\ m^{-3}$)	11	1.975	2.071	1.152	0.795	1.06
B(a)P (ppb)	13	0.00087	0.00141	0.00317	0.00454	1
Sum PAHs (ppb)	13	0.1081	0.1474	0.2219	0.3905	1
$PM_{2.5}$:PM_{10} mass	9	0.718	0.186	0.574	0.251	4.68
Outdoors						
Mass PM_{10} ($\mu g\ m^{-3}$)	8	36.25	25.58	33.7	23.33	0.97
Mass $PM_{2.5}$ ($\mu g\ m^{-3}$)	8	18.91	16.09	23.31	16.34	0.85
Abs PM_{10} ($m^{-1}\ 10^5$)	10	1.67	0.68	1.54	0.8	1.32
Abs $PM_{2.5}$ ($m^{-1}\ 10^5$)	10	1.33	0.42	1.31	0.7	1.43
Benzene ($\mu g\ m^{-3}$)	9	1.031	0.526	1.237	1.137	0.65
B(a)P (ppb)	14	0.00337	0.00517	0.00561	0.0084	1
Sum PAHs (ppb)	14	0.1653	0.2763	0.4389	0.8414	0.98
$PM_{2.5}$:PM_{10} mass	8	0.695	0.215	0.669	0.303	2.88

* Abs: absorbance

Ilgen *et al*. (2001) conducted a research into the impact of traffic on the levels of aromatic hydrocarbons in the atmospheric environment. This study was carried out in both indoor and outdoor environments in Northern Germany. The aromatic hydrocarbons they looked into were

benzene, toluene, ethyl benzene and the three isometric xylenes. This case study involved 115 non-smoking homes. Half of the experiments were conducted in rural homes with virtually no traffic and the other half in urban homes with a high traffic density. They used both environmental and bio-monitoring of the residents.

Figure 2-46 shows the annual variation in benzene, toluene and total xylenes in the outdoor air of both rural and urban areas. The concentrations of benzene and other aromatic hydrocarbons found in urban areas were 10 times higher than the rural areas. The overall measurements of benzene in both urban and rural areas showed a geometric mean of 3.1 $\mu g/m^3$ and 1.8 $\mu g/m^3$ respectively.

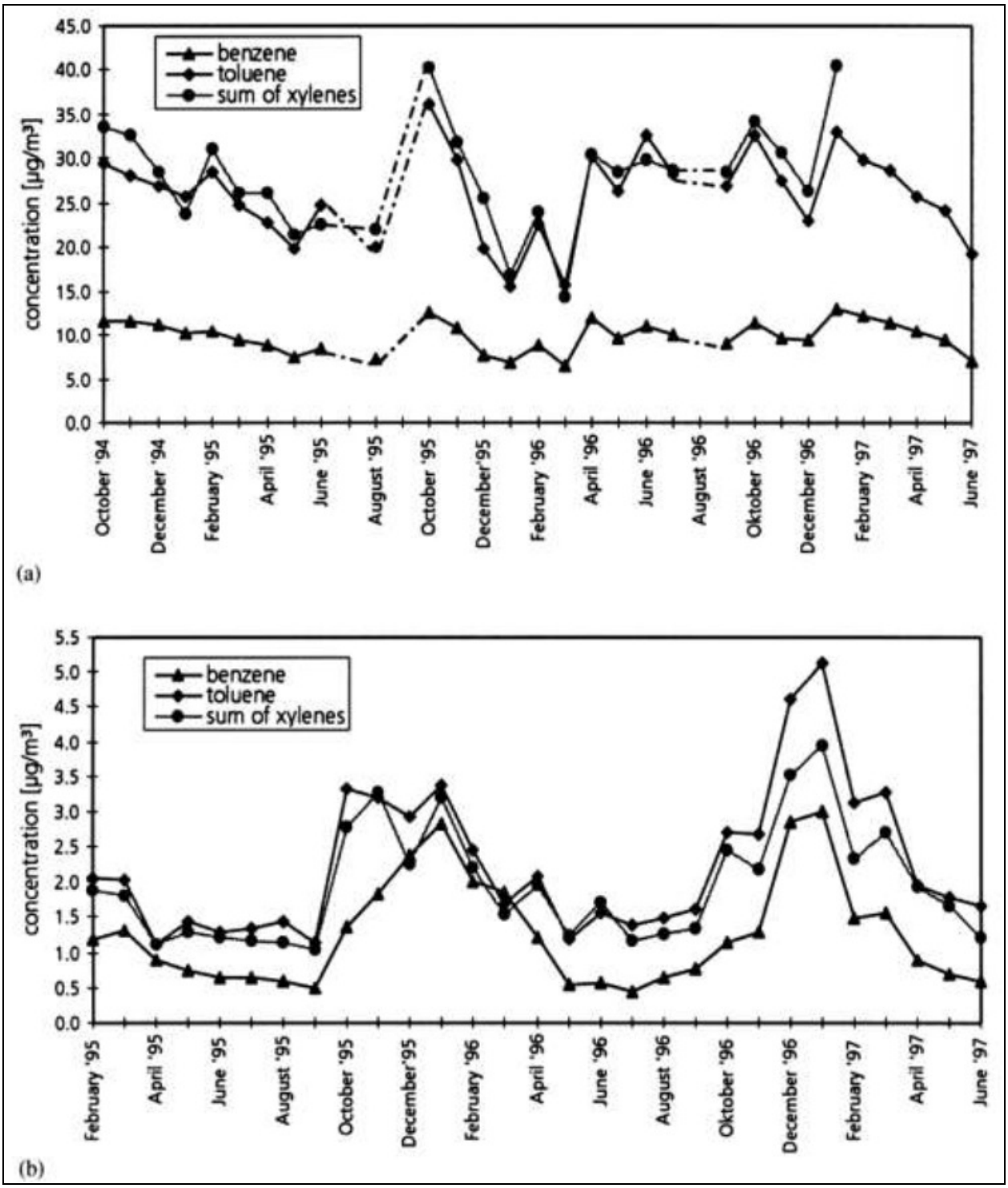

Figure 2-46: Annual variation in benzene, toluene and total xylenes in outdoor air of (a) the Hannover city centre, and (b) in a rural area (Ilgen *et al.*, 2001)

Table 2-26 shows the ratio of the indoor to outdoor concentrations of various aromatic hydrocarbons. The ratio for the city locations was close to 1, which implies the equilibrium between the indoor and outdoor air, except toluene. The ratio for toluene was 3.5, which showed a more significant effect from indoor sources rather than outdoor sources.

Table 2-26: Concentration ratios for indoor and outdoor (I/O) air (after Ilgen *et al*., 2001)

Species	Rural Area I/O Ratio	Urban Area I/O Ratios	
		Rooms Facing Street	Rooms to Backyards
Benzene	1.5	1.1	1.5
Toluene	9.2	3.5	5.3
Ethyl benzene	6.2	1.2	2.1
m/p-Xylene	6.6	1.2	2.0
o-Xylene	6.1	1.1	1.9
Total Xylenes	6.4	1.1	2.1

As presented in Table 2-26, the rooms facing the street have ratios implying the concentrations inside the building are almost equal to those on the street. The equilibrium theory is supported by the high correlation coefficient shown in Table 2-27, with the exception of toluene. The possible sources of the aromatic hydrocarbons at the back of the building is most likely from within the property.

Table 2-27: Correlation coefficients between indoor and outdoor air (after Ilgen *et al*., 2001)

Species	Rural Area I/O Ratio	Urban Area I/O Ratios	
		Rooms Facing Street	Rooms to Backyards
Benzene	0.78	0.62	0.63
Toluene	0.03	-0.23	-0.29
Ethyl benzene	0.26	0.55	0.32
m/p-Xylene	0.22	0.37	0.32
o-Xylene	0.29	0.45	-0.10
Total Xylenes	0.19	0.39	0.33

There may have been some transference from the outside (street side) through the property as the compounds were also present in the back yard side room (Figure 2-47). The ratios for the rural locations were between 6 and 9. This showed a high dependence on the indoor sources, except for benzene. It can be concluded that the outdoor air from low traffic areas still influenced the indoor air. Another finding is the outdoor benzene levels were very susceptible to temperature variations in rural areas and this relationship was not found in the urban areas (Figure 2-48).

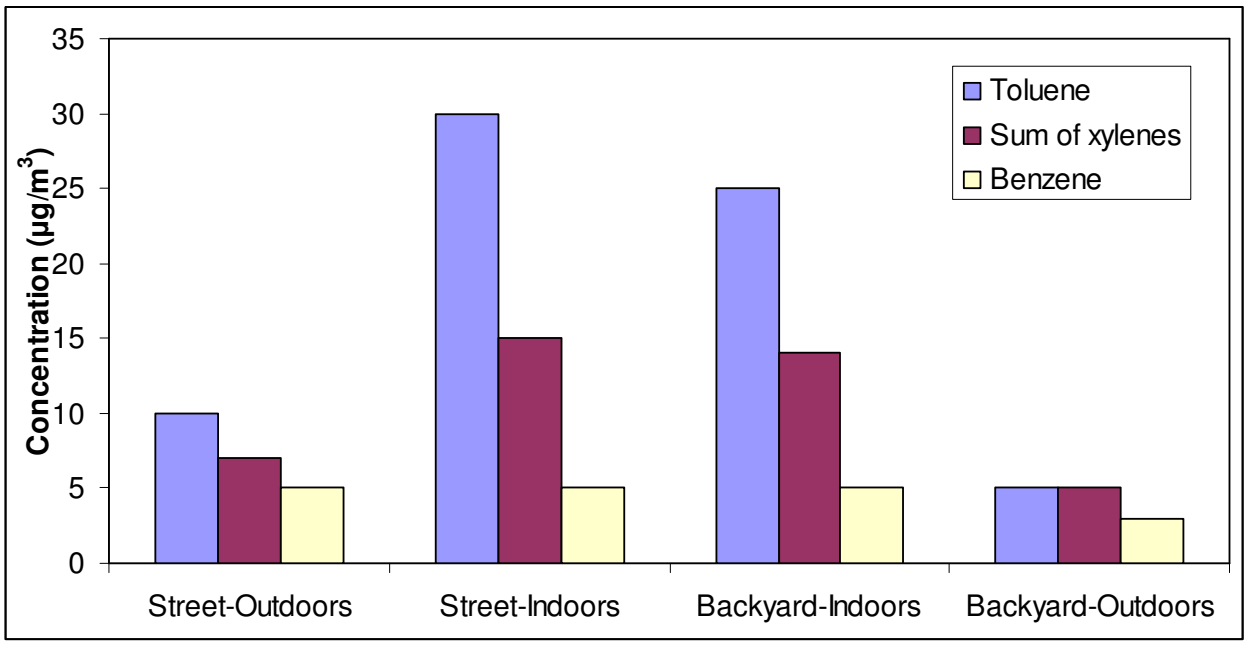

Figure 2-47: The interdependence of pollutant levels at street level, backyard and indoors (after Ilgen *et al*., 2001)

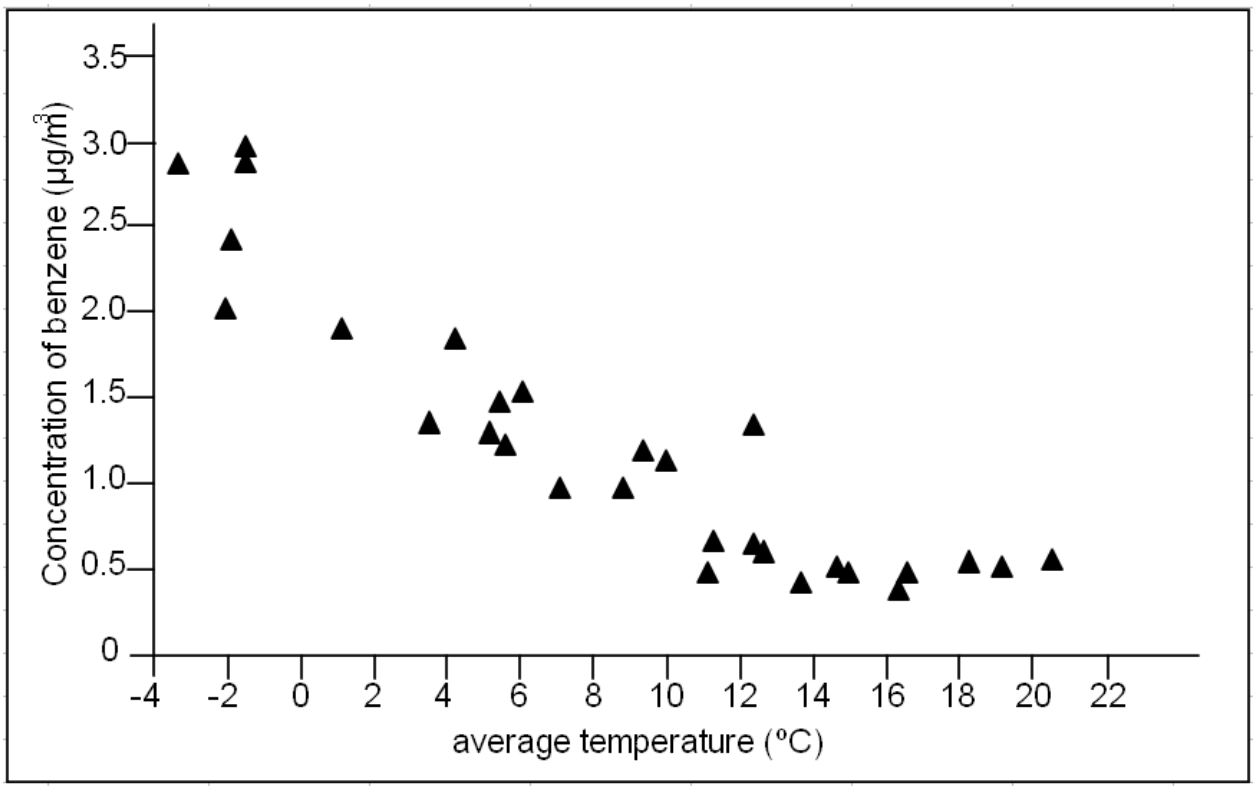

Figure 2-48: Benzene concentration in rural Germany with respect to temperature (after Ilgen *et al*., 2001)

2.9 SUMMARY

This chapter covered the introduction to various indoor air pollutants, health effects, their sources and releases. The indoor air pollutants from various heating systems were also discussed along with the emission rates. The relationship between the indoor and outdoor concentrations was also discussed. Computational fluid dynamics, which is widely used in predicting the particle trajectories, was included in this chapter. Finally this chapter reviewed the impacts of traffic and weather on indoor pollutant concentrations. Most of the previous research work only focused on one pollutant; however in this study, four pollutants were monitored and investigated at the same time for different residential buildings.

3

THEORETICAL BACKGROUND

The main focus of this study is to investigate the particulates emitted from various heating and cooking systems. It is therefore important to understand particle motion in the atmosphere. The theory of particle motion due to gravity and other forces is discussed below. The effects of air exchange rates and indoor emission rates on the indoor pollutant concentrations are presented. Several instruments were used to measure the concentrations of various indoor pollutants in this study: an Andersen Sampler, Scanning Electron Microscopy with Energy Dispersive X-ray Spectrometry (SEM/EDS), Inductively Coupled Plasma Optical Emission Spectrometry (ICP-OES), DustTrak™ II Aerosol Monitor, IAQ-CALC Indoor Air Quality Meter, Diffusion Tubes and Tenax TA Tubes. A detailed description of the principles of these instruments is given below.

3.1 PARTICLE MOTION THEORY

The movement of a particle in the atmosphere is subjected to various forces acting on the particle. The magnitude and direction of these forces are important in deciding the location of the particle in the atmosphere. To enable a particle to move through a fluid, three forces are involved. These forces are: (1) the external force (gravitational or centrifugal force), (2) the buoyant force, and (3) the drag force. A particle is drawn by the gravitational force at a constant rate. The buoyant force acts alongside the external force but in the contrary direction. When there is relative motion between the particle and the fluid, then the drag force will appear (Zhang, 2011).

When a particle is moving through a fluid, this can be expressed by:

$$m\frac{du}{dt} = F_e - F_B - F_D \tag{3-1}$$

where m = mass of a particle;

u = velocity of the particle relative to the fluid;

F_e = the external force;

F_B = the buoyant force; and

F_D = the drag force.

The external force can be expressed as follows:

$$F_e = ma_e \tag{3-2}$$

where a_e = acceleration of the particle.

By adopting the principle of Archimedes, the buoyant force is expressed as:

$$F_b = m\rho\, a_e/\rho_p \tag{3-3}$$

where m/ρ_p = Volume of the particle;

$(m/\rho_p)\rho$ = Mass of fluid displaced; and

ρ = Density of the fluid.

And, the drag force is:

$$F_D = C_D u^2 \rho\, A_p/2 \tag{3-4}$$

where C_D = Drag coefficient;

A_p = The projected area of the particle (perpendicular to the flow direction).

By substituting all forces (Equations 3-2, 3-3 & 3-4) into Equation 3-1, the following can be obtained:

$$\frac{du}{dt} = a_e - \frac{a_e\rho}{\rho_p} - \frac{C_D u^2 A_p \rho}{2m} = a_e\frac{\rho_p - \rho}{\rho_p} - \frac{C_D u^2 A_p \rho}{2m} \tag{3-5}$$

Thus, motion from the gravitational force is:

$$\frac{du}{dt} = g\frac{\rho_p - \rho}{\rho_p} - \frac{C_D u^2 A_p \rho}{2m} \tag{3-6}$$

where $a_e = g$ (in this case).

And, motion in a centrifugal field is:

$a_e = r\omega^2$

$$\frac{du}{dt} = r\omega^2 \frac{\rho_p - \rho}{\rho_p} - \frac{C_D u^2 A_p \rho}{2m} \tag{3-7}$$

where u = velocity of the particle (of which u is relative to the fluid and is directed outwardly along a radius).

Terminal Velocity

In a gravitational settling, terminal velocity is achieved when the downward force of gravity equals the upwards force of drag. The acceleration decreases with time and approaches zero (NASA, 2011).

$$\frac{du}{dt} = g\frac{\rho_p - \rho}{\rho_p} - \frac{C_D u^2 A_p \rho}{2m} = 0 \tag{3-8}$$

$$u_t = \sqrt{\frac{2g(\rho_p - \rho)m}{A_p \rho_p C_D \rho}} \tag{3-9}$$

If du/dt is neglected, then

$$u_t = \omega\sqrt{\frac{2r(\rho_p - \rho)m}{A_p \rho_p C_D \rho}} \tag{3-10}$$

The gas density is always smaller than the density of the particle in the atmosphere. If the shape of the particle is spherical (D_p = diameter), then

$m = \pi D_p^3 \rho_p / 6$

$A_p = \pi D_p^2 / 4$

By substituting m and A_p into Equation 3-10, the gravity settling of spheres is:

$$u_t = \sqrt{\frac{4g(\rho_p - \rho)D_p}{3C_D\rho}} \qquad (3\text{-}11)$$

3.2 THEORETICAL CALCULATIONS

The following section reviews the effects of air exchange rates and indoor emission rates on indoor pollutant concentrations and the relationship between outdoor and indoor concentrations.

3.2.1 Effects of Air Exchange Rates on Indoor Concentrations

Building air exchange rates are associated with wind and thermally induced pressure flows, as well as those associated with mechanical ventilation. Generally, air exchange rates can be measured using the tracer gas decay method, the constant injection or the constant concentration method (International Organization for Standardization, 2000).

The most widely used air exchange measuring technique is the concentration decay method. Initially, a tracer gas is injected into a space or building with the assumption that the tracer gas is well mixed in the building/space air (tracer gas technique). The decrease or decay of the tracer gas concentration is then measured over time:

$$C_t = C_0 \exp\left[-(Q/V)t\right] = C_0 \exp(-n \cdot t) \qquad (3\text{-}12)$$

where: C_t = the tracer gas concentration at the time t, µg/m^3 or ppmv;
C_0 = the tracer gas concentration at time t=0, µg/m^3 or ppmv;
V = the volume of room space, m^3;
Q = ventilation rate, m^3/hr; and
n = air exchange rate, 1/hr or ACH.

From these measurements, the air exchange rate n can be determined from the following equation:

$$n = \frac{\ln C(t_1) - \ln C(t_2)}{t_2 - t_1} \tag{3-13}$$

As mentioned above, tracer gas techniques are frequently used in measuring the air exchange rates in buildings. Tracer gases used in such measurements are characteristically nonreactive, nontoxic and easily measured at low concentrations. Sulphur hexafluoride and perfluorocarbons are commonly used to measure air exchange rates because they can be detected and quantitatively determined in the parts per billion ranges. On occasion, nitrous oxide (N_2O) or carbon dioxide (CO_2) is used.

Carbon dioxide has the advantage of being measured in real time with relatively inexpensive continuous monitors. It has the disadvantage however of being produced by humans. Thus it cannot be used when building spaces are occupied. Sulphur hexafluoride, perfluorocarbons and N_2O are collected using one-time sampling techniques and require analysis on sophisticated, expensive instruments. Perfluorocarbon measurements are usually made using permeation tubes as sources and passive samplers as collectors. As such, air exchange measurements based on perfluorocarbons typically provide seven-day averages.

In this study air exchange rates in the kitchens of the residential house and flats were measured in accordance with ISO 12569 (International Organization for Standardization, 2000). CO_2 was chosen as a tracer gas. The tracer gas decay method was employed to determine the air exchange rates in three kitchens.

A small volume of CO_2 was released, mixed and uniformly distributed in the kitchen, causing an initial concentration of approximately 1500 – 2000ppm. A CO_2 analyser (IAQ Calc 7545) was then used to record the CO_2 concentrations continuously for about 15–20min. In the measurements, the kitchen was assumed as a perfectly stirred reactor. This release-measurement program was repeated twice in each kitchen in order to minimize the effect of temporal and spatial fluctuations.

3.2.2 Effects of Indoor Emission Rates on Indoor Concentrations

Moschandreas *et al* (1987) reported that the pollutant emission rates from indoor sources can be measured using two techniques. One of the techniques is a direct measurement method

and the other technique is a mass balance method. The direct measurement method measures the pollutant emissions through directing the combustion effluents to an air sampling port. The mass balance method samples indoor air from strategically selected sampling sites and pollutant concentrations are measured. It was concluded that the results obtained from both methods were comparable under controlled conditions.

The mass balance method was adopted in this study to demonstrate the emission rates of indoor pollutants from various cooking activities. Mass-balance equations create a relationship between indoor and outdoor pollutant concentrations, air exchange rates, pollutant removal rates and source emission rates. The mass balance differential equation is shown below (Wallace *et al*, 2004):

$$\frac{dC_{in}}{dt} = p \cdot a \cdot C_{out} - (a+k) \cdot C_{in} + S_e / V \tag{3-14}$$

where: C_{in} = indoor mass concentration of pollutants ($\mu g/m^3$);
C_{out} = outdoor mass concentration of pollutants ($\mu g/m^3$);
p = penetration coefficient across building envelope;
a = air exchange rate (hr^{-1});
k = pollutant removal rate (hr^{-1});
V = volume of the room (m^3); and
S_e = emission rate ($\mu g/hr$).

The values p, a, k and S_e are assumed to be constant values in the mass balance differential equation. The outdoor concentration of a pollutant is also assumed as constant. Therefore, the relationship between indoor concentrations at time t_1 and t_2 can be obtained by integrating Equation (3-14), as shown by the following:

$$\int_{t_1}^{t_2} \frac{dC_{in}(t)}{C_{in}(t) - \frac{S}{V(a+k)} - \frac{p \cdot a \cdot C_{out}}{a+k}} = -(a+k) \int_{t_1}^{t_2} dt \tag{3-15}$$

Thus,

$$C_{in}(t_2) = \frac{p \cdot a \cdot C_{out} + S/V}{a+k} + \left(C_{in}(t_1) - \frac{p \cdot a \cdot C_{out} + S/V}{a+k} \right) \times \exp\left(-(a+k)(t_2 - t_1)\right) \tag{3-16}$$

The emission rate can be solved consequently from Equation (3-16),

$$S_e = \frac{\left(C_{in}(t_2) - \frac{p \cdot a \cdot C_{out}}{a+k} + \left(\frac{p \cdot a \cdot C_{out}}{a+k} - C_{in}(t_1) \right) \times \exp\left(-(a+k)(t_2 - t_1)\right) \right) \cdot V \cdot (a+k)}{\left(1 - \exp\left(-(a+k)(t_2 - t_1)\right)\right)} \tag{3-17}$$

In this study, the concentrations of $PM_{2.5}$ and CO were measured. The real-time values were monitored on a continuous basis. The emission rates of $PM_{2.5}$ and CO from indoor cooking activities can be obtained from Equation (3-17).

However, only average NO_2 and VOCs concentrations can be obtained. Hence, Equation (3-17) is not appropriate for calculating emission rates for these. By integrating each term of Equation (3-14) from the beginning of the sampling period:

$$\int_0^t dC_{in}(t) = p \cdot a \cdot \int_0^t C_{out}(t)dt - (a+k)\int_0^t C_{in}(t)dt + \int_0^t \frac{S_e}{V} dt \tag{3-18}$$

The average values of outdoor and indoor concentrations and of the pollutant emission rate can be given as:

$$\overline{C_{out}} = \frac{1}{t}\int_0^t C_{out}(t)dt \quad , \quad \overline{C_{in}} = \frac{1}{t}\int_0^t C_{in}(t)dt \quad , \quad \overline{S_e} = \frac{1}{t}\int_0^t S_e dt$$

Consequently, the average emission rate of an indoor pollutant can be calculated from the average indoor and outdoor concentrations, as follow:

$$\overline{S} = \frac{t}{\Delta t}\overline{S_e} = \frac{t}{\Delta t} \cdot V \cdot \left[(a+k)\overline{C_{in}} - p \cdot a \cdot \overline{C_{out}} + \frac{C_{in}(t) - C_{in}(0)}{t} \right] \tag{3-19}$$

where: t = sampling time; and

Δt = cooking time (corresponding to pollutants emissions).

Based on Equations (3-17) and (3-19), the indoor emission rates of CO, $PM_{2.5}$, NO_2 and VOCs can be calculated using the measured results for indoor pollutant concentrations.

3.3 ANDERSEN 8-STAGE AMBIENT SAMPLER INSTRUMENT

The multi-stage and multi-orifice cascade Andersen 1 ft^3/min (28.3 l/min) Ambient Particle Sizing Sampler has two main functions (Thermo Electron Corp., 2003). The first measures the size distribution of particles and the second determines the total concentration levels of particulate matter in the environment.

By calibrating the sampler with spherical particles with a unit density of 1g/cm^3, all particles collected are sized aerodynamically. They were similar to the reference particles, without taking their physical size, shape or density into consideration. These aerodynamic dimensions can contribute to determining the following:

(i) Particle behaviour in the atmosphere,
(ii) Particle deposition in the respiratory system,
(iii) Use of suitable equipment to collect the particle; and
(iv) Ensuring the particle concentration is within the exposure limit.

3.3.1 Description of Sample Instrument

The Andersen ambient sampler is shown in Figure 3-1. The sampler consists of eight stages, labelled from Stage 0 to Stage 7. A pre-separator is used to prevent particles greater than 10μm from entering the subsequent stages. This could help in minimizing particle bouncing and re-entrainment errors. There is an impactor chamber in the pre-separator with a 0.53 inch diameter inlet. To prevent overloading by particles and ensure a very low turbulence, three outlet tubes are designed 1 inch above the impaction surface. Three spring clamps are used to hold the eight aluminium stages together and each stage is gasketed with O-ring seals. Multiple orifices are drilled precisely within each impactor stage. In order to increase the orifice velocity, the size of the orifices in each stage is reduced from stage to stage (Figure 3-2). There are three supports for each stage to hold the stainless steel collection plates. When air is drawn through the sampler, the particles will be impacted onto the collection plate, then proceed to the succeeding stages.

The particles which are not retained in the eight stages are trapped on the final collection plate, which consists of a glass-fibre filter paper (Thermo Electron Corp., 2003).

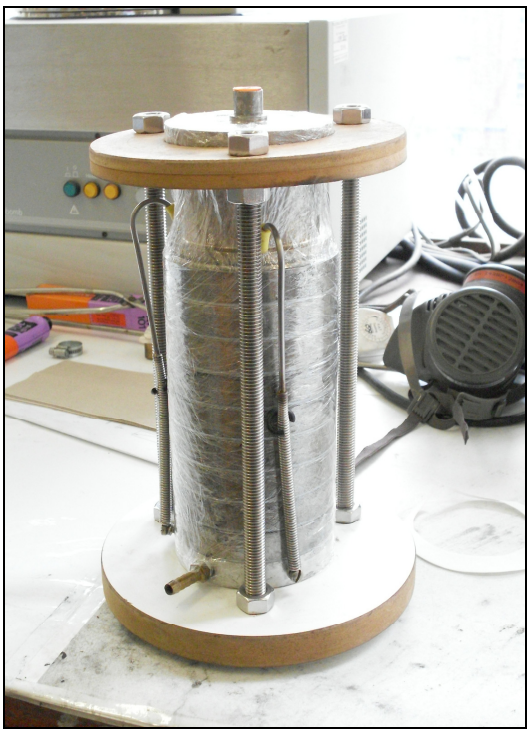

Figure 3-1: Andersen 8-Stage Ambient Sampler Instrument

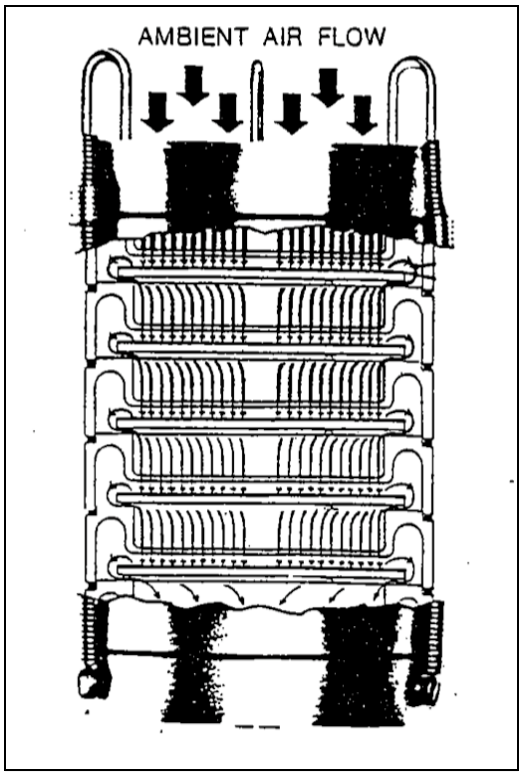

Figure 3-2: Schematic cross-section of the non-viable impactor stages with progressively smaller orifices (Thermo Electron Corp., 2003)

3.3.2 MARK II

The sampler used in this project was the Mark II version. The integral air inlet sections for Stages 0 and 1 consist of 96 orifices, which are arranged in a radial pattern for the Mark II version. The integral air inlet sections for Stages 2 to 6 contain 400 orifices and Stage 7 contains 201 orifices. The orifices from Stage 2 to 7 are arranged in a circular pattern. Table 3-1 shows the jet dimensions for the Mark II Andersen Ambient eight-stage Sampler. The orifices decrease in size from top to bottom. The diameters of the orifices range from 0.1004 inches to 0.0100 inches. There is a removable stainless steel collection plate (3.25 inches in diameter) for each stage. The unimpacted particles are directed to the next stage due to the existence of an exhaust section and it is approximately 0.75 inches larger in diameter than the collection plate.

Table 3-1: Jet dimensions for the Mark II Andersen Ambient 8-Stage Sampler (Thermo Electron Corp., 2003)

Stage	Orifice Diameter (inches)	Number of Orifices
0	0.1004	96
1	0.0743	96
2	0.0360	400
3	0.0280	400
4	0.0210	400
5	0.0135	400
6	0.0100	400
7	0.0100	201
F	0.1100	Filter Holder

3.3.3 Aerodynamic Particle Sizing

The main concept of the Andersen Non-Viable Ambient Particle Sizing Sampler is designed based on the fact that particle deposition in the human lung occurs as proposed by Andersen (1958). The respiratory tract is substituted by the sampling device, which acts as a dust collector. The sampling data can be used to predict the penetration ability of airborne particles into the human lung. The sampler classifies the particles based on the aerodynamic dimensions as the fraction of particles inhaled and retained in the human respiratory system. The physical properties of the particle and its behaviour determine the sites of deposition in the human lungs. The simulation of the human respiratory system by the Andersen Sampler was shown in Figure 1-1 (Thermo Electron Corp., 2003).

3.4 SCANNING ELECTRON MICROSCOPY WITH ENERGY DISPERSION X-RAY SPECTROMETRY (SEM/EDS)

To characterise the morphology of particulate matter effectively, suitable equipment is required. Srivastava and Jain (2007) used scanning electron microscopy (SEM) in an indoor environment study in Delhi, India, to characterise the suspended particles. SEM is a powerful instrument to characterize heterogeneous organic and inorganic materials. Berube *et al* (2004) also used SEM in a study to investigate the spatial and temporal variations in PM_{10} concentrations at six homes in Wales and Cornwall. In this section, an overview of the analytical techniques available to test for morphology (shape and size) is introduced.

Scanning Electron Microscopy (SEM) can be used to observe and characterize the bulk specimen from the nanometer (nm) to micrometer (μm) scale. The principle of SEM is shown in Figure 3-3. SEM is capable of displaying three-dimensional-like images for a wide range of solid materials. Electrons are accelerated through a voltage difference between an anode and cathode, ranging from 0.1 keV to 50 keV (Reimer, 1998).

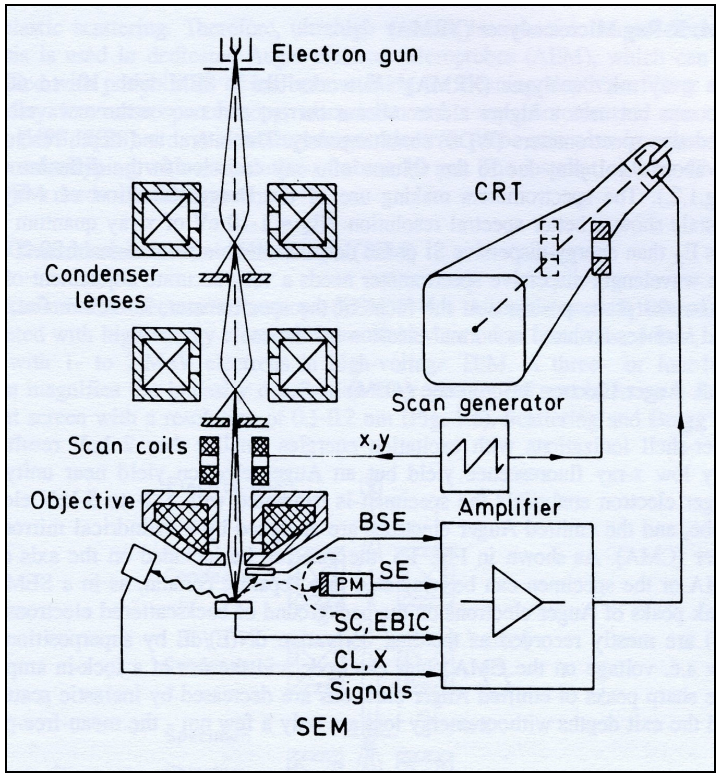

Figure 3-3: Schematic cross-section of a scanning electron microscope (SEM) (Reimer, 1993)

Figure 3-4 shows the JEOL JSM6400 Scanning Electron Microscope with Energy Dispersion X-ray Spectrometry (SEM/EDS) instrument used in this study. The instrument has a

wide magnification from 10x to 10,000x. The main advantage of SEM is that a large variety of electron-specimen interactions can be used to form images and to provide qualitative and quantitative information besides the backscattered and secondary electrons (Reimer, 1998).

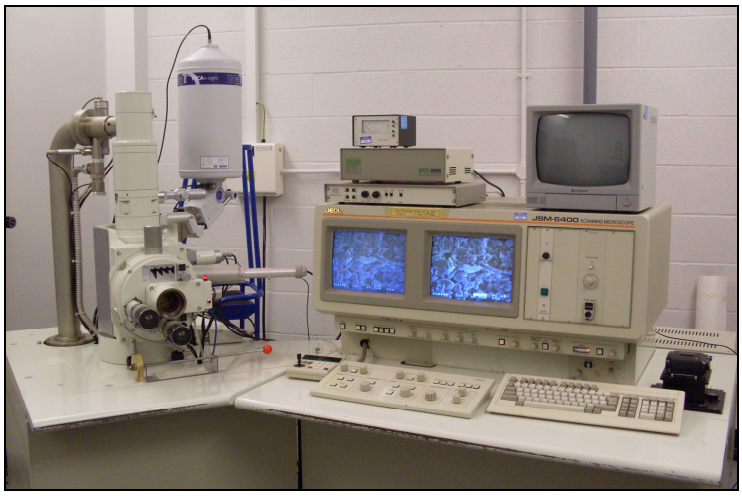

Figure 3-4: Scanning Electron Microscopy with Energy Dispersion X-ray Spectrometry (SEM/EDS) (Model: JEOL JSM6400)

SEM consists of two major components: an electron column and a control console (Figure 3-5). The electron column is comprised of two or more electron lenses and an electron gun. The base of the column is usually operated under vacuum conditions (10^{-4} Pa). The control console is made up of two cathode ray tube (CRT) viewing screens, knobs and computer keyboard that control the electron beam (Goldstein *et al*., 2003).

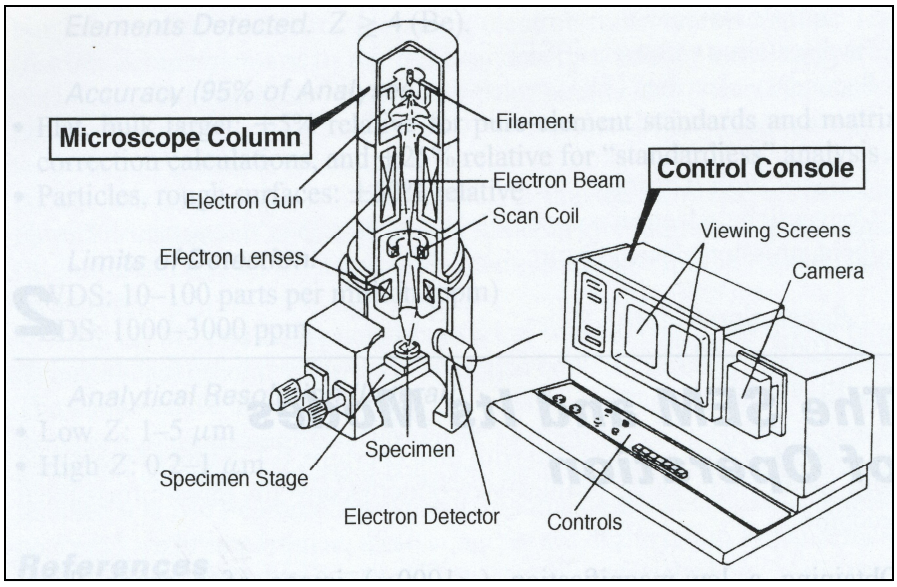

Figure 3-5: The two major parts of the SEM (i.e. microscope column and control console) (Goldstein *et al*., 2003)

3.4.1 Functions of the SEM Subsystems

The main functions of the SEM subsystems will be described in the following sub-sections.

(i) Electron gun and lenses

The main function of this system is to produce a small electron beam. The electron generated by the electron gun is accelerated to an energy level ranging from 0.1 to 30 keV. The tungsten filament gun produces a large spot size on the specimen. Electron lenses are used to place a smaller focus on the specimen and to demagnify the unclear image, as shown in Figure 3-6. In order to produce a higher quality image, the electron beam should have a spot size less than 10nm and contain sufficient probe current on the specimen (Goldstein *et al*., 2003).

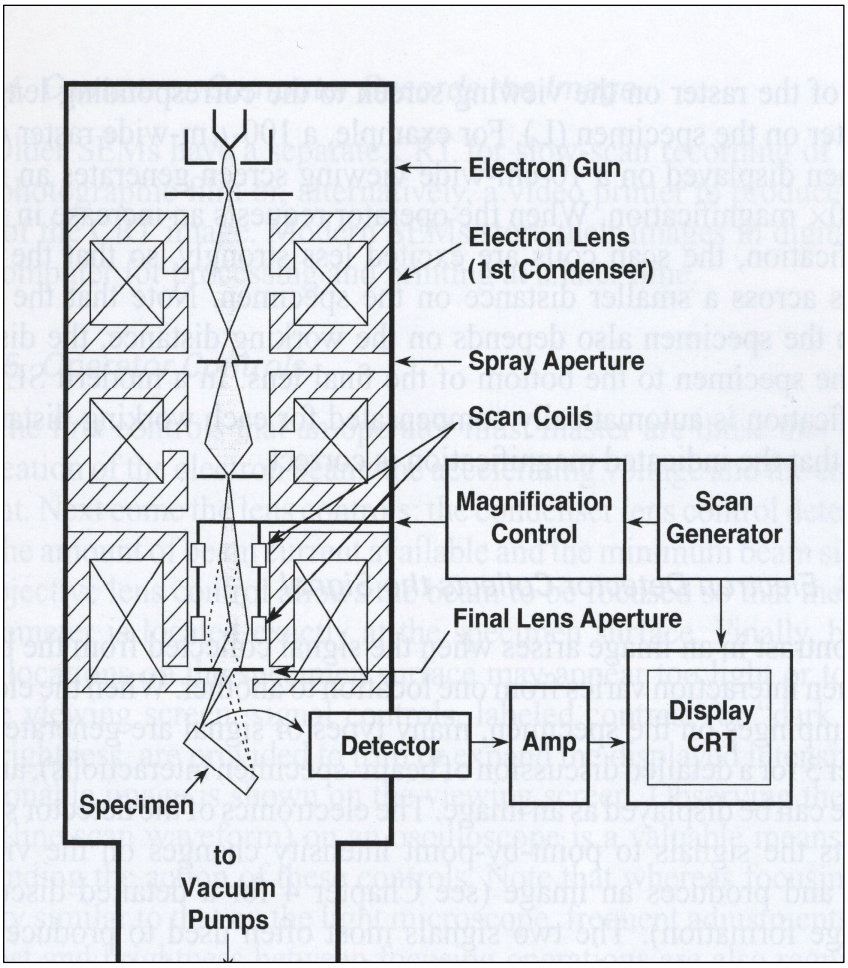

Figure 3-6: Schematic drawing of the electron column (Goldstein *et al*., 2003)

(ii) Deflection system

The main function of the deflection system is to control magnification. The scanned image is formed point by point. The deflection system accelerates the beam to form a rectangular raster on the specimen. At the same time, a similar raster is created on the viewing screen. Two pairs of electromagnetic deflection coils are used to sweep the beam across the specimen. The beam is deflected off the optical axis of the microscope by these two pairs of coils. Then they bend the beam back to the axis of the scan (Figure 3-7). Working distance (W) is the distance between the specimen and the bottom of the final lens pole-piece. It also plays an important role in magnification (Goldstein *et al*., 2003).

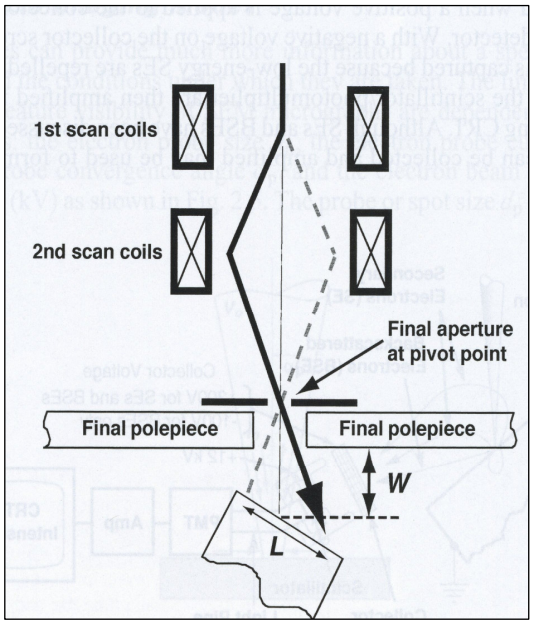

Figure 3-7: Deflect systems inside the final lens (Goldstein *et al*., 2003)

(iii) Electron detector

The main function of the electron detector is to collect the signal. Various types of signals are generated when the electron beam spots on the specimen. Any of these signals can be displayed as an image. The signals formed will be converted by the detector system to produce an image on the viewing screen. Secondary electrons (SE) and backscattered electrons (BSE) are the most common signals used to produce SEM images (Goldstein *et al*., 2003).

3.4.2 Secondary Electrons

Incident electrons interacting with weakly bound conduction-band electrons in the atom of the specimen will produce SE. This interaction to form the SE is mainly based on kinetic

energy. These electrons usually have an energy of less than 50eV. The SE created will set into motion and propagate through the solid. Some of them will intersect the surface and escape. SE are usually emitted from the atoms occupying the top surface. It usually produces a higher quality readable image of the surface as it consists of a smaller diameter of the primary electron beam (Goldstein *et al*., 2003).

3.4.3 Backscattered Electrons

Backscattered electrons (BSE) are defined as the beam electrons which escape from the surface of the specimen when their trajectories are intercepted with a specimen. This only happens when the deviation from the incident beam path has accumulated to a certain degree when the electrons intersect through numerous elastic scattering events. A large-angle elastic scattering (>90º) event will lead to the formation of BSE from time to time. The total energy of the primary beam will be reduced significantly by BSE. Additional secondary radiation products will be produced in the absence of the backscattering effect (Goldstein *et al*., 2003). Figure 3-8 shows the schematic illustration of the origin of the two sources of secondary electron generation in the sample.

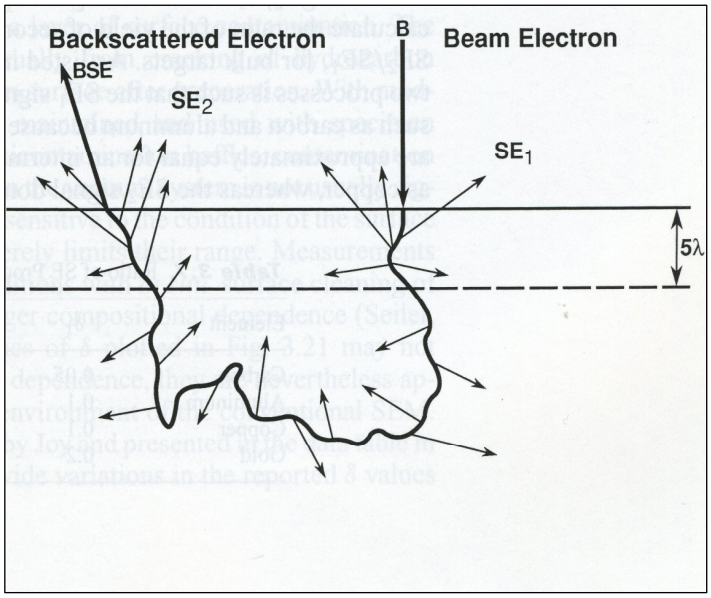

Figure 3-8: Schematic illustration of the origin of two sources of secondary electron generation in the sample (Goldstein *et al.*, 2003)

3.5 INDUCTIVELY COUPLED PLASMA OPTICAL EMISSION SPECTROMETRY (ICP-OES)

A spectrometer is an instrument that is used to measure the spectral intensities with the use of photoelectric detectors, but not photographic plates. It was further developed in the USA in 1940 (Slickers, 1993). Inductively Coupled Plasma-based (ICP) techniques have been widely used as this technique is ideal for high sensitivity analysis. Optical Emission Spectrometry (OES) is time-consuming in most ICP-based analysis as samples are required to be dissolved.

An Inductively Coupled Plasma Optical Emission Spectrometer (ICP-OES) is shown in Figure 3-9. It is a technique used to determine multiple element concentrations in solution. It is a 'wet' sampling method, as the samples are analysed in various aqueous matrices. The instrument uses an ICP source to dissociate the sample to form its constituent atoms or ions. The ICP source can generate temperatures up to 8000ºC. At this temperature, the atoms or ions in the solution become excited to a level which emits light at characteristic wavelengths. The spectrometer converges the light which passes through a diffraction grating. Then the light is resolved into a spectrum according to its constituent wavelengths. The diffracted light is then collected according to its wavelength inside the spectrometer. An intensity measurement is yielded at this stage. The intensity measurement is then converted to an elemental concentration by comparing it with the calibration standards. This equipment is typically suitable for determinations of the lighter elements in the periodic table, such as Li, Be, Si, P, S and others (Green, 2009; Mennim, 2009; Evans Analytical Group, 2009).

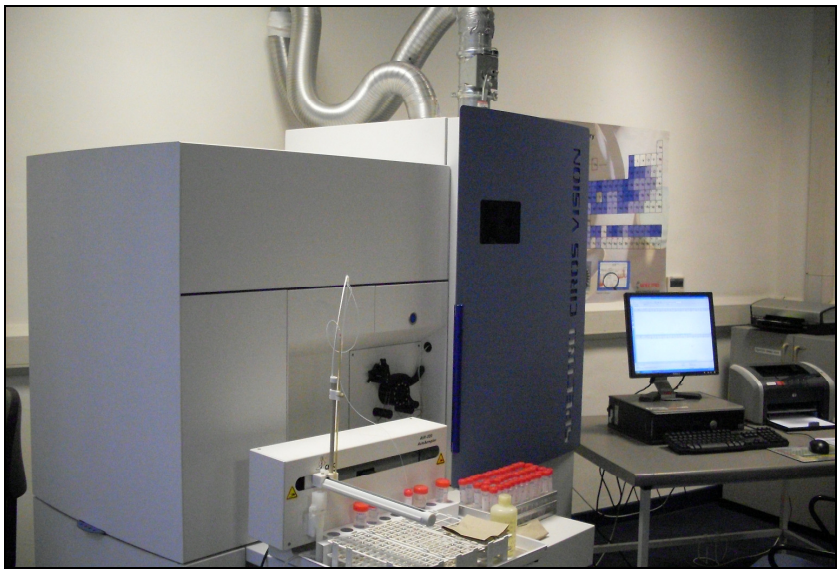

Figure 3-9: Inductively Coupled Plasma Optical Emission Spectrometer (ICP-OES)

3.6 DUSTTRAK™ II AEROSOL MONITOR

The TSI DustTrak™ II Aerosol Monitor is a real-time direct-reading analyser that uses light scattering technology. This aerosol monitor is ideal for measuring aerosol contaminants (e.g. fumes, smoke, dust, mists etc). It can provide real-time mass readings of aerosols by its light scattering laser photometers. The aerosol is kept isolated in the optics chamber with the help of the sheath air system. Therefore, this equipment is not only suitable to be used in clean indoor environments but also in heavy industry workplaces and construction sites. Figure 3-10 shows the internal components of the DustTrak™ II Aerosol Monitor.

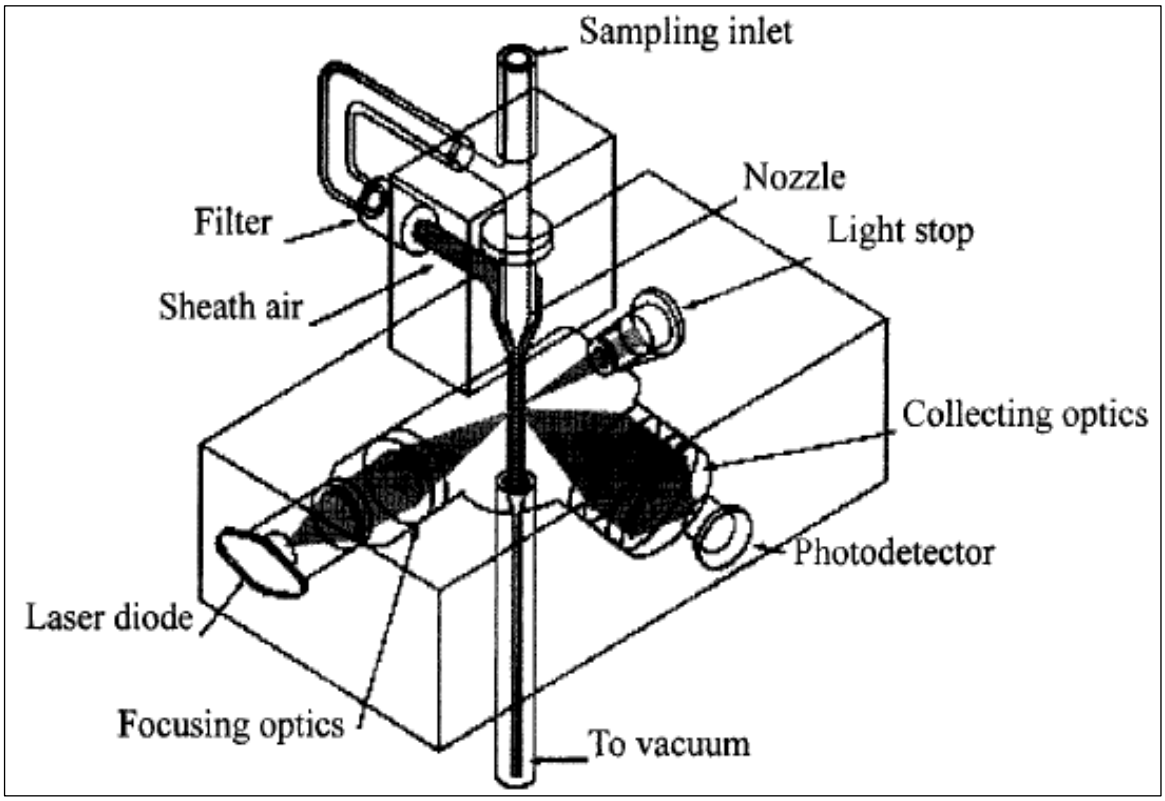

Figure 3-10: Internal components of a DustTrak™ II Aerosol Monitor (Niu *et al*., 2002)

The DustTrak™ II Aerosol Monitor is lightweight and portable. With the capability to collect single point data, it is perfect for indoor air quality measurements and for baseline trending and screening. The main feature of the equipment is that it can perform in-line gravimetric analysis for custom reference calibrations, where a 37mm filter cassette is used together with the aerosol stream (TSI, 2008). The DustTrak™ II Aerosol Monitor was designed with a set of impactors, with the size of 1μm, 2.5μm, 4μm and 10μm. This helps in performing size-selective sampling. The impactors are designed to be easily attached to the inlet of the

equipment. All of the impactors are operated at 3.0 L/min. Figure 3-11 shows the DustTrak™ II Aerosol Monitor used in a kitchen to measure particle concentrations.

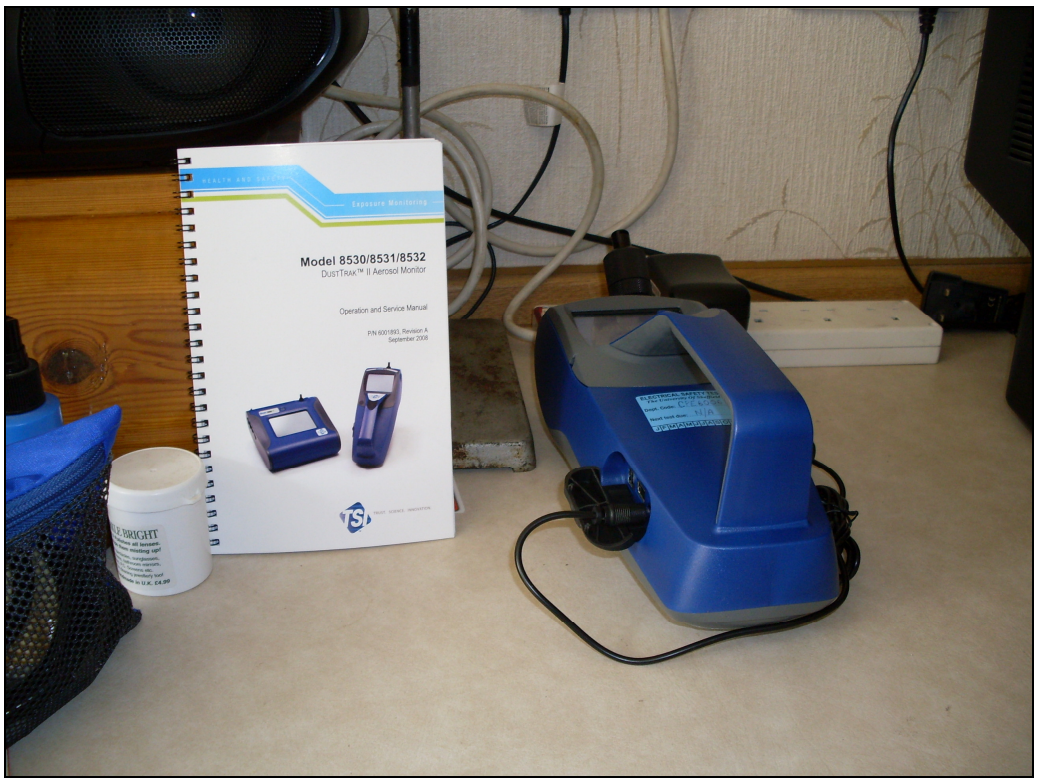

Figure 3-11: DustTrak™ II Aerosol Monitor

The DustTrak™ II Aerosol Monitor is a photometric instrument used to determine real-time aerosol concentrations. The aerosol is drawn into the sensing chamber by using a diaphragm pump in a continuous stream. The aerosol stream is divided into two parts. One part is the aerosol stream split before the sensing chamber, which passes through a High-Efficiency Particulate Air (HEPA) filter. This flow is then injected back into the chamber as sheath flow. The other part is the aerosol stream, which enters the sensing chamber by passing through the inlet of the equipment. The laser diode will then form a sheet of laser light and illuminate the aerosol stream. The laser light will penetrate both the collimating lens and the cylindrical lens. A thin sheet of light will be created. After that, a significant amount of light which is scattered by the particles will be captured by a gold coated spherical mirror. Then it will be focused onto a photo detector. The current detected is proportional to the aerosol concentration over total concentrations. A calibration constant is used to multiply with the voltage. This calibration constant is obtained from the ratio of a known mass concentration of the Arizona Test Dust to the current response of the equipment (TSI, 2008). Figure 3-12 shows the schematic cross-section of a DustTrak™ II Aerosol Monitor.

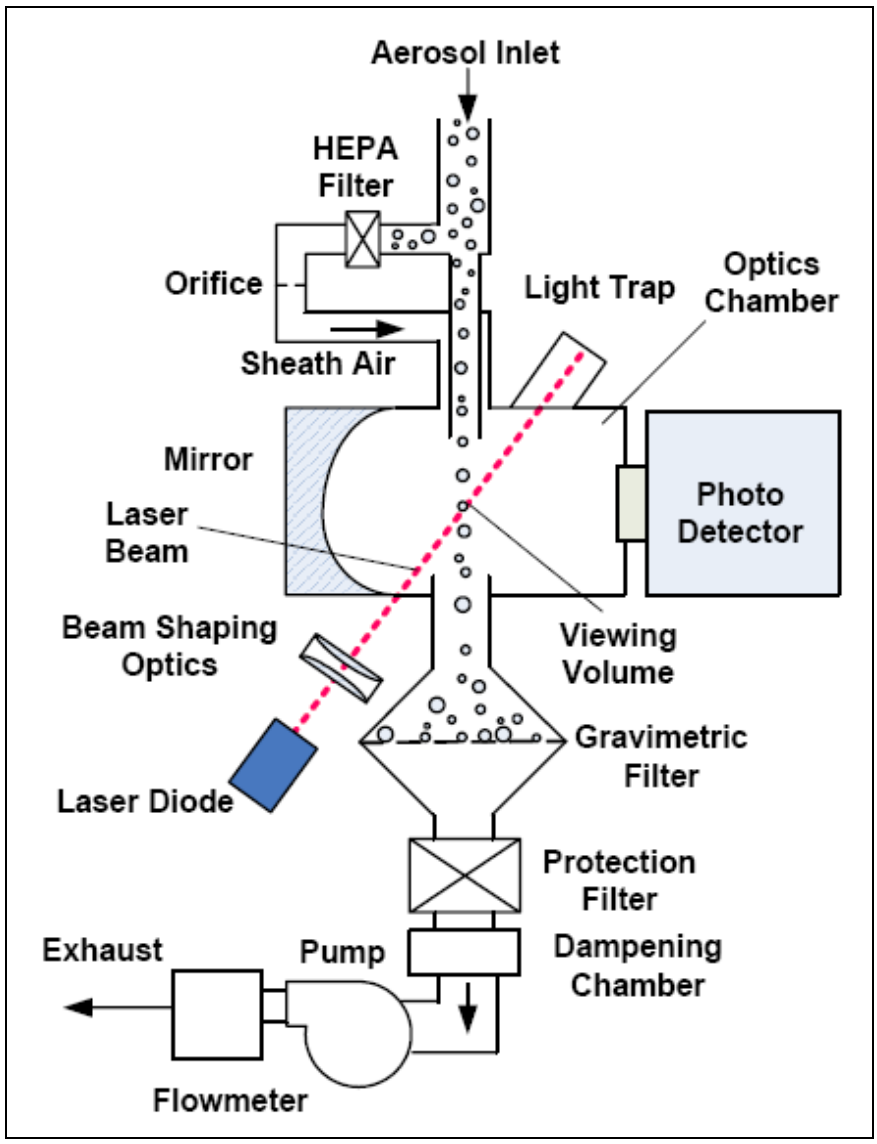

Figure 3-12: Schematic cross-section of a DustTrak™ II Aerosol Monitor (TSI, 2008)

3.7 IAQ-CALC INDOOR AIR QUALITY METER

The instrument used to measure the CO in this study was a TSI IAQ-CALC Meter (Figure 3-13). This is an instrument for the measurement of indoor air quality. The parameters include CO, CO_2, temperature, humidity, calculated dew point and wet bulb temperature. The instrument can measure and log multiple parameters simultaneously. By being equipped with an electrochemical sensor, it gives a more stable and accurate CO reading (TSI, 2007).

Figure 3-13: TSI's IAQ-CALC Meter (TSI, 2011)

TSI's IAQ-CALC Meter is also capable in conducting indoor air quality evaluations. Furthermore, it can verify the Heating, Ventilation and Air Conditioning (HVAC) system performance of a building. It can examine indoor air quality conditions in order to optimise productivity and comply with regulations and guidelines.

The CO sensor is of an electro-chemical type, which was calibrated to a range of 0 to 500 ppm. For monitoring the carbon monoxide, an electrochemical sensor was used. An anode and a cathode were set-up, which is similar to the set-up of a fuel cell. When CO reduction takes effect at the anode, it causes an electric current to pass through the circuit. A carbon cathode is consumed to produce CO_2. The size of the current produced represents the amount of CO. CO_2 is measured through the Nondispersive Infrared Sensor (NDIR) technique. During the indoor measurements, the logging interval of the concentrations was 1 minute. The resolution is 0.1ppm and its accuracy is ±3.0% of the reading or ±3ppm (whichever is greater). The response time of the instrument is <60 sec to 90% step change.

The NDIR sensor (Figure 3-14) measures the CO_2 level by pumping or allowing the sample gas to diffuse through the detection chamber. It is also known as a light tube, where an infra-red beam is passed through the gas.

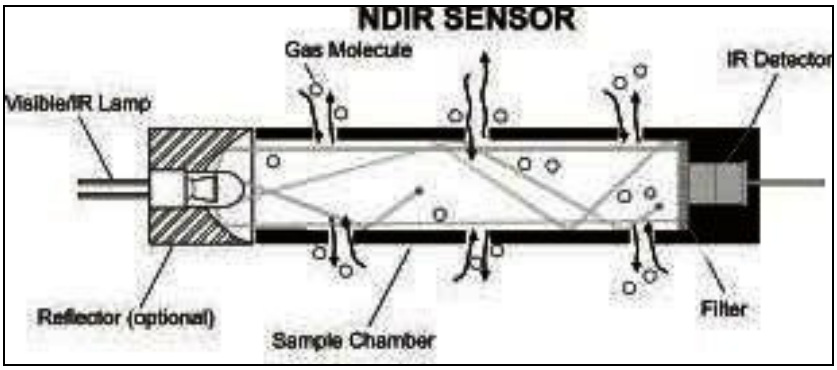

Figure 3-14: NDIR Sensor (International Light Technologies Inc., 2011)

A thermistor, which is made from a temperature sensitive resistor material, was used to monitor the temperature. The resistance of the material changes proportionally with the increase in temperature, which would then alter the electrical output of the sensor. To measure the relative humidity, a relative humidity sensor was used. It is a thin film capacitive sensor, which uses monolithic signal conditioning circuitry containing an electrode and a thin film of hygroscopic polymer material. Both of these materials were then integrated into a substrate. The dielectric constant of the hygroscopic material changes with the fluctuation of the relative humidity, which would then alter the capacitance and be represented by an electrical output change.

3.8 DIFFUSION TUBES

To measure the ambient concentration of nitrogen dioxide (NO_2), Palmes-type diffusion tubes has been the most popular choice since 1976 (DEFRA, 2012). The diffusion tube is considered a passive sampler as it absorbs the pollutant from the ambient air without the use of electricity. Passive samplers can be deployed in large quantities as they are relatively inexpensive when compared to other automatic monitoring techniques. The passive sampler is easy to use and has made a popular choice in recent years (DEFRA, 2012).

Passive sampling originated from the occupational exposure monitoring field. After years of testing and developing, diffusion sampling techniques have been widely used in ambient air quality monitoring. The NO_2 diffusion sampler is designed as a small plastic tube, of 7cm in length. It contains a chemical reagent. The chemical reagent is used to absorb the pollutant from the ambient air. The absorbent used in the Palmes-type diffusion tubes is triethanolamine (TEA). TEA is placed at the closed end with stainless-steel mesh grids. The water-based or acetone-

based solution of TEA is coated onto the mesh grids. Figure 3-15 shows the components of NO_2 diffusion tubes.

Figure 3-15: The components of NO_2 diffusion tubes (DEFRA, 2012)

Two methods are used to apply the TEA to the grids. First is to dip the grids into a TEA water-based or acetone-based solution. Once the grids have dried they are assembled in the tubes. Second is to pipet the TEA or acetone solution onto the grids situated in the caps, then placing them on the tube and putting a cap on the other end.

During sampling, one end of the diffusion sampler is open and the other closed. An absorbent is placed at the closed end for the monitoring of NO_2. After the monitoring period, a colorimetric or spectrophotometric technique, i.e. ion chromatography, is used to analyse the exposed tube.

The principle of diffusion tube analysis using colorimetry is less complicated. The nitrite collected on the grids is slightly dissolved by a mixture of water and reagent added to the tube after agitation. A purple compound will be formed after the reagent reacts with the nitrite in solution. Then spectrophotometry will be used to measure the intensity of the resulting purple compound. By calibrating with a set of standard nitrite solutions, the concentration of nitrite in the sample can be determined.

The diffusion sampler works on the basis of molecular diffusion. The gas molecules will diffuse from a high concentration region to a low concentration region. The high concentration region is referred to as the open end of the samplers and the low concentration region is referred to as the absorbent end of the sampler.

Sometimes, the accuracy of the sampler is affected by several factors. One of the factors is the exposure period. Several studies report that the absorbed nitrite becomes degraded after the exposure period was increased. Other factors include the nitrite extracted from the grids is insufficient and light causing the photochemical degradation of the triethanolamine-nitrite complex

Palmes-type diffusion tubes are particularly useful for identifying high NO_2 concentrations in areas of traffic where emissions are reasonably consistent over time. However, it is not suitable to be used in areas with specific emission sources such as industrial plants. This is due to the incapability of diffusion tubes to identify the short-term fluctuations in NO_2, especially the fluctuation in wind direction.

There are two limitations of diffusion tubes. First is that they are an indicative monitoring technique and not as accurate as automatic monitoring techniques. Secondly the results obtained are incomparable with the air quality standards as the exposure period of diffusion tubes is typically several weeks.

3.9 TENAX TA TUBES

DIFTXTA (Gradko International) VOC diffusion tubes are used to measure VOC concentrations in the environment. The sampler consisted of a stainless steel tube (6.3mm OD × 5.0mm ID × 90mm length) filled with a solid polymer absorbent – TENAX TA. The tube is then sealed with Swagelok compression joint caps (Gradko International, 2011).

The sample is collected when pollutants in the air diffuse from the entrance opening of a cylindrical sampler to the surface of a solid sorbent in the sampler. The pollutant concentration is assumed to be negligible when compared to the bulk air concentration. The diffusion distance is adjusted to a suitable position. Ideally, the sampling flow rate should follow Fick's First Law of Diffusion. It should be determined by the geometry of the sampler and diffusion coefficient of the pollutants. The passive sampling device is smaller as it does not require pump and flow regulation system. Therefore, it is suitable to be used for both personal and environmental samplings.

3.10 SUMMARY

There are three forces affecting the movement of particles through the fluid, which are the external force (gravitational or centrifugal force), the buoyant force and the drag force. The effect of air exchange rates and indoor emission rates on the pollutant concentrations and the relationship between the indoor and outdoor concentrations were discussed. The mass balance method was adopted in this study to determine the emission rates of various indoor pollutants. During the experimental work, an Andersen ambient sampler was used to determine the particle size distribution. Scanning Electron Microscopy with Energy Dispersion X-ray Spectrometry (SEM/EDS) was used to define the morphology of particles. Inductively Coupled Plasma Optical Emission Spectrometry (ICP-OES) was used to determine the elemental composition of the samples. A DustTrak^{TM} II Aerosol Monitor was used to measure the concentrations of $PM_{2.5}$. An IAQ-CALC Indoor Air Quality Meter was used to measure the CO concentrations. To measure the ambient concentration of nitrogen dioxide (NO_2), Palmes-type diffusion tubes were used. Tenax TA tubes were used to measure the VOC concentrations in this study. The principles and functions of each instrument were discussed in detail in this chapter.

4

EXPERIMENTAL PROGRAMME

The concentrations of $PM_{2.5}$ – solid-phase particulate matter ≤2.5 μm – as well as gaseous pollutants (CO, NO_2 and VOCs), were measured in the kitchens and outdoor environments at all three sampling sites. The methods for these measurements are described below. Additional particulates were collected and tested for Cases 1 and 3.

4.1 ANDERSEN SAMPLER

A multi-stage, multi-orifice cascade Andersen 1 ft^3/min (28.3 l/min) Ambient Particle Sizing Sampler (Mark II version, Thermo Electron Corp.) was used to collect PM samples from the kitchen (Cases 1 and 3), as well as the lounge, a bedroom and the outdoor environment (Case 1 only) in order to establish the particle size distribution. The sampler was calibrated with 1 g/cm^3 spherical particles.

4.1.1 Experimental Set-up

The Andersen sampler consists of eight stages, labelled from Stage 0 to Stage 7. A collection plate is placed between each stage of the Andersen Sampler in order to collect the particles by impaction (Figure 4-1). A substrate was used for the ease of collecting particles. An aluminium substrate was placed above the collection plate. Aluminium foil was selected as it is durable and easily made into discs. In addition, the particles collected can be easily removed from

the aluminium foil into specimen containers. The aluminium foil was cut into 80mm diameter discs which were placed on top of the collection plates. At the final stage, a glass fibre filter was used which was also 80mm in diameter. Surgical gloves with no powder were worn at all times to avoid excess moisture and oil from human skin appearing on top of the substrates and collection plates.

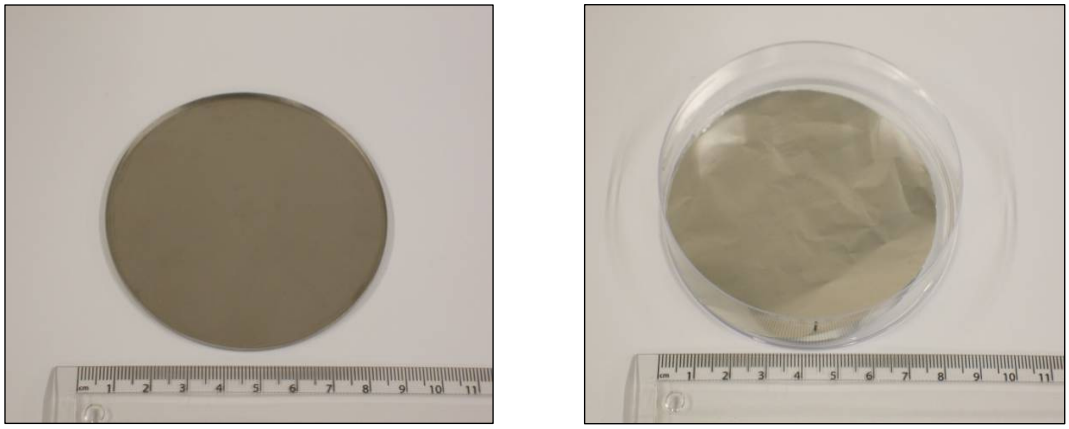

(a) (b)

Figure 4-1: (a) Collection plate for each impactor, (b) Manufactured aluminium collection substrate disc stored in a petri dish

A pre-separator was used to prevent particles greater than 10 μm from entering the subsequent stages. Before sampler assembly, the orifice stages, pre-separator and collection plates were cleaned with a mild detergent and warm water. The soap was completely removed by immersing the stages and plates in an ultrasonic cleaner. Acetone was used to remove the water on top of the stages and plates effectively. A lint-free wiping paper was used to remove slight traces of film on the stages and plates. To prevent getting skin oil on the orifice and collection surfaces the stages and plates were handled by the edges. Each stage was examined for any material in the holes. If holes were plugged, a jet blast of dry air was used to clean the holes effectively (Thermo Electron Corp., 2003). Then each substrate was weighed using a Precisa 205A scales. The data was recorded and the substrate was placed into the collection plate. The sampler was then assembled carefully while weighing progressed. Once assembled, the sampler was ready to be transported to the collection site (Figure 4-2). Care was taken to prevent any collection plate or substrate being misplaced within the sampler.

Figure 4-2: Andersen sampler ready for transport to sampling location

4.1.2 Operating Procedures

During the sampling, the substrates and collection plates of the Andersen Sampler were assembled accordingly. Once assembled, a continuous duty, carbon-vane vaccum pump was connected to Andersen Sampler. The pump was used to provide 1 ACFM (Actual cubic foot per minute) of constant air flow to the sampler. An adjustable bleed valve was used on the pump to control the air flow rate. After the pump was switched on, ambient gases then entered the inlet cone and cascaded from Stage 0 to Stage 7. The successively higher orifice velocities made the smaller particles inertially impact onto the collection plates. The sub-micrometer particles were then caught in the backup filter if they were not collected by the last collection plate. At the same time, the clean gases flowed through the vacuum tube and pump and were subsequently exhausted. The sampling time was recorded after the sampling was completed. The collection plates and backup filter were then removed for weighing. The concentration levels were determined and the size distribution was plotted.

4.1.3 Accuracy

Due to re-entrainment problems, 10mg of particulate matter on any one stage was considered as the upper limit in each sampling. Overloading could be detected by visual

inspection, indicated by the sample depositing on the edge of the plate. Since this would affect the results, this sample was discarded.

To ensure the measurement accuracy of the Andersen sampler, all the collection media, such as collection plates and substrates for each stage, were preconditioned prior to weighing. The most effective method was storing the collection media in a desiccator both before and after a sampling cycle as airborne particulates had hygroscopic characteristics. The filter weighing was made to an accuracy of ±0.02mg whereas the precision was ±0.01mg.

4.2 SCANNING ELECTRON MICROSCOPY WITH ENERGY DISPERSION X-RAY SPECTROMETRY (SEM/EDS)

All PM samples collected were analysed to determine the particle morphology and composition. The morphology of the PM_{10} samples was studied using scanning electron microscopy (SEM) with energy dispersive X-ray spectroscopy (EDS) (See Figure 3-5), which characterised the bulk specimen from 1 to 100 μm. The EDS is capable in X-ray mapping and microanalysis. Various software packages available on the computer were used to link the SEM in order to acquire digital images.

4.2.1 Experimental Set-up

To prepare the specimen stub, the cylinder stub needed to be in a clean condition. The size of the cylinder stub is 12.5mm x 10mm. A carbon tab with a 12mm diameter was stuck on top of the stub. A coax stick was used to pull out the transparent sticker in order to make the surface become adhesive. After that, the stub was put on top of the sample gently to ensure the sample adhered well on the carbon sticker. The samples were then coated using an Edwards Carbon Coating Unit, as shown in Figure 4-3.

Figure 4-3: Edwards Carbon Coating Unit (Model: 12E6/1598)

The samples were put on the platform, which was ready for carbon coating. It took about 30 minutes for the sample to be coated. The coated specimen stubs were ready for use with JEOL JSM6400 Scanning Electron Microscope (SEM).

4.2.2 Operating Procedures

For image acquisition, SEM/EDS was used in this study. The default settings were inspected before the start of each experimental work. The following settings were adopted:

- Image acquisition working distance = 8 – 15 mm
- Image acquisition accelerating voltage = 7 – 15 keV

For each sample, several random particles were subjected to analysis, ranging from 1µm to 100µm. Magnification was adjusted in order to obtain the clearest image.

4.3 DUSTTRAK™ II AEROSOL MONITOR

The TSI DustTrak™ 8532 aerosol monitor was used to measure the real-time $PM_{2.5}$ concentrations in each indoor and outdoor environment.

4.3.1 Experimental Set-up

The inlet cap of the DustTrak™ II Aerosol Monitor was put over the instrument when the sampling was taking place. It can prevent large objects from plugging the inlet hole and stop direct light, which skew the results during sampling. A size-selective impactor can help to control the size range of the particles entering the instrument. The sizes available include PM_1, $PM_{2.5}$, PM_4 (respirable) and PM_{10}. It was placed at the inlet of the instrument. 3.0 l/min (factory default setting) of air was drawn through the instrument to ensure the correct cut points were achieved. The cap, impaction plate and bottom are the three main parts of the size selective impactor. The cut size of the impactor was determined by the selection of the cap. The particle cut size (1μm, 2.5 μm, 4.0 μm or 10 μm) was clearly labelled on each cap. The impaction plate and bottom used for all impactor sizes are the same. The assembled impactor was then attached in place and the instrument was ready to be used.

4.3.2 Operating Procedures

Prior to using the instrument, it was zero calibrated using a zero calibration function and zero filter. In these tests, the 2.5μm filter was attached to the instrument, which allows only particles under this size to pass into the detection area. To set this up, the filter was dismantled and the impact plate oiled with two drops of impactor oil, then placed inside the filter assembly. The assembly was attached to the instrument and was then ready for the investigation. The test setting used was Test 1 with the parameters of continuous testing for 2-4 weeks from a specified start date to finish date, with a sample result being logged every 30 seconds.

4.3.3 Accuracy

The detection range of this instrument was 0.001-150 mg/m^3. The resolution was set to 0.1% of the reading. The log interval of the concentration data was set at 30 s. Although the particle size range of the instrument was 0.1-10 μm, during these measurements a size-selective impactor (cut size 2.5 μm) was attached to the inlet, which pre-conditioned the size range of particles (<2.5 μm) entering the instrument.

4.4 IAQ-CALC INDOOR AIR QUALITY METER

CO concentrations were measured for all three cases using a TSI IAQ-Calc Model7545 analyser. This instrument is a hand-held portable device that simultaneously measures CO, CO_2, temperature and relative humidity. The logging interval was 30 seconds for both species.

As Table 4-1 shows, carbon dioxide was analysed by a low drift non-dispersive infra-red CO_2 sensor with an accuracy of around 50ppm.

Table 4-1: Sensor and accuracies on the IAQ-Calc Monitor (TSI, 2011)

Parameters	Sensor	Range	Accuracy	Resolution	Response Time
CO_2	Dual-Wavelength NDIR	0 to 5000ppm	±3.0% or ±50ppm	1ppm	20s
Temperature	Thermistor	0 to 60ºC	±0.6ºC	0.1ºC	30s
Relative Humidity	Thin Film Capacitive	5% to 95%	±3.0%	0.1% RH	20s
CO	Electro-chemical	0 to 500ppm	±3.0% or 3ppm	0.1ppm	<60s

In addition, the IAQ-CALC Indoor Air Quality Meter is a sensing probe which relied on the diffusion of air. To produce the best results, the sensing probe was kept surrounded by moving air. It was prohibited from breathing on the probe as humans can exhale CO_2 at levels exceeding 10,000ppm and it might take time for the probe to re-stabilize. A probe holder was used to support the probe when in continuous data logging mode.

4.5 DIFFUSION TUBES

Different types of diffusion tubes were deployed to monitor NO_2 and VOCs in this study. To measure NO_2 concentrations, Palmes-type diffusion tubes (Gradko International, 20% Triethanolamine) were used. The tube material is colourless clear or translucent plastic. Stainless steel grids were used to hold the TEA solution with two grids for each tube. The end caps are made of flexible plastic. Glassware used throughout is at least Grade B. The TEA solution available is either 50% v/v TEA/acetone, or 20% v/v TEA/water. The diffusion tubes are recommended to be used within 4 months of preparation.

4.5.1 Experimental Set-up

The passive tests were set up at the beginning of the test period and reassembled at the end. The final result from these tests gives a total result for the 2-4 weeks period. Both sets of tubes were purchased from Gradko International who will, upon completion of the experiment, re-analyse the tubes to determine the amount of absorbed pollutant.

Detailed Siting of Diffusion Tube

During sampling, the open end of diffusion tube was held vertically and faced downwards (Figure 4-4). The open end of the tube was exposed to freely circulating air. A holder was used to hold the diffusion tube and the tube could be changed and adjusted to a desired height easily at each site. The tube was not fixed directly to walls as certain surfaces might act as absorbers for NO_2. This would lead to a thin layer of reduced atmospheric concentrations. A spacer was used between the wall and tube.

It was recommended to avoid the opposite extreme such as areas of higher than usual turbulence, sink of NO_2, disturbance to the airflow, low level balanced heater flues, air conditioning outlets, underground ventilation shafts and others.

Figure 4-4: The open end of diffusion tube was held vertically facing downwards

Exposing Diffusion Tube to Collect Sample

There were several procedures to be followed before exposing the diffusion tube at the sampling site. This was to ensure the samples collected were within appropriate quality assurance. The procedures included:

- Diffusion tube was removed from the refrigerator only on the day of sampling and each tube was clearly labeled with a unique identification number. The label should be weatherproof.
- The tube was placed in a sealable plastic bag or container when transporting the tube to sampling site.
- The start date and time of the exposure period and any site irregularities were clearly recorded.
- The end caps of the tube were kept safe, so that it can be used again when the exposure period was complete.

4.5.2 Operating Procedures

The tubes were stored in a sealed container in a refrigerator prior to use. During the investigation, the diffusion tube was held vertically with the open end faced downwards. NO_2 was absorbed into the tubes as nitrite. The lower end cap was replaced after exposure for 2 to 4 weeks time. The NO_2 concentration was quantitatively determined using UV spectrophotometry (UVS04 Camspec M550). This gave the average concentration over the entire exposure period for each case study.

4.5.3 Accuracy

The analytical expanded measurement uncertainty for the diffusion tubes in this study was ±3.69%. The detection limit was 0.4 ppb (or 0.34 $\mu g/m^3$) over a two-week exposure period in each environment. The colour reagents used for the analysis need to be accurately prepared to ensure the measurement accuracy of diffusion tubes. Besides that, the diffusion tube should be used within the lifetime of the tube. To produce the most accurate results, the tube was recommended to be used within four months of preparation. Apart from that, diffusion tube was analysed in manageably sized batches to ensure the consistency was maintained throughout.

4.6 TENAX TA TUBES

The Tenax TA tubes are used to determine time-weighted average concentrations of VOCs present in the environment, as shown in Figure 4-5.

Figure 4-5: Gradko VOC Diffusion Tube (Gradko International, 2011)

4.6.1 Experimental Set-up

During passive sampling, an aluminium air diffuser was fitted to the sampling end of the tube. After 3-4 weeks exposure, the absorbent in the tubes was analysed. The analytical measurement error was ±14.8%. It should be noted that the average VOC concentration over the period of exposure is measured using this method.

4.6.2 Operating Procedures

During the investigation, the Tenax TA tube's cap which was marked with an orange dot, was removed and replaced with an air diffuser. Once completed, the cap was replaced and the tube was tested at Gradko International. It was analysed using gas chromatography with either flame ionisation detection or mass spectroscopy, to determine the top 20 VOCs present.

4.7 TSI DP-CALC MICRO-MANOMETER

To measure the air pressure difference between the interior and exterior of the buildings, a TSI DP-CALC Micromanometer Model 5825 (Figure 4-6) was chosen. This allows the differential pressure to be measured across a boundary, but it is also capable of measuring static, total and velocity pressures. For the differential pressure, it has a range of -15 to +15 in. H_2O (-3735 to +3735 Pa), an accuracy of ±1% of the reading or ±0.005 in. H_2O, and a resolution of 0.001 in. H_2O, (0.1Pa), and is capable of a logging interval ranging from 1 second to 1 hour (TSI, 2011).

Figure 4-6: TSI DP-Calc Air Pressure Monitor (TSI, 2011)

4.8 SAMPLE LOCATIONS AND MEASUREMENTS

Experiments have been conducted to determine the species, concentrations, sources and emission rates of various indoor gaseous and solid-phase pollutants. Three different domestic environments were chosen for the experimental studies. These were: (i) a stone-built detached house in a rural area with an electrical cooking system; (ii) a flat in a city centre with gas heating and cooking systems; and (iii) a flat on a main road in an urban area, also with gas heating and cooking systems. As well as varying the locations of the properties, the sources of energy were also different; electric and gas appliances could thus be compared. The Andersen sampler was used to collect particulate matter samples from the bedroom, kitchen, lounge and outdoor of Case

1 and from the kitchen of Case 3. Various indoor pollutant ($PM_{2.5}$, CO, NO_2 and VOCs) measurements were conducted at all three sites.

4.8.1 Experimental Measurement Periods and Corresponding Activities

The measurement periods for various samples collected from Cases 1 and 3 are showed in Table 4-2. Results obtained from full elemental analysis and morphology analytical work are presented in the following chapters.

Table 4-2: Measurement periods for various samples collected from Cases 1 and 3

Sampling		**Measurement Period (s)**		
		Andersen Sampler	**Morphology Analysis**	**Full Elemental Analysis**
Hathersage (Case 1)	Bedroom	06/02/09 - 22/03/09	17/04/09	07/04/09
	Kitchen	23/03/09 - 21/04/09	02/06/09	11/06/09
	Lounge	18/07/09 - 18/08/09	14/09/09	05/10/09
	Outdoor	15/05/09 - 29/06/09	15/07/09	16/09/09
Sheffield (Case 3)	Kitchen	22/11/10 - 18/12/10	13/01/11	11/01/11

Tests were also carried out outside the buildings (outdoor environment). Air exchange rates were also measured in the kitchens. Table 4-3 presents the timetable for indoor pollutant measurements at all sites.

Table 4-3: Timetable for pollutant measurements

Pollutant	**Instrument**	**Residential house in Hathersage**		**Residential flat near Sheffield Centre**		**Residential flat on a main road in Sheffield**	
		Indoor	**Outdoor**	**Indoor**	**Outdoor**	**Indoor**	**Outdoor**
$PM_{2.5}$	TSI DustTrak 8532	13/7/09 – 24/7/09	15/5/09 – 29/06/09	27/7/09 – 11/8/09	27/8/09	15/9/10 – 29/9/10	11/10/10 – 25/10/10
CO	TSI IAQ Calc 7545	9/7/09 – 24/7/09	24/7/09	27/7/09 – 3/8/09	27/8/09	15/9/10 – 29/9/10	11/10/10 – 25/10/10
NO_2	Diffusion tubes	29/6/09 – 27/7/09	29/6/09 – 27/7/09	28/7/09 – 20/8/09	28/7/09 – 20/8/09	15/9/10 – 15/10/10	15/9/10 – 15/10/10
VOCs	Tenax TA tubes	29/6/09 – 27/7/09	29/6/09 – 27/7/09	29/5/09 – 18/6/09	4/6/09 – 21/6/09	15/9/10 – 15/10/10	15/9/10 – 15/10/10
Air exchange rate	TSI IAQ Calc 7545	24/7/09	–	27/8/09	–	25/10/10	–

4.9 SUMMARY

An extensive series of experimental tests were conducted in three residential buildings. Various items of equipment were used to collect and analyse the samples. An Andersen Sampler was used to collect PM samples from the kitchen (Cases 1 and 3), as well as the lounge, a bedroom and the outdoor environment (Case 1 only) in order to establish the particle size distribution. The morphology of the PM_{10} samples was studied using SEM/EDS. The TSI DustTrak^{TM} 8532 aerosol monitor was used to measure the real-time $PM_{2.5}$ concentrations in each indoor and outdoor environment. CO concentrations were measured for all three cases using a TSI IAQ-Calc Model7545 analyser. Palmes-type diffusion tubes were used to measure the ambient NO_2 concentrations. Tenax TA Tubes were used to determine the VOCs concentrations. A TSI DP-CALC Micromanometer Model 5825 was used to measure the air pressure difference between the interior and exterior of the building.

5

CASE STUDY 1: EXPERIMENTS IN A STONE-BUILT DETACHED HOUSE IN HATHERSAGE

A diverse investigation was conducted in a residential house in Hathersage. The house had an electric cooker. The tests conducted including constant measurements of $PM_{2.5}$ and CO concentrations. The levels of NO_2 and VOCs were monitored over a period of time in the kitchen using passive diffusion tubes. Air exchange rates were also measured in the kitchen. The emission rates of various indoor pollutants ($PM_{2.5}$, CO, NO_2 and VOCs) were calculated by using a mass balance method. The details of the case study location and results obtained are discussed below.

5.1 SITE DESCRIPTIONS

This case study focussed on a stone-built detached house in Hathersage. Hathersage is located in the Hope Valley, Derbyshire (Figure 5-1). It is a village in the Peak District National Park (Figure 5-2), just over 10 miles west of Sheffield.

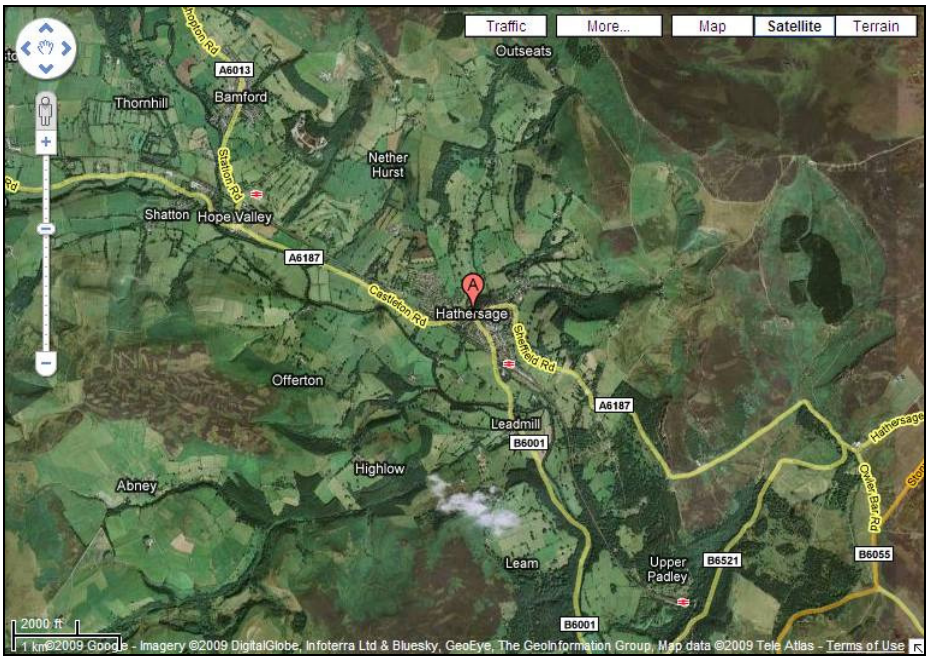

Figure 5-1: Location of Hathersage (Google, 2009)

The village is centred around a busy road junction above the River Derwent. There is an industrial cement manufacturing plant 4 miles away from the house and a reservoir about 3 miles northwest. There is also a busy diesel-operated railway line 0.1 mile away and a busy road that lies 50 metres northwest. The sampling location is situated about 0.2 miles from the A6187 and the B6001.

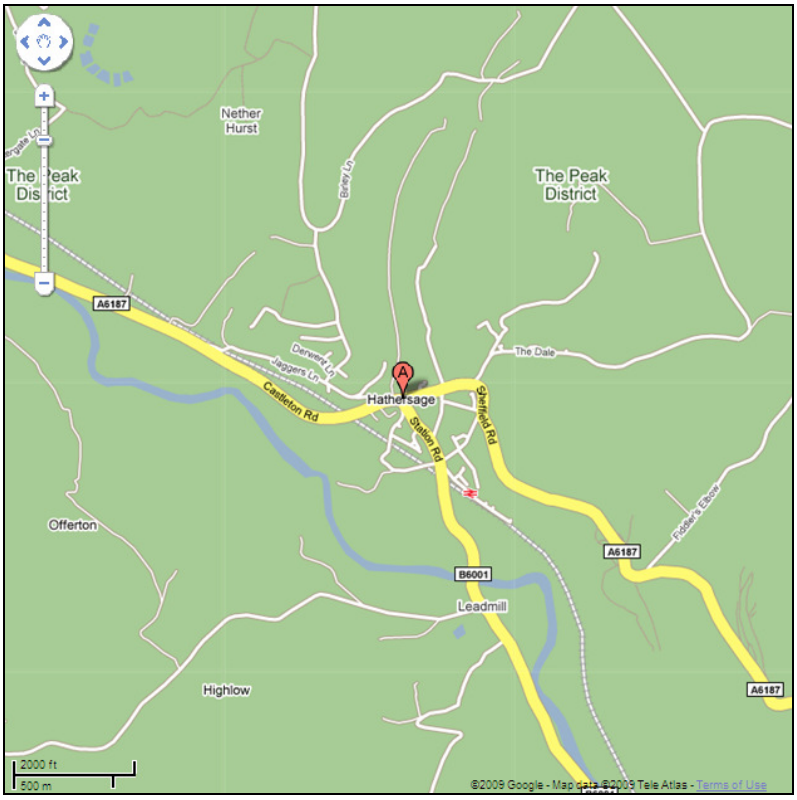

Figure 5-2: Proximity of Hathersage to the Peak District (Google, 2009)

Hathersage is situated about 12 miles south east of Buxton on the A625 Buxton to Sheffield road and is also part of the Sheffield/Chesterfield commuter belt. Figure 5-3 shows the River Derwent near the sampling location. General views of Hathersage are shown in Figures 5-4 and 5-5.

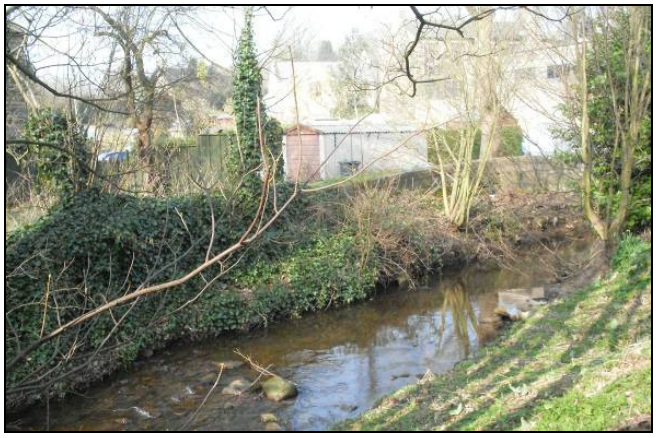

Figure 5-3: The River Derwent closes to the sampling site

Figure 5-4: General view of Hathersage 1

Figure 5-5: General view of Hathersage 2

Figure 5-6 shows the aerial view of Hathersage and the location of the test site. The sampling site is a 200 year-old stone-built detached house, Figure 5-7. The house has a natural gas heating system of 23.5–85 kW capacity, Figure 5-8. Figure 5-9 shows the layout of the kitchen of the residential house in Hathersage.

Figure 5-6: Location of the test site (Google, 2009)

Figure 5-7: A 200 years old stone-built detached house

Figure 5-8: Natural gas heating system (type SPG 146 – 1, 23.5 to 85 kW capacities)

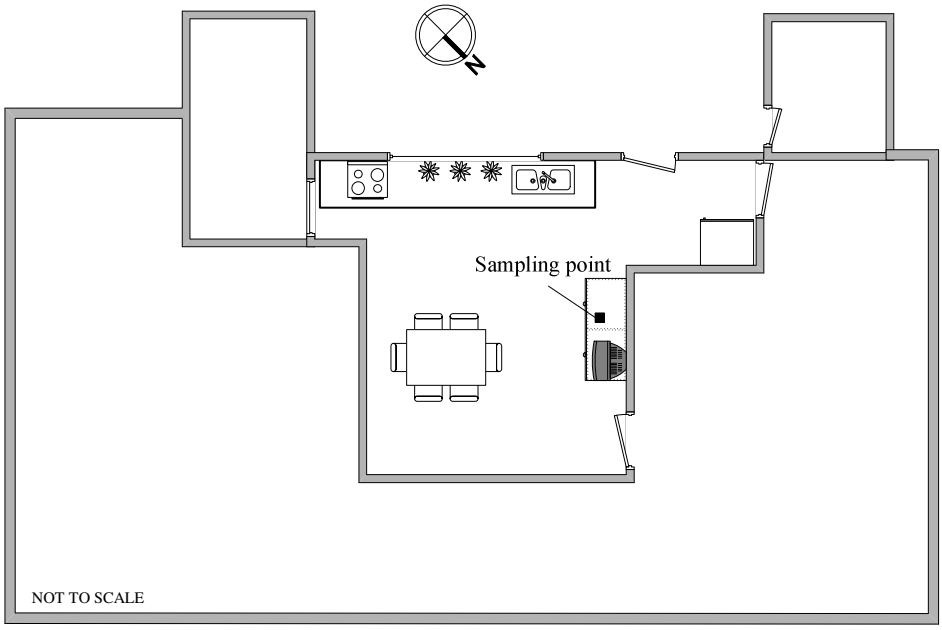

Figure 5-9: Layout of the kitchen for Case 1

5.2 PARTICULATE MEASUREMENTS AND ANALYSIS

5.2.1 Bedroom

The bedroom that was monitored is shown in Figures 5-10 and 5-11. The dimensions of the bedroom were 3m length x 4m width x 2.5 m height. There was only one window. The Andersen Sampler was brought to the sampling location and connected to the transformer and pumps, Figure 5-12. The sampling position was at the centre of the room at a height of about

1.0m from the floor, as shown in Figure 5-13. The sampler was left at the sampling location for a period of 6 weeks. Sampling started on 06/02/2009 at 10.30am and ended on 22/03/2009 at 10.29am, which is equal to approximately 1,008 hours.

Figure 5-10: Bedroom chosen for conducting the experiment

Figure 5-11: Bedroom interior

Figure 5-12: Installation of Andersen Sampler

Figure 5-13: Andersen Sampler was placed about 1m from floor level

5.2.1.1 Particle Size Distribution

The concentration of particles collected from each stage is presented in Table 5-1. Overall, 5.7 mg of particulate matter was collected from the chosen unoccupied bedroom. From Figure 5-14 it can be seen that the particulate matter data for the bedroom sampling gave a normal particle size distribution. The concentrations of $PM_{2.5}$ and PM_{10} were about 2.16µg/m^3 and 3.33µg/m^3 respectively. The results obtained were expected as larger particles only remain in the atmosphere for a short period of time. The majority of these particles arose from vehicle combustion and disc brake dust. Some other possible sources were secondary particles and by-products from a cement plant nearby.

Table 5-1: The concentrations of particles collected from each stage (Bedroom)

Stage	Mass Size Distribution (µm)	PM (mg)	Concentration (µg/m^3)	%
0	9.0-10	0	0.00	0.00
1	5.8-9.0	0	0.00	0.00
2	4.7-5.8	0.4	0.23	7.02
3	3.3-4.7	0.5	0.29	8.77
4	2.1-3.3	1.1	0.64	19.30
5	1.1-2.1	1.7	0.99	29.82
6	0.7-1.1	0.8	0.47	14.04
7	0.4-0.7	0.6	0.35	10.53
Filter	0-0.4	0.6	0.35	10.53
Total		**5.7**	**3.33**	**100**

Test time	60,480mins (≈1,008hours)
Air volume (m^3)	1712.61
$PM_{2.5}$ concentration (µg/m^3)	2.16
PM_{10} concentration (µg/m^3)	3.33

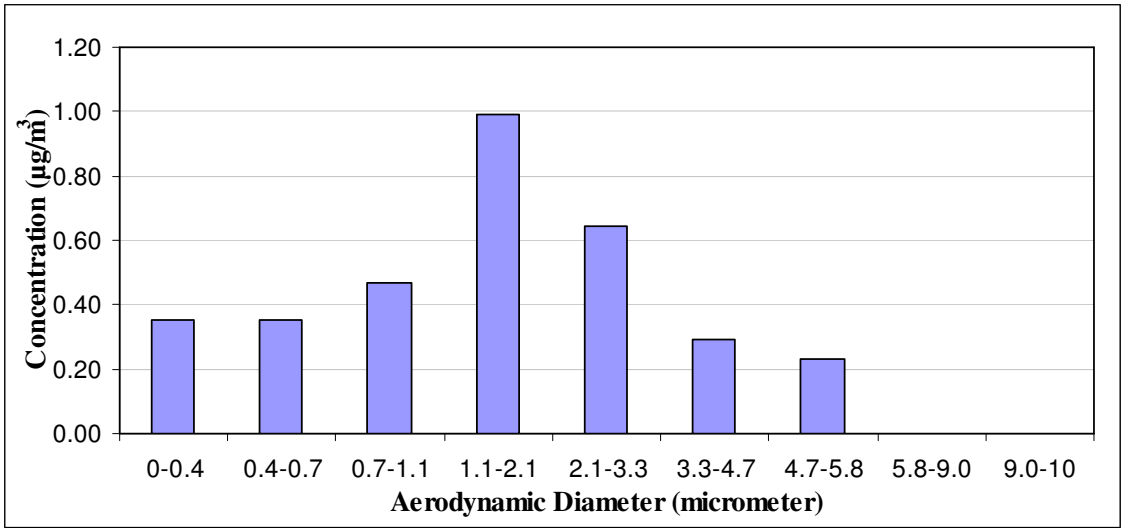

Figure 5-14: Particle size distribution for bedroom sampling

5.2.1.2 Full Elemental Analysis

All the filter samples were analysed at the Centre for Analytical Science (CAS), Department of Chemistry. ICP-OES was used for the elemental analysis. The acid solvent used to

digest the sample was *Aqua Regia*, a mix of three parts of HNO_3 and one part of HCl. The use of HCl meant that the chlorine measurements were not accurate due to the sensitivity limitations of the system.

Figure 5-15 presents the elemental composition for particles collected from the bedroom. The samples were mainly composed of Na, Fe, S and Zn. The most likely source of Na, given that the sampling was carried out in winter, was from road grit being carried into the house on footwear. Fe is a product of brake pad wear. The most likely source of S is from fuel combustion, both vehicles and trains, as the sampling location was close to a busy main road and railway line. The most like source of Zn was from paint (where zinc oxide is one of the white pigments used).

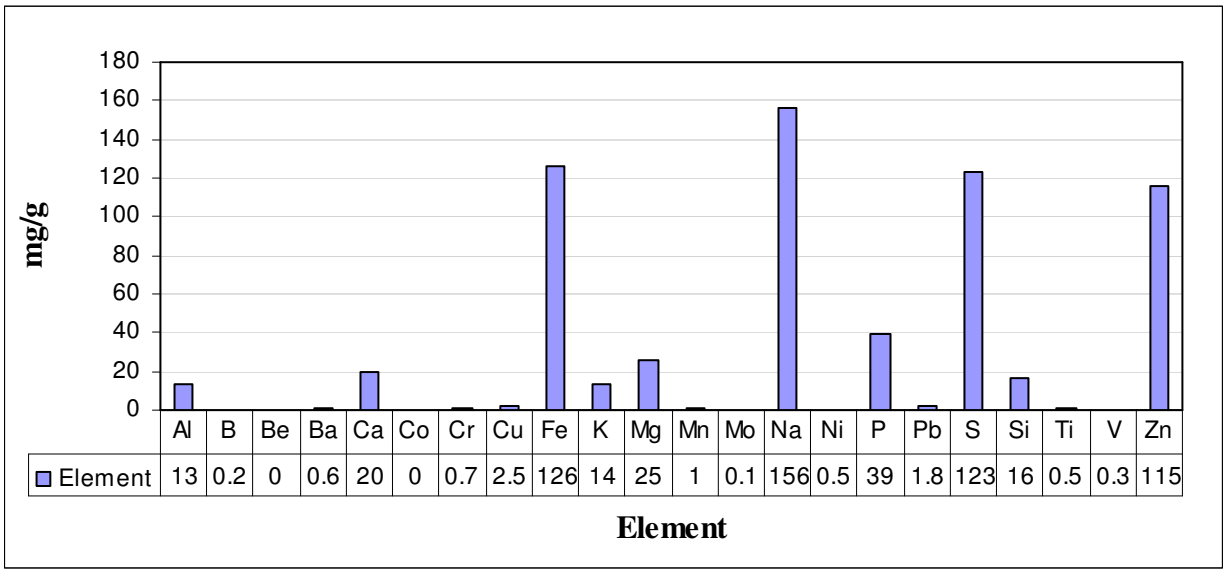

Figure 5-15: Element contents for bedroom sampling

5.2.1.3 Morphology Analysis

The morphology of individual particles was obtained by using SEM/EDS. The particles for each stage are presented along with a brief description. The particles collected possess different structures and sizes.

Stage 4 (2.1 – 3.3 µm):

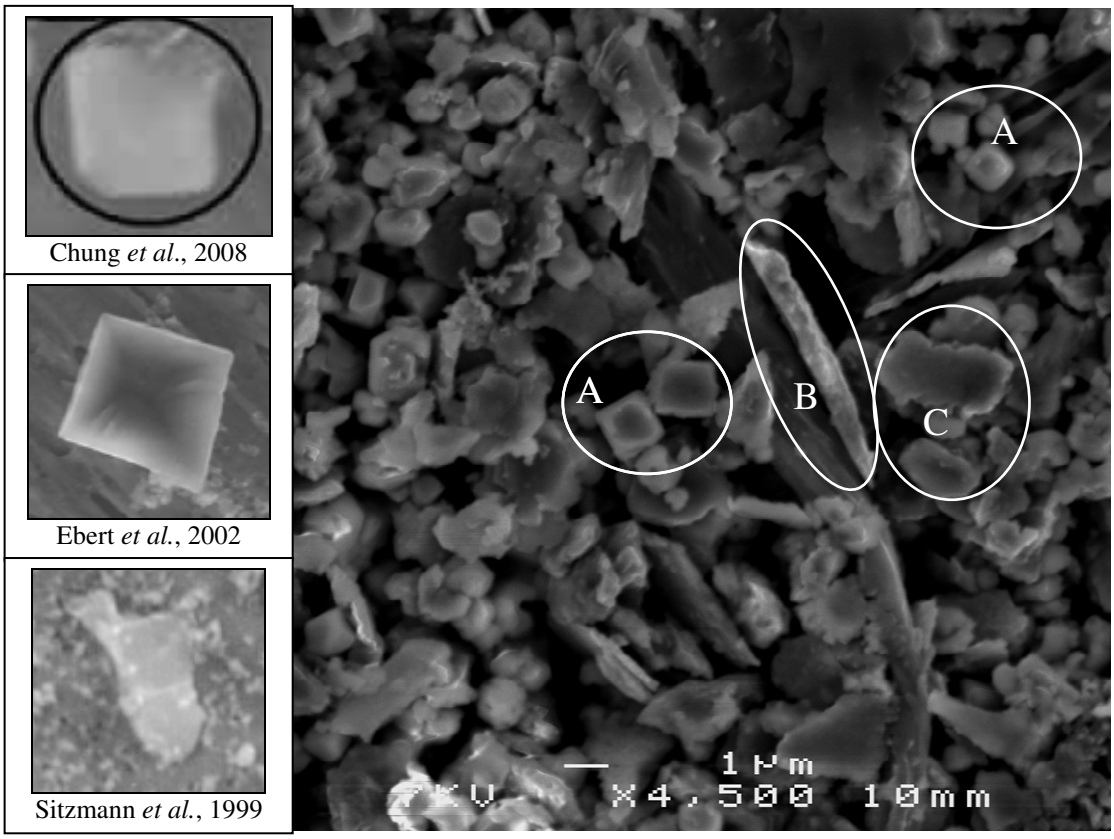

Figure 5-16: SEM image of PM at 1µm

Particles A in Figure 5-16 are approximately 1–2µm in length with a cubic shape. The morphology of these particles suggests that they were salt crystals and salt related particles (Chung *et al*., 2008; Ebert *et al*., 2002). The elemental composition suggests that the particle was a mixture of very fine salt fused together or a particle was growing at high relative humidity. These particles originated from road gritting as the sampling was collected during winter and grit salt is used extensively in this season. The presence of salt particles was confirmed by EDS analysis (Cl peak).

Particle B in Figure 5-16 is a fibre-shaped particle of several microns. It was a mineral fibre from outdoors or a textile fibre from indoors. Particle C in Figure 5-16 is a plate-like particle of approximately 3µm with a rectangular shape. It was either a rust compound from vehicles or a result of brake abrasion from the nearby transportation (Sitzmann *et al*., 1999).

Stage 4 (2.1 – 3.3 µm):

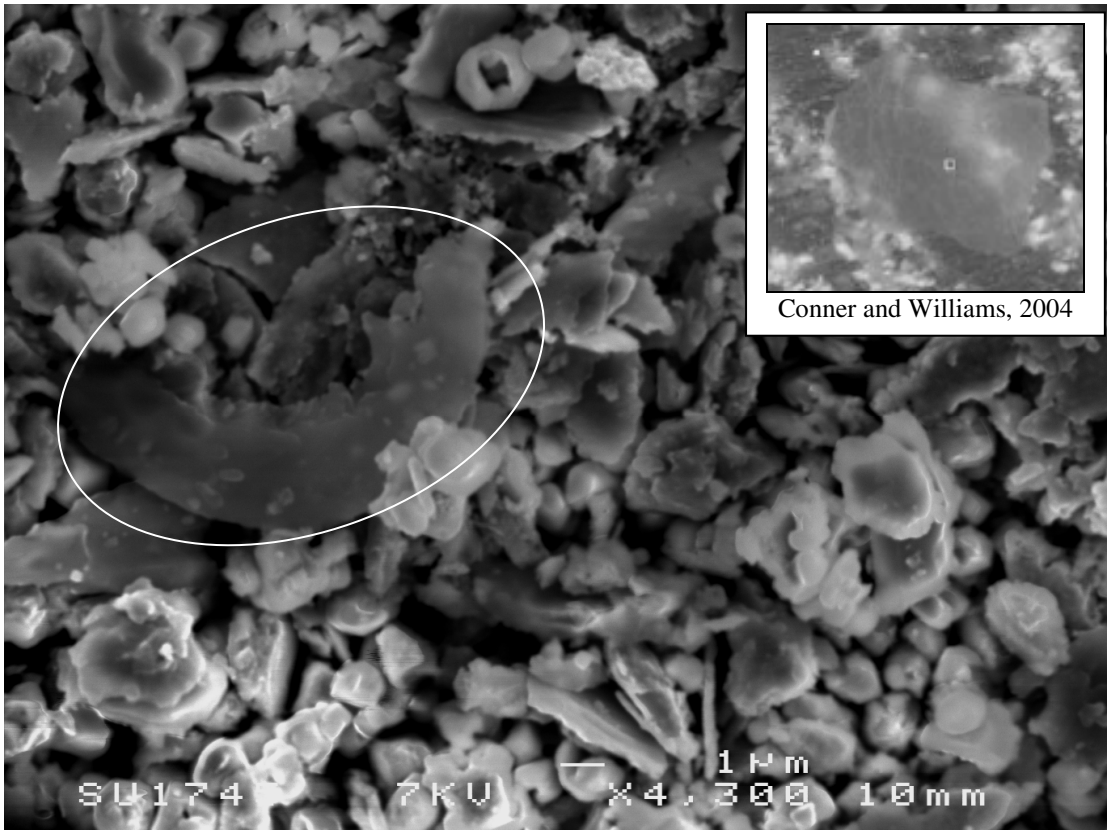

Figure 5-17: SEM image of PM at 1µm

The particle of interest in Figure 5-17 is possibly of biological origin. The plate-like and semi-transparent appearance of this particle indicates that it is a skin flake (Conner and Williams, 2004). EDS analysis of this particle gave traces of S, Cl and Si.

Stage 4 (2.1 – 3.3 µm):

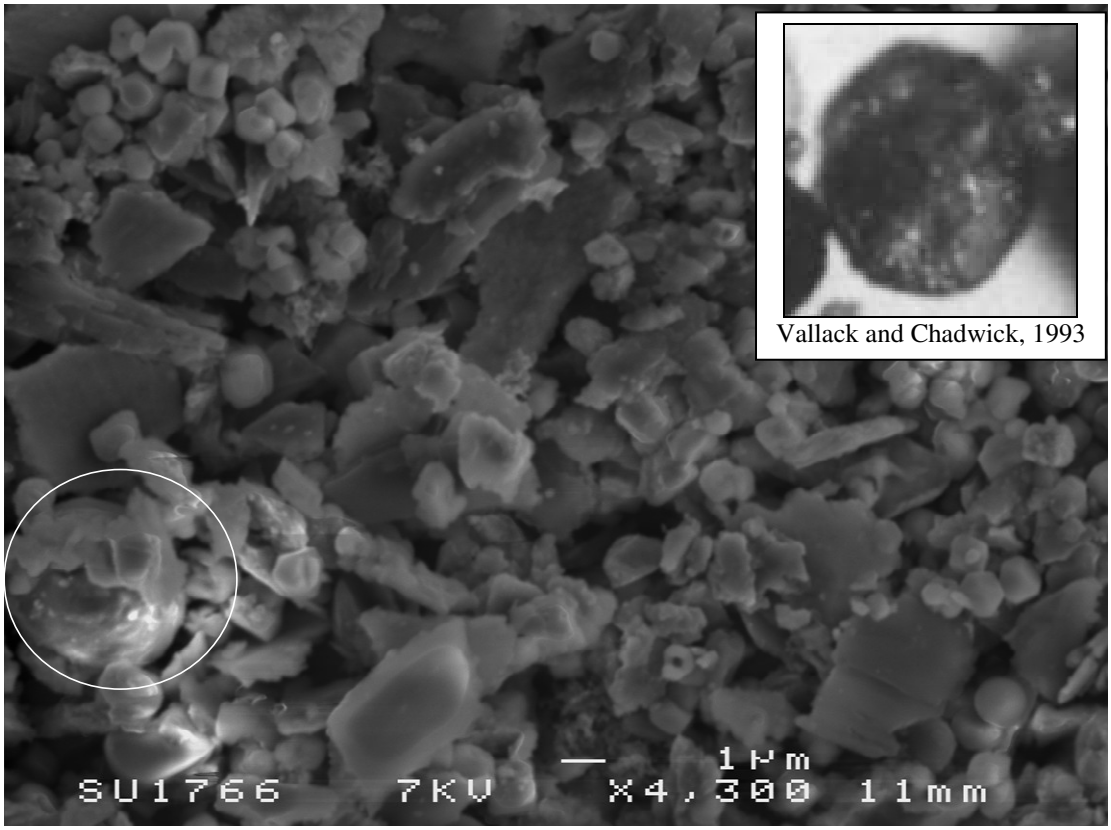

Figure 5-18: SEM image of PM at 1µm

In Figure 5-18, the particle of interest is marked with a circle. The morphology of this particle is a sphere and this suggests that the particle originated from high temperature sources (Vallack and Chadwick, 1993). The diameter of this particle is around 3 µm with a smooth surface texture. The round edges of the particle suggest that it was formed during a high temperature process. EDS analysis of this particle gave high amounts of Si, Ca and Fe.

Stage 2 (4.7 – 5.8 µm):

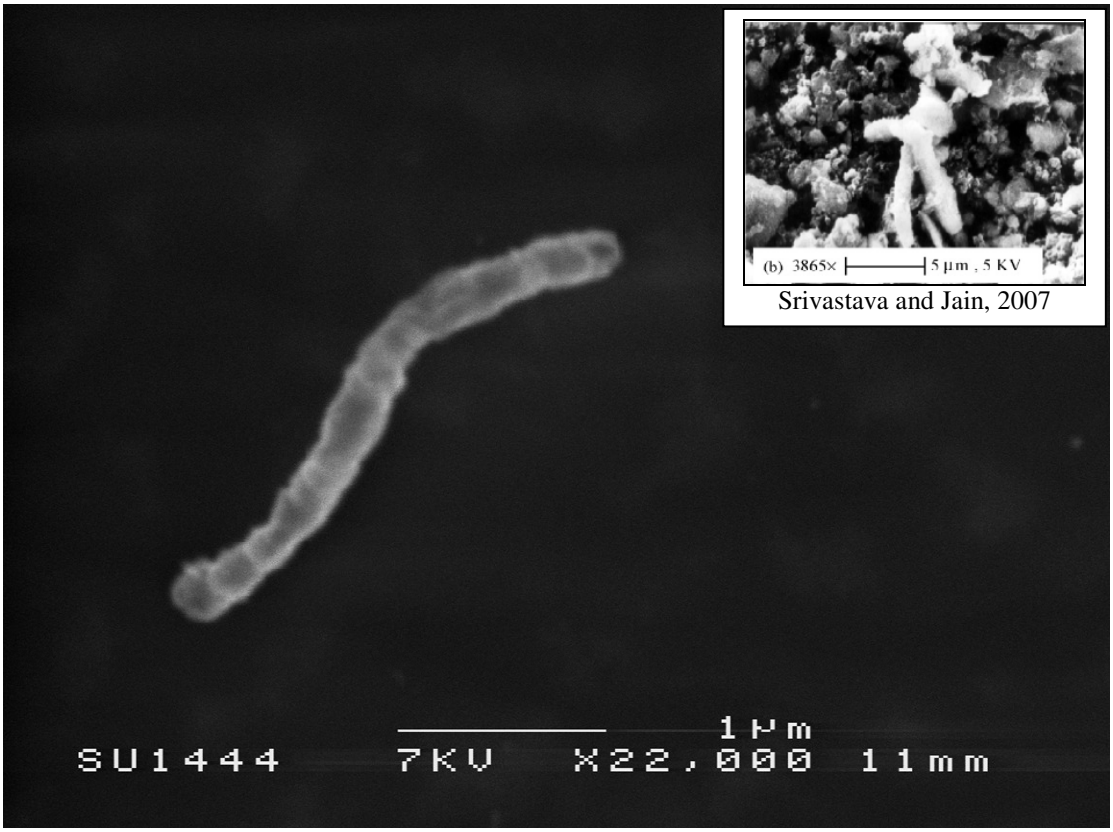

Srivastava and Jain, 2007

Figure 5-19: SEM image of PM at 1µm

The particle featured in Figure 5-19 appears fibrous in nature. The morphology of this particle indicates that it is a fibre. This kind of particle typically has a high amount of Cl with lower amounts of P, S and K. During the EDS analysis, the agglomerates of the particles were not visible. However, upon closer inspection of the image, it could be concluded that the rod-like particle is an organic compound (Srivastava and Jain, 2007).

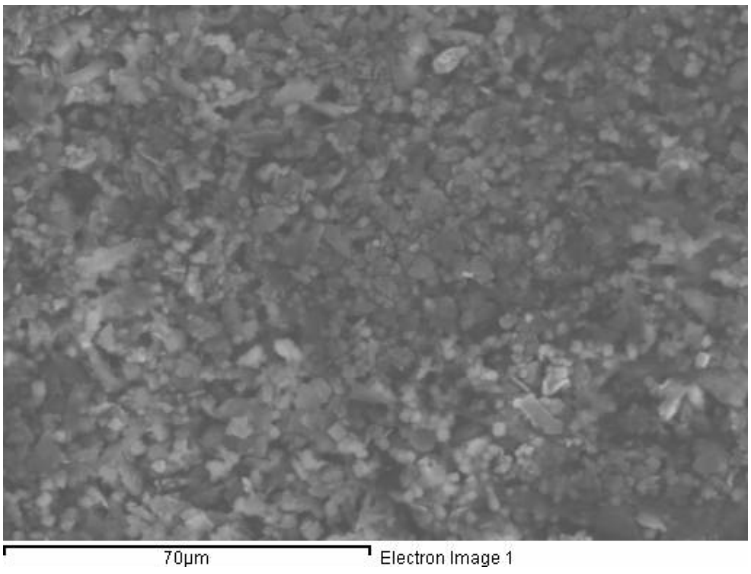

(a)

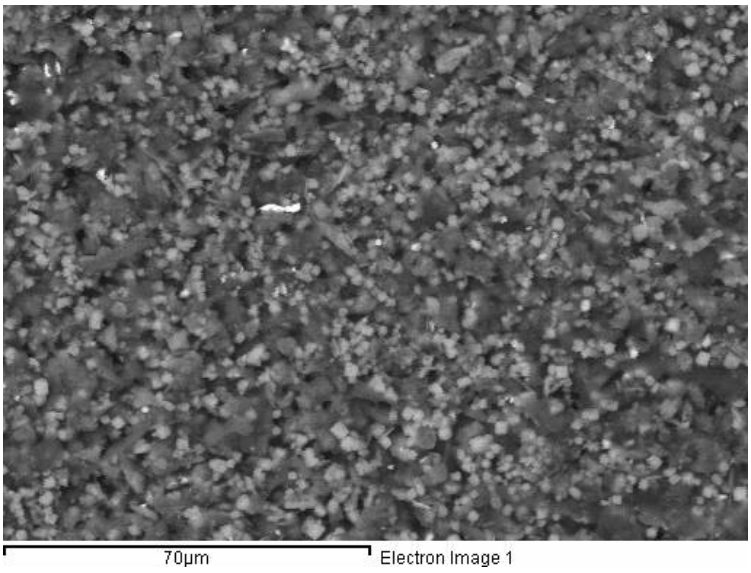

(b)

Figure 5-20: SEM/EDS images captured using (a) secondary electron mode; and (b) back-scattered mode (Bedroom sampling, Stage 3)

Figure 5-20(a) shows the SEM/EDS images captured using Secondary Electron (SE) mode and Figure 5-20(b) was captured by using Back-Scattered (BS) mode. SE mode gave the morphology of the sample and BS mode gave the different elemental contents of the sample. In BS mode, the higher the atomic weight, the brighter the element. The elemental content for the particles in Figure 5-20 were further analysed by using EDS and shown in Figure 5-21.

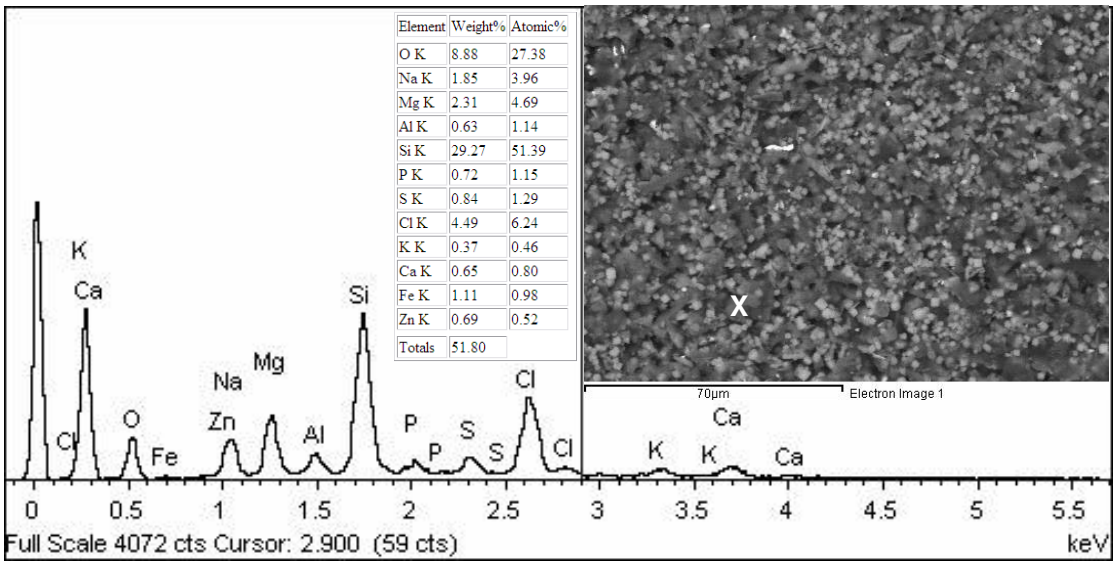
Element Weight% Atomic%
O K 8.88 27.38
Na K 1.85 3.96
Mg K 2.31 4.69
Al K 0.63 1.14
Si K 29.27 51.39
P K 0.72 1.15
S K 0.84 1.29
Cl K 4.49 6.24
K K 0.37 0.46
Ca K 0.65 0.80
Fe K 1.11 0.98
Zn K 0.69 0.52
Totals 51.80
70µm
Electron Image 1
Full Scale 4072 cts Cursor: 2.900 (59 cts)
keV

(a)

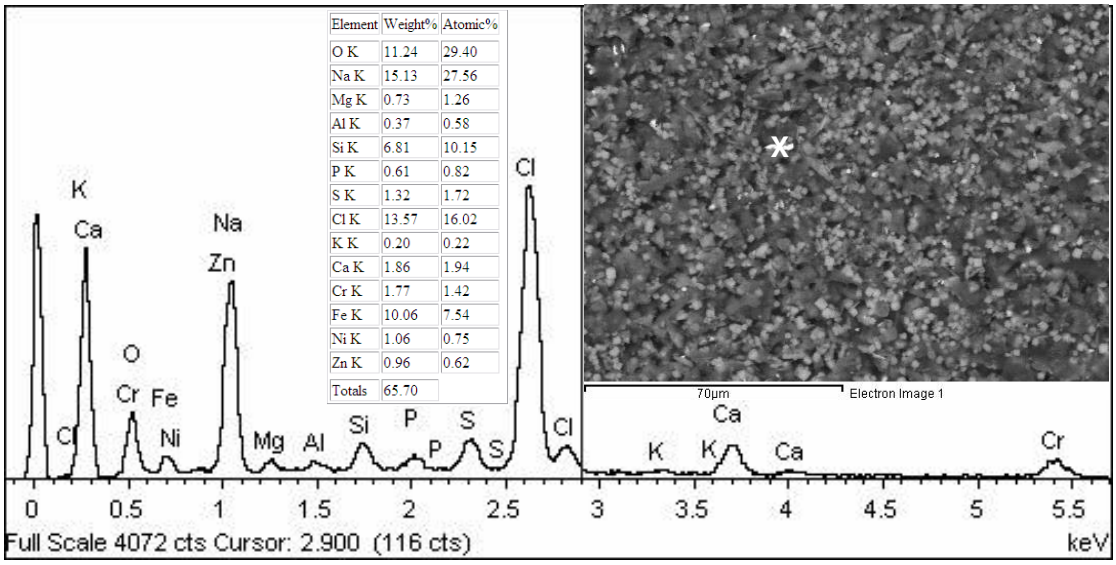
Element Weight% Atomic%
O K 11.24 29.40
Na K 15.13 27.56
Mg K 0.73 1.26
Al K 0.37 0.58
Si K 6.81 10.15
P K 0.61 0.82
S K 1.32 1.72
Cl K 13.57 16.02
K K 0.20 0.22
Ca K 1.86 1.94
Cr K 1.77 1.42
Fe K 10.06 7.54
Ni K 1.06 0.75
Zn K 0.96 0.62
Totals 65.70
70µm
Electron Image 1
Full Scale 4072 cts Cursor: 2.900 (116 cts)
keV

(b)

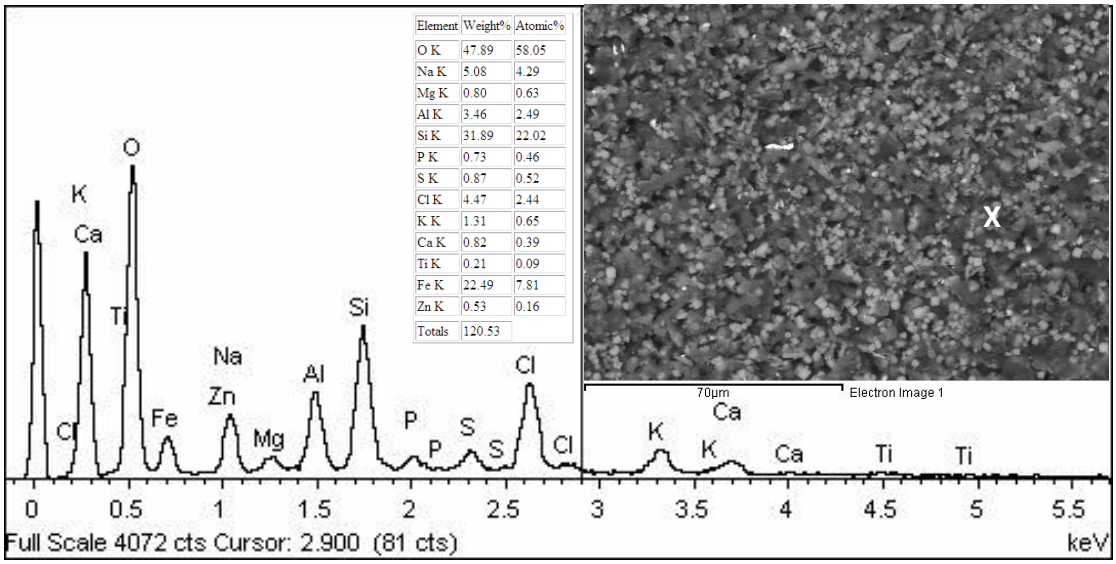
Element Weight% Atomic%
O K 47.89 58.05
Na K 5.08 4.29
Mg K 0.80 0.63
Al K 3.46 2.49
Si K 31.89 22.02
P K 0.73 0.46
S K 0.87 0.52
Cl K 4.47 2.44
K K 1.31 0.65
Ca K 0.82 0.39
Ti K 0.21 0.09
Fe K 22.49 7.81
Zn K 0.53 0.16
Totals 120.53
70µm
Electron Image 1
Full Scale 4072 cts Cursor: 2.900 (81 cts)
keV

(c)

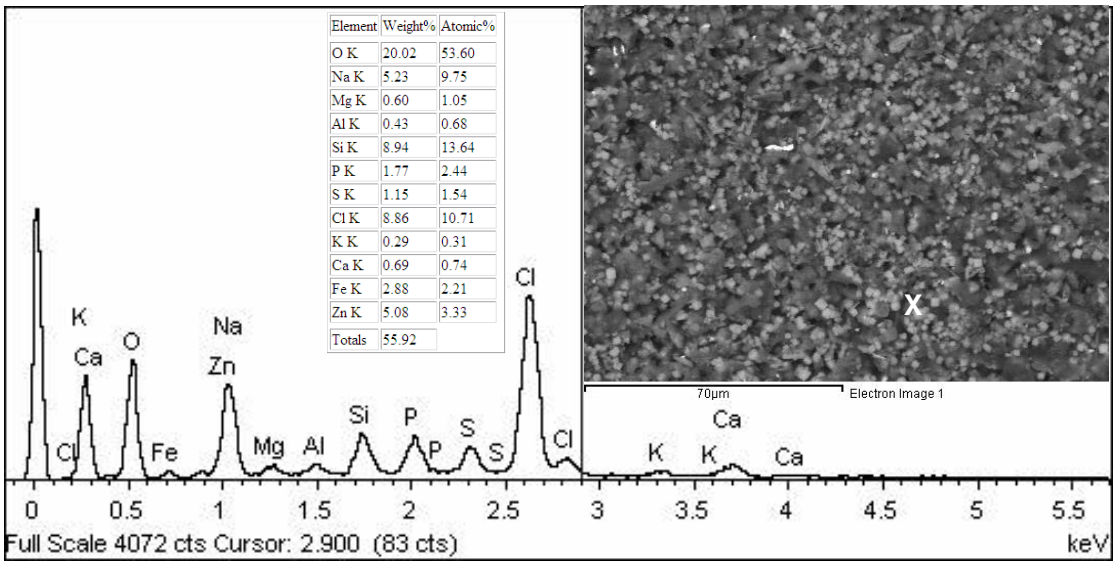

(d)

Figure 5-21: SEM/EDS analysis on bedroom sampling Stage 3 at 70 µm

Figure 5-21 shows the SEM/EDS analysis of the bedroom sampling at 70 µm. The mark in red is the location and size of the beam when the particles were subjected to EDS analysis. The particle marked "X" in Figure 5-21(a) shows high amounts of Si (51.39% atomic weight) and O (27.38% atomic weight). This particle is most likely to be silicon dioxide (SiO_2). SiO_2 is commonly found in nature as sand (silica). Thus, it was believed that this particle was from the outdoor environment. This particle would enter the bedroom through the window which was opened once while the bedroom was occupied by someone before the experiment was conducted.

The particle marked "X" in Figure 5-21(b) shows high amounts of O (29.40% atomic weight), Na (27.56% atomic weight) and Si (10.15% atomic weight). The elemental contents of this particle suggest that it is either SiO_2 or albite. Albite is a plagioclase feldspar mineral which is white in colour and consists of Na in its compound (Anthony *et al.*, 2011). The particle in Figure 5-21(b) is white in colour. This further confirmed that the particle is albite. Both SiO_2 and albite are widely present in the natural environment.

The particle marked "X" in Figure 5-21(c) has high amounts of O (58.05% atomic weight) and Si (22.02% atomic weight). The combination of Si and O suggested that the particle is SiO_2. The particle marked "X" in Figure 5-21(d) also shows high amounts of O (53.60% atomic weight) and Si (13.64% atomic weight). Thus, this particle is SiO_2 as well.

Since the elemental contents for the particles in Figure 5-21 are similar, it can be concluded that all other particles are about the same. Most of them are sand which is easily found in the outdoor environment. This sample also gave small amounts of Fe and Zn. The Fe originated either from the abrasion disc brakes or from vehicle rust since the sample was collected from a location near to busy road traffic. Brake dust is gradually ground off the brake pads when a braking force is applied. The rust was formed when iron reacted with oxygen due to high moisture contents in the atmosphere.

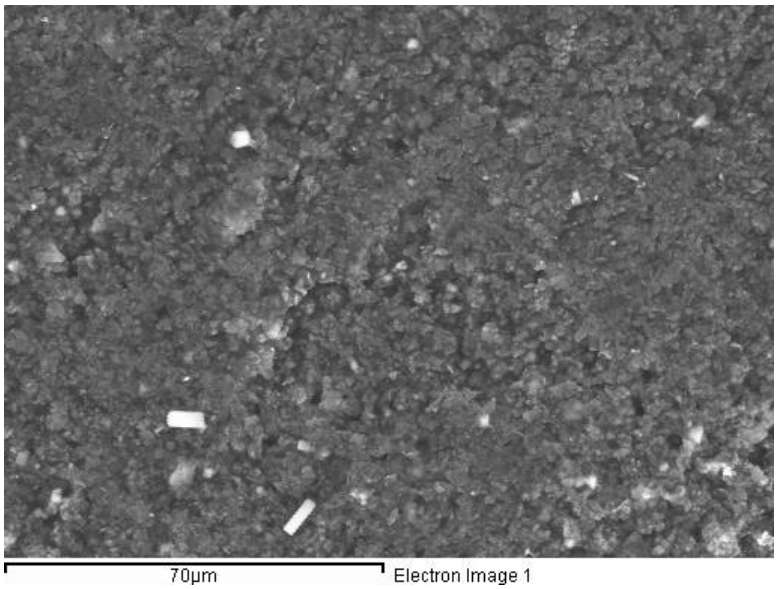

(a)

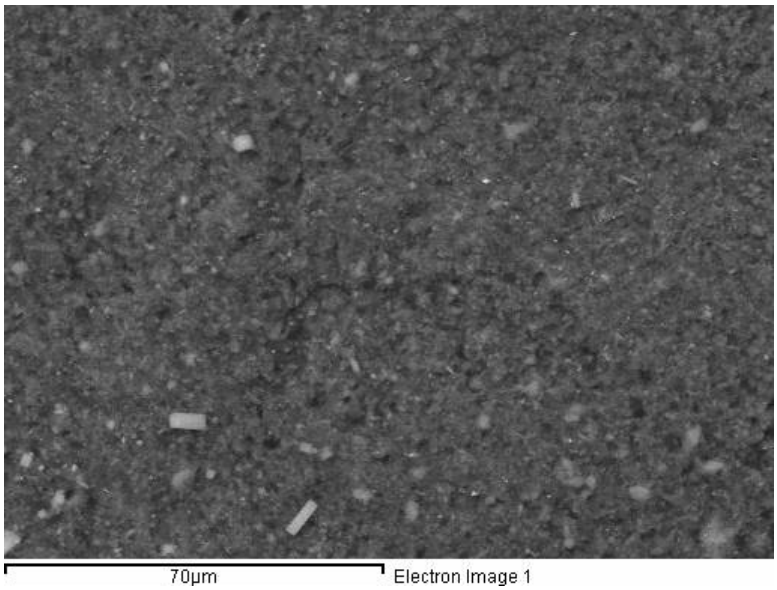

(b)

Figure 5-22: SEM/EDS images captured using (a) secondary electron mode; and (b) back-scattered mode (Bedroom sampling, Stage 5)

Figure 5-22(a) shows the SEM/EDS images captured using secondary electron mode and Figure 5-22(b) was captured by using back-scattered mode. The elemental contents for the particles in Figure 5-22 were further analysed by using EDS and shown in Figure 5-23.

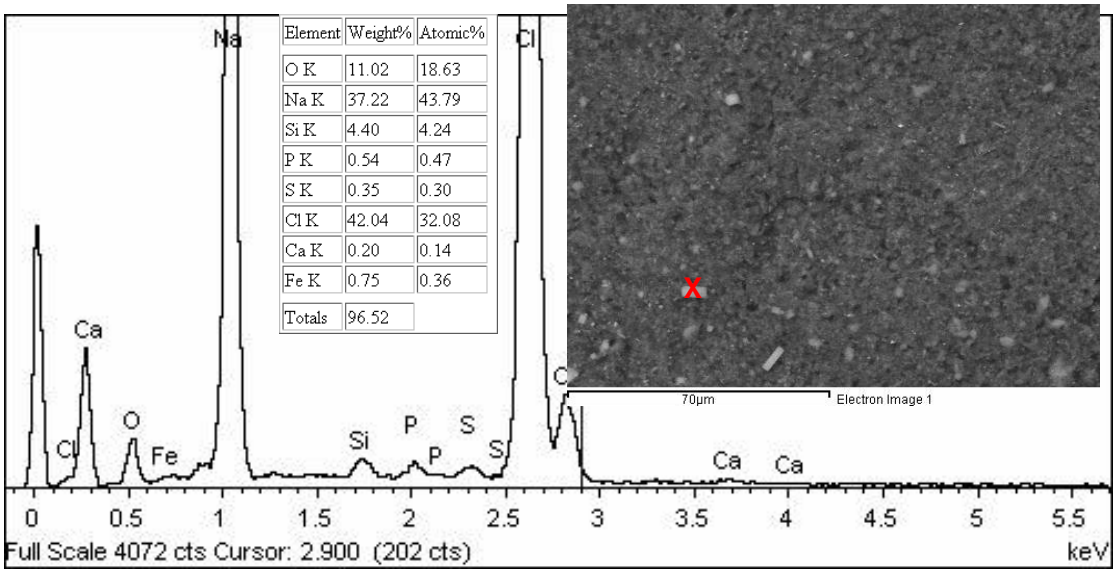

(a)

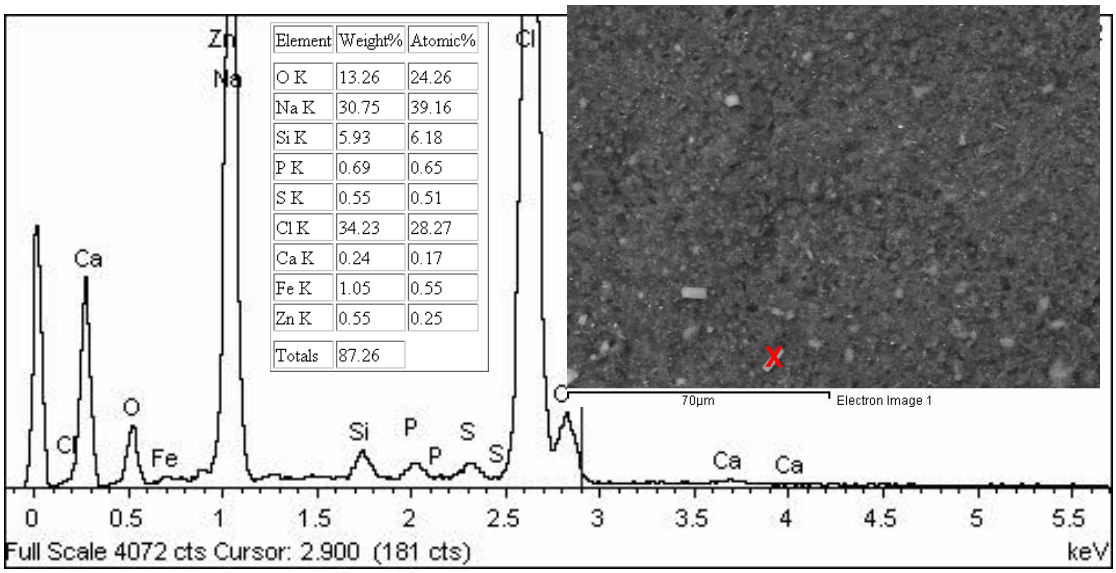

(b)

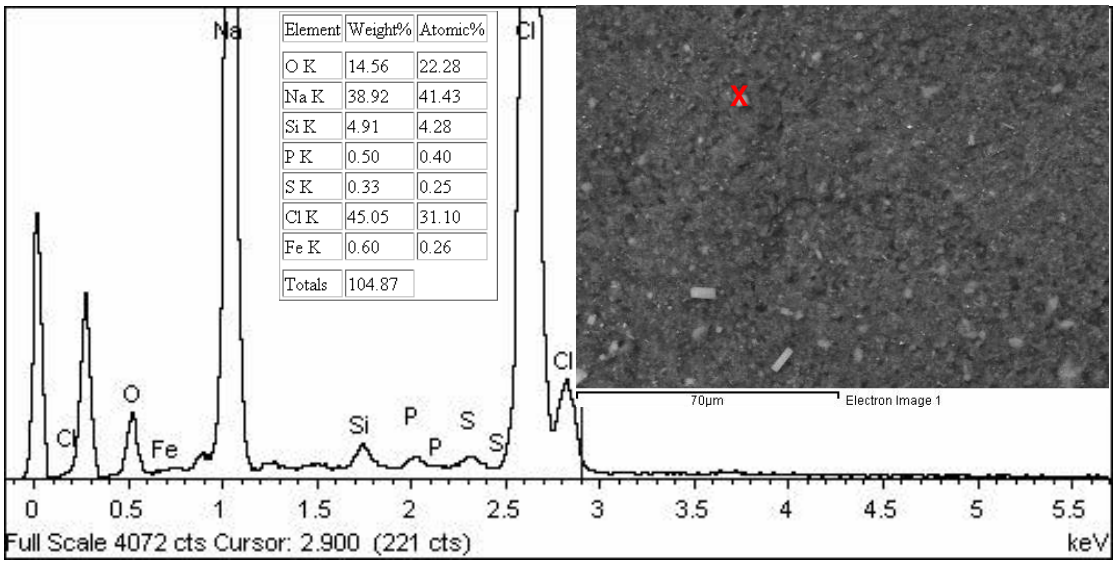
Element Weight% Atomic%
O K 14.56 22.28
Na K 38.92 41.43
Si K 4.91 4.28
P K 0.50 0.40
S K 0.33 0.25
Cl K 45.05 31.10
Fe K 0.60 0.26
Totals 104.87
Na
Cl
O
Fe
Si
P
S
70µm
Electron Image 1
Full Scale 4072 cts Cursor: 2.900 (221 cts)
keV

(c)

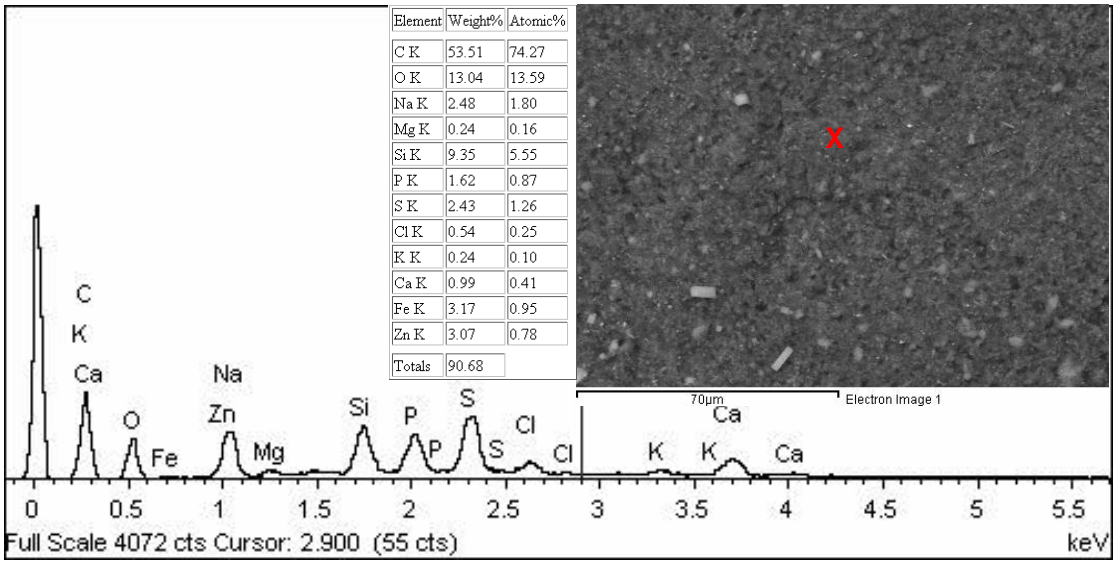
Element Weight% Atomic%
C K 53.51 74.27
O K 13.04 13.59
Na K 2.48 1.80
Mg K 0.24 0.16
Si K 9.35 5.55
P K 1.62 0.87
S K 2.43 1.26
Cl K 0.54 0.25
K K 0.24 0.10
Ca K 0.99 0.41
Fe K 3.17 0.95
Zn K 3.07 0.78
Totals 90.68
C
K
Ca
Na
Zn
O
Fe
Mg
Si
P
S
Cl
K
Ca
70µm
Electron Image 1
Full Scale 4072 cts Cursor: 2.900 (55 cts)
keV

(d)

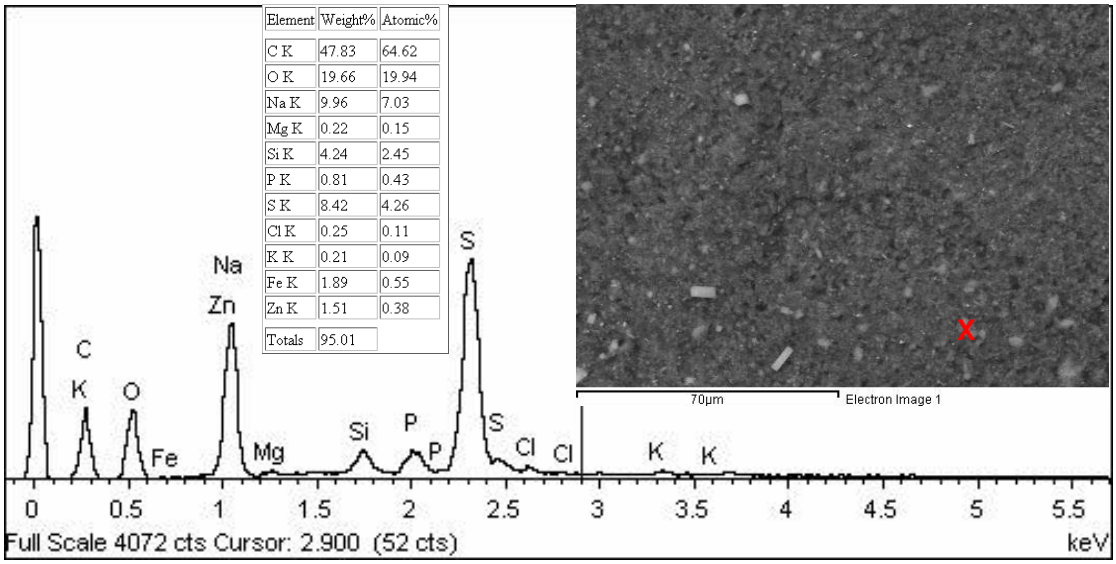
Element Weight% Atomic%
C K 47.83 64.62
O K 19.66 19.94
Na K 9.96 7.03
Mg K 0.22 0.15
Si K 4.24 2.45
P K 0.81 0.43
S K 8.42 4.26
Cl K 0.25 0.11
K K 0.21 0.09
Fe K 1.89 0.55
Zn K 1.51 0.38
Totals 95.01
C
K
O
Fe
Na
Zn
Mg
Si
P
S
Cl
K
70µm
Electron Image 1
Full Scale 4072 cts Cursor: 2.900 (52 cts)
keV

(e)

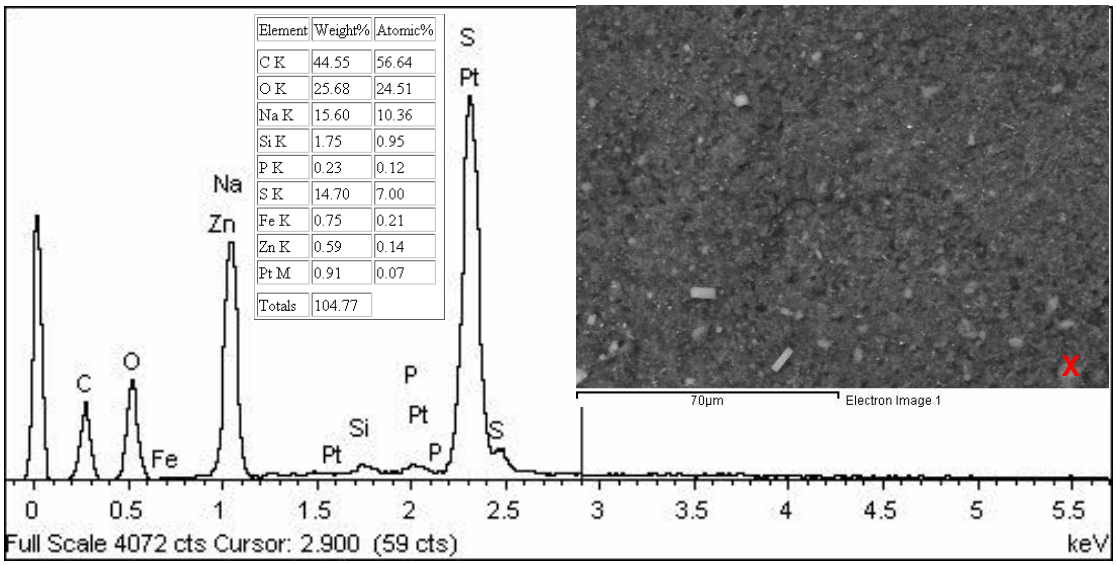

(f)

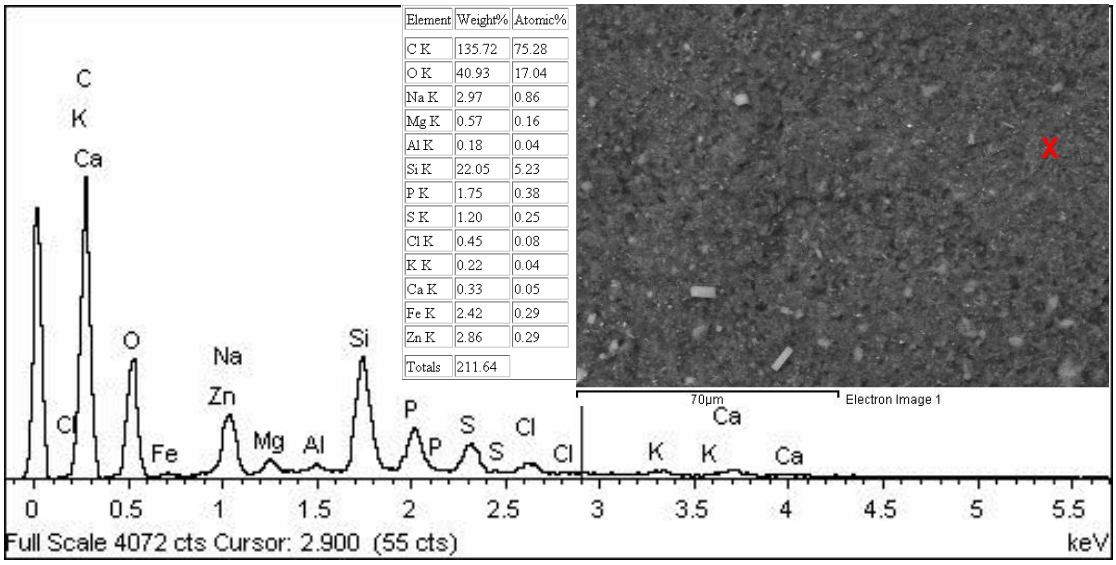

(g)

Figure 5-23: SEM/EDS analysis for bedroom sampling Stage 5 at 70 µm

Figure 5-23 shows the SEM/EDS analysis for bedroom sampling at 70 µm. The particle marked "X" in Figure 5-23(a) shows high amounts of Na (43.79% atomic weight) and Cl (32.08% atomic weight). The cube-like particle structure suggests that it is a salt crystal. Again, this particle is most likely to be from road gritting. This result was expected as the sample was collected during winter. Grit salt is widely used in this season.

The particle marked "X" in Figure 5-23(b) is similar to particle in Figure 5-23(a). EDS analysis confirmed that both of these particles have the same surface structures and characteristic compositions, except that the particle in Figure 5-23(b) contains a minor amount of zinc (0.25%

atomic weight). The elements like Na (39.16% atomic weight) and Cl (28.27% atomic weight), which form salt crystals also exist here.

EDS analysis was then performed on the particle which showed significant metallic concentrations. The particle was marked as "X" in Figure 5-23(c). It is a spherical particle with the same colour as particles in Figures 5-23(a) and (b). Although this particle has a different shape compared to the particle in Figure 5-23(a), their element contents were similar, except that the particle in Figure 5-23(c) lacked Ca.

The particle marked "X" in Figure 5-23(d) is completely different from the particles shown in Figures 5-23(a), (b) and (c). This particle shows high amounts of C (74.27% atomic weight) and O (13.59% atomic weight). These elements originate from carbonaceous fuel due to incomplete combustion in a vehicle engine. The main source of these particles is diesel-operated vehicles (e.g. trains, trucks, etc.) in this case. The main derivatives of the incomplete combustion process are carbon monoxide (CO) and soot that could lead to vascular dysfunction, especially for particles released from diesel-operated vehicles (Tomqvist *et al.*, 2007).

The particle marked "X" in Figure 5-23(e) shows an amorphous looking surface which could either be carbonaceous or biological. Upon EDS analysis, this particle gave a high amount of C (64.62% atomic weight). Apart from that, it also had a high amount of SiO_2 (19.94% O and 2.45% Si). Thus, it is confirmed that this particle is a carbonaceous particle probably covered with silica. This means that the particle originated from vehicle combustion, but mixed with silica during the particle transmission process. S (4.26% atomic weight) originated from fuel combustion. This result was expected as the sampling location is close to busy traffic. This type of particle can easily enter into the bedroom through the window or door gap.

The particle marked "X" in Figure 5-23(f) shows high amounts of C (56.64% atomic weight), O (24.51% atomic weight), Na (10.36% atomic weight) and S (7% atomic weight). Apart from these few elements, this particle also shows a low amount of Pt (0.07% atomic weight). The platinum originated from either fine wire, as Pt acts as an alloying agent, vehicle catalysts or electrical contacts and jewellery.

The particle marked "X" in Figure 5-23(g) shows high amounts of C (75.28% atomic weight) and O (17.04% atomic weight). Thus, it can be concluded that this particle is a

carbonaceous particle from incomplete combustion, especially from diesel-operated vehicles. EDS analysis was performed on this particle, however it did not give any significant information to suggest any metallic concentrations.

5.2.1.4 Summary of Findings

The results of the PM tests to collect and determine the size distribution (Andersen Sampler), morphology (SEM/EDS) and chemical composition (ICP-OES) of particulate matter in the bedroom can be summarised as follows:

(i) Approximately 30% of particles collected were 1.1 – 2.1µm,
(ii) The majority of the particles were composed mainly of Fe, Na, Zn and S,
(iii) The particles found were salt crystals, mineral fibres and skin flakes. Others were rust compounds from vehicles, brakepad wear and from high temperature sources.

5.2.2 Kitchen

Figure 5-24 illustrates the kitchen conditions inside the chosen house for the installation of the Andersen Sampler. The kitchen has an estimated volume of 70 m^3. As shown in Figure 5-24, there is an electric cooker installed in the kitchen, which is used once or twice a day (around 1.5 hours each time).

Figure 5-24: Kitchen worktop and appliances

As shown in Figure 5-25, the sampler was placed on top of a cupboard at a height of about 1.5m from the floor. The sampler was placed in the sampling location for about 4 weeks.

Sampling started on 23/03/2009 at 10.30am and ended on 21/04/2009 at 8.35am, which is equal to approximately 718 hours.

Figure 5-25: The Andersen Sampler was placed about 1.5m from floor level

5.2.2.1 Particle Size Distribution

Table 5-2 shows the concentration of particles collected from each stage. 15.7mg of particulate matter was collected from the kitchen. The concentrations of $PM_{2.5}$ and PM_{10} were 7.95µg/m^3 and 12.87µg/m^3 respectively. From Figure 5-26, it can be seen that approximately 25% of the particulate matter collected from the kitchen were within the range of 1.1-2.1µm. In general, larger particles do not stay in the atmosphere. Therefore, these results were expected. The major source of these particles can be attributed to cooking activities, for example using the stove and burnt food, as well as other common household activities, like cleaning.

Table 5-2: The concentrations of particles collected from each stage (Kitchen)

Stage	Mass Size Distribution (µm)	PM (mg)	Concentration (µg/m^3)	%
0	9.0-10	1.2	0.98	8
1	5.8-9.0	1.2	0.98	8
2	4.7-5.8	0.6	0.49	4
3	3.3-4.7	1.5	1.23	10
4	2.1-3.3	1.5	1.23	10
5	1.1-2.1	4.0	3.29	25
6	0.7-1.1	2.3	1.89	15
7	0.4-0.7	1.2	0.98	8
Filter	0-0.4	2.2	1.80	14
Total		15.7	12.87	100
Test time		43,085mins (≈718hours)		
Air volume (m^3)		1220.04		
$PM_{2.5}$ concentration (µg/m^3)		7.95		
PM_{10} concentration (µg/m^3)		12.87		

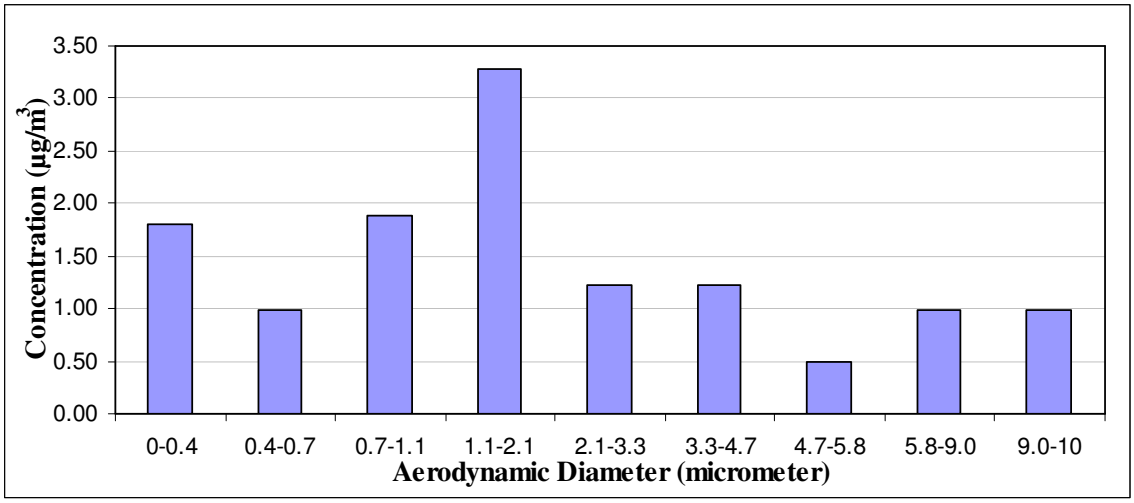

Figure 5-26: Particle size distribution for kitchen sampling

5.2.2.2 Full Elemental Analysis

Figure 5-27 presents the elemental composition for particles collected from the kitchen. The samples were mainly composed of Si, Na, B and Ca. These were generated from a range of

different sources, including various cooking activities or the ingression of pollutants from outdoor sources.

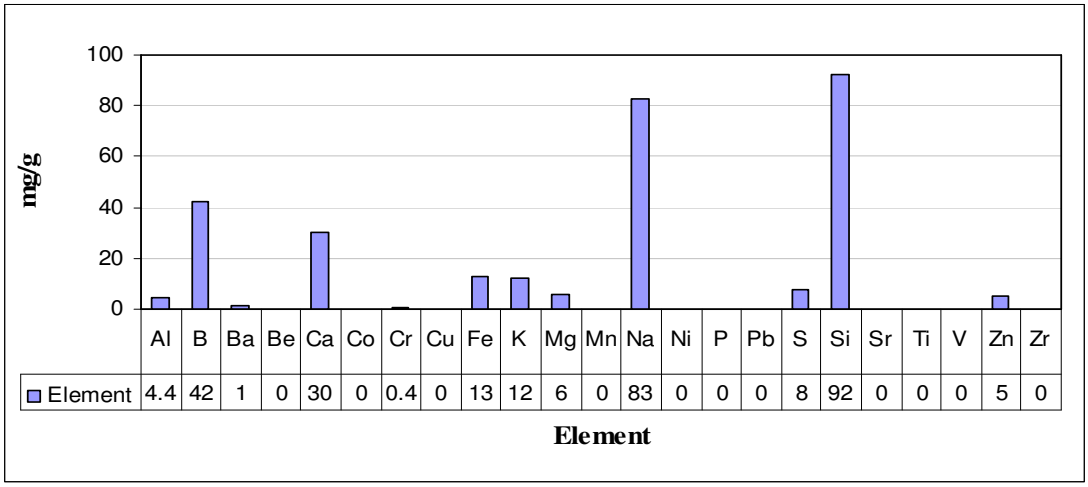

Figure 5-27: Element contents for kitchen sampling

5.2.2.3 Morphology Analysis

SEM/EDS was used to determine the morphology of individual particles. The particles collected were mainly comprised of Ca, C, O, Si, Fe, S, K, Na, Cl, Mg and B.

Stage 0 (9.0 – 10 µm):

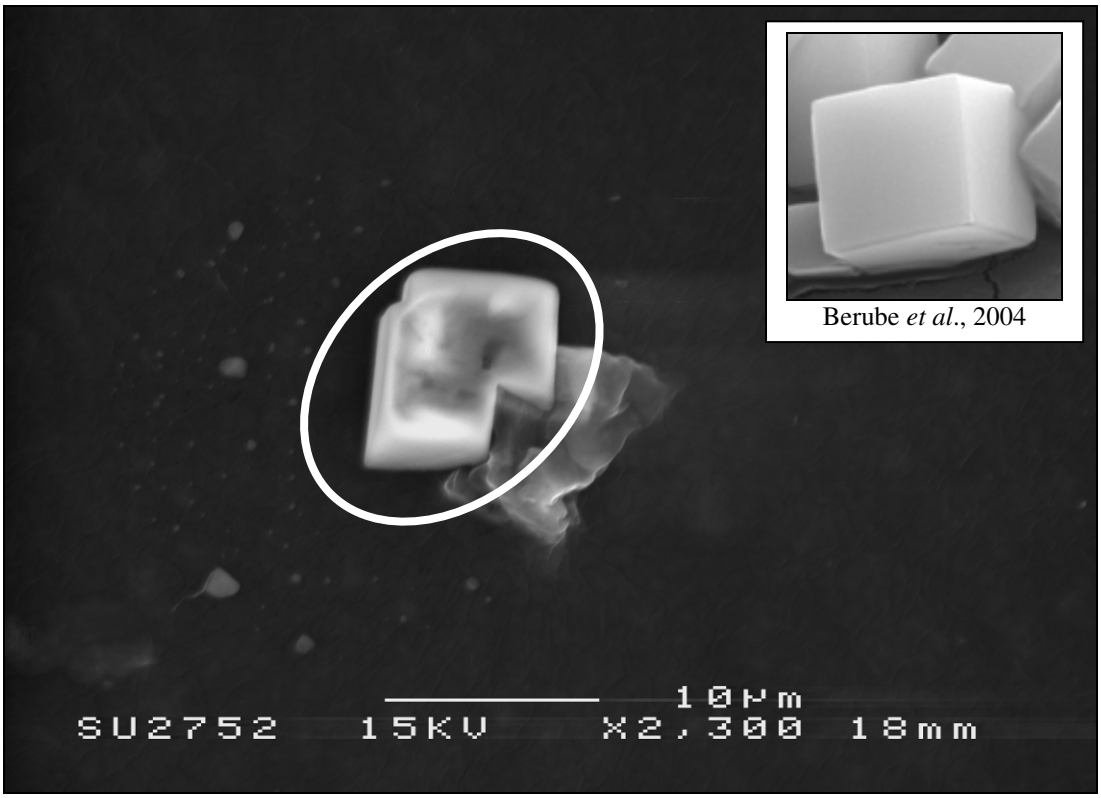

Figure 5-28: SEM image of PM at 10µm from Stage 0 (9.0 - 10µm)

In Figure 5-28, the particle of interest is marked with a circle. The particle is approximately 10µm in length with a cubic shape. The morphology of this particle suggests that it was salt crystal or salt related particle (Berube *et al.*, 2004). The smooth area in the middle of the particle was subjected to EDS analysis and the results showed high amounts of Na and Cl. The elemental composition also reaffirmed that the particle contains high amounts of Na and Cl. The particle is likely to be from cooking activities as a large amount of salt particles could easily melt due to high cooking temperatures. However, it will recrystallise when the temperature drops. It will then form a smaller particle and spread elsewhere in the kitchen.

Stage 0 (9.0 – 10 µm):

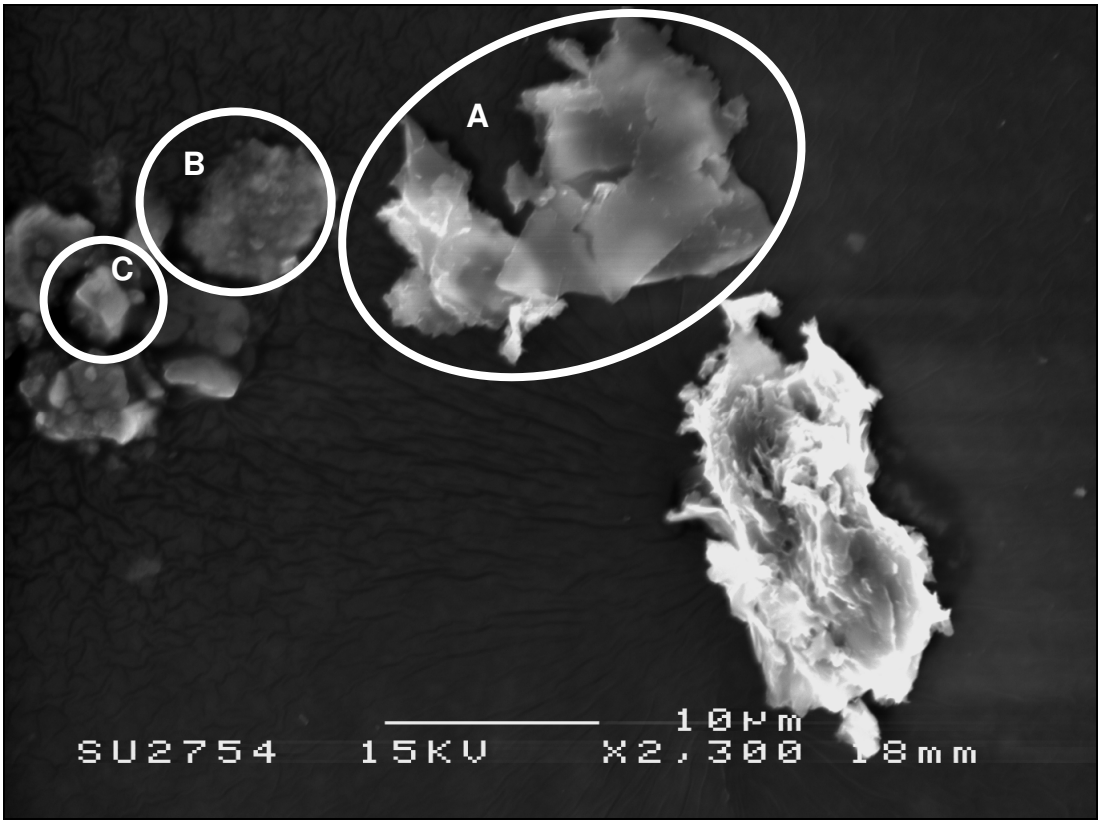

Figure 5-29: SEM image of PM at 10µm from Stage 0 (9.0 - 10µm)

In this stage (Stage 0), most of the particles observed were larger than 10µm although the pre-separator was used to prevent particles with aerodynamic diameter greater than 10µm from entering the instrument. The possible reason was the accumulation of smaller particles within the moist environment to produce larger particles, e.g. Particle A, as shown in Figure 5-29.

Particle A is a plate-like particle with high luminosity. The particle is greater than 10µm in size with an irregular shape. The morphology of this particle suggests that the particle

originated from high temperature sources. EDS analysis was conducted on Particle A and it gave a high count of C. The surface texture of this particle showed more indication of layering effects rather than particle accumulation.

Particle B in Figure 5-29 is approximately 8µm in size with an irregular shape. EDS analysis confirmed that Particle B was mainly composed of Fe and O. This particle was rust or a product of brake wear.

Particle C was detected containing high amounts of C and O with lower amounts of Ca and Si. The diameter of this particle is around 3µm with an unsmooth surface texture. The elemental composition suggests that the particle was either a mixture of $CaCO_3$ and SiO_2 fused together or the particle was growing at high relative humidity.

Stage 1 (5.8 – 9.0 µm):

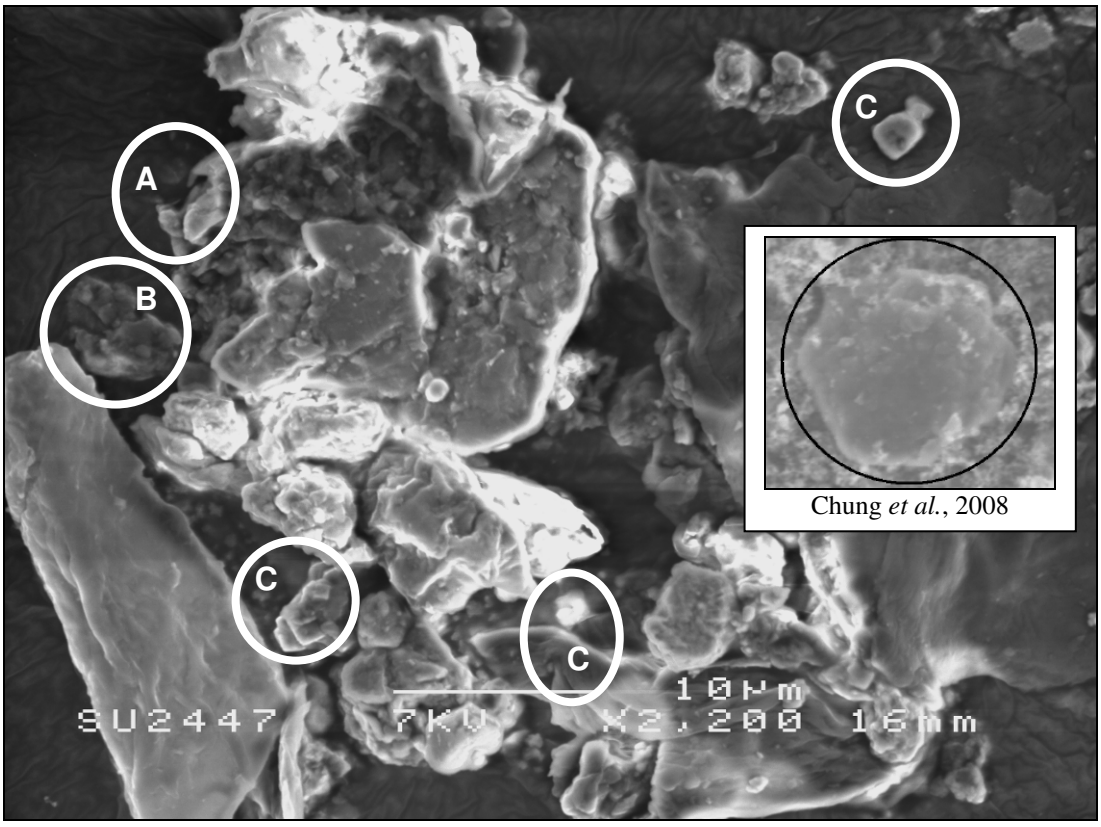

Figure 5-30: SEM image of PM at 10µm from Stage 1 (5.8 – 9.0µm)

In Figure 5-30, the particles of interest are marked with several circles. Particle A is irregular in shape with a smooth surface. The round edge of the particle suggests that it was formed during a high temperature process. As reported by Lai and Ho (2008), a large amount of

smoke fumes could easily be generated from oil due to high cooking temperatures and cooking practice. The fumes nucleate and will then form ultrafine particles inside the kitchen.

Particle B featured in Figure 5-30 appears to be a cluster of irregularly shaped particles accumulated together. The morphology of these suggests that they were dust components (Chung *et al.*, 2008).

Particles C in Figure 5-30 are approximately 1-2µm in length with a cubic shape. The morphology of these particles suggests that they were salt crystals or salt related particles. The formation of these particles was a result of moisture accumulating on a high concentration salt area. All the particles C shown in Figure 5-30 were confirmed by EDS analysis and the results showed a high amount of Cl. These particles originated from table salt since the samples were collected from the kitchen.

Stage 1 (5.8 – 9.0 µm):

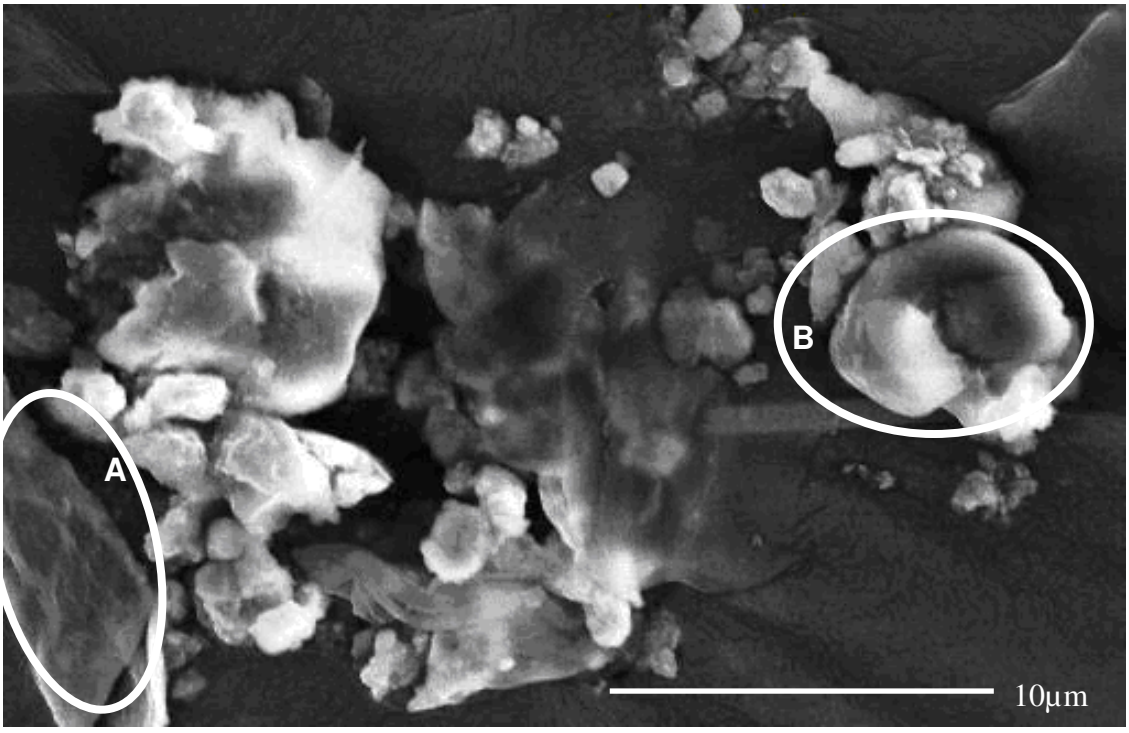

Figure 5-31: SEM image of PM at 10µm from Stage 1 (5.8 – 9.0µm)

Particle A in Figure 5-31 is a cluster of angular particles accumulated together. EDS results for the featured particles gave high amounts of C and O and a low amount of P. The morphology and elemental composition suggest that it originated from a high temperature process.

Particle B is a round-edged particle with smooth surface. The diameter of this spherical particle is about 5µm. The morphology of this particle suggests that it originated from high temperature sources. EDS analysis on this particle gave high amounts of C and O.

Both particles A and B originated from burned food since the particles were collected from the kitchen. Most coarse particles are generated by frying and spattering processes during cooking (Lai and Ho, 2008).

Stage 2 (4.7 - 5.8 µm):

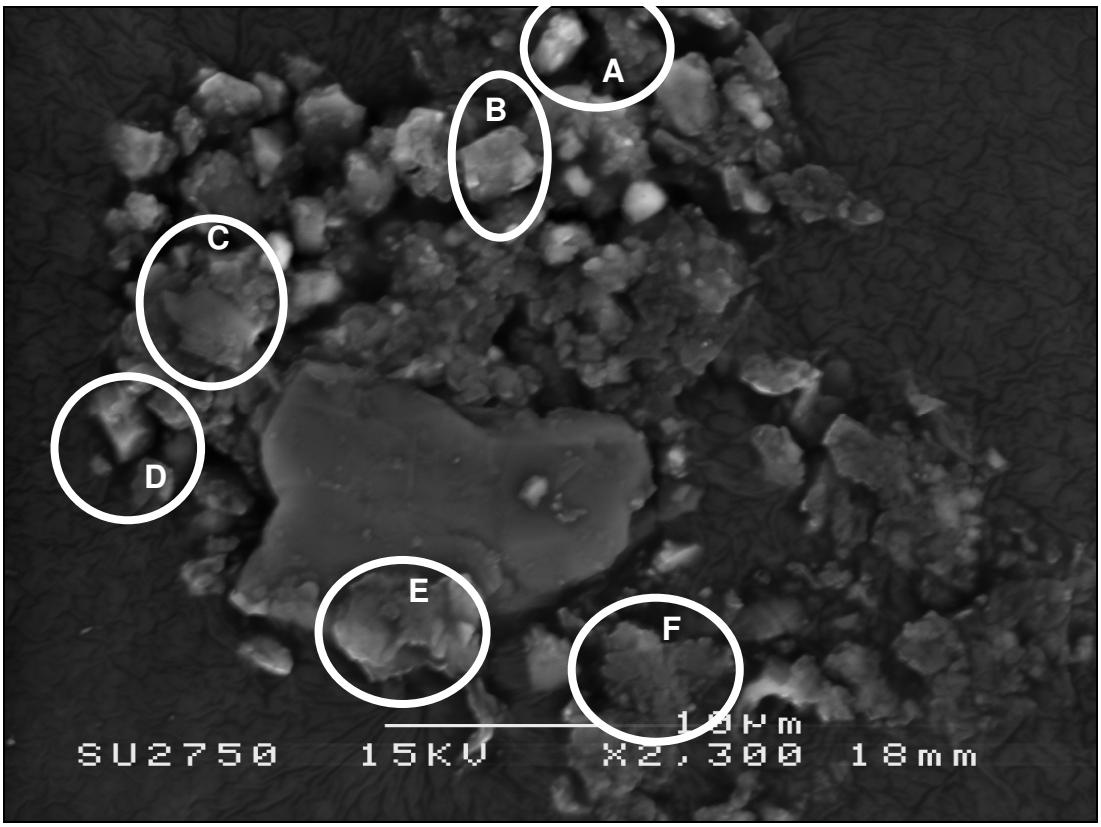

Figure 5-32: SEM image of PM at 10µm from Stage 2 (4.7 - 5.8µm)

Particle A in Figure 5-32 appears to be a large number of accumulated particles. It did not provide a clearer surface image although increased magnification was used. The particle has an irregular shape with a semi-transparent appearance. This particle is mainly composed of O with a low amount of Mg. This originated from the substrate, however the surface morphology suggests otherwise.

Particle B is a cubic particle, 2-3µm in length. The morphology of this particle suggests that it was a salt crystal or salt related particle. Particle C gave high amounts of Si, Ca and O

under EDS analysis. The EDS analysis on Particle D found in Figure 5-32 gave high amounts of Ca and O. Both of these plate-like particles, C and D, were generated from high temperature sources. Particle E was mainly composed of B (boron). Boron is a component of fibreglass insulation. Particle F has an irregular shape with an accumulation of finer particles on top of its surface structure. This suggests that it was a dust component.

Stage 3 (3.3 – 4.7 µm):

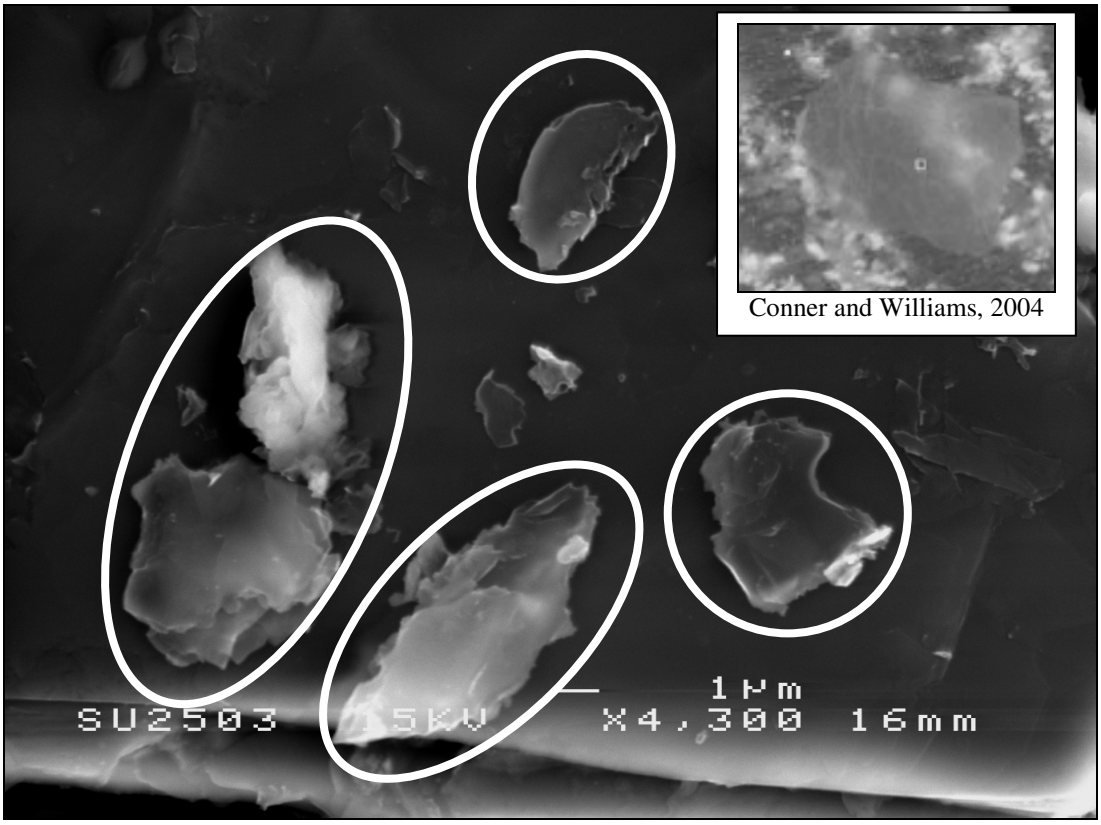

Figure 5-33: SEM image of PM at 1µm from Stage 3 (3.3 – 4.7µm)

All the particles subjected to EDS analysis are marked with a circle, as shown in Figure 5-33. Particles in Figure 5-33 are plate-like particles with smooth surface. All these particles vary in size, which range from 4µm to greater than 10µm. Each of these plate-like particles is surrounded by an irregular edge. The particles are semi-transparent in appearance. EDS analysis on these particles gave high amounts of C and O and moderate amounts of Mg and Si. The morphology of these particles suggests that they were skin flakes (Conner and Williams, 2004).

Stage 4 (2.1 – 3.3 µm):

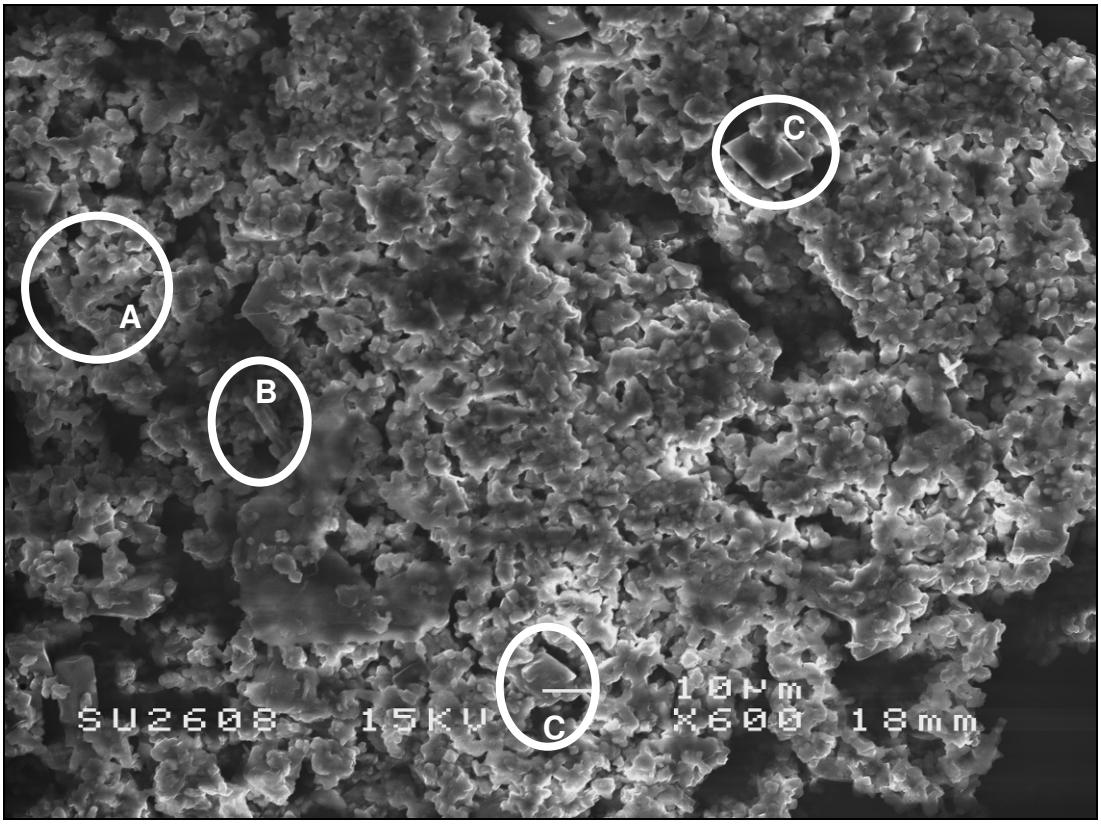

Figure 5-34: SEM image of PM at 10µm from Stage 4 (2.1 – 3.3µm)

Particle A in Figure 5-34 is cubical in shape and approximately 1-2µm in length. Upon analysis with EDS, the highest amount registered was Si, followed by S, Cl and Ca. Particle B in Figure 5-34 is a fibre-shaped particle of several microns. It was either a mineral fibre from outdoors or a textile fibre from indoors.

Particles C retain an angular structure, such as a solid cube or cuboid. The particle is approximately 1–2µm in length. The darker region of the particle is the deeper part of the particle. The morphology of this particle suggests that it was a salt crystal. Upon EDS analysis, it was confirmed that these particles have high amounts of Na and Cl.

Stage 5 (1.1 – 2.1 µm):

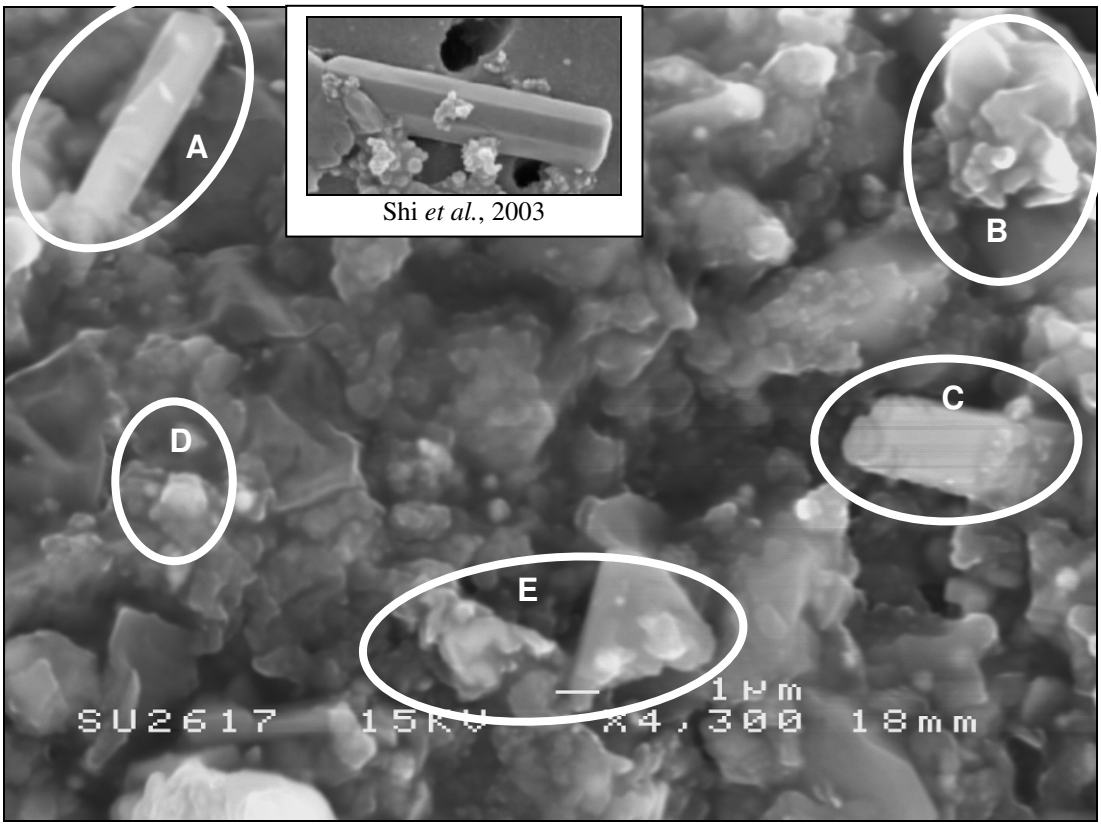

Figure 5-35: SEM image of PM at 1µm from Stage 5 (1.1 – 2.1µm)

Particle A in Figure 5-35 is a rod-like particle, several microns in length. The elongated particle has a smooth surface with slight luminosity. EDS analysis on this rod-like particle gave a high amount of O and moderate amounts of Na, S, Ca and K. This particle was formed by secondary atmospheric reactions (Shi *et al.*, 2003).

Particle B is an irregularly shaped particle with a smooth surface. This particle was generated from high temperature sources. EDS analysis confirmed that the particle has high amounts of C and O.

Particle C is a particle of 4–5µm in length. The rectangular shape of this particle suggests that it is a salt related particle. Upon EDS analysis, it was confirmed that the particle gave high amounts of Na and Cl. Particle D was mainly comprised of B and O. Similar to Particle B, Particle E has a smooth surface, with an irregular shape. EDS analysis gave a high elemental composition of C and O.

Stage 6 (0.7 – 1.1 µm):

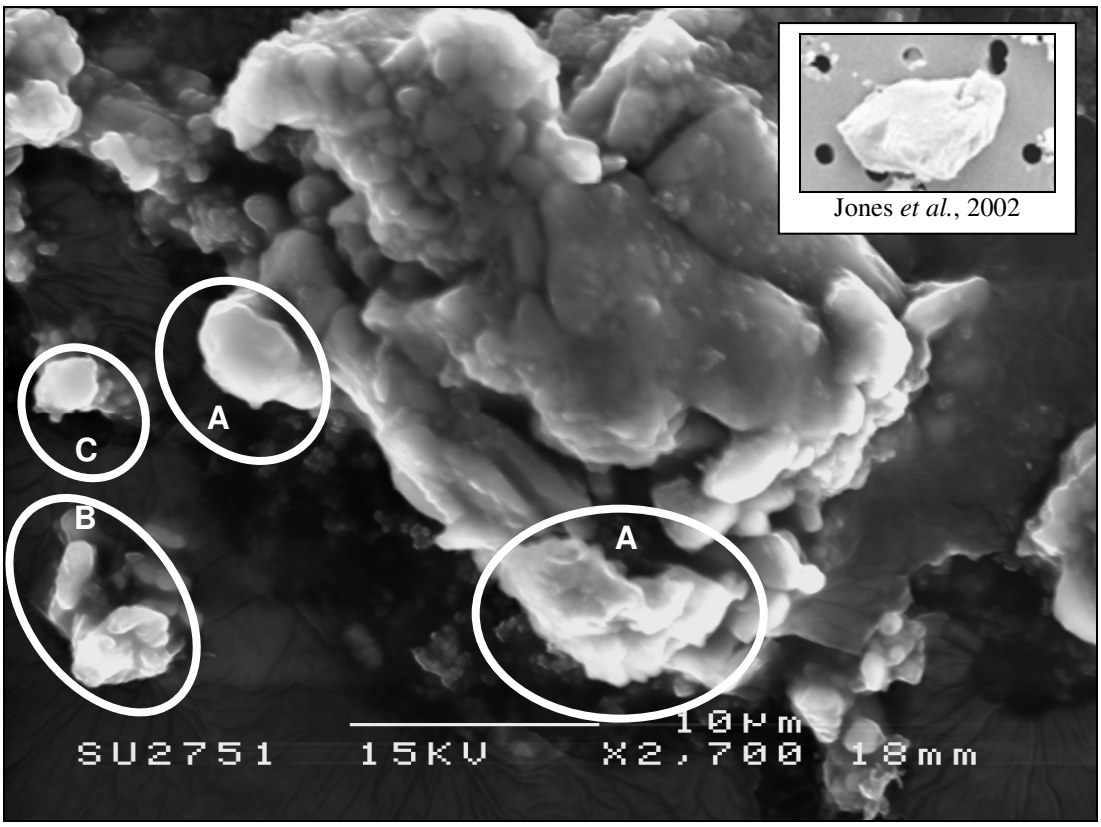

Figure 5-36: SEM image of PM at 10µm from Stage 6 (0.7 – 1.1µm)

Particles A in Figure 5-36 are approximately 3–10µm in size. The particle size varies due to the accumulation of finer particles. These particles have smooth surfaces and with a semi-transparent appearance. The morphology of these particles suggests that they were mineral grains (Jones *et al.*, 2002). The EDS results gave high concentrations of O and Mo with a low amount of K. Upon EDS analysis, particle B has a high amount of O, a moderate amount of S and minimal amounts of Na and Ca. As for Particle C, it gave a high amount of B (boron) and slightly smaller amounts of S and O.

Stage 7 (0.4 – 0.7 µm):

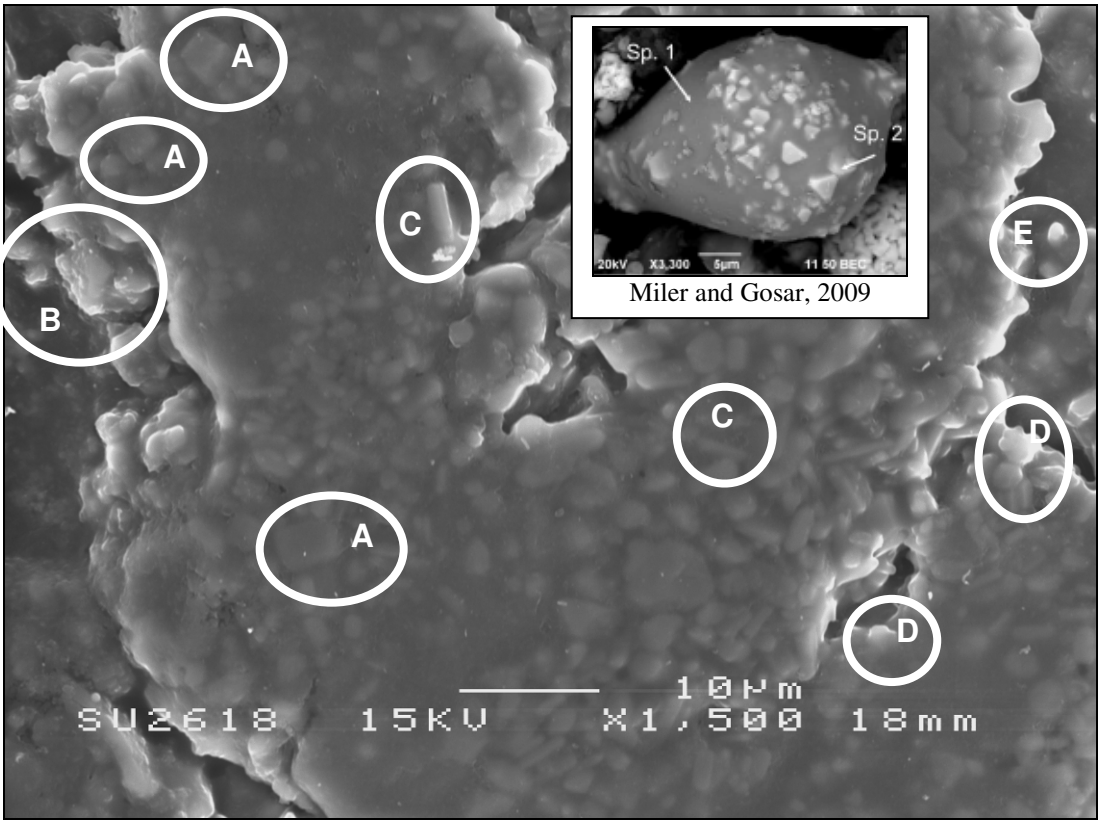

Miler and Gosar, 2009

Figure 5-37: SEM image of PM at 10µm from Stage 7 (0.4 – 0.7µm)

Particles A in Figure 5-37 were detected to have high amounts of Na and Cl with a low amount of K. This is very similar to the other cubical particles found in earlier stage. The morphology of these particles and EDS analysis confirmed that they were salt crystals or salt related particles.

As for Particle B, the morphology suggests that it originated from high temperature sources (Miler and Gosar, 2009). The particle has a smooth surface and is spherical in shape.

Particles C have a rod-like shape, several microns length. Upon EDS analysis, Particles C gave high concentrations of C and O and with lower concentration of S. The rod-like particles are very similar to the other rod-like particles found in earlier stages. These particles were mineral fibres or textile fibres generated from different sources.

Similar to Particle B, Particle D has a smooth surface and with a semi-transparent appearance. The morphology of this particle suggests that it was generated from high temperature sources. EDS analysis was performed and it gave significant amounts of C and O. EDS analysis

was also performed on Particle E and the results gave an extremely high concentration of B (boron).

5.2.2.4 Summary of Findings

The results of PM tests to collect and determine the size distribution (Andersen Sampler), morphology (SEM/EDS) and chemical composition (ICP-OES) of particulate matter in the kitchen are summarised as follows:

(i) Approximately 25% of particles collected were 1.1 – 2.1µm,
(ii) The majority of the particles were mainly composed of B, Ca, Na and Si,
(iii) The particles were mainly salt crystals, mineral fibres and grains, skin flakes and dust components. Others were the result of stove use, burned food, high cooking temperatures and other common household activities.

5.2.3 Lounge

Figure 5-38 illustrates the lounge conditions inside the chosen house for the installation of the Andersen Sampler. The size of the lounge is 18 x 12 ft. The house owners normally have their breakfast in the lounge.

Figure 5-38: The conditions inside the lounge

As shown in Figure 5-39, the sampler was placed on top of a chair at a height of about 0.8m from the floor. The sampler was placed in the sampling location for about 4 weeks.

Sampling started on 18/07/2009 at 9.00am and ended on 18/08/2009 at 3.00pm, which is equal to approximately 750 hours.

Figure 5-39: The Andersen Sampler was placed about 0.8m from floor level

5.2.3.1 Particle Size Distribution

Table 5-3 shows the concentration of particles collected from each stage. 13.8mg of particulate matter was collected from the lounge. The concentrations of $PM_{2.5}$ and PM_{10} were 4.16µg/m^3 and 10.84µg/m^3 respectively. From Figure 5-40, it can be seen that approximately 17% of the particulate matter collected from the lounge were within the range of 3.3-4.7µm. In general, larger particles do not stay in the atmosphere for a long period of time. Therefore, these results were expected. The major sources of these particles were attributed to the car porch, which is located near the lounge. They were either a result of brake abrasion or rust compounds from vehicles from nearby transportation. Other possible sources include ventilation of outdoor air and other common household activities.

Table 5-3: The concentrations of particles collected from each stage (Lounge)

Stage	Mass Size Distribution (µm)	PM (mg)	Concentration (µg/m^3)	%
0	9.0-10	1.3	1.02	9
1	5.8-9.0	2.2	1.73	16
2	4.7-5.8	1.0	0.79	7
3	3.3-4.7	2.4	1.89	17
4	2.1-3.3	1.6	1.26	13
5	1.1-2.1	1.3	1.02	9
6	0.7-1.1	1.5	1.18	11
7	0.4-0.7	0.5	0.38	4
Filter	0-0.4	2.0	1.57	14
Total		13.8	10.84	100
Test time		44,950mins (≈750hours)		
Air volume (m^3)		1272.85		
$PM_{2.5}$ concentration (µg/m^3)		4.16		
PM_{10} concentration (µg/m^3)		10.84		

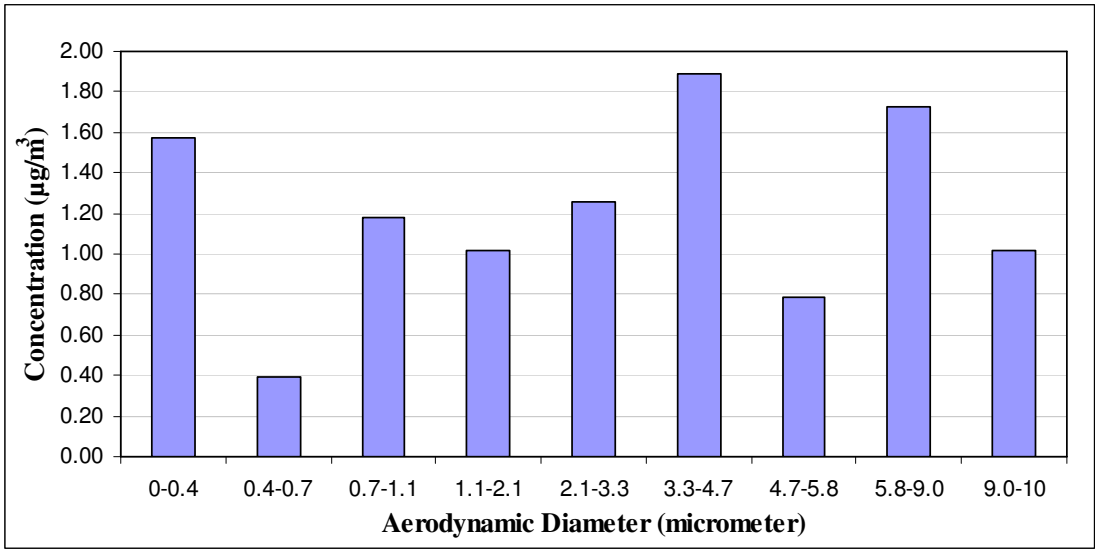

Figure 5-40: Particle size distribution for lounge sampling

5.2.3.2 Full Elemental Analysis

Figure 5-41 presents the elemental composition for particles collected from the lounge. The samples were mainly composed of Fe, Ca and Zn. They could arise from combustion and

brakepad wear from vehicles as the lounge is located near the car porch. However, they could be generated from other indoor or outdoor sources.

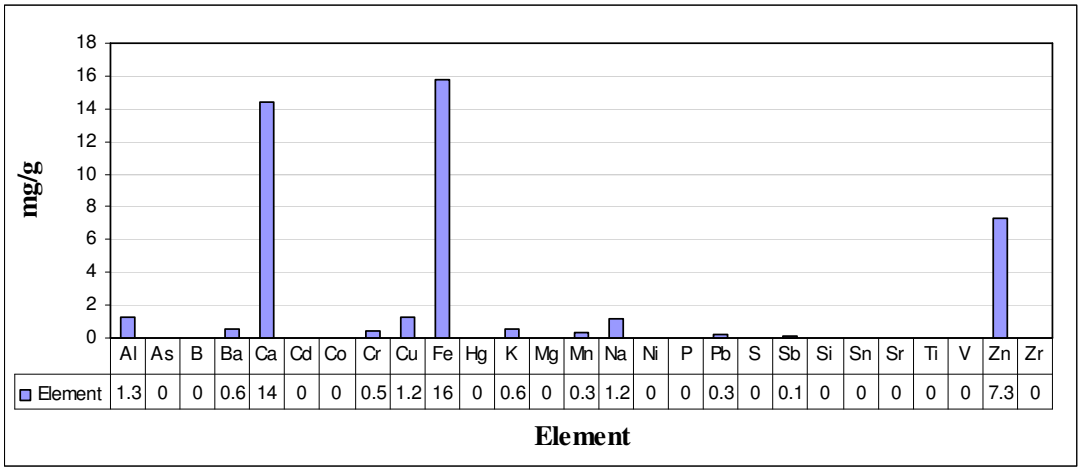

Figure 5-41: Element contents for lounge sampling

5.2.3.3 Morphology Analysis

The morphology of individual particles was determined by using SEM/EDS. These particles were mainly comprised of Ca, Na, C, O, P, Si, Fe, Zn, S and Cl.

Stage 0 (9.0 – 10 µm):

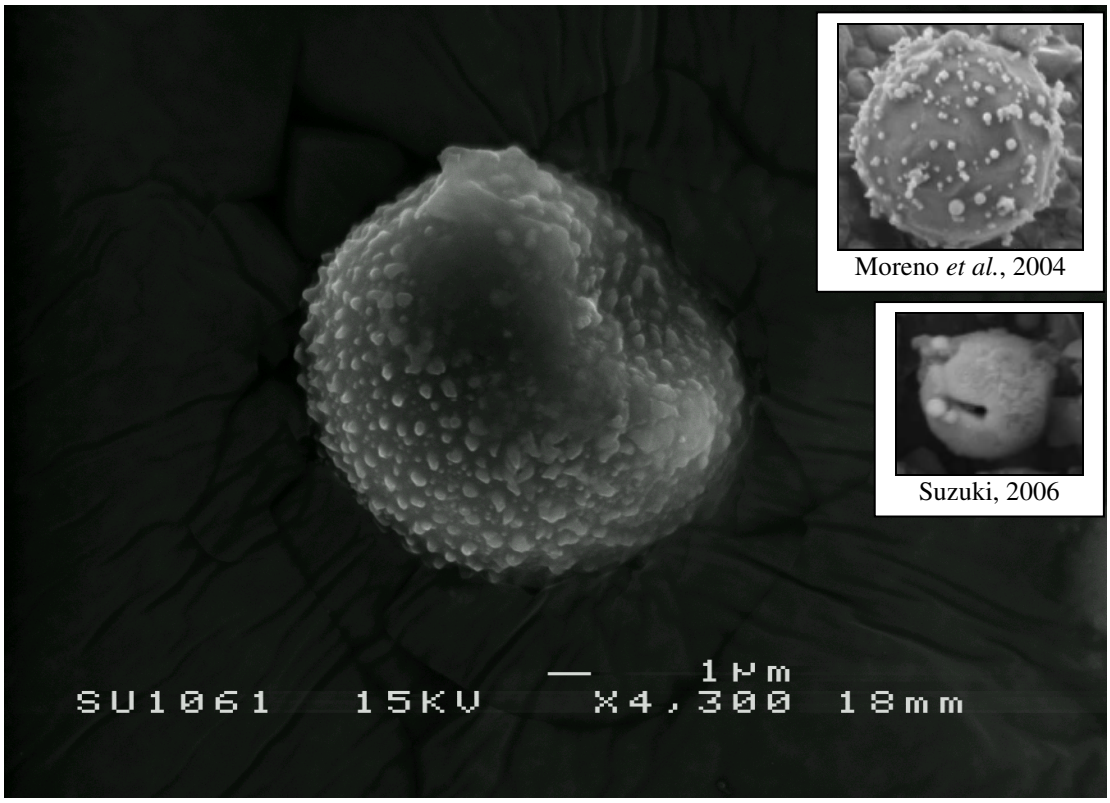

Figure 5-42: SEM image of PM from Stage 0 (9.0 - 10µm)

In Figure 5-42, the particle is spherical with crustal materials stuck on it. The particle is approximately 10µm in diameter. This particle appears to be an iron spherule (Suzuki, 2006; Moreno *et al.*, 2004). The sphere shape of the particle indicates that it is a product from a high temperature source. Part of the particle is shaded with a darker colour compared to the other amorphous looking particles. This is due to its uneven surface. With increased of magnification, the surface of the particle shows that there is some crustal material nucleating on the iron spherule. Upon EDS analysis, the particle was shown to contain O, Na, P, S, Cl, Fe and K. The crustal materials stuck on the surface of the spherical particle could have been included in the analysis.

Stage 1 (5.8 – 9.0 µm):

Figure 5-43: SEM image of PM from Stage 1 (5.8 – 9.0µm)

In Figure 5-43, the particles of interest are marked with a circle. The particles are plate-like with high luminosity. All these particles vary in size. Each of these plate-like particles is surrounded by an irregular edge. The surface texture of these particles showed more indication of layering effects rather than particle accumulation. EDS analysis was conducted on theses particles which gave a high amount of O with low amounts of Ca, Na, Al, Si, S and Cl. The morphology of these particles indicates that they were skin flakes or a product of brake wear.

Stage 2 (4.7 - 5.8 µm):

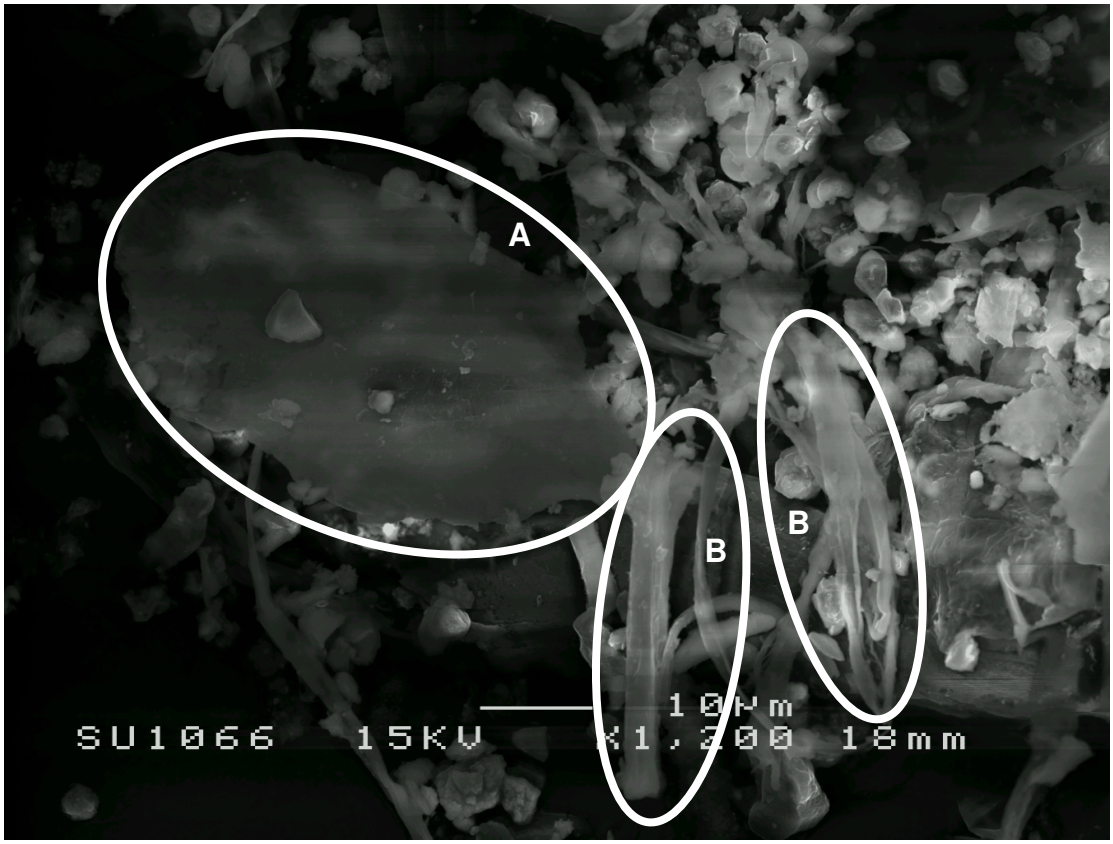

Figure 5-44: SEM image of PM from Stage 2 (4.7 - 5.8µm)

Particle A in Figure 5-44 is a plate-like particle with an irregular edge. The morphology of this particle suggests that it was skin flake. EDS analysis on particle A gave a high amount of O with moderate amounts of Ca, Na, Cl, Al, Si, K and S.

Particles B are fibre-shaped particles, several microns in length. EDS analysis confirmed that these particles have a high amount of O, followed by Ca, S, Cl, Si, Na, Al and In. These particles were either mineral fibres or textile fibres.

Stage 3 (3.3 – 4.7 µm):

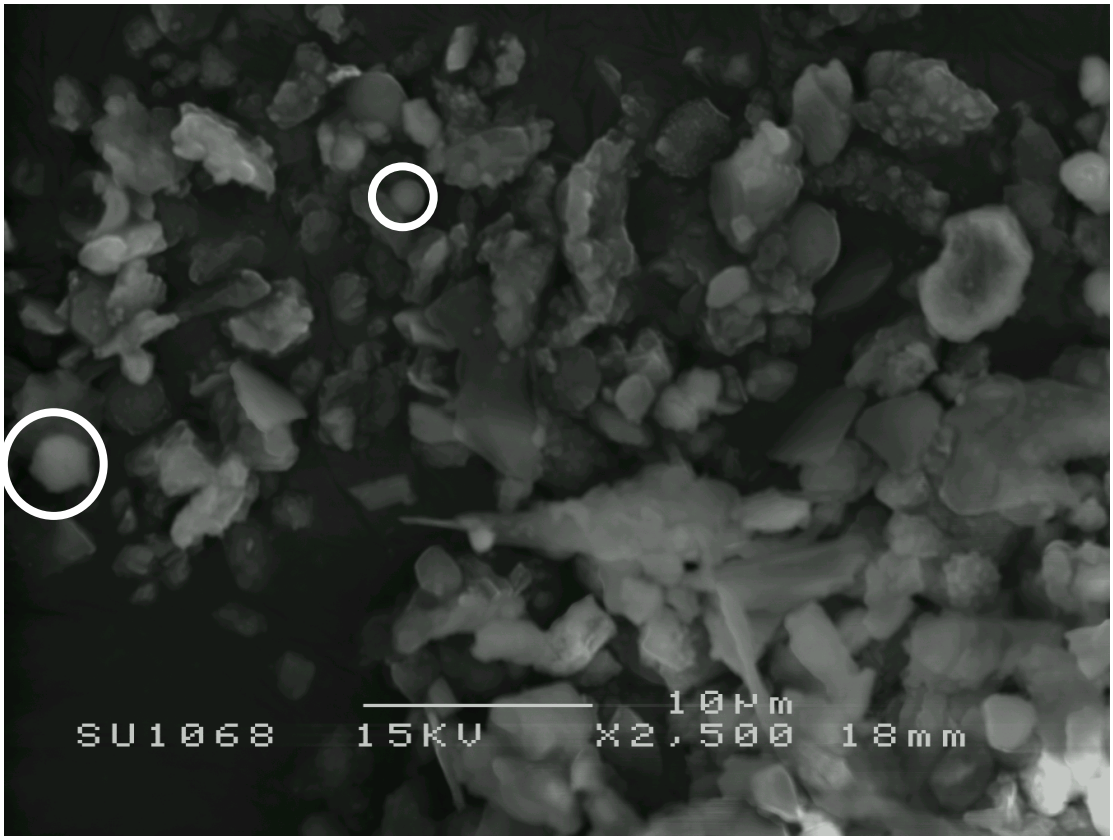

Figure 5-45: SEM image of PM from Stage 3 (3.3 – 4.7µm)

The spherical particles shown in Figure 5-45 seem to be a common type of particle for this sampling location. A similar surface morphology and structure has been observed in earlier sample filters. The feature particles highlighted in Figure 5-45 are spherical, which originated from high temperature sources. EDS analysis on these particles gave high amounts of O and C with lower amounts of Si, Al and K. The particles vary in size, from 1.5µm to 2.5µm.

Stage 4 (2.1 – 3.3 µm):

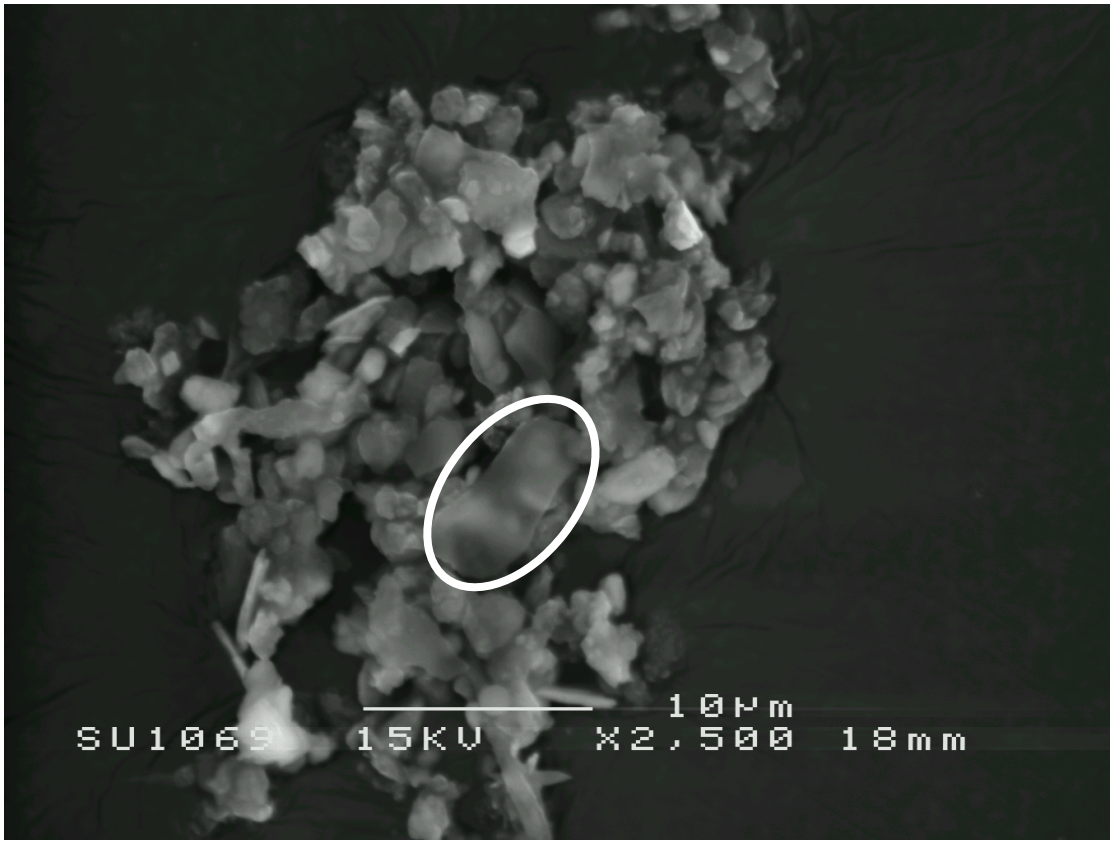

Figure 5-46: SEM image of PM from Stage 4 (2.1 – 3.3µm)

The particle in Figure 5-46 appears to be a plate-like particle with a smooth surface. The surface texture of this particle shows more indication of a layering effect as seen in the previous image. The particle is semi-transparent in appearance. EDS analysis on this particle gave a high amount of O with moderate amounts of Na, Si, P, S, Cl, Ca and Fe. The morphology of this particle suggests that it was either skin flake or rust. It could also be a product resulting from brake abrasion.

Stage 5 (1.1 – 2.1 µm):

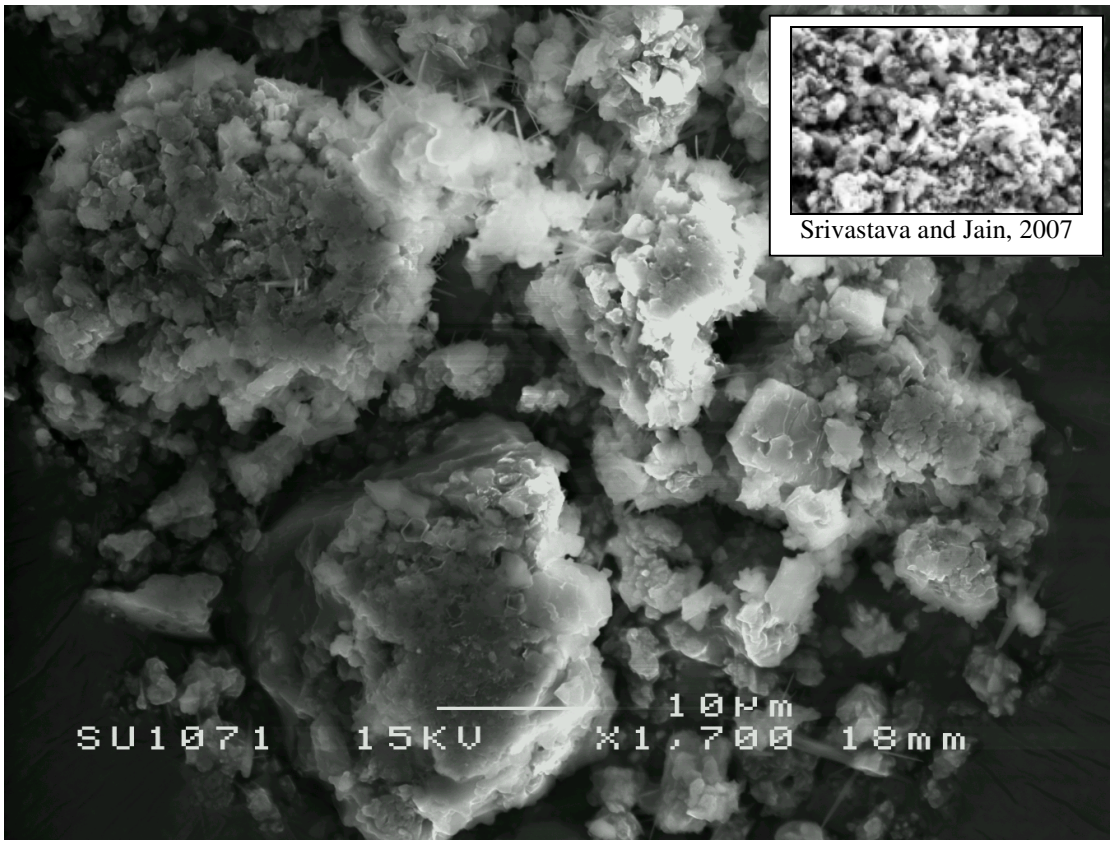

Figure 5-47: SEM image of PM from Stage 5 (1.1 – 2.1µm)

Figure 5-47 appears to be a cluster of irregularly shaped particles that have accumulated together. Increased magnification was used to provide a clearer surface image. The morphology of these particles suggests that they were soot and silicate particles (Srivastava and Jain, 2007). All the particles vary in size. The particle sizes varied due to the accumulation of finer particles. EDS analysis confirmed that these particles have high amounts of S and O with low amounts of Na, Al, Si, Cl, Ca, Fe and In.

Stage 6 (0.7 – 1.1 µm):

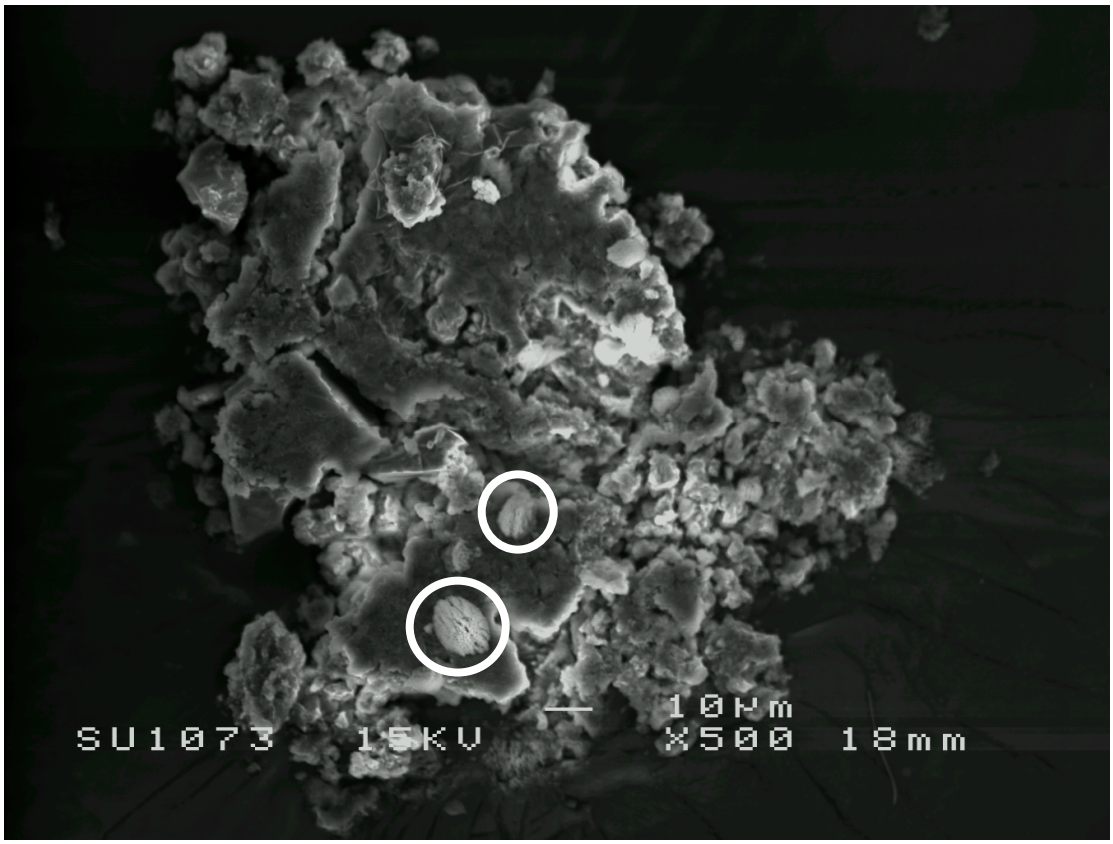

Figure 5-48: SEM image of PM from Stage 6 (0.7 – 1.1µm)

Figure 5-48 is an image of a cluster of irregularly shaped particles accumulated together. Particles highlighted in Figure 5-48 gave only high amounts of S, O and K with lower amounts of Al, Si, Fe and Zn. The morphology of these particles suggests that they were soot particles since on closer inspection there were a lot of amorphous looking particles.

Stage 7 (0.4 – 0.7 µm):

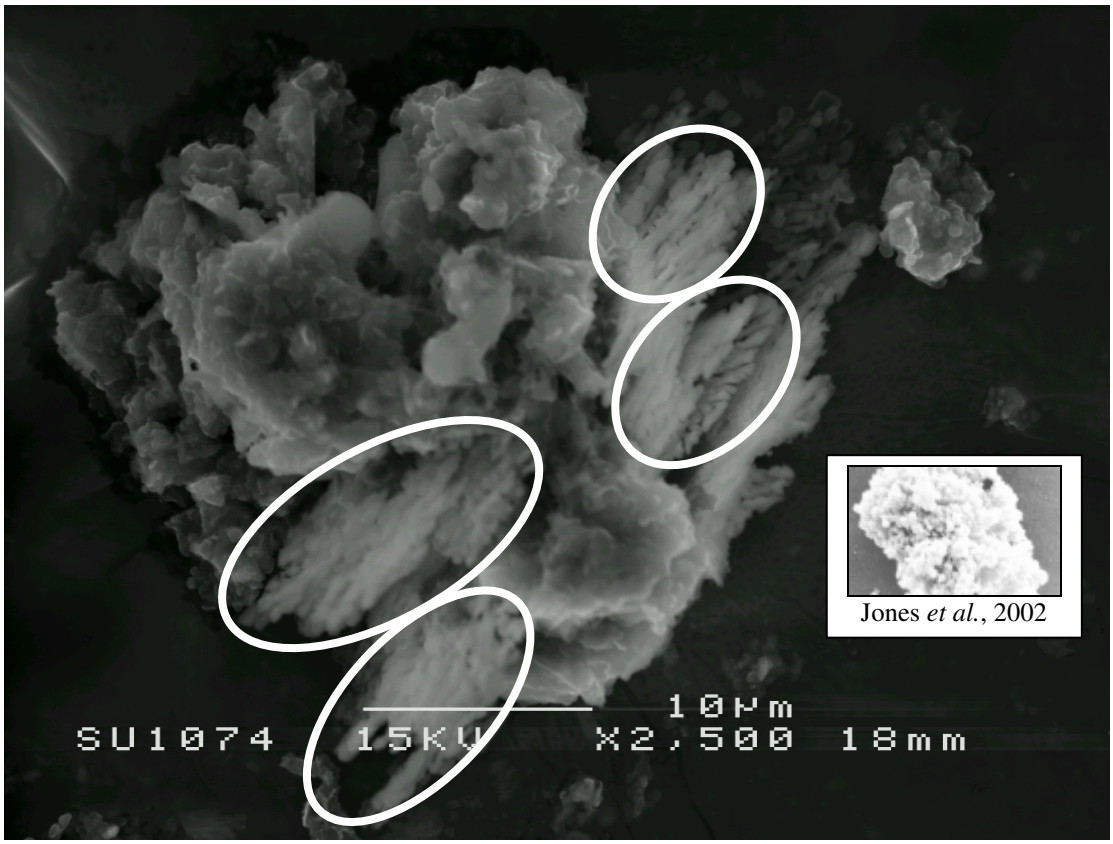

Figure 5-49: SEM image of PM from Stage 7 (0.4 – 0.7µm)

The surface texture of the particles in Figure 5-49 showed more indication of particle accumulation than layering effects. The particles are approximately 10µm in size although the preseparator was used to prevent restricted particles with an aerodynamic diameter greater than 10µm from entering the later stages. The possible reason could be the accumulation reaction of smaller particles in the moist environment. EDS analysis was conducted on these particles and it gave high amounts of C, S and O with a lower amount of K. The particles appear to be vehicle exhaust particles (Jones *et al.*, 2002).

5.2.3.4 Summary of Findings

The results of PM tests to collect and determine the size distribution (Andersen Sampler), morphology (SEM/EDS) and chemical composition (ICP-OES) of particulate matter in the lounge are summarised as follows:

(i) Approximately 17% of particles collected were 3.3-4.7µm,

(ii) The majority of the particles were mainly composed of Fe, Ca, and Zn,

(iii) The particles were mainly skin flakes, mineral fibres, soot and silicate particles and iron spherules. Others were rust compounds from vehicles, brakepad wear and also resultants from high temperature sources due to the lounge being located close to the car porch. Also, they may have been generated from activities in the lounge.

5.2.4 Outdoor

Figure 5-50 illustrates the outdoor conditions of the stone-built detached house. As shown in Figure 5-51, the Andersen Sampler was placed on top of a ladder at a height of about 2.0m from the floor. A 1.5m tube was connected to the sampler at one end and the other was placed outside the store room to collect particles. The sampler was placed in the store room for about 6 weeks. Sampling started on 15/05/2009 at 10.30am and ended on 29/06/2009 at 3.00pm, which is equal to approximately 1,085 hours.

Figure 5-50: Outdoor conditions

Figure 5-51: The Andersen Sampler was placed about 2.0m from floor level

5.2.4.1 Particle Size Distribution

Table 5-4 shows the concentration of particles collected from each stage. 26.9mg of particulate matter was collected from the outdoors. The concentrations of $PM_{2.5}$ and PM_{10} were 9.23µg/m^3 and 14.6µg/m^3 respectively. From Figure 5-52, it can be seen that approximately 29% of the particulate matter collected from outdoors were within the range of 0-0.4µm. The major sources of these particles were attributed to vehicle combustion, brake discs, brake pad wear and the nearby cement plant. Other possible sources include pollen, either from local plants or it could have migrated from the other plants outside the village.

Table 5-4: The concentrations of particles collected from each stage (Outdoor)

Stage	**Mass Size Distribution (µm)**	**PM (mg)**	**Concentration (µg/m^3)**	**%**
0	9.0-10	1.4	0.76	5
1	5.8-9.0	1.9	1.03	7
2	4.7-5.8	1.1	0.60	4
3	3.3-4.7	3.0	1.63	11
4	2.1-3.3	2.5	1.36	9
5	1.1-2.1	4.3	2.33	16
6	0.7-1.1	3.2	1.74	12
7	0.4-0.7	2.0	1.09	7
Filter	0-0.4	7.5	4.07	29
Total		26.9	14.60	100

Test time	65,070mins (≈1,085hours)
Air volume (m^3)	1842.58
$PM_{2.5}$ concentration (µg/m^3)	9.23
PM_{10} concentration (µg/m^3)	14.60

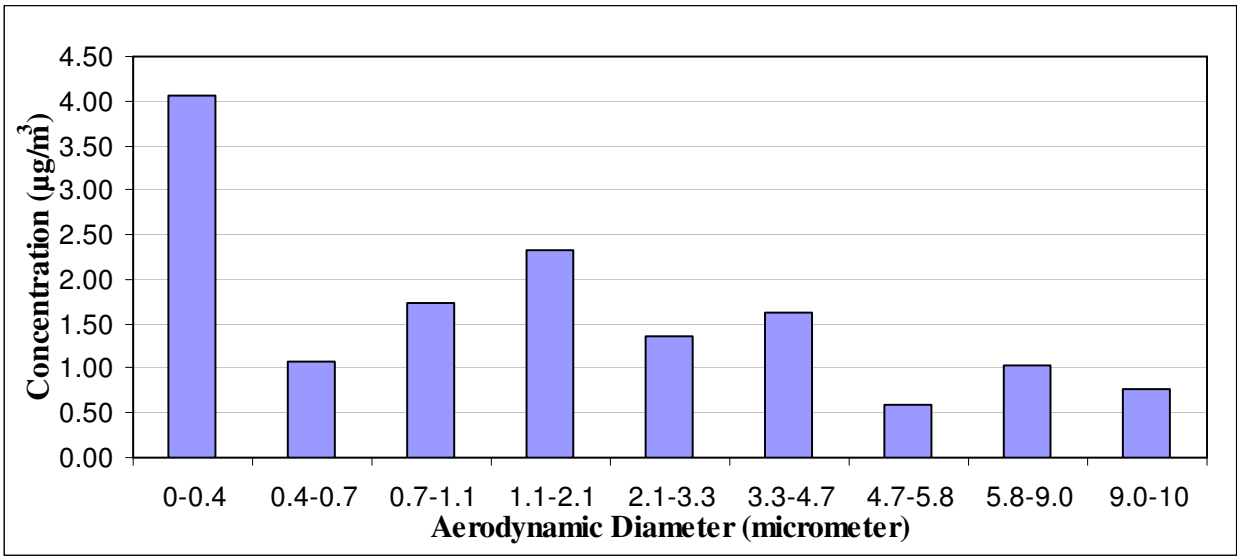

Figure 5-52: Particle size distribution for outdoor sampling

5.2.4.2 Full Elemental Analysis

Figure 5-53 presents the elemental composition for particles collected from outdoors. The outdoor PM_{10} samples were mainly composed of S, Na and K, which are likely to be from the cement plant nearby.

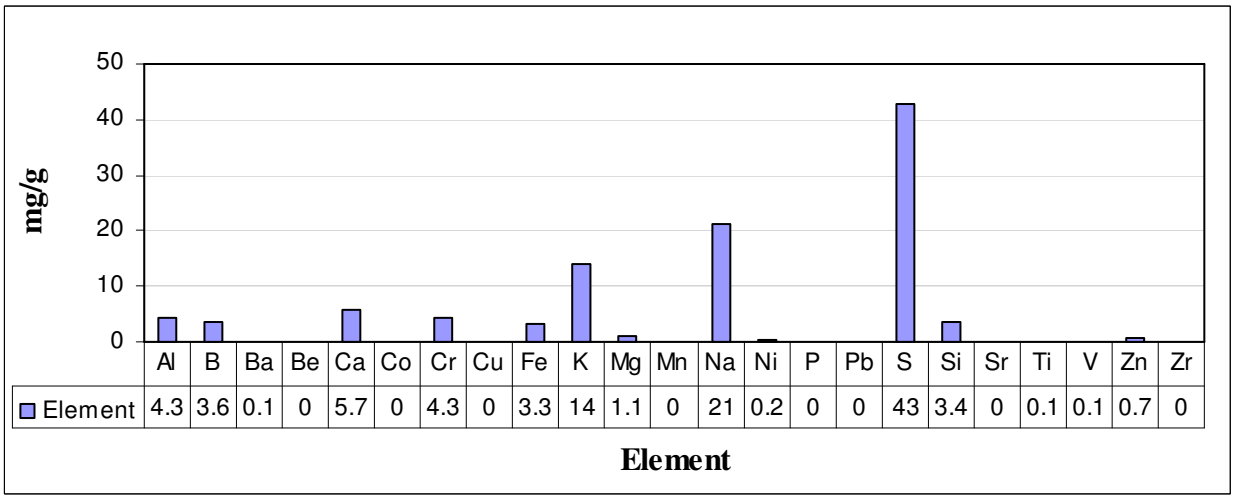

Figure 5-53: Element contents for outdoor sampling

5.2.4.3 Morphology Analysis

SEM/EDS was adopted to determine the morphology of individual particles. These particles were mainly comprised of C, O, Na, Cl, Ca, S, Mg and Si.

Stage 0 (9.0 – 10 µm):

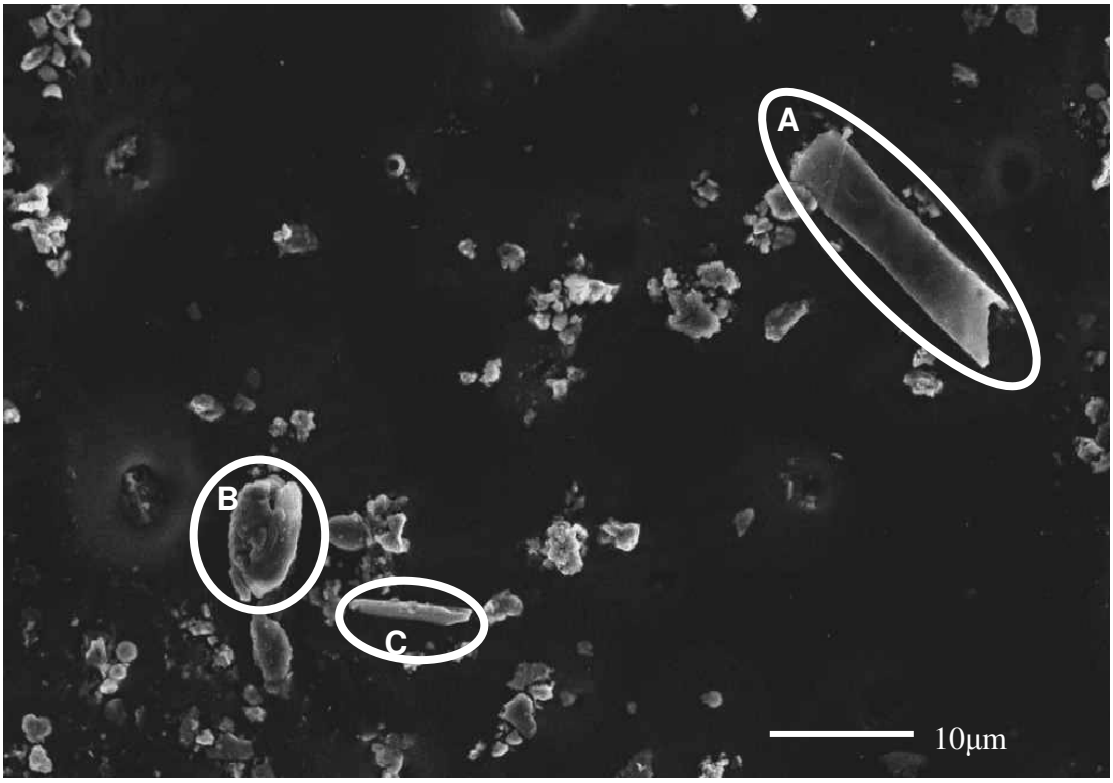

Figure 5-54: SEM image of PM from Stage 0 (9.0 - 10µm)

Particle A in Figure 5-54 retains an angular structure. The particle is approximately 20µm in length. The darker region of the particle is the deeper part of the particle. The morphology of this particle suggests that it was from local minerals. Upon EDS analysis, it was confirmed that this particle has high amounts of C and O with lower amounts of Na, S and Cl.

Particle B has an irregular shape with an accumulation of finer particles on top of its surface structure. This suggests that it was a carbonate mineral. EDS analysis confirmed that this particle has high amounts of C and O.

Particle C in Figure 5-54 is a fibre-shaped particle of several microns in length. It was a mineral fibre from outdoors.

Stage 1 (5.8 – 9.0 µm):

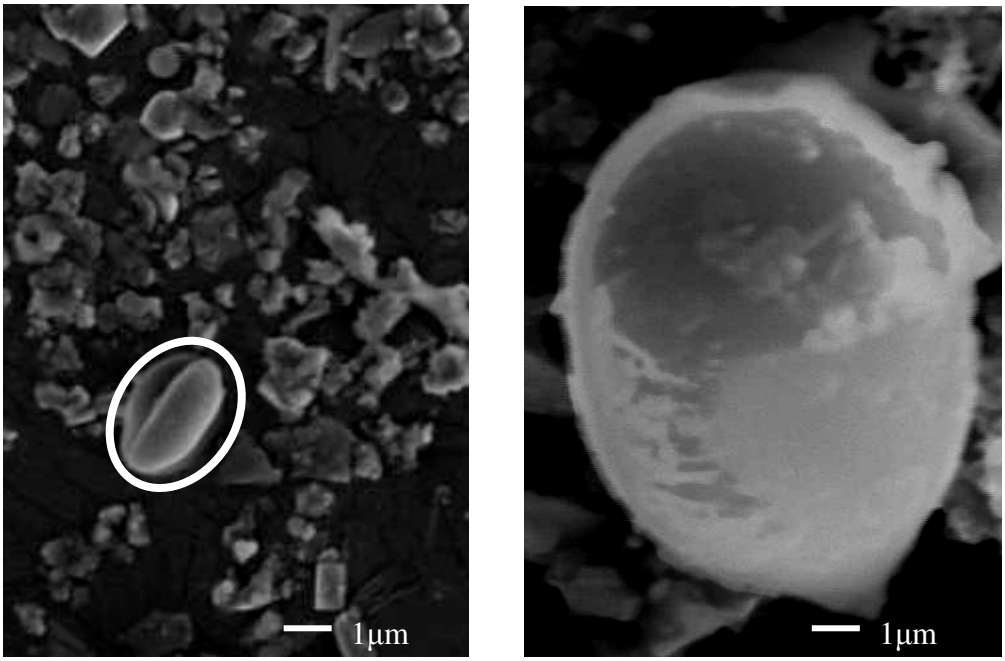

(a) **(b)**

Figure 5-55: SEM image of PM from Stage 1 (5.8 – 9.0µm)

The image shown in Figure 5-55(a) is a particle with smooth surface. The darker region of the particle is the deeper part of the particle. EDS analysis was conducted on this particle and it gave high amounts of C and O. This was either a pollen or a carbonate particle from local plants. Alternatively it could have migrated from the other locations such as the cement works.

The particle of interest in Figure 5-55(b) is a spherical particle. The morphology of the particle suggests that it is a cenosphere. Results from EDS analysis showed high amounts of C and O. The round edge suggested that it probably formed during high temperature processes. However, the shape could also have formed by weathering or erosion during migration from its source.

Stage 2 (4.7 - 5.8 µm):

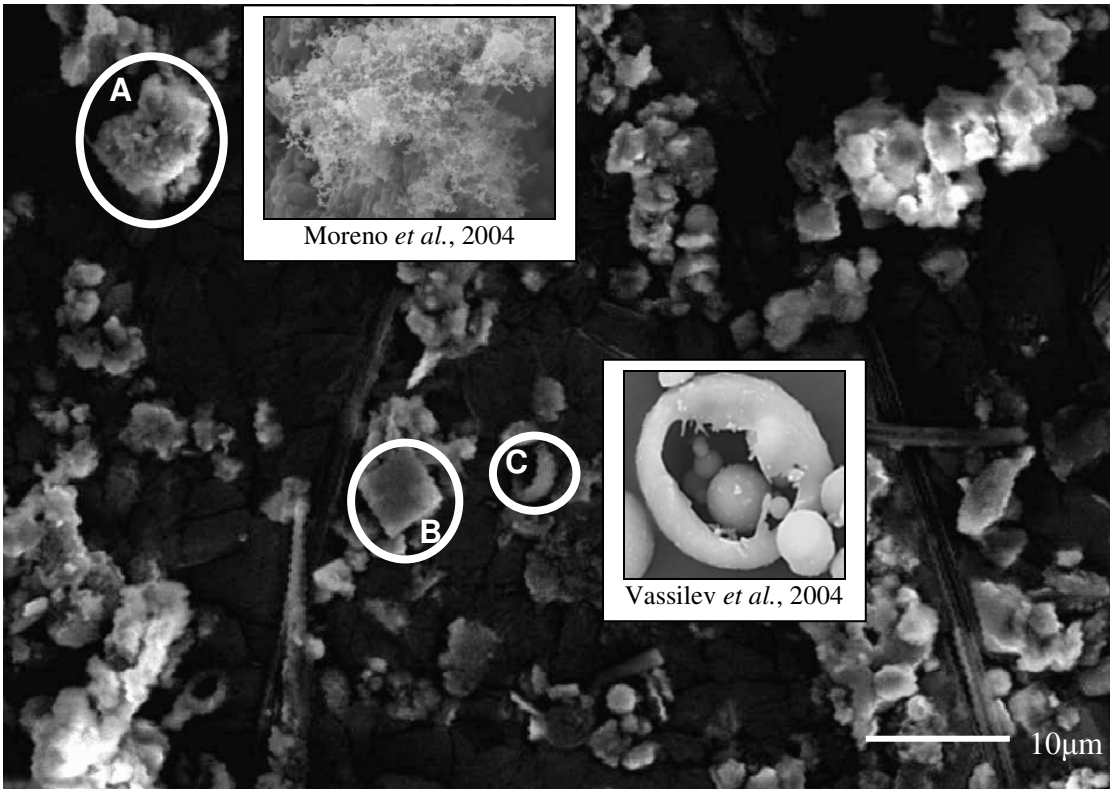

Figure 5-56: SEM image of PM from Stage 2 (4.7 - 5.8µm)

Particle A in Figure 5-56 is approximately 8µm in size with an irregular shape. EDS analysis confirmed that Particle A was mainly composed of C and O with a lower amount of S. This was a soot particle (Moreno *et al.*, 2004).

Particle B is approximately 4-5µm in length with a cubic shape. The morphology of this particle suggests that it was a salt crystal or salt related particle. The smooth area in the middle of the particle was subjected to EDS analysis and the result was high amounts of Na and Cl with lower amounts of C and O. The elemental composition also reaffirmed that the particle contains high amounts of Na and Cl. The particle is likely to be from road gritting.

Particle C has a symmetrical sphere shape with a semi-transparent appearance. The structure was observed in SEM mode and then the equipment was reset to EDS mode in order to determine its elemental composition. Its elemental composition revealed mainly C and O and with a lower amount of Na. This particle appears to be a cenosphere with surface crystallisation (Vassilev *et al.*, 2004).

Stage 3 (3.3 – 4.7 µm):

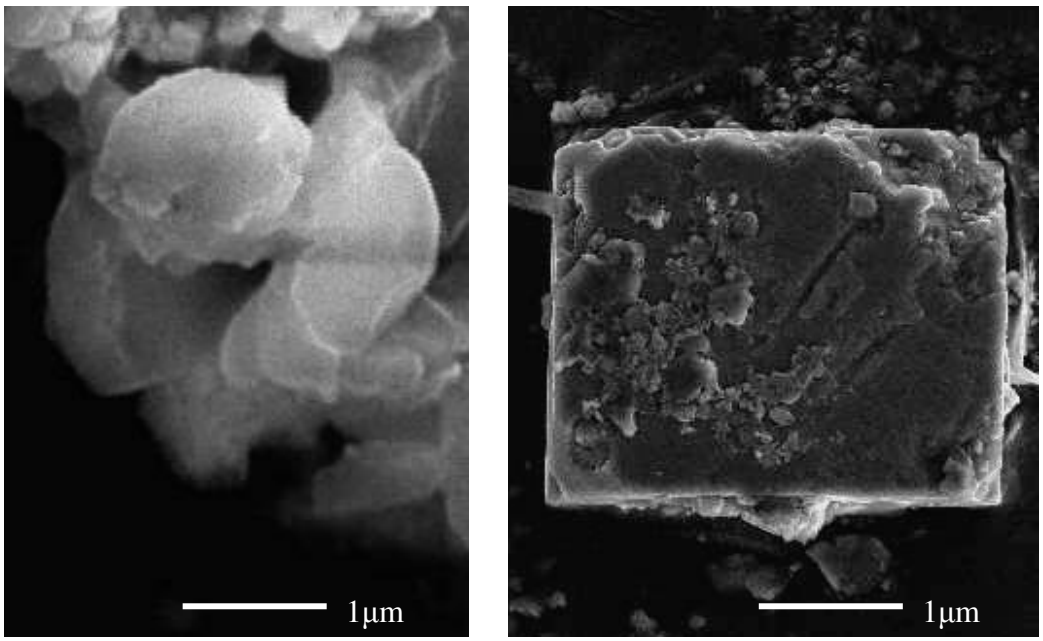

(a) (b)

Figure 5-57: SEM image of PM from Stage 3 (3.3 – 4.7µm)

The particle of interest in Figure 5-57(a) is spherical with a smooth surface. The morphology of this particle suggests that the particle could have originated from high temperature sources. EDS analysis of this particle gave only high amounts of C and O and with a lower amount of Si. The diameter of this particle is around 3 µm with a smooth surface texture.

The image shown in Figure 5-57(b) is a cube-like particle with minor particles nucleating on it. This is very similar to the other cubical particles found in earlier stages. The morphology of this particle and EDS analysis confirmed that it was a salt crystal or salt related particle. This particle was found to have high amounts of Na, Cl and C. It originated from road gritting.

Stage 4 (2.1 – 3.3 µm):

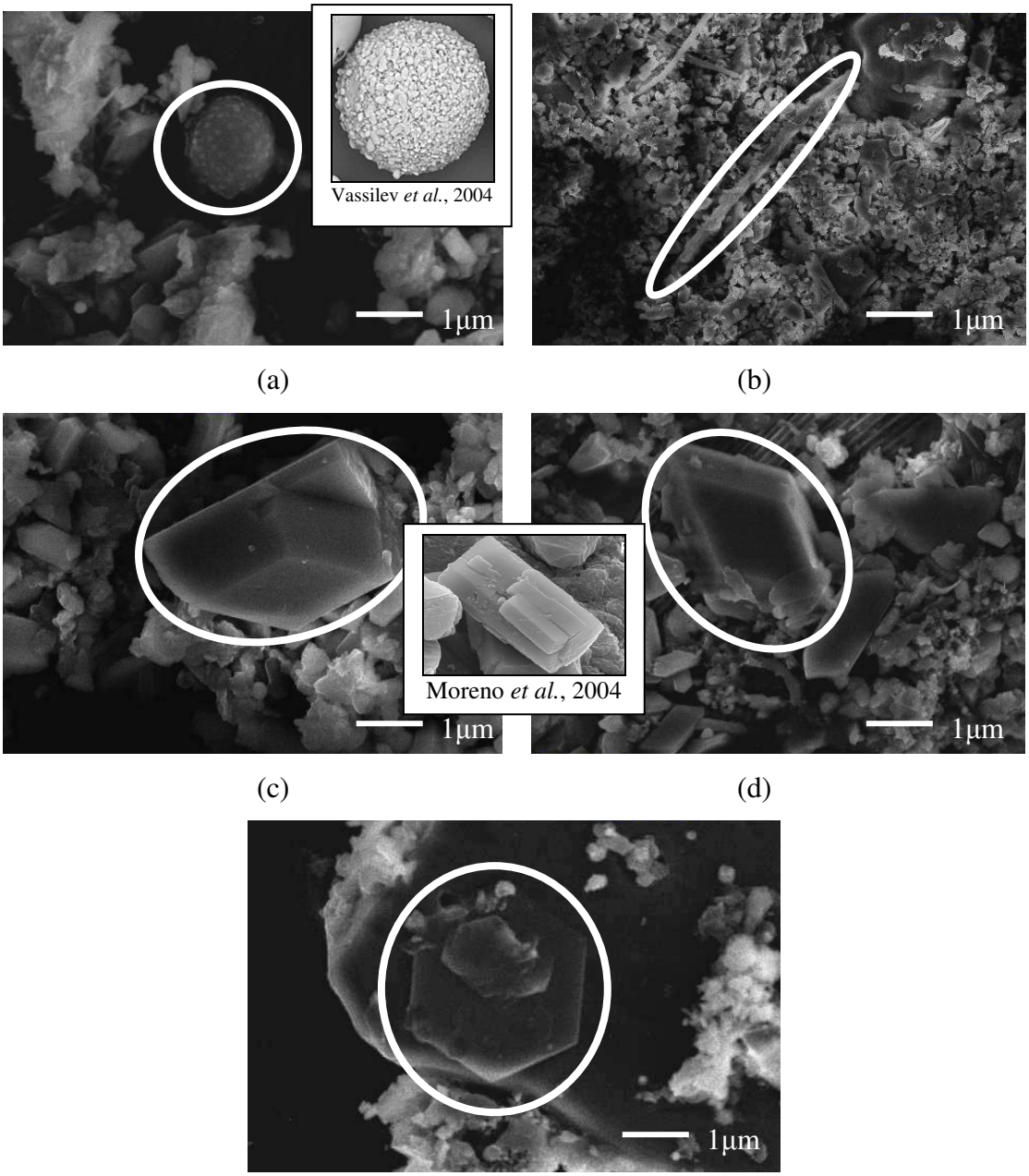

Figure 5-58: SEM image of PM from Stage 4 (2.1 – 3.3µm)

The particle in Figure 5-58(a) is a spherical particle with high amounts of C and O from the EDS analysis. This particle is approximately 2µm in diameter. This particle was a cenosphere (Vassilev *et al.*, 2004). The particle in Figure 5-58(b) is a fibre-shaped particle of several microns. It was a mineral fibre from outdoors.

Both cube-like particles shown in Figures 5-58(c) and (d) have sizes of around 3-4µm. Results from the EDS analysis for both particles gave high amounts of Ca, C, S and O elements.

These particles are $CaSO_4$ crystals, which are commonly found in the environment (Moreno *et al.*, 2004).

The image shown in Figure 5-58(e) is a hexagonal shaped particle. This particle was detected containing high amounts of Na and O with lower amounts of Mg, S and K. The hexagonal particle has signs of abrasion from a larger particle. Initial observations suggest that it was a sulphate or carbonate crystal. EDS analysis did not indicate the presence of Ca element.

Stage 5 (1.1 – 2.1 µm):

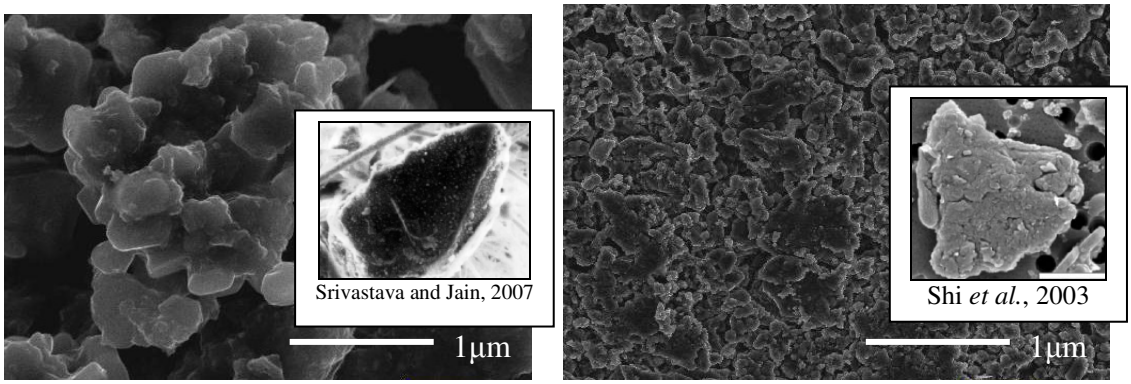

(a) (b)

Figure 5-59: SEM image of PM from Stage 5 (1.1 – 2.1µm)

Figure 5-59(a) shows a macroscopic image of typical clusters of soot and carbonaceous particles. EDS analysis confirmed that this particle have high amounts of C and O with a lower amount of Si. This particle appears to be silicate with a crystalline shape (Srivastava and Jain, 2007).

Particles shown in Figure 5-59(b) are irregular mineral particles, which were geologically sourced (Shi *et al.*, 2003). EDS analysis of the particles resulted in high amounts of C, O and S with low amounts of Na and K.

Stage 6 (0.7 – 1.1 µm):

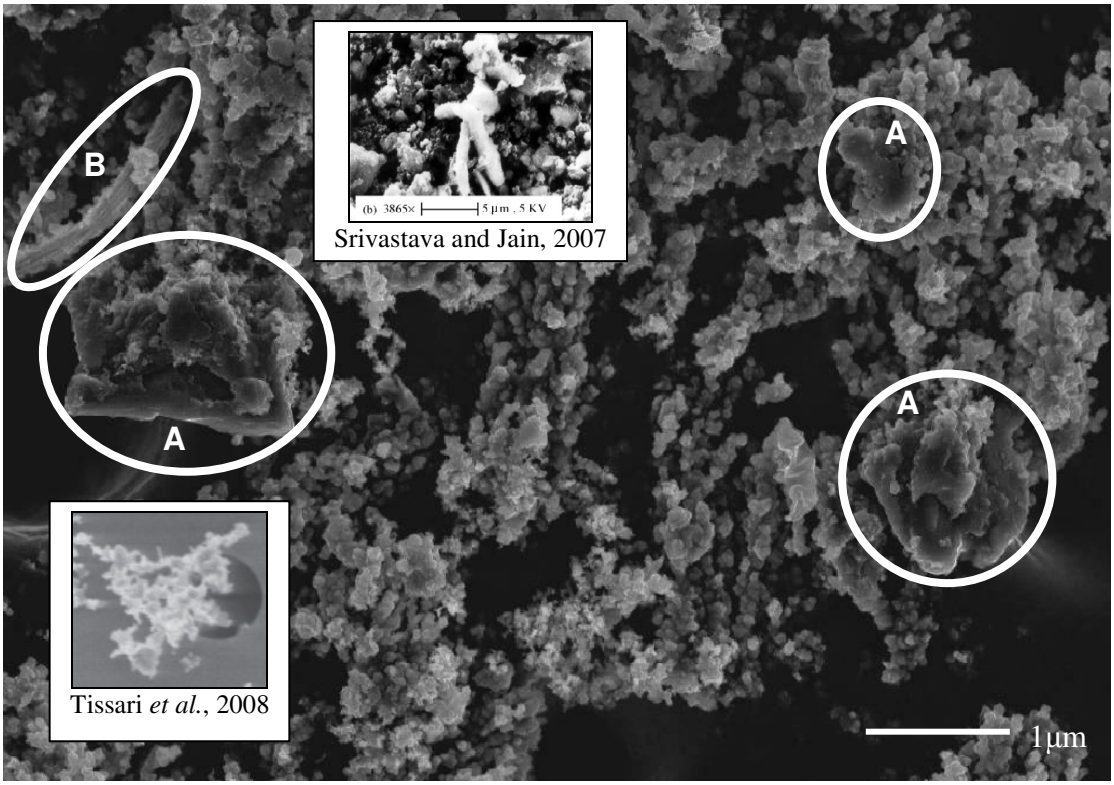

Figure 5-60: SEM image of PM from Stage 6 (0.7 – 1.1µm)

Particles A in Figure 5-60 have plate-like characteristics. The surface texture of these particles showed more indication of layering effects rather than particle accumulation. The size of these particles ranged from 1-3µm. Upon EDS analysis, these particles were found to have high amounts of C and O. The morphology of these particles and EDS analysis confirmed that they were a result of combustion processes (Tissari *et al.*, 2008).

Particle B is a fibrous shaped particle, 1µm in length. The surface of the particle is coated with dust fragments. EDS analysis on several locations of the particle confirmed high amounts of C and O with a low amount of S. This particle was a fibre (Srivastava and Jain, 2007).

5.2.4.4 Summary of Findings

The results of PM tests to collect and determine the size distribution (Andersen Sampler), morphology (SEM/EDS) and chemical composition (ICP-OES) of particulate matter at the outdoor environment are summarised as follows:

(i) Approximately 29% of particles collected were 0 – 0.4µm,

(ii) The majority of the particles were mainly composed of S, Na and K,

(iii) The particles were mainly dust fragments, cenospheres, pollen, carbonate and sulphate minerals, salt crystals and mineral fibres. Others were the result of high temperature processes, combustion processes and from the cement works.

5.3 NO_2, VOC, CO AND $PM_{2.5}$ MEASUREMENTS

Various analytical instruments were placed inside the kitchen to monitor indoor pollutant concentrations. The instruments for measuring $PM_{2.5}$, CO, NO_2 and VOCs were placed on the top of a sideboard (Figure 5-61) at a height of about 1.2m from the floor and a distance of about 3.5m away from the cooker.

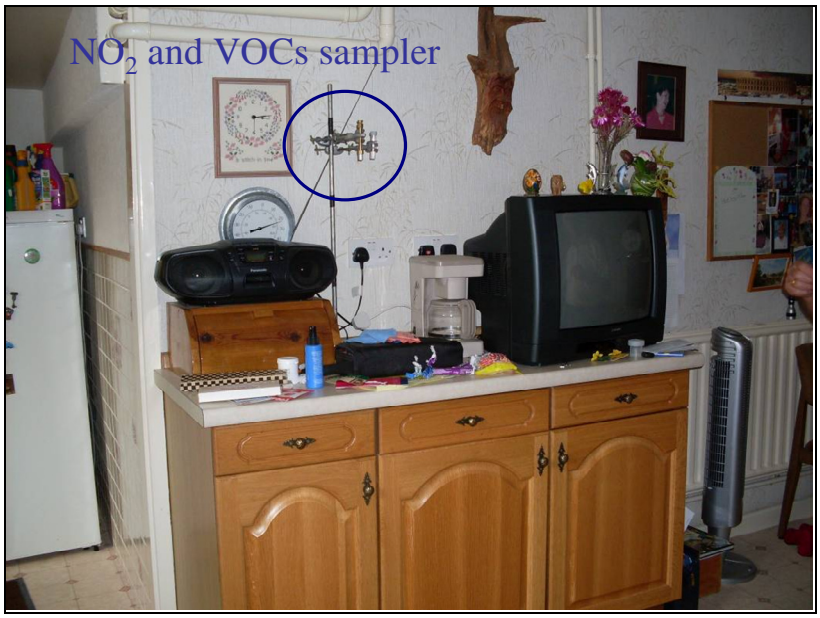

Figure 5-61: Position of instruments for measurement

5.3.1 Indoor and Outdoor Concentrations of Pollutants

5.3.1.1 $PM_{2.5}$

Figure 5-62 shows the indoor $PM_{2.5}$ concentration in the kitchen of the residential house in Hathersage, Case 1. The data was collected from 13 to 24 July 2009. The indoor $PM_{2.5}$ concentration remained constant at around 10-12 µg/m^3 during the initial measurement period (13 to 18 July 2009); this is most likely due to the fact that the house was unoccupied during this part of the sampling period. $PM_{2.5}$ concentrations in the kitchen were found to increase when there

were more indoor activities taking place. This created a positive relationship between indoor activities and indoor $PM_{2.5}$ concentration. As shown on Figure 5-62, the highest value achieved was 198 $\mu g/m^3$, where the spikes coincided with cooking activities. Overall, the average indoor $PM_{2.5}$ concentration was 16 $\mu g/m^3$. This was slightly higher than the value obtained using the Andersen sampler. The Andersen Sampler suggested that the average indoor $PM_{2.5}$ concentration was 8-9 $\mu g/m^3$. The outdoor $PM_{2.5}$ concentration near the house was about 10 $\mu g/m^3$, similar to the indoor background levels.

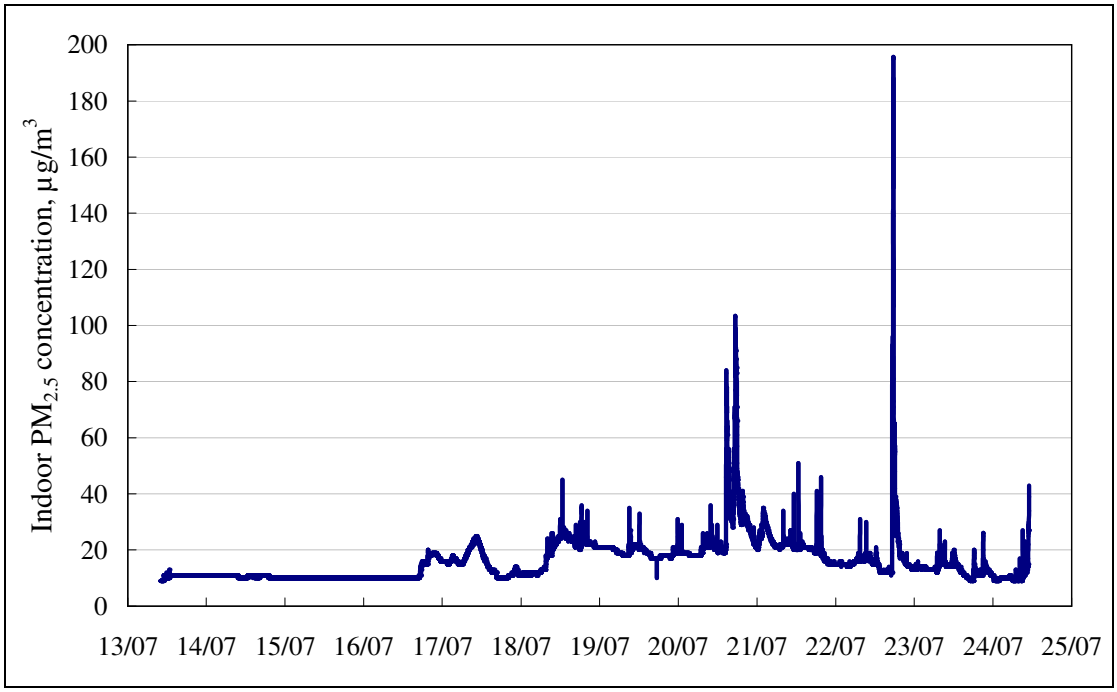

Figure 5-62: Real time concentrations of indoor $PM_{2.5}$ in the kitchen

5.3.1.2 CO

Figure 5-63 presents the real-time concentrations of indoor CO in the kitchen of the rural house, Case 1. The measured CO concentrations for Case 1 were very low, fluctuating between 0.9 and 1.3 ppm. In order to investigate the effect of the gas-fired central heating system on the indoor CO concentration, the gas boiler at the rural house was turned on at the end of the testing period. It was shown that the gas-fired heating system had no effect on the indoor CO concentration, as seen on Figure 5-63. This is to be expected since the flue gases from the boiler were discharged to the outdoor environment through well-insulated and sealed ducts and not released in or near the kitchen. Although no significant CO emission source existed in the kitchen of this rural house (Case 1), the average indoor CO concentration was still about 1.0 ppm.

The outdoor CO concentration at this site was zero, which implies that the outdoor CO at this location is dispersed rapidly. The monthly average CO concentration in Sheffield city centre was only 0.2-0.3ppm during the summer of 2009, as reported in the UK National Air Quality Archive (DEFRA, 2009).

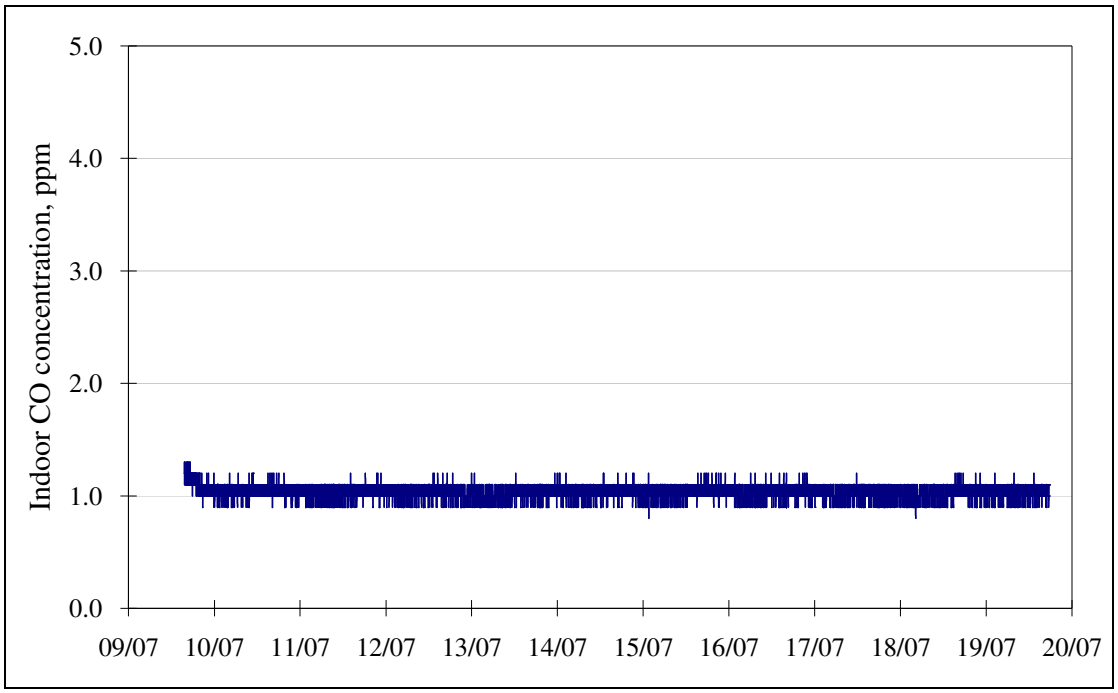

Figure 5-63: Real time concentrations of indoor CO from the kitchen

5.3.1.3 NO_2

As shown in Table 5-5, the indoor and outdoor NO_2 concentrations measured using diffusion tubes were almost identical in the rural area (Case 1), since there was no significant source of indoor NO_2.

Table 5-5: Indoor and outdoor NO_2 concentrations measured at Hathersage

Sampling Site	Indoor	Outdoor
Residential house in Hathersage, µg/m^3	10.2	10.8

5.3.1.4 VOCs

Table 5-6 shows the indoor and outdoor concentrations of Σ20 VOCs – the sum of the top 20 VOCs obtained from the analysis of the TENAX TA Tubes deployed at Hathersage (Case 1).

At this site, the indoor Σ20 VOC concentrations were notably higher than the outdoor concentrations, as shown. This result was expected since any high outdoor VOC concentrations will be rapidly dispersed and diluted in the outdoor environment. The possible sources of the indoor VOCs include household products, carpets, the electric oven and wood-based furniture, as well as consumer products. In this kitchen, all the furniture (e.g. cabinets, dining table, sideboards etc.) are made from wood. A small piece of carpet was placed in front of the cabinet. All these are the possible sources of indoor VOCs. Moreover, various household cleaning products were used in this kitchen.

Table 5-6: Indoor and outdoor VOC concentrations

Sampling Site	Indoor	Outdoor
Residential house in Hathersage, µg/m^3	221.5	42.6

The top 20 VOC compounds found at Case 1 are shown in Figure 5-64. Toluene was by far the most common VOC to be found in the indoor environment for this case study. The concentrations of this aromatic hydrocarbon reached over 80µg/m^3 at this rural house. This was also one of the most common VOCs found in the outdoor environment. Toluene is from paints or lacquers.

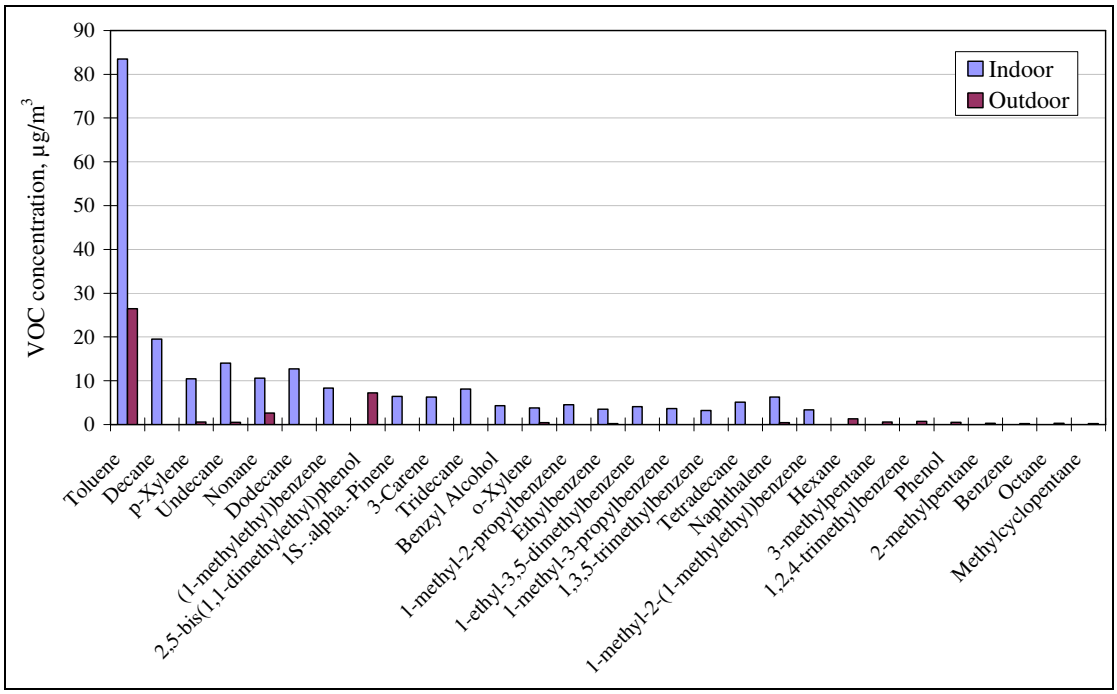

Figure 5-64: Top 20 VOCs sampled (µg/m^3)

5.3.2 Indoor Temperature and Relative Humidity

The real time temperature recordings taken in the kitchen of Case 1 are presented in Figure 5-65. The temperatures recorded ranged from ~18 ºC to 23 ºC. The temperature variations could be due to the cooking activities.

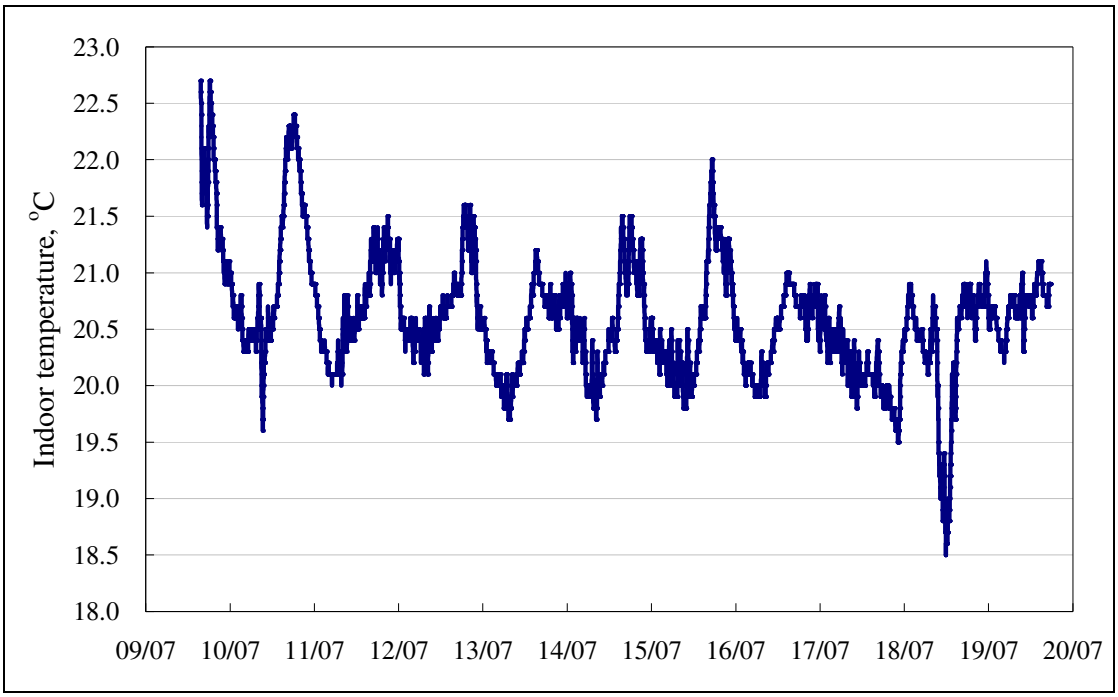

Figure 5-65: Real time temperature recordings in the kitchen of the residential house in Hathersage

Figure 5-66 presents the real time recordings of the relative humidity in the kitchen of the Case 1 house. The range of indoor humidity levels was 40% to ~65%. Cooking activities could be the main contributors of the increasing humidity levels.

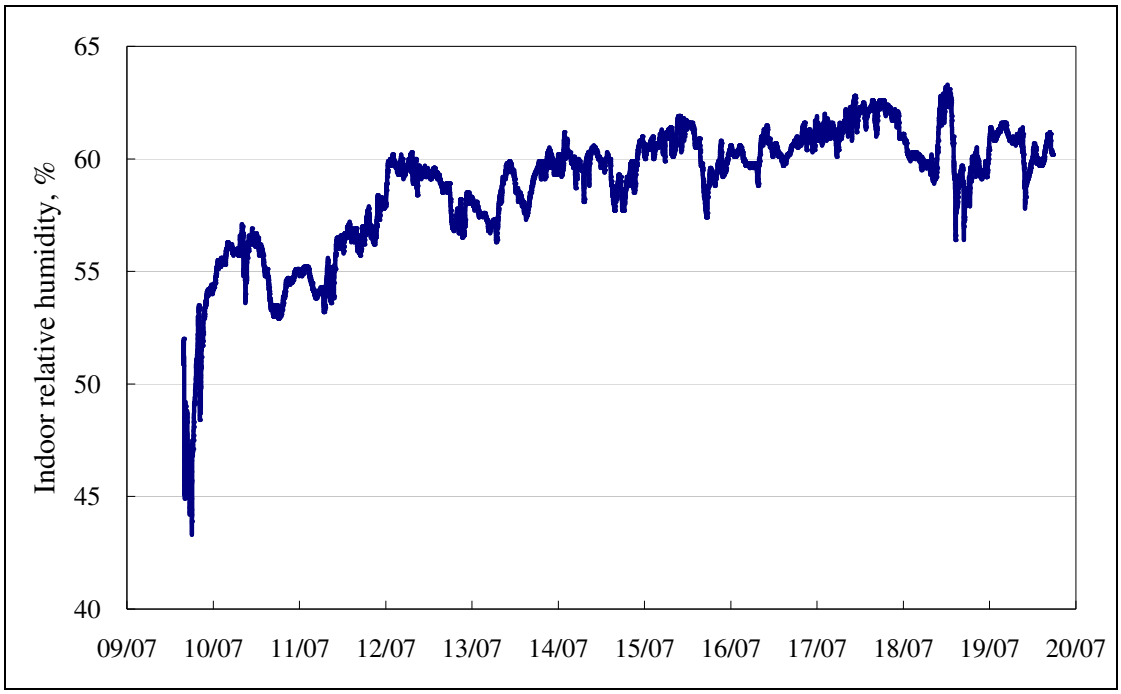

Figure 5-66: Real time recordings of the relative humidity in the kitchen of the residential house in Hathersage

5.3.3 Air Exchange Rate

In order to allow the determination of the emission rates for each pollutant from the previous tests, the air exchange rate was calculated. Figure 5-67 shows the typical decay curves for the CO_2 concentration during the air exchange rate tests in the kitchen of the rural house (Case 1). As seen in Figure 5-67, the indoor CO_2 concentration was increased to approximately 1500 ppm when CO_2 was released and well mixed in the kitchen of the rural house. The CO_2 concentration then slowly decreased. The air exchange rate in the kitchen of Case 1 was 1.5±0.2 air changes per hour (hr^{-1}).

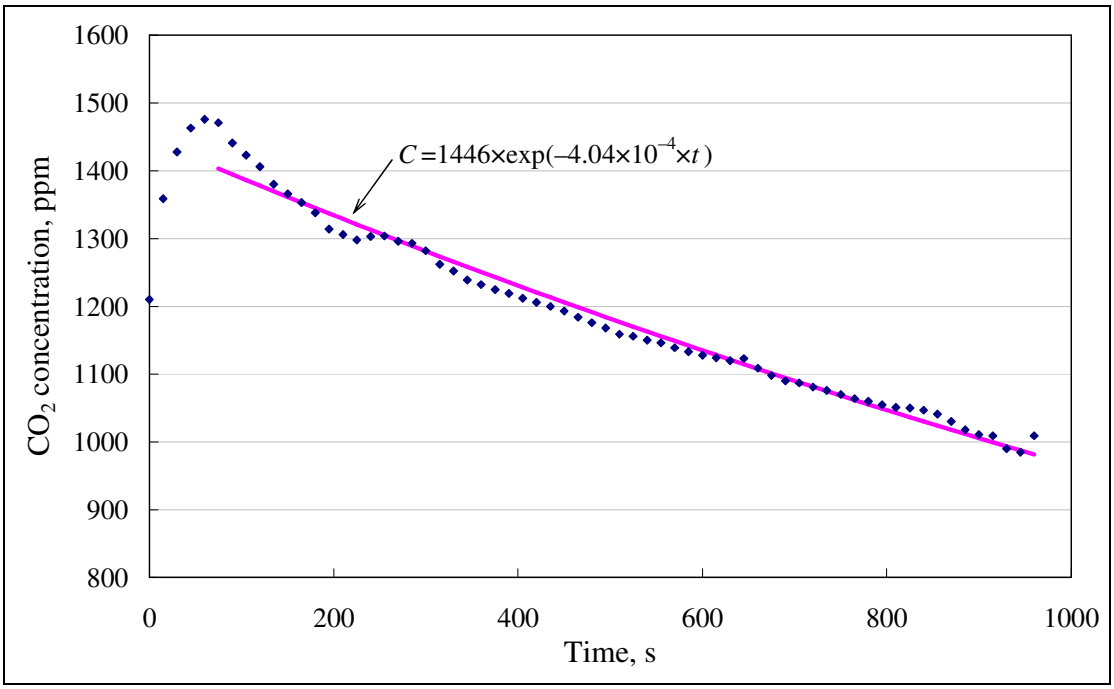

Figure 5-67: CO_2 concentration decay in the kitchen
(Air exchange rate = 1.5±0.2 air changes per hour (hr^{-1}))

5.3.4 Emission Rates of Indoor Pollutants

5.3.4.1 $PM_{2.5}$

The $PM_{2.5}$ emission rates for the cooking periods in this kitchen were determined based on the CO_2 decay curve and the subsequent air exchange rate that was calculated. Figure 5-68 shows the average emission rates of $PM_{2.5}$ during three cooking periods in the kitchen of Case 1. The emission rates for this case study varied significantly and ranged from 5 to 23 mg/hr. On 20th of July, the emission rates were relatively low. The average emission rates during these two events were approximately 5.4–6.4mg/hr. On 22nd of July, however, the emission rates during the cooking period increased significantly with an average of 22.5mg/hr (i.e. much higher than the rates recorded on 20th of July). This may be due to the differences in the food preparation methods and cooking activities during the measurement periods.

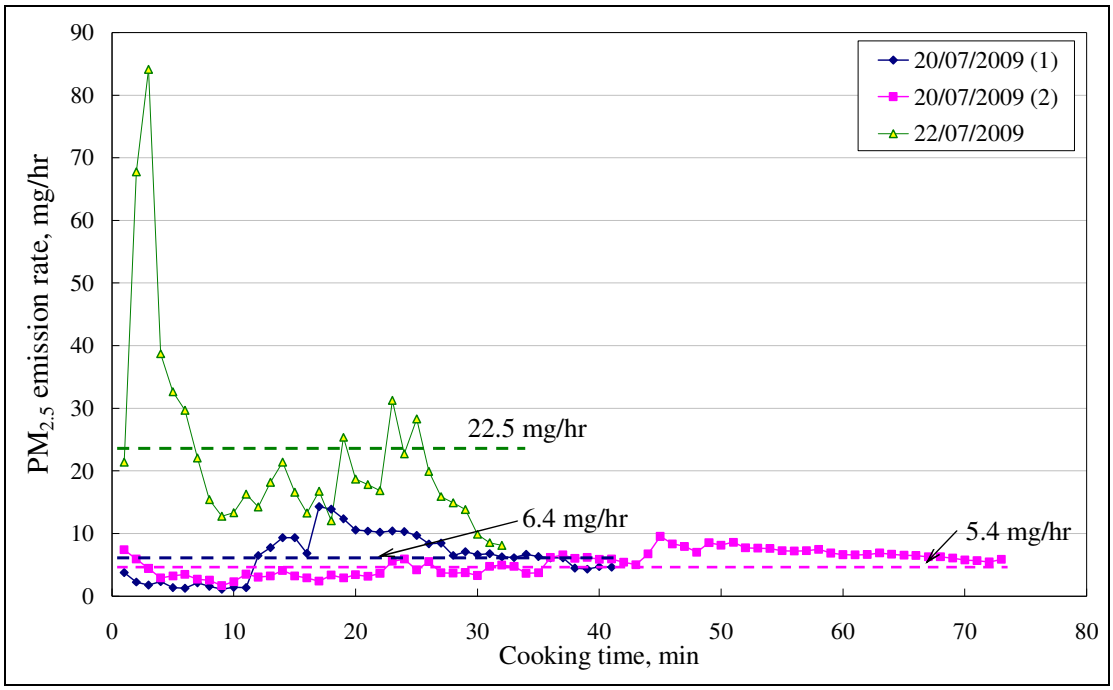

Figure 5-68: The emission rates of $PM_{2.5}$ during the cooking events in the kitchen of a residential house in Hathersage

5.3.4.2 CO

Although there was no significant CO emission source in the kitchen of the residential house in Hathersage, the average indoor CO concentration was still 1.0 ppm. Theoretically, the emission rate was calculated to be 0.091g/hr.

5.3.4.3 NO_2 & VOCs

The indoor emission rates of NO_2 and VOCs calculated in the residential house in Hathersage are listed in Table 5-7. The higher indoor Σ20 VOC concentrations at this location resulted in much higher VOC emissions rates, of 13mg/hr. The reason for the elevated Σ20 VOC concentration in the rural house (Case 1) is most likely due to the wood-based furniture and cleaning products used.

Table 5-7: Indoor emission rates of NO_2 and VOCs at Hathersage

Date	Average emission rates of NO_2 (mg/hr)	Average emission rates of VOCs (mg/hr)
Residential house in Hathersage	LoD*	13.0

**** LoD = Limit of detection***

5.4 COMPUTATIONAL FLUID DYNAMICS MODELLING OF THE FLOWFIELDS INSIDE THE KITCHEN

Determining the particle flowfields in an indoor environment is important to ensure a healthier and pleasant environment. Theoretical modelling using CFD software was conducted for Case 1. Firstly, Gambit 2.2.30, a mesh-generating tool, was used to construct the geometry of the kitchen. Figure 5-69 shows the overall geometry and computational mesh developed for use in this investigation. In this study, a Cooper mesh was adopted and was uniformly generated over the geometry. The minimum size of the mesh was 0.065 m. As shown, there were five inlets (4 doors and 1 roof) and one outlet (door to the rest of the property). The total number of nodes was 270,000.

It is obvious why the doors and windows in the kitchen were classed as inlets. In this case, however, the roof was also considered as one of the inlets, for several reasons. The first of these is buoyancy. The floor, which is not well-sealed, tends to make the particles or pollutants rise from the floor and move upwards. The location of the house is the second reason; the house faces west and in UK, the wind is mostly from this direction. The external air comes into the house (into the kitchen and the bedroom above it) through the windows and can also come into the indoor environment through the other inlet (the door in the kitchen). In addition, the ceiling in the kitchen is not well-sealed, thus the air inside the bedroom above it (which faces west) could also leak in from this source. Furthermore, the thermophoresis phenomenon could also play a role; this is where warmer molecules push colder molecules to the cooler side of the environment.

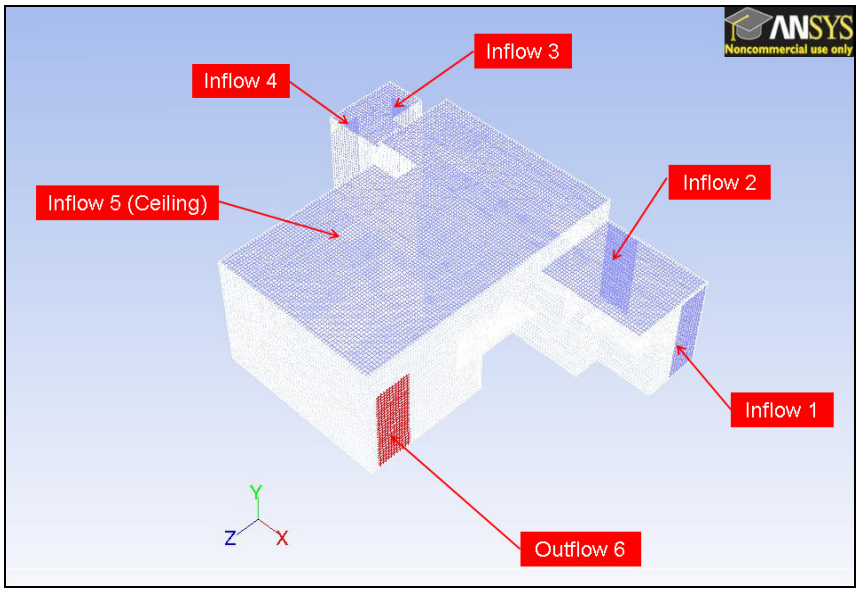

Figure 5-69: The geometry and computational grids for the kitchen in the rural house – Case 1

FLUENT Ansys 12 was then utilised for performing the calculations – to evaluate the velocity magnitude, flowfields and particle trajectories within the kitchen. The standard *k-epsilon* model was adopted for this study, with the turbulent intensity set to 1%. The various boundary conditions selected for the CFD simulations are presented in Table 5-8. As detailed, the mass flowrate at the door inlet was set at 0.008022 kg/s, whereas the mass flowrate for the roof (inlet) was half of this. The mass flowrate was calculated from the volumetric flowrate of the kitchen. The temperature was assumed to be 15ºC.

Table 5-8: Overview of the values for various parameters used as the boundary conditions for the mathematical CFD modelling for Case 1

Boundary Conditions	Parameters
Mass-flow-inlet	mass flowrate (door): 0.008022 kg/s mass flowrate (roof): 0.004011 kg/s
	hydraulic diameter (door): 1.0830 m hydraulic diameter (roof): 0.9799 m
	temperature: 288 K
	mass fraction (O_2): 0.233
Outflow	flow rate weighting = 1

5.4.1 Air Flow Pattern

Contours of velocity magnitude for various horizontal and vertical sections of the kitchen in the rural house are presented in Figure 5-70. Figures 5-70a and 5-70b show the horizontal airflow pattern for the lower (0.4 m from the floor) and upper (1.9 m from floor level) parts of the kitchen respectively. The air entered the kitchen through the various inlets, mainly the door leading to the outside environment, although also through the windows, and moved randomly through the kitchen at a variety of velocities (from 0.006 m/s to 0.011 m/s) towards the outlet – the door leading from the kitchen to the rest of the house. This may be one of the main causes of pollutant ingression from the outdoor environment; this would also explain why outdoor pollutants and those from the kitchen are found in the rest of the house, e.g. the bedrooms and lounge.

As shown, there was some limited recirculation that occurred, mainly in the corners of the kitchen. Airflow velocities near the walls and corners were very slow – generally less than 0.001 m/s. Furthermore, the furniture, such as wall cabinets, the dining table and cupboards were found to limit the movement of the incoming air towards the outlet. A large circulating region of air (recirculation zone) with low air velocities was formed behind the cupboards and dining table. This region was marked by the deep blue colour in the figures (the slowest velocity) and occupied most parts of the kitchen due to the presence of furniture.

Figures 5-70c and 5-70d present the FLUENT modelling results for the vertical airflow patterns at the centre of the kitchen and near the outlet point (the door leading from the kitchen to the rest of the house). These diagrams also show that the fastest velocities were seen at or close to the outflow – the door from the kitchen to the rest of the home (identified as the yellow, orange and red colours, which indicate velocities of up to 0.024 m/s). The airflow coming from the inlet door moved both horizontally and vertically in the kitchen and finally exited at the outlet.

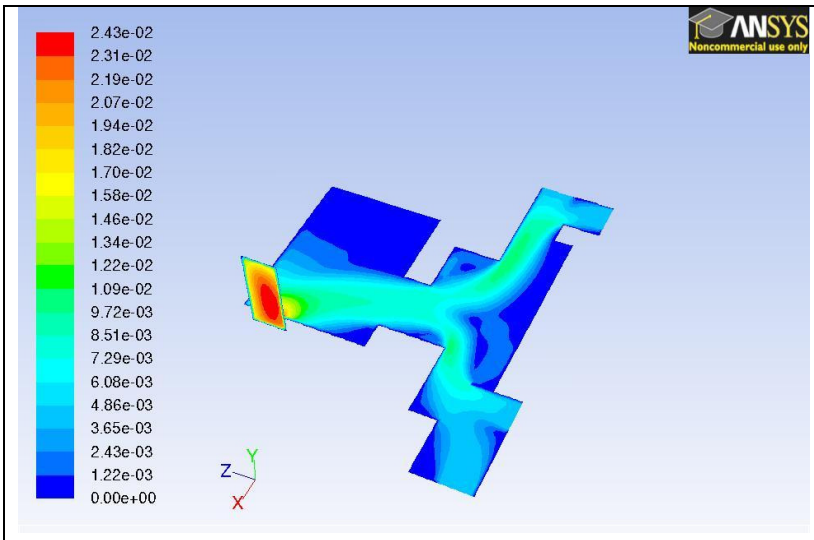
2.43e-02
2.31e-02
2.19e-02
2.07e-02
1.94e-02
1.82e-02
1.70e-02
1.58e-02
1.46e-02
1.34e-02
1.22e-02
1.09e-02
9.72e-03
8.51e-03
7.29e-03
6.08e-03
4.86e-03
3.65e-03
2.43e-03
1.22e-03
0.00e+00
ANSYS
Noncommercial use only
Y
Z
X

(a)

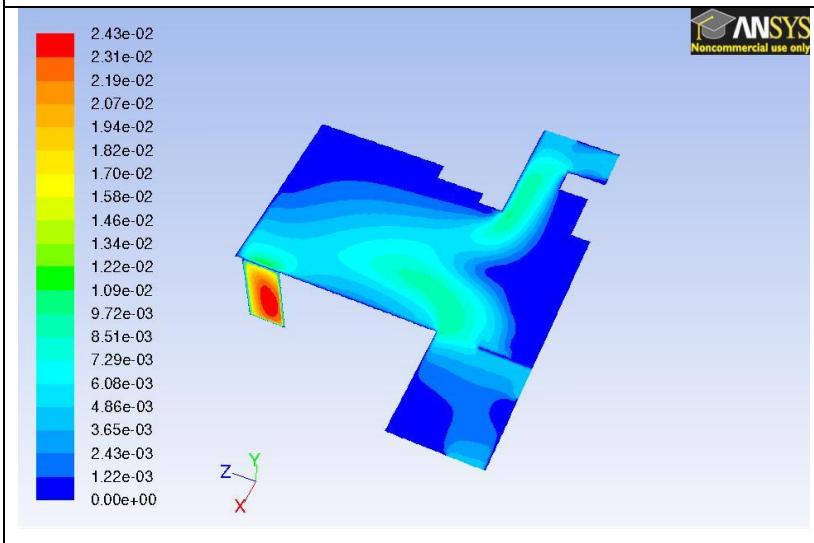
2.43e-02
2.31e-02
2.19e-02
2.07e-02
1.94e-02
1.82e-02
1.70e-02
1.58e-02
1.46e-02
1.34e-02
1.22e-02
1.09e-02
9.72e-03
8.51e-03
7.29e-03
6.08e-03
4.86e-03
3.65e-03
2.43e-03
1.22e-03
0.00e+00
ANSYS
Noncommercial use only
Y
Z
X

(b)

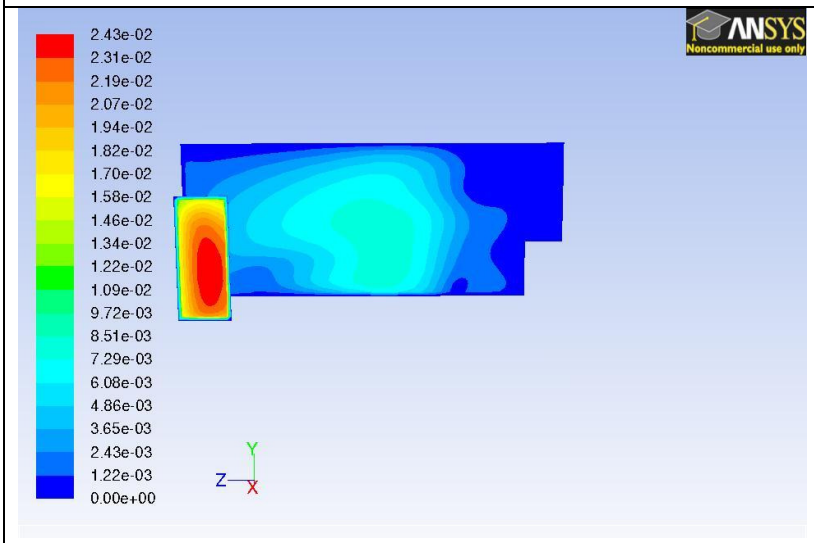
2.43e-02
2.31e-02
2.19e-02
2.07e-02
1.94e-02
1.82e-02
1.70e-02
1.58e-02
1.46e-02
1.34e-02
1.22e-02
1.09e-02
9.72e-03
8.51e-03
7.29e-03
6.08e-03
4.86e-03
3.65e-03
2.43e-03
1.22e-03
0.00e+00
ANSYS
Noncommercial use only
Y
Z
X

(c)

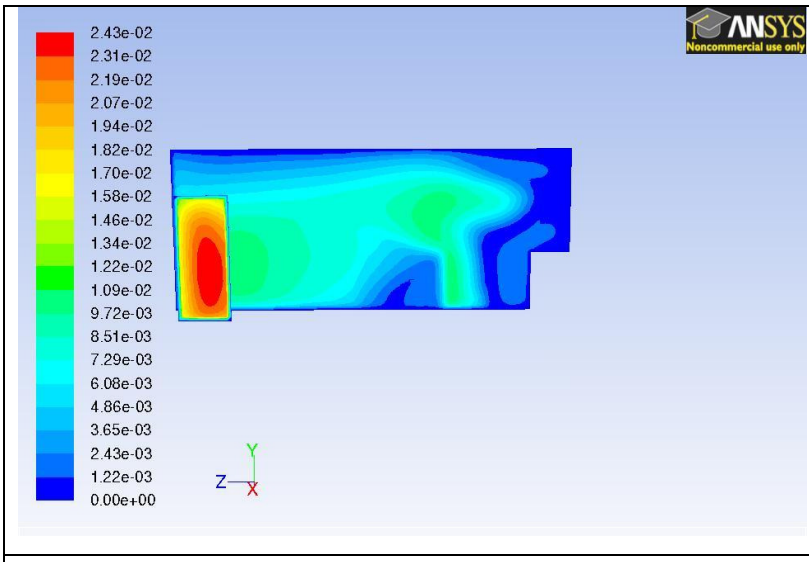

(d)

Figure 5-70: Velocity magnitude contours (m/s) for the kitchen: (a) 0.4 m above floor level, (b) 1.9 m above floor level, (c) centre of kitchen and (d) near the outlet at the rural house

5.4.2 Particle Injection

Once the velocity magnitude had been modelled, approximately 800 particles of 1 μm diameter were injected into the kitchen to monitor the flow fields. The quantity of particles injected into the kitchen depended on the number of grid meshes constructed for the inlets. Figure 5-71 shows the particle traces from different inlet points. The particles were injected from the roof and doors that lead to the outdoor environment; all particles were transferred through the kitchen from these inlets to the outflow – the door to the rest of the house. This is further conformation that particles from both the outdoor environment and the kitchen can migrate through the property.

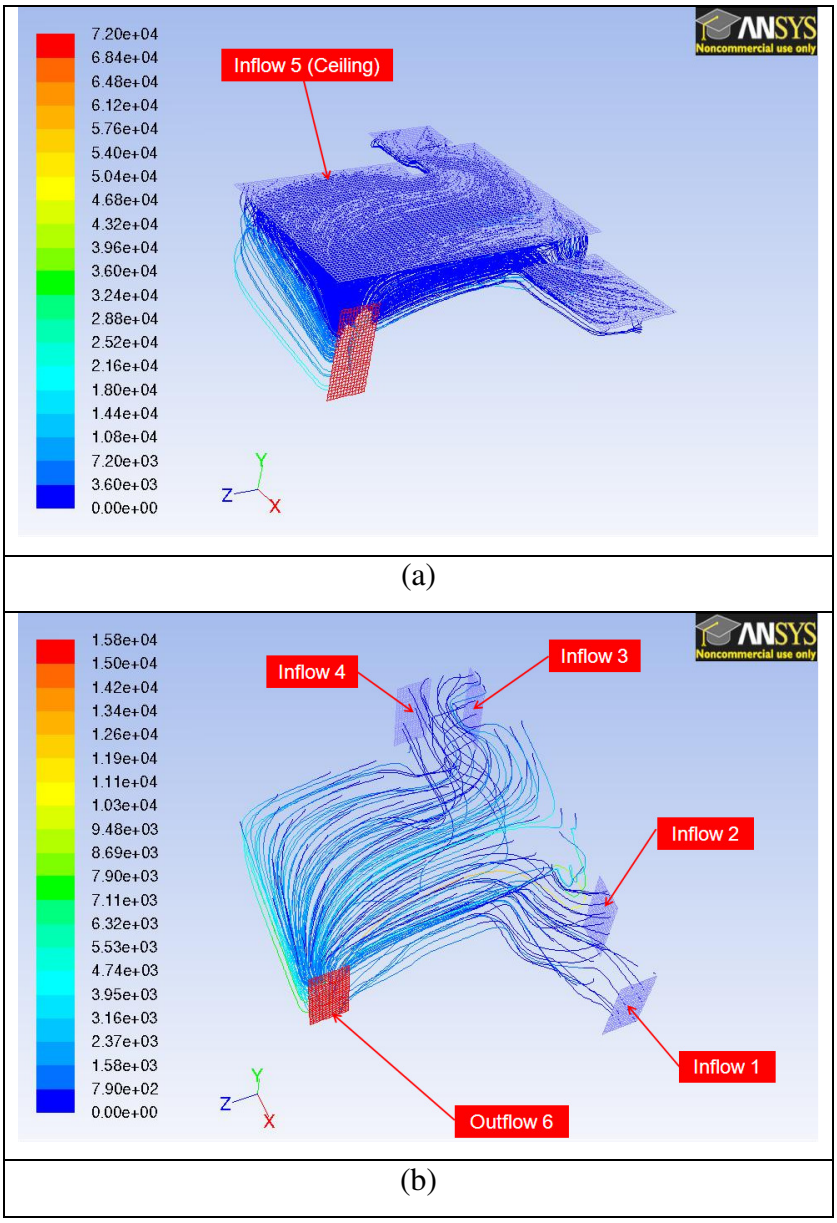

Figure 5-71: The particle traces coloured by particle residence time (s) from (a) roof; and (b) different doors (inlet points), in the kitchen of Case 1

Most of the particles were expelled out of the kitchen with the airflow. However, some of them settled on the floor or walls. Finer particles possess only small inertia, which limits them from accumulating rebound energy; these particles are thus easily deposited on the floor or walls (Zhang and Chen, 2006; Chang and Hu; 2008). Moreover, there were some particles which became trapped in the eddies inside the kitchen, thus the particle-tracking process is longer than any other region in the house. The particles entering the kitchen from these different inlets have a range of particle residence times. The theoretical residence time was calculated based on the size and volumetric flowrate of the kitchen. The theoretical residence time for this kitchen was 2,483

seconds (approximately 42 minutes). This means that the particles would stay up to 42 minutes in the kitchen before they were removed through the outlet.

In reality, there are many factors affecting the airflow and particle trajectories within the kitchen; these include the gap between the windows and walls, doors opening and extractor fans and heating which can set up convection currents, among others. In this model, only the basic factors were considered, as the kitchen was assumed to be a perfect stirred reactor. Thus, the calculated theoretical residence time was not suitable to be used to compare with the experimental results.

5.5 SUMMARY

Various experimental tests were conducted in a residential house in Hathersage. The concentrations of NO_2, VOCs, CO and $PM_{2.5}$ were measured in the kitchen and outdoor environment at this site. Additional particle collection and analysis was conducted using the Andersen Sampler. The PM were analysed for particle size distribution, elemental composition and morphology.

Most of the particles collected from the indoor environment (bedroom, kitchen and lounge) were within the range of 1.1 to 2.1µm. As for the outdoor environment, approximately 29% of the particles collected had a particle size of less than 0.4µm. The morphology of the particles collected from the indoor environment mainly comprised of salt crystals, mineral fibres, skin flakes and dust fragment. As for the outdoor environment, the particles were mainly dust fragments, cenospheres, pollen, salt crystals, mineral fibre and carboneous material. The chemical compositions of the particles collected from the indoor environment were mainly Fe, Na, Zn, S, B, Ca and Si. The majority of the particles collected from the outdoor environment contained S, Na and K.

The average indoor (kitchen) and outdoor $PM_{2.5}$ concentrations were 16 $\mu g/m^3$ and 10 $\mu g/m^3$ respectively. The average emission rate of $PM_{2.5}$ for the different cooking periods varied from 5.4 to 6.4 mg/hr. The average indoor CO concentration was 1.0 ppm, whilst the outdoor CO concentration at this site was zero. The CO emission rate was 0.091g/hr.

The indoor and outdoor NO_2 concentrations were 10.2 µg/m^3 and 10.8 µg/m^3 respectively. The emission rate of NO_2 at this property was zero. The indoor Σ20 VOC concentration was 221.5 µg/m^3 and the outdoor concentration was 42.6 µg/m^3. The emission rate of VOCs was 13.0 mg/hr. Toluene was the most common VOC for this case study. The air exchange rate in this kitchen was 1.5±0.2 air changes per hour (hr^{-1}).

6

CASE STUDY 2: EXPERIMENTS IN A RESIDENTIAL FLAT NEAR SHEFFIELD CITY CENTRE

A series of extensive emissions tests were carried out in a residential flat near Sheffield city centre. The flat was equipped with a gas-fired cooker. Concentrations of $PM_{2.5,}$ CO, NO_2 and VOCs were measured in this kitchen. Air exchange rates were also measured in this flat (i.e. kitchen). By using the mass balance method, the emission rates of indoor pollutants ($PM_{2.5}$, CO, NO_2 and VOCs) from various cooking activities were calculated. The case study environment and results obtained are described below.

6.1 SITE DESCRIPTIONS

The second case study environment was a residential flat near Sheffield city centre (Figure 6-1). The flat was on the second floor in a residential building near a street in the vicinity of the Crookes Valley Park. Figure 6-2 presents the street view and the outdoor sampling point (i.e. balcony of flat).

Figure 6-1: Aerial view showing the location of the residential flat in Sheffield (Google, 2009)

Figure 6-2: Street view of the flat in Sheffield

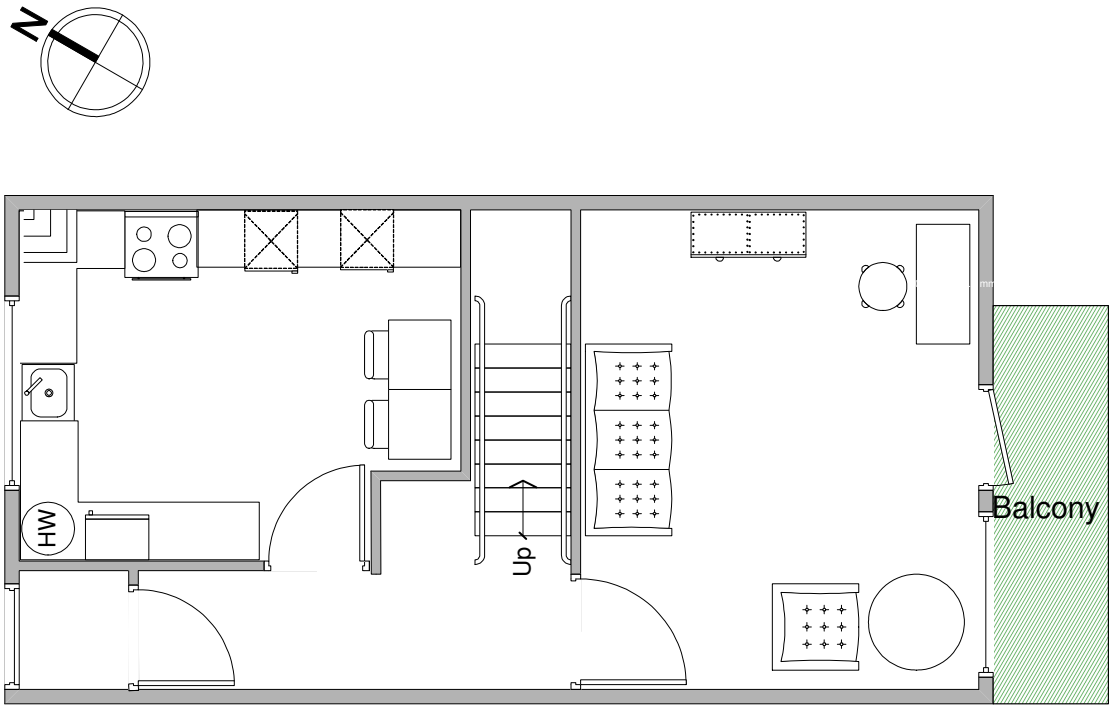

Figure 6-3: Layout of the kitchen and the living room of the flat

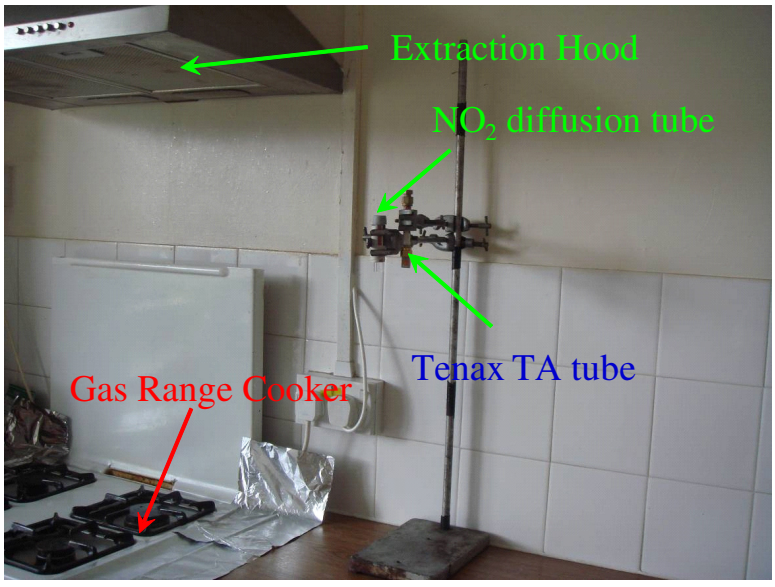

Figure 6-4: Cooker, extraction hood and installation of sampling equipment

Figure 6-3 shows the layout of the kitchen and the living room in the flat. The estimated kitchen volume is 36 m^3. A natural gas-fired boiler (Glow-worm Betacom c, 30kW) is installed in the kitchen, which provides hot water (presented as HW in Figure 6-3). The flue gases from the boiler are discharged to the outdoor environment via a vent above the boiler. Also in this kitchen, there is a gas cooker approximately 3 m from the boiler. A hood (extractor fan) is installed one metre above the cooker to improve ventilation during cooking (Figure 6-4). For this case, the

analytical instruments were placed 0.5 m from the cooker, at a height of about 1.5 m from the floor. The doors to the main entrance and balcony were closed.

6.2 NO_2, VOC, CO AND $PM_{2.5}$ MEASUREMENTS

6.2.1 Indoor and Outdoor Concentrations of Pollutants

6.2.1.1 $PM_{2.5}$

The real time indoor $PM_{2.5}$ concentrations in the kitchen of the city-centre flat are presented in Figure 6-5. As shown, the $PM_{2.5}$ spikes were much higher than those for Case 1, often by an order of magnitude. This is due to the type of cooker used – the city-centre flat has a gas cooker compared to an electric cooker in the rural house (Case 1). Other possible sources of such high $PM_{2.5}$ concentrations may include burnt food and different cooking techniques, such as more frying with cooking oil. Frequent deep-frying is one of the Chinese cooking traditions. Indoor cooking oil pollution is one of the main causes of lung cancer in China (Zhao *et al.*, 2006). This flat was owned by a Chinese family. Therefore a large amount of cooking oil was frequently used in this kitchen with a high cooking temperature. They have stir-fried food almost everyday. The fumes emitted from frying pans can nucleate, forming ultrafine particles inside the kitchen. Most coarse particles generated in the kitchen are known to be from frying and spattering during cooking. This scenario agreed well with the research conducted by Lai and Ho (2008). The average indoor $PM_{2.5}$ concentration in this kitchen was 40.6 $\mu g/m^3$, much higher than Case 1, whereas the average outdoor $PM_{2.5}$ concentration near the flat was 14 $\mu g/m^3$, which is more similar, but still slightly elevated compared to the rural house.

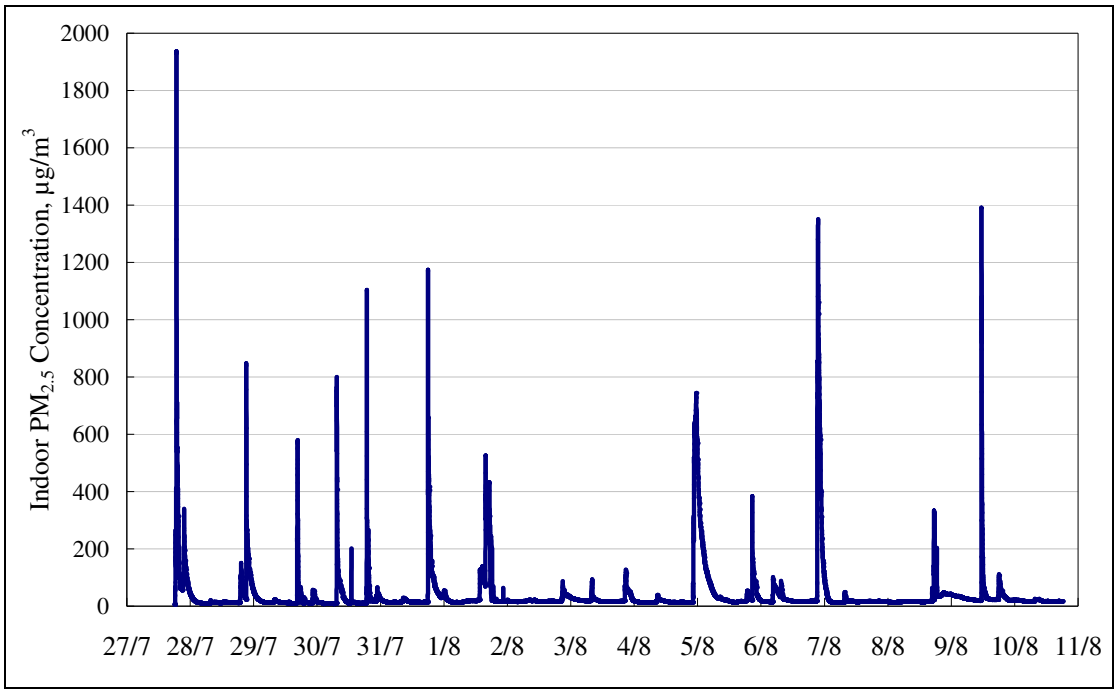

Figure 6-5: Real time concentrations of indoor $PM_{2.5}$ in the kitchen

6.2.1.2 CO

The real time concentration of indoor CO in the kitchen of the city-centre flat (Case 2) is shown in Figure 6-6. CO spikes occurred whenever any cooking activity was conducted, thus the source of CO emissions would be the gas cooker used in the kitchen. The average indoor CO concentration during the entire monitoring period was 2 ppm, though peaks of 14-22 ppm were recorded, as shown in Figure 6-6. The gas-fired cooker used in this kitchen is quite old, thus the possibility of CO emissions to the atmosphere is higher compared to the gas cooker used in Case 3 (as detailed in Chapter 7). It can be concluded that indoor air quality in a kitchen using this gas cooker (Case 2) is generally poorer than a kitchen using electric cooker (Case 1).

The outdoor CO concentration at this site was zero, as measured by the TSI IAQ-Calc 7545. This implies that the outdoor CO at this location is dispersed rapidly. As reported in the UK National Air Quality Archive, during the summer of 2009, the monthly average CO concentration in Sheffield city centre was only 0.2-0.3ppm (DEFRA, 2009).

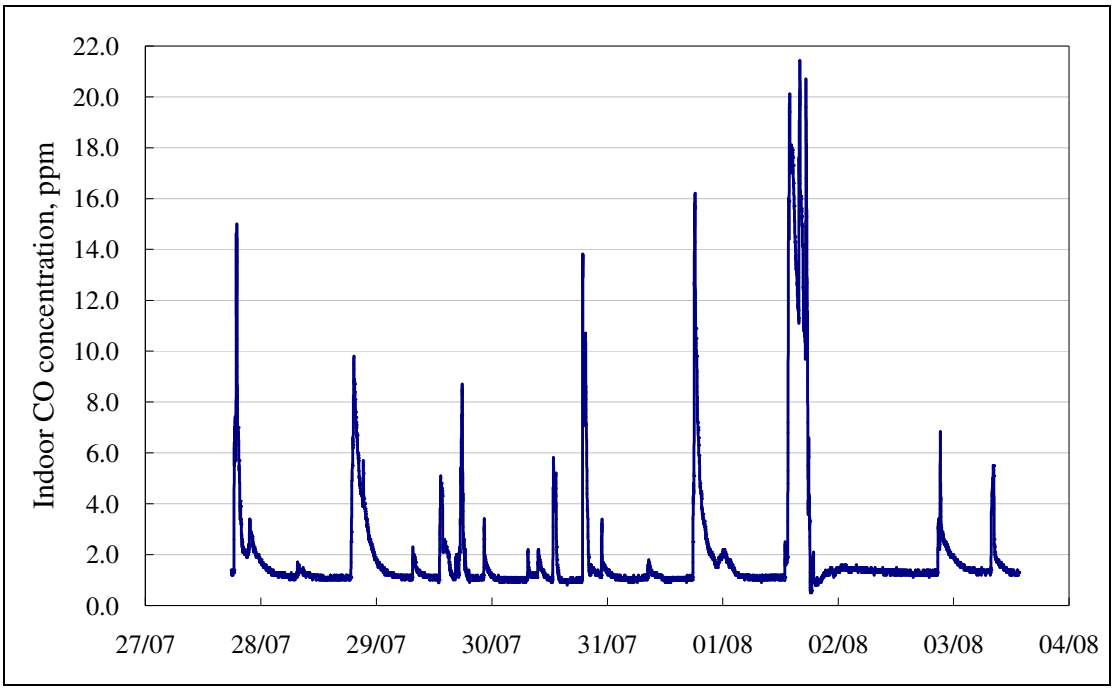

Figure 6-6: Real time concentrations of indoor CO from the kitchen

6.2.1.3 NO_2

The indoor and outdoor NO_2 concentrations measured using NO_2 diffusion tubes are shown in Table 6-1. The NO_2 concentration inside the city-centre flat (Case 2) was 3.5 times higher than the outdoor NO_2 concentration – 47.1 µg/m^3 compared to 14.7 µg/m^3. This is attributed to the use of a gas cooker in the flat. NO_2 was produced when nitrogen and oxygen reacted during combustion processes. In addition, the main constituents of air are nitrogen (78%) and oxygen (21%). Thus, NO_2 was formed as long as the gas cooker was turned on. Therefore, the cooker is the major source of indoor NO_2.

Table 6-1: Indoor and outdoor NO_2 concentrations

Sampling Site	Indoor	Outdoor
Residential flat near Sheffield Centre, µg/m^3	47.1	14.7

6.2.1.4 VOCs

Table 6-2 presents the indoor and outdoor concentrations of the Σ20 VOCs obtained from the analysis of the TENAX TA Tubes deployed at this sampling location. The indoor Σ20 VOC concentration (430.7 µg/m^3) was notably higher than the outdoor concentration (65.4 µg/m^3). The reason for the elevated Σ20 VOC concentration in this kitchen is most likely due to the difference

in cooking styles, as well as subtle differences in the gas cooker used. The possible sources of these indoor VOCs include combustion by-products (gas stoves) and cooking activities (emissions from food), as well as cleaning products. Other possible sources of the indoor VOCs include building materials, kitchen furnishings and consumer products. The building materials here refer to floor coverings, paints and lacquers used on the kitchen's wall and furniture. Consumer products such as electrical goods, plastics, cleaning detergents and air freshers were widely used in this kitchen.

Table 6-2: Indoor and outdoor VOC concentrations

Sampling Site	Indoor	Outdoor
Residential flat near Sheffield Centre, µg/m^3	430.7	65.4

The top 20 VOCs sampled from the indoors and outdoors using Tenax TA Tubes are presented in Figure 6-7. Toluene was by far the most common VOC to be found in the indoor environment for this case study. The concentrations of this aromatic hydrocarbon exceeded 200 µg/m^3 inside this city-centre flat (Case 2). On the other hand, Heptadecane, probably from vehicles, was one of the most common VOCs found in the outdoor environment at Case 2.

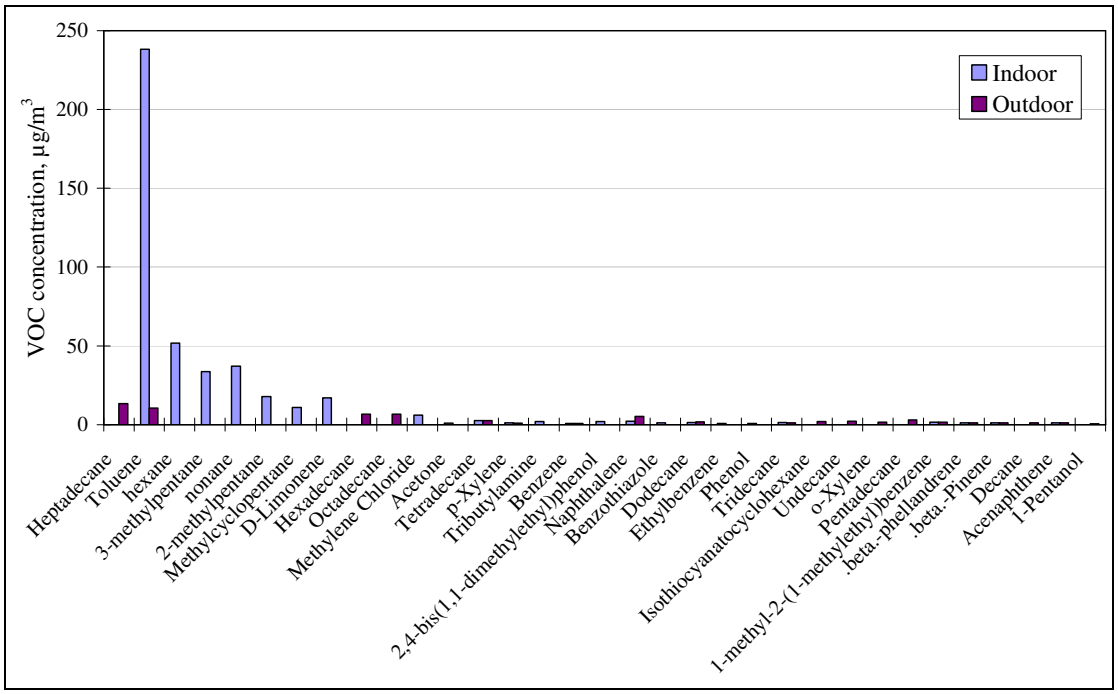

Figure 6-7: Top 20 VOCs sampled (µg/m^3)

6.2.2 Indoor Temperature and Relative Humidity

Figure 6-8 shows the real time temperature recordings taken in the kitchen of Case 2. The temperature recorded ranged from ~21 to 32 ℃. Cooking activities could be the main contributor to the temperature variations.

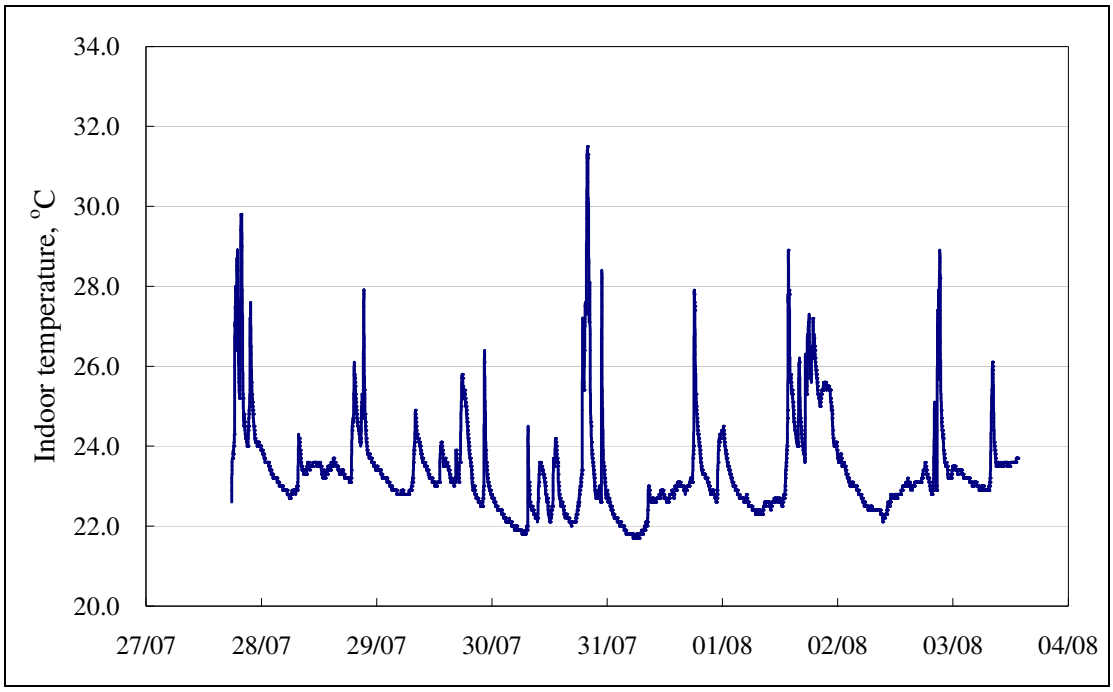

Figure 6-8: Real time temperature recordings in the kitchen

Figure 6-9 presents the real time recordings of the relative humidity in the kitchen of the Case 2 flat. The range of indoor humidity levels was 25% to ~85%. The great increases in humidity levels were due to cooking activities.

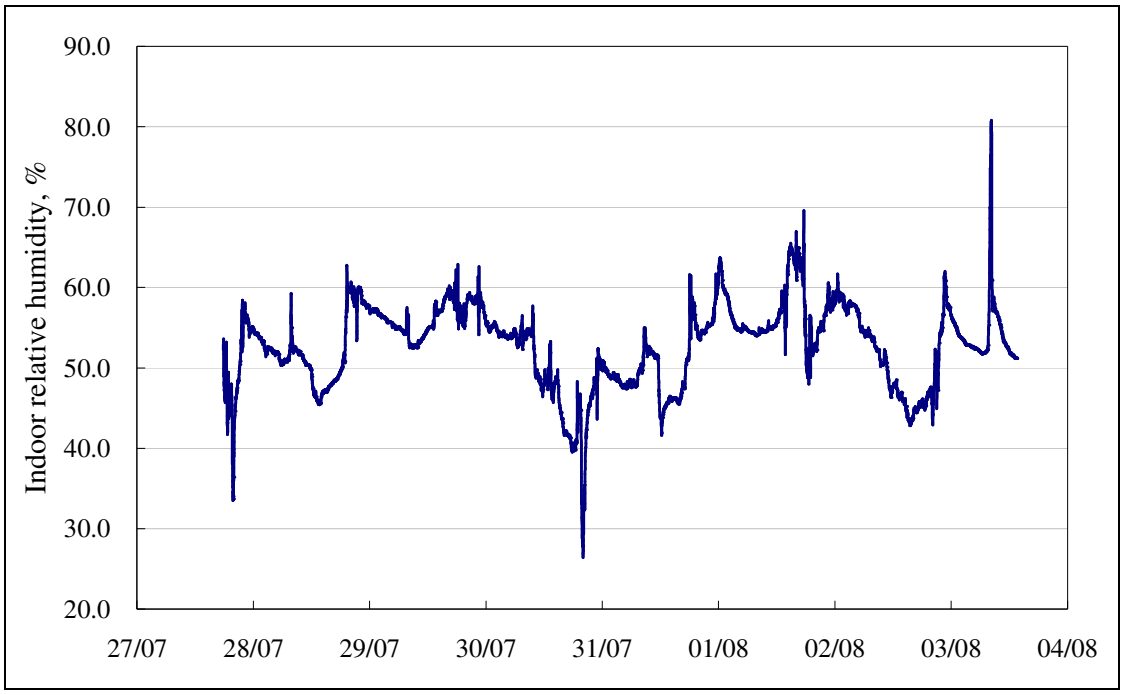

Figure 6-9: Real time recordings of the relative humidity in the kitchen

6.2.3 Air Exchange Rate

The air exchange rate was calculated in order to allow the determination of the emission rates for each pollutant from the previous tests. The CO_2 concentration decay curve measured in the kitchen of the city-centre flat (Case 2) is shown in Figure 6-10. The air exchange rate in this kitchen was 3.3±0.6 air changes per hour (hr^{-1}). The higher air exchange rate in this case study was expected. This is due to the presence of an air extraction fan above the cooker (the extractor oven fan was on during the cooking process). This value is much higher than the values for the kitchens in both Cases 1 and 3.

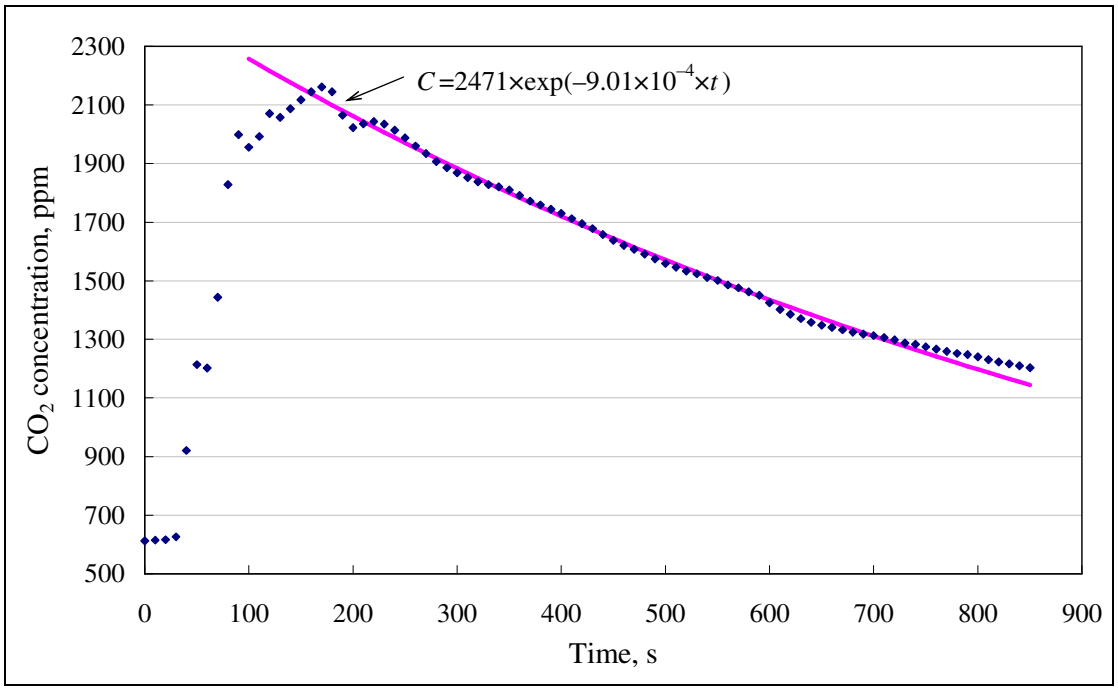

Figure 6-10: CO_2 concentration decay in the kitchen
(Air exchange rate = 3.3±0.6 air changes per hour (hr^{-1}))

6.2.4 Emission Rates of Indoor Pollutants

6.2.4.1 $PM_{2.5}$

Based on the CO_2 decay curve and the subsequent air exchange rate that was calculated, $PM_{2.5}$ emission rates could thus be determined for the cooking periods in this kitchen (Case 2). The tests for Case 2 also showed that there was a considerable range in emission rates in the kitchen. The emission rates of $PM_{2.5}$ during five cooking periods in the kitchen are presented in Figure 6-11. Particles emitted from food preparation or frying are the main contributor to the emission rate variations. This was further confirmed by the high peaks of emission rates on 27th and 31st of July, 2009, as shown in Figure 6-11. During these two days, deep frying was done by the Chinese family with a large amount of cooking oil. Cooking fumes (submicron-sized particulate matter) were then generated during the frying process.

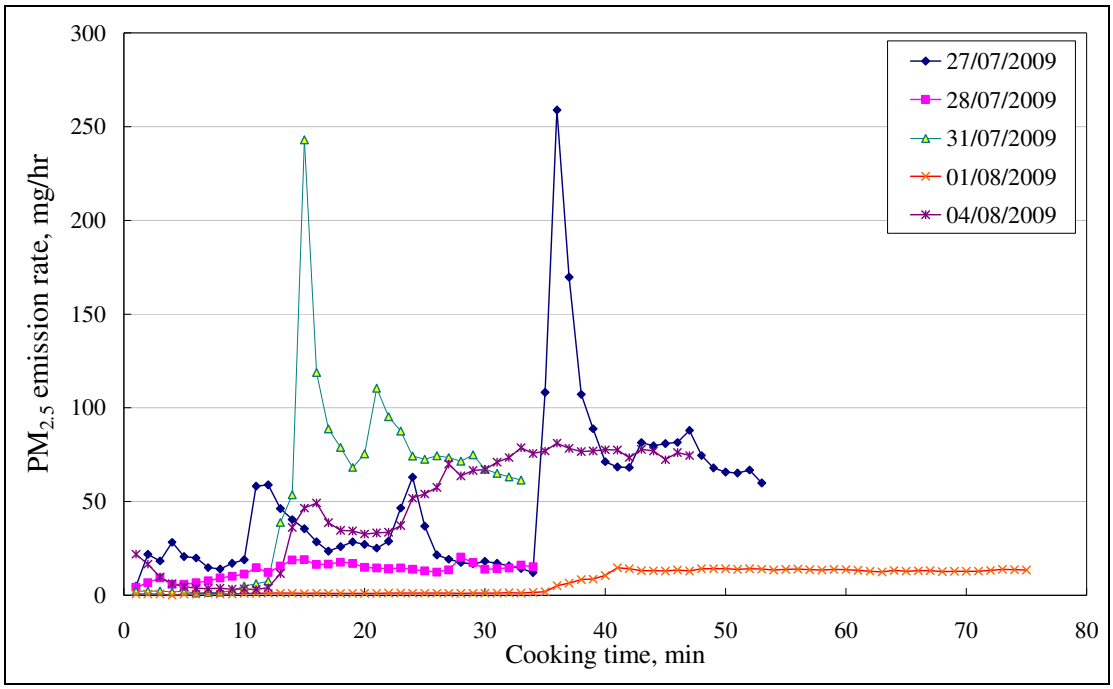

Figure 6-11: The emission rates of $PM_{2.5}$ during the cooking events in the kitchen

The average emission rates for each cooking period are listed in Table 6-3. As presented in Table 6-3, the average emission rate of $PM_{2.5}$ for the different cooking periods varied from 7 to 54 mg/hr. Traynor *et al* (1982) reported that the emission rates of $PM_{2.5}$ from range-top burners (domestic cookers) were in the region of 0.24-1.62 µg/kJ. This is similar to the low range of the results obtained in this study, which were calculated to be in the region of 0.60-4.5 µg/kJ, when normalised to the amount of fuel consumed during the cooking period.

Table 6-3: Average emission rates of $PM_{2.5}$ in the kitchen of the residential flat near Sheffield City Centre

Date	**Average emission rates of $PM_{2.5}$**	
	mg/hr	**µg/kJ**
27/07/2009	50.1	4.14
28/07/2009	13.2	1.08
31/07/2009	54.4	4.50
01/08/2009	7.31	0.60
04/08/2009	46.8	3.86

6.2.4.2 CO

Figure 6-12 shows the variations in CO emission rates during several cooking periods in the kitchen for Case 2. The CO emissions were attributed to the presence and use of the gas cooker.

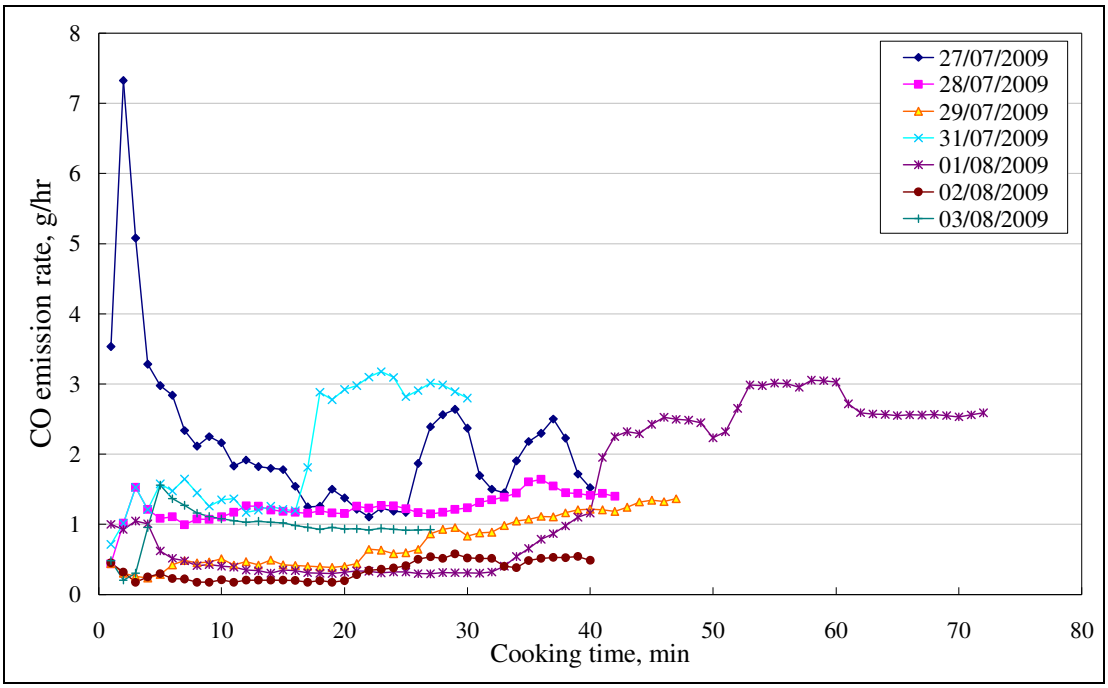

Figure 6-12: CO emission rates during the cooking events in the kitchen of the residential flat near Sheffield City Centre

Table 6-4 lists the average CO emission rates for each cooking period. The emission rates based on unit fuel consumption (μg/kJ) are also given in this table. During cooking periods, the CO emission rates from the gas cooker ranged from 0.3 to 2.2 g/hr (i.e. 28.4-179.4 μg/kJ). These values are well within the range (9.9-243.8 μg/kJ) reported by Moschandreas *et al* (1987). The CO emission rates obtained from range-top burners by Traynor *et al* (1982) were 200-226 μg/kJ, slightly higher than those for Case 2 in this study.

Table 6-4: Average CO emission rates in the kitchen

Date	Average emission rate of CO	
	g/hr	µg/kJ
27/07/2009	2.17	179.4
28/07/2009	1.24	102.6
29/07/2009	0.74	61.4
31/07/2009	2.02	167.6
01/08/2009	1.44	119.2
02/08/2009	0.34	28.4
03/08/2009	0.96	79.4

6.2.4.3 NO_2 & VOCs

The indoor emission rates of NO_2 and VOCs calculated in the flat are shown in Table 6-5. The NO_2 emissions in the kitchen of the city-centre flat are attributed to gas combustion (gas-fuelled cooker). As seen in Table 6-5, the emission rate of NO_2 at this property was 65.5 mg/hr, which was calculated from the measured NO_2 concentrations during cooking and the air exchange rate for this kitchen. When normalised to the amount of fuel consumed during the cooking period, the emission rate of NO_2 is 5.42 µg/kJ. This value is within the range (4.98-7.03 µg/kJ) reported by Traynor *et al* (1982).

The higher indoor Σ20 VOC concentrations at this location resulted in higher VOC emissions rates. The reason for the elevated Σ20 VOC concentration in the city-centre flat (Case 2) is most likely to be due to the gas cooker used; emission rates of around 42.7 mg/hr were calculated for such species here.

Table 6-5: Indoor emission rates of NO_2 and VOCs

Date	Average emission rates of NO_2	Average emission rates of VOCs
	(mg/hr)	(mg/hr)
Residential flat in Sheffield	65.5	42.7

6.3 SUMMARY

A number of experimental tests were conducted in a residential flat near Sheffield city centre. The tests include NO_2, VOC, CO and $PM_{2.5}$ measurements. The average indoor and outdoor $PM_{2.5}$ concentrations were 40.6 $\mu g/m^3$ and 14 $\mu g/m^3$ respectively. The average emission rate of $PM_{2.5}$ for the different cooking periods varied from 7 to 54 mg/hr. The possible sources of such high $PM_{2.5}$ concentrations may include burnt food and different cooking techniques. The average indoor CO concentration was 2 ppm, whilst the outdoor CO concentration at this site was zero. The source of CO emissions would be the gas cooker used in the kitchen. The CO emission rates from the gas cooker ranged from 0.3 to 2.2 g/hr (i.e. 28.4-179.4 µg/kJ). The indoor and outdoor NO_2 concentrations at this flat were 47.1 $\mu g/m^3$ and 14.7 $\mu g/m^3$ respectively. The emission rate of NO_2 at this property was 65.5 mg/hr. This is attributed to the use of a gas cooker in the flat where NO_2 was produced during the combustion process. The indoor Σ20 VOC concentration was 430.7 $\mu g/m^3$ and the outdoor concentration was 65.4 $\mu g/m^3$. The emission rate of VOCs was 42.7 mg/hr. The possible sources include the use of the gas cooker, differences in cooking styles, combustion by-products, cleaning products, building materials, kitchen furnishings and consumer products. Toluene was the most common VOC for this case study. The air exchange rate in this kitchen was 3.3±0.6 air changes per hour (hr^{-1}).

7

CASE STUDY 3: EXPERIMENTS IN A RESIDENTIAL FLAT ON A MAIN ROAD IN SHEFFIELD

An investigation was conducted in a residential flat on a main road in Sheffield. The kitchen used a gas cooker. Constant active measurements of $PM_{2.5}$ and CO concentrations were conducted. NO_2 and VOCs concentrations were monitored over a period of time in the kitchen. Air exchange rates were also measured in the flat. A mass balance method was used to calculate the emission rates of various indoor pollutants ($PM_{2.5}$, CO, NO_2 and VOCs) and an Andersen Sampler was used for conducting additional particle collection and analysis. The PM were then analysed for size distribution, elemental contents and morphology. The details of the case study location and results obtained are presented in this chapter.

7.1 SITE DESCRIPTIONS

The third case study was carried out in a residential flat on a main road in Sheffield (Figure 7-1). The flat is in a three-storey building located above shops in an urban area of Sheffield (Figure 7-2).

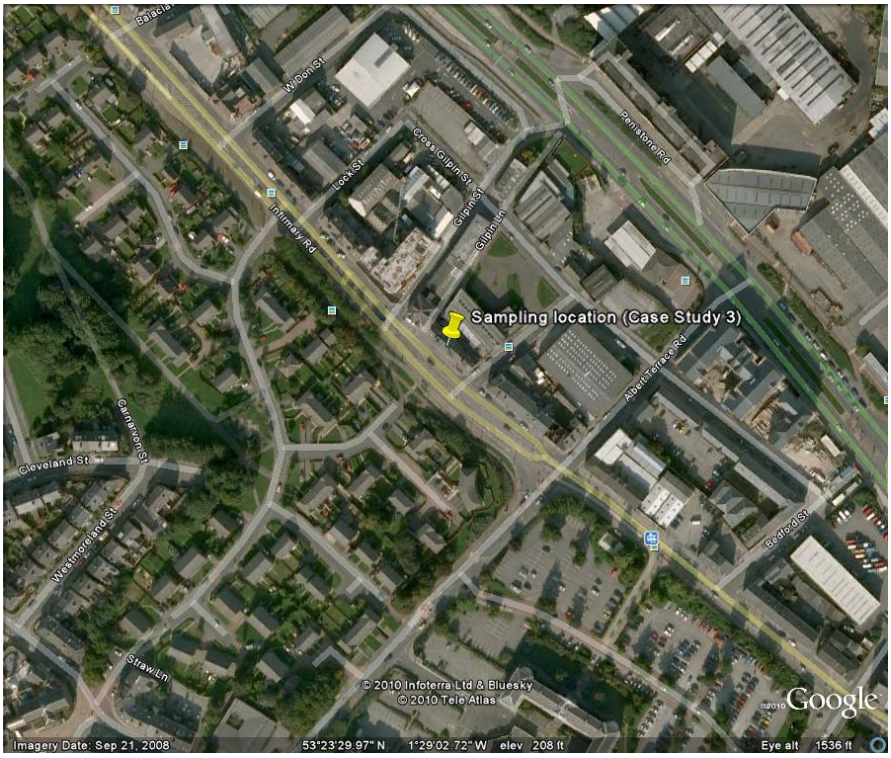

Figure 7-1: Aerial view of the residential flat on a main road in Sheffield (Google, 2010)

Figure 7-2: Sampling location for Case 3

The main road is regularly used by buses, trams and cars/lorries (Figure 7-3). Figure 7-4 shows the surroundings of the sampling location.

Figure 7-3: Street view of the residential flat for Case 3

Figure 7-4: General view of the sampling location

The kitchen is located on the first floor. Figure 7-5 shows the layout of the kitchen in the flat. The estimated volume of the kitchen is 30 m^3.

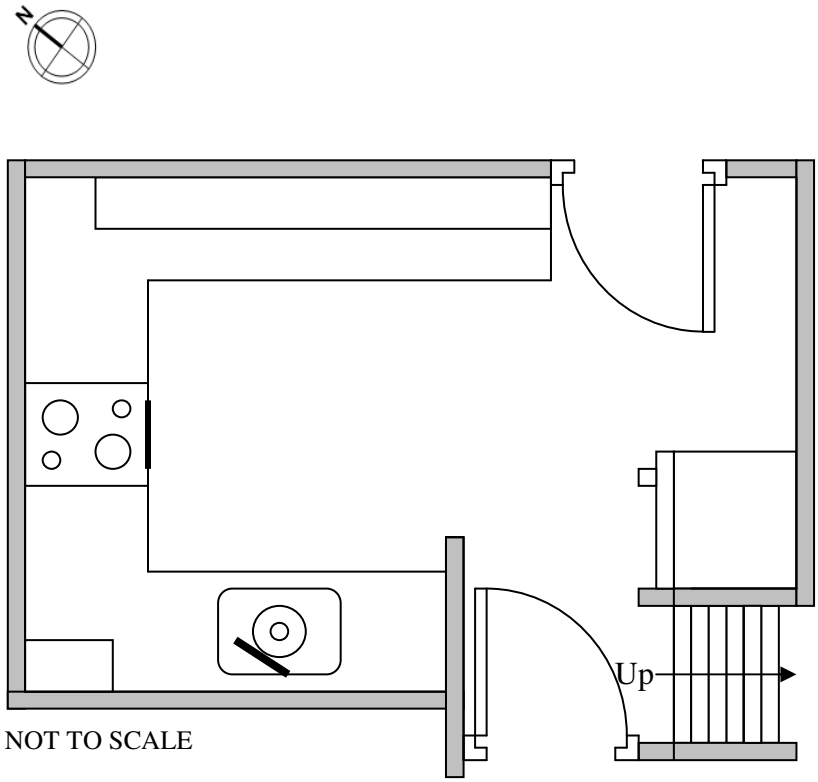

Figure 7-5: Layout plan of kitchen

Figure 7-6 illustrates the conditions inside the kitchen. A natural gas boiler (Ferroli Boilers type Optima 700, 22.3 kW; Figure 7-7a) vented to the outdoor environment is installed in one corner of the kitchen, about 1 m from the gas cooker (Leisure type 2100 SEL WH, 3-4.5 kW; Figure 7-7b), which does not have an extractor fan above it.

Figure 7-6: The conditions inside the kitchen

(a) (b)

Figure 7-7: (a) Natural gas heating system (Ferroli Boilers type Optima 700, 22.3kW), and (b) natural gas cooker (Leisure type 2100 SEL WH, 3 – 4.5kW)

During the measuring period, the analytical instruments were placed approximately 0.5 m away from the cooker at a height of about 1 m (Figure 7-8). The doors to the main entrance and living room were closed. The equipment was placed in the kitchen for four weeks. Sampling started on 15/09/2010 at 11.30am.

Figure 7-8: Installation of sampling equipment inside the kitchen

7.2 PARTICULATE MEASUREMENTS AND ANALYSIS

An Anderson Sampler/Impactor was used to collect particulate matter of all sizes. The sampler separates the particles using their mass, thus a particle size distribution could be established, including the proportion of particles smaller than 2.5 µm. The sampler was installed in between the cooker and the boiler at a height of about 1 m from the floor, as shown in Figure 7-9. The sampler was placed at the sampling location over a period of 4 weeks. Sampling started on 22/11/2010 at 10.30am and ended on 18/12/2010 at 5.00pm, which is equal to approximately 630.5 hours.

Figure 7-9: Installation of Andersen Sampler inside the kitchen

7.2.1 Particle Size Distribution

Table 7-1 shows the concentration of particles collected from the various stages of the Andersen Sampler. A total of 29.9 mg of particulates were collected from the kitchen during the entire monitoring period. The total test time was 630.5 hours, during which 1071.2 m^3 of air was sampled. The concentrations of $PM_{2.5}$ and PM_{10} were 11.95 µg/m^3 and 27.91 µg/m^3 respectively. It can be seen that the average amount of particulate matter collected from each stage of the Andersen sampler was evenly distributed. This is significantly different from Case 1, as the majority of the PM collected from both the kitchen and bedroom was within the range of 1.1-2.1 µm. The major sources of these particles were attributed to general cooking activities (fuel use and emissions from food) since a gas cooker was used in this kitchen. Other possible sources

were emissions from vehicles, including fuel combustion and from the wear of disc brakes. This is due to the sampling location being located on a main road.

Table 7-1: The concentrations of particles collected from each stage (Kitchen)

Stage	Mass Size Distribution (µm)	PM (mg)	Concentration (µg/m^3)	%
0	9.0-10	2.8	2.6138	9
1	5.8-9.0	3.4	3.1739	12
2	4.7-5.8	3.0	2.8005	10
3	3.3-4.7	3.9	3.6407	13
4	2.1-3.3	4.0	3.7340	13
5	1.1-2.1	3.5	3.2673	12
6	0.7-1.1	3.7	3.4540	12
7	0.4-0.7	2.7	2.5205	9
Filter	0-0.4	2.9	2.7072	10
Total		**29.9**	**27.9119**	**100.00**

Test time	37,830 mins (≈630.5 hours)
Air volume (m^3)	1071.23
$PM_{2.5}$ concentration (µg/m^3)	11.95
PM_{10} concentration (µg/m^3)	27.91

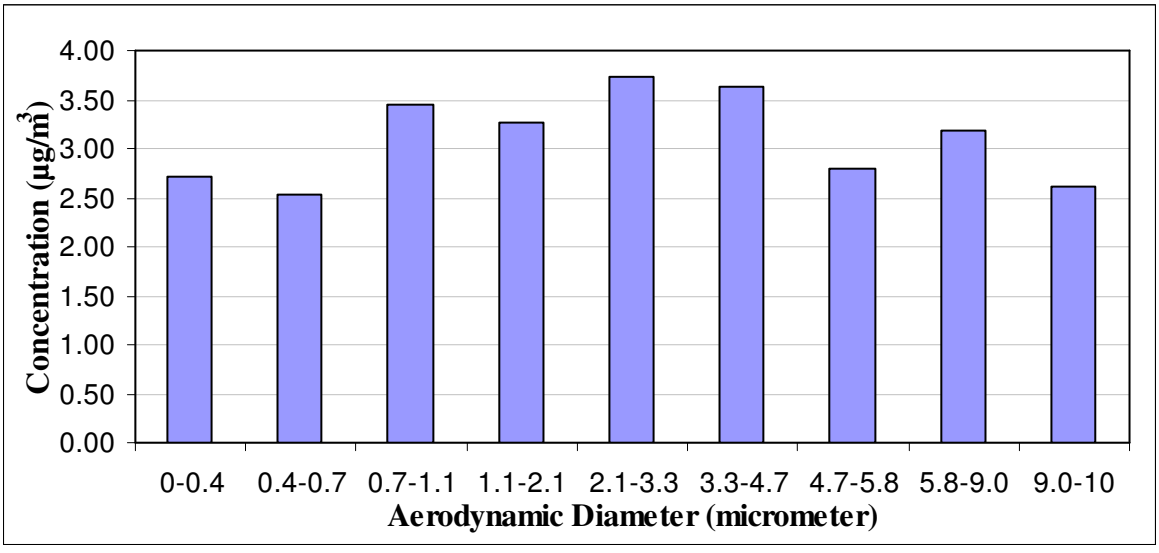

Figure 7-10: Particle size distribution for kitchen sampling

7.2.2 Full Elemental Analysis

In addition to the size distribution, the composition of the particles collected was also analysed. Figure 7-11 presents the elemental composition for the particles collected from the kitchen. As shown, the samples were mainly composed of Al, Na, Ca and Fe, with smaller amounts of Si, S, K and Mg, which could all be generated from either indoor or outdoor sources. Indoor sources may include cooking (for example salt particles, burnt food and particles from various cooking methods such as frying) and cleaning products, while outdoor sources were likely to be due to the nearby busy road. The traffic could result in a range of particles migrating into the house from sources including vehicle combustion and the wear of disc brakes, as the flat is located on a main road.

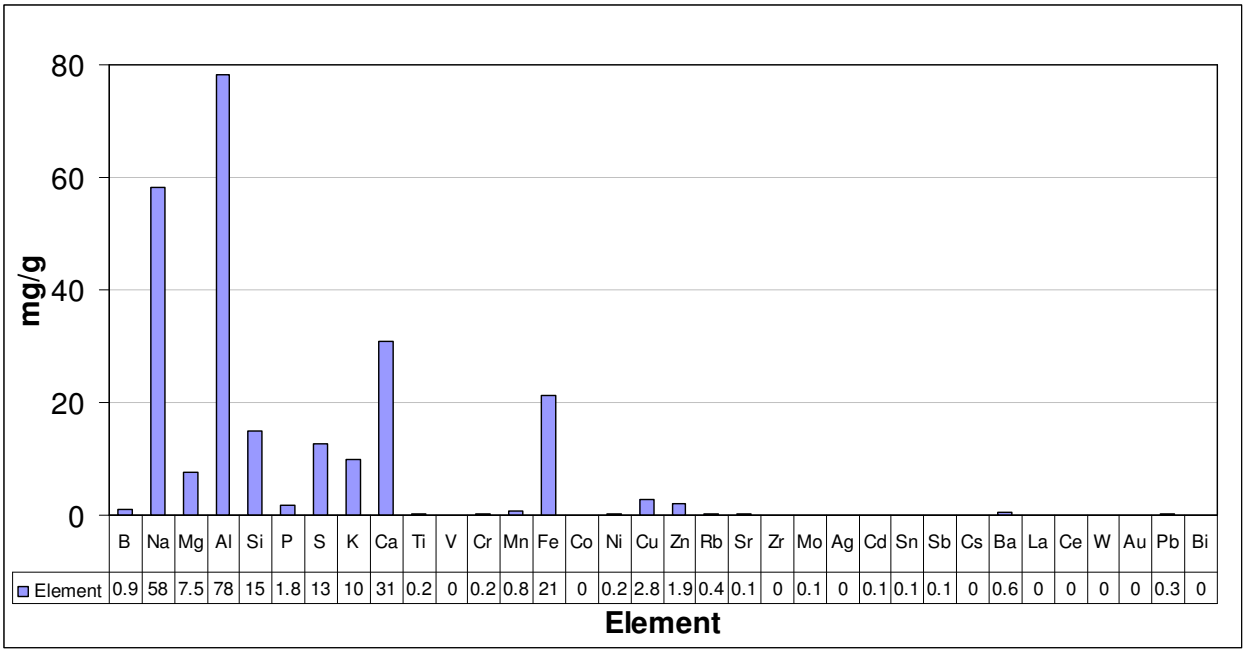

	B	Na	Mg	Al	Si	P	S	K	Ca	Ti	V	Cr	Mn	Fe	Co	Ni	Cu	Zn	Rb	Sr	Zr	Mo	Ag	Cd	Sn	Sb	Cs	Ba	La	Ce	W	Au	Pb	Bi
Element	0.9	58	7.5	78	15	1.8	13	10	31	0.2	0	0.2	0.8	21	0	0.2	2.8	1.9	0.4	0.1	0	0.1	0	0.1	0.1	0.1	0	0.6	0	0	0	0	0.3	0

Figure 7-11: Element composition of the particulates collected in the kitchen

7.2.3 Morphology Analysis

After the elemental composition of the overall sample was determined, the morphology of individual particles was then examined using SEM/EDS. The particles for each stage are presented along with a brief description.

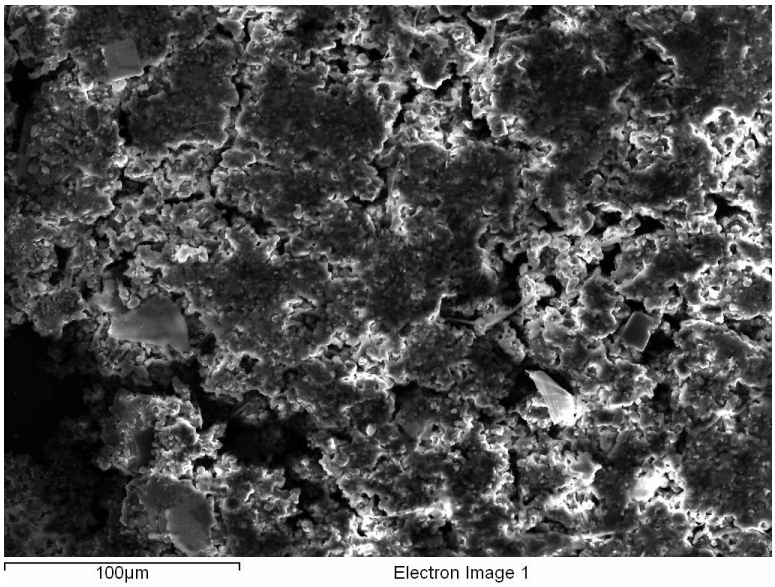

(a)

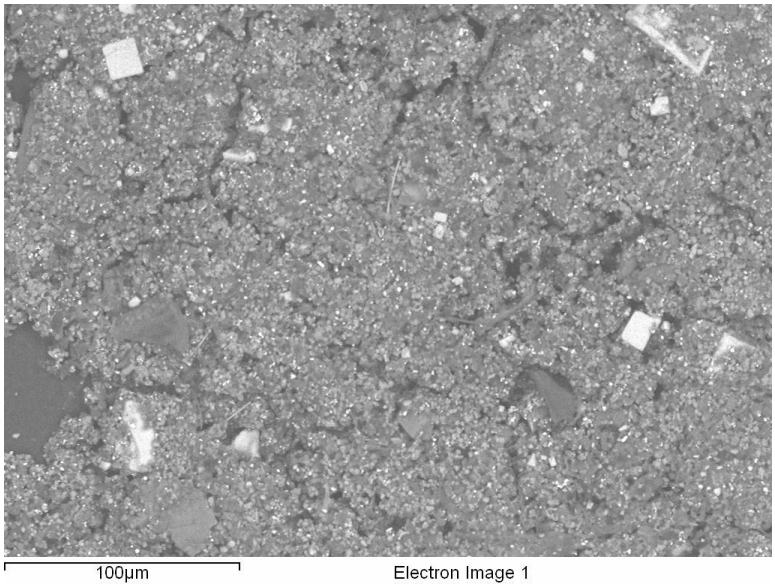

(b)

Figure 7-12: SEM/EDS images captured using (a) secondary electron mode; and (b) back-scattered mode (Kitchen sampling, Stage 4)

Figure 7-12(a) shows the SEM/EDS images captured using SE mode, and Figure 7-12(b) was captured using BS mode. SE mode shows the morphology of the sample and BS mode highlights the difference in atomic weight – the brighter the part of the image the higher the atomic weight. The elemental contents for the particles in Figure 7-12 were further analysed by using EDS, Figure 7-13.

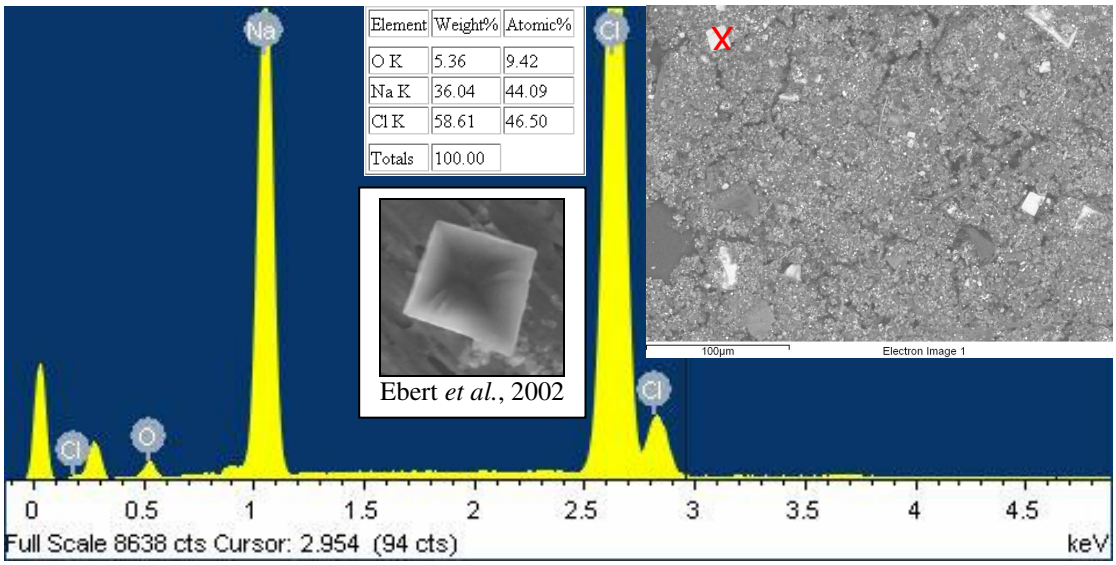

(a)

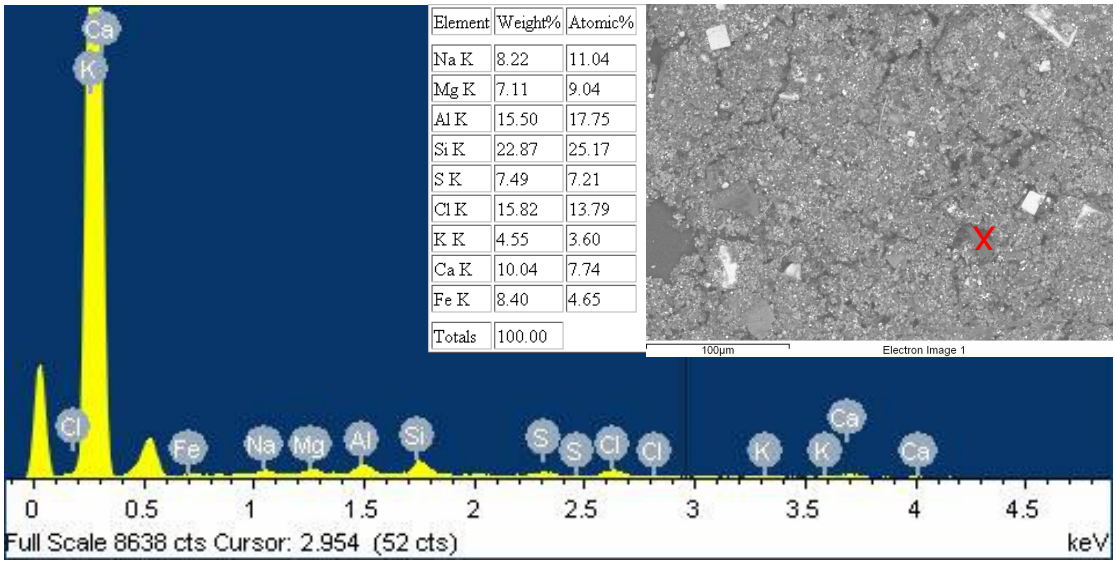

(b)

Figure 7-13: SEM/EDS analysis on kitchen sampling Stage 4 at 100 µm

Figure 7-13 shows the SEM/EDS analysis on kitchen sampling at 100 µm. The particle marked "X" in Figure 7-13(a) shows high amounts of Na (44.09% atomic weight) and Cl (46.50% atomic weight). The cube-like particle suggests that it is a salt crystal (NaCl). The shape of this particle is similar to the SEM images of NaCl particles from the literature (e.g. Ebert *et al.*, 2002) and the previous case here. The source of this particle is most likely from cooking activities since the equipment was placed very close to the cooker during the sampling period.

The particle marked "X" in Figure 7-13(b) shows a mixture of various metals. EDS analysis revealed high amounts of Si (25.17% atomic weight) and Al (17.75% atomic weight). These elements indicated that the particles were earth crustal materials (e.g. soil). EDS analysis

also revealed minor amounts of Cl (13.79% atomic weight), Na (11.04% atomic weight), Mg (9.04% atomic weight), Ca (7.74% atomic weight), S (7.21% atomic weight), Fe (4.65% atomic weight) and K (3.60% atomic weight). These minor elements from the analysis suggest that the particles are possibly tire/road wear or brake dust with soil grains on the top surface (Abu-Allaban *et al.*, 2003). This result was as expected as the sampling location is situated on a busy main road in Sheffield.

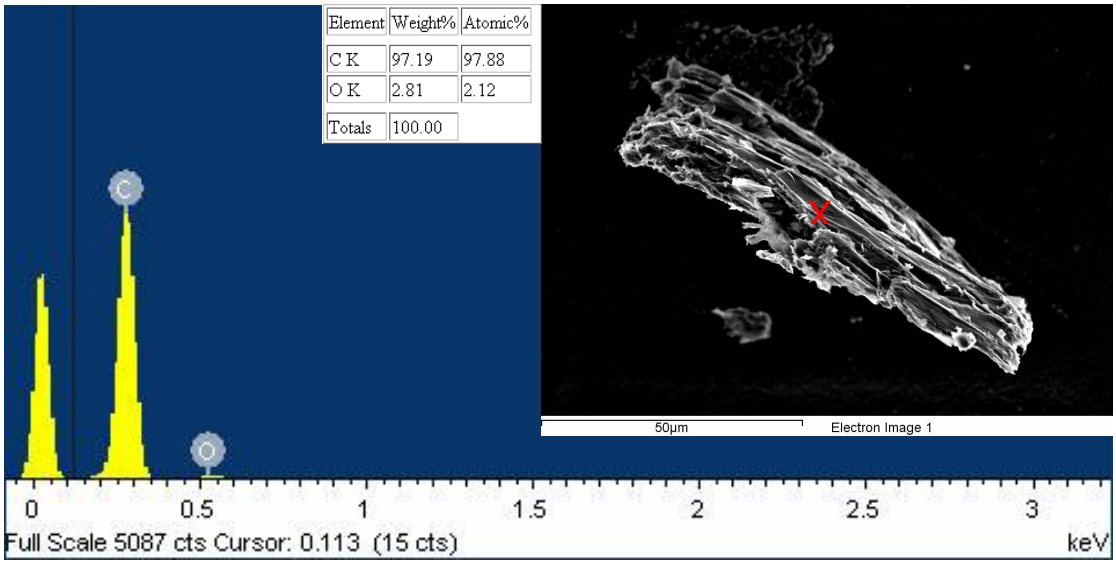

(a)

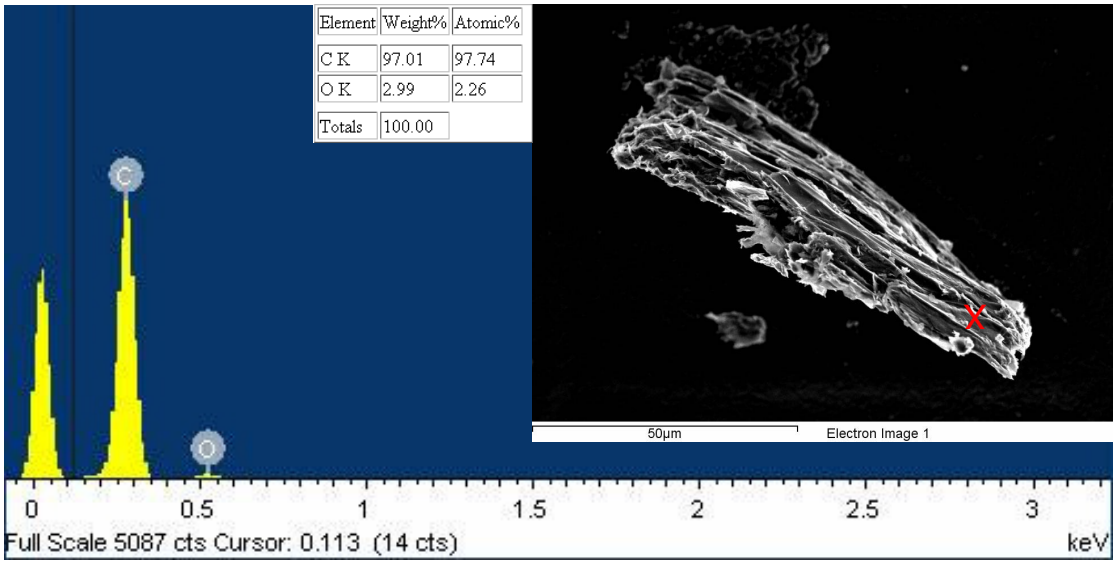

(b)

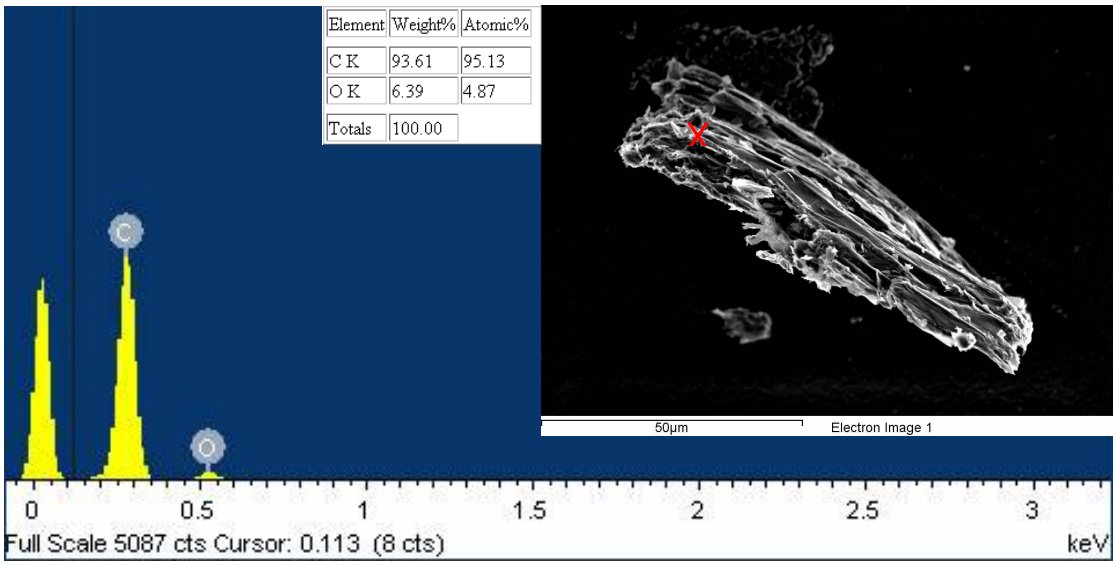

(c)

Figure 7-14: SEM/EDS analysis on kitchen sampling Stage 5 at 50 µm

EDS analysis was conducted on a particle collected from the kitchen of Case 3. The particle marked "X" in Figure 7-14(a) shows a high amount of C (97.88% atomic weight) and a low amount of O (2.12% atomic weight). This suggests that the carbon-rich particles are soot, resulting from the incomplete combustion of hydrocarbons (Moreno *et al.*, 2004). In this case, they were produced by the internal combustion of diesel and petrol in vehicles since the sampling location is close to a busy main road in Sheffield. Various vehicles (e.g. lorries, trucks, etc) passed by the sampling location in a regular basis. The soot particles could also arise from vehicles which were parked next to the sampling location. The soot particles were released when the engines were turned on and off at the site. EDS analysis was then conducted on two other locations of the particle, as shown in Figures 7-14(b) and (c). EDS results revealed a similar composition to Figure 7-14 (a) – a high amount of C and a low amount of O. Therefore it can be concluded that the particles are probably from the same source.

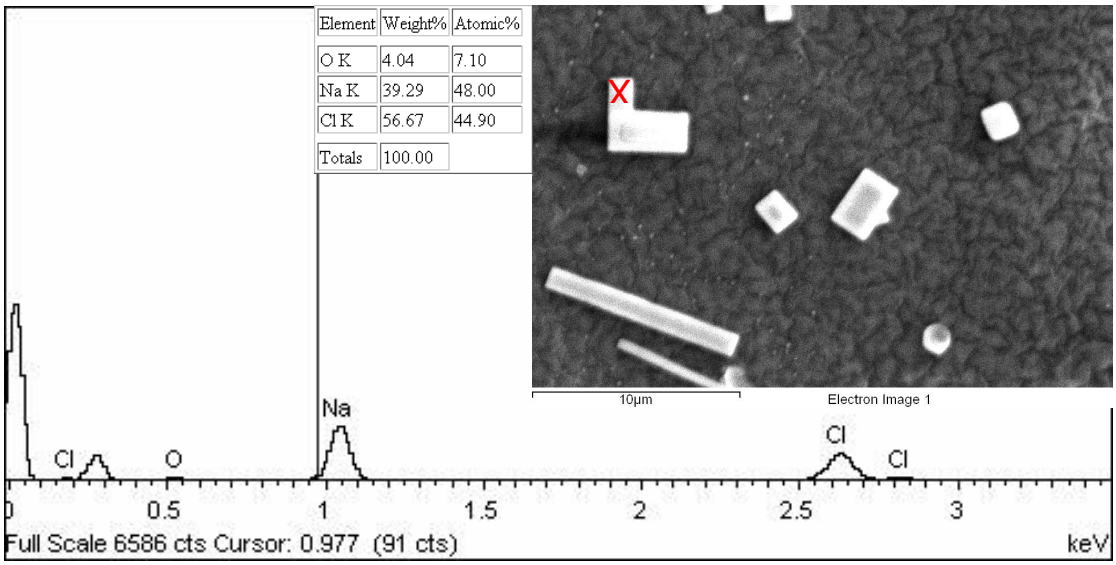
Element Weight% Atomic%
O K 4.04 7.10
Na K 39.29 48.00
Cl K 56.67 44.90
Totals 100.00
X
10µm
Electron Image 1
Na
Cl
O
Cl
Cl
0 0.5 1 1.5 2 2.5 3
Full Scale 6586 cts Cursor: 0.977 (91 cts)
keV

(a)

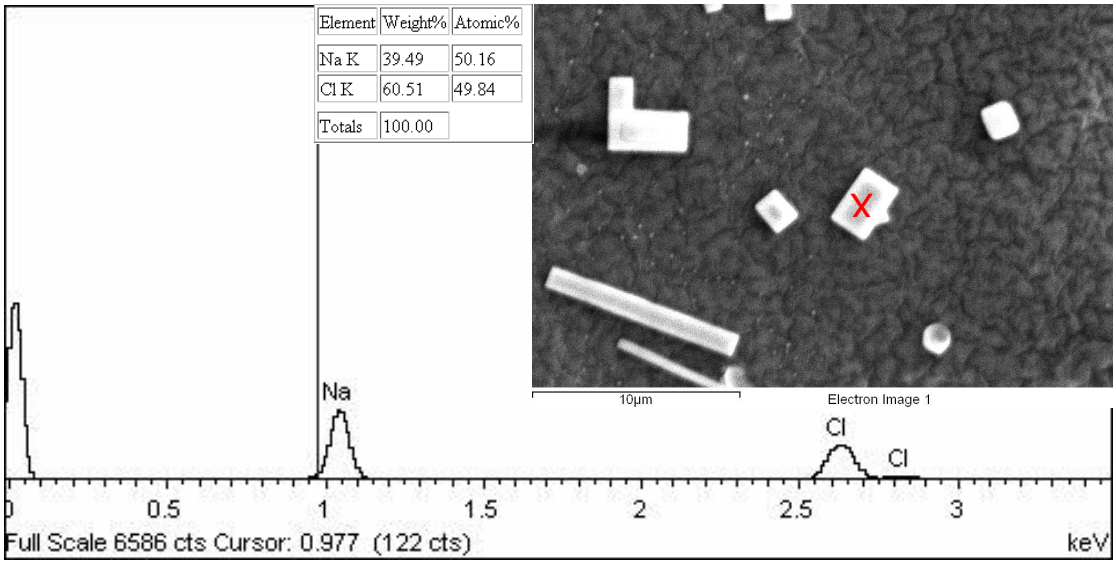
Element Weight% Atomic%
Na K 39.49 50.16
Cl K 60.51 49.84
Totals 100.00
X
10µm
Electron Image 1
Na
Cl
Cl
0 0.5 1 1.5 2 2.5 3
Full Scale 6586 cts Cursor: 0.977 (122 cts)
keV

(b)

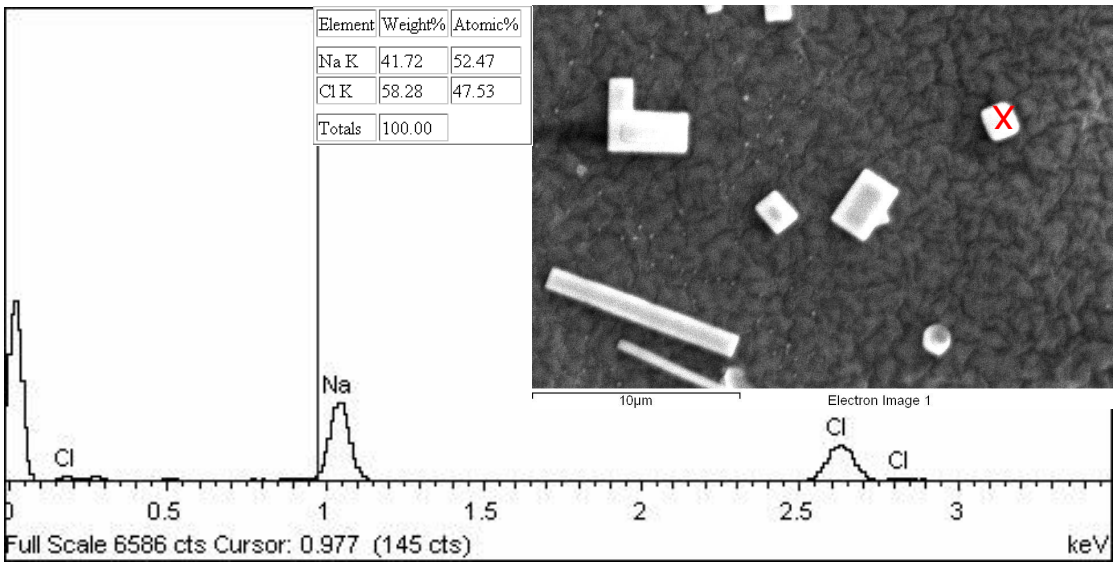
Element Weight% Atomic%
Na K 41.72 52.47
Cl K 58.28 47.53
Totals 100.00
X
10µm
Electron Image 1
Na
Cl
Cl
Cl
0 0.5 1 1.5 2 2.5 3
Full Scale 6586 cts Cursor: 0.977 (145 cts)
keV

(c)

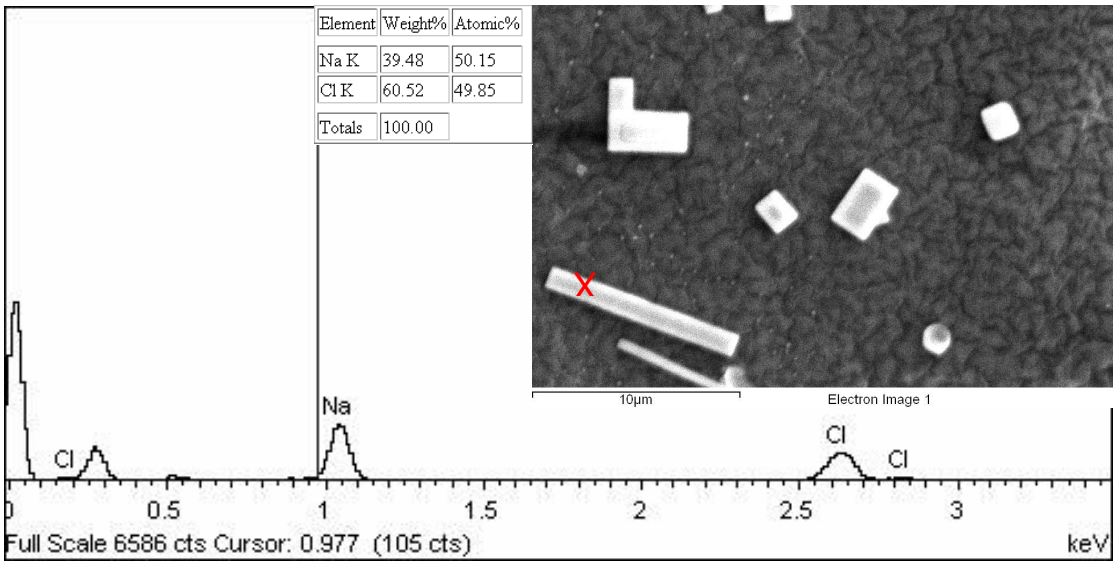

(d)

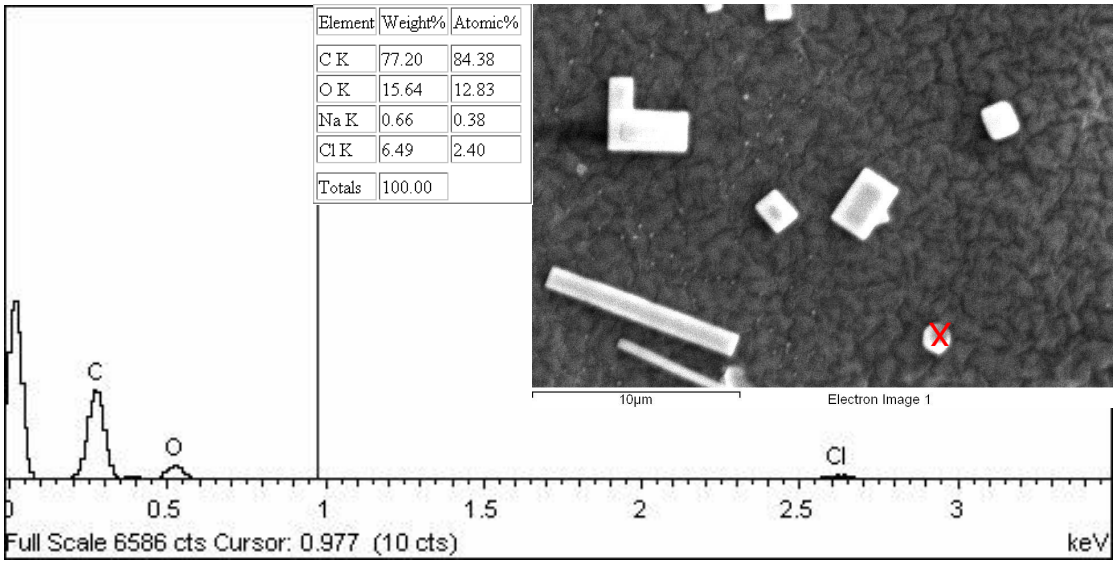

(e)

Figure 7-15: SEM/EDS analysis on kitchen sampling Stage 7 at 10 µm

The particle marked "X" in Figure 7-15(a) shows high amounts of Na (48.0% atomic weight) and Cl (44.9% atomic weight). The perfect cube-like particle structure suggests that it was a salt crystal, NaCl (Berube *et al.*, 2004). EDS analysis was then conducted on the particles marked "X" in Figure 7-15(b), (c) and (d). All the particles gave high amounts of Na and Cl. Thus it can be confirmed that all these particles were salt crystals. The results were as expected since the samples were collected from the kitchen of Case 3.

The particle marked "X" in Figure 7-15(e) shows a spherical particle with smooth surface. Upon the EDS analysis, this particle gave high amounts of C (84.38% atomic weight) and O (12.83% atomic weight). This suggests that the particle is a carbon-rich particle, a by-product of a

high temperature process (Vallack and Chadwick, 1993). This type of particle originated from vehicle combustion since the location of particle sampling is close to a busy road with no other major high temperature activities in the surroundings.

7.3 NO_2, VOC, CO AND $PM_{2.5}$ MEASUREMENTS

7.3.1 Indoor and Outdoor Concentrations of Pollutants

7.3.1.1 $PM_{2.5}$

Figure 7-16 shows the real time concentrations of indoor $PM_{2.5}$ in the kitchen of Case 3. The average indoor $PM_{2.5}$ concentration measured in this environment was 38 µg/m^3, similar to Case 2 and again much greater than Case 1. The indoor $PM_{2.5}$ concentrations remained fairly constant for much of the monitoring period, though it was slightly increased during indoor activities, especially cooking (spikes of 300-700 µg/m^3). A peak of around 2000 µg/m^3 was reached when food was deliberately burned. The average outdoor $PM_{2.5}$ concentration near the flat was 42 µg/m^3. Both the indoor and outdoor $PM_{2.5}$ concentrations for Case 3 were higher than the tests in the rural house, Case 1. Nevertheless, the indoor concentrations were slightly lower than the kitchen of Case 2, although the outdoor PM levels were higher, due to the effects of the main road nearby. The indoor $PM_{2.5}$ concentrations were most likely to be caused by cooking activities in the kitchen and also possibly due to the use of deodorant sprays elsewhere in the house.

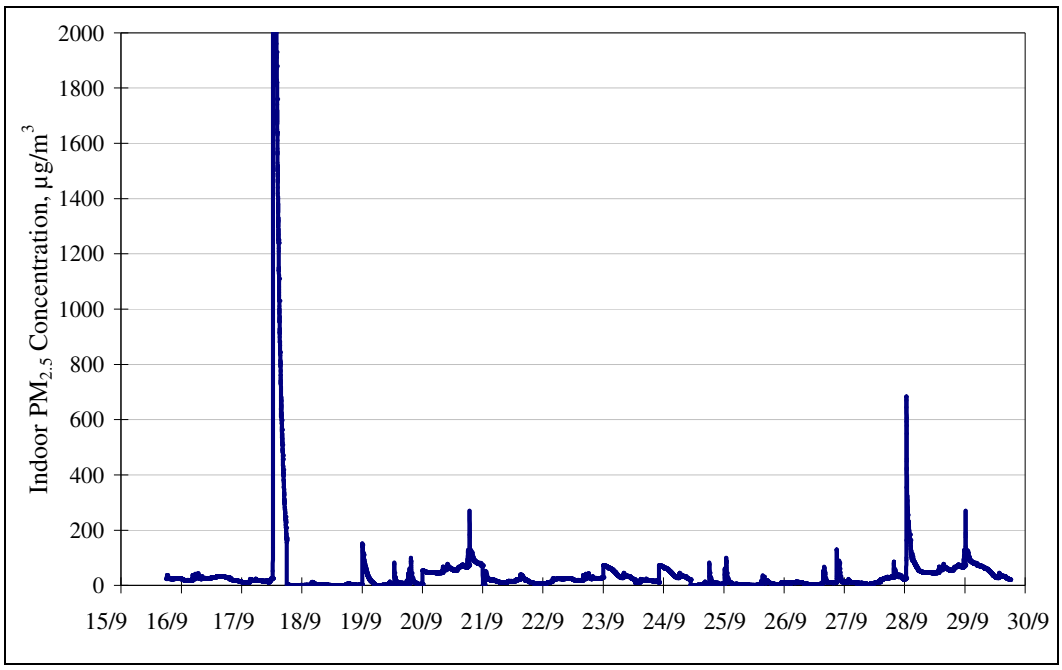

Figure 7-16: Real time concentrations of indoor $PM_{2.5}$ in the kitchen

7.3.1.2 CO

The real time concentrations of indoor CO in the kitchen of Case 3 are presented in Figure 7-17. The average indoor CO concentration here was 1.1 ppm – lower than Case 2 (2 ppm) and similar to Case 1 (1 ppm). The CO concentration reached the highest point during one of the cooking periods, at 12 ppm. The baseline for the CO concentration in this kitchen is 1 ppm. Again, the source of CO emissions is the gas cooker used in the kitchen, as the spikes coincided with cooking episodes. The gas boiler is unlikely to elevate indoor CO concentrations for two main reasons: (i) combustion is highly controlled and thus CO emissions are likely to be low; and (ii) it is a vented system so all combustion products are sent via a flue to the outdoor environment.

The outdoor CO concentration at this site was zero, similar to Cases 1 and 2. Again, this implies that the outdoor CO at these locations is dispersed rapidly.

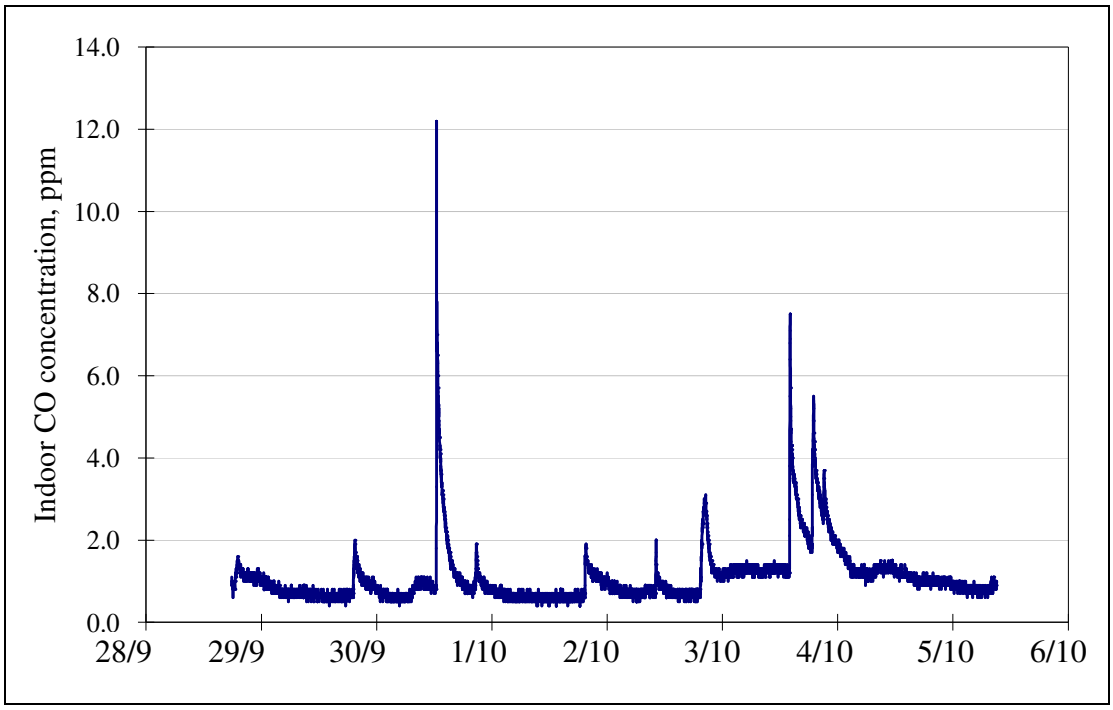

Figure 7-17: Real time concentrations of indoor CO in the kitchen

7.3.1.3 NO_2

The indoor and outdoor NO_2 concentrations measured using the NO_2 diffusion tubes are shown in Table 7-2. The outdoor NO_2 concentration for this case study (Case 3) was 23.37 µg/m^3, slightly higher than the indoor concentration at this location (20.69 µg/m^3). Both the indoor and

outdoor NO_2 concentrations measured here were higher than the values obtained for Case 1. Compared to Case 2 however, whilst the indoor concentration was significantly lower, the outdoor concentration of NO_2 was in fact slightly higher. Nonetheless, the outdoor NO_2 concentrations measured in this case study still met the EU annual limit values (European Commission-Environment, 2011) and the UK Air Quality Strategy objectives (DEFRA, 2007) for NO_2 of 40 $\mu g/m^3$. NO_2 is released into the atmosphere when fuels are burned. In this case, petrol or diesel combustion in a vehicle engine was the main contributor of NO_2 as there were various types of diesel-operated vehicles (i.e. trucks, buses) passing-by the sampling location during the measurement period. As reported by DEFRA (2004), road transport is the largest source of NO_x emission in the UK. NO_x contributed 49% of total emissions in 2000. A slow-moving diesel-operated vehicle could cause an extra 25% of NO_2 emissions in the local atmosphere. Another possible source is the domestic natural gas boiler located in the kitchen.

Table 7-2: Indoor and outdoor NO_2 concentrations

Sampling Site	Indoor	Outdoor
Residential flat in Sheffield, $\mu g/m^3$	20.69	23.37

7.3.1.4 VOCs

The indoor and outdoor concentrations of the Σ20 VOCs obtained from this sampling location are shown in Table 7-3. At this site, the outdoor concentration (32.6 $\mu g/m^3$) was lower than the indoor Σ20 VOC concentration (49.7 $\mu g/m^3$). This result was expected since any high outdoor Σ20 VOC concentrations would be rapidly dispersed and diluted in the outdoor environment. The main contributor of indoor VOCs in this kitchen is the cleaning agents. The owner cleans the kitchen almost everyday using various types of cleaning products (e.g. dusting spray, dishwasher detergent, oven cleaner, air freshener, floor polish etc). Other possible sources include combustion of fuel, furnishings, furniture and carpet adhesives.

Table 7-3: Indoor and outdoor VOC concentrations

Sampling Site	Indoor	Outdoor
Residential flat in Sheffield, $\mu g/m^3$	49.7	32.6

The top 20 VOCs sampled from indoors and outdoors using Tenax TA Tubes are presented in Figure 7-18. Undecane and pentadecane appeared to be the most common VOCs found in the indoor and outdoor environment of Case 3 respectively. Undecane reached indoor levels of 6 µg/m^3, whereas pentadecane exceeded 12 µg/m^3 in the outdoor environment. Indoors, there were generally higher levels of most of the VOCs sampled (Nonane, 1-methyl-2-(1-methylethyl)benzene, Toluene, m/p-Xylene and 1,2,4-trimethylbenzene). Most of the VOCs sampled inside this residential environment had concentrations greater than 1 µg/m^3. Outdoors, where there generally were much lower VOC levels (often less than 1 µg/m^3 for specific VOCs).

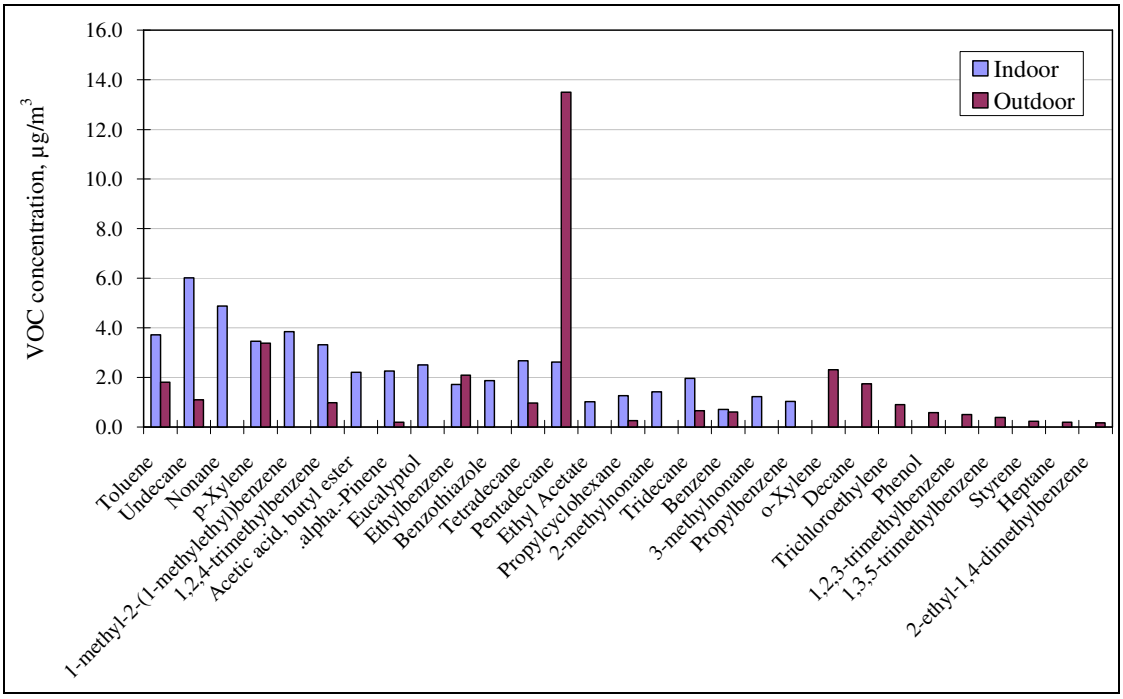

Figure 7-18: Top 20 VOCs sampled (µg/m^3)

7.3.2 Indoor Temperature and Relative Humidity

The real-time temperature recordings taken in the kitchen of the flat on the main road are presented in Figure 7-19. The temperature variations were relatively small; the temperatures recorded ranged from ~18 °C to 23 °C. The slight increases in temperature were due to cooking activities, since the probe was located close to the cooker.

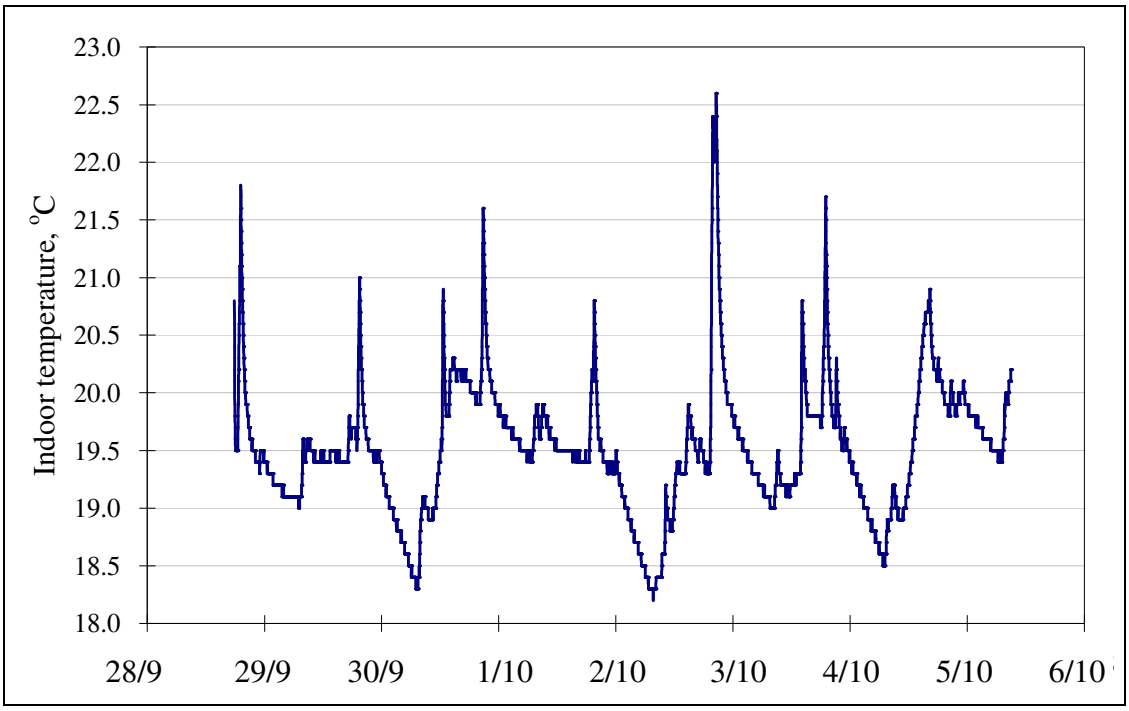

Figure 7-19: Real time temperature recordings in the kitchen

Figure 7-20 shows the real-time recordings of the relative humidity in the kitchen of the Case 3 flat. The range of indoor humidity levels was 55% to ~70%. Humidity levels in the kitchen could also have been increased by cooking activities – especially boiling water – either in the kettle or for cooking food (e.g. pasta).

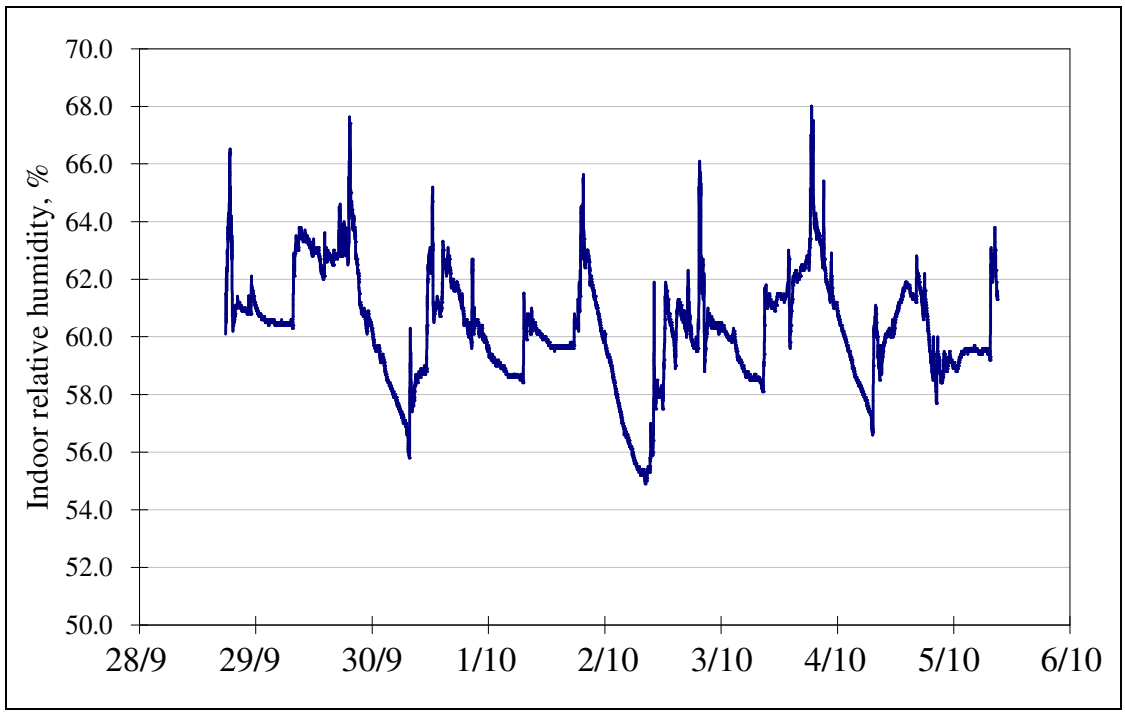

Figure 7-20: Real time recordings of the relative humidity in the kitchen

7.3.3 Air Exchange Rate

Figure 7-21 presents a typical decay curve of the CO_2 concentration during the air exchange rate tests in the kitchen of Case 3; the air exchange rate here was 0.9±0.1 air changes per hour (hr^{-1}). The air exchange rate in this case study was expected since the kitchen is well sealed and rather airtight. Thus, the airflow inside the kitchen is slower.

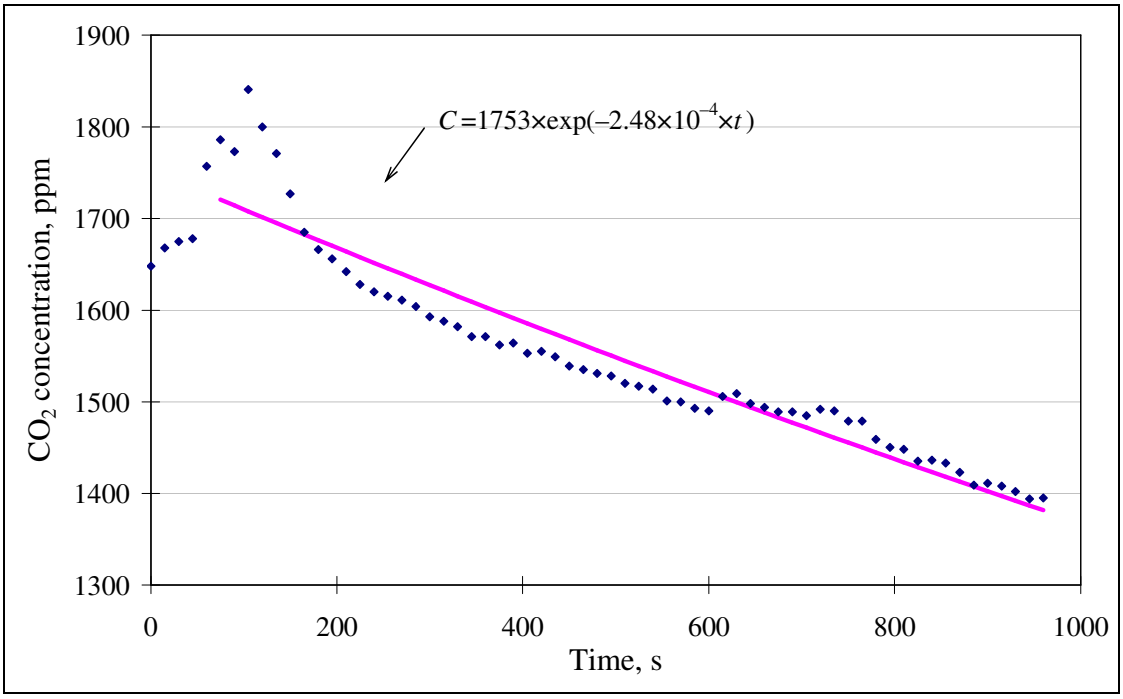

Figure 7-21: CO_2 concentration decay in the kitchen
(Air exchange rate = 0.9±0.1 air changes per hour (hr^{-1}))

7.3.4 Emission Rates of Indoor Pollutants

Based on the above data regarding the indoor pollutant concentrations ($PM_{2.5}$, CO, VOCs and NO_2) and the air exchange rate, the emission rates of these could be calculated.

7.3.4.1 $PM_{2.5}$

The emission rates of $PM_{2.5}$ during five cooking periods in the kitchen of Case 3 are presented in Figure 7-22. There were often peaks of relatively high particulate concentrations, as shown. The emission rates here also varied significantly due to the differences in cooking styles

and food preparation methods. Particles emitted from food, for example during frying or grilling, greatly contribute to the variation in emission rates found here – particularly if food is burned.

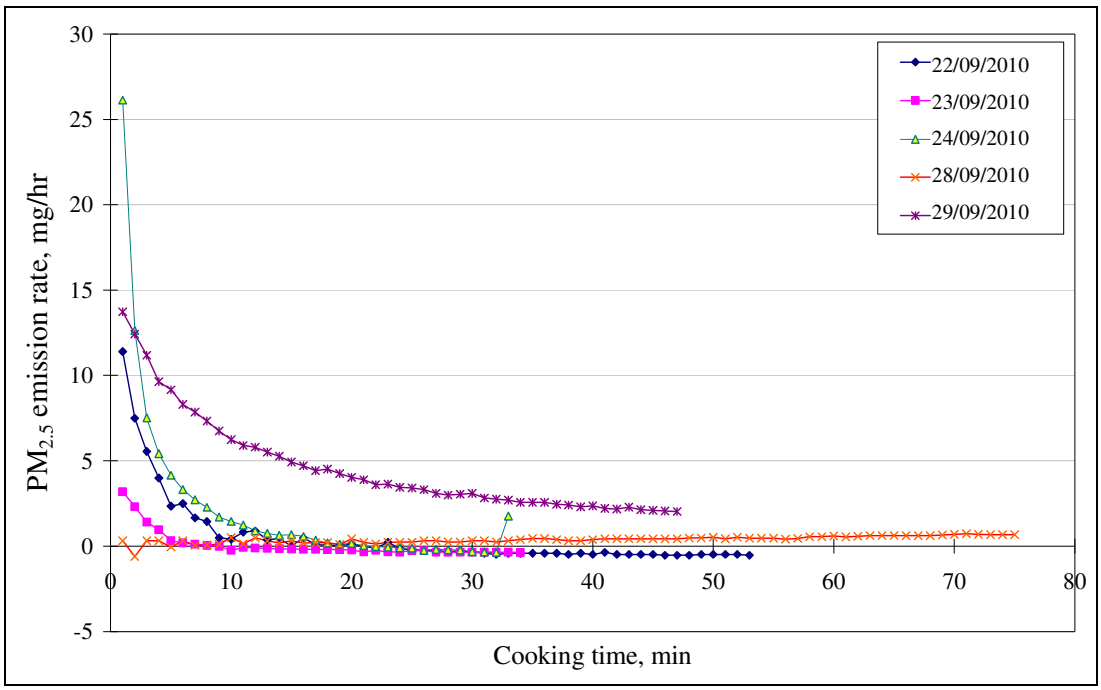

Figure 7-22: The emission rates of $PM_{2.5}$ during the cooking events in the kitchen

The $PM_{2.5}$ emission rates on 29th of September were relatively high when compared to the other cooking periods; the average $PM_{2.5}$ emission rate for this cooking period was approximately 4.6 mg/hr. On 24th of September, the emission rates were around 2.2 mg/hr during the cooking period. The average emission rate for each cooking period is listed in Table 7-4. This table also shows the emission rates when normalised to the amount of gas used during cooking.

Table 7-4: Average emission rates of $PM_{2.5}$ in the kitchen of the residential flat on a main road in Sheffield

Date	**Average emission rate of $PM_{2.5}$**	
	mg/hr	**µg/kJ**
22/09/2010	0.53	7.77
23/09/2010	0.06	0.91
24/09/2010	2.20	32.09
28/09/2010	0.39	5.68
29/09/2010	4.60	67.09

7.3.4.2 CO

Figure 7-23 shows the variations in CO emission rates during several cooking periods in the kitchen of Case 3 when the gas-fired cooker was being used. Again, the CO emissions were most likely due to the incomplete burning of the gas during cooking. The maximum CO emission rate was 0.5 g/hr (during one of the cooking periods), whereas the average emission rate for the whole monitoring period was ~0.1 g/hr.

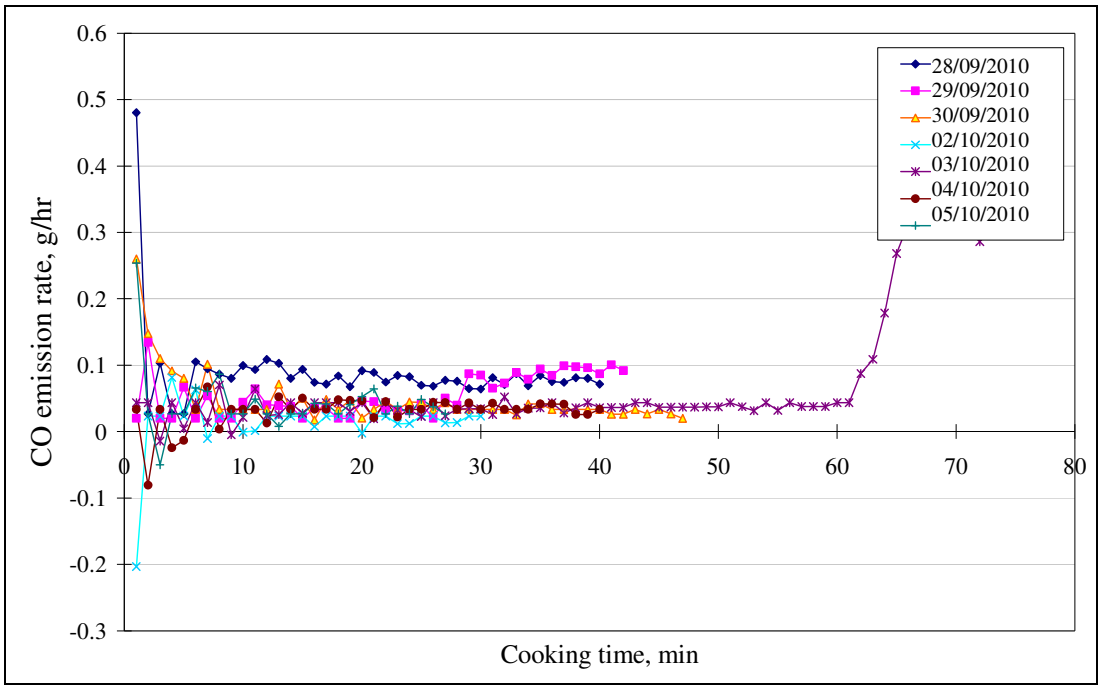

Figure 7-23: CO emission rates during the cooking events in the kitchen of the residential house in Sheffield

7.3.4.3 NO_2 and VOCs

Since there was no significant NO_2 emission source in the kitchen (even though there was a gas cooker), the concentrations were very low. No emission rates were therefore calculated for this species.

The indoor emission rates of the VOCs calculated in the house are listed in Table 7-5. The small increase in indoor Σ20 VOC levels at the flat on a main road (50 µg/m^3) compared to the outdoor concentration (33 µg/m^3) meant that the emission rate here was very low, just 0.46 mg/hr. This was attributed to the gas combustion emitting VOCs during the use of the gas-fired cooker.

Table 7-5: Indoor emission rates of NO_2 and VOCs of the flat in Sheffield

Sampling Site	Average emission rates of NO_2 (mg/hr)	Average emission rates of VOCs (mg/hr)
Residential house in Sheffield	*LoD**	0.46
* *LoD = Limit of detection*		

7.4 SUMMARY

Concentrations and emission rates of a range of pollutants have been measured previously in two case study environments. Various tests have now also been conducted in a third case study environment – an urban flat on a main road – to determine the indoor and outdoor concentrations and indoor emission rates of various pollutants. The results from this case study could be compared with those previously obtained from Case 1 (a rural detached house) and Case 2 (a city-centre flat).

Particulate matter was collected using an Andersen Sampler. The concentration of particles in each of the nine stages of the Andersen Sampler was about the same (9-12% per stage), which resulted in particulate concentrations of 2.5-3.7 $\mu g/m^3$ for each size range. The particles collected in the kitchen were mainly composed of Na, Al, C and O; the morphological analysis revealed that these were likely to be salt crystals, carbonaceous particles, soot and particles generated from the traffic of the busy road outside (such as brake wear). The indoor sources of the pollutants were cooking activities and other common household activities, like cleaning or using sprays, such as deodorants.

The average indoor $PM_{2.5}$ concentration in the kitchen was 38 $\mu g/m^3$. This was higher than the value obtained for Case 1 (16 $\mu g/m^3$), but slightly lower than the value obtained for Case 2 (40.6 $\mu g/m^3$). This may be due to the type of cooker used; both flats (Cases 2 and 3) had natural gas-fired cookers, whereas an electric cooker was used in a rural house (Case 1). There were also differences in the type of cooking conducted in each residential environment. The emission rates of $PM_{2.5}$ for Case 3 were relatively low compared to the other case study environments. Here, the $PM_{2.5}$ emission rate peaked at 4.6 mg/hr, but could be as low as 0.06 mg/hr. The $PM_{2.5}$ emission

rates for Case 1 ranged from 5 to 23 mg/hr, although the highest values were found for Case 2, which had $PM_{2.5}$ emission rates of 7 to 54 mg/hr.

The CO concentration fluctuated more often for Case 3 than the tests in both Cases 1 and 2. In Case Study 1, the CO concentration ranged from 0.9 to 1.3 ppm. As for Case Study 2, the average indoor CO concentration was 2 ppm. In this experimental work, the CO concentration reached the highest point at 12 ppm. This value is higher than the value obtained in the other two case studies. The possible source of CO emissions is the boiler and the gas fired cooker used in the kitchen. As mentioned previously, the kitchen in the Hathersage house had an electric cooker whereas the kitchens in both the flat and the house in Sheffield had gas cookers. The CO emission rates in the kitchens with a gas cooker were much higher than the emission rates in the kitchen with an electric cooker.

NO_2 was measured using diffusion tubes, which gave the overall concentration during the whole monitoring period. The indoor NO_2 concentration was found to be 20.7 $\mu g/m^3$, whereas the outdoor NO_2 concentration was slightly higher – around 23.4 $\mu g/m^3$. Both the indoor and outdoor NO_2 concentrations measured in this case study were higher than for Case 1; this residential environment had indoor and outdoor NO_2 concentrations of 10.2 and 10.8 $\mu g/m^3$ respectively. Whilst the concentration of NO_2 in the kitchen of Case 3 was slightly higher than for Case 2 (14.7 $\mu g/m^3$), the outdoor concentration was significantly lower (47.1 $\mu g/m^3$). No emission rates were calculated for NO_2 since the levels were very low.

The indoor Σ20 VOC concentrations for all three cases studied were higher than the outdoor concentrations. The possible sources include cleaning products, combustion of fuel, furnishings, furniture and carpet adhesives. The emission rate of VOCs for this case study was 0.46 mg/hr. The emission rates of VOCs for both Case Study 1 and 2 were higher than the emission rate of this case study.

The air exchange rate in this kitchen was 0.9±0.1 air changes per hour (hr^{-1}). The temperature (~18°C to 23 °C) and relative humidity (55% to ~70%) were both found to increase slightly during cooking periods in this case study environment, since the monitor was located next to the cooker. This is most likely to be due to the fact that cooking using a gas cooker will generate both heat and water vapour. Additional moisture could come from cooking activities that involved boiling water.

8

DISCUSSION

Three detailed UK-based case studies were completed in different residential buildings to assess both solid-phase (PM) and gaseous (CO, NO_2 and VOCs) emissions associated with fuel and energy usage within domestic environments. Although there has been a great deal of research examining the effects of various pollutants in the indoor environment, limited indoor air pollutant emissions data and the associated emission rates from heating and/or cooking appliances have been reported in the literature. As part of this research, it is essential to investigate the concentration of indoor air pollutants generated by various heating and cooking systems in residential buildings. This is the first study to focus specifically on PM. In particular, the levels of $PM_{2.5}$ – particulate matter that is less than 2.5 μm in diameter – were assessed, as these particles are classed as the respirable fraction; they are small enough to be inhaled and may have significant negative consequences on human health.

Homes with gas and electric cookers were monitored, in addition to those in urban and rural settings, where data was collected, analysed and compared for both the indoor (mainly in the kitchens) and outdoor environments at each location. Real-time concentrations of $PM_{2.5}$ were measured in each kitchen and outdoor environment using a TSI DustTrak™ 8532 aerosol monitor, with additional particle collection of PM_{10} at two of the case study environments. For this, particles were accumulated over a 4-week period with a multi-stage, multi-orifice cascade Andersen Ambient Particle Sizing Sampler; the particles were then analysed for morphology and composition via SEM/EDS and ICP emission spectrometry respectively. Most particulates found

in the kitchens were small (<2.5 μm) and would thus be respirable – consequently having potential health implications. The elemental analysis of the indoor PM collected revealed high metal concentrations (especially of Fe, Na and Zn), whilst their morphologies indicated these were present as salt crystals, mineral fibres and skin flakes, which could have come from a range of indoor and outdoor sources.

Data was collected for both the indoor and outdoor environments for each property. The kitchen in the rural house with an electric cooker (Case 1) appears to have much lower concentrations and emission rates of various indoor air pollutants, during the cooking periods, than the urban flats (Cases 2 and 3), which both had gas appliances. The monitoring of the outdoor environments at these locations did not result in such significant differences in emissions as the indoor concentrations reveal, thus it can be safely assumed that the elevated pollutant levels found in the indoor environments are the result of particular activities, such as fuel use, especially during cooking.

Due to the higher indoor concentrations of the different pollutants, the emission rates of CO, $PM_{2.5}$ and NO_2 in the kitchens with a gas-fired cooker were generally much higher than those in the kitchen with an electric cooker, most noticeably during the cooking periods. Variations in cooking styles (e.g. frying/grilling compared to boiling) may have also impacted the concentrations and emission rates – especially those of the PM – during the cooking periods monitored.

In this chapter, an overall discussion will be presented to show the relationship of indoor and outdoor concentrations of air pollutants, the influence of cooker types and the effect of cooking styles on indoor air quality, as well as the impact of weather on particle size distribution and elemental composition. Finally the problems and errors encountered in this research study will be discussed.

8.1 INDOOR AND OUTDOOR CONCENTRATIONS OF AIR POLLUTANTS

The emissions of various pollutants associated with fuel and energy usage in residential buildings were monitored for three case studies. Concentrations of $PM_{2.5}$, CO, NO_2 and VOCs were measured in the kitchens and outdoor environments. $PM_{2.5}$ is mostly emitted by cooking

activities. The average indoor and outdoor pollutant concentrations in all case studies are presented in Figure 8-1. The average indoor levels of $PM_{2.5}$ ranged from 10 to 42 μg/m^3. The highest indoor levels of $PM_{2.5}$ were found in Case 3. The ratios between indoor and outdoor $PM_{2.5}$ concentrations for both Cases 1 and 2 exceeded 1.0. As shown in Figures 8-1(a), the indoor and outdoor concentrations of $PM_{2.5}$ for Case 1 are similar. However, for Case 2, the indoor concentrations varied significantly compared to outdoor concentrations. As for Case 3, the outdoor concentrations are slightly higher than the indoor concentrations.

Gas-fired central heating systems, which vent their combustion products to the outdoor environment through well-insulated and sealed ducts, had no effect on indoor CO levels in any of the properties with such a heating system. Outdoor CO concentrations were minimal at all sites (~0 ppm, or lower than the detection limit on the TSI IAQ Calc 7545 monitor), thus any CO found in the homes came from indoor sources. Rural homes, with limited outdoor pollutant levels indicated the significance of indoor activities in these environments. The indoor air quality in homes in urban areas (near main roads or city centres) was notably affected by outdoor pollution sources, like transport and industry, in additional to the impacts of indoor air pollutant emissions; this indicates that air ingression, particularly in urban areas can be a significant influence on overall indoor pollutant levels and indoor air quality.

NO_2 and VOCs were passively sampled using diffusion tubes and Tenax TA tubes, respectively. A comparison of indoor and outdoor levels of NO_2 for all case studies is presented in Figure 8-1(b). It was found that the NO_2 concentrations were greater inside in the city-centre flat (Case 2) than outdoors, whilst for the rural house (Case 1), the concentrations were much lower overall and the indoor and outdoor environments were more similar. The outdoor concentrations are slightly higher than the indoor concentrations for Case 3.

Figure 8-1(c) shows the comparison of indoor and outdoor levels of VOCs for all case studies. The VOCs concentration inside the rural detached house (Case 1) was significantly elevated compared to its outdoor environment. The same was also found for the urban flats (Cases 2 and 3), although there were generally much greater concentrations in the city centre (Case 2).

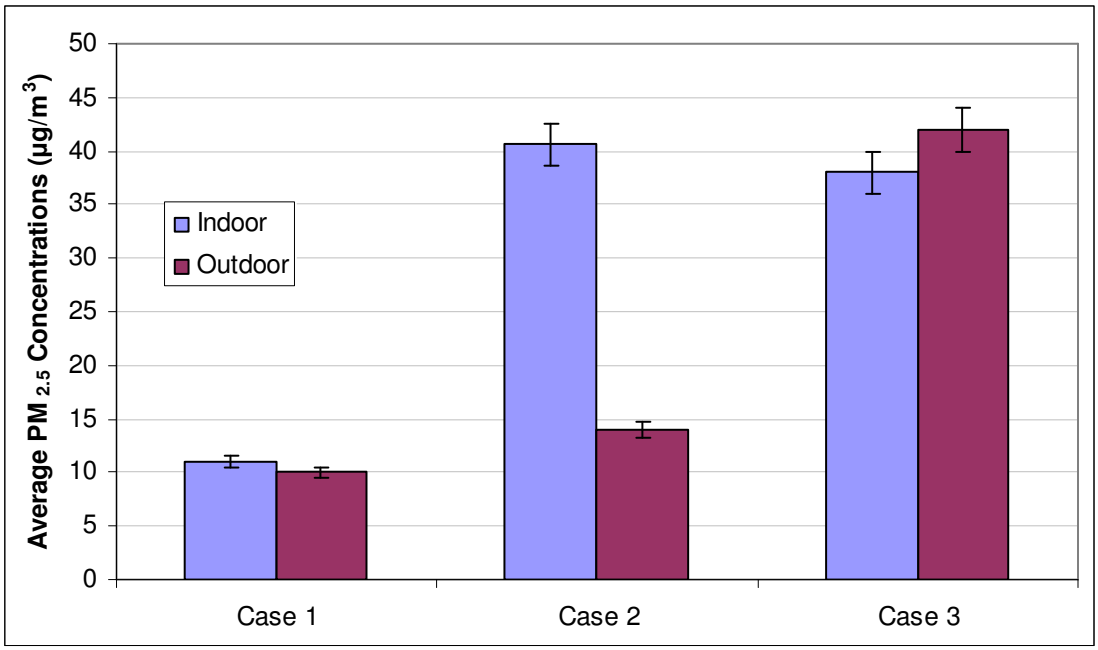
Average PM 2.5 Concentrations (µg/m3)
50
45
40
35
30
25
20
15
10
5
0
Indoor
Outdoor
Case 1
Case 2
Case 3

(a)

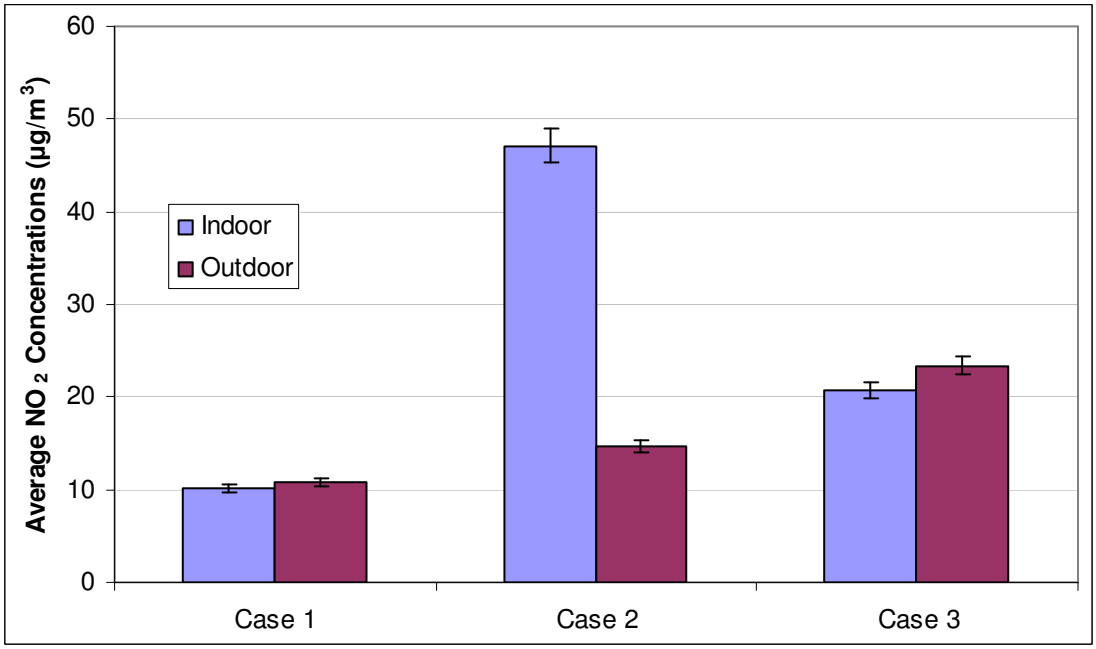
Average NO 2 Concentrations (µg/m3)
60
50
40
30
20
10
0
Indoor
Outdoor
Case 1
Case 2
Case 3

(b)

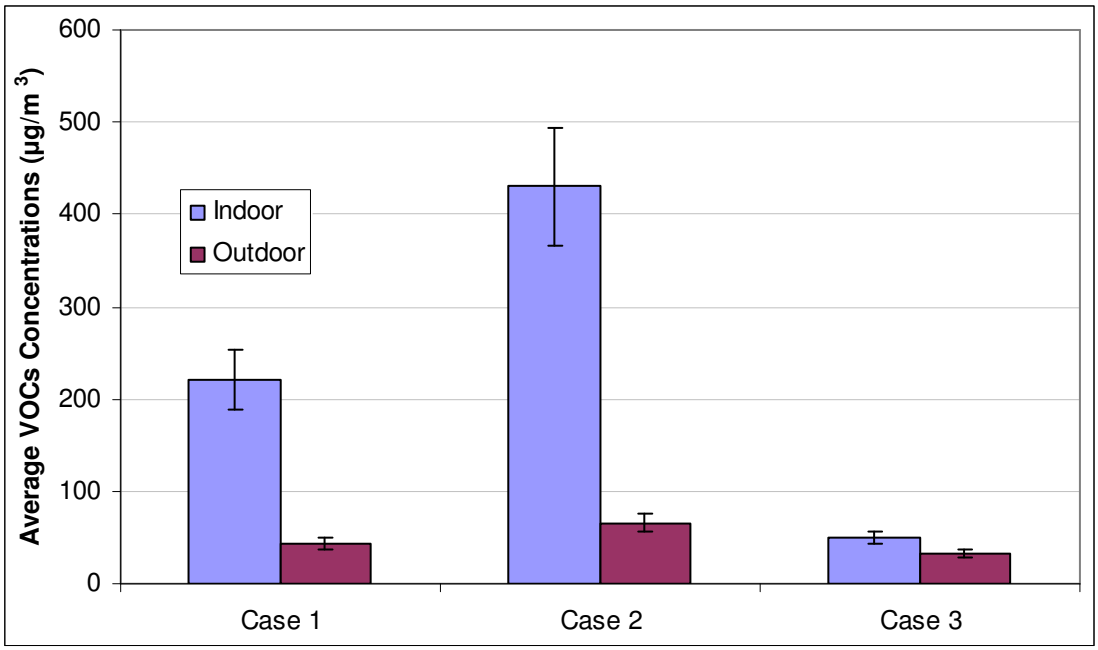

(c)

Figure 8-1: Comparison of indoor and outdoor levels of targeted pollutants for all case studies

8.2 INFLUENCE OF COOKER TYPES ON INDOOR AIR QUALITY

A range of analysers were used to measure particulate species, in addition to carbon monoxide, oxides of nitrogen and volatile organic compounds. Figure 8-2 shows the concentrations of various pollutants in kitchens using different fuels type. $PM_{2.5}$ are classed as the respirable fraction, as they are small enough to be inhaled; these may have negative health consequences, as toxic species, such as polycyclic aromatic hydrocarbons and heavy metals, tend to accumulate here. $PM_{2.5}$ concentrations were monitored continuously, using a TSI DustTrak™ II 8532. As shown in Figure 8-2, the average indoor $PM_{2.5}$ concentrations were greater in the kitchens of the home using the gas cooker than the house using an electric cooker.

The kitchen of Case 2 has higher concentrations of various pollutants compared to Case 3, although both of these kitchens used gas-fired cookers. As discussed before, this is probably due to the fact that the cooker used in Case 2 was quite old compared to the cooker used in Case 3. Thus, it can be concluded that the type of cooker used in the kitchen does have an effect on the indoor pollutant concentrations. Gas-fired cookers generally have a greater impact than an electric cooker. Such gas cooking appliances were also found to be considerable emitters of NO_2 and VOCs for kitchens of Cases 2 and 3.

CO aids greenhouse gas formation and is highly toxic. There was no difference in the CO levels recorded between the cooking and non-cooking periods in the home with the electric cooker, whereas small spikes occurred whenever any cooking activity was conducted in homes with gas appliances, thus the source of CO emissions would be the gas cooker.

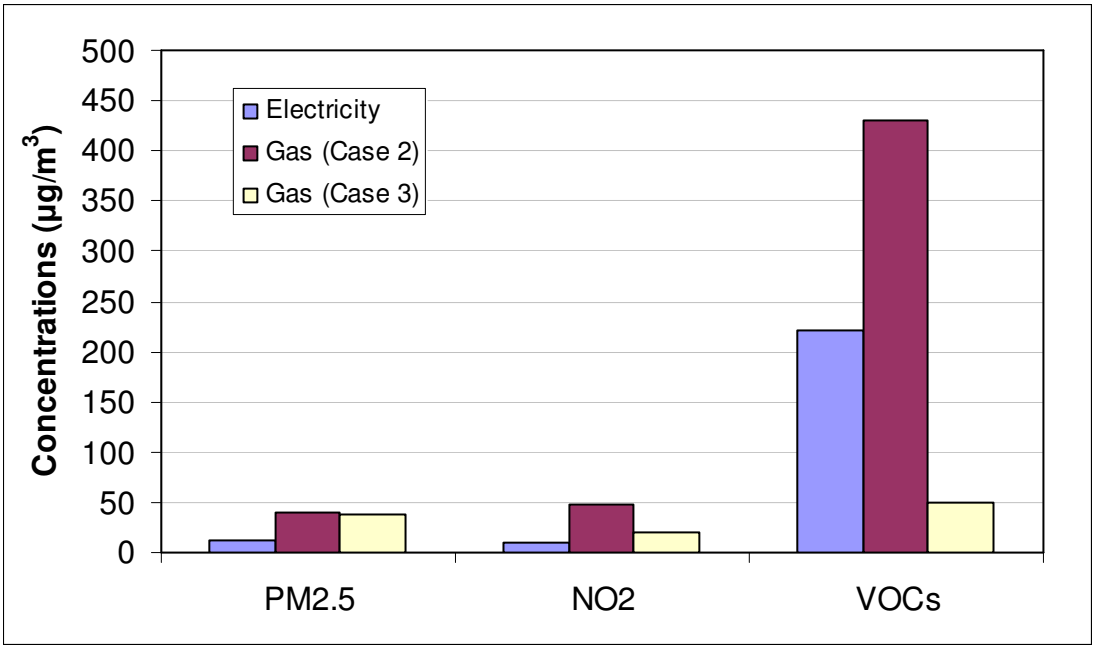

Figure 8-2: The concentrations of various pollutants in kitchens by fuel use

8.3 EFFECT OF COOKING STYLES ON INDOOR AIR QUALITY

Cooking sources, especially burning food, appeared to be the most significant contributor to PM emissions in the kitchens. For instance, $PM_{2.5}$ concentrations could peak at over 16,400 µg/m^3, from an average of 40 µg/m^3 in homes with gas or electric cookers, where the location of the home (urban or rural) had little impact. Changing the cooking style would thus have a much greater impact on PM concentrations than modal switching (from gas to electricity). Based on the measured $PM_{2.5}$ concentrations, the $PM_{2.5}$ emission rates were calculated for the various cooking periods in each home, after the sizes of the kitchens were measured and the air exchange rates determined using the standard concentration decay method. The $PM_{2.5}$ emission rates were also considerably affected by cooking method, where frying and grilling notably increased emission rates and burning food significantly elevated PM concentrations (200+ µg/m^3 compared to background levels of 38 µg/m^3) and emission rates (up to 34 µg/hr compared to 0 µg/hr, when there was no cooking source). This applied to Case 2 as well. As discussed in Chapter 6, the Chinese family did a lot of stir-frying by using a large amount of cooking oil with high cooking

temperatures. Therefore both the solid-phase and gaseous emissions in this city-centre flat appeared to be the highest among the kitchens.

Modal switching would thus appear to only impact gaseous species (like CO and NO_2), whereas changing the cooking style would have a much greater impact on PM concentrations (as considered above) and less effect on gaseous species. However, VOCs found in the indoor environment, collected with DIFTXTA Tenax TA diffusion tubes, tended to be from cleaning products and construction materials used in the buildings, rather than from fuel/energy use, although these may have made a small contribution to overall levels.

8.4 IMPACT OF WEATHER ON PARTICLE SIZE DISTRIBUTION

Figure 8-3 shows the particle size ratio for samples collected in different seasons. As shown, the kitchen and lounge sampling of Case 1 was conducted during the spring and summer respectively. For the kitchen sampling of Case 3, particles were collected during the autumn and bedroom sampling for Case 1 was conducted during winter. As can be seen from the figure, fewer particles were collected in winter. This agreed well with the study conducted by Gao *et al.* (2007) as less photochemical promotion occurs in winter. The cooler weather restricted the formation of new particles due to the lower intensity of solar radiation.

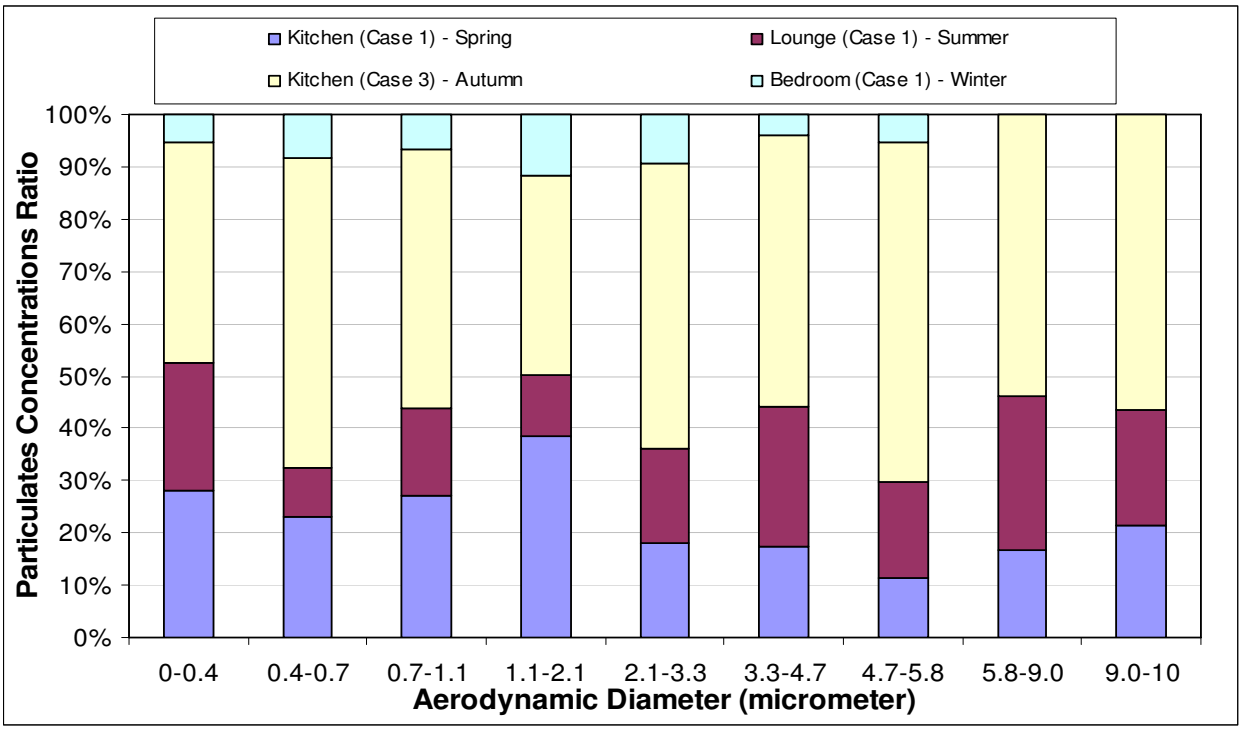

Figure 8-3: Particle size ratio for samples collected according to seasons

8.5 ELEMENTAL COMPOSITION

Particulates, again focusing particularly on $PM_{2.5}$, were analysed using various techniques, including an Anderson Impactor for particle size distribution, ICP-OES for elemental analysis and SEM/EDS for particle morphology. Figure 8-4 presents the elemental composition of the particles collected from the kitchen, bedroom and outdoor environment for Case 1 and kitchen of Case 3.

The Anderson Impactor showed that most particles in the kitchen of Case 1 had a diameter less than 2.5 μm and were mainly within the size range of 1.1-2.1 μm. Most particles were thus respirable and may have negative health impacts if inhaled. The elemental analysis revealed that the most common elements were B, Ca, Na and Si (up to 90 mg/g), with smaller amounts (<15 mg/g) of sulphur and various metals, like Al, Ba, Fe, K, Mg and Zn. The particle morphology identified that most particles were either salt crystals or salt-related particles (containing sodium and chlorine) or dust and skin flakes (comprised of carbon, oxygen, silicon and magnesium).

The analysis of the PM_{10} samples from the bedroom of Case 1 revealed that the particles contained high concentrations of Fe, Na (up to 150 mg/g), S and Zn, whereas the outdoor PM_{10} samples were mainly composed of S (up to 50 mg/g), Na and K. The samples collected from the kitchen of Case 3 were mainly composed of Al (up to 80 mg/g), Na, Ca and Fe, with smaller amounts of Mg, Si, S and K. It can be noted that the most common element that exists in all four samples was Na. It could be generated either from indoor or outdoor sources. Indoors, it could arise from various cooking activities; outdoors, it was most likely to be from road gritting as some of the experiments were conducted in winter.

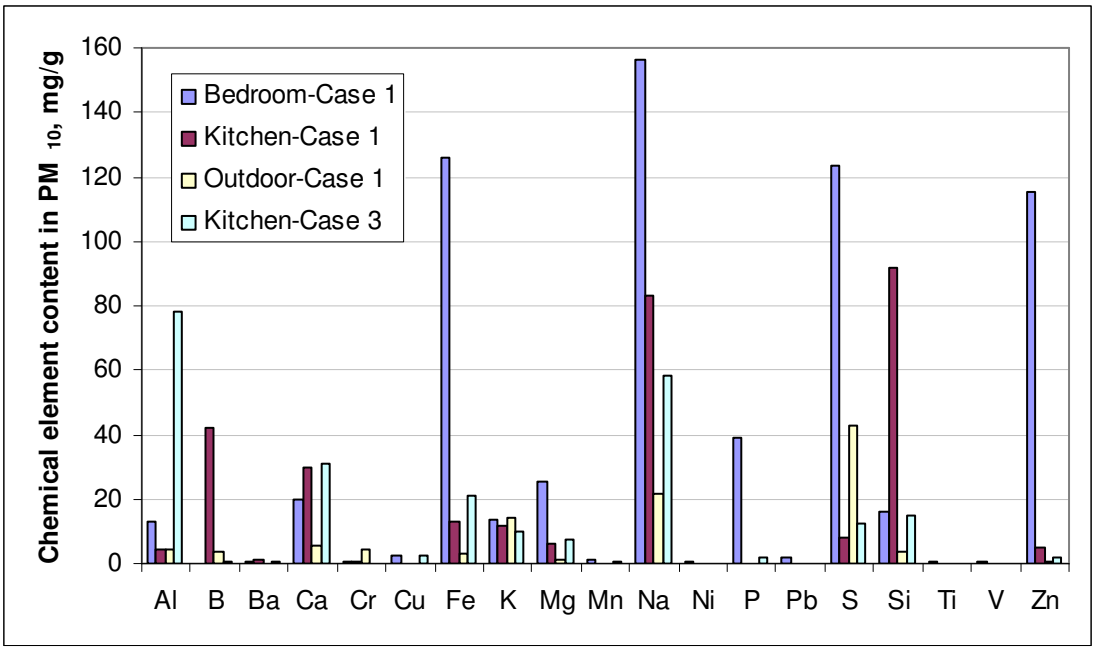

Figure 8-4: Chemical composition of the PM_{10} samples collected from the bedroom, kitchen and the outdoor environment of the rural house – Case 1 and kitchen of Case 3 using ICP-OES

8.6 SAMPLING PROGRAMME

8.6.1 Andersen Sampling

In the Andersen sampling experiments, all the particles collected using the Andersen Sampler looked identical at all times. Hence, it was difficult to determine if the amount of particles collected were sufficient for subsequent analysis. The most particles collected were from the kitchen of Case 3 (≈29.9mg) and the least particles collected were from the bedroom of Case 1 (≈5.7mg). Most of the particles collected from Case 1 were less than 2.5μm ($PM_{2.5}$). This further confirmed that finer particles tend to remain in the atmosphere for a long period of time and they are able to migrate further. Although a preseparator was used to restrict particles larger than 10 μm from entering the later stages of the Andersen Sampler, there were still some particles greater than 10 μm detected under the SEM. This was probably due to the particles starting to accumulate and grow while they were being sampled.

8.6.2 Morphology Analysis

All the particles collected from both Case Studies 1 and 3 managed to give sufficient particle counts to be tested using the SEM/EDS for all stages. The Al count rate detected from the EDS however could have originated from the substrate used in the Andersen Sampler.

Nonetheless, if the detected Al was from the aluminium substrate, it would have shown a much higher count rates. Futhermore, the substrate is comprised of other elements, such as magnesium, copper, nickel etc. If the detected Al was from the substrate, then these components would have also appeared in each test conducted by using the SEM/EDS. However, this did not happen. Therefore, it can be concluded that all the Al detected was from the samples.

8.7 PROBLEMS AND ERRORS

A few problems and errors were encountered during the sampling programme. The first was the use of aluminium substrates in the Andersen Sampling. The aluminium substrate could help in reducing the weighing error as it is lighter compared to the stainless steel collection plates. Nevertheless, transferring the particles to specimen stubs is rather difficult. The particles can adhere to the aluminium substrate and this might give an inaccurate elemental composition for the samples with the presence of Al. Second is the limitation of SEM/EDS. Some particles in the specimen might disintegrate upon analysis since the Back-Scattered Electron method has a very high energy. Moreover, EDS is limited to detect hydrogen and unable to segregate particles. Thus, the actual elemental composition cannot be determined from the EDS chart. Only some major and minor components could be identified based on the count rates.

8.8 SUMMARY

The highest indoor levels of $PM_{2.5}$ were found in Case 3. The ratios between indoor and outdoor $PM_{2.5}$ concentrations for both Cases 1 and 2 exceeded 1.0. The indoor air quality in homes in urban areas (near main roads or city centres) was notably affected by outdoor pollution sources. The type of cooker used in the kitchen also has an effect on the indoor pollutants concentrations. A gas-fired cooker generally has a greater impact than an electric cooker. Cooking style has a much greater impact on PM concentrations. Fewer particles were collected in winter due to the cold weather restricting the formation of new particles. The most common element that was present in all samples was Na, originating from either cooking activities or road gritting, as some samples were collected in winter. A few problems and errors were encountered during the sampling programme (i.e. the use of aluminium substrates and limitation of SEM/EDS). A summary of the research findings is presented in Table 8-1.

Table 8-1: A summary of the research findings

Indoor Pollutants	Equipment (Model)	Case 1: Rural House			Case 2: City-Centre Flat			Case 3: Main Road Flat			Sources	Health Effects	Exposure Limit (COMEAP)
		Indoor Concentration	Outdoor Concentration	Emission Rates	Indoor Concentration	Outdoor Concentration	Emission Rates	Indoor Concentration	Outdoor Concentration	Emission Rates			
$PM_{2.5}$	TSI DustTrak™ 8532	11 µg/m^3	10 µg/m^3	5.4 – 6.4 mg/hr	40.6 µg/m^3	14 µg/m^3	7.31 – 54.4 mg/hr	38 µg/m^3	42 µg/m^3	0.06 – 4.6 mg/hr	1. Type of cooker used – gas/electric cooker, 2. Burnt food, 3. Different cooking technique, 4. Emitted from food preparation or frying (cooking fumes) (e.g. more frying with cooking oil, frequent deep-frying, stir-fry etc.), 5. From road traffic, 6. From cement plant [Case 1],	- Decrease lung function among asthmatics and increase mortality. - Irritate respiratory tissues and more seriously, decrease the lung function and cause cancer. - Cause allergic reactions and infectious diseases in human body.	-
CO	TSI IAQ-Calc Model7545	1.0 ppm (1.15 mg/m^3)	0 ppm	0.1 g/hr	2.0 ppm (2.29 mg/m^3)	0 ppm	0.1 g/hr	1.1 ppm (1.26 mg/m^3)	0 ppm	0.1 g/hr	1. Type of cooker used – gas cooker, 2. From road traffic,	- Form carboxyhaemoglobin and disrupting oxygen transport. - Cause blurred vision, loss of muscle control and flu-like symptoms. - Cause influenza, tiredness, migraine, vomiting and cognitive impairment. - Cause nervous system impairment and amnesia.	25 ppm (30 mg/m^3) - 1 hour average
NO_2	Palmes-type Diffusion tubes	10.2 µg/m^3	10.8 µg/m^3	Nil	47.1 µg/m^3	14.7 µg/m^3	65.5 mg/hr	20.7 µg/m^3	23.4 µg/m^3	Nil	1. Type of cooker used – gas cooker, 2. Produced from combustion process (78% of N_2 in air), 3. Gas combustion (gas-fuelled cooker),	- Damage the lungs and increase susceptibility to colds and respiratory illness. - Cause irritation to mucous membrane, exacerbation of asthma, respiratory infections and decreased lung function. - Acute exposure may result in bronchial reactivity.	150 ppb (300 µg/m^3) - 1 hour average
VOCs	Tenax TA tubes	221.5 µg/m^3	42.6 µg/m^3	13.0 mg/hr	430.7 µg/m^3	65.4 µg/m^3	42.7 mg/hr	49.7 µg/m^3	32.6 µg/m^3	0.5 mg/hr	1. Difference in cooking styles, 2. Gas cooker used, 3. Combustion by-products (gas stove), 4. Cooking activities (Emission from food), 5. Cleaning products, 6. Building materials (e.g. floor coverings, paints, lacquers etc), 7. Kitchen furnishings, 8. Consumer products (e.g. electrical goods, plastics, cleaning detergents, air freshers etc).	- Result in sick building syndrome. - Cause eye and throat irritation, liver damage, and in serious way, destruction to the central nervous system. - Cause irritation to airways and respiratory system, rhinitis, and increase allergic sensitisation.	(i) Benzene: 1.6 ppb (5.0 µg/m^3) - Annual average (ii) Benzo[a]pyrene: 0.25 ng/m^3 - Annual average*

** Provisional Guidelines*

9

CONCLUSIONS AND RECOMMENDATIONS FOR FUTURE WORK

This investigation into indoor air pollutants in different residential buildings has shown that there are variations in both gaseous and solid-phase emissions in the indoor and outdoor environments. Three locations and housing types were compared, which had either electric or gas cooking appliances in the kitchen. Although these factors may have been the primary influence, differences in cooking styles may have also impacted the results, particularly for PM.

9.1 CONCLUSIONS

The main conclusions from this research study are summarised as follows:

PM:

- PM_{10} samples collected from the indoor environment (bedroom and kitchen) of the rural house were mostly composed of small particles <2.5 µm. In contrast, particulates from the outdoor environment at this property were also small, but generally <0.5 µm. These particles are all within the respirable size range and thus could have detrimental health implications if inhaled.

- The elemental analysis of the PM_{10} samples revealed high metal concentrations (Fe, Na and Zn), whereas their morphologies, determined by SEM-EDS analysis, indicated that the particles were mainly salt crystals, mineral fibres, skin flakes and dust fragments, which could thus have come from a range of indoor and outdoor sources.
- Cooking activities were found to directly contribute to $PM_{2.5}$ emissions in the indoor environment. In the kitchen of the rural house with the electrical cooker, $PM_{2.5}$ emission rates ranged from 5 to 22 mg/hr. The city centre flat with a gas cooker had higher $PM_{2.5}$ concentrations and thus also greater emission rates (up to 54 mg/hr).

CO:

- CO concentrations were generally quite low – around 1-2 ppm in all three residential environments. During cooking however, the CO levels became elevated in the kitchens with the gas cookers (Cases 2 and 3), as this was a significant source of this species; levels often peaked at 10-20 ppm during cooking.
- For Case 1, where an electric cooker was installed, there was no difference in CO levels during cooking and non-cooking periods.
- Although average emission rates for the entire monitoring period were low for all cases, the emission rates in the kitchens with the gas cookers during cooking were much higher than in the kitchen with the electric cooker. CO emission rates from the gas cookers were 0.3-2.0 g/hr.

NO_2:

- In the rural house (Case 1), since there was no source of NO_2 emissions inside, the indoor and outdoor NO_2 concentrations were the same, around 10-11 $\mu g/m^3$.
- However in the city-centre flat (Case 2), the gas cooker was found to be a significant source of NO_2 and thus the indoor concentration was much greater than the outdoor levels (47 $\mu g/m^3$ compared to 15 $\mu g/m^3$) and the resultant indoor emission rate was also high – up to 65.5 mg/hr.

VOCs:

- The VOC concentrations were consistently higher in the indoor environments at all locations compared to outdoor levels. The highest emission rate for VOCs was for the kitchen of Case 2, the city-centre flat (~ 43 mg/hr).

Overall this study has achieved the goal of investigating the indoor air pollutants, namely PM, CO, NO_x and VOCs, related to the generation, conservation and use of energy in buildings, focussing especially the particulate matter emitted from various heating and cooking systems. In conclusion, this study has clearly demonstrated that the indoor air quality in kitchens using gas cookers is generally poorer than those using electric cookers – most noticeably in terms of particles ($PM_{2.5}$), NO_2 and CO. Furthermore, these pollutants can migrate through the rest of the residential environment.

9.2 RECOMMENDATIONS FOR FUTURE WORK

Based on the results obtained, the following recommendations have been made:

- Carry out further experimental tests in other residential buildings with different cooking systems (e.g. LPG, biogas, kerosene, charcoal, firewood, gasoline etc.).
- Investigate the impact of weather (e.g. windspeed, pressure etc.) and traffic on the emissions of indoor pollutants in residential buildings.
- Look into the existing models available for the indoor environment that link sources and pollutants to the associated environmental effects.
- Review organic matter removal technologies as a pre-treatment for electron microscopy analysis to obtain better images of individual particles (SEM tests).
- Study the effect of other energy options such as heat pumps, micro-CHP (Micro combined heat and power), tri-generation, photovoltaics, wind turbines, fuel cells and solar water heating on the emission of indoor pollutants.
- Conduct experimental tests looking into the effects on particulate concentrations from:
  - Burning food (i.e. meat, vegetable etc);
  - Using different types of cooking oil (i.e. sesame oil, sunflower oil etc);
  - Placing the equipment in different locations;
  - Measuring under different circumstances (i.e. cooker on and off); and
  - Supplying different gas consumption rates to the cooker (i.e. turn the dials from zero to fully turn on).

REFERENCES

Abu-Allaban, M., Gillies, J.A., Gertler, A.W., Clayton, R., and Proffitt, D. (2003) Tailpipe, resuspended road dust, and brake-wear emission factors from on-road vehicles, **Atmospheric Environment**, Vol. 37, 5283-5293.

Agelopoulos, N. G., Pickett, J. A., Wadhams, L. J., and Woodcock, C. M. (2000) **Flower Emissions of Oilseed Rape**, Ministry of Agriculture, Fisheries and Food, Final Project Report.

American Lung Association (2008) **Indoor air quality**, [Online] Pennsylvania, Washington: American Lung Association. Available at: <URL: http://www.HealthHouse.org>.

Andersen, A.A. (1958) New sampler for the collection, sizing and enumeration of viable airborne particles, **Journal of Bacteriol**, Vol. 76, 471.

Anderson, I. (1972) Relationship between indoors and outdoors air pollution, **Atmospheric Environment**, Vol. 6, 275.

Anthony, J.W., Bideaux, R. A., Bladh, K.W., and Nichols, M.C. (2011) **Handbook of Mineralogy**, [Online] Chantilly, Virginia: Mineralogical Society of America. Available at: <URL: http://www.handbookofmineralogy.org/pdfs/albite.pdf>.

Bady, M., Kato, S., and Huang, H. (2008) Towards the application of indoor ventilation efficiency indices to evaluate the air quality of urban areas, **Building and Environment**, Vol. 43, 1991-2004.

Baek, S.-O., Kim, Y.-S., and Perry, R. (1996) Indoor air quality in homes, offices and restaurants in Korean urban areas – indoor/outdoor relationships, **Atmospheric Environment**, Vol. 31, 529-544.

Baker, A.J., Roy, A., and Kelso, R.M. (1994a) CFD Experiment characterization of airborne contaminant transport for two practical 3-D room air flow fields, **Building and Environment**, Vol. 29, 253-259.

Baker, A.J., Williams, P.T., and Kelso, R.M. (1994b) Development of a robust finite element CFD procedure for predicting indoor room air motion, **Building and Environment**, Vol. 29, 261-273.

Berube, K.A., Sexton, K.J., Jones, T.P., Moreno, T., Anderson, S. and Richards, R.J. (2004) The spatial and temporal variations in PM_{10} mass from six UK homes, **Science of the Total Environment**, Vol. 324, 41-53.

Bluyssen, P.M., and Cox, C. (2002) Indoor environment quality and upgrading of European office buildings, **Energy and Buildings**, Vol. 34, 155-162.

Brown, S.K., Mahoney, K.J., and Cheng, M. (2004) Room chamber assessment of the pollutant emission properties of (nominally) low-emission unflued gas heaters, **Indoor Air**, Vol. 14, 84-91.

Chang, T.-J., and Hu, T.-S. (2008) Transport mechanisms of airborne particulate matters in partitioned indoor environment, **Building and Environment**, Vol. 43, 886-895.

Charles K., Magee R.J., Won D. and Lusztyk E. (2005) **Indoor air quality guidelines and standards**, Canada: National Research Council.

Chen J., Lin H., Chiang T., Hsu J., Ho H., Lee Y. and Wang C. (2008) Gaseous Nitrogen Oxide promotes human lung cancer cell line A549 migration, invasion, and metastasis via iNOS-mediated MMP-2 production, **Toxicological Sciences**, Vol. 106, 364-375.

Chiang C. and Lai C. (2002) A study on the comprehensive indicator of indoor environment assessment for occupants' health in Taiwan, **Building and Environment**, Vol. 37, 387-392.

Chiang C.M., Chou P.C., Lai C.M. and Li Y.Y. (2001) A methodology to assess the indoor environment in care centers for senior citizens, **Building and Environment**, Vol. 36, 561-568.

Chiang, C.-M., Lai, C.-M., Chou, P.-C., and Li, Y.-Y. (2000) The influence of an architectural design alternative (transoms) on indoor air environment in conventional kitchens in Taiwan, **Building and Environment**, Vol. 35, 579-585.

Christoforou C. (2007) **Air pollution**, [Online] Available at: <URL: http://www.pollutionissues.com/A-Bo/Air-Pollution.html>.

Chung, W., Sharifi, V.N., Swithenbank, J., Osammor, O., and Nolan, A. (2008) Characterisation of airborne particulate matter in a city environment, **Modern Applied Science**, Vol. 2, 17-32.

COMEAP: Committee on the Medical Effects of Air Pollutants (2004) **Guidance on the effects on health of indoor air pollutants**, [Online] London: Department of Health. Available at: <URL:http://comeap.org.uk/images/stories/Documents/Reports/Effects_on_Health_on_Indoor_Pollutants.pdf>.

COMEAP: Committee on the Medical Effects of Air Pollutants (2008) **The mortality effects of long-term exposure to particulate air pollution in the United Kingdom**, [Online] London:

Department of Health. Available at: <URL: http://www.comeap.prg.uk/images/stories/ Documents/Reports/comeap the mortality effects of long-term exposure to particulate air pollution in the UK 2010.pdf>.

COMEAP: Committee on the Medical Effects of Air Pollutants (2012) **Particles**, [Online] London: Department of Health. Available at: <URL: http://www.comeap.prg.uk/component/ content/article/28-page-linking/126-particles. html>.

Conner, T.L., and Williams, R.W. (2004) Identification of possible sources of particulate matter in the personal cloud using SEM/EDX, **Atmospheric Environment**, Vol. 38, 5305-5310.

Daisey, J.M., Hershman, R.J., and Kneip, T.J. (1982) Ambient levels of particulate organic matter in New York City in winter and summer, **Atmospheric Environment**, Vol. 16, 2161-2168.

DEFRA: Department for Environment, Food and Rural Affairs (2004) **Nitrogen Dioxide in the United Kingdom** by the Air Quality Expert Group, [Online] Available at: <URL: http://archive.defra.gov.uk/environment/qulaity/air/airquality/ publications/nitrogen- dioxide/nd-summary.pdf>.

DEFRA: Department for Environment, Food and Rural Affairs (2007) **The Air Quality Strategy for England, Scotland, Wales and Northern Ireland (Volume 1)**, [Online] Available at: <URL: http://archieve.defra.gov.uk/environment/quality/air/air quality/strategy/documents/air-qualitystrategy-vol1.pdf >.

DEFRA: Department for Environment, Food and Rural Affairs (2009) **UK National Air Quality Archive** by the AEA Energy and Environment Group, [Online] Available at: <URL: http://webarchieve.nationalarchieves.gov.uk/20090507124904/http://www.airquality.co.uk/networks_home.php>.

DEFRA: Department for Environment, Food and Rural Affairs (2012) **Diffusion tubes for ambient NO_2 monitoring: practical guidance for Laboratories and Users** by the AEA Energy and Environment Group, [Online] Available at: <URL: http://laqm.defra.gov.uk/documents/ 0802141004_NO2_WG_PracticalGuidance_Issue1a.pdf>.

Destaillats H., Maddalena R.L., Singer B.C., Hodgson A.T. and McKone T.E. (2008) Indoor pollutants emitted by office equipment: A review of reported data and information needs, **Atmospheric Environment**, Vol. 42, 1371-1388.

Ebert, M., Inerle-Hof, M., and Weinbruch, S. (2002) Environmental scanning electron microscopy as a new technique to determine the hygroscopic behaviour of individual aerosol particles, **Atmospheric Environment**, Vol. 36, 5909-5916.

Edwards C. A. (2007) **Pesticides**, [Online] Available at: <URL: http://www.pollutionissues.com/ Na-Ph/Pesticides.html>.

Ekberg L. (2007) **Revised Swedish Guidelines for the Specification of Indoor Climate Requirements** released by SWEDVAC, Proceedings of Clima 2007 Well Being Indoor, Sweden: CIT Energy Management AB.

European Commission-Environment (2011) **EU Air Quality Standards**, [Online] Available at: <URL: http://ec.europa.eu/environment/air/quality/standards.htm>.

European Commission Joint Research Centre (2005), **The INDEX Project: Critical appraisal of the setting and implementation of indoor exposure limits in the EU**, Italy: Institute for Health and Consumer Protection, Physical and Chemical Exposure Unit.

Evans Analytical Group LLC (2009) **Inductively Coupled Plasma Spectroscopy (ICP-OES/MS)**, [Online] Available at: <URL: http://www.eaglabs.com/techniques/analytical_techniques/icp_oes_ms.php>.

Fan, Y. (1995) CFD modelling of the air and contaminant distribution in rooms, **Energy and Buildings**, Vol. 23, 33-39.

Finnish Housing and Building Department (2003) **Finnish Building Code Section D2: Indoor climate and ventilation of buildings Regulations and Guidelines 2003**, Finland: Ministry of the Environment.

FiSIAQ: Finnish Society of Indoor Air Quality and Climate (2002) **Finish classification of indoor climate: revised target values**, Indoor Air Proceedings, Finland: FiSIAQ Publication.

Gadgil, A.J., Lobscheid, C., Abadie, M.O., and Finlayson, E.U. (2003) Indoor pollutant mixing time in an isothermal closed room: an investigation using CFD, **Atmospheric Environment**, Vol. 37, 5577-5586.

Gao, J., Wang, J., Cheng, S.-H., Xue, L.-K., Yan, H.-Z., Hou, L.-J., Jiang, Y.-Q., and Wang, W.-X. (2007) Number concentration and size distributions of submicron particles in Jinan urban area: characteristics in summer and winter, **Journal of Environmental Sciences**, Vol. 19, 1466-1473.

Geng Q., Guo Q., Cao C. and Wang H. (2008) Investigation into photocatalytic degradation of gaseous Benzene in a Circulated Photocatalytic Reactor (CPCR), **Chemical Engineering Technology**, Vol. 31, 1023-1030.

Giess, P. (1998) Respirable particulates and oxides of nitrogen measured inside a building alongside a busy road, **Indoor and Built Environment**, Vol. 7, 308-314.

Gillespie-Bennett, J., Pierse, N., Wickens, K., Crane, J., Nicholls, S., Shields, D., Boulic, M., Viggers, H., Baker, M., Woodward, A. and Howden-Chapman, P. (2008) Sources of nitrogen dioxide (NO_2) in New Zealand homes: findings from a community randomized controlled trial of heater substitutions, **Indoor Air**, Vol. 18, 521-528.

Godish, T. (2001) **Indoor environmental quality**, CRC Press, LLC.

Goldstein, J., Newbury, D., Joy, D., Lyman, C., Echlin, P., Lifshin, E., Sawyer, L. and Michael, J. (2003) **Scanning electron microscopy and x-ray microanalysis**, 3rd ed., United States of America; Spinger.

Google (2009) **Google Maps**, [Online] Available at: <URL: http://maps.google.co.uk/>.

Google (2010) **Google Maps**, [Online] Available at: <URL: http://maps.google.co.uk/>.

Gradko International (2011) **Gradko International Introduction**, [Online] Available at: <URL: http://www.gradko.co.uk/introduction.shtml>.

Green, D. (2009) **PerkinElmer Optima 4300 DV ICP-OES**, [Online] Available at: <URL: http://www.noc.soton.ac.uk/geochem/Facilities%20Links/icp-oes.htm>.

Hamilton I.S. (2007) **Radon**, [Online] Available at: <URL: http://www.pollutionissues.com/Pl-Re/Radon.html>.

Hastie D.R. (2007) **Smog**, [Online] Available at: <URL: http://www.pollutionissues.com/Re-Sy/Smog.html>.

Health Canada (1987) **Exposure guidelines for residential indoor air quality: a report of the federal-provincial advisory committee on environmental and occupational health - revised 1989**, Canada: Ministry of Supply and Services.

Hoek, G., Forsberg, B., Borowska, M., Hlawiczka, S., Vaskovi, E., Welinder, H., Branis, M., Benes, I., Kotesovec, F., Hagen, L.O., Cyrys, J., Jantunen, M., Roemer, W., and Brunekreef, B. (1997) Wintertime PM_{10} and black smoke concentrations across Europe: results from the peace study, **Atmospheric Environment**, Vol. 31, 3609-3622.

Hoek, G., Kos, G., Harrison, R., Hartog, J., Meliefste, K., Brink, H., Katsouyanni, K., Karakatsani, A., Lianou, M., Kotronarou, A., Kavouras, I., Pekkanen, J., Vallius, M., Kulmala, M., Puustinen, A., Thomas, S., Meddings, C., Ayres, J., van Wijnen, J., and Hameri, K. (2008) Indoor-outdoor relationships of particle number and mass in four European cities, **Atmospheric Environment**, Vol. 42, 156-169.

HPA: Health Protection Agency (2005) **The burden of disease attributable to environmental pollution**, [Online] London: Department of the Environment. Available at: <URL: http://www.hpa.org.uk/webc/HPAwebFile/ HPAweb_C/1194947365630>.

HPA: Health Protection Agency (2007a) **6-Environmental Pollution**, [Online] London: Department of the Environment. Available at: <URL: http://www.hpa.org.uk/webc/HPAwebFile/HPAweb_C/1194947360849>.

HPA: Health Protection Agency (2007b) **Development of a UK Children's Environment and Health Strategy**, [Online] London: Department of the Environment. Available at: <URL: http://www.hpa.org.uk/webc/HPAwebFile/ HPAweb_C/1194947331041>.

HPA: Health Protection Agency (2011) **Report of a workshop to identify needs for research on the Health Effects of Nitrogen Dioxide – London 2-3 March 2011**, [Online] London: Department of the Environment. Available at: <URL: http://www.hpa.org.uk/webc/HPAwebFile/HPAweb_C/1315371918587>.

HPA: Health Protection Agency (2012) **Air Quality Factsheet 6: Particles – PM_{10} & $PM_{2.5}$**, [Online] London: Department of the Environment. Available at: <URL: http://www.hpa.org.uk/webc/HPAwebFile/HPAweb_C/1294740079203>.

Hun, D.E., Corsi, R.L., Morandi, M.T., and Siegel, J.A. (2011) Automobile proximity and indoor residential concentrations of BTEX and MTBE, **Building and Environment**, Vol. 46, 45-53.

Ilgen, E., Karfich, N., Levsen, K., Angerer, J., Schneider, P., Heinrich, J., Wichmann, H.-E., Dunemann, L., and Begerow, J. (2001) Aromatic hydrocarbons in the atmospheric environment: part 1. indoor versus outdoor sources, the influence of traffic, **Atmospheric Environment**, Vol. 35, 1235-1252.

Illinois Department of Public Health (2008) **Guidelines for indoor air quality**, [Online] Illinois: Division of Environmental Health. Available at: <URL: http://www.idph.state.il.us/envhealth/factsheets/indoorairqualityguide_fs.htm>.

Indoor Air Quality Management Group (2003), **Guidance notes for the management of indoor air quality in offices and public places**, The Government of the Hong Kong Special Administrative Region.

Institute of Environmental Epidemiology (1996) **Guidelines for good indoor air quality in office premises**, Singapore: Ministry of the Environment.

International Light Technologies Inc. (2011) **NDIR Gas Sensors**, [Online] Available at: <URL: http://www.intl-lighttech.com/applications/light-source-apps/ndir-gas-sensor>.

International Organization for Standardization (2000) **ISO12569: 2000. Thermal Performance of Buildings – Determination of Air Change in Buildings – Tracer Gas Dilution Method**, International Organization for Standardization: Geneva.

IRK: Indoor Air Hygiene Commission (2009) **Guide values for indoor air quality**, [Online] Germany: Health and Environmental Hygiene. Available at: <URL: http://www.umweltbundesamt.de/gesundheit-e/irk.htm>.

Jedrychowski, W.A., Perera, F.P., Pac, A., Jacek, R., Whyatt, R.M., Spengler, J.D., Dumyahn. T.S., and Sochacka-Tatara, E. (2006) Variability of total exposure to $PM_{2.5}$ related to indoor and outdoor pollution sources Krakow study in pregnant women, **Science of the Total Environment**, Vol. 366, 47-54.

Jones, T., Blackmore, P., Leach, M., Berube, K., Sexton, K., and Richards, R. (2002) Characterisation of airborne particles collected within and proximal to an opencast coalmine: South Wales, UK, **Environmental Monitoring and Assessment**, Vol. 75, 293-312.

Keatinge, W.R., and Donaldson, G.C. (2001) Mortality related to cold and air pollution in London after allowance for effects of associated weather patterns, **Environmental Research Section A**, Vol. 86, 209-216.

Kingham, S., Briggs, D., Elliott, P., Fischer, P., and Lebret, E. (2000) Spatial variations in the concentrations of traffic related pollutants in indoor and outdoor air in Hundersfield England, **Atmospheric Environment**, Vol. 34, 905-916.

Kumar A., and Kumar R. (2007) **Indoor air pollution**, [Online] Available at: <URL: http://www.pollutionissues.com/Ho-Li/Indoor-Air-Pollution.html>.

Kwong C.W., Chao Christopher Y.H., Hui K.S. and Wan M.P. (2008) Removal of VOCs from indoor environment by ozonation over different porous material, **Atmospheric Environment**, Vol. 42, 2300-2311.

Lai, A.C.K. and Ho, Y.W. (2008) Spatial concentration variation of cooking-emitted particles in a residential kitchen, **Building and Environment**, Vol. 43, 871-876.

Lawrence, A.J., Masih, A., and Taneja, A. (2004) Indoor/outdoor relationships of carbon monoxide and oxides of nitrogen in domestic homes with roadside, urban and rural locations in a central Indian region, **Indoor Air**, Vol. 15, 76-82.

Lawson, S.J., Galbally, I.E., Powell, J.C., Keywood, M.D., Molloy, S.B., Cheng, M., and Selleck, P.W. (2011) The effect of proximity to major roads on indoor air quality in typical Australian dwellings, **Atmospheric Environment**, Vol. 45, 2252-2259.

Leaderer, B.P., Naeher, L., Jankun, T., Balenger, K., Holford, T.R., Toth, C., Sullivan, J., Wolfson, J.M. and Koutrakis, P. (1999) Indoor, outdoor and regional summer and winter concentrations of PM_{10}, $PM_{2.5}$, SO_4^{2-}, H^+, NH_4^+, NO_3, NH_3 and nitrous acid in homes with and without kerosene space heaters, **Environmental Health Perspectives**, Vol. 107, 223-231.

Lebowitz, M.D., Toyama, T., and McCarroll, J. (1973) The relationship between air pollution and weather as stimuli and daily mortality as responses in Tokyo, Japan, with comparisons with other cities, **Environmental Research**, Vol. 6, 327-333.

McCormack M.C., Breysse P.N., Hansel N.N., Matsui E.C., Tonorezos E.S., Curtin-Brosnan J., Williams D'A. L., Buckley T.J., Eggleston P.A. and Diette G. B. (2008) Common household activities are associated with elevated particulate matter concentrations in bedrooms of inner-city Baltimore pre-school children, **Environmental Research**, Vol. 106, 148-155.

Meininghaus R., Gunnarsen L. and Knudsen H. N. (2000) Diffusion and sorption of volatile organic compounds in building materials – Impact on indoor air quality, **Environmental Science and Technology**, Vol. 34, 3101-3108.

Mennim, A. (2009) **ICP-OES**, [Online] Edinburgh: School of Geosciences, The University of Edinburgh. Available at: <URL: http://www.geos.ed.ac.uk/facilities/ chem/ICP.html>.

Mestl, H.E.S., Aunan, K., Seip, H.M., Wang, S., Zhao, Y. and Zhang, D. (2007) Urban and rural exposure to indoor air pollution from domestic biomass and coal burning across China, **Science of the Total Environment**, Vol. 377, 12-26.

Miler, M. and Gosar, M. (2009) Characterisation of solid airborne particles in urban snow deposits from Ljubljana by means of SEM/EDS, **RMZ-Materials and Geoenvironment**, Vol. 56, 266-282.

Milner, J.T., Dimitroulopoulou, C., and ApSimon, H.M. (2004) **Indoor concentrations in buildings from sources outdoors**, UK Atmospheric Dispersion Modelling Liaison Committee, ADMLC/2004/2.

Molnar, P., Gustafson, P., Johannesson, S., Boman, J., Barregard, L. and Sallsten, G. (2005) Domestic wood burning and $PM_{2.5}$ trace elements: Personal exposures, indoor and outdoor levels, **Atmospheric Environment**, Vol. 39, 2643-2653.

Moreno, T., Jones, T.P., and Richards, R.J. (2004) Characterisation of aerosol particulate matter from urban and industrial environments: examples from Cardiff and Port Talbot, South Wales, UK, **Science of the Total Environment**, Vol. 334-335, 337-346.

Moriske, H.-J., Drews, M., Ebert. G., Menk, G., Scheller, C., Schondube, M. and Konieczny, L. (1996) Indoor air pollution by different heating systems: coal burning, open fireplace and central heating, **Toxicology Letters**, Vol. 88, 349-354.

Moschandreas, D.J., Relwani, S.M., Billick, I.H., and Macriss, R.A. (1987) Emission rates from range-top burners – assessment of measurement methods, **Atmospheric Environment**, Vol. 21, 285-289.

Mumford, J.L., Williams, R.W., Walsh, D.B., Burton, R.M., Svendsgaard, D.J., Chuang, J.C., Houk, V.S. and Lewtas, J. (1991) Indoor air pollutants from unvented kerosene heater emissions in mobile homes: studies on particles, semivolatile organics, carbon monoxide and mutagenicity, **Environmental Science and Technology**, Vol. 25, 1732-1738.

NASA (2011) **Terminal Velocity**, [Online] Washington, United States. Available at: <URL: http://www.grc.nasa.gov/WWW/K-12/airplane/termv.html>.

Nerisson, P., Simonin, O., Ricciardi, L., Douce, A., and Fazileabasse, J. (2011) Improved CFD transport and boundary conditions models for low-inertia particles, **Computers & Fluids**, Vol. 40, 79-91.

Niu, J., Lu, B.M.K., Tung, T.C.W. (2002) Instrumentation issue in indoor air quality measurements: the case with respirable suspended particulates, **Indoor Built Environment**, Vol. 11, 162-170.

Norton, T., Grant, J., Fallon, R., and Sun, D.-W. (2010a) Improving the representation of thermal boundary conditions of livestock during CFD modelling of the indoor environment, **Computers and Electronics in Agriculture**, Vol. 73, 17-36.

Norton, T., Grant, J., Fallon, R., and Sun, D.-W. (2010b) Optimising the ventilation configuration of naturally ventilated livestock buildings for improved indoor environmental homogeneity, **Building and Environment**, Vol. 45, 983-995.

Noullett, M., Jackson, P.L., and Brauer, M. (2006) Winter measurements of children's personal exposure and ambient fine particle mass, sulphate and light absorbing components in a northern community, **Atmospheric Environment**, Vol. 40, 1971-1990.

O'Connell, S., Au-Yeung, H.-K.C., Gregory, C.J., and Matthews, I.P. (2008) Outdoor and indoor respirable air particulate concentrations in differing urban traffic microenvironments, **Journal of Toxicology and Environment Health, Part A: Current Issues**, Vol. 71, 1069-1072.

Palmgren, F., Wahlin, P., Kildeso, Afshari, A., and Fogh, C.L. (2003) Characterisation of particle emissions from the driving car fleet and the contribution to ambient and indoor particle concentrations, **Physics and Chemistry of the Earth**, Vol. 28, 327-334.

Parikh, J., Balakrishnan, K., Laxmi, V., and Biswas, H. (2001) Exposure from cooking with biofuels: pollution monitoring and analysis for rural Tamil Nadu, India, **Energy**, Vol. 26, 949-962.

Park, K., Park, J.Y., Kwak, J.-H., Cho, G.N., and Kim, J.-S. (2008) Seasonal and diurnal variations of ultrafine particle concentration in urban Gwangju, Korea: observation of ultrafine particle events, **Atmospheric Environment**, Vol. 42, 788-799.

Parra M.A., Elustondo D., Bermejo R. and Santamaria J.M. (2008) Quantification of indoor and outdoor volatile organic compounds (VOCs) in pubs and cafes in Pamplona, Spain, **Atmospheric Environment**, Vol. 42, 6647-6654.

Pastuszka J.S., Paw U.K.T., Lis D.O., Wlazlo A. and Ulfig K. (2000) Bacterial and fungal aerosol in indoor environment in Upper Silesia, Poland, **Atmospheric Environment**, Vol. 34, 3833-3842.

Reimer, L. (1993) **Image formation in low-voltage scanning electron microscopy**, Volume TT 12, United States of America: SPIE Optical Engineering Press.

Reimer, L. (1998) **Scanning electron microscopy: physics of image formation and microanalysis**, 2nd ed., Germany: Spinger-Verlag.

Rohdin, P., and Moshfegh, B. (2007) Numerical predictions of indoor climate in large industrial premises: a comparison between different k-e models supported by field measurements, **Building and Environment**, Vol. 42, 3872-3882.

Roorda-Knape, M.C., Janssen, N.A.H., De Hartog, J.J., Van Vliet, P.H.N., Harssema, H., and Brunekreef, B. (1998) Air pollution from traffic in city districts near major motorways, **Atmospheric Environment**, Vol. 32, 1921-1930.

Roulet, C.-A. (2001) Indoor environment quality in buildings and its impact on outdoor environment, **Energy and Buildings**, Vol. 33, 183-191.

Russo, J.S., and Khalifa, H.E. (2010) CFD assessment of intake fraction in the indoor environment, **Building and Environment**, Vol. 45, 1968-1975.

Sekhar, S.C., and Willem, H.C. (2004) Impact of airflow profile on indoor air quality - a tropical study, **Building and Environment**, Vol. 39, 255-266.

Shi, Z.-B., He, K.-B., Yu, X.-C., Yao, Z.-L., Yang, F.-M., Ma, Y.-L., Ma, R., Jia, Y.-T., and Zhang, J. (2007) Diurnal variation of number concentration and size distribution of ultrafine particles in the urban atmosphere of Beijing in winter, **Journal of Environmental Sciences**, Vol. 19, 933-938.

Shi, Z., Shao, L., Jones, T.P., Whittaker, A.G., Lu, S., Berube, K.A., He, T., and Richards, R.J. (2003) Characterisation of airborne individual particles collected in an urban area in Beijing, 2001, **Atmospheric Environment**, Vol. 37, 4097-4108.

Sitzmann, B., Kendall, M., Watt, J., and Williams, I. (1999) Characterisation of airborne particles in London by computer-controlled scanning electron microscopy, **The Science of the Total Environment**, Vol. 241, 63-73.

Sivastava, A. and Jain, V.K. (2007) A study to characterise the suspended particulate matter in an indoor environment in Delhi, India, **Building and Environment**, Vol. 42, 2046-2052.

Slickers, K. (1993) **Automatic atomic-emission-spectroscopy**, 2nd ed., Germany: Giessen.

Sone H., Fugetsu B., Tsukada T. and Endo M. (2008) Affinity-based elimination of aromatic VOCs by highly crystalline multi-walled carbon nanotubes, **Talanta**, Vol. 74, 1265-1270.

Sorensen, D.N., and Weschler, C.J. (2002) Modelling-gas phased reactions in indoor environments using computational fluid dynamics, **Atmospheric Environment**, Vol. 36, 9-18.

Srebric, J., Vukovic, V., He. G., and Yang, X. (2008) CFD boundary conditions for contaminant dispersion, heat transfer and airflow simulations around human occupants in indoor environments, **Building and Environment**, Vol. 43, 294-303.

Srivastava, A., and Jain, V.K. (2007) A study to characterise the suspended particulate matter in an indoor environment in Delhi, India, **Building and Environment**, Vol. 42, 2046-2052.

Stamou, A., and Katsiris, I. (2006) Verification of a CFD model for indoor airflow and heat transfer, **Building and Environment**, Vol. 41, 1171-1181.

Stedman D. (2007) **VOCs (Volatile Organic Compounds)**, [Online] Available at: <URL: http://www.pollutionissues.com/Ve-Z/VOCs-Volatile-Organic-Compounds. html>.

Steeman, H.J., Janssens, A., Carmeliet, J., and De Paepa, M. (2009) Modelling indoor air and hygrothermal wall interaction in building simulation: comparison between CFD and a well-mixed zonal model, **Building and Environment**, Vol. 44, 572-583.

Sun, Z., and Wang, S. (2010) A CFD-based test method for control of indoor environment and space ventilation, **Building and Environment**, Vol. 45, 1441-1447.

Susin, R.M., Lindner, G.A., Mariani, V.C., and Mendonca, K.C. (2009) Evaluating the influence of the width of inlet slot on the prediction of indoor airflow: comparison with experimental data, **Building and Environment**, Vol. 44, 971-986.

Suzuki, K. (2006) Characterisation of airborne particulates and associated trace metals deposited on tree bark by ICP-OES, ICP-MS, SEM-EDX and laser ablation ICP-MS, **Atmospheric Environment**, Vol. 40, 2626-2634.

Teodosiu, C., Hohota, R., Rusaouen, G., and Woloszyn, M. (2003) Numerical prediction of indoor air humidity and its effect on indoor environment, **Building and Environment**, Vol. 38, 655-664.

Thermo Electron Corporation (2003) **Series 20-800 Eight Stage Non-Viable Impactor – Instruction Manual P/N 100073-00**, pp1-16, Massachusetts: Thermo Electron Corporation Environmental Instruments.

Tian, Z.F., Tu, J.Y., Yeoh, G.H., and Yuen, R.K.K. (2006) On the numerical study of contaminant particle concentration in indoor airflow, **Building and Environment**, Vol. 41, 1504-1514.

Tissari, J., Lyyranen, J., Hytonen, K., Sippula, O., Tapper, U., Frey, A., Saarnio, K., Pennanen, A.S., Hillamo, R., Salonen, R.O., Hirvonen, M.-R., and Jokiniemi, J. (2008) Fine particle and gaseous emissions from normal and smouldering wood combustion in a conventional masonry heater, **Atmospheric Environment**, Vol. 42, 7862-7873.

Tomqvist, H., Mills, N.L., Gonzalez, M., Miller, M.R., Robinson, S.D., Megson, I.L., MacNee, W., Donaldson, K., Soderberg, S., Newby, D.E., Sandstrom, T., and Blomberg, A. (2007)

Persistent endothelial dysfunction in humans after diesel exhaust inhalation, **American Journal of Respiratory and Critical Care Medicine**, Vol. 176, 395.

Traynor, G.W., Anthon, D.W., and Hollowell, C.D. (1982) Technique for determining pollutant emissions from a gas-fired range, **Atmospheric Environment**, Vol. 16, 2979-2987.

TSI Incorporated (2007) **IAQ-CALC™ Indoor air quality meters**, United States of America.

TSI Incorporated (2008) **DustTrak™ ll aerosol monitor**, United States of America.

TSI Incorporated (2008) **DustTrak II Aerosol Monitor – Theory of Operation –Application Note EXPMN-001**, [Online] Available at: <URL: http://www.tsi.com/uploadedFiles/Product_Information/Literature/Application_Notes/EXPMN-001_DustTrakII_Theory__of_Operation.pdf>.

TSI Incorporated (2011) **TSI Performance Measurement Tools and Precision Measurement Tools**, [Online] Available at: <URL: http://www.tsi.com/en-1033/indes.aspx>.

USEPA: United State Environmental Protection Agency (2009) **A guide to indoor air quality**, [Online] Washington, United States. Available at: <URL: http://www.epa.gov/iaq/pubs/insidest.html>.

Vallack, H.W., and Chadwick, M.J. (1993) Monitoring airborne dust in a high density coal-fired power station region in North Yorkshire, **Environmental Pollution**, Vol. 80, 177-183.

Van Dijken F., Van Bronswijk J.E.M.H. and Sundell J. (2006) Indoor environment and pupils' health in primary school, **Building Research and Information**, Vol. 34, 437-446.

Vassilev, S.V., Menendez, R., Diaz-Somoano, M., and Martinez-Tarazona, M.R. (2004) Phase-mineral and chemical composition of coal fly ashes as a basis for their multicomponent utilization. 2. Characterization of ceramic cenosphere and salt concentrates, **Fuel**, Vol. 83, 585-603.

Vincent G., Marquaire P.M. and Zahraa O. (2008) Abatement of volatile organic compounds using an annular photocatalytic reactor: Study of gaseous acetone, **Journal of Photochemistry and Photobiology A: Chemistry**, Vol. 197, 177-189.

Wallace, L. (1996) Indoor particles: a review, **Journal of the Air and Waste Management Association**, Vol. 46, 98-126.

Wallace, L.A., Emmerich, S.J., and Howard-Reed, C. (2004) Source strength of ultrafine and fine particles due to cooking with a gas stove, **Environmental Science and Technology**, Vol. 38, 2304-2311.

Wang, L., and Wong, N.H. (2009) Coupled simulations for naturally ventilated rooms between building simulation (BS) and computational fluid dynamics (CFD) for better prediction of indoor thermal environment, **Building and Environment**, Vol. 44, 95-112.

Wang, S., Ang, H.M., and Tade, M.O. (2007) Volatile organic compounds in indoor environment and photocatalytic oxidation: state of the art, **Environment International**, Vol. 33, 694-705.

Ward, T. and Noonan, C. (2008) Results of a residential indoor $PM_{2.5}$ sampling program before and after a woodstove changeout, **Indoor Air**, Vol. 18, 408-415.

WHO: World Health Organization (2000) **Air quality guidelines for Europe**, 2nd edition, World Health Organization Regional Office for Europe, Copenhagen, WHO Regional Publications, European Series, No. 91.

WHO: World Health Organization (2002) **The health effects of indoor air pollution exposure in developing countries**, WHO/SDE/OEH/02.05, Geneva, Switzerland.

WHO: World Health Organization (2005), **WHO air quality guidelines for particulate matter, ozone, nitrogen dioxide and sulfur dioxide: summary of risk assessment**, Global update 2005: Report on a working group meeting, Bonn, Germany, 18 – 20 October 2005, WHO Regional Office for Europe, Copenhagen.

Yamanaka, S., Hirose, H., and Takada, S. (1979) Nitrogen oxides emissions from domestic kerosene-fired and gas-fired appliances, **Atmospheric Environment**, Vol. 13, 407-412.

Yan, W., Zhang, Y., Sun, Y., and Li., D. (2009) Experimental and CFD study of unsteady airborne pollutant transport within an aircraft cabin mock-up, **Building and Environment**, Vol. 44, 34-43.

Yi, O., Hong, Y.-C., and Kim, H. (2010) Seasonal effect of PM_{10} concentrations on mortality and morbidity in Seoul, Korea: A temperature-matched case-crossover analysis, **Environmental Research**, Vol. 110, 89-95.

Zhang, J. (2011) **Particle Technology**, [Online] Available at: <URL: http://lorien.ncl.ac.uk/ming/particle/cpe124p2.html>.

Zhang, Z., and Chen, Q. (2006) Experimental measurements and numerical simulations of particle transport and distribution in ventilated rooms, **Atmospheric Environment**, Vol. 40, 3396-3408.

Zhang, Z., and Chen, Q. (2009) Prediction of particle deposition onto indoor surfaces by CFD with a modified Lagrangian method, **Atmospheric Environment**, Vol. 43, 319-328.

Zhao, B., Chen, C., and Tan, Z. (2009) Modelling of ultrafine particle dispersion in indoor environments with an improved drift flux model, **Aerosol Science**, Vol. 40, 29-43.

Zhao, B., Li, X., and Yan, Q. (2003) A simplified system for indoor airflow simulation, **Building and Environment**, Vol. 38, 543-552.

Zhao Y., Chen B., Guo Y., Peng F. and Zhao J. (2004) Indoor air environment of residential buildings in Dalian, China, **Energy and Buildings**, Vol. 36, 1235-1239.

Zhao, Y., Wang, S., Aunan, K., Seip, H.M., and Hao, J. (2006) Air pollution and lung cancer risks in China – a meta-analysis, **Science of the Total Environment**, Vol. 366, 500-513.

Zuraimi M.S. and Tham K.W. (2008) Indoor air quality and its determinants in tropical child care centers, **Atmospheric Environment**, Vol. 42, 2225-2239.

Appendix I

LIST OF PUBLICATIONS AND PRESENTATIONS

Publications

- Caren C.L. Tan, Karen N. Finney, Qun Chen, Nigel V. Russell, Vida N. Sharifi and Jim Swithenbank, Experimental investigation of indoor air pollutants in residential buildings, **Journal of Indoor and Built Environment** (Accepted for publication on 15 February 2012) – See Page 268

EPSRC Progress Reports

- INTRAWISE Sheffield Indoor Air Tests, May 2009, by Caren Tan
- Indoor Particulates: Experimental Tests in the Bedroom of a Stone-Built Detached House, May 2009, by Caren Tan
- Indoor Particulates: Experimental Tests in the Kitchen of a Stone-Built Detached House, July 2009, by Caren Tan
- Measured Emission Rates of $PM_{2.5}$, CO, NO_2 and VOCs: Two Case Studies – A Residential House in Hathersage and a Flat near Sheffield City Centre, October 2009, by Caren Tan, Dr Qun Chen and Dr Xiaohui Zhang
- Outdoor Particulates: Experimental Tests at the Outdoors of a Stone-Built Detached House, October 2009, by Caren Tan
- Indoor Air Pollutants: Distributed and Centralised Energy Provision for Households, February 2010, by Dr Qun Chen, Caren Tan, Dr Xiaohui Zhang and Dr Karen Finney

- Case Study 1: Hathersage – Additional CO and $PM_{2.5}$ Measurements (with and without cooking activities), February 2010, by Caren Tan, Dr Qun Chen and Dr Xiaohui Zhang
- Air Exchange Between Indoor and Outdoor Environments, September 2010, by Caren Tan
- Experimental Case Study: Concentrations and Emission Rates of VOCs, CO, NO_2 and $PM_{2.5}$ in a Residential Building, January 2011, by Caren Tan and Dr Karen Finney
- Experimental Case Study: Measured Concentrations and Calculated Emission Rates of NO_2 and $PM_{2.5}$ in a Residential Building, April 2011, by Caren Tan and Dr Karen Finney
- FLUENT Modelling Report: Airflow Patterns and Particle Trajectories in the Kitchen of a Stone-Built House in Hathersage, September 2011, by Caren Tan and Dr Karen Finney

Poster Events

- C Tan, Q Chen, X Zhang, K Finney, V Sharifi, J Swithenbank, Experimental Investigation of Indoor Air Pollutants, 2010 Annual UK Review Meeting on Outdoor and Indoor Air Pollution Research at Cranfield University, UK, 13-14th April 2010
- C Tan, K Finney, Q Chen, V Sharifi, J Swithenbank, Experimental Investigation of Indoor Air Pollutants in Residential Buildings, 2011 Annual UK Review Meeting on Outdoor and Indoor Air Pollution Research at Cranfield University, UK, 10-11th May 2011

Conference Papers

- J Swithenbank, W Chung, Q Chen, C Tan, X Zhang, V Sharifi. Particulates in the Urban Environment. 12th Annual UK Review Meeting on Outdoor & Indoor Air Pollution at Cranfield University, UK, 20-21st April 2009
- C Tan, Q Chen, X Zhang, K Finney, V Sharifi, J Swithenbank. Experimental Investigation of Indoor Air Pollutants. 2010 Annual UK Review Meeting on Outdoor and Indoor Air Pollution Research at Cranfield University. UK, 13-14th April 2010
- C Tan, K Finney, Q Chen, V Sharifi, J Swithenbank. Experimental investigation of indoor air pollutants in residential buildings. 2011 Annual UK Review Meeting on Outdoor and Indoor Air Pollution Research at Cranfield University. UK, 10-11th May 2011

Departmental Seminars and Events

- 24-month Departmental Poster Presentation, Experimental Investigation of Indoor Air Pollutants, Sir Robert Hadfield Building, Department of Chemical and Biological Engineering, University of Sheffield, 10th November 2010
- 30-month Departmental Oral Presentation, Experimental Investigation of Indoor Air Pollutants in Residential Buildings, Sir Robert Hadfield Building, Department of Chemical and Biological Engineering, University of Sheffield, 2nd November 2011

Original Paper

Indoor and Built Environment

Indoor Built Environ 2012;000;000:1–19

Accepted: February 15, 2012

Experimental Investigation of Indoor Air Pollutants in Residential Buildings

Caren C.L. Tan Karen N. Finney Qun Chen
Nigel V. Russell Vida N. Sharifi Jim Swithenbank

Sheffield University Waste Incineration Centre, Department of Chemical and Biological Engineering, University of Sheffield, UK

Key Words

Air exchange rate · Emission rates · Indoor air pollution · Particle composition · Particle morphology · Particulate matter

Abstract

Indoor air quality is affected by many factors, including energy provision/use. The main objective of this research was to investigate indoor air pollutant emissions due to energy use in residential buildings, with a specific focus on particulate matter (PM). Three environments were compared: (a) a rural house with an electric cooker; (b) a city-centre flat with a gas cooker; and (c) an urban flat on a main road, also with gas appliances. Concentrations of PM, CO, NO_2 and VOCs were measured in the kitchens and emission rates were calculated for cooking periods. Although there has been a great deal of research examining the effects of gaseous pollutants in the indoor environment, this is one of the first studies to specifically focus on PM. Most particles were small ($\leq$2.5 μm) and thus respirable. The elemental analysis of the PM revealed high metal concentrations (Fe/Na/Zn), whilst their morphologies indicated these were present as salt, skin and particles of biological origin. Gaseous emissions, particularly NO_2 and CO, were more prevalent in homes with gas appliances, since these are a significant source of both pollutants.

Nomenclature

a = Air exchange rate (h^{-1})
C_{in} = Indoor mass concentration of pollutants ($\mu g \cdot m^{-3}$)
C_{out} = Outdoor mass concentration of pollutants ($\mu g \cdot m^{-3}$)
EDS = Energy dispersion X-ray system
k = Pollutant removal rate (h^{-1})
NO_x = Oxides of nitrogen
p = Penetration coefficient across building envelope
PM = Particulate matter
S_e = Emission rate ($\mu g \cdot h^{-1}$)
SEM = Scanning electron microscopy
t = Sampling time (h)
V = Volume of the room (m^3)
VOCs = Volatile organic compounds
Δt = Cooking time (h)
ΣVOCs = Sum (total) of top 20 volatile organic compounds

DOI: 10.1177/1420326X12441806
Accessible online at http://ibe.sagepub.com

Karen N. Finney,
Sheffield University Waste Incineration Centre, Department of Chemical and Biological Engineering, University of Sheffield, Mappin Street, Sheffield, S1 3JD, UK Tel. 44 (0)114 222 7563, Fax. 44 (0)114 222 7501
E-Mail k.finney@sheffield.ac.uk

Introduction

We spend the vast majority of our time indoors – on average 90%. We control these indoor environments for health, thermal comfort and productivity. However, maintaining the quality of the environment in buildings can have considerable consequences both on human health and on the local and global environment. The quality of the indoor environment is affected by many factors, including the design of buildings, ventilation, energy provision/use, thermal insulation and household activities such as cleaning.

Indoor Air Pollution

Although ambient air has a significant impact on the quality of the indoor environment [1], several field studies have shown that indoor pollutant levels can be approximately two to five times (and occasionally more than 100 times) higher than outdoor levels [2,3]. In addition to outdoor sources of pollutants, which ingress to the indoor environment, there are also various indoor sources of air pollution, for example from combustion, building materials (vapours from carpets, pressed wood furniture) and household cleaning products [4]. Recently, increasing the airtightness of buildings has become a significant issue – mainly as part of a drive to provide improved thermal comfort and reduce energy consumption. However, as dwellings are made more airtight, internal pollution sources (such as heating and cooking systems) can have a greater impact on indoor air quality and occupants may experience adverse health effects due to the increased exposure. Most indoor air pollution comes from sources inside the building [5]. The sources listed above generate or release pollutants either continuously (building materials and household fragrance products) or intermittently (smoking or the use of solvents for cleaning).

In addition to the above sources, another major contributor to indoor air pollution is the use of energy, specifically for cooking and heating. When gas cookers are used in kitchens, various pollutants, like carbon monoxide, oxides of nitrogen (NO_x) and particulate matter (PM) can be emitted. Many different types of appliance are used for heating, cooking and supplying hot water [6]. Several studies have been carried out to investigate indoor air pollution from various heating systems [7–9]. Gas cooking appliances are not vented to the outdoors and as a result, they are a potentially significant source of indoor air contamination.

Rationale for the Experiments

Indoor air pollutants, such as those listed above, can have significant health implications. CO is highly toxic and even short-term low exposure can negatively impact health. Volatile organic compounds (VOCs) are also toxic and many are carcinogenic. Acid gas emissions, like NO_x, can dissolve in water to form corrosive acids or can become attached to small particles. It has been suggested that the inhalation of such gases or particles can initiate or exacerbate existing respiratory problems. PM, if inhaled, can cause chronic cardiovascular, respiratory and pulmonary illnesses; smaller particles, particularly sub-micron PM, can penetrate deeper into the lungs, having greater health effects. Limited data for indoor air pollutant levels and the associated emission rates from heating or cooking appliances have been reported in the literature. Since we spend most of our time indoors, more detailed information on pollutant levels in homes is vital for understanding how emission concentrations can be reduced, thus limiting personal exposure and minimising detrimental health impacts.

The main objective of this research programme was therefore to investigate the concentrations and emission rates of indoor air pollutants, namely PM, CO, NO_x and VOCs, generated from various heating and cooking systems in three residential buildings, especially in the kitchens of these environments. This paper presents the experimental results obtained from this study, focusing primarily on PM.

Materials and Methods

Site Descriptions

A series of extensive emissions tests were carried out in three different residential buildings. Case 1 was a rural house with an electric cooker. Cases 2 and 3 were both flats with gas-fired cookers in Sheffield. Case 2 was located in the city centre, whereas Case 3 was in an urban area, but situated on a main road. Each of these case study environments are described in the following sections.

Case 1

This was a stone-built detached house in Hathersage – a village in the Peak District National Park, just over 10 miles west of Sheffield. There is an industrial cement manufacturing plant 4 miles away from the house and a reservoir about 3 miles northwest. There is also a busy diesel-operated railway line 0.1 mile away and a busy road that lies 50 m northwest. Although there is a natural gas

heating system with a capacity of 23.5–85 kW, the boiler is not located in the kitchen. There is an electric cooker installed in the kitchen (Figure 1(a)) which is used once or twice a day (around 1.5 h each time). The kitchen has an estimated volume of 50 m^3.

Various analytical instruments were placed inside the kitchen of each study environment to monitor indoor pollutants. The sampling points were located at strategic sites in the kitchens to represent the personal exposure of the person cooking. In Case 1, the instruments were placed on the top of a sideboard at a height of about 1.2 m above the floor and a distance of 3.5 m away from the cooker (Figure 1(a)).

Case 2

This case study environment was a second floor flat in a residential building, located near Sheffield city centre. The estimated kitchen volume is 36 m^3. A natural gas-fired boiler (30 kW capacity) is installed in the kitchen, which provides hot water. The flue gases from the boiler are discharged to the outdoor environment via a vent above the boiler. Also in this kitchen, there is a gas cooker approximately 3 m from the boiler (Figure 1(b)). A hood (extractor fan) is installed 1 m above the cooker to improve ventilation during cooking. For this case, the analytical instruments were placed 0.5 m from the cooker, at a height of about 1.5 m from the floor.

Case 3

The third case study environment was in a three-storey residential building located on top of shops in an urban area of Sheffield. The flat is situated on a main road, which is regularly used by buses, trams and cars/lorries. The kitchen is located on the first floor. The estimated volume of the kitchen is 30 m^3. A natural gas-fired boiler (22.3 kW) vented to the outdoor environment is installed in one corner of the kitchen, about 1 m from the gas cooker (3–4.5 kW), which does not have an extractor fan above it. The analytical instruments were placed approximately 0.5 m away from the cooker, at a height of about 1 m (Figure 1(c)).

Experimental Methodologies and Equipment

The concentrations of $PM_{2.5}$ – solid-phase PM $\leq$2.5 μm – as well as gaseous pollutants (CO, NO_2 and VOCs) were measured in the kitchens and outdoor environments at all three sampling sites. The methods for these measurements are described in the following sections. Additional particles were collected and tested for Cases 1 and 3.

Particulate Matter

The TSI Dust-Trak 8532 aerosol monitor was used to measure the real-time $PM_{2.5}$ concentrations in each indoor and outdoor environment. The detection range was 0.001–150 $mg \cdot m^{-3}$ and the resolution was 0.1% of the reading. The log interval of the concentration data was set at 30 s. Although the particle size range of the instrument was 0.1–10 μm, during these measurements a size-selective impactor was attached to the inlet (with a cut size of 2.5 μm), which pre-conditioned the size range of particles ($<$2.5 μm) entering the instrument.

For Cases 1 and 3, additional particle collection and analysis was conducted. A multi-stage, multi-orifice cascade Andersen 0.0283 $m^3 \cdot min^{-1}$ Ambient Particle Sizing Sampler (Mark II version, Thermo Electron Corp.) was used to collect PM samples from the kitchen (Cases 1 and 3), as well as a bedroom and the outdoor environment (Case 1 only) in order to establish the particle size distribution. The sampler was calibrated with 1 $g \cdot cm^{-3}$ spherical particles. A pre-separator was used to prevent particles greater than 10 μm from entering the subsequent stages, which could help minimise particle bouncing and re-entrainment errors. In each of the eight stages of the Andersen sampler, aluminium foil was used as the collection substrate and was placed on top of the collection plates. The bedroom that was monitored for Case 1 had dimensions of $4 \times 3 \times 2.5$ m^3. There was only one window in this room. The sampling position was at the centre of the room at a height of 1 m. Samples were collected in the bedroom over a period of 6 weeks (1008 h). PM_{10} samples in the outdoor environment were collected over a period of 1085 h, at a height of 2 m from the ground. Indoor samples were taken over a monitoring period of 4 weeks in each case.

All PM samples collected were then analysed to determine the particle morphology and composition. The morphology of the PM_{10} samples was studied using scanning electron microscopy (SEM) with energy dispersive X-ray spectroscopy (EDS). It was used to characterise the bulk specimen from 1 to 100 μm. The EDS allowed both qualitative and quantitative microanalysis and X-ray mapping. Digital images were acquired using various software packages available on the computer linked to the SEM. In addition, the chemical composition (elemental analysis) of the PM_{10} samples was determined using a Spectro Ciros inductively coupled plasma (ICP) emission spectrometer.

Gaseous Pollutants

CO concentrations were measured for all three cases using a TSI IAQ-Calc Model 7545 analyser. This

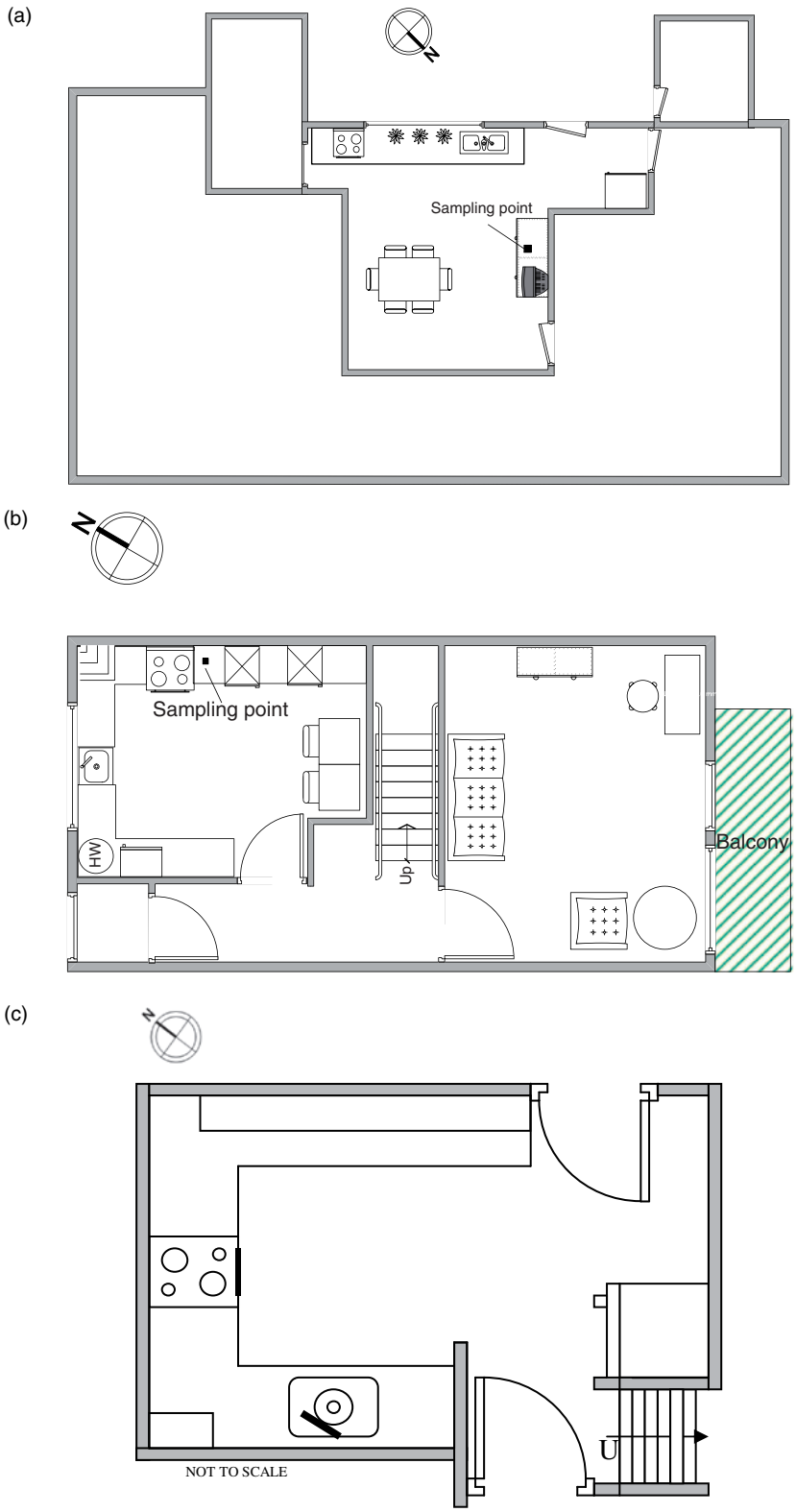

Fig. 1. Layout of the kitchen for each case study environment: (a) the rural house – Case 1; (b) the city-centre flat – Case 2; and (c) the urban flat on a main road – Case 3.

instrument is a hand-held portable device that simultaneously measures CO, CO_2, temperature and relative humidity. The CO sensor/detector was electro-chemical, which was calibrated to a range of 0 to 500 ppm. CO_2 was measured using the non-dispersive infrared spectrometry technique. The logging interval was 30 s for both species.

Different types of diffusion tubes were deployed to monitor NO_2 and VOCs. To measure NO_2 concentrations, Palmes-type diffusion tubes (Gradko International, 20% triethanolamine) were used, which are widely utilised in the UK for determining ambient nitrogen dioxide (NO_2) concentrations [10]. The analytical expanded measurement uncertainty for the diffusion tubes in this study was ±3.69%. The detection limit was 0.4 ppb (or 0.34 $\mu g \cdot m^{-3}$) over a 2-week exposure period in each environment. The tubes were stored in a sealed container in a refrigerator prior to use. The tube was vertically mounted with the open end at the bottom. NO_2 was absorbed as nitrite in the tubes. After exposure for 2–4 weeks, the lower end cap was replaced and the NO_2 concentration was quantitatively determined using UV spectrophotometry (UVS04 Camspec M550). This gave the average concentration over the entire exposure period for each case study.

For VOCs, DIFTXTA (Gradko International) VOC diffusion tubes were used. The VOC sampler consisted of a stainless steel tube (6.3 mm OD × 5.0 mm ID × 90 mm length) filled with a solid polymer absorbent (TENAX TA) with two brass Swagelok caps. During passive sampling, an aluminium air diffuser was fitted to the sampling end of the tube. After 3–4 weeks exposure, the diffusion tubes were returned to Gradko for analysis and the results were given as VOC concentrations. The absorbent in the tubes was analysed through thermal desorption and mass spectroscopy. The masses of the top 20 VOCs were identified. The analytical measurement error was ±14.8%. It should be noted that the average VOC concentration over the period of exposure was measured using this method.

Air Exchange Rate

Air exchange rates for the kitchen in each residential building were also determined to aid the calculation of pollutant emission rates. Building air exchange rates are associated with the wind and thermally induced pressure flows, as well as mechanical ventilation. The air exchange rate can be measured through the tracer gas decay method, the constant injection method or the constant concentration method. The concentration decay method is the most widely used air exchange measuring technique and this is the method employed in this study to determine the air exchange rates of all three kitchens. The air exchange rate was measured in accordance with ISO 12569 [11], where CO_2 was chosen as a tracer gas. A small volume of CO_2 was released, mixed and uniformly distributed in each kitchen, causing initial concentrations of approximately 1500–2000 ppm. A CO_2 analyser (the IAQ Calc 7545, used also for the analysis of the CO and CO_2 concentrations, as described above) was used to record the CO_2 levels continuously for about 15–20 min or until the reading had dropped by several hundred ppm. In this study, it was assumed that the kitchens were perfectly stirred reactors. Tests were repeated three times in each kitchen to minimise the effects of temporal and spatial fluctuations.

Emission Rates of Indoor Air Pollutants

A mass balance method was used to determine the emission rates of indoor pollutants from various cooking activities. Mass balance equations establish relationships between changes over time in the pollutant concentration in the air of a well-mixed room and the outdoor concentration, source emission rates, air exchange rates and removal rates. A mass balance differential equation for a certain period of time (t) is shown in Equation (1) [12]:

$$\frac{dC_{in}}{dt} = p \cdot a \cdot C_{out} - (a + k) \cdot C_{in} + S_e/V \qquad (1)$$

where C_{in} is the indoor mass concentration of pollutants ($\mu g \cdot m^{-3}$), C_{out} the outdoor mass concentration of pollutants ($\mu g \cdot m^{-3}$), p the penetration coefficient across the building envelope, a the calculated air exchange rate (h^{-1}), k the pollutant removal rate (h^{-1}), S_e the emission rate ($\mu g \cdot h^{-1}$) and V the volume of the room (m^3).

Given the constant values for p, a, k and S_e and the outdoor concentration, C_{out}, the relationship between indoor concentrations at times t_1 and t_2 can be obtained by integrating Equation (1), as shown in Equations (2) to (4):

$$\int_{t_1}^{t_2} \frac{dC_{in}(t)}{C_{in}(t) - \frac{S}{V(a+k)} - \frac{p \cdot a \cdot C_{out}}{a+k}} = -(a + k) \int_{t_1}^{t_2} dt \qquad (2)$$

Thus,

$$C_{in}(t_2) = \frac{p \cdot a \cdot C_{out} + S/V}{a + k} + \left(C_{in}(t_1) - \frac{p \cdot a \cdot C_{out} + S/V}{a + k} \right) \times \exp(-(a + k)(t_2 - t_1)) \qquad (3)$$

The emission rate of a particular pollutant can consequently be solved from Equation (4):

$$S_e = \frac{\left(\left(C_{in}(t_2) - \frac{p\cdot a\cdot C_{out}}{a+k} + \left(\frac{p\cdot a\cdot C_{out}}{a+k} - C_{in}(t_1)\right)\right.\right.}{\left.\left.\times \exp\left(-(a+k)(t_2-t_1)\right)\right)\cdot V\cdot(a+k)\right)} \quad (4)$$

In this study, the concentrations of both CO and $PM_{2.5}$ were measured; real-time values were monitored on a continuous basis. The emission rates of CO and $PM_{2.5}$ from indoor cooking activities can therefore be obtained from Equation (4). For NO_2 and VOCs, however, only average concentrations can be obtained from the method used (different types of diffusion tubes). Integrating each term of Equation (1) over the sampling period gives Equation (5):

$$\int_0^t dC_{in}(t) = p\cdot a\cdot\int_0^t C_{out}(t)dt - (a+k)\int_0^t C_{in}(t)dt + \int_0^t \frac{S_e}{V}dt \quad (5)$$

Since the average values of outdoor and indoor concentrations are known, the average pollutant emission rate can be defined by Equation (6):

$$\overline{C_{out}} = \frac{1}{t}\int_0^t C_{out}(t)dt, \quad \overline{C_{in}} = \frac{1}{t}\int_0^t C_{in}(t)dt, \quad \overline{S_e} = \frac{1}{t}\int_0^t S_e(t)dt \quad (6)$$

Subsequently, the average emission rate of an indoor pollutant can be calculated from the average indoor and outdoor concentrations, as shown by Equation (7):

$$\bar{S} = \frac{t}{\Delta t}\overline{S_e} = \frac{t}{\Delta t}\cdot V\cdot\left[(a+k)\overline{C_{in}} - p\cdot a\cdot\overline{C_{out}} + \frac{C_{in}(t)-C_{in}(0)}{t}\right] \quad (7)$$

where t is the sampling time and Δt the cooking time (corresponding to the pollutant emissions). Based on Equations (4) and (7), the indoor emission rates of $PM_{2.5}$, CO, NO_2 and VOCs can be calculated using the indoor pollutant concentrations determined in the experimental phase of this study.

Results and Discussion

Determining the Air Exchange Rates

The air exchange rates were calculated first in order to allow the determination of the emission rates for each pollutant from the subsequent tests. Figure 2 shows the typical decay curves for the CO_2 concentration during the air exchange rate tests in the kitchens of all three buildings. As observed for Case 1, the indoor CO_2 concentration was increased to approximately 1500 ppm when CO_2 was released and well mixed in the kitchen of the rural house. The CO_2 concentration then slowly decreased. The air exchange rate in the kitchen of Case 1 was 1.5 ± 0.2 hr^{-1}. The air exchange rate measured in the kitchen of the city-centre flat (Case 2) was 3.3 ± 0.6 hr^{-1} and the air exchange rate in the kitchen of Case 3

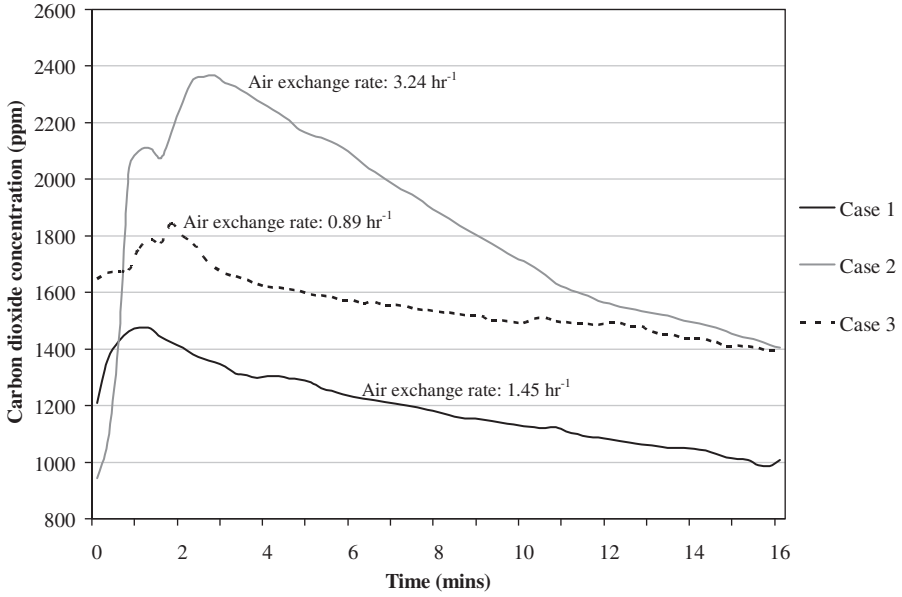

Fig. 2. CO_2 concentration decay curves in the kitchens of all residential case study environments.

was 0.9 ± 0.1 hr^{-1}. The air exchange rates in all three case studies were expected.

Particulate Emissions

Comparison of $PM_{2.5}$ for all Three Case Study Environments

$PM_{2.5}$ Concentrations

Figure 3 shows the real-time concentrations of indoor $PM_{2.5}$ in the kitchens for all three case studies. Figure 3(a) shows that the indoor $PM_{2.5}$ concentration in the rural house, Case 1, remained constant at around 10–12 $\mu g \cdot m^{-3}$ during the initial measurement period; this is most likely due to the fact that the house was unoccupied during this part of the sampling period. This unoccupied period gave a background reading for this case study environment.

$PM_{2.5}$ concentrations in the kitchen were found to increase when there were more indoor activities taking place. As shown in Figure 3(a), the highest value achieved was 198 $\mu g \cdot m^{-3}$, where the spikes coincided with cooking activities. Overall, the average indoor $PM_{2.5}$ concentration was 16 $\mu g \cdot m^{-3}$. This was slightly higher than the value obtained using the Andersen sampler. The Andersen sampler suggested that the average indoor $PM_{2.5}$ concentration was 8–9 $\mu g \cdot m^{-3}$. The outdoor $PM_{2.5}$ concentration near the house was about 10 $\mu g \cdot m^{-3}$, similar to the indoor background levels.

The real-time indoor $PM_{2.5}$ concentrations in the kitchen of the city-centre flat are presented in Figure 3(b) – Case 2. As shown, the $PM_{2.5}$ spikes were much higher than those for Case 1, often by an order of magnitude. This is due to the type of cooker used – the city-centre flat has a gas cooker compared to an electric cooker in the rural house. Other possible sources of such high $PM_{2.5}$ concentrations may include burnt food and different cooking techniques, such as more frying with cooking oil. The fumes emitted from frying pans can nucleate, forming ultrafine particles inside the kitchen. Most coarse particles generated in the kitchen are known to be from frying and spattering during cooking [13]. The average indoor $PM_{2.5}$ concentration in this kitchen was 40.6 $\mu g \cdot m^{-3}$, much higher than Case 1, whereas the average outdoor $PM_{2.5}$ concentration near the flat was 14 $\mu g \cdot m^{-3}$, which is more similar, but still slightly elevated compared to the rural house. Figure 3(c) shows the real-time concentrations of indoor $PM_{2.5}$ in the kitchen of Case 3 – the urban flat on a main road. The average indoor $PM_{2.5}$ concentration measured in this environment was 38 $\mu g \cdot m^{-3}$, similar to Case 2 and again much greater than Case 1. The indoor $PM_{2.5}$ concentrations remained fairly constant for much of the monitoring period, though it was slightly increased during indoor activities, especially cooking (spikes of 300–700 $\mu g \cdot m^{-3}$). A peak of around 2000 $\mu g \cdot m^{-3}$ was reached when food was deliberately burned. The average outdoor $PM_{2.5}$ concentration near the flat was 42 $\mu g \cdot m^{-3}$. Both the indoor and outdoor $PM_{2.5}$ concentrations for Case 3 were higher than the tests in the rural house, Case 1. The indoor concentrations were slightly lower than the kitchen of Case 2, although the outdoor PM levels were higher, due to the effects of the main road nearby.

$PM_{2.5}$ Emission Rates

Based on the CO_2 decay curves and the subsequent air exchange rates that were calculated, the $PM_{2.5}$ emission rates could thus be determined for the cooking periods in each residential environment. Figure 4(a) shows the average emission rates of $PM_{2.5}$ during three cooking periods in the kitchen of Case 1, which varied significantly, from 5 to 23 $mg \cdot h^{-1}$. This may be due to the differences in the food preparation methods and cooking activities during the measurement periods. The tests for Case 2 also showed that there was a considerable range in emission rates in the kitchen. Particles emitted from food preparation or frying could be the main contributors. As shown in Figure 4(b), the average emission rate of $PM_{2.5}$ for the different cooking periods varied from 7 to 54 $mg \cdot h^{-1}$. Traynor et al. [8] reported that the emission rates of $PM_{2.5}$ from range-top burners were in the region of 0.24–1.62 $\mu g \cdot kJ^{-1}$. This is similar to the results obtained in this study, which were calculated to be in the region of 0.60–4.5 $\mu g \cdot kJ^{-1}$, when normalised to the amount of fuel consumed during the cooking period. The emission rates of $PM_{2.5}$ during five cooking periods in the kitchen of Case 3 are presented in Figure 4(c). The emission rates here also significantly varied due to the differences in cooking styles and food preparation methods. Particles emitted from food, for example during frying or grilling, greatly contribute to the variation in emission rates found here.

Properties and Composition of PM_{10} for Cases 1 and 3

Besides $PM_{2.5}$ concentration measurements using the TSI Dust-Trak, additional particle collection and analysis were conducted for Cases 1 and 3 using the Andersen sampler. The PM were analysed for particle size distribution, elemental composition and morphology.

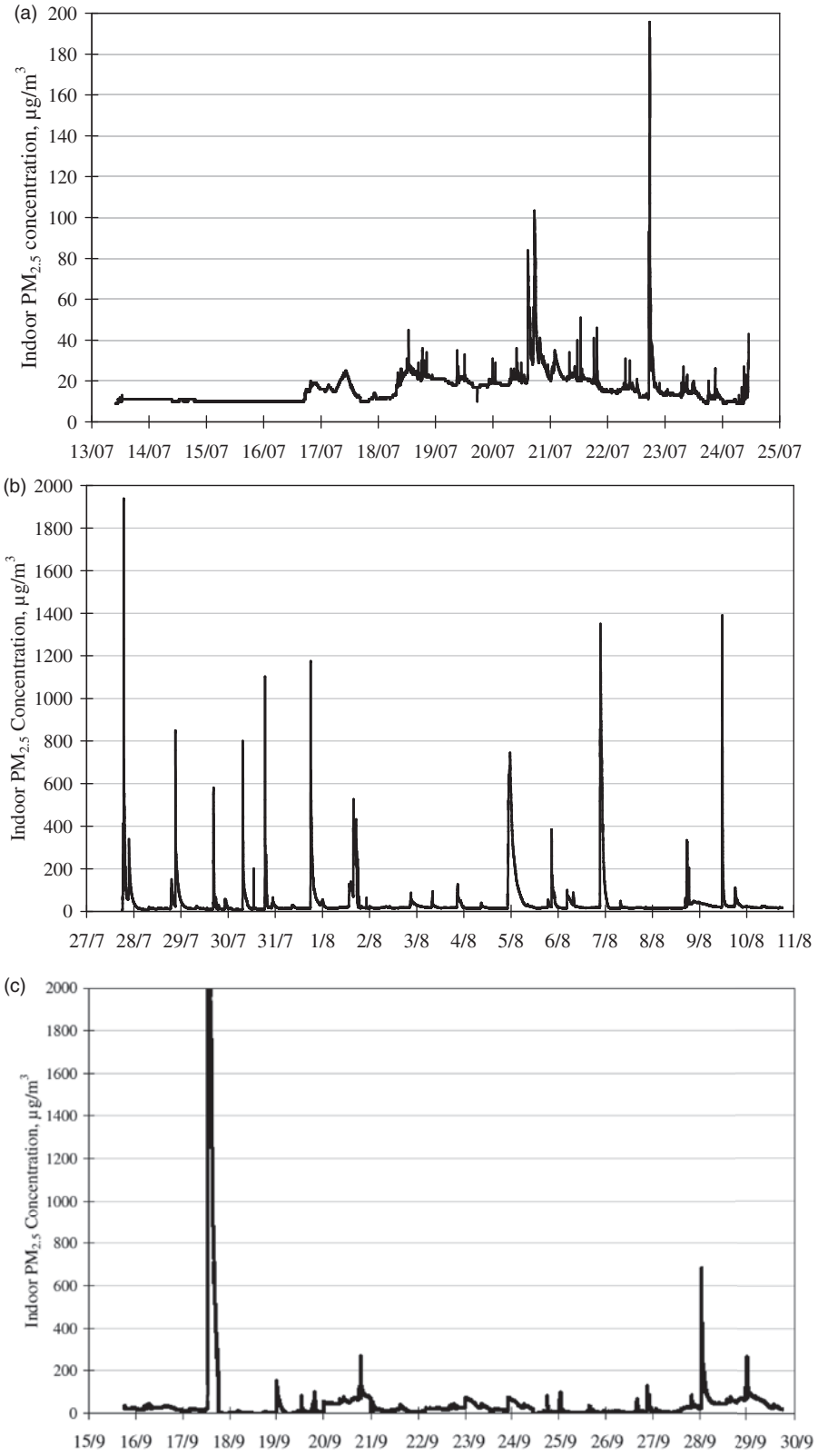

Fig. 3. Real-time concentrations of indoor $PM_{2.5}$ in the kitchens of (a) the rural house – Case 1; (b) the city-centre flat – Case 2; and (c) the urban flat on a main road – Case 3.

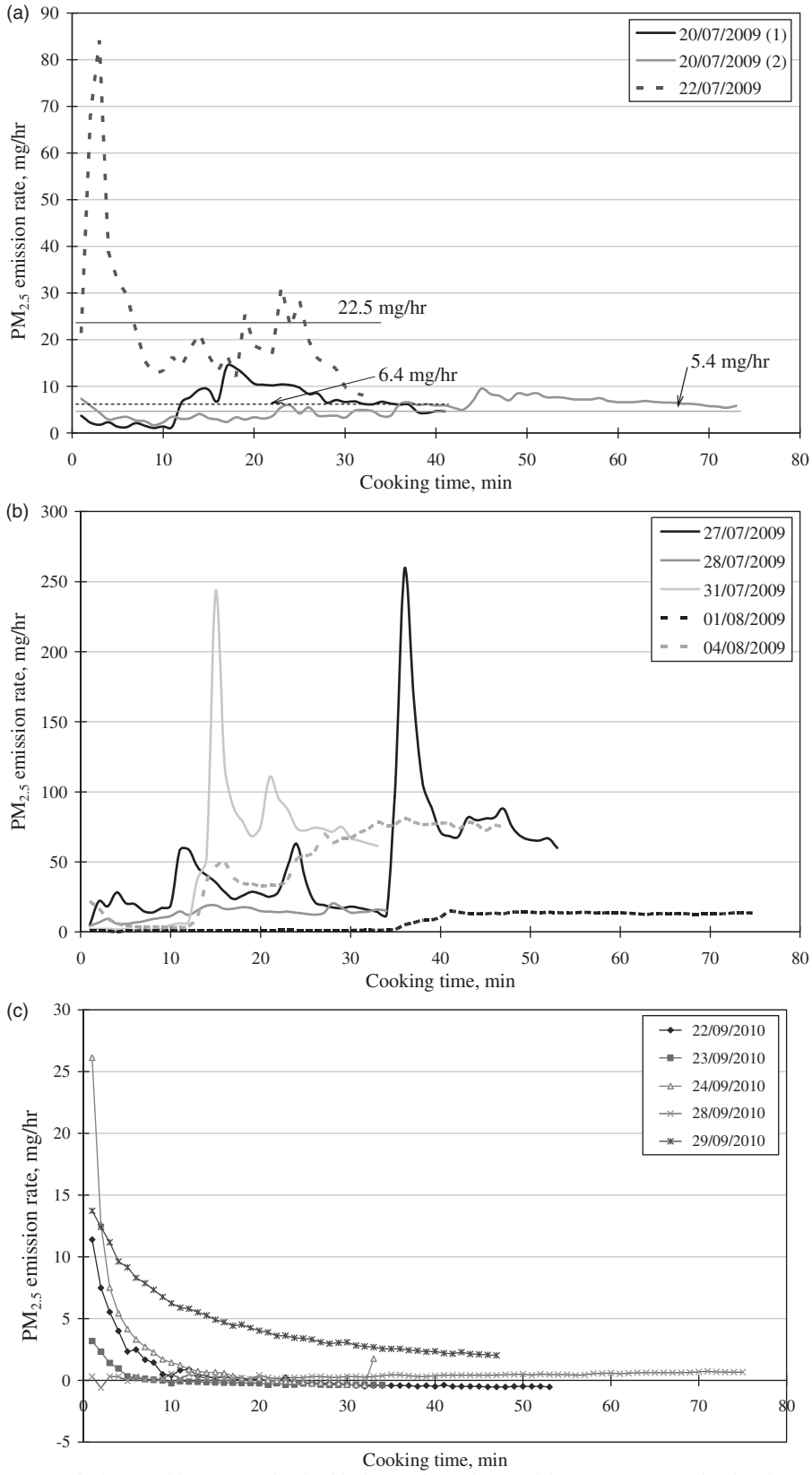

Fig. 4. $PM_{2.5}$ emission rates during cooking events in the kitchens of (a) the rural house – Case 1; (b) the city-centre flat – Case 2; and (c) the urban flat on a main road – Case 3.

Particle Size Distribution

Samples of PM, which were generally smaller than 10 μm, were collected in the kitchen of Case 1 and this was compared to samples taken from a bedroom in the same house and the outdoor environment. The mass concentrations/distributions of PM_{10} collected for the three locations at Case 1 and the kitchen of Case 3 are presented in Figure 5.

Figure 5(a) displays the size distribution for the particles collected in the kitchen in Case 1. The concentrations of $PM_{2.5}$ and PM_{10} were 8.0 and 12.9 $\mu g \cdot m^{-3}$, respectively. The major source of these particles is attributed to cooking activities, for example using the stove and burnt food, as well as other common household activities, like cleaning.

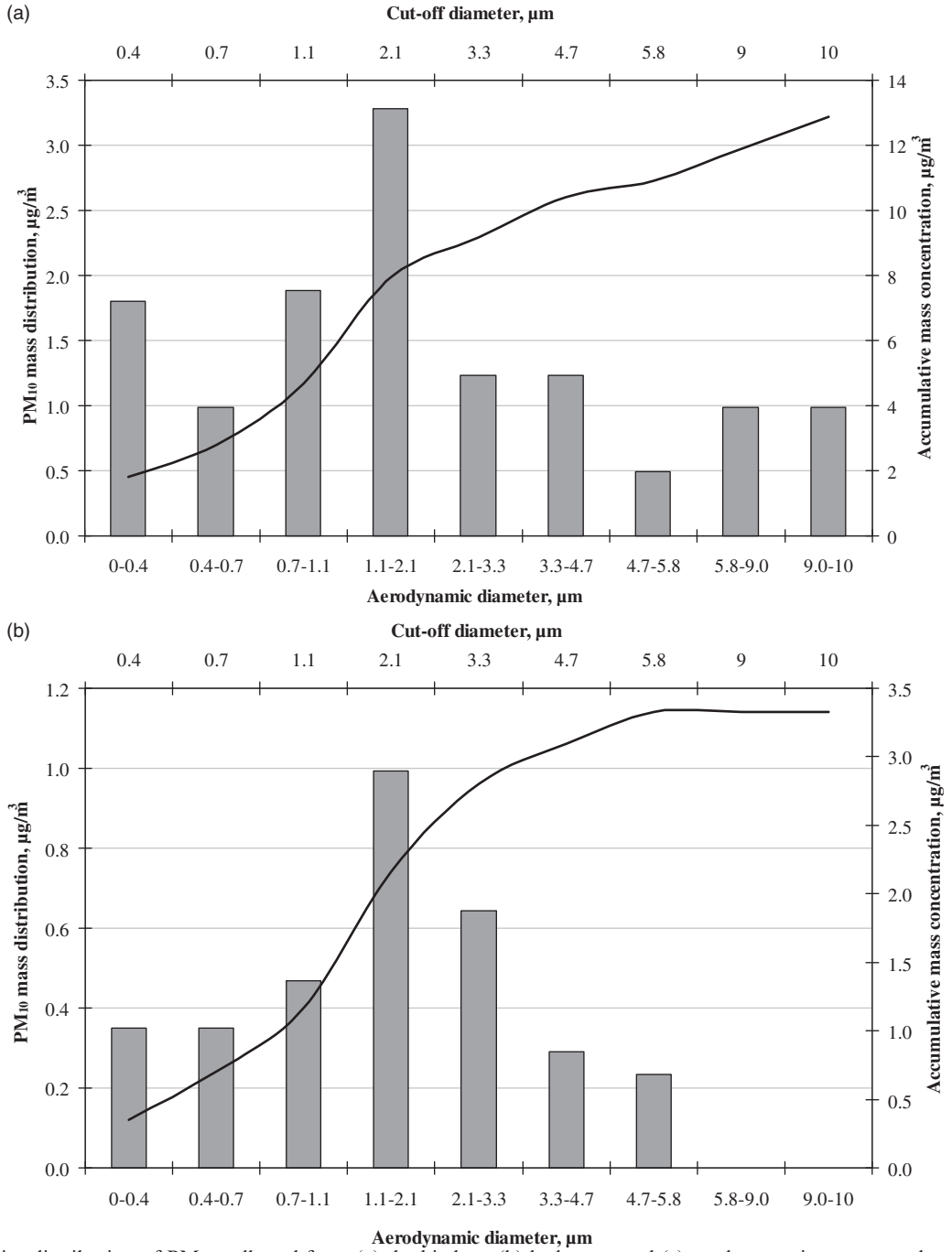

Fig. 5. Mass size distribution of PM_{10} collected from (a) the kitchen; (b) bedroom; and (c) outdoor environment at the rural Hathersage house – Case 1; and (d) the kitchen at the urban Sheffield flat – Case 3.

Figure 5(b) shows that the sampling conducted in the bedroom (Case 1) collected PM that had a normal particle size distribution. The concentrations of $PM_{2.5}$ and PM_{10} were 2.2 and 3.4 $\mu g \cdot m^{-3}$, respectively. The concentrations of PM in the outdoor environment at Case 1 were higher than indoors: outdoor concentrations of $PM_{2.5}$ and PM_{10} were 9.2 and 14.6 $\mu g \cdot m^{-3}$, respectively. From Figure 5(c), it can be observed that approximately 29% of the PM collected was in the sub-micron range. Particles in this size range had the highest concentration, whereas for the indoor environments, particles of 1.2–2.1 μm were most prominent.

Figure 5(d) presents the sampling conducted in the kitchen of an urban flat in Sheffield (Case 3). The concentrations of $PM_{2.5}$ and PM_{10} were 12 and 27.9 $\mu g \cdot m^{-3}$, respectively. It can be observed that the

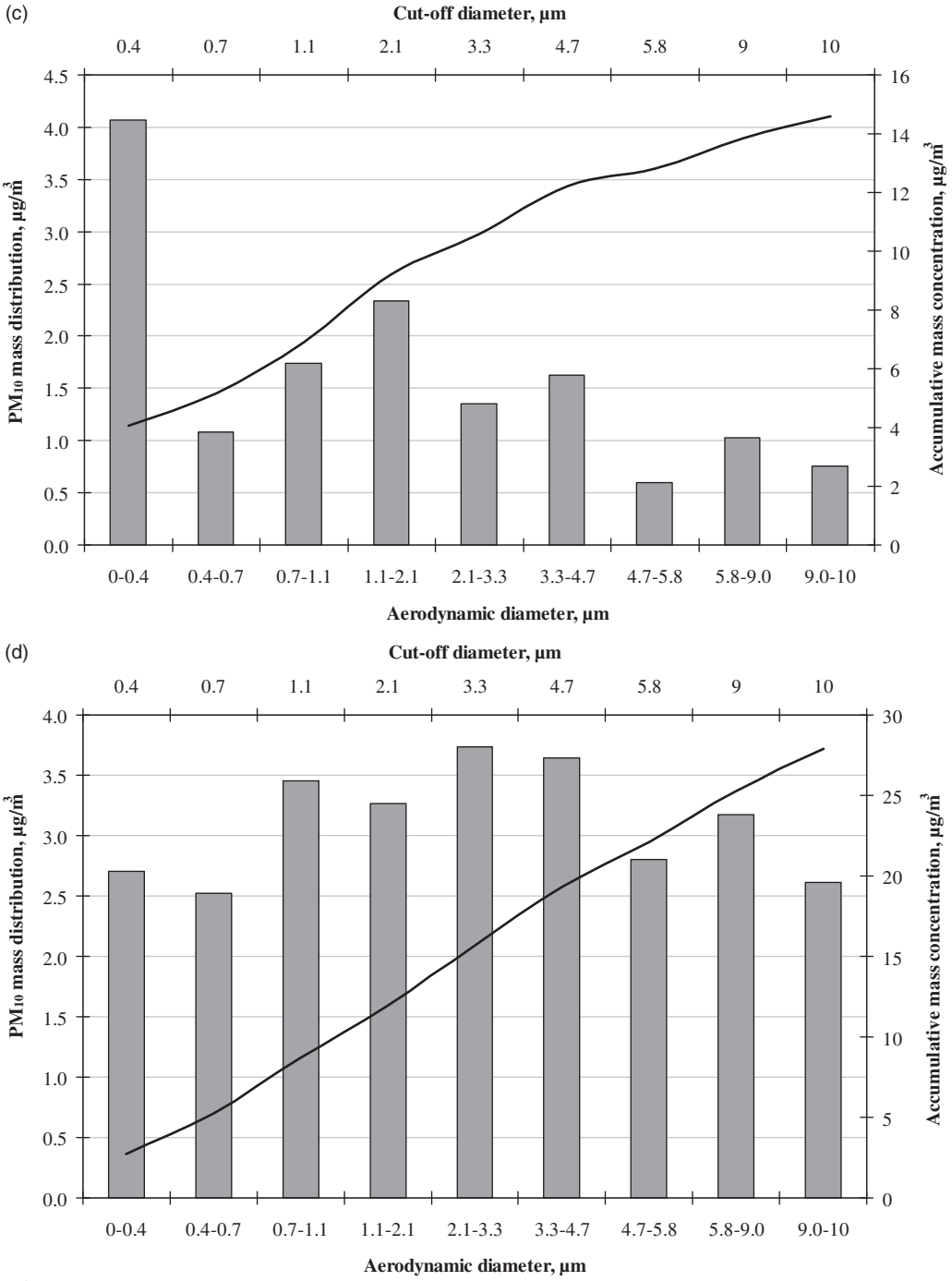

Fig. 5. Continued.

average amount of PM collected from each stage of the Andersen sampler was fairly even here. This is significantly different from Case 1, as the majority of the PM collected from both the kitchen and bedroom was within the range of 1.1–2.1 μm. The results obtained were expected, as larger particles would remain in the atmosphere only for a short period of time. The majority of these particles would arise from vehicles, including fuel combustion and from the wear of disc brakes and the vehicle body. Another possible source was the nearby cement plant.

Particle Composition

In addition to the size distribution, the composition of the particles collected was also analysed. Figure 6 presents the elemental composition of the particles collected from the kitchen, bedroom and outdoor environment for Case 1 and kitchen of Case 3. The PM_{10} samples from the bedroom were mainly composed of Fe, Na, Zn and S, which was attributed to mould or the ingression of pollutants from the outdoor environment. The analysis of the PM_{10} samples from the kitchen revealed that the particles contained high concentrations of B, Ca, Na and Si. These could have been generated from a range of different sources, including various cooking activities (such as the use of salt) or the ingression of pollutants from outdoor sources. The outdoor PM_{10} samples were mainly composed of S, Na and K, which are likely to be due to the road nearby (e.g. car exhaust and brake wear). As shown in Figure 6, the samples collected from the kitchen of Case 3 were mainly composed of Al, Na, Ca and Fe, with smaller amounts of Mg, Si, S and K, which could all be generated from either indoor or outdoor sources. Indoor sources may include cooking (like salt particles, burned food and particles from various cooking methods, like frying) and cleaning products, whilst outdoor sources are likely to be due to the nearby busy road.

Particle Morphology

Since the PM could originate from different sources, the PM_{10} collected possessed different structures and morphologies and thus had different chemical compositions. Figures 7 and 8 present the SEM/EDS analysis of various particles from the PM_{10} samples collected from Cases 1 and 3, respectively. The particle in Figure 7(a) is around 10 μm in length with a cubic shape and was common in this sample. The crystal was identified by EDS as NaCl, salt. The particle is likely to have been generated from cooking activities, since it was found in the kitchen; salt particles can easily melt due to high temperature cooking, which can then re-crystallise when the temperature has dropped. Particles of interest in Figure 7(b) are plate-like with smooth surfaces. They all vary in size, ranging from 4 μm to greater than 10 μm, and have irregular edges. EDS analysis on these gave high peaks of C and O, with moderate amounts of Mg and Si – the morphology of these particles suggest that they are skin flakes.

Particles A and B in Figure 7(c) are possibly of biological origin. The plate-like appearance of particle A

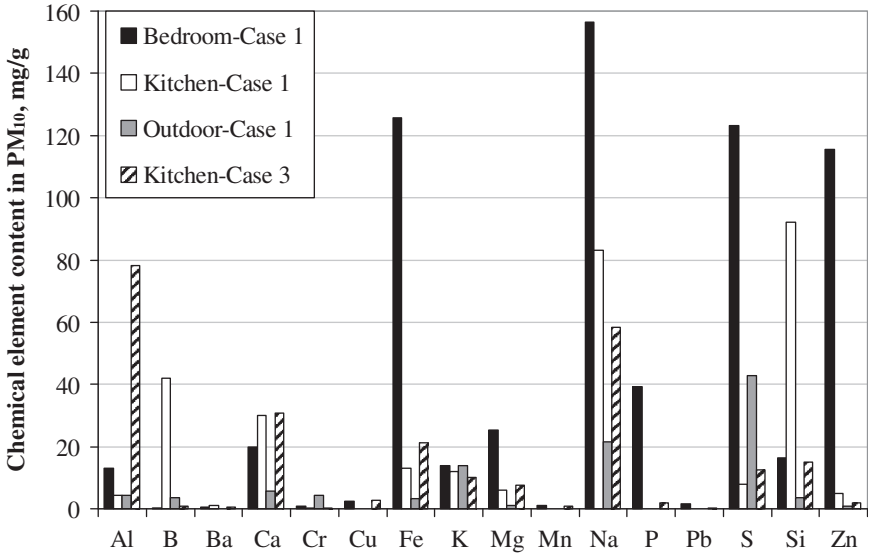

Fig. 6. Chemical composition of the PM_{10} samples collected from the bedroom, kitchen and the outdoor environment of the rural house – Case 1 and kitchen of Case 3 using ICP-OES.

suggests it is a skin flake [14]. Particle B is a form of microorganism, which could be an example of either a bacterium or an environmental microorganism known as biofilm [15]. Since this particle is approximately 7 μm in diameter, there is a possibility that it will penetrate into the human respiratory system, which could lead to detrimental health impacts. This particular biofilm particle was found to have high amounts of S and Cl, with moderate amounts of Ca and K. The cube-like particle shown in Figure 7(d) is 3–4 μm. Results from the EDS analysis gave a high count rate of C, O, Ca and S, thus it is likely that this is $CaSO_4$ crystal, which is abundant in the environment.

An example of the results of the SEM/EDS analysis for various particles from the PM_{10} samples collected from Case 3 is shown in Figure 8. As shown, the circled particle gave high count rates for both Na and Cl. This confirmed the visual observation that this particle was a salt crystal. This commonly arises from cooking activities. The EDS results obtained in this study are similar to those reported by other researchers [15].

Gas-Phase Emissions for all Three Case Study Environments

Measured Concentrations and Calculated Emission Rates of Carbon Monoxide

Figure 9 presents the real-time concentrations of indoor CO in the kitchens of the city-centre flat (Case 2) and the urban flat on a main road (Case 3). The measured CO concentrations for Case 1 were very low, fluctuating between 0.9 and 1.3 ppm. In order to investigate the effect of the gas-fired central heating system on the indoor CO concentration, the gas boiler at the rural house was turned on at the end of the testing period. It was found that the gas-fired heating system had no effect on the indoor CO concentration. This is to be expected since the flue gases from the boiler were discharged to the outdoor environment through well-insulated and sealed ducts and not released in or near the kitchen. Although no significant CO emission source existed in the kitchen of this rural house (Case 1), the average indoor CO concentration was still about 1.0 ppm. Based on this data and the air

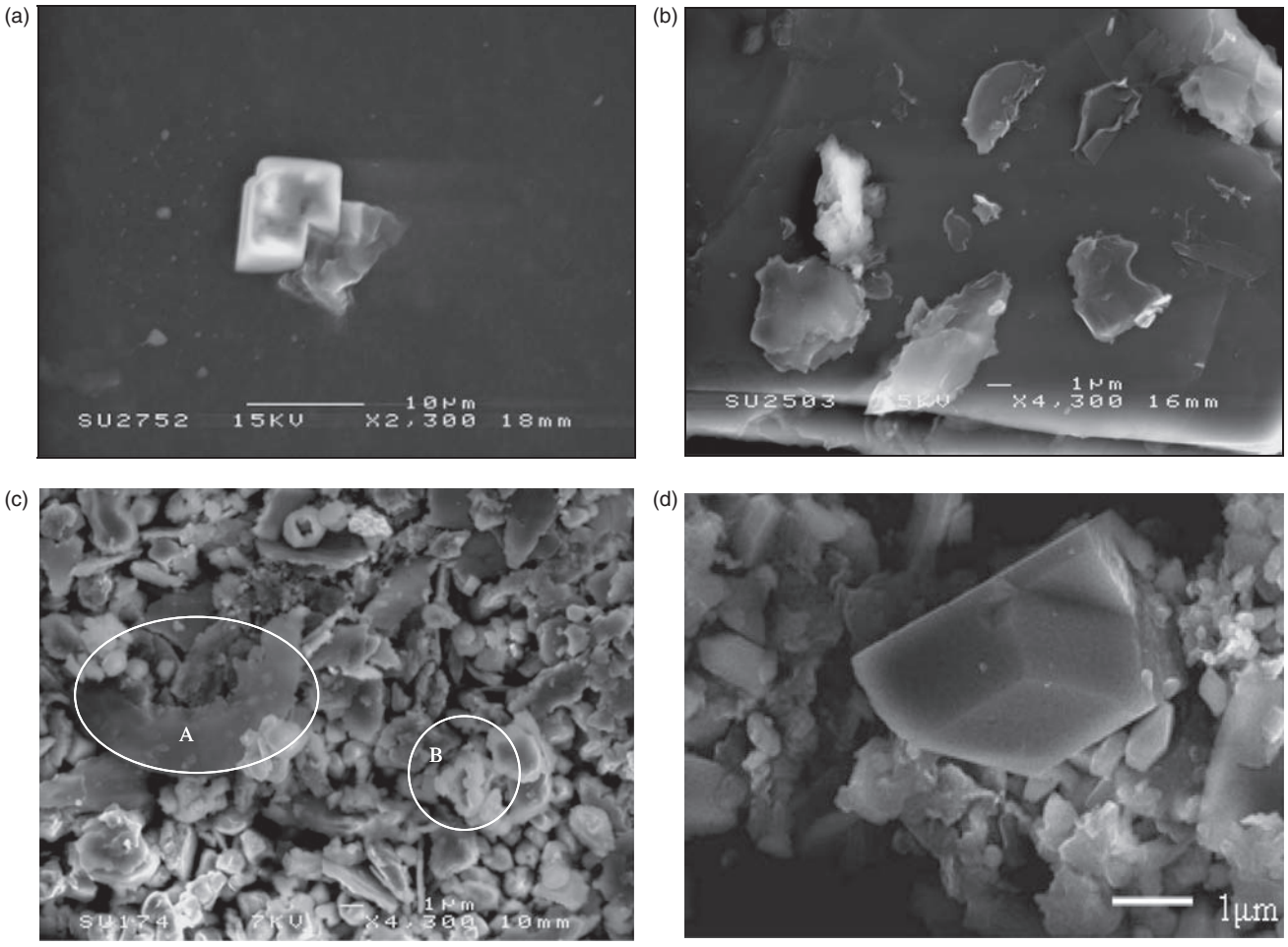

Fig. 7. Morphology of the PM collected from (a and b) the kitchen; (c) bedroom; and (d) the outdoor environment of rural house – Case 1.

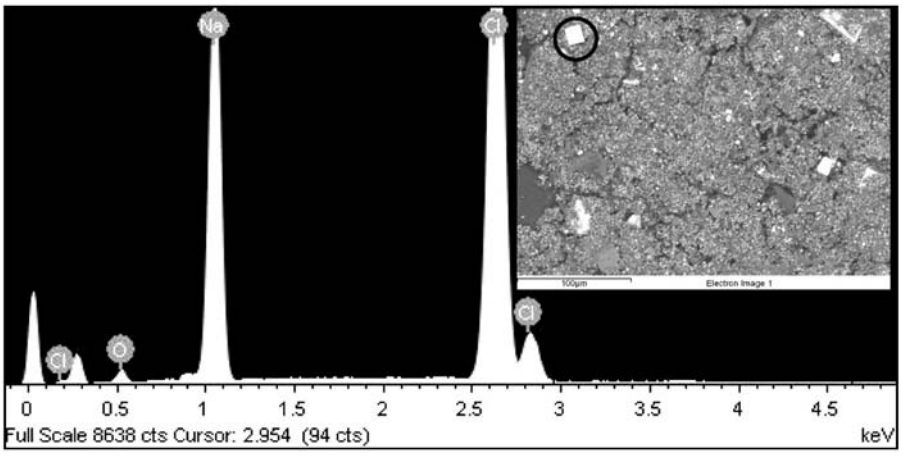

Fig. 8. An example of the EDS analysis of the PM collected from the kitchen of Case 3.

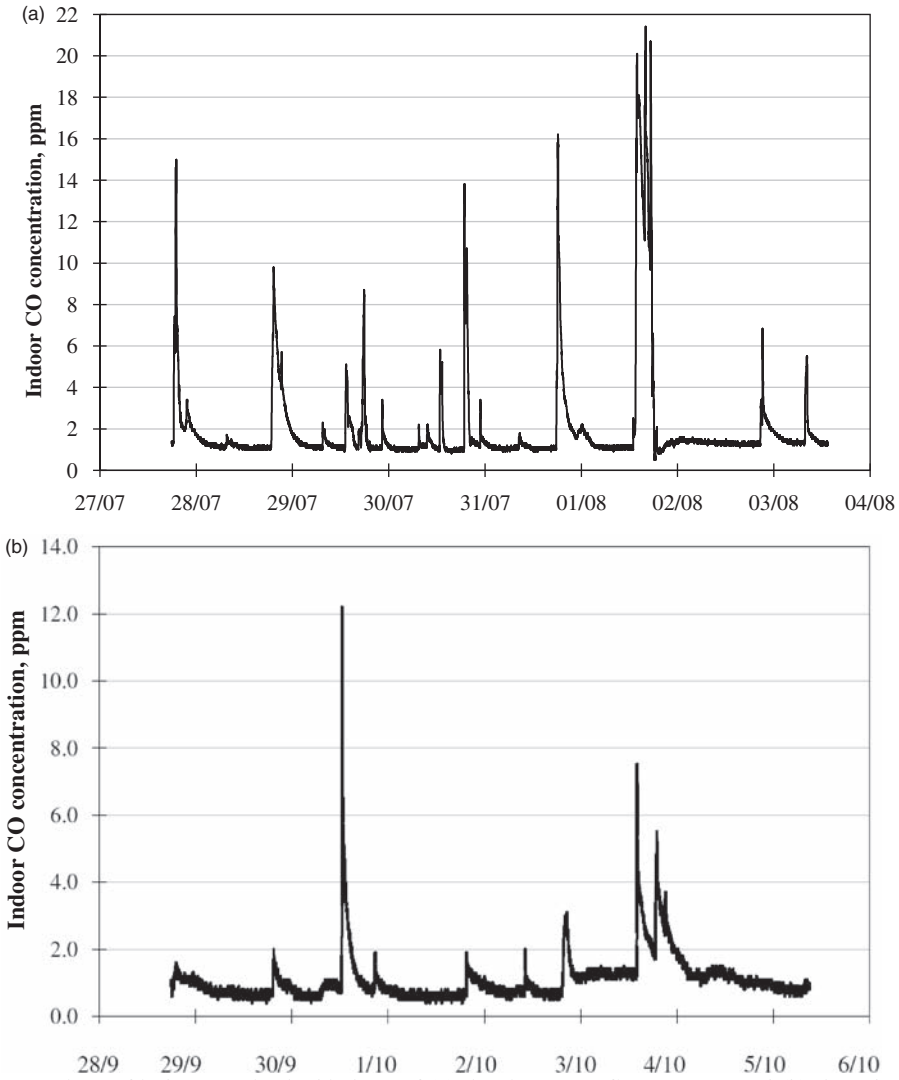

Fig. 9. Real-time concentrations of indoor CO in the kitchens of (a) the city-centre flat – Case 2 and (b) the urban flat on a main road – Case 3.

Table 1. Average indoor and outdoor concentrations and emission rates of carbon monoxide, nitrogen dioxide and total VOCs at the three study locations

	Case 1: rural house		Case 2: city-centre flat		Case 3: main road flat	
	Indoor	Outdoor	Indoor	Outdoor	Indoor	Outdoor
CO						
Average concentration (ppm)	1.0	–	2.0	–	1.1	–
Average emission rate ($g \cdot h^{-1}$)	0.1	–	0.1	–	0.1	–
NO_2						
Average concentration ($\mu g \cdot m^{-3}$)	10.2	10.8	47.1	14.7	20.7	23.4
Average emission rate ($mg \cdot h^{-1}$)	–	–	65.5	–	–	–
Σ*20 VOCs*						
Average concentration ($\mu g \cdot m^{-3}$)	221.5	42.6	430.7	65.4	49.7	32.6
Average emission rate ($mg \cdot h^{-1}$)	13.0	–	42.7	–	0.5	–

exchange rate calculated above, the average emission rate of CO in this kitchen was thus estimated to be $0.091\ g \cdot h^{-1}$ (Table 1). There was no difference in the CO levels recorded between the cooking periods and the non-cooking periods.

The real-time concentration of indoor CO in the kitchen of the city-centre flat (Case 2) is shown in Figure 9(a). CO spikes occurred whenever any cooking activity was conducted, thus the source of CO emissions would be the gas cooker used in the kitchen. The average indoor CO concentration during the entire monitoring period was 2 ppm, as presented in Table 1, though peaks of 14–22 ppm were recorded, as shown in Figure 9(a). The real-time concentration of indoor CO in the kitchen of Case 3 is presented in Figure 9(b). The average indoor CO concentration here was 1.1 ppm – lower than Case 2 and similar to Case 1 (as outlined in Table 1). The CO concentration reached the highest point during one of the cooking periods, at 12 ppm. Again, the source of CO emissions is the gas cooker used in the kitchen, as the spike coincided with a cooking episode. The gas boiler is unlikely to elevate indoor CO concentrations for two main reasons: (a) combustion is highly controlled and thus CO emissions are likely to be low and (b) it is a flued system so all combustion products are vented to the outdoor environment.

The outdoor CO concentrations at all the three sites were zero, as measured by the TSI IAQ-Calc 7545. This implies that the outdoor CO at these locations is rapidly dispersed, even at the Case 2 flat location in the city centre. As reported in the UK National Air Quality Archive, during the summer of 2009, the monthly average CO concentration in Sheffield city centre was only 0.2–0.3 ppm [16].

Figure 10(a) shows the variations in CO emission rates during several cooking periods in the kitchen of Case 2. The CO emissions were attributed to the presence and use of the gas cooker. During the entire measurement period, the average CO emission rate was $0.1\ g \cdot h^{-1}$ (Table 1). During cooking periods, however, the emission rates from the gas cooker ranged from 0.3 to $2.2\ g \cdot h^{-1}$ (i.e. 28.4–179.4 $\mu g \cdot kJ^{-1}$). These values are well within the range (9.9–243.8 $\mu g \cdot kJ^{-1}$) reported by Moschandreas et al. [9]. The CO emission rates obtained from range-top burners by Traynor et al. [8] were 200–226 $\mu g \cdot kJ^{-1}$, slightly higher than those for Case 2 in this study. Figure 10(b) shows the variations in CO emission rates during several cooking periods in the kitchen of Case 3 when the gas-fired cooker was being used. Again, the CO emissions were most likely due to the burning of the gas during cooking. The maximum CO emission rate was $0.5\ g \cdot h^{-1}$ (during one of the cooking periods), whereas the average emission rate for the whole monitoring period was $\sim 0.1\ g \cdot h^{-1}$ (Table 1).

Measured Concentrations and Calculated Emission Rates of 'Oxides of Nitrogen'

As given in Table 1, the indoor and outdoor NO_2 concentrations were almost identical in the rural area (Case 1), since there was no significant source of indoor NO_2. The NO_2 concentrations inside the city-centre flat (Case 2) were 3.5 times higher than the outdoor values – $47\ \mu g \cdot m^{-3}$ compared to $15\ \mu g \cdot m^{-3}$. This can be attributed to the use of a gas cooker in the flat. The outdoor NO_2 concentration for Case 3, the flat on a main road, was $23\ \mu g \cdot m^{-3}$, slightly higher than the indoor value at this location ($21\ \mu g \cdot m^{-3}$). Both the indoor and outdoor NO_2 concentrations measured here were higher than the values obtained for Case 1. Compared to Case 2 however, whilst the indoor concentrations was significantly lower, the outdoor concentrations of NO_2 was in fact slightly higher. The NO_2 emissions in the

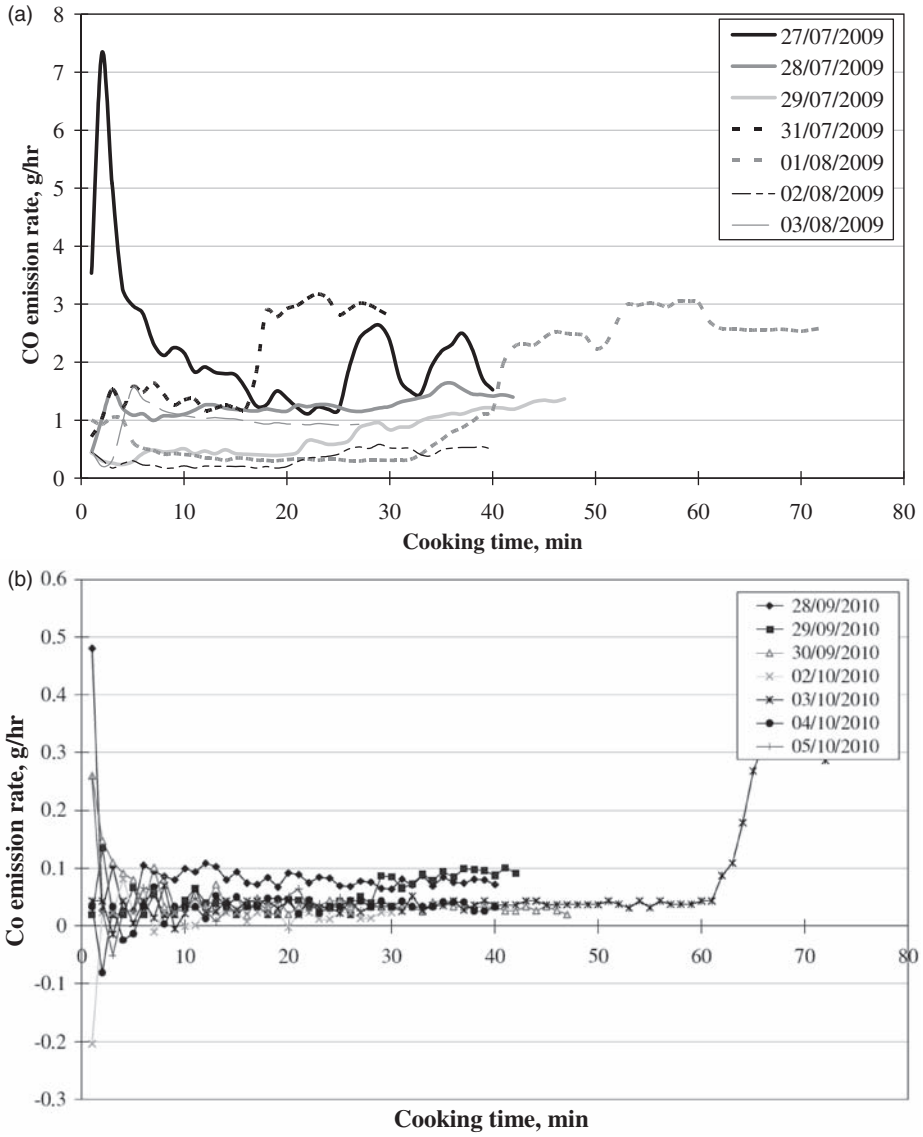

Fig. 10. CO emission rates during the cooking events in the kitchen of (a) the city-centre flat – Case 2 and (b) the urban flat on a main road – Case 3.

kitchen of the city-centre flat could be attributed to gas combustion (gas-fuelled cooker). As observed from Table 1, the emission rate of NO_2 at this property was 65.5 mg·h^{-1} (or 5.42 μg·kJ^{-1}), which was calculated from the measured NO_2 concentrations during cooking and the air exchange rate for this kitchen. This value is very similar to the results of NO_2 emission rates (4.98–7.03 μg·kJ^{-1}) obtained by Traynor et al. [8].

Measured Concentrations and Calculated Emission Rates of 'Volatile Organic Compounds'

Table 1 also presents the indoor and outdoor concentrations and emission rates of Σ20 VOCs – the sum of the top 20 VOCs obtained from the analysis of the Tenax TA tubes deployed at the three residential environments. At all the three sites, the indoor Σ20 VOCs concentrations were notably higher than the outdoor concentrations, considerably so for Cases 1 and 2, as shown. These results were expected since any high outdoor Σ20 VOCs concentrations will be rapidly dispersed and diluted in the outdoor environment. The higher indoor Σ20 VOCs concentrations at these two locations resulted in much higher VOC emissions rates for Cases 1 and 2 compared to Case 3. The small increase in indoor VOC levels at the flat on a main road (50 μg·m^{-3}) compared to the outdoor concentration (33 μg·m^{-3}) meant that the emission rate here was

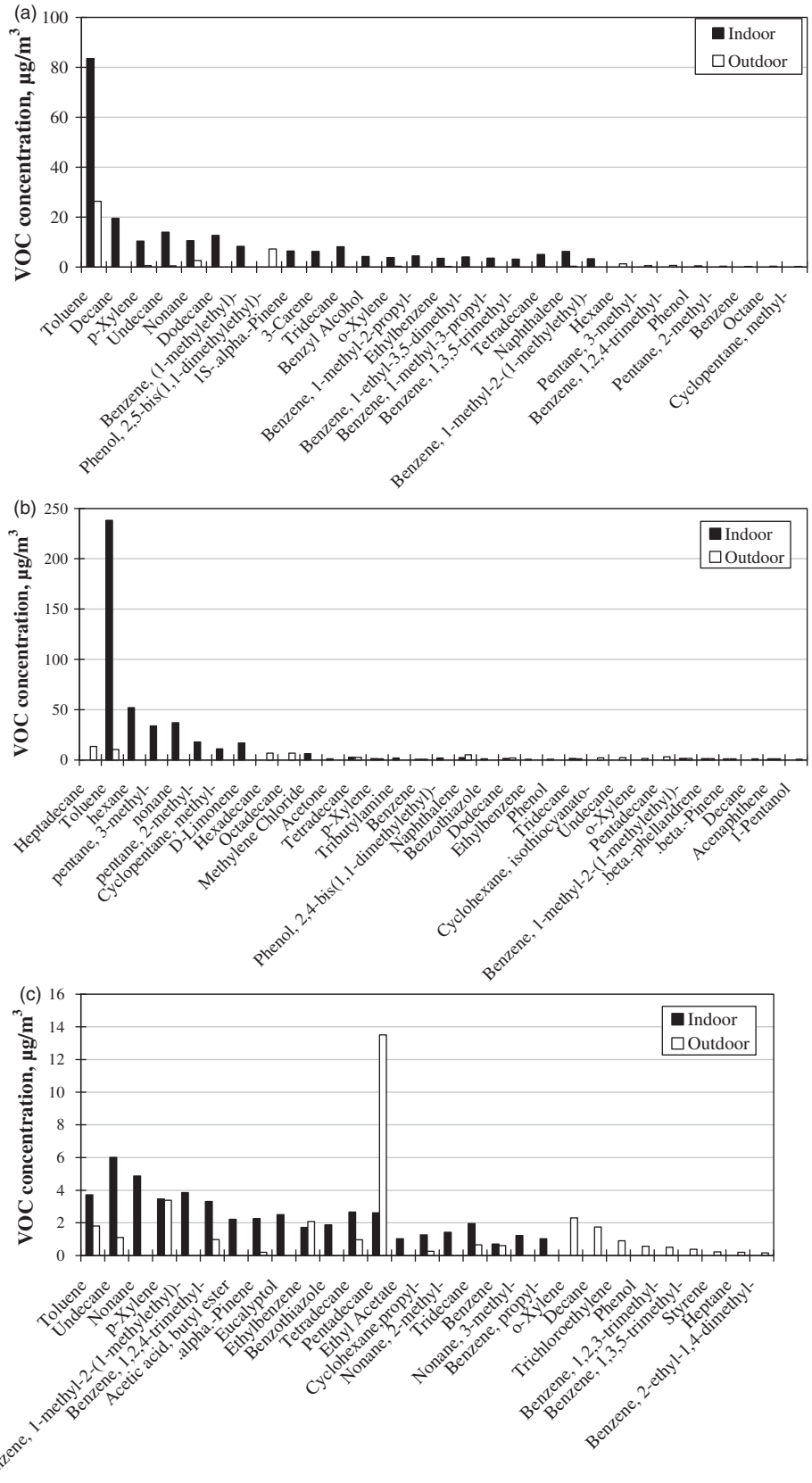

Fig. 11. Top 20 VOCs in the samples taken from indoor and outdoor environments at (a) the rural house – Case 1; (b) city flat – Case 2; and (c) urban flat on a main road in Sheffield – Case 3.

very low, just 0.5 mg·h^{-1} (Table 1). The reason for the elevated Σ20 VOCs concentration in the city-centre flat (Case 2) is most likely to be due to the difference in cooking styles, as well as subtle differences in the gas cookers used; emission rates of around 43 mg·h^{-1} were calculated for such species here. The possible sources of these indoor VOCs include combustion by-products (gas stoves) and cooking activities (emissions from food), as well as cleaning products and the various construction materials used in the buildings.

The top 20 VOCs found at Cases 1, 2 and 3 are shown in Figure 11. Toluene was by far the most common VOC to be found in the indoor environment for both Cases 1 and 2: concentrations of this aromatic hydrocarbon reached over 80 μg·m^{-3} at the rural house (Case 1), whereas levels exceeded 200 μg·m^{-3} inside the city-centre flat (Case 2). This was also one of the most common VOCs found in the outdoor environment at Case 1. Undecane and pentadecane appeared to be the most common VOCs found in the indoor and outdoor environment of Case 3, respectively. Undecane reached indoor levels of 6 μg·m^{-3}, whereas pentadecane exceeded 12 μg·m^{-3} in the outdoor environment. A number of other hydrocarbons were also found – mainly alkanes, such as decane, nonane and hexane.

Conclusions

This investigation into indoor air pollutants in different residential buildings has shown that there are variations in both the gaseous and solid-phase emissions in the indoor and outdoor environments, as illustrated by the three case studies presented herein. The main conclusions from this experimental work are as follows:

- PM collected from the indoor environment of the rural house were mostly composed of small particles <2.5 μm; those from the outdoor environment tended to be sub-micron in size (<0.5 μm). Most particles were therefore within the respirable size range and thus could have detrimental health implications if inhaled.
- The elemental analysis of the PM_{10} samples revealed high metal concentrations (Fe, Na and Zn), whilst SEM/EDS analysis identified the particles as salt crystals, mineral fibres, skin flakes, dust fragments, biofilms, bacteria and mould fungus spores.
- Cooking activities directly contributed to $PM_{2.5}$ emissions.
- Background CO concentrations were low at 1–2 ppm in all three cases, although CO levels during cooking became elevated in the kitchens with the gas cookers (Cases 2 and 3); peaking at 10–20 ppm. CO emission rates from the gas cookers were 0.3–2.0 g·h^{-1}.
- Gas cookers were also found to be a significant source of NO_2 and thus the indoor concentration was much greater than the outdoor levels (47 μg·m^{-3} compared to 15 μg·m^{-3}); indoor emission rates peaked at 65.5 mg·h^{-1}.
- VOC concentrations were consistently higher in the indoor environments at all locations compared to outdoor levels.

This study has clearly demonstrated that the indoor air quality in kitchens using gas cookers is generally poorer than those using electric cookers – most noticeably in terms of particles, NO_2 and CO. Furthermore, these pollutants can migrate through the rest of the residential environment.

Acknowledgement

The authors thank the UK Engineering and Physical Sciences Research Council (EPSRC PUrE Intrawise Consortium (grant reference no.: EP/F007132/1): Pollutants in the Urban Environment – Integrated Framework for Improving Sustainability of the Indoor Environment) for their financial and technical support for this research study.

References

1 Parra MA, Elustondo D, Bermejo R, Santamaria JM: Quantification of indoor and outdoor volatile organic compounds (VOCs) in pubs and cafes in Pamplona, Spain: Atmos Environ 2008;42:6647–6654.
2 Kumar A, Kumar R: Indoor air pollution. Available at: pollutionissues.com/Ho-Li/Indoor-Air-Pollution.html (accessed February 2009).
3 Wang S, Ang HM, Tade MO: Volatile organic compounds in indoor environment and photo-catalytic oxidation: State of the art: Environ Int 2007;33:694–705.
4 US Environmental Protection Agency: The inside story: a guide to indoor air quality. Available at: epa.gov/iaq/pubs/insidest.html (accessed June 2011).
5 Agelopoulos NG, Pickett JA, Wadhams LJ, Woodcock CM: Flower emissions of oilseed rape: Final Project Report, Ministry of Agriculture, Fisheries and Food, 2000.
6 Godish T: Indoor Environmental Quality. Boca Raton, FL: CRC Press LLC, 2001.
7 Yamanaka S, Hirose H, Takada S: Nitrogen oxides emissions from domestic kerosene-fired and gas-fired appliances: Atmos Environ 1979;13:407–412.
8 Traynor GW, Anthon DW, Hollowell CD: Technique for determining pollutant emissions from a gas-fired range: Atmos Environ 1982;16:2979–2987.

9 Moschandreas DJ, Relwani SM, Billick IH, Macriss RA: Emission rates from range-top burners – assessment of measurement methods: Atmos Environ 1987;21:285–289.
10 Targa J, Loader A: Diffusion tubes for ambient NO_2 monitoring: Practical guidance for laboratories and users: Report to UK Department for Environment, Food & Rural Affairs and the Devolved Administrations, 2008.
11 ISO 12569:2001: Thermal performance of buildings–determination of air change in buildings–tracer gas dilution method, International Organization for Standardisation, Geneva, 2000.
12 Wallace LA, Emmerich SJ, Howard-Reed C: Source strength of ultrafine and fine particles due to cooking with a gas stove: Environ Sci Technol 2004;38:2304–2311.
13 Lai ACK, Ho YW: Spatial concentration variation of cooking-emitted particles in a residential kitchen: Build Environ 2008;43:871–876.
14 Conner TL, Williams RW: Identification of possible sources of particulate matter in the personal cloud using SEM/EDX: Atmos Environ 2004;38:5305–5310.
15 Chung W, Sharifi VN, Swithenbank J, Ossamor O, Nolan A: Characterisation of airborne particulate matter in a city environment: Mod Appl Sci 2008;2:17–32.
16 AEA Energy & Environment: UK national air quality archive: Report to UK Department for Environment, Food & Rural Affairs and the Devolved Administrations, 2009.

Appendix II

GUIDELINE VALUES FOR ORGANIC CHEMICALS IN INDOOR AIR (INDUSTRIAL AND NON-INDUSTRIAL SETTINGS)

(Charles et al., 2005)

#	Substances	CAS #	ACGIH [1] mg/m³	OSHA [2] mg/m³	OEHHA [3] mg/m³	WHO [4] mg/m³	Japan [5] mg/m³	HK [6] mg/m³	Germany [7] mg/m³
1	Acetaldehyde	75-07-0	(C)45	360	0.009	0.05 [1 yr]	0.048		
2	Acetic acid	64-19-7	25	25					
3	Acetic anhydride	108-24-7	21	20					
4	Acetone	67-64-1	1188	2400		n.p.			
5	Acetone cyanohydrin	75-86-5	(C)5						
6	Acetonitrile	75-05-8	34	70					
7	2-Acetylaminofluorene	53-96-3		Carcinogen					
8	Acetophenone	98-86-2	49						
9	Acetylene	74-86-2	207640						
10	Acetylene tetrabromide	79-27-6	14	14					
11	Acetylsalicylic acid	50-78-2	5						
12	Acrolein	107-02-8	(C)0.23	0.3	0.00006	0.05 [30 min]			
13	Acrylamide	79-06-1	0.03	0.3					
14	Acrylic acid	79-10-7	6						
15	Acrylonitrile	107-13-1	4	4	0.005				
16	Adipic acid	124-04-9	5						
17	Adiponitrile	111-69-3	9						
18	Aldrin	309-00-2	0.3	0.3					
19	Allyl alcohol	107-18-6	1	5					
20	Allyl chloride	107-05-1	3	3					
21	Allyl glycidyl ether	106-92-3	5	(C)45					
22	Allyl propyl disulfide	2179-59-1	3	12					
23	4-Aminodiphenyl	92-67-1	A1	Carcinogen					
24	2-Aminopyridine	504-29-0	2	2					
25	Amitrole	61-82-5	0.2						
26	Ammonium perfluorooctanoate	3825-26-1	0.01						
27	tert-Amyl methyl ether [TAME]	994-05-8	84						
28	Aniline	62-53-3	8	19					
29	o-Anisidine	90-04-0	0.5	0.5					
30	p-Anisidine	104-94-9	0.5	0.5					
31	ANTU	86-88-4	0.3	0.3					
32	Arsenic, organic compounds (as As)	7440-38-2		0.5					
33	Atrazine	1912-24-9	5						
34	Azinphos-methyl	86-50-0	0.2	0.2					
35	Benz[a]anthracene	56-55-3	A2						
36	Benzene	71-43-2	2	32	0.06	n.v.		0.0161	
37	Benzidine	92-87-5	A1	Carcinogen					
38	Benzo[b]fluoranthene	205-99-2	A2						
39	Benzo[a]pyrene	50-32-8	A2						
40	Benzotrichloride	98-07-7	0.8						
41	Benzoyl chloride	98-88-4	(C)3						
42	Benzoyl peroxide	94-36-0	5	5					
43	Benzyl acetate	140-11-4	61						
44	Benzyl chloride	100-44-7	5	5					
45	Biphenyl	92-52-4	1	1					
46	Bis(2-dimethylaminoethyl) ether [DMAEE]	3033-62-3	0.3						
47	Bromacil	314-40-9	10						

#	Substances	CAS #	ACGIH [1] mg/m³	OSHA [2] mg/m³	OEHHA [3] mg/m³	WHO [4] mg/m³	Japan [5] mg/m³	HK [6] mg/m³	Germany [7] mg/m³
48	1,3-Butadiene	106-99-0	4	2	0.02				
49	Butane	106-97-8	2378						
50	n-Butanol	71-36-3	61	300					
51	see-Butanol	78-92-2	303	450					
52	tert-Butanol	75-65-0	303	300					
53	2-Butoxyethanol	111-76-2	97	240		13.1 [1 wk]			
54	2-Butoxyethyl acetate	112-07-2	131						
55	n-Butyl acetate	123-86-4	713	710					
56	see-Butyl acetate	105-46-4	951	950					
57	tert-Butyl acetate	540-88-5	951	950					
58	n-Butyl acrylate	141-32-2	10						
59	n-Butylamine	109-73-9	(C)15	(C)15					
60	Butylated hydroxytoluene [BHT]	128-37-0	2						
61	tert-Butyl chromate (as CrO3)	1189-85-1	(C)0.1	(C)0.1					
62	n-Butyl glycidyl ether [BGE]	2426-08-6	133	270					
63	n-Butyllactate	138-22-7	30						
64	n-Butyl mercaptan	109-79-5	2	35					
65	o-sec-Butylphenol	89-72-5	31						
66	p-tert-Butyltoluene	98-51-1	6	60					
67	Camphor - Synthetic	76-22-2	12	2					
68	Caprolactam	105-60-2	5						
69	Captafol	2425-06-1	0.1						
70	Captan	133-06-2	5						
71	Carbaryl	63-25-2	5	5					
72	Carbofuran	1563-66-2	0.1						
73	delta-3-Carene [3,7,7-Trimethyl bicyclohep-3-ene]	13466-78-9	112						
74	Catechol	120-80-9	23						
75	Chlordane	57-74-9	0.5	0.5					
76	Chlorinated camphene	8001-35-2	0.5	0.5					
77	o-Chlorinated diphenyl oxide	31242-93-0	0.5						
78	Chloroacetaldehyde	107-20-0	(C)3	(C)3					
79	Chloroacetone	78-95-5	(C)4						
80	2-Chloroacetophenone	532-27-4	0.3	0.3					
81	Chloroacetyl chloride	79-04-9	0.2						
82	Chlorobenzene	108-90-7	46	350	1	0.5 [1 yr]			
83	o-Chlorobenzylidene malononitrile	2698-41-1	(C)0.4	0.4					
84	Chlorobromomethane	74-97-5	1059	1050					
85	Chlorodifluoromethane [FC-2]	75-45-6	3539						
86	Chlorodiphenyl (42% chloride)	53469-21-9	1	1					
87	Chlorodiphenyl (54% chloride)	11097-69-1	0.5	0.5					
88	Chloroform	67-66-3	49	(C)240	0.3			0.163	
89	bis(Chloromethyl) ether	542-88-1	0.005	Carcinogen					
90	Chloromethyl methyl ether	107-30-2	A2	Carcinogen					

#	Substances	CAS #	ACGIH [1] mg/m³	OSHA [2] mg/m³	OEHHA [3] mg/m³	WHO [4] mg/m³	Japan [5] mg/m³	HK [6] mg/m³	Germany [7] mg/m³
91	1-Chloro-1-nitropropane	600-25-9	10	100					
92	Chloropentafluoroethane	76-15-3	6321						
93	Chloropicrin	76-06-2	0.7	0.7	0.0004				
94	beta-Chloroprene	126-99-8	36	90					
95	1-Chloro-2-propanol	127-00-4	4						
96	2-Chloro-1-propanol	78-89-7	4						
97	2-Chloropropionlc acid	598-78-7	0.4						
98	o-Chlorostyrene	2039-87-4	284						
99	o-Chlorotoluene	95-49-8	259						
100	Chlorpyrifos	2921-88-2	0.1				0.0001 (children), 0.001 (others)		
101	Chrysene	218-01-9	A3						
102	Clopidol	2971-90-6	10						
103	o-Cresol	95-48-7	22						
104	m-Cresol	108-39-4	22						
105	p-Cresol	106-44-5	22						
106	Cresol - Mixture of isomers	1319-77-3	22	22	0.6				
107	Crotonaldehyde	4170-30-3	(C)0.9	6					
108	Crufomate	299-86-5	5						
109	Cumene	98-82-8	246	245					
110	Cyanamide	420-04-2	2						
111	Cyanogen	460-19-5	21						
112	Cyanogen chloride	506-77-4	(C)0.8						
113	Cyclohexane	110-82-7	344	1050					
114	Cyclohexanol	108-93-0	205	200					
115	Cyclohexanone	108-94-1	80	200					
116	Cyclohexene	110-83-8	1008	1015					
117	Cyclohexylamine	108-91-8	41						
118	Cyclonite	121-82-4	0.5						
119	Cyclopentadiene	542-92-7	203	200					
120	Cyclopentane	287-92-3	1722						
121	Cyhexatin	13121-70-5	5						
122	2,4-D [2,4-Dichlorophenoxyacetic acid	94-75-7	10	10					
123	DDT [Dichlorodiphenyltrichloroethane]	50-29-3	1	1					
124	Demeton	8065-48-3	0.05	0.1					
125	Demeton-S-methyl	919-86-8	0.05						
126	Diacetone alcohol	123-42-2	238	240					
127	Diazinon	333-41-5	0.01				0.00029		
128	Diazomethane	334-88-3	0.3	0.4					
129	1,2-Dibromo-3-chloropropane (DBCP)	96-12-8		0.010					
130	2-N-Dibutylaminoethanol	102-81-8	4						
131	Dibutyl phenyl phosphate	2528-36-1	4						
132	Dibutyl phosphate	107-66-4	9	5					
133	Dibutyl phthalate	84-74-2	5	5			0.22		
134	Dichloroacetylene	7572-29-4	(C)0.4						

#	Substances	CAS #	ACGIH [1] mg/m³	OSHA [2] mg/m³	OEHHA [3] mg/m³	WHO [4] mg/m³	Japan [5] mg/m³	HK [6] mg/m³	Germany [7] mg/m³
135	o-Dichlorobenzene	95-50-1	150	(C)300				0.5	
136	p-Dichlorobenzene	106-46-7	60	450	0.8	1 [1 yr]	0.24	0.2	
137	3,3' -Dichlorobenzidine	91-94-1	A3	Carcinogen					
138	1,4-Dichloro-2-butene	764-41-0	0.03						
139	Dichlorodifluoromethane [FC-12]	75-71-8	4948	4950					
140	1,3-Dichloro-5,5-dimethyl hydantoin	118-52-5	0.2	0.2					
141	1,1-Dichloroethane	75-34-3	405	400					
142	1,2-Dichloroethylene, cis-isomer	156-59-2	794						
143	1,2-Dichloroethylene, sym-isomer	540-59-0	794	790					
144	1,2-Dichloroethylene, trans-isomer	156-60-5	794						
145	Dichloroethyl ether	111-44-4	29	(C)90					
146	Dichlorofluoromethane [FC-21]	75-43-4	42	4200					
147	Dichloromethane	75-09-2	174	87	0.4	3 [24 hr]			2 / 0.2 [24 h]*
148	1,1-Dichloro-1-nitroethane	594-72-9	12	(C)60					
149	1,3-Dichloropropene	542-75-6	5						
150	2,2-Dichloropropionic acid	75-99-0	5						
151	Dichlorotetrafluoroethane [Cryofluorane]	76-14-2	6995	7000					
152	Dichlorvos [DDVP]	62-73-7	0.1	1					
153	Dicrotophos	141-66-2	0.05						
154	Dicyclopentadiene	77-73-6	27						
155	Dieldrin	60-57-1	0.3	0.3					
156	Diesel fuel - Vapor & aerosol	68334-30-5	100						
157	Diesel fuel No.2 - Vapor & aerosol	68476-34-6	100						
158	Diesel fuel No.4 (Marine disel) - Vapour & Aerosol	77650-28-3	100						
159	Diethanolamine	111-42-2	2		0.003				
160	Diethylamine	109-89-7	15	75					
161	2-Diethylaminoethanol	100-37-8	10	50					
162	Diethylene triamine	111-40-0	4						
163	Di(2-ethylhexyl)phthalate [DEHP]	117-81-7	5	5			0.12		
164	Diethyl ketone	96-22-0	705						
165	Diethyl phthalate	84-66-2	5						
166	Difluorodibromomethane	75-61-6	859	860					
167	Diglycidyl ether [DGE]	2238-07-5	0.5	(C)2.8					
168	Diisobutyl ketone	108-83-8	146	290					
169	Diisopropylamine	108-18-9	21	20					
170	N,N-Dimethylacetamide	127-19-5	36	35					
171	Dimethylamine	124-40-3	9	18					
172	Dimethylaniline	121-69-7	25	25					
173	4-Dimethylaminoazo-benzene	60-11-7		Carcinogen					
174	2,2-Dimethylbutane	75-83-2	1763						
175	2,3-Dimethylbutane	79-29-8	1763						

#	Substances	CAS #	ACGIH [1] mg/m³	OSHA [2] mg/m³	OEHHA [3] mg/m³	WHO [4] mg/m³	Japan [5] mg/m³	HK [6] mg/m³	Germany [7] mg/m³
176	Dimethyl carbamoyl chloride	79-44-7	A2						
177	Dimethylethoxysilane	14857-34-2	2						
178	Dimethylformamide	68-12-2	30	30	0.08				
179	1,1-Dimethylhydrazine	57-14-7	0.02	1					
180	Dimethyl phthalate	131-11-3	5	5					
181	Dimethyl sulfate	77-78-1	0.5	5					
182	Dimethyl sulfide	75-18-3	25						
183	Dinitolmide	148-01-6	5						
184	o-Dinitrobenzene	528-29-0	1	1					
185	m-Dinitrobenzene	99-65-0	1	1					
186	p-Dinitrobenzene	100-25-4	1	1					
187	Dinitro-o-cresol	534-52-1	0.2	0.2					
188	Dinitrotoluene	25321-14-6	0.2	2					
189	1,4-Dioxane	123-91-1	72	360	3				
190	Dioxathion	78-34-2	0.1						
191	1,3-Dioxolane	646-06-0	61						
192	Diphenylamine	122-39-4	10						
193	Dipropyl ketone	123-19-3	234						
194	Diquat	2764-72-9	0.5						
195	Diquat	2764-72-9	0.1						
196	Disulfiram	97-77-8	2						
197	Disulfoton	298-04-4	0.05						
198	Diuron	330-54-1	10						
199	Divinyl benzene	1321-74-0	53						
200	Dodecyl mercaptan	112-55-0	0.8						
201	Endosulfan	115-29-7	0.1						
202	Endrin	72-20-8	0.1	0.1					
203	Enflurane	13838-16-9	566						
204	Epichlorohydrin	106-89-8	2	19	0.003				
205	EPN	2104-64-5	0.1	0.5					
206	Epoxybutane (1,2-)	106-88-7			0.02				
207	Ethane	74-84-0	1231						
208	Ethanol	64-17-5	1885	1900					
209	Ethanolamine	141-43-5	7	6					
210	Ethion	563-12-2	0.05						
211	2-Ethoxyethanol [EGEE]	110-80-5	18	740	0.07	n.p.			
212	2-Ethoxyethyl acetate [EGEEA]	111-15-9	27	540	0.3	n.p.			
213	Ethyl acetate	141-78-6	1442	1400					
214	Ethyl acrylate	140-88-5	20	100					
215	Ethylamine	75-04-7	9	18					
216	Ethyl amyl ketone	541-85-5	131	130					
217	Ethyl benzene	100-41-4	434	435	2	22 [1 yr]	3.8	1.447	
218	Ethyl bromide	74-96-4	22	890					
219	Ethyl tert-butyl ether [ETBE]	637-92-3	21						
220	Ethyl butyl ketone	106-35-4	234	230					
221	Ethyl chloride	75-00-3	264	2600	30				
222	Ethyl cyanoacrylate	7085-85-0	1						
223	Ethylene	74-85-1	223441						
224	Ethylene chlorohydrin	107-07-3	(C)3	16					
225	Ethylenediamine	107-15-3	25	25					
226	Ethylene dibromide	106-93-4	A3		0.0008				

#	Substances	CAS #	ACGIH [1] mg/m³	OSHA [2] mg/m³	OEHHA [3] mg/m³	WHO [4] mg/m³	Japan [5] mg/m³	HK [6] mg/m³	Germany [7] mg/m³
227	Ethylene dichloride	107-06-2	41		0.4				
228	Ethylene glycol - Aerosol	107-21-1	(C)100		0.4				
229	Ethylene glycol dinitrate [EGDN]	628-96-6	0.3	(C)1					
230	Ethylene oxide	75-21-8	2	2	0.03				
231	Ethylenimine	151-56-4	0.9	Carcinogen					
232	Ethyl ether	60-29-7	1213	1200					
233	Ethyl formate	109-94-4	303	300					
234	2-Ethylhexanoic acid	149-57-5	5						
235	Ethylidene norbornene	16219-75-3	(C)25						
236	Ethyl mercaptan	75-08-1	1	(C)25					
237	N-Ethylmorpholine	100-74-3	24	94					
238	Ethyl silicate	78-10-4	85	850					
239	Fenamiphos	22224-92-6	0.1						
240	Fensulfothion	115-90-2	0.1						
241	Fenthion	55-38-9	0.2						
242	Ferbam	14484-64-1	10						
243	Fenobucarb	3766-81-2					0.033		
244	Fonofos	944-22-9	0.1						
245	Formaldehyde	50-00-0	(C)0.4	0.9	0.003	0.1 [30 min]	0.1		
246	Formamide	75-12-7	18						
247	Formic acid	64-18-6	9	9					
248	Fuel oil No.2 - Vapor & aerosol	68476-30-2	100						
249	Fuel oil No.4 - Vapor & aerosol	68476-31-3	100						
250	Furfural	98-01-1	8	20					
251	Furfuryl alcohol	98-00-0	40	200					
252	Gasoline - Bulk handling	86290-81-5	300 ppm						
253	Glutaraldehyde	111-30-8	(C)0.2		0.00008				
254	Glycidol	556-52-5	6	150					
255	Glyoxal	107-22-2	0.1						
256	Halothane	151-67-7	404						
257	Heptachlor	76-44-8	0.05	0.5					
258	Heptachlor epoxide	7024-57-3	0.05						
259	Heptane - All isomers		1640						
260	n-Heptane		1640	2000					
261	Hexachlorobenzene [HCB]	118-74-1	0.002						
262	Hexachlorobutadiene	87-68-3	0.2						
263	Hexachlorocyclopentadiene	77-47-4	0.1						
264	Hexachloroethane	67-72-1	10	10					
265	Hexachloronaphthalene	1335-87-1	0.2	0.2					
266	Hexafluoroacetone	684-16-2	0.7						
267	Hexahydrophthalic anhydride	85-42-7	(C)0.005						
268	Hexahydrophthalic anhydride - cis-isomer	13149-00-3	(C)0.005						
269	Hexahydrophthalic anhydride - trans-isomer	14166-21-3	(C)0.005						
270	1,6-Hexamethylene diisocyanate [HDI]	822-06-0	0.03						

#	Substances	CAS #	ACGIH [1] mg/m³	OSHA [2] mg/m³	OEHHA [3] mg/m³	WHO [4] mg/m³	Japan [5] mg/m³	HK [6] mg/m³	Germany [7] mg/m³
271	Hexamethyl phosphoramide	680-31-9	A3						
272	n-Hexane	110-54-3	176	1800	7				
273	Hexane, other isomers excluding n-hexane		500 ppm						
274	1,6-Hexanediamine		2						
275	1-Hexene	592-41-6	172						
276	sec-Hexyl acetate	108-84-9	295	300					
277	Hexylene glycol	107-41-5	(C)121						
279	Hydrogenated terphenyls - Nonirradiated	61788-32-7	5						
278	Hydrogen cyanide (as CN)	74-90-8	(C)5	11	0.009				
280	Hydroquinone	123-31-9	2	2					
281	2-Hydroxypropyl acrylate	999-61-1	3						
282	Indene	95-13-6	48						
283	Isoamyl alcohol	123-51-3	361	360					
284	Isobutane	75-28-5	2378						
285	Isobutyl acetate	110-19-0	713	700					
286	Isobutyl alcohol	78-83-1	152	300					
287	Isobutyl nitrite	542-56-3	(C)4						
288	Isooctane	540-84-1	1402						
289	Isooctyl alcohol	26952-21-6	266						
290	Isopentane	78-78-4	1772						
291	Isopentyl acetate	123-92-2	266	525					
292	Isophorone	78-59-1	(C)28	140	2				
293	Isophorone diisocyanate	4098-71-9	0.05						
294	2-Isopropoxyethanol	109-59-1	107						
295	Isopropyl acetate	108-21-4	418	950					
296	Isopropylamine	75-31-0	12	12					
297	N-Isopropylaniline	768-52-5	11						
298	Isopropyl ether	108-20-3	1045	2100					
299	Isopropyl glycidyl ether [IGE]	4016-14-2	238	240					
300	Jet fuels		200						
301	Kerosene		200						
302	Kerosene - Hydrodesulferized	64742-81-0	200						
303	Ketene	463-51-4	0.9	0.9					
304	Lindane	58-89-9	0.5	0.5					
305	Liquified petroleum gas [L.P.G .]	68476-85-7	1743	1800					
306	Malathion	121-75-5	1	15					
307	Maleic anhydride	108-31-6	0.4	1	0.0007				
308	Manganese cyclopentadienyl tricarbonyl (as Mn)	12079-65-1	0.1						
309	Mesityl oxide	141-79-7	60	100					
310	Methacrylic acid	79-41-4	70						
311	Methane	74-82-8	656						
312	Methanol	67-56-1	262	260	4				
313	Methomyl	16752-77-5	3						
314	Methoxychlor	72-43-5	10	15					
315	2-Methoxyethanol	109-86-4	16	80	0.06	n.p.			
316	2-Methoxyethyl acetate	110-49-6	24	120	0.09				

#	Substances	CAS #	ACGIH [1] mg/m³	OSHA [2] mg/m³	OEHHA [3] mg/m³	WHO [4] mg/m³	Japan [5] mg/m³	HK [6] mg/m³	Germany [7] mg/m³
317	(2-methoxymethylethoxy)propanal [DPGME]	34590-94-8	606	600					
318	4-Methoxyphenol	150-76-5	5						
319	1-Methoxy-2-propanol [PGME]	107-98-2	369		7				
320	Methyl acetatE	79-20-9	639	610					
321	Methyl acetylene	74-99-7	1640	1650					
322	Methyl acetylene-propadiene mixture [MAPP]	59355-75-8	1640						
323	Methyl acrylate	96-33-3	7	35					
324	Methylacrylonitrile	126-98-7	3						
325	Methylal	109-87-5	3114	3100					
326	Methylamine	74-89-5	6	12					
327	Methyl n-amyl ketone	110-43-0	234	465					
328	N-Methyl aniline	100-61-8	2	9					
329	Methyl bromide	74-83-9	4	(C)80	0.005				
330	Methyl tert-butyl ether [MTBE]	1634-04-4	180		8				
331	2-Methylbutyl acetate	624-41-9	266						
332	Methyl n-butyl ketone	591-78-6	20	410					
333	Methyl chloride	74-87-3	103	207					
334	Methyl chloroform	71-55-6	1911	1900	1				
335	Methyl 2-cyanoacrylate	137-05-3	0.9						
336	Methylcyclohexane	108-87-2	1607	2000					
337	Methylcyclohexanol	25639-42-3	234	470					
338	o-Methylcyclohexanone	583-60-8	230	460					
339	2-Methylcyclopentadienyl manganese tricarbonyl	12108-13-3	0.2						
340	Methyl demeton	8022-00-2	0.5						
341	Methylene bisphenyl isocyanate [MDI]	101-68-8	0.05	(C)0.2	0.0007				
342	4,4'-Methylene bis(2-chloroaniline) [MBOCA]	101-14-4	0.1						
343	Methylene bis(4-cyclohexylisocyanate)	5124-30-1	0.05						
344	4,4'-Methylene dianiline	101-77-9	0.8		0.02				
345	Methyl ethyl ketone [MEK]	78-93-3	590	590					
346	Methyl ethyl ketone peroxide [MEKP]	1338-23-4	(C)0.6						
347	Methyl formate	107-31-3	246	250					
348	Methyl hydrazine	60-34-4	0.02	(C)0.35					
349	Methyl iodide	74-88-4	12	28					
350	Methyl isoamyl ketone	110-12-3	234	475					
351	Methyl isobutyl carbinol	108-11-2	105	100					
352	Methyl isobutyl ketone	108-10-1	205	410					
353	Methyl isocyanate	624-83-9	0.05	0.05	0.001				
354	Methyl isopropyl ketone	563-80-4	705						
355	Methyl mercaptan	74-93-1	1.0	(C)20					
356	Methyl mercury (as Hg)	22967-92-6	0.01						
357	Methyl methacrylate	80-62-6	205	410		0.2 [1 yr]			

#	Substances	CAS #	ACGIH [1] mg/m³	OSHA [2] mg/m³	OEHHA [3] mg/m³	WHO [4] mg/m³	Japan [5] mg/m³	HK [6] mg/m³	Germany [7] mg/m³
358	Methyl parathion	298-00-0	0.2						
359	2-Methyl pentane	107-83-5	1763						
360	3-Methyl pentane	96-14-0	1763						
361	Methyl propyl ketone	107-87-9	705	700					
362	Methyl silicate	681-84-5	6						
363	alpha-Methyl styrene	98-83-9	242	(C)480					
364	Methyl vinyl ketone	78-94-4	(C)0.6						
365	Metribuzin	21087-64-9	5						
366	Mevinphos	7786-34-7	0.01	0.1					
367	Monocrotophos	6923-22-4	0.05						
368	Morpholine	110-91-8	71	70					
369	Naled	300-76-5	0.1	3					
370	Naphthalene	91-20-3	52	50	0.009				0.02 / 0.002
371	alpha-Naphthylamine	134-32-7		Carcinogen					
372	beta-Naphthylamine	91-59-8	A1	Carcinogen					
373	Natural gas	8006-14-2	1000 ppm						
374	Natural rubber latex	9006-04-6	0.001						
375	Nicotine	54-11-5	0.5	0.5					
376	p-Nitroaniline	100-01-6	3	6					
377	Nitrobenzene	98-95-3	5	5					
378	p-Nitrochlorobenzene	100-00-5	0.6	1					
379	4-Nitrodiphenyl	92-93-3	A2	Carcinogen					
380	Nitroethane	79-24-3	307	307					
381	Nitroglycerin [NG]	55-63-0	0.5	(C)2					
382	Nitromethane	75-52-5	50	250					
383	1-Nitropropane	108-03-2	91	90					
384	2-Nitropropane	79-46-9	36	90					
385	N-Nitrosodimethylamine	62-75-9	A3	Carcinogen					
386	Nitrotoluene - o-isomer	88-72-2	11	30					
387	Nitrotoluene - m-isomer	99-08-1	11	30					
388	Nitrotoluene - p-isomer	99-99-0	11	30					
389	Nonanal	124-19-6					0.041 (interim due to data gap)		
390	Nonane - All isomers	111-84-2	1050						
391	Octachloronaphthalene	2234-13-1	0.1	0.1					
392	n-Octane	111-65-9	1402	2350					
393	Oxalic acid	144-62-7	1	1					
394	p,p'-Oxybis(benzenesulfonyl hydrazide)	80-51-3	0.1						
395	Paraquat	4685-14-7	0.1						
396	Paraquat	4685-14-7	0.5						
397	Parathion	56-38-2	0.05	0.1					
398	Pentachloronaphthalene	1321-64-8	0.5	0.5					
399	Pentachloronitrobenzene	82-68-8	0.5						
400	Pentachlorophenol	87-86-5	0.5	0.5					0.001 / 0.0001
401	Pentane - All isomers		1772						
402	n-Pentane		1772	2950					
403	tert-Pentane [Neopentane]	463-82-1	1772						
404	Pentyl acetate - All isomers		266						

#	Substances	CAS #	ACGIH [1] mg/m³	OSHA [2] mg/m³	OEHHA [3] mg/m³	WHO [4] mg/m³	Japan [5] mg/m³	HK [6] mg/m³	Germany [7] mg/m³
405	1-Pentyl acetate		266	525					
406	2-Pentyl acetate	626-38-0	266	650					
407	3-Pentyl acetate	620-11-1	266						
408	tert-Pentyl acetate	625-16-1	266						
409	Perchloromethyl mercaptan	594-42-3	0.8	0.8					
410	Perfluorobutyl ethylene [PFBE]	19430-93-4	1007						
411	Perfluoroisobutylene	382-21-8	(C)0.08						
412	Phenol	108-95-2	19	19	0.2				
413	Phenothiazine	92-84-2	5						
414	o-Phenylenediamine	95-54-5	0.1						
415	m-Phenylenediamine	108-45-2	0.1						
416	p-Phenylenediamine	106-50-3	0.1	0.1					
417	Phenyl ether - Vapor	101-84-8	7	7					
418	Phenyl ether-biphenyl mixture, vapor			7					
419	Phenyl glycidyl ether [PGE]		0.6	60					
420	Phenylhydrazine	100-63-0	0.4	22					
421	Phenyl mercaptan	108-98-5	0.5						
422	N-Phenyl-beta-naphthylamine	135-88-6	A4						
423	Phenyl phosphine	638-21-1	(C)0.2						
424	Phorate	298-02-2	0.05						
425	Phthalic anhydride	85-44-9	6	12	0.02				
426	m-Phthalodinitrile	626-17-5	5						
427	Picric acid	88-89-1	0.1	0.1					
428	Pindone	83-26-1	0.1	0.1					
429	alpha-Pinene	80-56-8	112						2 / 0.2 (terpenes) **
430	beta-Pinene	127-91-3	112						
431	Piperazine dihydrochloride	142-64-3	5						
432	Propane	74-98-6	1804	1800					
433	Propane sultone	1120-71-4	A3						
434	n-Propanol	71-23-8	492	500					
435	2-Propanol	67-63-0	492	980	7	n.p.			
436	Propargyl alcohol	107-19-7	2						
437	beta-Propiolactone	57-57-8	1	Carcinogen					
438	Propionaldehyde	123-38-6	48						
439	Propionic acid	79-09-4	30						
440	Propoxur	114-26-1	0.5						
441	n-Propyl acetate	109-60-4	836	840					
442	Propylene	115-07-1	335800		3				
443	Propylene dichloride	78-87-5	347	350					
444	Propylene glycol dinitrate	6423-43-4	0.3						
445	Propylene imine	75-55-8	5	5					
446	Propylene oxide	75-56-9	5	240	0.03				
447	n-Propyl nitrate	627-13-4	108	110					
448	Pyrethrum	8003-34-7	5	5					
449	Pyridine	110-86-1	3	15					
450	Quinone	106-51-4	0.4	0.4					
451	Resorcinol	108-46-3	45						

#	Substances	CAS #	ACGIH [1] mg/m³	OSHA [2] mg/m³	OEHHA [3] mg/m³	WHO [4] mg/m³	Japan [5] mg/m³	HK [6] mg/m³	Germany [7] mg/m³
452	Ronnel [Fenchlorphos]	299-84-3	10	15					
453	Rosin core solder thermal decomposition products (colophony)	8050-09-7	sensitization						
454	Rotenone (commercial)	83-79-4	5	5					
455	Rubber solvent (Naphtha)	8030-30-6	1588	400					
456	Sesone	136-78-7	10						
457	Sodium fluoroacetate	62-74-8	0.05	0.05					
458	Stoddard solvent	8052-41-3	573	2900					
459	Strychnine	57-24-9	0.2	0.2					
460	Styrene - monomer	100-42-5	85	426	0.9	0.26 [1 wk]	0.22		0.3 / 0.03
461	Subtilisins [Proteolytic enzymes]	1395-21-7	(C)0.00006						
462	Sulfometuron methyl	74222-97-2	5						
463	Sulfotepp [TEDP]	3689-24-5	3						
464	Sulprofos	35400-43-2	1						
465	2,4,5- T [2,4,5-Trichlorophenoxyacetic acid]	93-76-5	10						
466	Temephos	3383-96-8	10						
467	Terbufos	1307-79-9	0.01						
468	Terephthalic acid	100-21-0	10						
469	o-Terphenyl	84-15-1	(C)5						
470	m-Terphenyl	92-06-8	(C)5						
471	p-Terphenyl	92-94-4	(C)5						
472	Terphenyl- Mixed isomers	26140-60-3	(C)5	(C)9					
473	1,1,1,2-Tetrachloro-2,2-difluoroethane [FC-112a]	76-11-9	4171	4170					
474	1,1,2,2-Tetrachloro-1,2-difluoroethane [FC-112]	76-12-0	4171	4170					
475	1,1,2,2-Tetrachloroethane	79-34-5	7	35					
476	Tetrachloroethylene [Perchlorophthalene]	127-18-4	170	679	0.035	0.25 [24 hr]		0.25	
477	Tetrachloronaphthalene	1335-88-2	2	2					
478	Tetradecane	629-59-4					0.33		
479	Tetraethyllead (as Pb)	78-00-2	0.1	0.08					
480	Tetraethyl pyrophosphate [TEPP]	107-49-3	0.05	0.05					
481	Tetrafluoroethylene	116-14-3	8						
482	Tetrahydrofuran	109-99-9	590	590					
483	Tetramethyllead (as Pb)	75-74-1	0.2	0.08					
484	Tetramethyl succinonitrile	3333-52-6	3	3					
485	Tetranitromethane	509-14-8	0.04	8					
486	Tetryl	479-45-8	2	2					
487	Thimerosal	54-64-8	0.1						
488	4,4'- Thiobis(6-tert-butyl-m-cresol)	96-69-5	10						
489	Thioglycolic acid	68-11-1	4						
490	Thiram	137-26-8	1	5					
491	Tin - Organic compounds (as Sn)	7440-31-5	0.1	0.1					
492	o-Tolidine	119-93-7	A3						
493	Toluene	108-88-3	189	754	0.3	0.26 [1 wk]	0.26	1.092	3 / 0.3

#	Substances	CAS #	ACGIH [1] mg/m³	OSHA [2] mg/m³	OEHHA [3] mg/m³	WHO [4] mg/m³	Japan [5] mg/m³	HK [6] mg/m³	Germany [7] mg/m³
494	Toluene-2,4-diisocyanate [2,-4-TDI]	584-84-9	0.04	(C)0.14	0.00007				
495	Toluene-2,6-diisocyanate [2,6-TDI]	91-08-7	0.2						
496	Toluene diisocyanate - Mixed isomers	26471-62-5	0.04						
497	o-Toluidine	95-53-4	9	22					
498	m-Toluidine	108-44-1	9						
499	p-Toluidine	106-49-0	9						
500	Tributyl phosphate	126-73-8	2	5					
501	Trichloroacetic acid	76-03-9	7						
502	1,2,4-Trichlorobenzene	120-82-1	(C)37						
503	1,1 ,2-Trichloroethane	79-00-5	55	45					
504	Trichloroethylene	79-01-6	269	538	0.6	n.v		0.77	
505	Trichlorofluoromethane [FC-11]	75-69-4	(C)5600	5600					
506	Trichloronaphthalene	1321-65-9	5	5					
507	1,2,3-Trichloropropane	96-18-4	60	300					
508	1,1 ,2-Trichloro-1 ,2,2-trifluoroethane [FC-113]	76-13-1	7669	7600					
509	Trichlorphon	52-68-6	1						
510	Triethanolamine	102-71-6	5						
511	Triethylamine	121-44-8	4	100	0.2				
512	Trifluorobromomethane [F-13B1]	75-63-8	6094	6100					
513	1,3,5- Triglycidyl-s-triazinetrione	2451-62-9	0.05						
514	Trimellitic anhydride	552-30-7	(C)0.04						
515	Trimethylamine	75-50-3	33						
516	1,2,3- Trimethyl benzene	526-73-8	123						
517	1,2,4- Trimethyl benzene	95-63-6	123						
518	1,3,5- Trimethyl benzene [Mesitylene]	108-67-8	123						
519	Trimethyl benzene - Mixed isomers	25551-13-7	123						
520	Trimethyl phosphite	121-45-9	10						
521	2,4,6- Trinitrotoluene [TNT]	118-96-7	0.1	2					
522	Triorthocresyl phosphate	78-30-8	0.1	0.1					
523	Triphenyl amine	603-34-9	5						
524	Triphenyl phosphate	115-86-6	3	3					
525	Tris(2-chloroethyl)phosphate	115-96-8							0.05 / 0.005
526	Turpentine	8006-64-2	111	560					
527	n-Valeraldehyde	110-62-3	176						
528	Varnish makers' & Printers'	8032-32-4	1400						
529	Vinyl acetate	108-05-4	35		0.2				
530	Vinyl bromide	593-60-2	2						
531	Vinyl chloride	75-01-4	3	3					
532	4-Vinyl cyclohexene	100-40-3	0.4						
533	Vinyl cyclohexene dioxide	106-87-6	0.6						
534	Vinyl fluoride	75-02-5	2						
535	Vinylidene chloride	75-35-4	20		0.07				

#	Substances	CAS #	ACGIH [1] mg/m³	OSHA [2] mg/m³	OEHHA [3] mg/m³	WHO [4] mg/m³	Japan [5] mg/m³	HK [6] mg/m³	Germany [7] mg/m³
536	Vinylidene fluoride	75-38-7	1310						
537	N-Vinyl-2-pyrrolidone	88-12-0	0.2						
538	Vinyl toluene [Methyl styrene] - Mixed isomers	25013-15-4	242	480					
539	Warfarin	81-81-2	0.1	0.1					
540	o-Xylene	95-47-6	434						
541	m-Xylene	108-38-3	434						
542	p-Xylene	106-42-3	434						
543	Xylene - Mixed isomers	1330-20-7	434	435	0.7	4.8 [24 hr]	0.87	1.447	
544	m-Xylene alpha,alpha'-diamin	1477-55-0	(C)0.1						
545	Xylidine - Mixed isomers	1300-73-8	2	25					
546	TVOC						0.4	0.6	0.2 - 0.3 ***

1 ACGIH TLV *(ACGIH, 2004)*
- TLV: threshold limit value set by American Conference of Governmental Industrial Hygienists. The time-weighted average conc. of a substance to which most workers can be exposed without adverse effects.
- A1 (confirmed human carcinogen), A2 (suspected human carcinogen), A3 (confirmed animal carcinogen w/ unknown relevance to humans) & A4 (not classifiable as a human carcinogen)
- Ref: ACGIH (2004) "TLVs and BEIs with other worldwide occupational exposure values 2004 CD-ROM"
2 OSHA PEL *(OSHA, 2004 a & 2004 b)*
- PEL: permissible exposure level set by the Occupational Safety and Health Administration (OSHA), US Department of Labor to protect workers against the health effects of exposure to hazardous substances over a normal 8-h workday or a 40-h workweek.
- PELs are regulatory limits on the amount or conc. of a substance in the air & are based on an 8-hour time weighted average (TWA) exposure.
- (C) denotes a ceiling limit.
- Ref: http://www.osha.gov/pls/oshaweb/owadisp.show_document?p_table=STANDARDS&p_id=9992
http://www.osha.gov/pls/oshaweb/owadisp.show_document?p_table=STANDARDS&p_id=9993
3 CREL *(OEHHA, 2005)*
- Non-caner chronic reference exposure level, Office of Env. Health Hazard Assessment (OEHHA), California EPA.
- CRELs are available at http://www.oehha.org/air/chronic_rels/AllChrels.html.
- CREL of a chemical is the airborne concentration that would pose no significant health risk to the general public.
4 WHO Guidelines for Air Quality *(WHO, 1999)*
- Guidelines for air pollutants with non-carcinogenic and carcinogenic health endpoints.
- Ref: http://www.who.int/environmental_information/Air/Guidelines/Chapter3.htm#3.2
- n.p.: not provided, n.v.: no value is given for chemicals with cancer health endpoints, Number in brackets [ ] is averaging time.
5 Japan - MHLW IAQ Guidelines *(MHLW, 2004)*
- IAQ Guidelines by Ministry of Health, Labour and Welfare of Japan
- The values are mainly based on long-term exposure except for formaldehyde.
- Ref: http://www.nihs.go.jp/mhlw/ocs/sickhouse/rep-eng4.pdf
6 Hong Kong - IAQ Guidelines *(Hong Kong, 2003)*
- Guidelines for Good Class IAQ set by the Government of the Hong Kong Special Administrative Region
- Ref: http://www.iaq.gov.hk/cert/doc/CertGuide-eng.pdf
7 Germany - IAQ Guidelines *(Umwelt Bundes Amt, 2005)*
- IAQ Guidelines set by an ad hoc working group of members of the Federal Environmental Agency's Indoor Air Hygiene Commission (IRK) & the Working Group of the Health Ministries of the Länder (AOLG) of Germany.
- Ref: http://www.umweltbundesamt.de/uba-info-daten/daten/irk.htm & http://www.umweltbundesamt.de/uba-info-daten-e/daten-e/irk.htm#4
** Guide value II / Guide value I [averaging time]*
*** The value is for the sum of several terpenes.*
**** These values of TVOC are for the maximum long-term average.*
Note: *- Some of the values were converted from ppm to mg/m3 at 25 oC and 1 atm.*